NANOSIZED DRUG DELIVERY SYSTEMS: COLLOIDS AND GELS FOR SITE SPECIFIC TARGETING

EDITED BY: Francesco Cellesi, Martin Ehrbar and Filippo Rossi
PUBLISHED IN: Frontiers in Bioengineering and Biotechnology

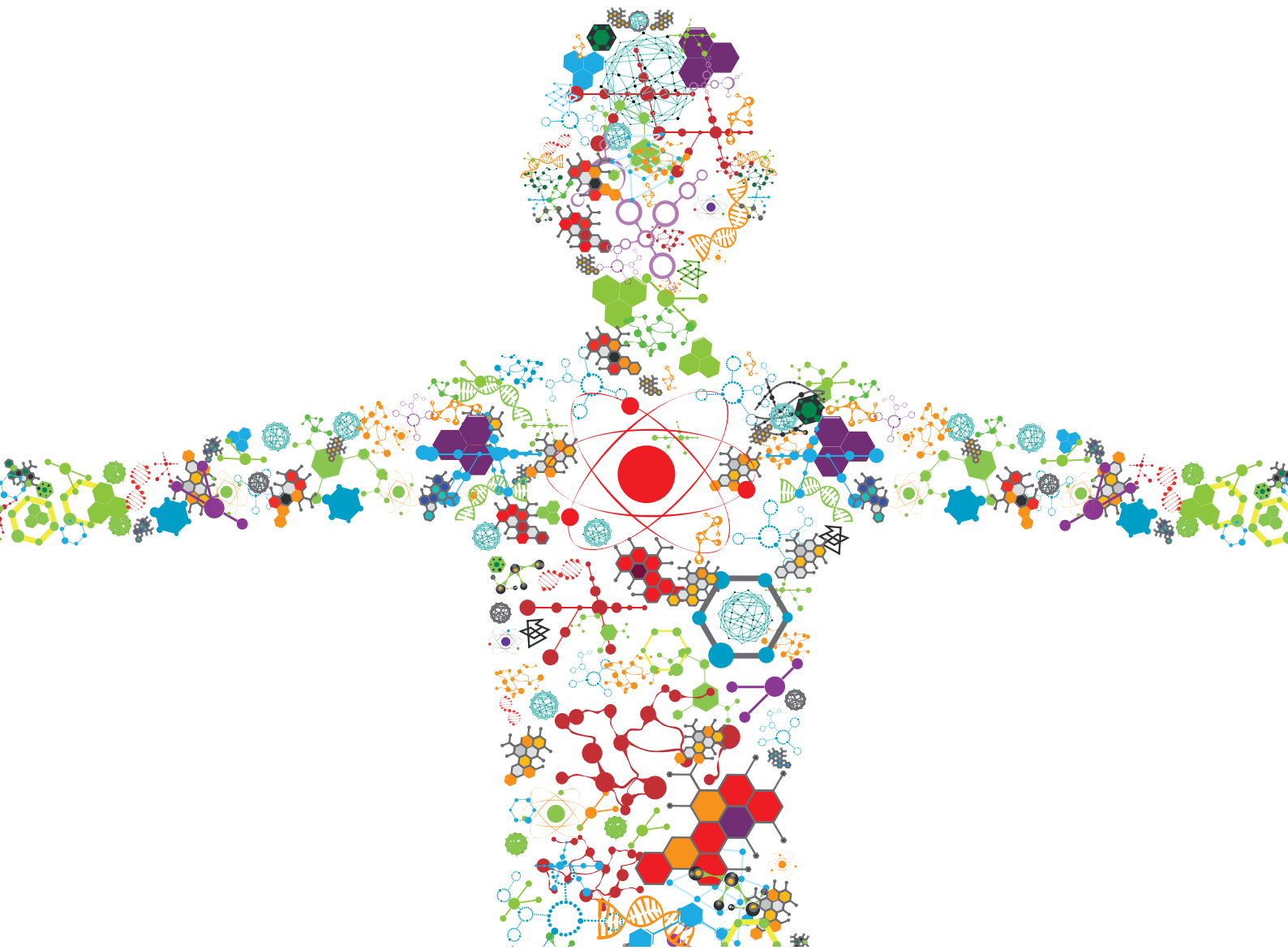

frontiers Research Topics

ISSN 1664-8714
ISBN 978-2-88966-022-3
DOI 10.3389/978-2-88966-022-3

About Frontiers

Frontiers is more than just an open-access publisher of scholarly articles: it is a pioneering approach to the world of academia, radically improving the way scholarly research is managed. The grand vision of Frontiers is a world where all people have an equal opportunity to seek, share and generate knowledge. Frontiers provides immediate and permanent online open access to all its publications, but this alone is not enough to realize our grand goals.

Frontiers Journal Series

The Frontiers Journal Series is a multi-tier and interdisciplinary set of open-access, online journals, promising a paradigm shift from the current review, selection and dissemination processes in academic publishing. All Frontiers journals are driven by researchers for researchers; therefore, they constitute a service to the scholarly community. At the same time, the Frontiers Journal Series operates on a revolutionary invention, the tiered publishing system, initially addressing specific communities of scholars, and gradually climbing up to broader public understanding, thus serving the interests of the lay society, too.

Dedication to Quality

Each Frontiers article is a landmark of the highest quality, thanks to genuinely collaborative interactions between authors and review editors, who include some of the world's best academicians. Research must be certified by peers before entering a stream of knowledge that may eventually reach the public - and shape society; therefore, Frontiers only applies the most rigorous and unbiased reviews.
Frontiers revolutionizes research publishing by freely delivering the most outstanding research, evaluated with no bias from both the academic and social point of view. By applying the most advanced information technologies, Frontiers is catapulting scholarly publishing into a new generation.

What are Frontiers Research Topics?

Frontiers Research Topics are very popular trademarks of the Frontiers Journals Series: they are collections of at least ten articles, all centered on a particular subject. With their unique mix of varied contributions from Original Research to Review Articles, Frontiers Research Topics unify the most influential researchers, the latest key findings and historical advances in a hot research area! Find out more on how to host your own Frontiers Research Topic or contribute to one as an author by contacting the Frontiers Editorial Office: researchtopics@frontiersin.org

NANOSIZED DRUG DELIVERY SYSTEMS: COLLOIDS AND GELS FOR SITE SPECIFIC TARGETING

Topic Editors:
Francesco Cellesi, Politecnico di Milano, Italy
Martin Ehrbar, University of Zurich, Switzerland
Filippo Rossi, Politecnico di Milano, Italy

Citation: Cellesi, F., Ehrbar, M., Rossi, F., eds. (2020). Nanosized Drug Delivery Systems: Colloids and Gels for Site Specific Targeting. Lausanne: Frontiers Media SA. doi: 10.3389/978-2-88966-022-3

Table of Contents

frontiers in Bioengineering and Biotechnology

EDITORIAL
published: 04 August 2020
doi: 10.3389/fbioe.2020.00803

Editorial: Nanosized Drug Delivery Systems: Colloids and Gels for Site Specific Targeting

Martin Ehrbar[1], *Filippo Rossi*[2] *and Francesco Cellesi*[2]*

[1] Department of Obstetrics, University Hospital Zurich, University of Zurich, Zurich, Switzerland, [2] Department of Chemistry, Materials and Chemical Engineering, Politecnico di Milano, Milan, Italy

Keywords: nanomedicine, drug delivery, nanocarrier (nanoparticle), colloids, gels, targeting, growth factors

Editorial on the Research Topic

Nanosized Drug Delivery Systems: Colloids and Gels for Site Specific Targeting

Recent advances in nanomedicine and biomaterials have provided new promising tools for *in vitro* models and targeted drug administration *in vivo*, aiming to increase efficacy while limiting side effects. Nanosized drug delivery systems are designed to modify the biodistribution of therapeutic agents, in order to enhance their accumulation in the pathological site. Bioactive molecules can be either conjugated to or entrapped into colloidal nanocarriers. Biocompatible nanoparticles (NPs), polymer nanotherapeutics, lipid-based nanomaterials may enhance the stability and the targeted delivery of low molecular weight drugs, as well as nucleic acids and therapeutic proteins. Once administered *in vivo*, these colloids will face sequential biological barriers, which represent a major challenge for site specific drug delivery. A fine control of key physicochemical characteristics of the nanocarriers, including size, drug loading, and functionality, may lead to a successful barrier penetration and an effective release at the targeted site.

Thomas and Weber review current limitations of NP-based drug delivery by focusing on cancer treatments. While enhanced permeability and retention (EPR) can result in drug accumulation in malignant tissues, this effect is highly dependent on tumor type and location. In order to improve drug delivery, drugs, and NPs with long half-lives are obtained by conjugation or coating with hydrophilic polymers. Controlled activation approaches and active targeting to cancer cells or specific cellular compartments are discussed in view of possible future developments.

Naturally derived polymers are increasingly used in therapeutics and diagnostics. Chitosan NPs are known to be promising vehicles for drug, protein, and gene delivery. Their main drawback resides in their low physical and chemical stability under biological conditions. In order to overcome this limitation, Saeed et al. grafted chitosan to phthalic or phenylsuccinic acids and then used polyphosphoric acid, hexametaphosphate, or tripolyphosphate to achieve ionotropic complexation and covalent crosslinking by carbodiimide chemistry. The NPs showed high stability and reproducibility, as well as cytotoxic activity once loaded with the chemotherapic doxorubicin.

Vashist et al. developed a smart strategy to prepare auto-fluorescent hydrogel NPs made of hydroxyethyl cellulose and chitosan, using water-in-oil emulsion polymerization. These nanoparticles guaranteed biocompatibility, stability, proper cellular uptake, and the ability to cross a model of blood brain barrier. Moreover, their auto-fluorescence in a wide range of wavelengths may be exploited in the field of theranostics to develop image-guided therapies for the central nervous system.

OPEN ACCESS

Edited and reviewed by:
Gianni Ciofani,
Italian Institute of Technology (IIT), Italy

***Correspondence:**
Francesco Cellesi
francesco.cellesi@polimi.it

Specialty section:
This article was submitted to Nanobiotechnology, a section of the journal Frontiers in Bioengineering and Biotechnology

Received: *16 June 2020*
Accepted: *22 June 2020*
Published: *04 August 2020*

Citation:
Ehrbar M, Rossi F and Cellesi F (2020) Editorial: Nanosized Drug Delivery Systems: Colloids and Gels for Site Specific Targeting. Front. Bioeng. Biotechnol. 8:803. doi: 10.3389/fbioe.2020.00803

Recently, polymeric NPs have been tested as therapeutic cancer vaccines, i.e., medical tools which are capable of educating the immune system to fight tumors and prevent cancer diseases. Briquez et al. discuss in their review the principles and current strategies to engineer therapeutic cancer vaccines, with a particular focus on the use of site-specific targeting nanomaterials. They outline the type of immune responses triggered by vaccination, with an overview of the main components of cancer vaccines, describing how nanomaterials can be engineered to improve pharmacokinetics and pharmacodynamics of the vaccine.

Current barriers to clinical translation of NPs are mainly related to the limited control over NP physicochemical properties and robust scale-up of their production. Bovone et al. engineered an automated coaxial jet mixer for the production of stable and size-controlled polymeric NPs from chemically diverse block copolymers. The jet mixer allowed a fine tuning of the flow conditions and mixing of the copolymer-containing organic phase and an aqueous stream, for the continuous nanoprecipitation of polymeric NPs.

The advantage of protecting active compounds from the environment during storage and transport, while achieving a safe and controlled release, are also relevant for applications which are far from healthcare. Vega-Vásquez et al. describe different types of nanocarriers developed in the biomedical field which may find applications in agriculture, specifically in the area of plant breeding, growth promotion, disease control, and post-harvest quality control, in order to improve plant and food production, while reducing the impact on the environment.

Moncalvo et al. describe in their review the recent research progress on nanosized delivery systems for therapeutic proteins, highlighting future directions and challenges. Although the impact of protein therapeutics in healthcare is steadily increasing, their safety and efficacy are often limited by instability, short half-life, and immunogenicity. Covalent attachment of biocompatible polymers, as well as protein nanoencapsulation in colloidal systems, are currently being investigated for overcoming these limitations, with the potential to develop next-generation protein therapeutics.

Smart hydrogels with highly ordered structures at the nano-scale have been extensively investigated as advanced delivery systems. These gels can act as efficient drug protectors, especially for peptides and proteins with limited half-life, and as targeted drug carriers for *in situ* controlled delivery. These characteristics are particularly appealing in tissue engineering, where extracellular matrix (ECM) mimetic biomaterials are required for controlled release of soluble factors to stimulate tissue regeneration.

Ren et al. review growth factor (GF) engineering strategies for tissue regeneration. GF binding to provisional biomaterials or even natural ECM serves as slow-delivery approach. The stability of GFs may be enhanced by site specific PEGylation, by the optimization of the primary structure or the modification of proteolytic sites. GF signaling may also be improved by modulating the receptor binding site, creating hybrid proteins which engage alternative signaling pathways, or controlling the GF availability to cell-surface receptors.

Hwang et al. review ECM-mimetic biomaterials for targeted and sustained drug release. The broad repertoire of ECM interactions with different cell-surface receptors can facilitate cell-targeted delivery and improve the therapeutic efficiency of drugs. In addition, the interaction between ECM components and cellular receptors are exploited for intracellular delivery, which may have a significant impact on disease treatment and tissue regeneration.

Fattah and Ranga present the latest advances in engineering organoids through a modular and orthogonal design of biomimetic materials, and the use of NPs which are able to modulate matrix and tissue mechanical stresses. Magnetic NPs enable the localized mechanical manipulation of cells and biomaterials during the establishment of organoids. Once internalized by target cells, these NPs become tools for cell stimulation and assembly of complex tissue structures.

AUTHOR CONTRIBUTIONS

All authors listed have made a substantial, direct and intellectual contribution to the work, and approved it for publication.

Conflict of Interest: The authors declare that the research was conducted in the absence of any commercial or financial relationships that could be construed as a potential conflict of interest.

frontiers in Bioengineering and Biotechnology

BRIEF RESEARCH REPORT
published: 17 December 2019
doi: 10.3389/fbioe.2019.00423

Automated and Continuous Production of Polymeric Nanoparticles

*Giovanni Bovone, Fabian Steiner, Elia A. Guzzi and Mark W. Tibbitt**

Macromolecular Engineering Laboratory, Department of Mechanical and Process Engineering, ETH Zürich, Zurich, Switzerland

Polymeric nanoparticles (NPs) are increasingly used as therapeutics, diagnostics, and building blocks in (bio)materials science. Current barriers to translation are limited control over NP physicochemical properties and robust scale-up of their production. Flow-based devices have emerged for controlled production of polymeric NPs, both for rapid formulation screening ($\sim\mu$g min^{-1}) and on-scale production ($\sim$mg min^{-1}). While flow-based devices have improved NP production compared to traditional batch processes, automated processes are desired for robust NP production at scale. Therefore, we engineered an automated coaxial jet mixer (CJM), which controlled the mixing of an organic stream containing block copolymer and an aqueous stream, for the continuous nanoprecipitation of polymeric NPs. The CJM was operated stably under computer control for up to 24 h and automated control over the flow conditions tuned poly(ethylene glycol)-*block*-polylactide (PEG_{5K}-*b*-PLA_{20K}) NP size between ≈56 nm and ≈79 nm. In addition, the automated CJM enabled production of NPs of similar size ($D_h \approx$ 50 nm) from chemically diverse block copolymers, PEG_{5K}-*b*-PLA_{20K}, PEG-*block*-poly(lactide-*co*-glycolide) (PEG_{5K}-*b*-$PLGA_{20K}$), and PEG-*block*-polycaprolactone (PEG_{5K}-*b*-PCL_{20K}), by tuning the flow conditions for each block copolymer. Further, the automated CJM was used to produce model nanotherapeutics in a reproducible manner without user intervention. Finally, NPs produced with the automated CJM were used to scale the formation of injectable polymer–nanoparticle (PNP) hydrogels, without modifying the mechanical properties of the PNP gel. In conclusion, the automated CJM enabled stable, tunable, and continuous production of polymeric NPs, which are needed for the scale-up and translation of this important class of biomaterials.

Keywords: nanoparticles, drug delivery, flow-based synthesis, automated production, process engineering

OPEN ACCESS

Edited by:
Filippo Rossi, Politecnico di Milano, Italy

Reviewed by:
Clara Mattu, Politecnico di Torino, Italy
Pradipta Ranjan Rauta, University of Texas MD Anderson Cancer Center, United States

****Correspondence:***
Mark W. Tibbitt
mtibbitt@ethz.ch

Specialty section:
This article was submitted to Nanobiotechnology, a section of the journal Frontiers in Bioengineering and Biotechnology

Received: *30 September 2019*
Accepted: *29 November 2019*
Published: *17 December 2019*

Citation:
Bovone G, Steiner F, Guzzi EA and Tibbitt MW (2019) Automated and Continuous Production of Polymeric Nanoparticles. Front. Bioeng. Biotechnol. 7:423. doi: 10.3389/fbioe.2019.00423

1. INTRODUCTION

Nanoparticles (NPs) comprise a useful class of biomaterials in modern medicine for the encapsulation and delivery of small molecule drugs, proteins, and nucleic-acid therapies as well as for *in vivo* diagnosis or as agents for improved biomedical imaging (Anselmo and Mitragotri, 2016; Kamaly et al., 2016; Detappe et al., 2017; Shi et al., 2017). NPs are particularly attractive in drug delivery as they can increase the solubility of poorly blood-soluble drugs, enhance drug stability, extend circulation time, and aid transport across biological barriers (Langer, 1998; Tibbitt et al., 2016). Within the field of nanomedicine, aqueous stable polymeric NPs

are especially useful as carriers for hydrophobic small molecules, which can be encapsulated directly within the hydrophobic core of the NPs during production without the need for chemical modification of the drug (Cheng et al., 2007; Liu et al., 2010; Bertrand et al., 2017). Drug-loaded NPs can be self-assembled via nanoprecipitation of amphiphilic block copolymers, e.g., poly(ethylene glycol)-*block*-polylactide (PEG_{5K}-*b*-PLA_{20K}), PEG-*block*-poly(lactide-*co*-glycolide) (PEG_{5K}-*b*-$PLGA_{20K}$), or PEG-*block*-polycaprolactone (PEG_{5K}-*b*-PCL_{20K}). Core-shell NPs have been exploited for systemic delivery of therapeutics following parenteral or oral administration as well as for local delivery following targeted administration in the body (Gref et al., 1994; Song et al., 1997; Westedt et al., 2007; Pridgen et al., 2013, 2015). Beyond the use of core-shell NPs as a stand alone delivery vector, they have recently been exploited as building blocks in the assembly of shear-thinning and self-healing, polymer–nanoparticle (PNP) hydrogels for site specific delivery following local injection (Appel et al., 2015b). PNP hydrogels have also been used as nanocarrier bioinks for additive manufacturing, as a sprayable barrier to prevent tissue adhesion following cardiothoracic surgery, and as a depot for the local release of cytokines and recruitment of immune cells (Fenton et al., 2019; Guzzi et al., 2019; Lopez Hernandez et al., 2019; Stapleton et al., 2019).

Despite the versatility and significant potential of polymeric NPs in biomedicine, translation to the clinic often remains limited by uncontrolled and poorly scalable production (Hickey et al., 2015; Ragelle et al., 2017; Colombo et al., 2018). Clinical application of polymeric NPs, either as a delivery vehicle or as a building block in PNP hydrogels, requires precise control over NP size, efficient drug loading, and scalable production. Polymeric NPs are commonly produced from amphiphilic block copolymers, such as PEG_{5K}-*b*-PLA_{20K}, PEG_{5K}-*b*-$PLGA_{20K}$, and PEG_{5K}-*b*-PCL_{20K}, by adding a solution of a water-miscible organic solvent, the block copolymer, and, optionally, a hydrophobic drug dropwise to water under vigorous stirring (Fessi et al., 1989; Mora-Huertas et al., 2010). The solvent mixes rapidly with water and the NPs form as the hydrophobic blocks collapse into a kinetically trapped core surrounded by a hydrophilic corona (Nicolai et al., 2010). Conventionally, this nanoprecipitation is carried out in batch with relatively limited throughput as well as minimal control over the production parameters and, thus, NP size or drug loading (Murday et al., 2009). More recently, flow-based devices have been developed for the continuous and tunable production of polymeric NPs via controlled mixing of an organic stream containing the block copolymer and drug with an aqueous stream in micro- or milli-fluidic systems (Johnson and Prud'homme, 2003a; Karnik et al., 2008; Capretto et al., 2012). Precise regulation of the flow rates provides a handle to control NP properties, such as size, by tuning the mixing time (Johnson and Prud'homme, 2003b; Saad and Prud'homme, 2016). Microfluidic devices based on hydrodynamic flow focusing have been used for formulation screening (μg min^{-1}), while on-scale production (mg min^{-1} to g min^{-1}) was achieved with impinging jet mixers and coaxial jet mixers (CJMs) (Karnik et al., 2008; Lim et al., 2014; Hickey et al., 2015; Liu et al., 2015; Rode García et al., 2018). In our recent work, we developed a CJM from off-the-shelf components for flow-based production of NPs that enabled tunable NP size in both formulation screening mode ($\sim\mu$g min^{-1}) and scalable production mode ($\sim$mg min^{-1}) (Bovone et al., 2019). While flow-based devices have improved the process engineering and production of polymeric NPs, automated processes are needed to offer user-independent scale-up and to minimize human intervention during pharmaceutical production.

In this study, we automated the CJM for continuous, controlled, and scalable production of polymeric NPs. The system exploited computer-controlled syringe pumps to tune the flow rates of the block copolymer solution and aqueous streams within the flow-based device. NPs of specified diameters were formed by tuning the flow rates and the ratio of the two streams and the CJM was operated stably, without human intervention, for up to 24 h. PEG_{5K}-*b*-PLA_{20K} NPs were formed continuously during stable operation, and the size was tuned between ≈56 and ≈79 nm within a single production process. The automated CJM was then used to produce NPs from three distinct polymers, PEG_{5K}-*b*-PCL_{20K}, PEG_{5K}-*b*-PLA_{20K}, and PEG_{5K}-*b*-$PLGA_{20K}$, with a similar diameter, $D_h \approx 50$ nm. In contrast, standard batch nanoprecipitation of PEG_{5K}-*b*-PCL_{20K}, PEG_{5K}-*b*-PLA_{20K}, and PEG_{5K}-*b*-$PLGA_{20K}$ formed NPs of disparate diameters, $D_h \approx$ 55, 76, and 60 nm, respectively. Stable operation and tuning of NP size using flow conditions were demonstrated both for dilute (10 mg mL^{-1}) and concentrated (50 mg mL^{-1}) polymer solutions. In addition, the automated CJM controlled NP size during formulation screening and scale-up of NP production. Model nanotherapeutics were produced with a consistent NP size using the automated CJM and Oil Red O (OR) as a model hydrophobic small molecule drug. Finally, on-scale production of NPs enabled the formation of PNP hydrogels in 0.6 g and 6.0 g batches, without altering the rheological properties of the PNP gels. In total, the automated CJM enabled controlled and scalable production of polymeric NPs with minimal user input, which is essential for the design and translation of nanocarriers and PNP gels for site specific delivery of therapeutics.

2. MATERIALS AND METHODS

2.1. Materials

PEG_{5k}-*b*-PCL_{20k}, PEG_{5k}-*b*-PLA_{20k} and PEG_{5k}-*b*-$PLGA_{20k}$ were purchased from PolySciTech, a divison of Akina, Inc. (USA). Acetonitrile (ACN) and dimethylformamide (DMF) were purchased from VWR International AG (CH). Ultrapure deionized water (dH_2O) was freshly filtered using a Milli-Q IQ 7000 from Merck Millipore (CH). All components of the coaxial jet mixer were purchased from BGB Analytik (CH) or Cole-Parmer (US) and are listed in detail in our recent work (Bovone et al., 2019).

2.2. Batch Nanoparticle Formation

Block copolymer solutions of 10 mg mL^{-1} or 50 mg mL^{-1} were prepared by dissolving PEG_{5k}-*b*-PCL_{20k} or PEG_{5k}-*b*-PLA_{20k} in

ACN, and PEG_{5k}-*b*-$PLGA_{20k}$ in DMF. The organic solution to water ratio, *R*, was defined as

$$R = \frac{V_{organic}}{V_{H_2O}} \quad (1)$$

For each batch nanoprecipitation, 1 mL of block copolymer solution ($V_{organic}$) was added drop wise to 10 mL of dH_2O (V_{H_2O}; $R = 0.1$) under stirring at 650 RPM (Stir bar: 15 mm). All batch nanoprecipitation experiments were performed in triplicate.

2.3. Flow-Based Nanoparticle Formation

2.3.1. Experimental Set-Up

The CJM design was based on similar devices used for inorganic particle synthesis and a recently developed device from our group for the flow-based production of polymeric nanoparticles (Baber et al., 2015; Bovone et al., 2019). The CJM was assembled from off-the-shelf components within minutes. In brief, an inner fused silica capillary was centered coaxially to an outer PTFE tube (ID = 1/32"; OD = 1/16"; L = 12 cm). Two different fused silica capillaries were used depending on the selected *R* for NP production; for $R = 0.005$ the capillary dimensions were OD = 363 μm and ID = 100 μm, and for $R = 0.1$ the capillary dimensions were OD = 363 μm and ID = 150 μm. All components were assembled in a PEEK T-junction. The alignment of the capillary and the main channel was the most difficult step and extra care should be taken here to ensure proper alignment of the device. The effect of alignment on NP production was tested previously by disassembling and reassembling the device after each synthesis (Bovone et al., 2019). NP fabrication with different capillary alignments showed a variability of up to ±10 nm. As this issue was studied extensively in our previous work, each automated production experiment was conducted using the same device and the inner capillary was exchanged as needed. The CJM was designed such that the block copolymer solution flowed through the inner fused silica capillary and the dH_2O flowed through the outer PTFE channel. The fluid streams were delivered from 2.5, 10, or 50 mL gas-tight syringes (SETonic) operated by computer-controlled syringe pumps (CETONI NeMESYS Low Pressure 29:1 gear & CETONI NeMESYS Low Pressure 14:1 gear). The pumps, and thus the flow rates of the fluid streams, were controlled externally by a LabView (National Instruments, USA) script provided in the **Supplementary Material** (**Section S1.2**), which utilized functions from the Qmix software developement kit (CETONI).

2.3.2. CJM NP Formation

For nanoprecipitation in the CJM, the block copolymers PEG_{5k}-*b*-PCL_{20k}, PEG_{5k}-*b*-PLA_{20k}, or PEG_{5k}-*b*-$PLGA_{20k}$ were first dissolved in ACN or DMF at concentrations of 10 mg mL^{-1} for dilute NP formulation screening or 50 mg mL^{-1} for concentrated NP production. DMF was used for block copolymers that nanoprecipitate into larger NPs, i.e., PEG_{5k}-*b*-$PLGA_{20k}$, as NPs produced with DMF were smaller than those produced with ACN, in preliminary experiments. In CJM experiments, the organic solution to dH_2O ratio, *R*, was defined as:

$$R = \frac{Q_{organic}}{Q_{H_2O}} \quad (2)$$

where $Q_{organic}$ and Q_{H_2O} represent the volumetric flow rates of the respective fluid streams. NP formation in dilute conditions was performed at $R = 0.005$. Concentrated NP production was performed at $R = 0.1$. Volumetric flow rates of dH_2O used in our study ranged from ∼1 to ∼35 mL min^{-1}, whereas the organic solution volumetric flow rate ranged from ∼50 μL min^{-1} to ∼4 mL min^{-1}. The Reynolds number, *Re*, for each experiment was calculated by estimating the viscosity and density of the final solvent-water mixture from literature values (Aminabhavi and Gopalakrishna, 1995). For the *Re* calculations, the inner diameter of the water PTFE tube was used as the characteristic length. The velocity was calculated based on the inner cross-sectional area of the outer tube of the CJM. The experiments were performed in cycles, which were determined by the complete refill and dispensing of the syringes.

2.3.3. Automated NP Production

To automate NP production, the CJM was connected to computer-controlled syringe pumps that dispensed the block copolymer solution, optionally containing a model drug, and dH_2O (**Figure 1**). A graphical user interface (GUI) was designed in LabView to control syringe filling from reservoirs of the two solutions and dispensing through the CJM into a collection reservoir. This enabled NP production without user intervention outside of system set-up, sample collection, and formulation switching. The flow rates or Reynolds number, *Re*, as well as the ratio between the volumetric flow rates of the organic and aqueous streams, *R*, were varied to control NP size.

For process automation, the NP production process was divided into multiple operational steps, which were individually programmed in LabView. During the first steps, the set-up was paired to the LabView program, initialized, and all syringes and valves were mounted. The production cycle was initiated with the refill of the syringes with water and polymer solution. Prior to starting the NP production, the flow rates were gradually increased and both the water and NP precursor solution were collected back into the respective reservoirs. When the flow rates stabilized, the valves redirected the flow into the main channel for NP production until one of the syringes was emptied to 15% of its total volume. The valves switched the flow back to the reservoirs, the flow rates were gradually decreased, and the cycle started over with refilling both syringes. In some experiments, the polymer or formulation solution was changed in between cycles. In this case, the CJM was equilibrated over 3 cycles of washing to accommodate the new formulation solution. A detailed description of all steps and a summary of all data is provided in the **Supplementary Material** (**Sections S1.1** and **S2**).

2.4. NP Characterization

The hydrodynamic diameter, D_h, of the synthesized NPs was characterized via dynamic light scattering (DLS) on a ZetaSizer Nano ZS (Malvern, UK). A NP suspension volume of ∼1 mL was measured at a scattering angle of 173° at 25°C. NP suspensions

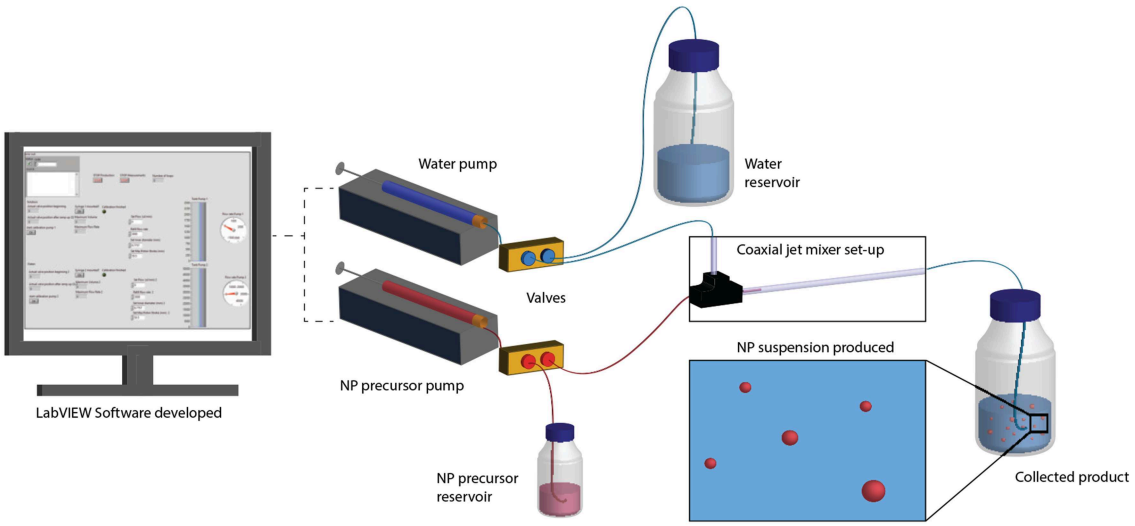

FIGURE 1 | NP production in the automated CJM. The set-up was designed for the production of NPs and included syringe pumps, valves, and reservoirs that were computer-controlled. A LabView program and a GUI enabled automation of the CJM to operate independently during NP production.

formed at $R = 0.1$ were diluted in dH_2O by a factor of 10. There was no change in observed D_h upon dilution (Bovone et al., 2019). NPs produced at $R = 0.005$ were analyzed as collected. The z-average hydrodynamic diameter, D_h, and the dispersity, Đ, were calculated over three measurements per sample. The dispersity was calculated according to ISO 22412:2017 (2017-02):

$$Đ = \frac{\sigma^2}{2\overline{\Gamma}} \tag{3}$$

where $\overline{\Gamma}$ represents the scattered light intensity-weighted average and σ represents the standard deviation of the distribution function.

2.5. Synthesis and Characterization of Drug Delivery Systems

2.5.1. Encapsulation of Small Molecules

A solution of OR (0.5 mg mL^{-1}) and PEG_{5K}-*b*-PLA_{20K} (50 mg mL^{-1}) in ACN was prepared to achieve a theoretical drug loading of 1%.

$$\text{Theoretical drug loading} = \text{tDL} = \frac{m_{\text{drug in formulation}}}{m_{\text{total formulation}}} \cdot 100\% \tag{4}$$

where $m_{\text{drug in formulation}}$ represents the total mass of model therapeutic used in the formulation and $m_{\text{total formulation}}$ is calculated by the sum of the block copolymer mass and of the model therapeutic mass. The formulation solution and dH_2O were injected into the CJM at ~3.2 mL min^{-1} and ~32 mL min^{-1}, respectively ($R = 0.1$, $Re = 1016$). Approximately three samples of 10 mL of the produced NPs were collected during each cycle. After NP production, the hydrodynamic diameter of each sample was measured via DLS. OR was quantified via UV-Vis spectroscopy at $\lambda = 520$ nm according to the protocol explained in the **Supplementary Material** (**Section S1.3**). The effective OR loading into the NPs was defined as

$$\text{Effective drug loading} = \text{eDL} = \frac{m_{\text{drug after filtration}}}{m_{\text{total formulation after filtration}}} \cdot 100\% \tag{5}$$

where $m_{\text{drug after filtration}}$ and $m_{\text{total formulation after filtration}}$ represent the respective residual mass of drug and of total matter after NP work-up.

2.5.2. Synthesis of Polymer–Nanoparticle Hydrogels

50 mg mL^{-1} PEG_{5K}-*b*-PLA_{20K} NPs were synthesized in the automated CJM with Q_{dH_2O} ~32 mL min^{-1} and $Q_{organic}$ ~ 3.2 mL min^{-1} ($R = 0.1$, $Re = 1016$). For the assembly of 0.6 g PNP hydrogels, ~15 mL of the NP suspension were utilized, and the remaining ~150 mL of the NP suspension were used for scaling up the PNP hydrogels to 6 g. The PNP hydrogels were composed by 2 %w/w hydroxypropylmethylcellulose (HPMC) and 15 %w/w PEG_{5K}-*b*-PLA_{20K} NPs (HPMC:NP, 2:15 %w/w). Further details on the synthesis of PNP hydrogels were reported in the **Supplementary Material** (**Section S1.4**).

2.5.3. Rheological Characterization of Polymer–Nanoparticle Hydrogels

Rheological tests were performed using a strain-controlled shear rheometer (MCR 502; Anton Paar; CH) fitted with a Peltier stage ($T = 37°C$). During the measurements, silicon oil was used to prevent evaporation. All experiments were performed using a 25 mm cone-plate geometry with a 2° truncation angle. The storage modulus, G', loss modulus, G'', and the loss factor, $\tan(\delta) = \frac{G''}{G'}$, were measured with an oscillatory strain amplitude sweep ($\gamma = 0.1$–1000%) at a constant angular frequency ($\omega = 10$ rad s^{-1}). Oscillatory step strain recovery experiments were performed at $\omega = 10$ rad s^{-1} to investigate the cyclic recovery

from a high strain interval (1000%, 4 min) followed by a low strain interval (0.3%, 8 min). The shear-thinning properties of PNP hydrogels were investigated with rotational shear rate ramp tests ($\frac{\delta\gamma}{\delta t} = 0.1–100\ s^{-1}$).

3. RESULTS AND DISCUSSION

3.1. Automated CJM for NP Production

A coaxial jet mixer (CJM) was assembled based on previous designs (Baber et al., 2015; Bovone et al., 2019) and automated for flow-based nanoprecipitation of polymeric NPs. The resulting NPs were compared to those produced by standard batch nanoprecipitation. A solution of PEG_{5K}-*b*-PLA_{20K} in ACN (50 mg mL^{-1}) was nanoprecipitated in dH_2O under flow ($R = 0.1$, $Re = 1016$). In the CJM, the PEG_{5K}-*b*-PLA_{20K} NPs formed with $D_h \approx 78$ nm (**Figure S7A**). The same polymer formed NPs with $D_h \approx 94$ nm via batch nanopreciptiation ($R = 0.1$). In both cases, the NPs formed with $Đ < 0.1$, indicating a narrow size distribution and effective NP formation. Thus, the CJM produced PEG_{5K}-*b*-PLA_{20K} NPs of similar size and quality to standard batch nanoprecipitation.

As the CJM was programmed with unit operations for automatic syringe filling and dispensing, the system could operate independent of an operator following set-up and filling of the organic and aqueous reservoirs. This enabled the CJM to produce NPs continuously with standard lab-scale syringes (up to 50 mL volume) over extended periods of time. For example, the respective reservoirs were filled with ∼830 mL of PEG_{5K}-*b*-PLA_{20K} in ACN (10 mg mL^{-1}) and 8.3 L of dH_2O and the automated CJM was programmed to produce NPs under flow ($R = 0.1$, $Re = 1016$) for 24 h without human intervention. The automated CJM operated stably without leaks or clogging over the 24 h experiment. The ability to operate continuously over extended periods of time is a major advantage of the automated CJM and is essential for scalable production of NPs.

3.2. Stable Operation of the CJM and Tuning of NP Size During Operation

In an initial test, we demonstrated that the automated CJM could operate without leaks or clogging for up to 24 h. Here, we investigated the stability of NP production over time and dynamic tuning of NP size during operation. First, NPs were produced from PEG_{5K}-*b*-PLA_{20K} in ACN (10 mg mL^{-1}). The CJM was operated ($Re = 1047$, $R = 0.005$) for 12 filling and dispensing cycles, equivalent to 80 min of operation time. Three discrete samples were collected directly from the exit stream of the CJM to monitor NP properties every second production cycle (**Figure 2A**). An additional sample was taken from the NP suspension collection reservoir after the 80 min of operation. During the course of continuous NP production, NP size remained stable with $D_h \approx 51$ nm and $Đ = 0.06 - 0.09$ for the discrete samples. The diameters from the discrete samples were consistent with the NP diameter of the samples from the collection reservoir. Thus, NP size and quality remained constant during continuous operation, highlighting the ability to produce NPs stably with the automated CJM, with dilute conditions.

Another useful feature of the automated CJM is the ability to modify the flow rates of the two fluid streams independently to control *Re* and *R* and, therefore, NP size (Bovone et al., 2019). Here, NPs were produced from PEG_{5K}-*b*-PLA_{20K} in ACN (10 mg mL^{-1}) with $D_h \approx 56$ nm at $Re = 1047$ over eight filling and dispensing cycles (**Figure 2B**). The size was then changed to $D_h \approx 79$ nm ($Re = 538$) for the next eight cycles and then back to 56 nm ($Re = 1047$) for an additional six cycles. These results demonstrated that NP size could be tuned dynamically during continuous operation by altering the flow conditions, such as *Re*.

3.3. Scalable and Automated NP Production

Beyond continuous and controlled NP prodution, scale-up remains a major hurdle to clinical translation of nanotherapeutics and PNP hydrogels for site specific delivery (Liu et al., 2015, 2018). To increase the NP production rate in the automated CJM, the block copolymer concentration was increased to 50 mg mL^{-1} and *R* was increased to 0.1. Here, NPs were produced from PEG_{5K}-*b*-PLA_{20K} in ACN under flow with the concentrated block copolymer solution. The CJM was operated ($Re = 1016$) for 6 filling and dispensing cycles, equivalent to 40 min of operation time. Discrete samples were collected directly from the exit stream of the CJM to monitor NP properties every cycle (**Figure 2C**). An additional sample was taken from the NP suspension collection reservoir after the 40 min of operation. During the course of continuous NP production, the NP size remained stable with $D_h \approx 75$ nm and $Đ = 0.07 - 0.08$ for the discrete samples. The D_h and Đ of the sample from the collection reservoir were 75 nm and 0.07, respectively. Thus, NP size and quality remained constant during continuous operation also in production mode. The increased size relative to the dilute condition was expected as C_{poly} and *R* are both known to influence NP size (Karnik et al., 2008; Bovone et al., 2019). With the current setup, a production rate of ∼40 g day^{-1} was possible. This calculation accounted for the downtime needed for the refilling steps, which was the most time consuming step in this design of the CJM. This is a significant improvement over the standard batch nanoprecipitation production rate. Further, a theoretical production rate of 230 g day^{-1} could be achieved with the automated CJM given additional syringes and pumps, such that some pumps could be refilling while others are dispensing. The CJM was tested for automated D_h tuning during concentrated NP production. NPs were produced at *Re* = 1016 for 4 cycles, followed by 4 cycles at $Re = 522$, and returning to $Re = 1016$ for a final 3 cycles (**Figure 2D**). These conditions produced PEG_{5K}-*b*-PLA_{20K} NPs of $D_h \approx 74$, 98, and 75 nm, respectively. The data demonstrates that the CJM retained the ability to tune NP size also during concentrated NP production.

3.4. Decoupling NP Formulation From Size

To further demonstrate the utility of flow control over NP size, the CJM was exploited to prepare NPs from three common block

copolymers used for drug delivery purposes, namely PEG_{5K}-*b*-PLA_{20K}, PEG_{5K}-*b*-PCL_{20K}, and PEG_{5K}-*b*-$PLGA_{20K}$. First, PEG_{5K}-*b*-PLA_{20K} and PEG_{5K}-*b*-PCL_{20K} were each dissolved in ACN and PEG_{5K}-*b*-$PLGA_{20K}$ was dissolved in DMF. NPs were prepared via dilute batch nanoprecipitation (10 mg mL^{-1} block copolymer solution, $R = 0.005$) with $D_h = 55 \pm 1$, 76 ± 1, and 60 ± 5 nm, for PEG_{5K}-*b*-PCL_{20K}, PEG_{5K}-*b*-PLA_{20K}, and PEG_{5K}-*b*-$PLGA_{20K}$ respectively (**Figure 3A**). All NPs formed with low dispersity ($Đ < 0.1$) and unimodal size distributions (**Figure 3B**). The results show that batch nanoprecipitation was able to produce NPs with low dispersity in a simple manner; however, formulations using different block copolymer chemistries resulted in NPs of distinct sizes. To test the ability of the CJM to decouple NP size from block copolymer chemistry, the device was used to produce NPs from each block copolymer with a similar size, $D_h \approx 50$ nm, by tuning the flow conditions (**Figure 3C**). This was achieved with $Re = 478$, 1047, and 591 for PEG_{5K}-*b*-PCL_{20K}, PEG_{5K}-*b*-PLA_{20K}, and PEG_{5K}-*b*-$PLGA_{20K}$, respectively. The resulting NP populations were similar both in their hydrodynamic diameter and in their size distribution (**Figure 3D**). This demonstrated that automated control of the flow conditions in the CJM was sufficient to produce NPs with similar size and dispersity from chemically distinct block copolymers, which formed NP of different size in batch nanoprecipitation. That is, the automated CJM was able to decouple D_h from the chemical composition of the NP.

Further, the CJM was tested on the stability of NP production with PEG_{5K}-*b*-PCL_{20K}, PEG_{5K}-*b*-PLA_{20K}, and PEG_{5K}-*b*-$PLGA_{20K}$ over time. NPs with $D_h \sim 50$ nm were produced from PEG_{5K}-*b*-PCL_{20K} in ACN (10 mg mL^{-1}) for six cycles ($Re = 478$) (**Figure 3E**). Then, NPs of a similar diameter were produced from PEG_{5K}-*b*-PLA_{20K} in ACN (10 mg mL^{-1}, $Re = 1{,}047$) and PEG_{5K}-*b*-$PLGA_{20K}$ in DMF (10 mg mL^{-1}, $Re = 591$) for an additional six cycles each. The automated CJM was also tested on the concentrated production of NPs using the same block copolymers. In concentrated batch nanoprecipitation, these polymers (50 mg mL^{-1}, $R = 0.1$) formed NPs with

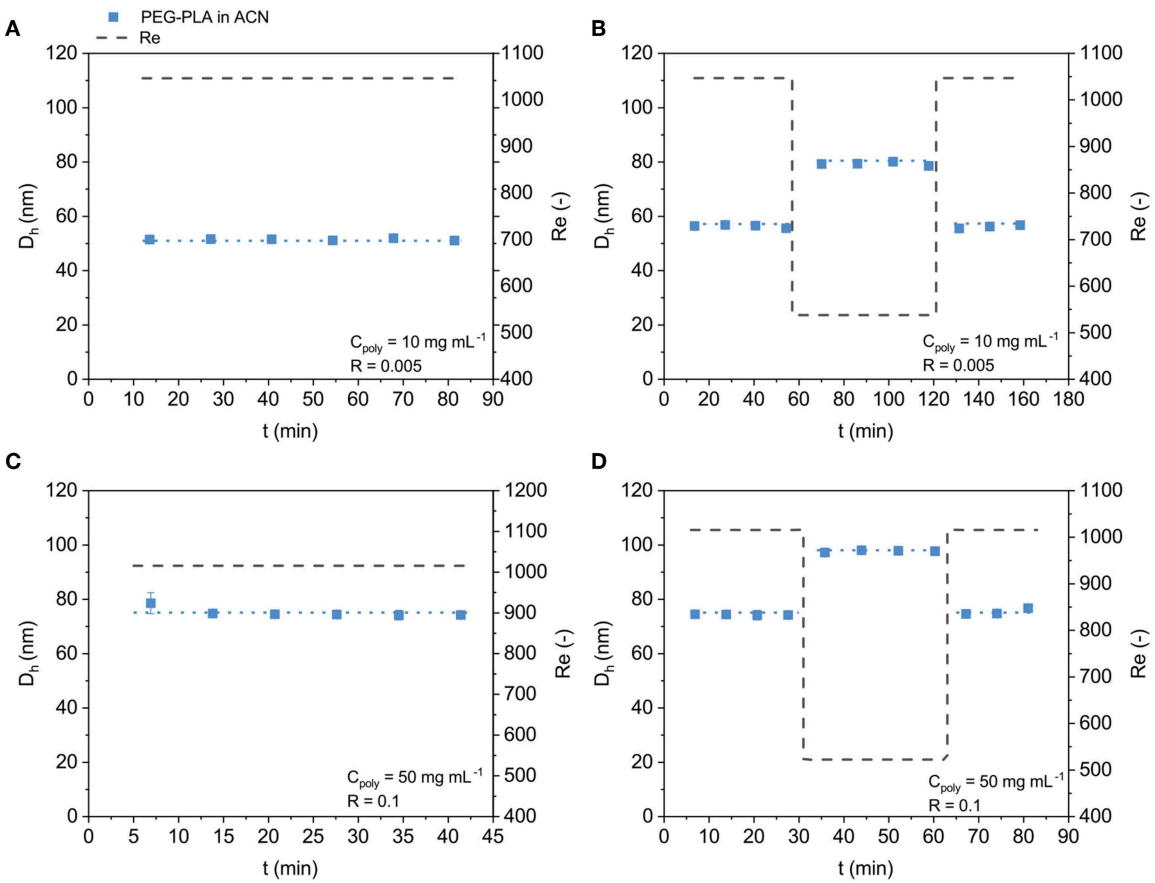

FIGURE 2 | Stable PEG_{5K}-*b*-PLA_{20K} NP production and size control in the automated CJM. **(A)** PEG_{5K}-*b*-PLA_{20K} was nanoprecipitated over several automated cycles ($Re = 1047$) showing reproducible and stable NP size over the whole production process. **(B)** Change in *Re* between 1,047 ($D_h \approx 56$ nm) and 538 ($D_h \approx 79$ nm) demonstrated control over NP size by altering flow conditions. **(C)** Concentrated automated production of NPs was carried out with commonly used block copolymers at 50 mg mL^{-1} and R = 0.1. PEG_{5K}-*b*-PLA_{20K} NP production remained stable ($Re = 1016$), $D_h \approx 75$ nm, with a production rate of ~40 g day^{-1}. **(D)** Re controlled NP size for the concentrated PEG_{5K}-*b*-PLA_{20K} formulations where $Re = 1016$ lead to $D_h \approx 74$ nm and $Re = 522$ lead to $D_h \approx 98$ nm.

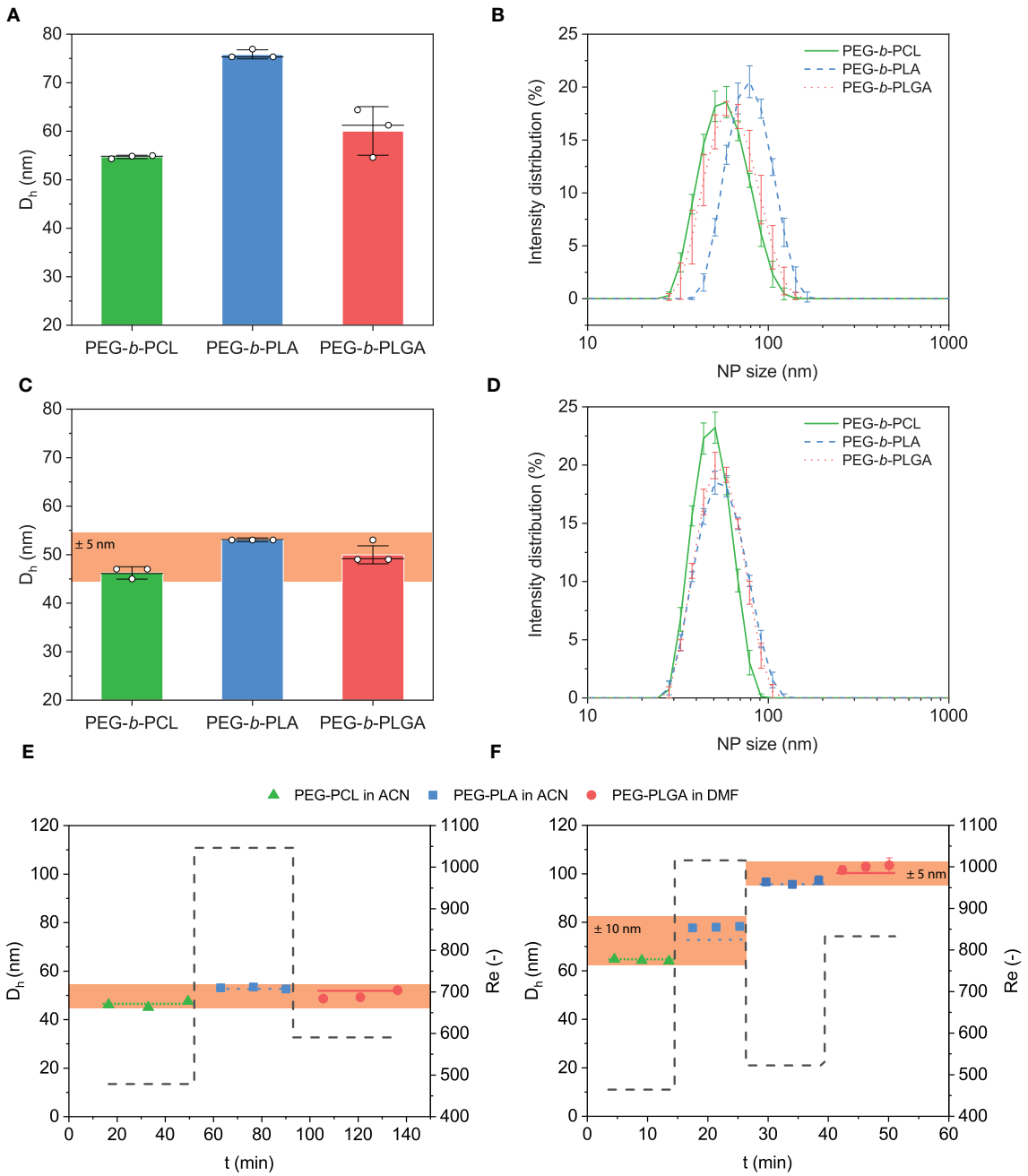

FIGURE 3 | Nanoprecipitation of common block copolymers via batch and with the automated CJM. **(A)** Diluted screening of NP size was carried out with commonly used block copolymers at concentrations of 10 mg mL^{-1} and $R = 0.005$. Batch nanoprecipitation (10 mg mL^{-1}, $R = 0.005$) of PEG$_{5K}$-*b*-PCL$_{20K}$ or PEG$_{5K}$-*b*-PLA$_{20K}$ dissolved in ACN and PEG$_{5K}$-*b*-PLGA$_{20K}$ dissolved in DMF produced NPs of $D_h \approx 76$, 55, and 60 nm, respectively with Đ < 0.1. **(B)** Corresponding size distribution of NPs produced in batch. **(C)** Flow control in the CJM enabled production of NPs with uniform size from chemically distinct formulations, $D_h = 50 \pm 5$ nm. NP production was carried out at $Re = 478$, 1047, and 591, respectively for PEG$_{5K}$-*b*-PCL$_{20K}$, PEG$_{5K}$-*b*-PLA$_{20K}$, and PEG$_{5K}$-*b*-PLGA$_{20K}$. **(D)** Relative size distribution of the CJM produced NPs. **(E)** The automated flow-controlled CJM enabled the continuous production of NPs with similar size $D_h \approx 50$ nm from the chemically distinct block copolymers over multiple cycles. **(F)** Concentrated automated production of NPs was carried out with commonly used block copolymers at 50 mg mL^{-1} and R = 0.1. Pairs of similar diameter but chemically distinct NPs were produced in the CJM. NPs were produced with $D_h \approx 65 - 78$ nm from PEG$_{5K}$-*b*-PCL$_{20K}$ ($Re = 478$) and PEG$_{5K}$-*b*-PLA$_{20K}$ ($Re = 1016$). Subsequently, NPs were produced with $D_h \approx 96 - 103$ nm from PEG$_{5K}$-*b*-PLA$_{20K}$ NPs ($Re = 522$) and PEG$_{5K}$-*b*-PLGA$_{20K}$ ($Re = 833$).

$D_h \approx$ 65, 94, and 127 nm, respectively (**Figure S7B**). Here, pairs of similar diameter but chemically diverse NPs were produced (**Figure 3F**). In the first 3 cycles, PEG$_{5K}$-*b*-PCL$_{20K}$ was nanoprecipitated at $Re = 464$ and PEG$_{5K}$-*b*-PLA$_{20K}$ at $Re = 1016$, producing NPs in the range of $D_h \approx 65 - 78$ nm. In the subsequent 3 cycles, the size of PEG$_{5K}$-*b*-PLA$_{20K}$ NPs

was increased ($Re = 522$) and matched to the one of PEG_{5K}-*b*-$PLGA_{20K}$ ($Re = 833$), forming NPs of $D_h \approx 96 - 103$ nm. These results confirmed that stable NP size control can be achieved in the automated CJM also for concentrated formulations, independent of the chemistry of the block copolymer. The CJM device decoupled NP size from the specific formulation, enabling the tuning of NP dimensions as a separate design parameter of polymeric NPs. These data further demonstrated the ability of the automated CJM to produce particles continuously and stably both in formulation screening and production modes.

3.5. Formation of Drug-Loaded NPs

One of the main applications of polymeric NPs is for the formation of drug-loaded nanotherapeutics. Here, we tested the ability of automated CJM to produce drug-loaded NPs in a stable manner. OR was selected as a model drug owing to its hydrophobicity and ease of detection. A solution of PEG_{5K}-*b*-PLA_{20K} (50 mg mL^{-1}) and OR (0.5 mg mL^{-1}) in ACN was used as the organic stream and NPs were nanoprecipitated from dH_2O under flow ($Re = 1016$, $R = 0.1$) in the automated CJM with a target OR loading of 1%. OR-loaded NPs were produced stably over four cycles, or 30 min of operation time, with $D_h \approx 89 - 99$

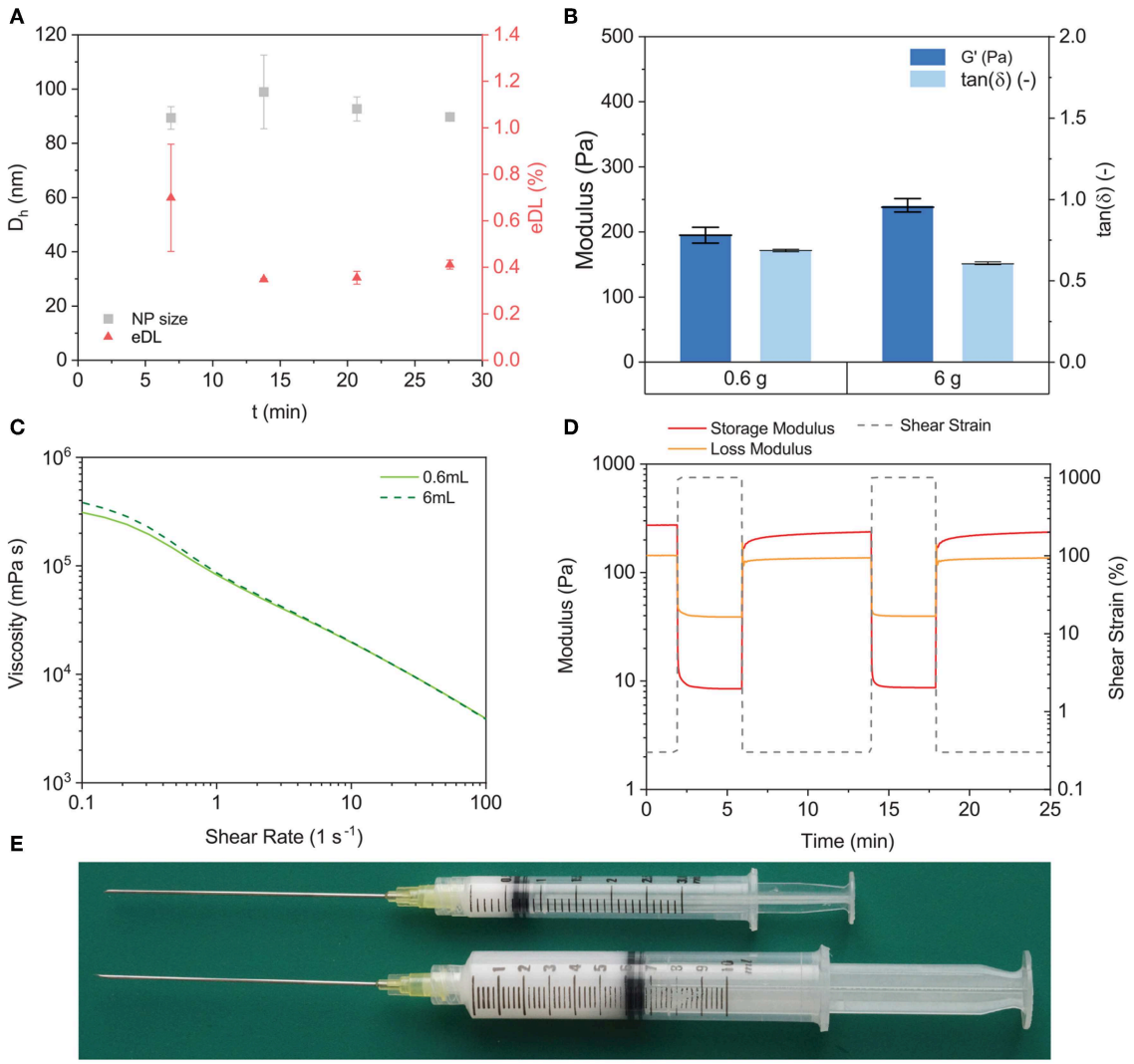

FIGURE 4 | Synthesis of nanotherapeutics and scale-up of PNP hydrogels. **(A)** PEG_{5K}-*b*-PLA_{20K} (50 mg mL^{-1}) and OR (0.5 mg mL^{-1}, *tDL* ≈ 1%) were nanoprecipitated at $Re = 1016$. NP size was stable over the production $D_h \approx 93$ nm and the eDL converged to ∼0.4%. **(B)** CJM NP synthesis allowed the production of PNP hydrogels (HPMC:NP, 2:15 wt%) on the 0.6 g and on the 6.0 g scale. Dynamic moduli were measured via oscillatory strain amplitude sweeps ($\gamma = 0.1$–1000%, $\omega = 10$ rad s^{-1}) **(C)** Rotational shear rate ramp ($\frac{d\gamma}{dt} = 0.1$–100 s^{-1}) of both the 0.6 g and of the 6.0 g PNP hydrogels showed decrease in viscosity with increasing shear rate demonstrating that the shear-thinning properties were retained at both scales. **(D)** The self-healing behavior of the 6.0 g PNP hydrogel was characterized with step strain measurements by alternating intervals of high (1000%, $\omega = 10$ rad s^{-1}) and low (0.3%, $\omega = 10$ rad s^{-1}) shear strain amplitude. The scaled-up PNP hydrogel demonstrated its ability to self-heal, as reported in literature and similarly to the 0.6 g hydrogel (**Figure S8**). **(E)** 0.6 g and 6.0 g PNP hydrogels were produced and loaded in plastic syringes.

nm (**Figure 4A**). The OR loading in the first cycle was ∼0.7 ± 0.2% and ∼0.4 ± 0.1% for each of the subsequent cycles. The reason for the discrepancy between the first and the subsequent cycles was not clear and we hypothesized that it was caused by a transient effect during the first phase of CJM operation. These results demonstrated that the automated CJM was also useful for the stable production of model nanotherapeutics.

3.6. Fabrication of Polymer–Nanoparticle (PNP) Hydrogels

An emerging application of polymeric NPs is as building blocks for the assembly of PNP hydrogels (Appel et al., 2015a,b; Guzzi et al., 2019; Lopez Hernandez et al., 2019; Stapleton et al., 2019; Steele et al., 2019). PNP hydrogels form spontaneously upon simple mixing of an appropriately paired polymer, e.g., hydroxypropylmethylcellulose (HPMC) or C12-functionalized hyaluonic acid, and a concentrated solution of core-shell NPs under aqueous conditions. PNP hydrogels are shear-thinning and self-healing owing to the reversible interactions between the polymers and NPs, and have been used for site specific delivery of therapeutics following injection *in vivo* (Appel et al., 2015b; Fenton et al., 2019; Steele et al., 2019). The clinical potential of these materials is significant; however, biomedical PNP gels are currently limited in the scale of their production. As PNP gels form via admixing of a polymer solution and a NP solution, the main limitation to scale is the availability of large amounts of high quality polymeric NPs (Yu et al., 2016). Therefore, we leveraged the automated CJM to produce ∼1 g of PEG_{5K}-*b*-PLA_{20K} NPs ($D_h \approx 80$ nm). The NPs were concentrated using centrifugal filter units (Amicon Ultra-15, Ultracel membrane, MWCO ≈ 50 kDa; Millipore) to a stock concentration of 20%w/w in dH_2O. From this suspension, two PNP gel samples were prepared at a final concentration of 2%w/w HPMC and 15%w/w NPs at a standard production of 0.6 g and a scaled production of 6.0 g. The rheological properties, $G' \approx 220$ Pa and a $\tan(\delta) \approx 0.65$, were consistent for the two scales (**Figure 4B**). The scaled version of the PNP gel maintained a high degree of shear-thinning (**Figure 4C**) and rapid self-healing (**Figure 4D** and **Figure S8**). This demonstrated that the automated CJM enabled more efficient and higher scale production of injectable PNP gels (**Figure 4E**), which could be useful for site specific delivery of therapeutics following local injection.

4. CONCLUSION

In this work, we engineered an automated CJM operated by computer-controlled syringe pumps and valves. A LabView program and a GUI were designed to enable external control over the cycles of refilling, dispensing, and washing and, therefore, NP production. The automated CJM was operated for up to 24 h without user intervention and enabled robust and stable production of PEG_{5K}-*b*-PLA_{20K} NPs. PEG_{5K}-*b*-PLA_{20K} NP diameter was tuned by controlling the flow conditions, $D_h \approx 56$ or 79 nm at $Re = 1047$ or 538, respectively. Flow-control in the automated CJM enabled nanoprecipitation of chemically diverse block copolymers, PEG_{5K}-*b*-PCL_{20K}, PEG_{5K}-*b*-PLA_{20K}, and PEG_{5K}-*b*-$PLGA_{20K}$, with similar size, $D_h \approx 50$ nm. Stable, robust, and controlled production of NPs was demonstrated both for dilute (10 mg mL^{-1}, $R = 0.005$, production rate ∼ 0.3 mg min^{-1} including refill time) as well as for concentrated NP formulations (50 mg mL^{-1}, $R = 0.1$, production rate ∼ 30 mg min^{-1} including refill time). A key application of the automated CJM would be for the production of nanotherapeutics, therefore, a model small molecule drug, OR, was encapsulated in PEG_{5K}-*b*-PLA_{20K} NPs. NPs of similar size, $D_h \approx 93$ nm, and effective OR loading, eDL ∼ 0.4%, were produced stably over several cycles with a production rate of ∼30 mg min^{-1}. NPs are not only attractive for systemic drug delivery, but also as a structural component for the formation of injectable PNP hydrogels for site specific drug release. NPs produced with the automated CJM were used for scale-up of PNP hydrogel formation from 0.6 g to 6.0 g. The mechanical properties of the PNP hydrogels were invariant of scale. Thus, the engineered CJM enabled automated, controlled, and continuous synthesis of various common polymeric NPs at different production rates, and for the synthesis of both systemic and local drug delivery systems. Further developments of these fluidic platforms could be instrumental for future translation of nanomaterials to production scales.

DATA AVAILABILITY STATEMENT

The datasets for this study are available upon request.

AUTHOR CONTRIBUTIONS

GB and MT conceived of the project and designed the experiments. GB, FS, and EG performed the experiments. FS developed the program to control the automated CJM. GB, FS, EG, and MT analyzed the data and prepared the figures. GB, FS, and MT wrote the manuscript.

FUNDING

This work was supported by the Swiss National Science Foundation under project number 200021_184697 and start-up funds from ETH Zürich.

ACKNOWLEDGMENTS

The authors acknowledge Particle Technology Lab (ETH) directed by Prof. Sotiris E. Pratsinis for providing access to their facilities.

SUPPLEMENTARY MATERIAL

The Supplementary Material for this article can be found online at: https://www.frontiersin.org/articles/10.3389/fbioe.2019.00423/full#supplementary-material

REFERENCES

Aminabhavi, T. M., and Gopalakrishna, B. (1995). Density, viscosity, refractive index, and speed of sound in aqueous mixtures of N,N-dimethylformamide, dimethyl sulfoxide, N,N-dimethylacetamide, acetonitrile, ethylene glycol, diethylene glycol, 1,4-dioxane, tetrahydrofuran, 2-methoxyethanol, and 2-ethox. *J. Chem. Eng. Data* 40, 856–861. doi: 10.1021/je00020a026

Anselmo, A. C., and Mitragotri, S. (2016). Nanoparticles in the clinic. *Bioeng. Translat. Med.* 1, 10–29. doi: 10.1002/btm2.10003

Appel, E. A., Tibbitt, M. W., Greer, J. M., Fenton, O. S., Kreuels, K., Anderson, D. G., et al. (2015a). Exploiting electrostatic interactions in polymer-nanoparticle hydrogels. *ACS Macro Lett.* 4, 848–852. doi: 10.1021/acsmacrolett.5b00416

Appel, E. A., Tibbitt, M. W., Webber, M. J., Mattix, B. A., Veiseh, O., and Langer, R. (2015b). Self-assembled hydrogels utilizing polymer-nanoparticle interactions. *Nat. Commun.* 6:6295. doi: 10.1038/ncomms7295

Baber, R., Mazzei, L., Thanh, N. T. K., and Gavriilidis, A. (2015). Synthesis of silver nanoparticles in a microfluidic coaxial flow reactor. *RSC Adv.* 5, 95585–95591. doi: 10.1039/C5RA17466J

Bertrand, N., Grenier, P., Mahmoudi, M., Lima, E. M., Appel, E. A., Dormont, F., et al. (2017). Mechanistic understanding of *in vivo* protein corona formation on polymeric nanoparticles and impact on pharmacokinetics. *Nat. Commun.* 8:777. doi: 10.1038/s41467-017-00600-w

Bovone, G., Guzzi, E. A., and Tibbitt, M. W. (2019). Flow-based reactor design for the continuous production of polymeric nanoparticles. *AIChE J.* 65:e16840. doi: 10.1002/aic.16840

Capretto, L., Cheng, W., Carugo, D., Katsamenis, O. L., Hill, M., and Zhang, X. (2012). Mechanism of co-nanoprecipitation of organic actives and block copolymers in a microfluidic environment. *Nanotechnology* 23:375602. doi: 10.1088/0957-4484/23/37/375602

Cheng, J., Teply, B. A., Sherifi, I., Sung, J., Luther, G., Gu, F. X., et al. (2007). Formulation of functionalized PLGA-PEG nanoparticles for *in vivo* targeted drug delivery. *Biomaterials* 28, 869–876. doi: 10.1016/j.biomaterials.2006.09.047

Colombo, S., Beck-Broichsitter, M., Bøtker, J. P., Malmsten, M., Rantanen, J., and Bohr, A. (2018). Transforming nanomedicine manufacturing toward quality by design and microfluidics. *Adv. Drug Deliv. Rev.* 128, 115–131. doi: 10.1016/j.addr.2018.04.004

Detappe, A., Thomas, E., Tibbitt, M. W., Kunjachan, S., Zavidij, O., Parnandi, N., et al. (2017). Ultrasmall silica-based bismuth gadolinium nanoparticles for dual magnetic resonance-computed tomography image guided radiation therapy. *Nano Lett.* 17, 1733–1740. doi: 10.1021/acs.nanolett.6b05055

Fenton, O. S., Tibbitt, M. W., Appel, E. A., Jhunjhunwala, S., Webber, M. J., and Langer, R. (2019). Injectable polymer-nanoparticle hydrogels for local immune cell recruitment. *Biomacromolecules* 20:4430–4436. doi: 10.1021/acs.biomac.9b01129

Fessi, H., Puisieux, F., Devissaguet, J., Ammoury, N., and Benita, S. (1989). Nanocapsule formation by interfacial polymer deposition following solvent displacement. *Int. J. Pharmaceut.* 55, R1–R4. doi: 10.1016/0378-5173(89)90281-0

Gref, R., Minamitake, Y., Peracchia, M. T., Trubetskoy, V., Torchilin, V., and Langer, R. (1994). Biodegradable long-circulating polymeric nanospheres. *Science* 263, 1600–1603. doi: 10.1126/science.8128245

Guzzi, E. A., Bovone, G., and Tibbitt, M. W. (2019). Universal nano-carrier ink platform for biomaterials additive manufacturing. *Small*. doi: 10.1002/smll.201905421. [Epub ahead of print].

Hickey, J. W., Santos, J. L., Williford, J.-M., and Mao, H.-Q. (2015). Control of polymeric nanoparticle size to improve therapeutic delivery. *J. Control. Release* 219, 536–547. doi: 10.1016/j.jconrel.2015.10.006

Johnson, B. K., and Prud'homme, R. K. (2003a). Flash nanoPrecipitation of organic actives and block copolymers using a confined impinging jets mixer. *Aust. J. Chem.* 56, 1021–1024. doi: 10.1071/CH03115

Johnson, B. K., and Prud'homme, R. K. (2003b). Mechanism for rapid self-assembly of block copolymer nanoparticles. *Phys. Rev. Lett.* 91:118302. doi: 10.1103/PhysRevLett.91.118302

Kamaly, N., Yameen, B., Wu, J., and Farokhzad, O. C. (2016). Degradable controlled-release polymers and polymeric nanoparticles: mechanisms of controlling drug release. *Chem. Rev.* 116, 2602–2663. doi: 10.1021/acs.chemrev.5b00346

Karnik, R., Gu, F., Basto, P., Cannizaro, C., Dean, L., Kyei-Manu, W., et al. (2008). Microfluidic platform for controlled synthesis of polymeric nanoparticles. *Nano Lett.* 8, 2906–2912. doi: 10.1021/nl801736q

Langer, R. (1998). Drug delivery and targeting. *Nature* 392(Suppl.), 145–146. doi: 10.1038/32337

Lim, J.-M., Swami, A., Gilson, L. M., Chopra, S., Choi, S., Wu, J., et al. (2014). Ultra-high throughput synthesis of nanoparticles with homogeneous size distribution using a coaxial turbulent jet mixer. *ACS Nano* 8, 6056–6065. doi: 10.1021/nn501371n

Liu, D., Cito, S., Zhang, Y., Wang, C.-F., Sikanen, T. M., and Santos, H. A. (2015). A versatile and robust microfluidic platform toward high throughput synthesis of homogeneous nanoparticles with tunable properties. *Adv. Mater.* 27, 2298–2304. doi: 10.1002/adma.201405408

Liu, D., Zhang, H., Fontana, F., Hirvonen, J. T., and Santos, H. A. (2018). Current developments and applications of microfluidic technology toward clinical translation of nanomedicines. *Adv. Drug Deliv. Rev.* 128, 54–83. doi: 10.1016/j.addr.2017.08.003

Liu, Y., Li, K., Liu, B., and Feng, S. S. (2010). A strategy for precision engineering of nanoparticles of biodegradable copolymers for quantitative control of targeted drug delivery. *Biomaterials* 31, 9145–9155. doi: 10.1016/j.biomaterials.2010.08.053

Lopez Hernandez, H., Grosskopf, A. K., Stapleton, L. M., Agmon, G., and Appel, E. A. (2019). Non-newtonian polymer-nanoparticle hydrogels enhance cell viability during injection. *Macromol. Biosci.* 19:1800275. doi: 10.1002/mabi.201800275

Mora-Huertas, C. E., Fessi, H., and Elaissari, A. (2010). Polymer-based nanocapsules for drug delivery. *Int. J. Pharmaceut.* 385, 113–142. doi: 10.1016/j.ijpharm.2009.10.018

Murday, J. S., Siegel, R. W., Stein, J., and Wright, J. F. (2009). Translational nanomedicine: status assessment and opportunities. *Nanomedicine* 5, 251–273. doi: 10.1016/j.nano.2009.06.001

Nicolai, T., Colombani, O., and Chassenieux, C. (2010). Dynamic polymeric micelles versus frozen nanoparticles formed by block copolymers. *Soft Matt.* 6, 3111–3118. doi: 10.1039/b925666k

Pridgen, E. M., Alexis, F., and Farokhzad, O. C. (2015). Polymeric nanoparticle drug delivery technologies for oral delivery applications. *Exp. Opin. Drug Deliv.* 12, 1459–1473. doi: 10.1517/17425247.2015.1018175

Pridgen, E. M., Alexis, F., Kuo, T. T., Levy-Nissenbaum, E., Karnik, R., Blumberg, R. S., et al. (2013). Transepithelial transport of Fc-targeted nanoparticles by the neonatal Fc receptor for oral delivery. *Sci. Translat. Med.* 5:213ra167. doi: 10.1126/scitranslmed.3007049

Ragelle, H., Danhier, F., Préat, V., Langer, R., and Anderson, D. G. (2017). Nanoparticle-based drug delivery systems: a commercial and regulatory outlook as the field matures. *Exp. Opin. Drug Deliv.* 14, 851–864. doi: 10.1080/17425247.2016.1244187

Rode García, T., García Ac, A., Lalloz, A., Lacasse, F.-X., Hildgen, P., Rabanel, J.-M., et al. (2018). Unified scaling of the structure and loading of nanoparticles formed by diffusion-limited coalescence. *Langmuir* 34, 5772–5780. doi: 10.1021/acs.langmuir.8b00652

Saad, W. S., and Prud'homme, R. K. (2016). Principles of nanoparticle formation by flash nanoprecipitation. *Nano Today* 11, 212–227. doi: 10.1016/j.nantod.2016.04.006

Shi, J., Kantoff, P. W., Wooster, R., and Farokhzad, O. C. (2017). Cancer nanomedicine: progress, challenges and opportunities. *Nat. Rev. Cancer* 17, 20–37. doi: 10.1038/nrc.2016.108

Song, C., Labhasetwar, V., Murphy, H., Qu, X., Humphrey, W., Shebuski, R., et al. (1997). Formulation and characterization of biodegradable nanoparticles for intravascular local drug delivery. *J. Control. Release* 43, 197–212. doi: 10.1016/S0168-3659(96)01484-8

Stapleton, L. M., Steele, A. N., Wang, H., Lopez Hernandez, H., Yu, A. C., Paulsen, M. J., et al. (2019). Use of a supramolecular polymeric hydrogel as an effective post-operative pericardial adhesion barrier. *Nat. Biomed. Eng.* 3, 611–620. doi: 10.1038/s41551-019-0442-z

Steele, A. N., Stapleton, L. M., Farry, J. M., Lucian, H. J., Paulsen, M. J., Eskandari, A., et al. (2019). A biocompatible therapeutic catheter-deliverable hydrogel for *in situ* tissue engineering. *Adv. Healthcare Mater.* 8:1801147. doi: 10.1002/adhm.201801147

Tibbitt, M. W., Dahlman, J. E., and Langer, R. (2016). Emerging frontiers in drug delivery. *J. Am. Chem. Soc.* 138, 704–717. doi: 10.1021/jacs.5b09974

Westedt, U., Kalinowski, M., Wittmar, M., Merdan, T., Unger, F., Fuchs, J., et al. (2007). Poly(vinyl alcohol)-graft-poly(lactide-co-glycolide) nanoparticles for local delivery of paclitaxel for restenosis treatment. *J. Control. Release* 119, 41–51. doi: 10.1016/j.jconrel.2007.01.009

Yu, A. C., Chen, H., Chan, D., Agmon, G., Stapleton, L. M., Sevit, A. M., et al. (2016). Scalable manufacturing of biomimetic moldable hydrogels for industrial applications. *Proc. Natl. Acad. Sci. U.S.A.* 113, 14255–14260. doi: 10.1073/pnas.1618156113

Conflict of Interest: The authors declare that the research was conducted in the absence of any commercial or financial relationships that could be construed as a potential conflict of interest.

frontiers in Bioengineering and Biotechnology

REVIEW
published: 17 December 2019
doi: 10.3389/fbioe.2019.00415

Overcoming Physiological Barriers to Nanoparticle Delivery—Are We There Yet?

Oliver S. Thomas[1,2,3] *and Wilfried Weber*[1,2,3]*

[1] Faculty of Biology, University of Freiburg, Freiburg, Germany, [2] Signalling Research Centres BIOSS and CIBSS, University of Freiburg, Freiburg, Germany, [3] Spemann Graduate School of Biology and Medicine, University of Freiburg, Freiburg, Germany

The exploitation of nanosized materials for the delivery of therapeutic agents is already a clinical reality and still holds unrealized potential for the treatment of a variety of diseases. This review discusses physiological barriers a nanocarrier must overcome in order to reach its target, with an emphasis on cancer nanomedicine. Stages of delivery include residence in the blood stream, passive accumulation by virtue of the enhanced permeability and retention effect, diffusion within the tumor lesion, cellular uptake, and arrival at the site of action. We also briefly outline strategies for engineering nanoparticles to more efficiently overcome these challenges: Increasing circulation half-life by shielding with hydrophilic polymers, such as PEG, the limitations of PEG and potential alternatives, targeting and controlled activation approaches. Future developments in these areas will allow us to harness the full potential of nanomedicine.

Keywords: nanomedicine, nanoparticle, nanocarrier, drug delivery, barrier, EPR effect, stimulus-responsive, PEG

OPEN ACCESS

Edited by:
Francesco Cellesi,
Politecnico di Milano, Italy

Reviewed by:
Hongwei Chen,
University of Michigan, United States
Clara Mattu,
Politecnico di Torino, Italy
Paolo Bigini,
Istituto Di Ricerche Farmacologiche Mario Negri, Italy

***Correspondence:**
Wilfried Weber
wilfried.weber@biologie.uni-freiburg.de

Specialty section:
This article was submitted to Nanobiotechnology, a section of the journal Frontiers in Bioengineering and Biotechnology

Received: *25 September 2019*
Accepted: *29 November 2019*
Published: *17 December 2019*

Citation:
Thomas OS and Weber W (2019) Overcoming Physiological Barriers to Nanoparticle Delivery—Are We There Yet? Front. Bioeng. Biotechnol. 7:415. doi: 10.3389/fbioe.2019.00415

1. INTRODUCTION

In the ever-continuing arms race between medical researchers and the ailments they are trying to tackle, nanotechnology has emerged as a useful ally. A nanoparticle (NP) is an object with dimensions in the nanometer range (**Figure 1**). A nanocarrier is a nanoparticle utilized for the transport of a cargo, for instance a therapeutic molecule. The diversity of available nanoparticles for drug delivery is considerable and includes polymeric nanoparticles, dendrimers, carbon nanotubes, quantum dots, metallic nanoparticles or lipid-based systems, such as micelles or liposomes (Hughes, 2005; Cho et al., 2008; Bogart et al., 2014; Matea et al., 2017). Liposomes were first described by Bangham et al. (1965) and would eventually prove to be a promising candidate for the encapsulation of therapeutic molecules. In fact, the first nanoparticulate drug to be approved by the US Food and Drug administration (FDA) has been Doxil (marketed as Caelyx outside the US) (Barenholz, 2012), a liposomal formulation of the cytostatic agent doxorubicin. Several liposomal drug products are now in clinical use (Bulbake et al., 2017), many of which are intended for the treatment of cancer, and new ones continue to reach approval status. In 2015, the FDA approved Onivyde (liposomal irinotecan) for the use in metastatic pancreatic cancer, a disease with a dismal prognosis for affected patients. The phase 3 trial showed an (albeit moderate) extension of overall survival (Wang-Gillam et al., 2016) that was confirmed in a recent follow-up study (Wang-Gillam et al., 2019). In 2017, Vyxeos (liposomal synergistic combination of daunorubicin and cytarabin) was approved for acute myeloid leukemia (Lancet et al., 2018). Innovative liposomal formulations also make their mark in disciplines other than oncology: Arikayce (liposomal amikacin) was FDA-approved in 2018 for the management of non-tuberculous mycobacteria infection (Griffith et al., 2018)—however, the application in Europe was withdrawn in 2016 (with intent to resubmit) after

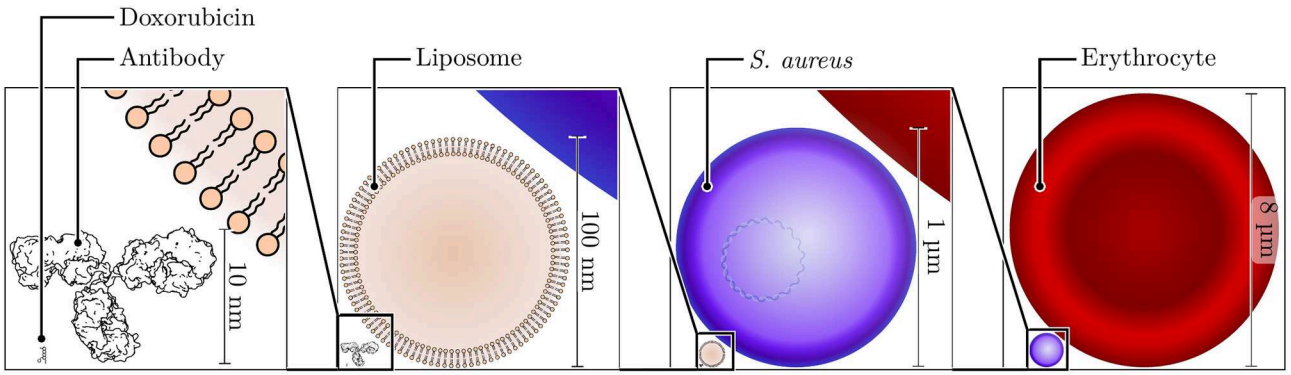

FIGURE 1 | Size comparison of nano- and microscale structures. Shown to the bottom left is the skeleton structure of doxorubicin, a typical cargo molecule for nanoparticle formulations, with a size of ∼1.5 nm. Adjacent to this small molecule, a typical antibody molecule (height of ∼10 nm) is shown next to a small unilamellar liposome with a diameter of 100 nm. The diameter of the bacterium *S. aureus* is ∼1 µm, and that of a human erythrocyte is ∼8 µm.

data from a phase 2 trial failed to convince the European Medicines Agency (EMA) of the drug's benefits. Also in 2018, a vaccine was approved for the prevention of Herpes Zoster in older patients, which contains a liposomally formulated adjuvant (Shingrix).

These examples highlight the potential of nanoparticulate formulations in general, and liposomally encapsulated drugs in particular. They also illustrate the breadth of applications (potential and actual) for these types of therapeutics, which is supported by an exhaustive overview of nanoparticles either approved clinically or undergoing clinical trials (Anselmo and Mitragotri, 2016, 2019).

This review aims to highlight the challenges faced by such formulations during their journey toward their destination and what strategies have been devised to try and circumvent these obstacles, with a focus on cancer therapy. Previous excellent reviews have considered related issues. For instance, Blanco et al. reviewed biological barriers to nanoparticle delivery, highlighting the influence of the physicochemical and geometric properties of nanoparticles (Blanco et al., 2015). Yu et al. considered numerous nano-scaled delivery devices with a focus on protein delivery and topical delivery modalities (Yu et al., 2016). This work is supposed to complement them with recent findings and developments of the last years. In particular, important progress has been made in attempts to quantitatively understand the processes leading to nanoparticle delivery and internalization. When examples are given for principles of nanoparticle design, we furthermore focused on systems which were efficacious clinically or at least in mammalian model organisms (as opposed to cell culture assays alone), whenever possible.

To illustrate the underlying principles, we will follow an injected nanoparticle from the site of injection toward the site of action. We first summarize the basis of the enhanced permeability and retention (EPR) effect and highlight its heterogeneous nature. We then shift the focus from the physiology of the disease to the characteristics of the nanoparticle and discuss shielding strategies, which are required to confer long half-lives on nanoparticles in order to exploit the EPR effect and allow arrival at the tumor. Furthermore, we consider options for stimulus-responsive designs of nanocarriers to maximize their capability of reaching (and interacting with) their target cells. Finally, we give an overview about targeting modalities to direct nanoparticles to their destined target cells within the tumor tissue and their intracellular sites of action.

Abbreviations: ABC, accelerated blood clearance; CDM, 2-propionic-3-methylmaleic anhydride; CT, computed tomography; EPR, enhanced permeability and retention effect; hGH, human growth hormone; HIF, hypoxia-inducible factor; HIFU, high-intensity focused ultrasound; HPMA, poly(N-[2-hydroxypropyl] methacrylamide); ID, injected dose; KS, Kaposi's sarcoma; LTSL, lyso-thermosensitive liposomes; MMP, matrix-metalloproteinase; Nbz, *o*-nitrobenzyl; NIR, near-infrared; NP, nanoparticle; PAcM, poly(N-acryloyl morpholine); PAE, poly-β-aminoester; PAMAM, polyamidoamine; PCL, polycaprolactone; PDMA, poly(N,N-dimethylacrylamide); PDT, photodynamic therapy; PEG, polyethylene glycol; PET, positron emission tomography; P-gp, P-glycoprotein; PLD, PEGylated liposomal doxorubicin; PLGA, poly(lactic-co-glycolic acid); PMOX, poly(2-methyl-2-oxazoline); POPE, 1-palmitoyl-2-oleoyl-sn-glycero-3-phosphoethanolamine; PPE, palmar-plantar erythrodysesthesia; PSar, polysarcosine; PVP, poly(vinylpyrrolidone); RBC, red blood cell; RFA, radio frequency ablation; ROS, reactive oxygen species; scFv, single-chain variable fragment; SIRP, signal-regulatory protein; SPION, superparamagnetic iron oxide nanoparticle; TAM, tumor-associated macrophage; UCNP, upconversion nanoparticle; VEGF, vascular endothelial growth factor.

2. CANCER NANOMEDICINE: FROM INJECTION TO TUMOR

A large amount of effort is being expended to enable and advance the application of nanotechnology-based drugs for the treatment of cancer. To exert their intended effect and eliminate malignant cells, these agents, like any drug, must first and foremost be capable of reaching the site of the lesion. A frequently cited, yet controversially discussed concept in research aimed at developing new nanocarriers for oncological treatments is the so-called enhanced permeability and retention (EPR) effect (Rosenblum et al., 2018). The term was coined by Matsumura and Maeda (1986) and describes the tendency of macromolecules and nano-sized-particles to accumulate in neoplastic tissues,

therefore facilitating passive targeting without the need for additional modifications of the carrier.

2.1. The Pathophysiological Basis of the EPR Effect

The underlying fundamental process toward the establishment of the EPR effect is neovascularization of the tumor tissue, an occurrence that was labeled as one of the hallmarks of cancer (Hanahan and Weinberg, 2011). It results in the sprouting of new vessels which are, however, of inferior quality compared to healthy vessels. The wall of regular capillaries is primarily made up of endothelial cells, which contain the blood flow toward their luminal side. In most tissues, endothelial cells are connected by tight junctions. In some specialized tissues (such as the kidney glomeruli, endocrine glands or the intestine), the endothelial wall is punctured by fenestrae, small pores of ∼60 nm in diameter covered by a negatively charged glycocalyx. The capillaries of the liver and bone marrow feature larger transcellular pores in the endothelial cells, allowing exchange of serum proteins with the interstitium, but this process is highly regulated (Stan, 2007). In the spleen, the capillaries display true intercellular gaps which allows extravasation of erythrocytes and requires them to be deformable enough to re-enter the venous system, filtering out aged and rigid cells (Mebius and Kraal, 2005).

As a tumor continues to grow, its demands increase regarding the acquisition of oxygen and nutrients on the one hand, and the expulsion of waste products on the other. Simultaneously, the distance to the nearest capillary increases. A normoxic environment persists in a radius of ∼100 μm around a vessel (Fang et al., 2008), with hypoxia becoming increasingly prevalent as the distance increases further. The hypoxia-inducible factor 1 (HIF-1) is a dimeric transcription factor, consisting of HIF-1α and HIF-1β (Eales et al., 2016). As O_2 levels decrease, HIF accumulates and induces transcription of its target genes, which includes the vascular endothelial growth factor (VEGF) family. The VEGFs are key players during angiogenesis, but by no means the only one. In tumors, the finely balanced microenvironment of angiogenic factors is disrupted, VEGF is not only upregulated by HIF via hypoxia, but also via the activation of oncogenes (Dvorak, 2003), resulting in aberrant vessels that are highly heterogeneous and differ from normal vessels in several important aspects (Less et al., 1991; Nagy et al., 2010; Azzi et al., 2013).

The induced vessels display gaps in between the endothelial cells (Hashizume et al., 2000) and are less selective regarding the permeability of particles. Around tumor vessels, the sheet of pericytes [a heterogeneous cell type which surrounds healthy vessels and is important for their proper functionality (Armulik et al., 2005; Attwell et al., 2016)] is not necessarily completely absent. However, their association with the endothelial wall is loose and their morphology differs from regular pericytes by the presence of protrusions away from the vessel wall, which are not seen in their regular counterparts (Morikawa et al., 2002). Likewise, the basal membrane of these vessels is compromised and differs in thickness, compactness and its cellular association (Baluk et al., 2003; Kalluri, 2003).

Additionally, tumors are frequently also sites of chronic inflammation to which a diverse array of different leukocytes is recruited (Hanahan and Weinberg, 2011; Coussens et al., 2013). They contribute to the production of tissue mediators of inflammation, which act on blood vessels to increase their permeability, further increasing leakiness, and agents modulating the relevant pathways can be used to modulate the EPR effect (Wu et al., 1998; Maeda et al., 2000).

These irregularities contribute to an inadequate blood supply of the tumor, creating a hypoxic and acidic milieu. They also account for the *enhanced permeability* component of the EPR effect and allow extravasation of macromolecules and particles up to ∼400 nm in size due to increased leakiness (Gerlowski and Jain, 1986; Yuan et al., 1995), but depending on the tumor type, this cutoff can be larger or smaller (Hobbs et al., 1998).

The second component, the *enhanced retention*, is a consequence of the aberrant lymphatic architecture (Stacker et al., 2014). Although metastatic spread frequently occurs by means of lymphatic dissemination, this appears to be mediated by lymphatic vessels in the periphery of the tumor mass, whereas internal vessels tend to collapse under the high tissue pressure (Leu et al., 2000; Padera et al., 2002). Consequently, tissue homeostasis within tumors is disrupted, and previously extravasated particles are not efficiently funneled back into the blood via lymphogenic transport through the ductus thoracicus (Noguchi et al., 1998).

Although the effects mentioned above were initially described in a static context, the tumor vasculature and the EPR effect appear to be subject to dynamic changes, as vents within the vessels open transiently to allow efflux of fluid into the surrounding tissues (Matsumoto et al., 2016). For larger particles, these events, termed eruptions, may be the only chance to leave the vessel lumen, and therefore allow them fewer opportunities to re-enter the circulation the way they left it, resulting in their entrapment (Ngoune et al., 2016).

In sum, both aspects (enhanced permeability and enhanced retention) can result in accumulation of particles, given sufficiently long circulation times of the particles in question for this process to take place.

2.2. Magnitude and Heterogeneity of the EPR Effect

Cancer is a generic term for the description of a large and heterogeneous class of diseases. The National Cancer Institute lists almost 200 types of cancers on their website. Likewise, the alterations described above are highly heterogeneous, within and between tumors, and the EPR effect cannot simply be generalized as a feature of all cancers (Maeda, 2015; Danhier, 2016). For less well-vascularized lesions, the efficiency of accumulation tends to be higher for small particles, whereas the influence of particle size diminishes as the lesion vascularization and leakiness increase (Cabral et al., 2011).

Broadly, many different factors influence the unique prevalence of the EPR effect in a given lesion, including the tumor type and stage, the characteristics of the individual patient under consideration, as well as the location of the tumor and

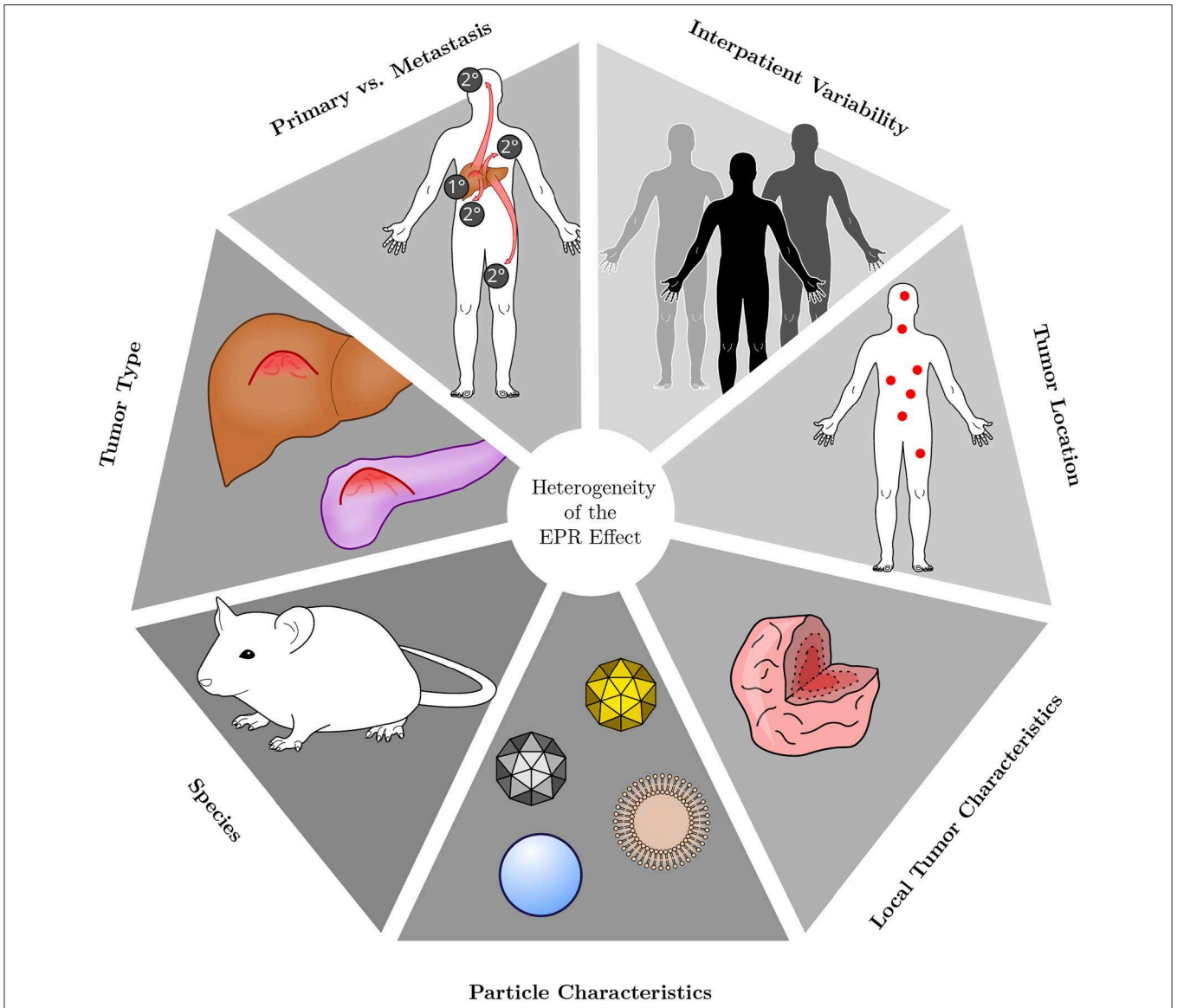

FIGURE 2 | Heterogeneity of the EPR effect. The EPR effect is a very heterogeneous phenomenon. Its presence and magnitude depend on the type of tumor under consideration, whether the lesion is of primary or metastatic origin and on the characteristics of each individual patient. Additionally, in which host tissue a lesion resides and where it is located is influential as well. Within a given tumor, accumulation of nanoparticle therapeutics may be heterogeneous owing to internal tissue composition and characteristics. Different types of particles are likewise heterogeneous in their behavior, owing to variations in, for instance, size, shape, charge or material. Most preclinical research is performed in small rodents, however, the species under investigation will also affect the EPR effect.

local properties in different zones of a tumor. For example, for Kaposi's sarcoma (KS), a sarcoma of vascular origin (Radu and Pantanowitz, 2013), doxorubicin levels in the lesion area were higher after treatment with Doxil compared to non-PEGylated doxorubicin (Northfelt et al., 1996) [but overall survival was not improved (Northfelt et al., 1998; Cooley et al., 2007; Udhrain et al., 2007)]. Contrary to KS, pancreatic adenocarcinomas tend to be hypovascular (Sofuni et al., 2005; Olive et al., 2009), potentially hampering the EPR effect [yet, a combination therapy of Onivyde plus 5-fluorouracil and leucovorin moderately improved overall survival in patients of metastatic pancreatic cancer (Wang-Gillam et al., 2016)]. Additionally, the features of the particle used to investigate the EPR effect will influence conclusions, and findings from laboratory animals are not necessarily transferable to the situation in humans (**Figure 2**).

In a comprehensive meta-analysis, the reported accumulation of nanoparticles in preclinical tumor models was analyzed and presented in terms of % injected dose (%ID) (Wilhelm et al., 2016). The published data (available from the paper's supplementary materials and the Cancer Nanomedicine Repository, http://inbs.med.utoronto.ca/CNR) also provides quantification of accumulation with a target quantity of

% injected dose per g of tissue (%ID/g), which was investigated here to facilitate comparison with other studies. This revealed that the median accumulation, normalized to tissue mass, was highest for pancreatic tumors (5.8 %ID/g, range 1.8–13.4) and lowest for lung tumors (1.1, 0.04–45.8). This observation stands in apparent contradiction to the aforementioned hypovascular characteristic of pancreatic cancers. However, as outlined above, a multitude of other factors, such as particle characteristics or the type of tumor model also influences tendencies of accumulation. For example, in their original investigation, Wilhelm et al. conducted a multivariate analysis over their full dataset, in which *p*-values for the effect of particle diameter and tumor model on delivery efficiency (%ID) were not significant individually (>0.05), but the interaction of both terms was. These observations and trends illustrate the heterogeneity of the EPR effect even in rodent models, for which it is generally well-accepted.

A large fraction of the injected dose is sequestered by tissue-resident macrophages before it can accumulate in the tumor tissue, and very small particles (below ∼5 nm in diameter) may also be cleared in the kidneys (**Figure 3**). When the macrophage populations of the liver and spleen were depleted by pretreatment with clodronate liposomes, the fraction of particles found in the liver and spleen were reduced or increased, respectively (Tavares et al., 2017). Concomitantly, plasma half-life and tumor accumulation of gold nanoparticles both increased significantly. However, although a large relative increase compared to the non-depleted condition was found, absolute accumulation of particles in the tumor still did not exceed 2% ID, emphasizing that premature clearance by macrophages is not the only mechanism preventing efficient accumulation. Overall, the effects of macrophage depletion were found to be polymorphic for the different xenografted tumor models of human origin used by the authors: in an orthotopic MDA-MB-435S (melanoma) model, no increased tumor accumulation (in terms of % injected dose) was observed. In the orthotopic MDA-MB-231 (mammary adenocarcinoma), the heterotopic SKOV3 (ovarian adenocarcinoma) and the heterotopic A549 (lung carcinoma) models, a 20-fold increase was observed, whereas a 100-fold increase was achieved in the orthotopic PC3 (prostate carcinoma) model.

Small animal models are useful for characterization of the EPR effect and verifying the efficacy of new nanotherapeutic formulations, but the situation is even more complicated and inadequately understood for larger animals and humans. More recently, quantification attempts of long-term accumulation have been made. In a study with dogs, $^{64}Cu^{2+}$-labeled liposomes with a lipid composition equivalent to Doxil were used to quantitatively measure their deposition in various cancers by Positron Emission Tomography (PET) and Computed Tomography (CT) (Hansen et al., 2015). Liposome uptake in tumors increased from 1 to 24 h in 6 out of 7 carcinomas, but not in sarcomas. One of the dogs had metastases in the lung and axillary lymph node, in which liposome accumulation occurred. The achieved concentrations 24 h after administration ranged between 0.0048 and 0.0231 %ID/g for the carcinomas, and between 0.0011 and 0.0038 %ID/g for the sarcomas.

$^{64}Cu^{2+}$-based PET imaging was also used in a clinical study involving MM-302, a PEGylated liposomal formulation of doxorubicin with targeting activity toward HER2 (a growth factor receptor overexpressed in many mammary carcinomas) for the treatment of breast cancer (Lee et al., 2017). Tumor deposition was heterogeneous both within lesions of the same patient and between patients, and varied between ∼0.001 and 0.01 %ID/g on day 2 after administration. A correlation between lesion size and carrier accumulation was not found. Deposition also occurred in normal liver, spleen and bone marrow, but not in other normal tissue, such as muscle.

Comparing the quantitative data of accumulation obtained from preclinical (rodent) studies (Wilhelm et al., 2016) and veterinary and human clinical observations (Hansen et al., 2015; Lee et al., 2017), a large discrepancy between both branches is evident, with rodent tumor models displaying a manifold higher uptake. This highlights the difficulty in translating observations from currently widely used investigative tools to the clinic due to profound differences in the underlying biological processes, such as the rate of growth or the size of malignancies relative to the host. Both of these are excessive in rodent models (Lammers et al., 2012a; Danhier, 2016). However, it has also been noted that focusing exclusively on the extent of accumulation omits other crucial parameters for the evaluation of drugs, such as their pharmacokinetic and toxicological properties, which can contribute to positive clinical outcomes, for instance by prolonging the exposure time to the compound (McNeil, 2016).

A big unmet need in cancer medicine is the effective extermination of metastases. In secondary lesions, the EPR effect will likely only be present in nodules that exceed the size threshold above which vascularization becomes a necessity, and will probably be equally heterogeneous. Although the physiological processes of abnormal vessel development underlying the EPR effect could be observed even in the initial phases of tumorigenesis (Hagendoorn et al., 2006), early and small lymphogenic metastases were not efficiently targeted by >150 nm liposomes (Mikada et al., 2017). However, 30 nm polymeric micelles loaded with a platinum complex suppressed lymph node metastases in a melanoma model, suggesting only a low grade EPR effect in these nodules (Cabral et al., 2015). In larger lesions, the EPR effect may eventually become significant, as exemplified by the efficiency of a pirarubicin-polymer against metastatic lung cancer (Tsukigawa et al., 2015) and the deposition of $^{64}Cu^{2+}$-labeled liposomes in secondary lesions (Lee et al., 2017).

The specific tumor microenvironment affects extravasation of nanoparticles to a large extent, but the inverse may also be true. Recently, inorganic TiO_2 nanoparticles were shown to promote gaps in between endothelial cells (Setyawati et al., 2017; Tay et al., 2017) and facilitate subsequent extravasation of cancer cells from the primary lesion to form metastases (Peng et al., 2019). Additionally, it has been suggested that liposomes not loaded with drug molecules may promote tumor growth and angiogenesis (Sabnani et al., 2015). Whether these are generalizable observations and whether they hold true for different types of inorganic or organic nanoparticles is presently

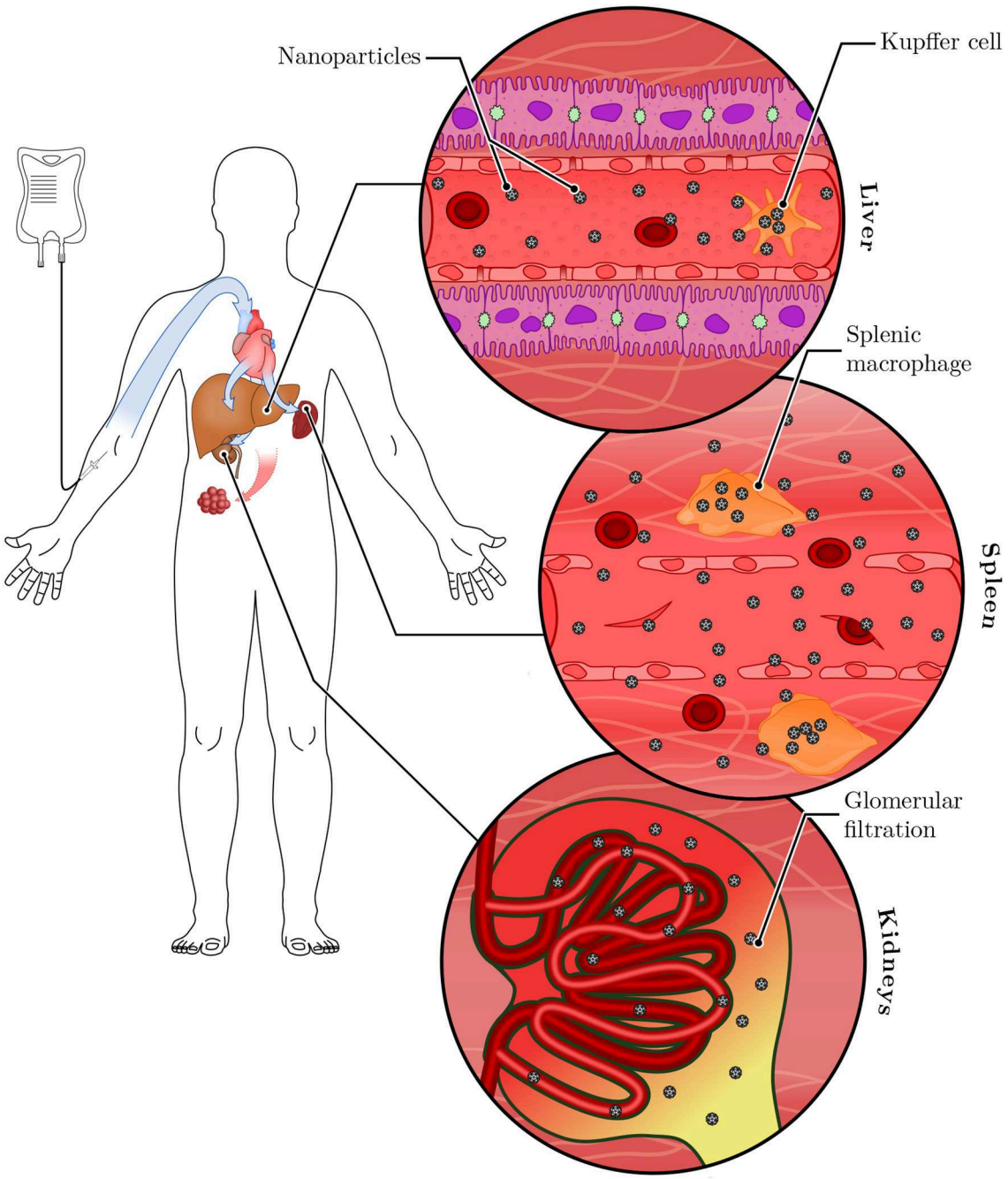

FIGURE 3 | Systemic clearance of nanoparticles. Following intravenous injection, nanoparticles are distributed systemically through the bloodstream. They reach the liver and the spleen, where tissue-resident macrophages (called Kupffer cells in the liver) sequester a large portion of the administered dose. Nanoparticles small enough to pass the glomerular filter (below ~5 nm) are excreted in the urine. Remaining nanoparticles have the opportunity to accumulate in tumor tissues.

unclear, but these questions are of potentially profound impact to the field of nanomedicine.

Thus, although the EPR effect is a reality in clinical settings, it is far from a simple manner and warrants critical evaluation (**Figure 2**). Exploiting it effectively remains a complicated challenge and will likely require individually tailored strategies in the clinic (Lammers et al., 2012b). Pharmaceutical interventions for enhancement of the EPR effect have been proposed (Fang et al., 2011), for instance by administration of hypertensive agents, such as angiotensin-II or by increasing vessel leakiness via NO-releasing compounds (such as nitroglycerine, which is used for the management of angina pectoris). On the other hand, inducing maturation of tumor vessels, for instance by inhibition of the VEGF signaling cascade, was reported to improve delivery of small and intermediately sized nanoparticles up to 40 nm to tumor tissue (Chauhan et al., 2012; Jiang

et al., 2015) due to a reduction in the interstitial pressure and consequent dominance of convection over the less efficient diffusion (see next section). However, the effect on larger particles (above 60 nm) was minimal (Chauhan et al., 2012), because normalization reduced pore sizes and prevented extravasation of larger particles. Interestingly, in another report, normalization of highly aberrant vasculature by sorafenib (a kinase inhibitor, acting on the VEGF-induced signaling cascade) increased tumor retention of FITC-Dextran with a hydrodynamic diameter of ∼50 nm. Conversely, the same inhibition in a tumor with vessels closer to the healthy state did reduce retention (Kano et al., 2009).

It has been suggested to use empty, non-drug loaded tracer particles, e.g., $^{64}Cu^{2+}$-labeled liposomes, for estimation of the EPR effect for the individual patient in order to gauge potential therapeutic efficacy of a nanocarrier (Lee et al., 2018). However, this approach might in practice be hampered by the accelerated blood clearance (ABC) phenomenon, in which PEGylated nanocarriers are cleared more rapidly from the circulation upon repeated administration (Ishida and Kiwada, 2008; Abu Lila et al., 2013).

2.3. Distribution of Nanoparticles in the Tumor Mass

After extravasation, the nanoparticles have not yet arrived at their final destination (**Figure 4**). They must be capable of maneuvering within the tumor mass to reach their target cells, a task made challenging by the difficult to navigate microenvironment of the tumor. One of the culprits is the high interstitial pressure in tumor tissue, to the elevation of which several factors contribute: Malignant cell proliferation results in an increase in cell mass, the overproduction of extracellular matrix components leads to fibrosis, and fluid pressure increases due to the leaky vasculature and the impaired lymphatic drainage (Chauhan et al., 2011). The increased interstitial pressure in tumor tissue diminishes the pressure gradient from circulation to tissue, especially in the central region of the lesion (Tong et al., 2004), where the lymphatics are more likely to be collapsed (Leu et al., 2000; Padera et al., 2002, 2004). This hampers convective transport processes and emphasizes undirected diffusion. Thus, all therapeutics achieve a slower net mass transport, contributing to their inefficient distribution in the tumor tissue, but this is especially problematic for nanoparticles due to their relatively larger sizes compared to free drug molecules, rendering their diffusion less efficient (Lane et al., 2015).

Centrally, the organization of extracellular matrix components, such as collagen or hyaluronic acid is also much more dense than in the periphery: Even within a few (1–2) millimeters from the surface of a murine B16 melanoma model, the diffusion capacity of macromolecules was substantially (up to several 100-fold) decreased compared to more superficial regions (Magzoub et al., 2007). This heterogeneity within one tumor is expanded by another layer of complexity in differences of diffusion for tumors of the same type, but at different localizations: When tumors derived from a glioblastoma or a melanoma were induced in mice, diffusion of macromolecules

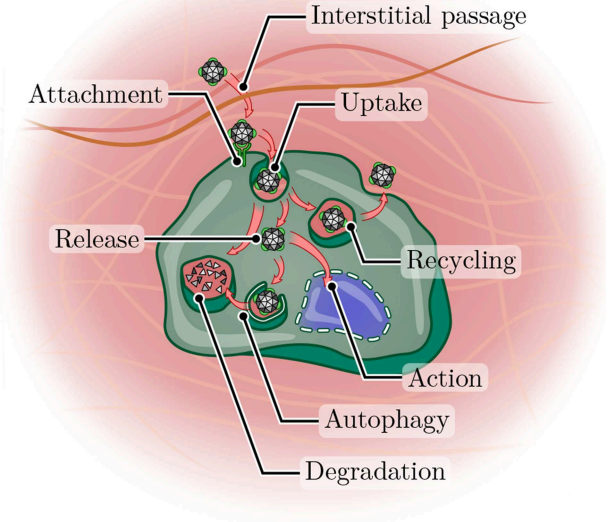

FIGURE 4 | Journey of a nanoparticle toward its site of action. After arriving in a tumor tissue, a nanoparticle must first overcome the often dense interstitium before it can attach to the surface of a cancer cell (potentially with the aid of a targeting ligand). Uptake can occur via a variety of pathways (not shown), but frequently leads to arrival in the endosomal compartment. From here, the nanoparticle may enter the recycling pathway and undergo exocytosis, be routed toward lysosomal degradation or achieve release into the cytoplasm. Even then, autophagy may still lead to degradation, or the particle (or its cargo) may arrive at its site of action and perform its function.

or liposomes was faster in tumors implanted at a cranial site compared to a dorsal site (Pluen et al., 2001).

Likewise, the distance that must be crossed also varies by tumor type (Smith et al., 2013): Based on the location of vessels, they were classified as "tumor vessels" (located close to cells) or "stromal vessels" (embedded within the stroma). For tumors rich in stromal vessels, diffusion distances to reach a target cell would be higher. This included colorectal, lung, prostate, and breast cancer model tumors, whereas vessels were closer to cells for renal, ovarian, hepatic, and thyroid cancers, as well as for a type of head and neck cancer and a glioma.

Recently, Zinger et al. proposed to utilize collagenase-loaded liposomes with slow release characteristics as a pretreatment to reduce the fibrotic character of pancreatic tumors and improve the delivery of secondary therapeutics (Zinger et al., 2019). They showed higher tumor weight reductions with the pretreatment and micellar paclitaxel, compared to micellar paclitaxel alone.

3. SHIELDING STRATEGIES TO IMPROVE CIRCULATION HALF-LIFE

For a therapeutic nanoparticle to be of use *in vivo*, it has to circulate for a sufficiently long time to reach its target and fulfill its intended function. This is especially important for carriers intended to exploit the EPR effect, in light of its apparent discontinuous and inefficient nature (Matsumoto et al., 2016), in order to give the agent ample time for accumulation to

occur. To confer long half-lives on nanoparticle formulations or proteins administered with a therapeutic intent, conjugation to polyethylene glycol (PEG) is by far the most common approach (Jokerst et al., 2011; Suk et al., 2016). The bulky, hydrophilic polymer increases the plasma half-life of modified particles by preventing excretion via the kidneys and blocking efficient uptake by phagocytic cells (Gref et al., 2000), in effect shielding them. The diminished cellular interaction is not exclusively due to steric hindrance. Upon exposure to biological fluids, nanoparticles acquire a new physicochemical identity due to the deposition of a dynamic layer of biomolecules on their surface, a process termed fouling which results in the establishment of a biocorona. It includes immunoglobulins, components of the complement system (Vu et al., 2019), coagulation factors and a plethora of other molecules, which fundamentally influences how cells perceive the coated particles (Giulimondi et al., 2019). It is now becoming increasingly appreciated that PEG alters the composition of the biocorona, which consequently influences cellular interactions and uptake modalities (Pelaz et al., 2015; Schöttler et al., 2016; Weiss et al., 2019). Notably, PEGylation is not a guaranteed way to raise biocompatibility, but its effect depends on the underlying material. For instance, PEGylation of two-dimensional graphene oxide nanosheets actually increased the cytokine levels secreted by challenged macrophages by facilitating diffusion and lodging within the cell membrane with subsequent activation of pro-inflammatory receptors (Luo et al., 2017).

3.1. Adverse Reactions to PEG

For many applications, PEG is generally considered biocompatible, safe and is successfully used clinically in many approved products (Webster et al., 2007, 2009; Jevševar et al., 2010). There is no doubt that PEG has made its mark on the market and is here to stay, however, it is not biologically inert and suffers from a number of issues. For instance, PEG is not biodegradable and has been shown to accumulate in the cytoplasm of renal cells, forming vacuoles whose impact on cell and organ function is unclear, but which may be of significance in the case of chronic applications (Bendele et al., 1998; Rudmann et al., 2013). Moreover, PEG may be more immunogenic than previously thought. Antibodies against PEG can be found after administration of PEGylated therapeutics, but also in more than 20% of naive healthy blood donors (Garay et al., 2012), as well as in naive pigs, with a potential source for priming being PEG contained in foods (Kozma et al., 2019). PEGylated asparaginase (PEG-ASNase) is used as a treatment for acute lymphoblastic leukemia. In a retrospective analysis of patient serum samples, the presence of anti-PEG was measured. In all of the samples in which anti-PEG could be detected, PEG-ASNase activity was undetectable, suggesting interference of these antibodies with the treatment (Armstrong et al., 2007). Considering the aforementioned potentially high prevalence of anti-PEG in the general population, such effects may be of considerable concern for the widespread use of PEG-modified nanocarriers. Apart from confounding treatment success, more immediately harmful effects were also seen: Hypersensitivity reactions were reported with PEG-containing therapeutics (Wenande and Garvey, 2016), both for PEG alone (used for instance for its laxative properties or as an excipient) or for bioconjugate products. Likewise, infusion reactions are prevalent for Doxil (Szebeni et al., 2002; Chanan-Khan et al., 2003). They occur in ∼11% of patients and vary in their intensity, ranging from flushing to anaphylactic shocks (Janssen Products, 2019). However, not all of these events must necessarily be attributable to PEG, since infusion reactions also occur for un-PEGylated nanomedicines (Szebeni et al., 2018).

The immunological response against PEG appears to be responsible for the aforementioned ABC phenomenon, thus hampering individual evaluation of the EPR effect with empty liposomes on a per patient basis. The first administration of PEGylated nanocarriers causes a priming effect with induction of IgM antibodies which have an opsonizing activity for subsequent doses, resulting in activation of the complement system and rapid clearance (Abu Lila et al., 2013; Kozma et al., 2019). The ABC phenomenon appears to be less pronounced or absent in liposomes containing cytotoxic drugs, because rapid elimination of injected liposomes was only observed when their administration was preceded by another dose of empty PEGylated liposomes, but not of doxorubicin-loaded liposomes (Laverman et al., 2001). Toxic effects of the loaded drugs on macrophages (Laverman et al., 2001) or splenic B cells (Ishida et al., 2006) have been suggested to be responsible for this observation. Concerning the situation in human patients, in a small clinical study with 12 participants involving three cycles of Doxil treatment, no increasing clearance was observed (La-Beck et al., 2012).

3.2. Alternatives to PEG

There are multiple approaches under investigation to reduce PEG-associated immunity. For instance, it was shown that the incorporation of gangliosides (a type of glycolipids natively present in cell membranes) into PEGylated liposomes reduced production of anti-PEG IgM in challenged mice, but only when both ligands were presented on the same particle (Mima et al., 2017). When these ganglioside-containing PEGylated liposomes were administered as a pretreatment, they also reduced anti-IgM production upon subsequent treatment with PEGylated liposomes without gangliosides. This raises the potential for upgrading PEG-containing therapeutics—nevertheless, there is an extensive body of research on other shielding polymers.

Synthetic hydrophilic polymers used for the extension of circulation half-life include poly(N-[2-hydroxypropyl] methacrylamide) (HPMA), poly(vinylpyrrolidone) (PVP), poly(2methyl-2-oxazoline) (PMOX), poly(N-acryloyl morpholine) (PAcM), and poly(N,N-dimethylacrylamide) (PDMA). When the half-life extensions of liposomes grafted with these compounds were evaluated in a comparative study, PMOX and PEG were found to have the largest effect (Kierstead et al., 2015). However, the authors note that an optimization of chain length and grafting had not been performed for polymers other than PEG, suggesting their performance may be improved. Notably, shielding efficiency was correlated to polymer viscosity, and the two most viscous polymers (PEG and PMOX) were the only ones to induce the ABC phenomenon in this study.

However, a causality of this observation was not shown, and it is thus only based on correlation.

A promising biological alternative to PEG is PAS: PAS is a heteropolymeric amino acid sequence incorporating the three monomers proline, alanine and serine (Schlapschy et al., 2013). These amino acids adopt an unfolded disordered conformation if assembled in a suitable manner, thus exposing the hydrophilic polypeptide backbone (with only a minor contribution of the serine hydroxy group to the overall hydrophilicity) (Breibeck and Skerra, 2018). One PAS unit consists of ∼20 monomers, and multiple PAS repeats can be chained to increase the shielding effect. The resulting polymeric sequence has biophysical properties which are similar to those of PEG, conferring an increased hydrodynamic radius on its fusion partners. As with PEG, this property varies with chain length, and a 400 residue PAS sequence is approximately equivalent to a 30 kDa linear PEG chain in its elution characteristics from a size exclusion matrix (Breibeck and Skerra, 2018).

Because PAS is an amino acid sequence, it can be genetically encoded. This obviates the need for post-translational chemical conjugation of therapeutic proteins, which carries the disadvantageous potential to alter their activity. Moreover, whereas preparations of PEG are polydisperse due to their synthesis, PAS is produced by the highly precise cellular machinery, reducing heterogeneity. From an economical point of view, PASylation likewise offers attractive prospects: Expensive raw materials are not necessary, and additional purification steps after conjugation, which reduce yields and are costly in themselves, are not required.

PAS has been used *in vivo* to extend the circulation half-life of proteins, for example of somatotropin (human growth hormone, hGH) (Schlapschy et al., 2013), antibody fragments (Mendler et al., 2015), leptins (Morath et al., 2015; Bolze et al., 2016), and interferon (Xia et al., 2019). For the hGH-PAS fusion protein, the immunogenicity of PAS was investigated—while antibodies against hGH-PAS did arise, epitope mapping revealed these were not reactive toward the PAS chain, but against epitopes of hGH, and no cross-reactivity to other PASylated proteins was found. However, given that antibody responses against multimeric epitopes are often strong due to their structural similarity to viral capsids (Bachmann and Zinkernagel, 1996; Yankai et al., 2006; Ogun et al., 2008), and in light of the inherent limitations of animal models for the investigation of immunogenicity, it is conceivable that antibodies against PAS or other immunological phenomena may be found if it is used in clinical practice. Nevertheless, data so far indicated that PAS was well-metabolizable and did not result in histological irregularities in the liver, spleen or kidneys of mice (Schlapschy et al., 2013).

PAS may also be an option for modification of nanoparticulate formulations other than therapeutic proteins. A protein nanocage composed of the ferritin heavy chain (HFt), utilized for the entrapment of doxorubicin, was PASylated by fusing its constituent monomers to 40 or 75 residue PAS sequences (Falvo et al., 2016). The PASylated variants showed chain-length dependent extended plasma half-lives of the entrapped doxorubicin in intravenously injected mice.

Polysarcosine (PSar) is a polymer of sarcosine (N-methylated glycine, an intermediate of glycine metabolism) in which tertiary amide bonds in the backbone confer resistance to proteolytic degradation compared to conventional peptides (Miller et al., 1995). Similar to PEG, PSar could be conjugated to lipids, potentially allowing the generation of PSar-protected liposomes and micelles (Weber et al., 2016). When PSar was grafted on a TiO_2 sheet, it reduced the amount of fibrinogen associated with the surface and prevented the attachment of mammalian and bacterial cells (Lau et al., 2012). In another study (Hu et al., 2018), interferon 2β was modified either with a 12 kDa PSar chain, or a 10 kDa PEG chain, which resulted in similar hydrodynamic radii and almost identical plasma half-lives. Accumulation in tumors of a murine OVCAR3 (ovarian carcinoma) model was slightly higher for the PSar-modified variant, culminating in an increased inhibition of tumor growth after 25 days, whereas liver deposition was lower. Data also suggested that less anti-IFN IgG was produced in response to PSar-IFN, but antibodies against PSar proper (i.e., antibodies binding directly to PSar) were not assessed. A block-copolymer consisting of poly(L-lactic acid) and PSar (lactosome) showed accumulation in murine tumor models of orthotopic hepatic and lung carcinomas, and a heterotopic pancreas carcinoma (Makino et al., 2009). However, upon repeated administration, lactosome was prone to an ABC phenomenon and was cleared rapidly from the circulation by hepatic sequestration (Hara et al., 2012). This metabolic clearance correlated with production of IgM and IgG3 which bound to PSar and persisted for 6 months after the first administration. Furthermore, the immunogenicity of PSar was found to vary with the type of particle (polymeric micelles or vesicular), the hydrodynamic diameter and the membrane elasticity (Kim et al., 2017).

An entirely different strategy to confer the ability to avoid rapid clearance on nanoparticles relies on the exploitation of the naturally occurring membrane composition of red blood cells (RBCs): RBCs were lysed, their membrane fraction was collected and subsequently grafted onto poly(lactic-co-glycolic acid) (PLGA) nanoparticles by passing the membrane suspension together with the particles through an extrusion device with a pore size of 100 nm. Following this treatment, the nanoparticles were covered in the RBC membrane and displayed increased *in vivo* half-life compared to conventionally PEGylated PLGA nanoparticles (Hu et al., 2011). In a subsequent study, the authors showed that this property was to some extent dependent on the presence of CD47 on the membrane surface, a glycosylated transmembrane protein which acts as a marker of "self" for the immune system and reduces uptake of the covered nanoparticles by macrophages due to binding SIRP (signal-regulatory protein) (Brown and Frazier, 2001). The increased half-life was not entirely abrogated upon blockade of CD47 by antibodies, however, suggesting involvement of other components which act as a shielding layer, e.g., the RBC glycocalyx, which was grafted in concert (Hu et al., 2013). In a different setup, adding an additional shielding layer by genetically engineering HEK293 (human embryonic kidney) cells to express PAS on their surface and grafting their membrane onto PLGA nanoparticles further increased the *in vivo* half-life in comparison to cell membranes

without PAS (Krishnamurthy et al., 2019). For human use, such an approach naturally begs the question of how to handle immune reactivity from different blood groups or potential contamination by pathogens. One option may be the use of autologous erythrocytes for personalized nanoparticle coatings.

3.3. The PEG Dilemma and Stimulus-Responsive Release

Irrespective of the strategy chosen for the avoidance of renal clearance and the MPS, there is a disadvantage associated with the prevention of cellular interactions: After successfully evading phagocytosis along the way and having arrived at its destined site of action, for instance by virtue of the EPR effect, the nanoparticle in question is now incapable of efficiently interacting with its target cells, such as tumor cells (Mishra et al., 2004). Furthermore, their efficient endosomal escape is impeded, resulting instead in the delivery of the particles into the degradative lysosomal pathway (Remaut et al., 2007; Dominska and Dykxhoorn, 2010).

As such, different strategies have been developed to allow nanoparticles to shed their protective coat or release their cargo in order to facilitate efficient uptake by their target cells (Hatakeyama et al., 2011; Zhu and Torchilin, 2013). For this purpose, nanoparticles have been engineered with the ability to change their properties in a stimulus-dependent fashion. Broadly speaking, such approaches can be divided into two distinct categories: Intrinsic and extrinsic stimulus-responsiveness (Mura et al., 2013; Jin et al., 2019).

Intrinsic stimulation relies on locally variable environmental circumstances (for instance in the tumor microenvironment), such as pH, redox potential or enzymatic activity. Contrarily, extrinsic stimulus-responsive nanocarriers are intended to react to cues applied externally by the treating physician at a precisely defined location and/or time, for instance by exposure to light, heat, ultrasonication or a magnetic field. Combinatorial approaches make for a monumental number of possible systems. A few recent illustrative examples highlighting the breadth of potential mechanisms are given below; For a more thorough overview, the interested reader is referred to other excellent reviews on this topic (Mura et al., 2013; Wang and Kohane, 2017; El-Sawy et al., 2018; Jin et al., 2019).

Nanocarriers may react to stimulation, whether extrinsic or intrinsic, either by the release of the free, low molecular weight drug, by shedding of the shielding layer (allowing facilitated uptake of the drug-loaded nanocarrier), or by altering their properties, such as size or geometry. Variants which keep the nanocarrier intact but facilitate its uptake, and therefore enable delivery of a bulk payload to target cells, bear the potential of overcoming drug resistance in resilient malignancies by three mechanisms: First, nanoparticles can deliver their payload via the endocytic internalization pathway, thus bypassing drug efflux pumps, such as P-glycoprotein (P-gp), which are localized in the plasma membrane, or exceeding their capacity after release of the active compound from the endosomal system (Davis et al., 2008; Wang et al., 2014). Second, by loading nanocarriers with synergistic combinations of compounds, therapeutic efficacy can be higher than for the individual drugs, and the evolution of drug resistance can be slowed down or prevented (Parhi et al., 2012). This is the principle behind Vyxeos, a liposomally encapsulated combination of cytarabine and daunorubicin (Lancet et al., 2018). Third, inhibitors of P-gp can be co-loaded with the therapeutic drug and delivered in concert (Saneja et al., 2014), for example chemical inhibitors (Tang et al., 2016) or siRNA (Zhang et al., 2016).

3.3.1. Intrinsic Stimulation

Matrix-metalloproteinases (MMPs) are a family of proteases involved in the progression of cancer, for instance by releasing growth factors from the extracellular matrix, mediating angiogenic processes, or facilitating invasive and migratory phenotypes by carving a path through the matrix (Kessenbrock et al., 2010). By conjugating PEG to a peptide comprising the recognition sequence of MMP-2, the PEG layer was rendered cleavable in the presence of this protease. The conjugate was then coupled to a cholesterol anchor and inserted into the lipid bilayer of liposomes by post-insertion (Wan et al., 2013). Encapsulating adenoviral vectors in these liposomes allowed higher transduction efficiencies of an MMP-2 secreting tumor cell line when cleavable PEG was grafted on the liposomes, compared to non-cleavable PEG.

Due to oxidative stress in the tumor area, increased amounts of the reducing tripeptide glutathione have been reported there. To exploit this phenomenon, a reduction-sensitive PEGylated lipid (1-palmitoyl-2-oleoyl-sn-glycero-3-phosphoethanolamine, POPE), linking PEG to a glycerophospholipid via a disulfide bridge (POPE-SS-PEG5000) was synthesized. As a second stimulus-responsive component, a lipopeptide mimicking the triple-helical structure of collagen which was cleavable by MMP-9 was incorporated into liposomes (Kulkarni et al., 2014). Exposure of these liposomes to glutathione resulted in the shedding of the PEG layer, subsequently providing access to the MMP-9 cleavage site of the lipopeptide, which destabilized the triple helix and allowed release of liposomally encapsulated contents. Notably, the destabilization process increased the size of the vesicles, possibly owing to aggregation resulting from the destabilization. In a heterotopic murine model of the human pancreatic cancer cell line PANC-1, these double-responsive liposomes showed preferential release of carboxyfluorescein at the tumor site. When liposomes were loaded with gemcitabine, treatment with vesicles containing the lipopeptide resulted in a moderately larger reduction of tumor growth compared to liposomes not responsive to MMP-9.

The pH in malignant lesions is typically lowered compared to healthy tissues because of their heightened metabolic activity, allowing potential discrimination of the tissue disease state (Lee et al., 2008). Additionally, the intracellular space is reducing, in contrast to the oxidizing extracellular compartment. One example of a pH and redox dual responsive nanocarrier is the iCluster system developed by Li et al. (2016). They linked polycaprolactone (PCL) and polyamidoamine (PAMAM) with a pH-sensitive linker (2-propionic-3-methylmaleic anhydride; CDM). The resulting PCL-CDM-PAMAM polymer was conjugated to a platinum prodrug and co-assembled with a PEG-PCL heteropolymer. The complete nanocarriers were

∼100 nm in size and exhibited a long plasma half-life by virtue of the incorporated PEG. Upon encounter of a slightly acidic milieu (pH 6.8), the CDM-based linker was cleaved, releasing substantially smaller PAMAM/Pt particles about 5 nm in size. The rationale behind this design was to facilitate diffusion through the tumor interstitium by size-reduction after accumulation at the site of interest via the EPR effect. The small particles were then taken up by cells and, upon encounter of the reducing conditions of the intracellular space, cisplatin was released from PAMAM/Pt, resulting in cytotoxicity. In murine models of heterotopic xenografts of Bx-PC3 human pancreatic tumor and a cisplatin-resistant A549R human lung tumor, the pH- and redox-sensitive cluster showed higher tumor growth inhibition and prolongation of survival compared to free cisplatin, PAMAM/Pt or a pH-insensitive cluster variant. An extension of median survival was also reported for an orthotopic allograft of the metastatic 4T1 mammary carcinoma.

A form of stimulus-responsiveness may also be involved in the mechanism of action of Doxil. Doxorubicin is remotely loaded into liposomes by means of an ammonium sulfate gradient, which allows the uncharged, unprotonated doxorubicin to diffuse through the membrane into the liposomal interior space, where a high ammonium sulfate concentration and low pH cause it to be protonated and form crystalline rods with the abundant sulfate ions (Haran et al., 1993; Wei et al., 2018). Extensive glutaminolysis at the tumor site could produce NH_3, which diffuses through the liposomal membrane, receives a proton from doxorubicin-NH_3^+ and allows the now uncharged doxorubicin to diffuse out of the liposome again (Silverman and Barenholz, 2015).

For passively stimulated nanoparticles, no exogenous input is required, and consequently, no information about the localization of a lesion is necessary to induce release. However, this could simultaneously be considered a blessing and a curse, since precise yet uncontrollable perturbations are required for the systems' functionality. As outlined above for the EPR effect, such tumor-related phenomena can be highly heterogeneous (Marusyk and Polyak, 2010; Alizadeh et al., 2015).

3.3.2. Extrinsic Stimulation

Conversely, active triggering does rely on external application of a stimulus. This requires knowledge about the target's location and extent, which renders this approach problematic for the eradication of very small and dispersed metastatic foci, but offers promising perspectives for the treatment of localized sites.

After allowing sufficient time for accumulation at the tumor site, suitably designed nanocarriers can be externally stimulated to induce efficient cargo release or allow cellular uptake. Light is a highly attractive modality for targeted activation due to the high spatiotemporal resolution of the stimulus. UV light is sufficiently energetic to cleave chemical bonds. However, for light-regulated systems, low-energy light in the far-red or near-infrared (NIR) region of the spectrum is most desirable for biological applications because it exhibits the highest capacity to penetrate tissues and is less cytotoxic compared to light of shorter wavelengths. For applications for which a high input of energy is nonetheless desirable, upconversion nanoparticles (UCNPs) offer tempting possibilities by virtue of an *anti-Stokes shift*, which converts multiple low energy input photons to higher energy output photons (Wen et al., 2018).

Photodynamic therapy (PDT) is a treatment modality which relies on the generation of cytotoxic reactive oxygen species (ROS) by means of photosensitizers after light illumination (Lucky et al., 2015). PDT is clinically tested for the treatment of malignancies for example of the skin, bladder, or esophagus, which are situated in proximity to an interior or exterior body lining (and therefore allow external illumination), but is of limited efficacy when the tumor harbors hypoxic regions. Conjugating photosensitizers to nanoparticles can improve their pharmacokinetic profile and bestow additional functionalities upon them. In an intricate setup (Xu et al., 2018), micelles of CPP (which is the PEG-modified photosensitizer chlorin e6 conjugated to a non-cytotoxic platinum(IV) diazido complex) were associated with UCNPs, which can convert inbound 980 nm light to emissions of 365 and 660 nm. Illumination with 980 nm light lead to formation of cytotoxic Pt(II) and O_2, allowing the generation of ROS even in the hypoxic tumor environment. The nanoparticles showed accumulation in the tumor and high anti-tumor activity in murine models of four different tumor cell lines upon illumination.

Shedding of PEG by NIR light was achieved by utilizing a UV-sensitive *o*-nitrobenzyl (Nbz) linker, connecting PEG to poly-β-aminoesters (PAE; PEG-Nbz-PAE-NBz-PEG). By incorporation of UCNPs, this setup allowed release of encapsulated doxorubicin in response to NIR illumination, which first led to removal of the PEG layer by the upconverted UV irradiation and also allowed cleavage of the pH sensitive PAE (Zhou et al., 2019).

To confer thermosensitivity on doxorubicin-loaded liposomes, a formulation that incorporated lyso-lipids into the phospholipid bilayer was developed (lyso-thermosensitive liposomes, LTSL; marketed as ThermoDox), which lowered the phase transition temperature and allowed rapid drug release (within 20 s) at moderately elevated temperatures of 39–40°C (Needham et al., 2000). Heating *in situ* can be achieved as a side-effect of radiofrequency ablation (RFA), which is based on the application of an alternating current to the tumor via an inserted probe. The invasiveness of this procedure depends on the route of access. In a clinical phase 3 study, LTSL were injected systemically to patients with unresectable hepatocellular carcinoma, and local release was induced by heating via RFA (Tak et al., 2018). An initial analysis did not find differences for overall or progression-free survival between patients treated with RFA and placebo, or with RFA and LTSL in combination. However, the original treatment protocol did not specify the exact duration of RFA treatment. When the analysis was restricted to patients who underwent RFA for more than 45 min, a significant improvement in overall survival was found for the RFA + LTSL arm. Since this analysis was performed *post-hoc* for hypothesis generation, a follow-up prospective study was planned and performed (NCT02112656), but results have not yet been made available.

In a phase 1 study with 10 patients suffering from primary or secondary liver tumors, the stimulus for heating in order to release doxorubicin from LTSL was applied externally by high-intensity focused ultrasound (HIFU), without the need for invasive placement of a probe, although the first part of the

study employed an implanted thermosensor to allow tuning of the ultrasound parameters to appropriate levels (Lyon et al., 2018). Biopsies of tumor tissue were taken after infusion of LTSL, and again after application of the ultrasound pulse. After application of ultrasound, doxorubicin levels were on average 3.3 times higher than before, and doxorubicin fluorescence co-localized with the nucleus in tissue sections of the HIFU-treated biopsies. Tumor sizes were monitored by PET-CT after the intervention. In some patients, tumors which had not been targeted by HIFU were visible on the same imaging plane as targeted tumors. Crucially, the targeted lesions shrank more substantially compared to the untargeted lesions, demonstrating the efficiency of the stimulation approach in a clinical setting with visible benefits.

4. TARGETING

For cancer nanomedicine, directing severely toxic drugs to their site of action is a goal of utmost importance. Partially, this is achievable as a consequence of the EPR effect, however, as outlined above, relying exclusively on this phenomenon may be insufficient, and more advanced approaches are under investigation.

Employing magnetism to influence suitably responsive particles carries great potential for non-invasive interventions (Prijic and Sersa, 2011; Tietze et al., 2015). Of these, mainly superparamagnetic iron oxide nanoparticles (SPIONs) are investigated for diagnostic or therapeutic purposes, for instance as contrast agents for magnetic resonance imaging or to induce local heating for hyperthermic ablation of tumor cells or other thermoresponsive systems. Additionally, their unique properties allow them to be locally targeted by the application of an external magnetic field. After promising preclinical results, this magnetic drug targeting had entered clinical trials for hepatocellular carcinoma in the form of MTC-Dox (magnetically targeted carriers with doxorubicin), particles of about 0.5–5 μm in size (hence not strictly meeting classification as nanoparticles) and composed of iron and carbon to which doxorubicin was adsorbed passively (Rudge et al., 2001). However, a therapeutic trial was terminated due to not achieving preset endpoints (NCT00034333). Notably, to prevent clearance and systemic distribution, these studies involved administration of the particles via an intraarterial catheter of the tumor-feeding artery, where extravasation was then induced by placing a magnet above the abdominal wall.

Magnetic targeting continues to be explored for its potential to achieve high local drug loads. For instance, a study with rabbits found over 50% of the applied drug load in the tumor tissue after intraarterial administration and magnetic targeting of 200 nm lauric acid coated SPIONs loaded with mitoxantrone to a superficial tumor grafted in the hind legs (Tietze et al., 2013). Al-Jamal et al. used PEGylated (thus longer circulating) nanoparticles with oil cores and varying amounts of incorporated SPIONs to quantitatively study magnetic particle targeting after intravenous injection (Al-Jamal et al., 2016). Extrapolating their mathematical model from murine data to potential human use, they suggest magnetic targeting under their conditions to be sufficient to achieve targeting in clinical practice.

A hitherto unsolved challenge is the magnetic targeting of deep tissues, due to issues with focusing magnetic fields and rapidly decaying magnetic field strength with distance (Shapiro et al., 2015). As such, the majority of studies conducted so far have focused on superficial tumors, which are easily reached by placing a magnet adjacent to the lesion.

One more dimension is added by kinetic targeting, which takes exploitation of the EPR effect a step further: In a pilot study involving 12 breast cancer patients and 3 ovarian cancer patients receiving PEGylated liposomal doxorubicin (PLD), extracorporeal plasmapheresis was applied 42–48 h after PLD treatment to remove residual circulating liposomes (Eckes et al., 2011). The treatment substantially reduced the doxorubicin plasma AUC by 50% and helped to alleviate undesirable side effects, such as palmar-plantar erythrodysesthesia (PPE, or hand-foot syndrome). PPE is a typical adverse reaction to PLD due to its pharmacokinetic profile, which allows accumulation of the drug in the skin especially of the hands and feet, where lesions can occur, but this accumulation is slower in skin compared to tumors (Charrois and Allen, 2003). PPE can be dose-limiting in some instances. During a total of 57 cycles of PLD and plasmapheresis, PPE occurred only in a single patient, whereas previous comparable trials without plasmapheresis reported occurrence in a total of 8/33 patients. No occurrence of grade IV neutropenia was reported (previous studies: 8/33). These data suggest an improvement of the toxicological profile of PLD and possibly other nanosized drug formulations by reducing systemic exposure to these agents via plasmapheresis. The response rate to the treatment appeared to be comparable to previously conducted studies, but in this pilot study, no comparative arm without plasmapheresis was included.

In addition to the approaches described here, which aim at improving the accumulation of particles in the tumor *tissue*, the next step is to target particles to individual tumor *cells* to improve uptake and cargo delivery.

4.1. Targeting Nanocarriers to Cancer Cells

Achieving cell-specific delivery is pursued by grafting targeting molecules onto the surface of nanoparticles. Many different monoclonal antibodies binding to cell surface molecules upregulated on cancer cells are now in clinical use, and similar approaches have been exploited for use in nanomedicine. MM-302 was briefly described above: It is a PEGylated liposomal formulation of doxorubicin to which a single chain variable fragment (scFv) against HER2 is bound via PEG as a spacer (Miller et al., 2016). ScFvs are synthetic proteins of the variable regions of an antibody molecule connected by a short peptide linker. Importantly, they lack the Fc region which interacts with Fc receptors of many immune cell populations, and only harbor the targeting activity. Other targeting ligands also exploit the overexpression of cancer antigens, such as the folate receptor (folic acid conjugated particles, e.g., Lu et al., 2012; Tang et al., 2018) or the transferrin receptor (transferrin conjugated particles, e.g., Sarisozen et al., 2014; Wei et al., 2019). Transferrin is also under investigation as a ligand to

induce transcytosis across the blood brain barrier, thus enabling cerebral delivery of nanotherapeutics (Ulbrich et al., 2009; Wiley et al., 2013; Clark and Davis, 2015). Furthermore, interaction between complementary DNA strands on liposomes and target cells were shown to improve delivery of the nanoparticles (Li et al., 2019), and grafting single-stranded DNA to antibodies facilitated their intracellular delivery in a sequence-independent fashion (Herrmann et al., 2019).

Alternatively, grafting complete cancer cell membrane fractions onto nanoparticles to allow homotypic interaction with the tumor cells by virtue of their adhesion molecules may be possible (Fang et al., 2014). This might enable more strictly personalized targeting, however, since a membrane source is required for such an approach, it would likely be reserved for accessible tumors in order to allow gathering sufficient material.

Although many preclinical studies report tremendously encouraging results using targeted nanoparticles, existing data also suggests heterogeneous efficacy of ligand-mediated targeting, where the targeting ligand was capable of improving cellular uptake and altering the uptake pathway (Pirollo and Chang, 2008; Clemons et al., 2018). However, localization of the particle to the tumor tissue was not necessarily improved, depending on particle size and the presence of PEG, with PEG potentially masking accumulation effects because of exploitation of the EPR effect (Pirollo and Chang, 2008; Choi et al., 2010). Moreover, caution should be exercised when extrapolating from *in vitro* to *in vivo* data, since the establishment of a biocorona can substantially impact targeting abilities (Salvati et al., 2013; Francia et al., 2019). The abrogation of targeting by serum protein binding can be alleviated by additionally grafting PEG, which is of lower molecular weight or length used to conjugate the targeting ligand to the particle surface. The polymer may then help to reduce fouling while not sterically hindering binding to the target molecule (Dai et al., 2014).

More recently, by using very small HER2-functionalized silica nanoparticles (∼7 nm), tumor targeting efficiencies of 10.3–17.2% ID/g were achieved in murine xenografts of HER2-positive BT-474 tumors, compared to 3.3–6.1% ID/g for HER2-negative tumors or untargeted particles (Chen et al., 2018). However, their fate after accumulation in the tumor was not further followed.

To address this question, Dai et al. quantitatively investigated the effects of active targeting (Dai et al., 2018). Using gold nanoparticles conjugated to trastuzumab (a monoclonal antibody against HER2), they used different particle sizes and tumor models to measure particle distribution in tumor tissue. For an ovarian SKOV-3 cancer model, xenografted subcutaneously to murine hosts, 0.59% of the injected targeted particle dose reached the tumor, whereas this amounted to 0.25% of untargeted particles. These values were in line with a previous meta-analysis of preclinical models published by the group earlier, where the median accumulation of actively targeted particles was 0.9% ID, versus 0.6% ID for passively targeted particles (Wilhelm et al., 2016). Strikingly, they found that even for particles that reached the tumor site, these were much more likely to be stuck in the acellular matrix (typically over 90% of all particles) of the tumor, or to be engulfed by tumor-associated macrophages (TAMs), than to be taken up by cancer cells. Furthermore, the difference in the fraction of particles taken up by cancer cells was not statistically significant between targeted and untargeted nanoparticles (0.001 vs. 0.003% ID for targeted and untargeted, respectively), and neither was the difference in the fraction of tumor cells that engulfed particles (0.96 vs. 0.42% for targeted and untargeted, respectively). These results were corroborated by follow-up experiments using other tumor models. When nanoparticles which were targeted to folate instead of HER2 were investigated, TAMs still dominantly engulfed nanoparticles. The authors suggest that this observation is in line with the perivascular localization of TAMs, making them more likely to first capture incoming nanoparticles, thus acting as a filter before malignant cells have an opportunity for interaction.

Moreover, targeting may not always be favorable, depending on the carrier: When small polymeric nanoparticles (10 nm) were actively targeted to tumor endothelium by grafting of RGD- or NGR-peptides, they were found to accumulate much more strongly in the tumor tissue than their non-targeted counter parts at early time points, up to 4 h after injection, before the EPR effect became significant. However, for later time points (24–72 h), this trend was reversed, and the passively targeted carriers actually accumulated to a higher degree over time (Kunjachan et al., 2014). In this instance, the targeted carriers were also more likely to be found at off-target sites.

Since targeting moieties attached to a nanoparticle's surface typically induce receptor-mediated endocytosis, the next stage of the journey is the cellular vesicular system.

4.2. Escaping the Endosome and the Vesicular System

In Kafka's novel "The Trial," the protagonist Josef K. is accused of committing an elusive crime, and subsequently desperately tries to navigate the intangible and confusing labyrinth of a convoluted court without ever reaching the higher tiers. It is a fate not quite unlike that of a nanocarrier, which, after finally reaching its target cell, has still not arrived at its ultimate goal.

Intact nanoparticles are principally believed to enter cells via the endocytic pathway, i.e., by attachment to the cell surface and subsequent incorporation into an intracellularly trafficked vesicle (Sahay et al., 2010; Zhang et al., 2015) (**Figure 4**). Roughly, endocytosis is divisible into two main branches (Dobrovolskaia and McNeil, 2007; Doherty and McMahon, 2009): Phagocytosis, which is the uptake of large particles or pathogens by specialized immune cells, and pinocytosis, which is the uptake of smaller particles and includes macropinocytosis and clathrin- or caveolin-dependent endocytosis.

Nanoparticle uptake depends on the dynamics of endocytosis, and on the dynamics of the attachment of particles to the cell surface. When nanoparticle uptake was investigated in two human cell lines using 8 nm quantum dots, the average number of nanoparticles found in a single endosome remained relatively constant with increasing concentration, however, the number of particle-containing endosomes was positively correlated with dose, at least in the range of doses and exposure times investigated (0.5–5 nM, and 0.5–2 h, respectively) (Rees et al., 2019).

Membrane scission of budding endocytic vesicle is typically induced by a family of dynamin GTPases. The primary vesicles then continue to fuse with early endosomes, which are the primary sorting station of the endosomal system and bear the potential to exclude a large fraction of incoming cargo by rerouting them toward exocytosis (Huotari and Helenius, 2011). Early endosomes mature to become late endosomes, with a concomitant drop in pH by the action of V-type ATPases, and eventually fuse with lysosomes, forming endolysosomes where enzymatic degradation of a variety of cargoes, such as nucleic acids, lipids and proteins occurs. The importance of these routes varies for different nanoparticle formulations: Stimulus-responsive systems which culminate in release of the free drug molecules at the disease site do not require endosomal escape, if the drug can diffuse across membrane barriers. However, for example for delivery of siRNA or DNA, the carrier has to be engulfed whole and needs a way to deliver its payload to the cytosol to prevent lysosomal degradation.

As briefly mentioned above, a large fraction of incoming cargo never proceeds very far into the endosomal system. For instance, for lipid nanoparticles (LNPs) intended for the delivery of siRNA, it was found that they entered cells via macropinocytosis, but about 70% of them were recycled and exocytosed by a mechanism involving the Niemann-Pick type C1 (NPC1) protein, which is a protein linked to a form of lysosomal storage disease (Sahay et al., 2013). Another study underscores that endosomal escape is an inefficient process: When siRNA-carrying lipid nanoparticles were traced, <2% were successful in reaching the cytosol (Gilleron et al., 2013).

Delivery of nucleic acids is often achieved by utilizing cationic polymers or lipids, such as poly(ethylene imine), which form complexes with the negatively charged phosphate backbone. The resulting polyplexes are believed to escape the endosome by exerting a "proton sponge" effect, in which the basic polymers buffer the proton influx during the acidification process, leading to a subsequent influx of chloride ions with a consequent endosomal swelling and rupture. However, this proposed mechanism is not undisputed and destabilization of the vesicular membrane by interaction with the polymer was proposed to induce endosomal leakage (Bus et al., 2018; Vermeulen et al., 2018).

Cationic lipid-based vesicles were more prone to aggregate in serum compared to their neutral counterparts, resulting in reduced tumor penetration and toxic side effects (Fischer et al., 2003; Zhao et al., 2011). Many approaches have been pursued to upgrade other materials with the capacity to effectively penetrate the endosome by swelling, membrane disruption, or potentially the proton sponge effect (Cupic et al., 2018; Smith et al., 2019). Many of these strategies rely on disruption of membrane integrity when the pH is lowered below physiological levels of the extracellular space, which might be hampered in the case of cancer nanomedicine due to the aforementioned lowered extracellular pH.

Even after successful endosomal escape, autophagy may pose a potential additional barrier. Autophagy (or, more precisely, macroautophagy, to distinguish this process from other forms of autophagy) is a cellular self-digestion mechanism which is induced upon starvation conditions to mobilize carbohydrates, lipids and proteins, but also contributes to the removal of damaged organelles (Levine et al., 2011). It involves the generation of a double isolation membrane (the phagophore) which encloses putative cargo and seals to form the autophagosome, which then fuses with lysosomes. In the resulting autolysosome, the vesicular contents are degraded. Cationic gene delivery polyplexes and liposomes were shown to be captured in autophagosomes, and in cells deficient for *atg5* (an essential regulator of autophagy), gene delivery was increased by a factor of eight (Roberts et al., 2013). Nanoparticles could also be captured by autophagosomes when they entered the cells via microinjection, bypassing the endosomal system, which suggests that once-escaped carriers may be removed from the cytosol again, limiting their time to perform a biological function (Remaut et al., 2014). Inhibition of autophagy by chloroquine was also reported to result in slower tumor growth of docetaxel-loaded PLGA nanocarriers (Zhang et al., 2014). However, because autophagy inhibitors are also investigated as cancer therapeutics (Kimura et al., 2013), it is unclear whether this was a result of a synergistic effect between the compounds leading to more efficient retention of the nanocarriers, or simply an enhancement by employing combination therapy. On the other hand, no major influence of *atg5* on knockdown efficiency was seen in a study involving LNPs and siRNA (Sahay et al., 2013).

4.3. Entering the Nucleus

Contrary to siRNA or mRNA, which can perform their function in the cytosol, DNA has to enter the nucleus to be transcribed. For the delivery of DNA, there are currently no approved non-viral vectors available, although clinical trials are in progress and intense research is underway, because synthetic alternatives promise advantages, such as reduced immunogenicity and oncogenic potential, as well as increased packaging capacity (Yin et al., 2014). Delivery of coding DNA is an attractive prospect for the generation of therapeutic proteins, such as monoclonal antibodies in the body of the patient, thus minimizing the tremendous costs associated with formulation, production, quality control and repeated administration of protein drugs (Deal and Balazs, 2015). For this purpose, intramuscular injections can be employed. Here, the physical availability of the target site allows efficient transfection by electroporation, but this is not possible for tumors or internal organs, such as the liver (Hollevoet and Declerck, 2017). For gene delivery into dividing cells, the DNA has the chance of entering the nucleus when the nuclear envelope is fragmented for mitosis. For post-mitotic cells, this is not an option. Furthermore, the passive diffusion of intact nanoparticles within the cytosol is minimal, as revealed by single-particle tracking (Remaut et al., 2014).

When the mechanism of DNA delivery by polyamine-containing agents was investigated, contributions of nuclear envelope permeabilization (consistent with their proposed action of endosomal permeabilization) and microtubule-directed transport were found, as well as dependency on cytosolic factors (Grandinetti and Reineke, 2012).

Apart from gene therapy approaches, other medications might also benefit from nuclear localization, such as anthracyclines,

which exert their effects in the nucleus. The nuclear envelope is interspersed with nuclear pore complexes. They allow passive transport by diffusion of small molecules, but macromolecules require an active mechanism to be translocated because strings of phenylalanine- and glycine-rich repeats block the pores (Strambio-De-Castillia et al., 2010). For endogenous proteins, this is achieved by a nuclear localization sequence (NLS) which engages the importing machinery. In the realm of nanoparticles, gold nanoparticles of ∼25 or 30 nm were modified with an NLS peptide to target them to the nucleus. Utilizing confocal microscopy, the particles were either found within the nucleus (Kang et al., 2010), or in the perinuclear region (Ali et al., 2017). Even such a perinuclear localization, however, would probably be quite efficient because it minimizes the necessary diffusion length of the cargo. With chitosan nanoparticles, heterogeneities in nuclear targeting deliveries were revealed: small particles of 25 nm entered the nucleus without the aid of an NLS. In non-malignant cell lines, 150 nm particles modified with low densities of NLS were more efficient at localizing nuclearly, whereas in a glioma cell line, this was most efficient for unmodified NPs, due to dysregulation of the nuclear import pathway (Tammam et al., 2017).

For nanoparticles, other approaches were also investigated, relying for instance on the HIV-derived Tat peptide which mediates nuclear import differently than the typical NLS-dependent mechanism and can deliver nanoparticles up to 90 nm into the nucleus (de la Fuente and Berry, 2005; Nitin et al., 2009). Functionalization of silica nanoparticles with the Tat peptide enabled them to enter the nucleus, whereas particles without Tat did not cross the nuclear envelope (Pan et al., 2013). Alternatively, modification of gold nanostars with the nucleolin-binding DNA aptamer AS1411 led to nuclear entry and morphological alterations of the nuclear envelope (Dam et al., 2012).

Finally, attempts at subcellular targeting are not limited to the nuclear compartment: Instead, approaches were developed, for example for targeting mitochondria, the endoplasmic reticulum or lysosomes, to deliver cargo precisely to its site of action (Jhaveri and Torchilin, 2016; Ma et al., 2016).

5. CONCLUSIONS

A principal attribute when discussing nanomedicine, emerging again and again at all levels and stages, is "heterogeneity." As such, precisely delivering a nanotherapeutic agent exactly to where it needs to be to exert its maximal efficacy is a monumentally challenging and complex task, requiring the collaborative expertise from many different disciplines, including medicine, biology, chemistry, physics, the materials sciences, and engineering. Numerous barriers must be overcome before a cargo is finally delivered. Considerable progress has been made, but we are not quite there yet. Although there are strategies in place for tackling barriers during individual stages of this process, an integrated approach will require new and ingenious solutions to advance the field of nanomedicine beyond its current state. Current formulations often profoundly improve the toxicity profile of a drug, but do not substantially increase overall survival of a patient population (Petersen et al., 2016). Doxil, for instance, dramatically reduced the cumulative cardiotoxicity compared to free doxorubicin, whereas treatment efficacy was comparable between both groups in the treatment of metastatic breast cancer (Safra et al., 2000; O'Brien et al., 2004). To have a chance of entering clinical trials and becoming reliable tools, nanomedicines must be capable of overcoming the astounding complexity of their sites of action and the plethora of challenges these impose. At the same time, they must be sufficiently simple in their formulation and design to allow large-scale production. Unifying these opposing requirements will be difficult, but allow strides toward the advancement of science and medicine.

AUTHOR CONTRIBUTIONS

OT wrote the manuscript and prepared the figures. WW supervised the work, critically discussed the literature, and edited the manuscript.

FUNDING

This study was supported in part by the Excellence Initiative of the German Research Foundation (GSC-4, Spemann Graduate School, BIOSS—EXC-294, and CIBSS—EXC-2189, Project ID 390939984).

ACKNOWLEDGMENTS

The authors would like to thank Maximilian Hörner, Ivo Schirmeister, and Hanna Wagner for productive discussions and helpful feedback.

REFERENCES

Abu Lila, A. S., Kiwada, H., and Ishida, T. (2013). The accelerated blood clearance (ABC) phenomenon: clinical challenge and approaches to manage. *J. Control. Release* 172, 38–47. doi: 10.1016/j.jconrel.2013.07.026

Ali, M. R. K., Wu, Y., Ghosh, D., Do, B. H., Chen, K., Dawson, M. R., et al. (2017). Nuclear Membrane-targeted gold nanoparticles inhibit cancer cell migration and invasion. *ACS Nano* 11, 3716–3726. doi: 10.1021/acsnano.6b08345

Alizadeh, A. A., Aranda, V., Bardelli, A., Blanpain, C., Bock, C., Borowski, C., et al. (2015). Toward understanding and exploiting tumor heterogeneity. *Nat. Med.* 21, 846–853. doi: 10.1038/nm.3915

Al-Jamal, K. T., Bai, J., Wang, J. T.-W., Protti, A., Southern, P., Bogart, L., et al. (2016). Magnetic drug targeting: preclinical *in vivo* studies, mathematical modeling, and extrapolation to humans. *Nano Lett.* 16, 5652–5660. doi: 10.1021/acs.nanolett.6b02261

Anselmo, A. C., and Mitragotri, S. (2016). Nanoparticles in the clinic. *Bioeng. Transl. Med.* 1, 10–29. doi: 10.1002/btm2.10003

Anselmo, A. C., and Mitragotri, S. (2019). Nanoparticles in the clinic: an update. *Bioeng. Transl. Med.* 4:e10143. doi: 10.1002/btm2.10143

Armstrong, J. K., Hempel, G., Koling, S., Chan, L. S., Fisher, T., Meiselman, H. J., et al. (2007). Antibody against poly(ethylene glycol) adversely affects PEG-asparaginase therapy in acute lymphoblastic leukemia patients. *Cancer* 110, 103–111. doi: 10.1002/cncr.22739

Armulik, A., Abramsson, A., and Betsholtz, C. (2005). Endothelial/pericyte interactions. *Circ. Res.* 97, 512–523. doi: 10.1161/01.RES.0000182903.16652.d7

Attwell, D., Mishra, A., Hall, C. N., O'Farrell, F. M., and Dalkara, T. (2016). What is a pericyte? *J. Cereb. Blood Flow Metab.* 36, 451–455. doi: 10.1177/0271678X15610340

Azzi, S., Hebda, J. K., and Gavard, J. (2013). Vascular permeability and drug delivery in cancers. *Front. Oncol.* 3:211. doi: 10.3389/fonc.2013.00211

Bachmann, M. F., and Zinkernagel, R. M. (1996). The influence of virus structure on antibody responses and virus serotype formation. *Immunol. Today* 17, 553–558. doi: 10.1016/s0167-5699(96)10066-9

Baluk, P., Morikawa, S., Haskell, A., Mancuso, M., and McDonald, D. M. (2003). Abnormalities of basement membrane on blood vessels and endothelial sprouts in tumors. *Am. J. Pathol.* 163, 1801–1815. doi: 10.1016/S0002-9440(10)63540-7

Bangham, A. D., Standish, M. M., and Watkins, J. C. (1965). Diffusion of univalent ions across the lamellae of swollen phospholipids. *J. Mol. Biol.* 13, 238–252.

Barenholz, Y. (2012). Doxil® — the first FDA-approved nano-drug: lessons learned. *J. Control. Release* 160, 117–134. doi: 10.1016/j.jconrel.2012.03.020

Bendele, A., Seely, J., Richey, C., Sennello, G., and Shopp, G. (1998). Short communication: renal tubular vacuolation in animals treated with polyethylene-glycol-conjugated proteins. *Toxicol. Sci.* 42, 152–157.

Blanco, E., Shen, H., and Ferrari, M. (2015). Principles of nanoparticle design for overcoming biological barriers to drug delivery. *Nat. Biotechnol.* 33, 941–951. doi: 10.1038/nbt.3330

Bogart, L. K., Pourroy, G., Murphy, C. J., Puntes, V., Pellegrino, T., Rosenblum, D., et al. (2014). Nanoparticles for imaging, sensing, and therapeutic intervention. *ACS Nano* 8, 3107–3122. doi: 10.1021/nn500962q

Bolze, F., Morath, V., Bast, A., Rink, N., Schlapschy, M., Mocek, S., et al. (2016). Long-acting PASylated leptin ameliorates obesity by promoting satiety and preventing hypometabolism in leptin-deficient Lep(ob/ob) mice. *Endocrinology* 157, 233–244. doi: 10.1210/en.2015-1519

Breibeck, J., and Skerra, A. (2018). The polypeptide biophysics of proline/alanine-rich sequences (PAS): recombinant biopolymers with PEG-like properties. *Biopolymers* 109:e23069. doi: 10.1002/bip.23069

Brown, E. J., and Frazier, W. A. (2001). Integrin-associated protein (CD47) and its ligands. *Trends Cell Biol.* 11, 130–135. doi: 10.1016/S0962-8924(00)01906-1

Bulbake, U., Doppalapudi, S., Kommineni, N., and Khan, W. (2017). Liposomal formulations in clinical use: an updated review. *Pharmaceutics* 9:E12. doi: 10.3390/pharmaceutics9020012

Bus, T., Traeger, A., and Schubert, U. S. (2018). The great escape: how cationic polyplexes overcome the endosomal barrier. *J. Mater. Chem. B.* 6, 6904–6918. doi: 10.1039/C8TB00967H

Cabral, H., Makino, J., Matsumoto, Y., Mi, P., Wu, H., Nomoto, T., et al. (2015). Systemic targeting of lymph node metastasis through the blood vascular system by using size-controlled nanocarriers. *ACS Nano* 9, 4957–4967. doi: 10.1021/nn5070259

Cabral, H., Matsumoto, Y., Mizuno, K., Chen, Q., Murakami, M., Kimura, M., et al. (2011). Accumulation of sub-100 nm polymeric micelles in poorly permeable tumours depends on size. *Nat. Nanotechnol.* 6, 815–823. doi: 10.1038/nnano.2011.166

Chanan-Khan, A., Szebeni, J., Savay, S., Liebes, L., Rafique, N. M., Alving, C. R., et al. (2003). Complement activation following first exposure to pegylated liposomal doxorubicin (Doxil®): possible role in hypersensitivity reactions. *Ann. Oncol.* 14, 1430–1437. doi: 10.1093/annonc/mdg374

Charrois, G. J. R., and Allen, T. M. (2003). Multiple injections of pegylated liposomal doxorubicin: pharmacokinetics and therapeutic activity. *J. Pharmacol. Exp. Ther.* 306, 1058–1067. doi: 10.1124/jpet.103.053413

Chauhan, V. P., Stylianopoulos, T., Boucher, Y., and Jain, R. K. (2011). Delivery of molecular and nanoscale medicine to tumors: transport barriers and strategies. *Annu. Rev. Chem. Biomol. Eng.* 2, 281–298. doi: 10.1146/annurev-chembioeng-061010-114300

Chauhan, V. P., Stylianopoulos, T., Martin, J. D., Popović, Z., Chen, O., Kamoun, W. S., et al. (2012). Normalization of tumour blood vessels improves the delivery of nanomedicines in a size-dependent manner. *Nat. Nanotechnol.* 7, 383–388. doi: 10.1038/nnano.2012.45

Chen, F., Ma, K., Madajewski, B., Zhuang, L., Zhang, L., Rickert, K., et al. (2018). Ultrasmall targeted nanoparticles with engineered antibody fragments for imaging detection of HER2-overexpressing breast cancer. *Nat. Commun.* 9, 1–11. doi: 10.1038/s41467-018-06271-5

Cho, K., Wang, X., Nie, S., Chen, Z. G., and Shin, D. M. (2008). Therapeutic nanoparticles for drug delivery in cancer. *Clin. Cancer Res.* 14, 1310–1316. doi: 10.1158/1078-0432.CCR-07-1441

Choi, C. H. J., Alabi, C. A., Webster, P., and Davis, M. E. (2010). Mechanism of active targeting in solid tumors with transferrin-containing gold nanoparticles. *Proc. Natl. Acad. Sci. U.S.A.* 107, 1235–1240. doi: 10.1073/pnas.0914140107

Clark, A. J., and Davis, M. E. (2015). Increased brain uptake of targeted nanoparticles by adding an acid-cleavable linkage between transferrin and the nanoparticle core. *Proc. Natl. Acad. Sci. U.S.A.* 112, 12486–12491. doi: 10.1073/pnas.1517048112

Clemons, T. D., Singh, R., Sorolla, A., Chaudhari, N., Hubbard, A., and Iyer, K. S. (2018). Distinction between active and passive targeting of nanoparticles dictate their overall therapeutic efficacy. *Langmuir* 34, 15343–15349. doi: 10.1021/acs.langmuir.8b02946

Cooley, T., Henry, D., Tonda, M., Sun, S., O'Connell, M., and Rackoff, W. (2007). A randomized, double-blind study of pegylated liposomal doxorubicin for the treatment of AIDS-related Kaposi's sarcoma. *Oncologist* 12, 114–123. doi: 10.1634/theoncologist.12-1-114

Coussens, L. M., Zitvogel, L., and Palucka, A. K. (2013). Neutralizing tumor-promoting chronic inflammation: a magic bullet? *Science* 339, 286–291. doi: 10.1126/science.1232227

Cupic, K. I., Rennick, J. J., Johnston, A. P., and Such, G. K. (2018). Controlling endosomal escape using nanoparticle composition: current progress and future perspectives. *Nanomedicine* 14, 215–223. doi: 10.2217/nnm-2018-0326

Dai, Q., Walkey, C., and Chan, W. C. W. (2014). Polyethylene glycol backfilling mitigates the negative impact of the protein corona on nanoparticle cell targeting. *Angew. Chemie Int. Ed.* 53, 5093–5096. doi: 10.1002/anie.201309464

Dai, Q., Wilhelm, S., Ding, D., Syed, A. M., Sindhwani, S., Zhang, Y., et al. (2018). Quantifying the ligand-coated nanoparticle delivery to cancer cells in solid tumors. *ACS Nano* 12, 8423–8435. doi: 10.1021/acsnano.8b03900

Dam, D. H. M., Lee, J. H., Sisco, P. N., Co, D. T., Zhang, M., Wasielewski, M. R., et al. (2012). Direct observation of nanoparticle–cancer cell nucleus interactions. *ACS Nano* 6, 3318–3326. doi: 10.1021/nn300296p

Danhier, F. (2016). To exploit the tumor microenvironment: since the EPR effect fails in the clinic, what is the future of nanomedicine? *J. Control. Release* 244, 108–121. doi: 10.1016/j.jconrel.2016.11.015

Davis, M. E., Chen, Z. G., and Shin, D. M. (2008). Nanoparticle therapeutics: an emerging treatment modality for cancer. *Nat. Rev. Drug Discov.* 7, 771–782. doi: 10.1038/nrd2614

de la Fuente, J. M., and Berry, C. C. (2005). Tat peptide as an efficient molecule to translocate gold nanoparticles into the cell nucleus. *Bioconj. Chem.* 16, 1176–1180. doi: 10.1021/bc050033+

Deal, C. E., and Balazs, A. B. (2015). Engineering humoral immunity as prophylaxis or therapy. *Curr. Opin. Immunol.* 35, 113–122. doi: 10.1016/j.coi.2015.06.014

Dobrovolskaia, M. A., and McNeil, S. E. (2007). Immunological properties of engineered nanomaterials. *Nat. Nanotechnol.* 2, 469–478. doi: 10.1038/nnano.2007.223

Doherty, G. J., and McMahon, H. T. (2009). Mechanisms of endocytosis. *Ann. Rev. Biochem.* 78, 857–902. doi: 10.1146/annurev.biochem.78.081307.110540

Dominska, M., and Dykxhoorn, D. M. (2010). Breaking down the barriers: siRNA delivery and endosome escape. *J. Cell. Sci.* 123, 1183–1189. doi: 10.1242/jcs.066399

Dvorak, H. F. (2003). How tumors make bad blood vessels and stroma. *Am. J. Pathol.* 162, 1747–1757. doi: 10.1016/S0002-9440(10)64309-X

Eales, K. L., Hollinshead, K. E. R., and Tennant, D. A. (2016). Hypoxia and metabolic adaptation of cancer cells. *Oncogenesis* 5:e190. doi: 10.1038/oncsis.2015.50

Eckes, J., Schmah, O., Siebers, J. W., Groh, U., Zschiedrich, S., Rautenberg, B., et al. (2011). Kinetic targeting of pegylated liposomal doxorubicin: a new approach to reduce toxicity during chemotherapy (CARL-trial). *BMC Cancer* 11:337. doi: 10.1186/1471-2407-11-337

El-Sawy, H. S., Al-Abd, A. M., Ahmed, T. A., El-Say, K. M., and Torchilin, V. P. (2018). Stimuli-responsive nano-architecture drug-delivery systems to solid tumor micromilieu: past, present, and future perspectives. *ACS Nano* 12, 10636–10664. doi: 10.1021/acsnano.8b06104

Falvo, E., Tremante, E., Arcovito, A., Papi, M., Elad, N., Boffi, A., et al. (2016). Improved doxorubicin encapsulation and pharmacokinetics of

ferritin–fusion protein nanocarriers bearing proline, serine, and alanine elements. *Biomacromolecules* 17, 514–522. doi: 10.1021/acs.biomac.5b01446

Fang, J., Nakamura, H., and Maeda, H. (2011). The EPR effect: unique features of tumor blood vessels for drug delivery, factors involved, and limitations and augmentation of the effect. *Adv. Drug Deliv. Rev.* 63, 136–151. doi: 10.1016/j.addr.2010.04.009

Fang, J. S., Gillies, R. D., and Gatenby, R. A. (2008). Adaptation to hypoxia and acidosis in carcinogenesis and tumor progression. *Semin. Cancer Biol.* 18, 330–337. doi: 10.1016/j.semcancer.2008.03.011

Fang, R. H., Hu, C.-M. J., Luk, B. T., Gao, W., Copp, J. A., Tai, Y., et al. (2014). Cancer cell membrane-coated nanoparticles for anticancer vaccination and drug delivery. *Nano Lett.* 14, 2181–2188. doi: 10.1021/nl500618u

Fischer, D., Li, Y., Ahlemeyer, B., Krieglstein, J., and Kissel, T. (2003). *In vitro* cytotoxicity testing of polycations: influence of polymer structure on cell viability and hemolysis. *Biomaterials* 24, 1121–1131. doi: 10.1016/S0142-9612(02)00445-3

Francia, V., Yang, K., Deville, S., Reker-Smit, C., Nelissen, I., and Salvati, A. (2019). Corona composition can affect the mechanisms cells use to internalize nanoparticles. *ACS Nano* 13, 11107–21. doi: 10.1021/acsnano.9b03824

Garay, R. P., El-Gewely, R., Armstrong, J. K., Garratty, G., and Richette, P. (2012). Antibodies against polyethylene glycol in healthy subjects and in patients treated with PEG-conjugated agents. *Expert Opin. Drug. Deliv.* 9, 1319–1323. doi: 10.1517/17425247.2012.720969

Gerlowski, L. E., and Jain, R. K. (1986). Microvascular permeability of normal and neoplastic tissues. *Microvasc. Res.* 31, 288–305.

Gilleron, J., Querbes, W., Zeigerer, A., Borodovsky, A., Marsico, G., Schubert, U., et al. (2013). Image-based analysis of lipid nanoparticle–mediated siRNA delivery, intracellular trafficking and endosomal escape. *Nat. Biotechnol.* 31, 638–646. doi: 10.1038/nbt.2612

Giulimondi, F., Digiacomo, L., Pozzi, D., Palchetti, S., Vulpis, E., Capriotti, A. L., et al. (2019). Interplay of protein corona and immune cells controls blood residency of liposomes. *Nat. Comm.* 10, 1–11. doi: 10.1038/s41467-019-11642-7

Grandinetti, G., and Reineke, T. M. (2012). Exploring the mechanism of plasmid DNA nuclear internalization with polymer-based vehicles. *Mol. Pharm.* 9, 2256–2267. doi: 10.1021/mp300142d

Gref, R., Lück, M., Quellec, P., Marchand, M., Dellacherie, E., Harnisch, S., et al. (2000). 'Stealth' corona-core nanoparticles surface modified by polyethylene glycol (PEG): influences of the corona (PEG chain length and surface density) and of the core composition on phagocytic uptake and plasma protein adsorption. *Colloids Surf. B* 18, 301–313. doi: 10.1016/S0927-7765(99)00156-3

Griffith, D. E., Eagle, G., Thomson, R., Aksamit, T. R., Hasegawa, N., Morimoto, K., et al. (2018). Amikacin liposome inhalation suspension for treatment-refractory lung disease caused by *Mycobacterium avium* complex (CONVERT). A prospective, open-label, randomized study. *Am. J. Respir. Crit. Care Med.* 198, 1559–1569. doi: 10.1164/rccm.201807-1318OC

Hagendoorn, J., Tong, R., Fukumura, D., Lin, Q., Lobo, J., Padera, T. P., et al. (2006). Onset of abnormal blood and lymphatic vessel function and interstitial hypertension in early stages of carcinogenesis. *Cancer Res.* 66, 3360–3364. doi: 10.1158/0008-5472.CAN-05-2655

Hanahan, D., and Weinberg, R. A. (2011). Hallmarks of cancer: the next generation. *Cell* 144, 646–674. doi: 10.1016/j.cell.2011.02.013

Hansen, A. E., Petersen, A. L., Henriksen, J. R., Boerresen, B., Rasmussen, P., Elema, D. R., et al. (2015). Positron emission tomography based elucidation of the enhanced permeability and retention effect in dogs with cancer using copper-64 liposomes. *ACS Nano* 9, 6985–6995. doi: 10.1021/acsnano.5b01324

Hara, E., Makino, A., Kurihara, K., Yamamoto, F., Ozeki, E., and Kimura, S. (2012). Pharmacokinetic change of nanoparticulate formulation "lactosome" on multiple administrations. *Int. Immunopharmacol.* 14, 261–266. doi: 10.1016/j.intimp.2012.07.011

Haran, G., Cohen, R., Bar, L. K., and Barenholz, Y. (1993). Transmembrane ammonium sulfate gradients in liposomes produce efficient and stable entrapment of amphipathic weak bases. *Biochim. Biophys. Acta* 1151, 201–215. doi: 10.1016/0005-2736(93)90105-9

Hashizume, H., Baluk, P., Morikawa, S., McLean, J. W., Thurston, G., Roberge, S., et al. (2000). Openings between defective endothelial cells explain tumor vessel leakiness. *Am. J. Pathol.* 156, 1363–1380. doi: 10.1016/S0002-9440(10)65006-7

Hatakeyama, H., Akita, H., and Harashima, H. (2011). A multifunctional envelope type nano device (MEND) for gene delivery to tumours based on the EPR effect: a strategy for overcoming the PEG dilemma. *Adv. Drug Deliv. Rev.* 63, 152–160. doi: 10.1016/j.addr.2010.09.001

Herrmann, A., Nagao, T., Zhang, C., Lahtz, C., Li, Y.-J., Yue, C., et al. (2019). An effective cell-penetrating antibody delivery platform. *JCI Insight* 4:e127474. doi: 10.1172/jci.insight.127474

Hobbs, S. K., Monsky, W. L., Yuan, F., Roberts, W. G., Griffith, L., Torchilin, V. P., et al. (1998). Regulation of transport pathways in tumor vessels: role of tumor type and microenvironment. *Proc. Natl. Acad. Sci. U.S.A.* 95, 4607–4612.

Hollevoet, K., and Declerck, P. J. (2017). State of play and clinical prospects of antibody gene transfer. *J. Transl. Med.* 15:131. doi: 10.1186/s12967-017-1234-4

Hu, C.-M. J., Fang, R. H., Luk, B. T., Chen, K. N. H., Carpenter, C., Gao, W., et al. (2013). 'Marker-of-self' functionalization of nanoscale particles through a top-down cellular membrane coating approach. *Nanoscale* 5, 2664–2668. doi: 10.1039/c3nr00015j

Hu, C.-M. J., Zhang, L., Aryal, S., Cheung, C., Fang, R. H., and Zhang, L. (2011). Erythrocyte membrane-camouflaged polymeric nanoparticles as a biomimetic delivery platform. *Proc. Natl. Acad. Sci. U.S.A.* 108, 10980–10985. doi: 10.1073/pnas.1106634108

Hu, Y., Hou, Y., Wang, H., and Lu, H. (2018). Polysarcosine as an alternative to PEG for therapeutic protein conjugation. *Bioconj. Chem.* 29, 2232–2238. doi: 10.1021/acs.bioconjchem.8b00237

Hughes, G. A. (2005). Nanostructure-mediated drug delivery. *Nanomed. Nanotechnol. Biol. Med.* 1, 22–30. doi: 10.1016/j.nano.2004.11.009

Huotari, J., and Helenius, A. (2011). Endosome maturation. *EMBO J.* 30, 3481–3500. doi: 10.1038/emboj.2011.286

Ishida, T., Ichihara, M., Wang, X., and Kiwada, H. (2006). Spleen plays an important role in the induction of accelerated blood clearance of PEGylated liposomes. *J. Control. Release* 115, 243–250. doi: 10.1016/j.jconrel.2006.08.001

Ishida, T., and Kiwada, H. (2008). Accelerated blood clearance (ABC) phenomenon upon repeated injection of PEGylated liposomes. *Int. J. Pharm.* 354, 56–62. doi: 10.1016/j.ijpharm.2007.11.005

Janssen Products (2019). *Doxil Prescribing Information*. Horsham, PA. Available online at: https://www.accessdata.fda.gov/drugsatfda_docs/label/2019/050718s055lbl.pdf

Jevševar, S., Kunstelj, M., and Porekar, V. G. (2010). PEGylation of therapeutic proteins. *Biotech. J.* 5, 113–128. doi: 10.1002/biot.200900218

Jhaveri, A., and Torchilin, V. (2016). Intracellular delivery of nanocarriers and targeting to subcellular organelles. *Expert Opin. Drug. Deliv.* 13, 49–70. doi: 10.1517/17425247.2015.1086745

Jiang, W., Huang, Y., An, Y., and Kim, B. Y. S. (2015). Remodeling tumor vasculature to enhance delivery of intermediate-sized nanoparticles. *ACS Nano* 9, 8689–8696. doi: 10.1021/acsnano.5b02028

Jin, Q., Deng, Y., Chen, X., and Ji, J. (2019). Rational design of cancer nanomedicine for simultaneous stealth surface and enhanced cellular uptake. *ACS Nano* 13, 954–977. doi: 10.1021/acsnano.8b07746

Jokerst, J. V., Lobovkina, T., Zare, R. N., and Gambhir, S. S. (2011). Nanoparticle PEGylation for imaging and therapy. *Nanomedicine* 6, 715–728. doi: 10.2217/nnm.11.19

Kalluri, R. (2003). Basement membranes: structure, assembly and role in tumour angiogenesis. *Nat. Rev. Cancer* 3, 422–433. doi: 10.1038/nrc1094

Kang, B., Mackey, M. A., and El-Sayed, M. A. (2010). Nuclear targeting of gold nanoparticles in cancer cells induces DNA damage, causing cytokinesis arrest and apoptosis. *J. Am. Chem. Soc.* 132, 1517–1519. doi: 10.1021/ja9102698

Kano, M. R., Komuta, Y., Iwata, C., Oka, M., Shirai, Y.-T., Morishita, Y., et al. (2009). Comparison of the effects of the kinase inhibitors imatinib, sorafenib, and transforming growth factor-beta receptor inhibitor on extravasation of nanoparticles from neovasculature. *Cancer Sci.* 100, 173–180. doi: 10.1111/j.1349-7006.2008.01003.x

Kessenbrock, K., Plaks, V., and Werb, Z. (2010). Matrix metalloproteinases: regulators of the tumor microenvironment. *Cell* 141, 52–67. doi: 10.1016/j.cell.2010.03.015

Kierstead, P. H., Okochi, H., Venditto, V. J., Chuong, T. C., Kivimae, S., Fréchet, J. M. J., et al. (2015). The effect of polymer backbone chemistry on the induction of the accelerated blood clearance in polymer modified liposomes. *J. Control. Release* 213, 1–9. doi: 10.1016/j.jconrel.2015.06.023

Kim, C. J., Hara, E., Watabe, N., Hara, I., and Kimura, S. (2017). Modulation of immunogenicity of poly(sarcosine) displayed on various nanoparticle surfaces due to different physical properties. *J. Peptide Sci.* 23, 889–898. doi: 10.1002/psc.3053

Kimura, T., Takabatake, Y., Takahashi, A., and Isaka, Y. (2013). Chloroquine in cancer therapy: a double-edged sword of autophagy. *Cancer Res.* 73, 3–7. doi: 10.1158/0008-5472.CAN-12-2464

Kozma, G. T., Mészáros, T., Vashegyi, I., Fülöp, T., Örfi, E., Dézsi, L., et al. (2019). Pseudo-anaphylaxis to polyethylene glycol (PEG)-coated liposomes: roles of anti-PEG IgM and complement activation in a porcine model of human infusion reactions. *ACS Nano* 13, 9315–9324. doi: 10.1021/acsnano.9b03942

Krishnamurthy, S., Muthukumaran, P., Jayakumar, M. K. G., Lisse, D., Masurkar, N. D., Xu, C., et al. (2019). Surface protein engineering increases the circulation time of a cell membrane-based nanotherapeutic. *Nanomed. Nanotechnol. Biol. Med.* 18, 169–178. doi: 10.1016/j.nano.2019.02.024

Kulkarni, P. S., Haldar, M. K., Nahire, R. R., Katti, P., Ambre, A. H., Muhonen, W. W., et al. (2014). MMP-9 responsive PEG cleavable nanovesicles for efficient delivery of chemotherapeutics to pancreatic cancer. *Mol. Pharm.* 11, 2390–2399. doi: 10.1021/mp500108p

Kunjachan, S., Pola, R., Gremse, F., Theek, B., Ehling, J., Moeckel, D., et al. (2014). Passive versus active tumor targeting using RGD- and NGR-modified polymeric nanomedicines. *Nano Lett.* 14, 972–981. doi: 10.1021/nl404391r

La-Beck, N. M., Zamboni, B. A., Gabizon, A., Schmeeda, H., Amantea, M., Gehrig, P. A., et al. (2012). Factors affecting the pharmacokinetics of pegylated liposomal doxorubicin in patients. *Cancer Chemother. Pharmacol.* 69, 43–50. doi: 10.1007/s00280-011-1664-2

Lammers, T., Kiessling, F., Hennink, W. E., and Storm, G. (2012a). Drug targeting to tumors: principles, pitfalls and (pre-) clinical progress. *J. Control. Release* 161, 175–187. doi: 10.1016/j.jconrel.2011.09.063

Lammers, T., Rizzo, L. Y., Storm, G., and Kiessling, F. (2012b). Personalized nanomedicine. *Clin. Cancer Res.* 18, 4889–4894. doi: 10.1158/1078-0432.CCR-12-1414

Lancet, J. E., Uy, G. L., Cortes, J. E., Newell, L. F., Lin, T. L., Ritchie, E. K., et al. (2018). CPX-351 (cytarabine and daunorubicin) liposome for injection versus conventional cytarabine plus daunorubicin in older patients with newly diagnosed secondary acute myeloid leukemia. *J. Clin. Oncol.* 36, 2684–2692. doi: 10.1200/JCO.2017.77.6112

Lane, L. A., Qian, X., Smith, A. M., and Nie, S. (2015). Physical chemistry of nanomedicine: understanding the complex behaviors of nanoparticles *in vivo*. *Annu. Rev. Phys. Chem.* 66, 521–547. doi: 10.1146/annurev-physchem-040513-103718

Lau, K. H. A., Ren, C., Sileika, T. S., Park, S. H., Szleifer, I., and Messersmith, P. B. (2012). Surface-grafted polysarcosine as a peptoid antifouling polymer brush. *Langmuir* 28, 16099–16107. doi: 10.1021/la302131n

Laverman, P., Carstens, M. G., Boerman, O. C., Dams, E. T. M., Oyen, W. J. G., van Rooijen, N., et al. (2001). Factors affecting the accelerated blood clearance of polyethylene glycol-liposomes upon repeated injection. *J. Pharmacol. Exp. Ther.* 298, 607–612. Available online at: http://jpet.aspetjournals.org/content/298/2/607.long

Lee, E. S., Gao, Z., and Bae, Y. H. (2008). Recent progress in tumor pH targeting nanotechnology. *J. Control. Release* 132, 164–170. doi: 10.1016/j.jconrel.2008.05.003

Lee, H., Gaddy, D., Ventura, M., Bernards, N., de Souza, R., Kirpotin, D., et al. (2018). Companion diagnostic 64Cu-liposome positron emission tomography enables characterization of drug delivery to tumors and predicts response to cancer nanomedicines. *Theranostics* 8, 2300–2312. doi: 10.7150/thno.21670

Lee, H., Shields, A. F., Siegel, B. A., Miller, K. D., Krop, I., Ma, C. X., et al. (2017). 64Cu-MM-302 Positron emission tomography quantifies variability of enhanced permeability and retention of nanoparticles in relation to treatment response in patients with metastatic breast cancer. *Clin. Cancer Res.* 23, 4190–4202. doi: 10.1158/1078-0432.CCR-16-3193

Less, J. R., Skalak, T. C., Sevick, E. M., and Jain, R. K. (1991). Microvascular architecture in a mammary carcinoma: branching patterns and vessel dimensions. *Cancer Res.* 51, 265–273. Available online at: http://cancerres.aacrjournals.org/content/51/1/265

Leu, A. J., Berk, D. A., Lymboussaki, A., Alitalo, K., and Jain, R. K. (2000). Absence of functional lymphatics within a murine sarcoma: a molecular and functional evaluation. *Cancer Res.* 60, 4324–4327. Available online at: https://cancerres.aacrjournals.org/content/60/16/4324.short

Levine, B., Mizushima, N., and Virgin, H. W. (2011). Autophagy in immunity and inflammation. *Nature* 469, 323–335. doi: 10.1038/nature09782

Li, H., Liu, Q., Crielaard, B. J., de Vries, J. W., Loznik, M., Meng, Z., et al. (2019). Fast, efficient, and targeted liposome delivery mediated by DNA hybridization. *Adv. Healthc. Mat.* 8:e1900389. doi: 10.1002/adhm.201900389

Li, H.-J., Du, J.-Z., Du, X.-J., Xu, C.-F., Sun, C.-Y., Wang, H.-X., et al. (2016). Stimuli-responsive clustered nanoparticles for improved tumor penetration and therapeutic efficacy. *Proc. Natl. Acad. Sci. U.S.A.* 113, 4164–4169. doi: 10.1073/pnas.1522080113

Lu, J., Li, Z., Zink, J. I., and Tamanoi, F. (2012). *In vivo* tumor suppression efficacy of mesoporous silica nanoparticles-based drug-delivery system: enhanced efficacy by folate modification. *Nanomed. Nanotechnol. Biol. Med.* 8, 212–220. doi: 10.1016/j.nano.2011.06.002

Lucky, S. S., Soo, K. C., and Zhang, Y. (2015). Nanoparticles in photodynamic therapy. *Chem. Rev.* 115, 1990–2042. doi: 10.1021/cr5004198

Luo, N., Weber, J. K., Wang, S., Luan, B., Yue, H., Xi, X., et al. (2017). PEGylated graphene oxide elicits strong immunological responses despite surface passivation. *Nat. Commun.* 8:14537. doi: 10.1038/ncomms14537

Lyon, P. C., Gray, M. D., Mannaris, C., Folkes, L. K., Stratford, M., Campo, L., et al. (2018). Safety and feasibility of ultrasound-triggered targeted drug delivery of doxorubicin from thermosensitive liposomes in liver tumours (TARDOX): a single-centre, open-label, phase 1 trial. *Lancet Oncol.* 19, 1027–1039. doi: 10.1016/S1470-2045(18)30332-2

Ma, X., Gong, N., Zhong, L., Sun, J., and Liang, X.-J. (2016). Future of nanotherapeutics: targeting the cellular sub-organelles. *Biomaterials* 97, 10–21. doi: 10.1016/j.biomaterials.2016.04.026

Maeda, H. (2015). Toward a full understanding of the EPR effect in primary and metastatic tumors as well as issues related to its heterogeneity. *Adv. Drug Deliv. Rev.* 91, 3–6. doi: 10.1016/j.addr.2015.01.002

Maeda, H., Wu, J., Sawa, T., Matsumura, Y., and Hori, K. (2000). Tumor vascular permeability and the EPR effect in macromolecular therapeutics: a review. *J. Control. Release* 65, 271–284. doi: 10.1016/S0168-3659(99)00248-5

Magzoub, M., Jin, S., and Verkman, A. S. (2007). Enhanced macromolecule diffusion deep in tumors after enzymatic digestion of extracellular matrix collagen and its associated proteoglycan decorin. *FASEB J.* 22, 276–284. doi: 10.1096/fj.07-9150com

Makino, A., Kizaka-Kondoh, S., Yamahara, R., Hara, I., Kanzaki, T., Ozeki, E., et al. (2009). Near-infrared fluorescence tumor imaging using nanocarrier composed of poly(l-lactic acid)-block-poly(sarcosine) amphiphilic polydepsipeptide. *Biomaterials* 30, 5156–5160. doi: 10.1016/j.biomaterials.2009.05.046

Marusyk, A., and Polyak, K. (2010). Tumor heterogeneity: causes and consequences. *Biochim. Biophys. Acta* 1805, 105–117. doi: 10.1016/j.bbcan.2009.11.002

Matea, C. T., Mocan, T., Tabaran, F., Pop, T., Mosteanu, O., Puia, C., et al. (2017). Quantum dots in imaging, drug delivery and sensor applications. *Int. J. Nanomed.* 12, 5421–5431. doi: 10.2147/IJN.S138624

Matsumoto, Y., Nichols, J. W., Toh, K., Nomoto, T., Cabral, H., Miura, Y., et al. (2016). Vascular bursts enhance permeability of tumour blood vessels and improve nanoparticle delivery. *Nat. Nanotechnol.* 11, 533–538. doi: 10.1038/nnano.2015.342

Matsumura, Y., and Maeda, H. (1986). A new concept for macromolecular therapeutics in cancer chemotherapy: Mechanism of tumoritropic accumulation of proteins and the antitumor agent smancs. *Cancer Res.* 46, 6387–6392. Available online at: https://cancerres.aacrjournals.org/content/46/12_Part_1/6387.short

McNeil, S. E. (2016). Evaluation of nanomedicines: stick to the basics. *Nat. Rev. Mater.* 1:16073. doi: 10.1038/natrevmats.2016.73

Mebius, R. E., and Kraal, G. (2005). Structure and function of the spleen. *Nat. Rev. Immunol.* 5:606. doi: 10.1038/nri1669

Mendler, C. T., Friedrich, L., Laitinen, I., Schlapschy, M., Schwaiger, M., Wester, H.-J., et al. (2015). High contrast tumor imaging with radio-labeled antibody Fab fragments tailored for optimized pharmacokinetics via PASylation. *mAbs* 7, 96–109. doi: 10.4161/19420862.2014.985522

Mikada, M., Sukhbaatar, A., Miura, Y., Horie, S., Sakamoto, M., Mori, S., et al. (2017). Evaluation of the enhanced permeability and retention effect

in the early stages of lymph node metastasis. *Cancer Sci.* 108, 846–852. doi: 10.1111/cas.13206

Miller, K., Cortes, J., Hurvitz, S. A., Krop, I. E., Tripathy, D., Verma, S., Riahi, K., et al. (2016). HERMIONE: a randomized Phase 2 trial of MM-302 plus trastuzumab versus chemotherapy of physician's choice plus trastuzumab in patients with previously treated, anthracycline-naïve, HER2-positive, locally advanced/metastatic breast cancer. *BMC Cancer* 16:352. doi: 10.1186/s12885-016-2385-z

Miller, S. M., Simon, R. J., Ng, S., Zuckermann, R. N., Kerr, J. M., and Moos, W. H. (1995). Comparison of the proteolytic susceptibilities of homologous L-amino acid, D-amino acid, and N-substituted glycine peptide and peptoid oligomers. *Drug Dev. Res.* 35, 20–32.

Mima, Y., Abu Lila, A. S., Shimizu, T., Ukawa, M., Ando, H., Kurata, Y., et al. (2017). Ganglioside inserted into PEGylated liposome attenuates anti-PEG immunity. *J. Control. Release* 250, 20–26. doi: 10.1016/j.jconrel.2017.01.040

Mishra, S., Webster, P., and Davis, M. E. (2004). PEGylation significantly affects cellular uptake and intracellular trafficking of non-viral gene delivery particles. *Eur. J. Cell Biol.* 83, 97–111. doi: 10.1078/0171-9335-00363

Morath, V., Bolze, F., Schlapschy, M., Schneider, S., Sedlmayer, F., Seyfarth, K., et al. (2015). PASylation of murine leptin leads to extended plasma half-life and enhanced *in vivo* Efficacy. *Mol. Pharm.* 12, 1431–1442. doi: 10.1021/mp5007147

Morikawa, S., Baluk, P., Kaidoh, T., Haskell, A., Jain, R. K., and McDonald, D. M. (2002). Abnormalities in pericytes on blood vessels and endothelial sprouts in tumors. *Am. J. Pathol.* 160, 985–1000. doi: 10.1016/S0002-9440(10)64920-6

Mura, S., Nicolas, J., and Couvreur, P. (2013). Stimuli-responsive nanocarriers for drug delivery. *Nat. Mater.* 12, 991–1003. doi: 10.1038/nmat3776

Nagy, J. A., Chang, S.-H., Shih, S.-C., Dvorak, A. M., and Dvorak, H. F. (2010). Heterogeneity of the tumor vasculature. *Sem. Throm. Hemost.* 36, 321–331. doi: 10.1055/s-0030-1253454

Needham, D., Anyarambhatla, G., Kong, G., and Dewhirst, M. W. (2000). A new temperature-sensitive liposome for use with mild hyperthermia: characterization and testing in a human tumor xenograft model. *Cancer Res.* 60, 1197–1201. Available online at: https://cancerres.aacrjournals.org/content/60/5/1197

Ngoune, R., Peters, A., von Elverfeldt, D., Winkler, K., and Pütz, G. (2016). Accumulating nanoparticles by EPR: a route of no return. *J. Control. Release* 238, 58–70. doi: 10.1016/j.jconrel.2016.07.028

Nitin, N., LaConte, L., Rhee, W. J., and Bao, G. (2009). Tat peptide is capable of importing large nanoparticles across nuclear membrane in digitonin permeabilized cells. *Ann. Biomed. Eng.* 37, 2018–2027. doi: 10.1007/s10439-009-9768-0

Noguchi, Y., Wu, J., Duncan, R., Strohalm, J., Ulbrich, K., Akaike, T., et al. (1998). Early phase tumor accumulation of macromolecules: a great difference in clearance rate between tumor and normal tissues. *Jpn. J. Cancer Res.* 89, 307–314.

Northfelt, D. W., Dezube, B. J., Thommes, J. A., Miller, B. J., Fischl, M. A., Friedman-Kien, A., et al. (1998). Pegylated-liposomal doxorubicin versus doxorubicin, bleomycin, and vincristine in the treatment of AIDS-related Kaposi's sarcoma: results of a randomized phase III clinical trial. *J. Clin. Oncol.* 16, 2445–2451.

Northfelt, D. W., Martin, F. J., Working, P., Volberding, P. A., Russell, J., Newman, M., et al. (1996). Doxorubicin encapsulated in liposomes containing surface-bound polyethylene glycol: pharmacokinetics, tumor localization, and safety in patients with AIDS-related Kaposi's sarcoma. *J. Clin. Oncol.* 36, 55–63.

O'Brien, M. E. R., Wigler, N., Inbar, M., Rosso, R., Grischke, E., Santoro, A., et al. (2004). Reduced cardiotoxicity and comparable efficacy in a phase III trial of pegylated liposomal doxorubicin HCl (CAELYX^{TM}/Doxil®) versus conventional doxorubicin for first-line treatment of metastatic breast cancer. *Ann. Oncol.* 15, 440–449. doi: 10.1093/annonc/mdh097

Ogun, S. A., Dumon-Seignovert, L., Marchand, J.-B., Holder, A. A., and Hill, F. (2008). The oligomerization domain of C4-binding protein (C4bp) acts as an adjuvant, and the fusion protein comprised of the 19-kilodalton merozoite surface protein 1 fused with the murine C4bp domain protects mice against malaria. *Infect. Immun.* 76, 3817–3823. doi: 10.1128/IAI.01369-07

Olive, K. P., Jacobetz, M. A., Davidson, C. J., Gopinathan, A., McIntyre, D., Honess, D., et al. (2009). Inhibition of Hedgehog signaling enhances delivery of chemotherapy in a mouse model of pancreatic cancer. *Science* 324, 1457–1461. doi: 10.1126/science.1171362

Padera, T. P., Kadambi, A., di Tomaso, E., Carreira, C. M., Brown, E. B., Boucher, Y., et al. (2002). Lymphatic metastasis in the absence of functional intratumor lymphatics. *Science* 296, 1883–1886. doi: 10.1126/science.1071420

Padera, T. P., Stoll, B. R., Tooredman, J. B., Capen, D., di Tomaso, E., and Jain, R. K. (2004). Pathology: cancer cells compress intratumour vessels. *Nature* 427:695. doi: 10.1038/427695a

Pan, L., Liu, J., He, Q., Wang, L., and Shi, J. (2013). Overcoming multidrug resistance of cancer cells by direct intranuclear drug delivery using TAT-conjugated mesoporous silica nanoparticles. *Biomaterials* 34, 2719–2730. doi: 10.1016/j.biomaterials.2012.12.040

Parhi, P., Mohanty, C., and Sahoo, S. K. (2012). Nanotechnology-based combinational drug delivery: an emerging approach for cancer therapy. *Drug Discov. Today* 17, 1044–1052. doi: 10.1016/j.drudis.2012.05.010

Pelaz, B., del Pino, P., Maffre, P., Hartmann, R., Gallego, M., Rivera-Fernández, S., et al. (2015). Surface functionalization of nanoparticles with polyethylene glycol: effects on protein adsorption and cellular uptake. *ACS Nano* 9, 6996–7008. doi: 10.1021/acsnano.5b01326

Peng, F., Setyawati, M. I., Tee, J. K., Ding, X., Wang, J., Nga, M. E., et al. (2019). Nanoparticles promote *in vivo* breast cancer cell intravasation and extravasation by inducing endothelial leakiness. *Nat. Nanotechnol.* 14:279. doi: 10.1038/s41565-018-0356-z

Petersen, G. H., Alzghari, S. K., Chee, W., Sankari, S. S., and La-Beck, N. M. (2016). Meta-analysis of clinical and preclinical studies comparing the anticancer efficacy of liposomal versus conventional non-liposomal doxorubicin. *J. Control. Release* 232, 255–264. doi: 10.1016/j.jconrel.2016.04.028

Pirollo, K. F., and Chang, E. H. (2008). Does a targeting ligand influence nanoparticle tumor localization or uptake? *Trends Biotechnol.* 26, 552–558. doi: 10.1016/j.tibtech.2008.06.007

Pluen, A., Boucher, Y., Ramanujan, S., McKee, T. D., Gohongi, T., di Tomaso, E., et al. (2001). Role of tumor–host interactions in interstitial diffusion of macromolecules: cranial vs. subcutaneous tumors. *Proc. Natl. Acad. Sci. U.S.A.* 98, 4628–4633. doi: 10.1073/pnas.081626898

Prijic, S., and Sersa, G. (2011). Magnetic nanoparticles as targeted delivery systems in oncology. *Radiol. Oncol.* 45, 1–16. doi: 10.2478/v10019-011-0001-z

Radu, O., and Pantanowitz, L. (2013). Kaposi sarcoma. *Arch. Pathol. Lab. Med.* 137, 289–294. doi: 10.5858/arpa.2012-0101-RS

Rees, P., Wills, J. W., Brown, M. R., Barnes, C. M., and Summers, H. D. (2019). The origin of heterogeneous nanoparticle uptake by cells. *Nat. Commun.* 10, 1–8. doi: 10.1038/s41467-019-10112-4

Remaut, K., Lucas, B., Braeckmans, K., Demeester, J., and De Smedt, S. C. (2007). Pegylation of liposomes favours the endosomal degradation of the delivered phosphodiester oligonucleotides. *J. Control. Release* 117, 256–266. doi: 10.1016/j.jconrel.2006.10.029

Remaut, K., Oorschot, V., Braeckmans, K., Klumperman, J., and De Smedt, S. C. (2014). Lysosomal capturing of cytoplasmic injected nanoparticles by autophagy: an additional barrier to non viral gene delivery. *J. Control. Release* 195, 29–36. doi: 10.1016/j.jconrel.2014.08.002

Roberts, R., Al-Jamal, W. T., Whelband, M., Thomas, P., Jefferson, M., van den Bossche, J., et al. (2013). Autophagy and formation of tubulovesicular autophagosomes provide a barrier against nonviral gene delivery. *Autophagy* 9, 667–682. doi: 10.4161/auto.23877

Rosenblum, D., Joshi, N., Tao, W., Karp, J. M., and Peer, D. (2018). Progress and challenges towards targeted delivery of cancer therapeutics. *Nat. Commun.* 9, 1–12. doi: 10.1038/s41467-018-03705-y

Rudge, S., Peterson, C., Vessely, C., Koda, J., Stevens, S., and Catterall, L. (2001). Adsorption and desorption of chemotherapeutic drugs from a magnetically targeted carrier (MTC). *J. Control. Release* 74, 335–340. doi: 10.1016/S0168-3659(01)00344-3

Rudmann, D. G., Alston, J. T., Hanson, J. C., and Heidel, S. (2013). High molecular weight polyethylene glycol cellular distribution and PEG-associated cytoplasmic vacuolation is molecular weight dependent and does not require conjugation to proteins. *Toxicol. Pathol.* 41, 970–983. doi: 10.1177/0192623312474726

Sabnani, M. K., Rajan, R., Rowland, B., Mavinkurve, V., Wood, L. M., Gabizon, A. A., et al. (2015). Liposome promotion of tumor growth is associated with angiogenesis and inhibition of antitumor immune responses. *Nanomed. Nanotechnol. Biol. Med.* 11, 259–262. doi: 10.1016/j.nano.2014.08.010

Safra, T., Muggia, F., Jeffers, S., Tsao-Wei, D. D., Groshen, S., Lyass, O., et al. (2000). Pegylated liposomal doxorubicin (doxil): reduced clinical cardiotoxicity in patients reaching or exceeding cumulative doses of 500 mg/m^2. *Ann. Oncol.* 11, 1029–1033. doi: 10.1023/A:1008365716693

Sahay, G., Alakhova, D. Y., and Kabanov, A. V. (2010). Endocytosis of nanomedicines. *J. Control. Release* 145, 182–195. doi: 10.1016/j.jconrel.2010.01.036

Sahay, G., Querbes, W., Alabi, C., Eltoukhy, A., Sarkar, S., Zurenko, C., et al. (2013). Efficiency of siRNA delivery by lipid nanoparticles is limited by endocytic recycling. *Nat. Biotechnol.* 31, 653–658. doi: 10.1038/nbt.2614

Salvati, A., Pitek, A. S., Monopoli, M. P., Prapainop, K., Bombelli, F. B., Hristov, D. R., et al. (2013). Transferrin-functionalized nanoparticles lose their targeting capabilities when a biomolecule corona adsorbs on the surface. *Nat. Nanotechnol.* 8, 137–143. doi: 10.1038/nnano.2012.237

Saneja, A., Dubey, R. D., Alam, N., Khare, V., and Gupta, P. N. (2014). Co-formulation of P-glycoprotein substrate and inhibitor in nanocarriers: an emerging strategy for cancer chemotherapy. *Curr. Cancer Drug Targets* 14, 419–433. doi: 10.2174/1568009614666140407112034

Sarisozen, C., Abouzeid, A. H., and Torchilin, V. P. (2014). The effect of co-delivery of paclitaxel and curcumin by transferrin-targeted PEG-PE-based mixed micelles on resistant ovarian cancer in 3-D spheroids and *in vivo* tumors. *Eur. J. Pharm. Biopharm.* 88, 539–550. doi: 10.1016/j.ejpb.2014.07.001

Schlapschy, M., Binder, U., Börger, C., Theobald, I., Wachinger, K., Kisling, S., et al. (2013). PASylation: a biological alternative to PEGylation for extending the plasma half-life of pharmaceutically active proteins. *Protein Eng. Des. Sel.* 26, 489–501. doi: 10.1093/protein/gzt023

Schöttler, S., Becker, G., Winzen, S., Steinbach, T., Mohr, K., Landfester, K., et al. (2016). Protein adsorption is required for stealth effect of poly(ethylene glycol)- and poly(phosphoester)-coated nanocarriers. *Nat. Nanotechnol.* 11, 372–377. doi: 10.1038/nnano.2015.330

Setyawati, M. I., Tay, C. Y., Bay, B. H., and Leong, D. T. (2017). Gold nanoparticles induced endothelial leakiness depends on particle size and endothelial cell origin. *ACS Nano* 11, 5020–5030. doi: 10.1021/acsnano.7b01744

Shapiro, B., Kulkarni, S., Nacev, A., Muro, S., Stepanov, P. Y., and Weinberg, I. N. (2015). Open challenges in magnetic drug targeting. *WIREs Nanomed. Nanobiotechnol.* 7, 446–457. doi: 10.1002/wnan.1311

Silverman, L., and Barenholz, Y. (2015). *In vitro* experiments showing enhanced release of doxorubicin from Doxil® in the presence of ammonia may explain drug release at tumor site. *Nanomed. Nanotechnol. Biol. Med.* 11, 1841–1850. doi: 10.1016/j.nano.2015.06.007

Smith, N. R., Baker, D., Farren, M., Pommier, A., Swann, R., Wang, X., et al. (2013). Tumor stromal architecture can define the intrinsic tumor response to VEGF-targeted therapy. *Clin. Cancer Res.* 19, 6943–6956. doi: 10.1158/1078-0432.CCR-13-1637

Smith, S. A., Selby, L. I., Johnston, A. P. R., and Such, G. K. (2019). The endosomal escape of nanoparticles: toward more efficient cellular delivery. *Bioconj. Chem.* 30, 263–272. doi: 10.1021/acs.bioconjchem.8b00732

Sofuni, A., Iijima, H., Moriyasu, F., Nakayama, D., Shimizu, M., Nakamura, K., et al. (2005). Differential diagnosis of pancreatic tumors using ultrasound contrast imaging. *J. Gastrroenterol.* 40, 518–525. doi: 10.1007/s00535-005-1578-z

Stacker, S. A., Williams, S. P., Karnezis, T., Shayan, R., Fox, S. B., and Achen, M. G. (2014). Lymphangiogenesis and lymphatic vessel remodelling in cancer. *Nat. Rev. Cancer* 14, 159–172. doi: 10.1038/nrc3677

Stan, R. V. (2007). Endothelial stomatal and fenestral diaphragms in normal vessels and angiogenesis. *J. Cell. Mol. Med.* 11, 621–643. doi: 10.1111/j.1582-4934.2007.00075.x

Strambio-De-Castillia, C., Niepel, M., and Rout, M. P. (2010). The nuclear pore complex: bridging nuclear transport and gene regulation. *Nat. Rev. Mol. Cell Biol.* 11, 490–501. doi: 10.1038/nrm2928

Suk, J. S., Xu, Q., Kim, N., Hanes, J., and Ensign, L. M. (2016). PEGylation as a strategy for improving nanoparticle-based drug and gene delivery. *Adv. Drug Deliv. Rev.* 99, 28–51. doi: 10.1016/j.addr.2015.09.012

Szebeni, J., Baranyi, L., Savay, S., Milosevits, J., Bunger, R., Laverman, P., et al. (2002). Role of complement activation in hypersensitivity reactions to doxil and hynic peg liposomes: experimental and clinical studies. *J. Liposome Res.* 12, 165–172. doi: 10.1081/LPR-120004790

Szebeni, J., Simberg, D., González-Fernández, Á., Barenholz, Y., and Dobrovolskaia, M. A. (2018). Roadmap and strategy for overcoming infusion reactions to nanomedicines. *Nat. Nanotechnol.* 13, 1100–1108. doi: 10.1038/s41565-018-0273-1

Tak, W. Y., Lin, S.-M., Wang, Y., Zheng, J., Vecchione, A., Park, S. Y., et al. (2018). Phase III HEAT study adding Lyso-thermosensitive liposomal doxorubicin to radiofrequency ablation in patients with unresectable hepatocellular carcinoma lesions. *Clin. Cancer Res.* 24, 73–83. doi: 10.1158/1078-0432.CCR-16-2433

Tammam, S. N., Azzazy, H. M. E., and Lamprecht, A. (2017). The effect of nanoparticle size and NLS density on nuclear targeting in cancer and normal cells; impaired nuclear import and aberrant nanoparticle intracellular trafficking in glioma. *J. Control. Release* 253, 30–36. doi: 10.1016/j.jconrel.2017.02.029

Tang, J., Howard, B. C., Mahler, M. S., Thurecht, J. K., Huang, L., and Ping Xu, Z. (2018). Enhanced delivery of siRNA to triple negative breast cancer cells *in vitro* and *in vivo* through functionalizing lipid-coated calcium phosphate nanoparticles with dual target ligands. *Nanoscale* 10, 4258–4266. doi: 10.1039/C7NR08644J

Tang, J., Zhang, L., Gao, H., Liu, Y., Zhang, Q., Ran, R., et al. (2016). Co-delivery of doxorubicin and P-gp inhibitor by a reduction-sensitive liposome to overcome multidrug resistance, enhance anti-tumor efficiency and reduce toxicity. *Drug Deliv.* 23, 1130–1143. doi: 10.3109/10717544.2014.990651

Tavares, A. J., Poon, W., Zhang, Y.-N., Dai, Q., Besla, R., Ding, D., et al. (2017). Effect of removing Kupffer cells on nanoparticle tumor delivery. *Proc. Natl. Acad. Sci. U.S.A.* 114, E10871–E10880. doi: 10.1073/pnas.1713390114

Tay, C. Y., Setyawati, M. I., and Leong, D. T. (2017). Nanoparticle density: a critical biophysical regulator of endothelial permeability. *ACS Nano* 11, 2764–2772. doi: 10.1021/acsnano.6b07806

Tietze, R., Lyer, S., Dürr, S., Struffert, T., Engelhorn, T., Schwarz, M., et al. (2013). Efficient drug-delivery using magnetic nanoparticles — biodistribution and therapeutic effects in tumour bearing rabbits. *Nanomed. Nanotechnol. Biol. Med.* 9, 961–971. doi: 10.1016/j.nano.2013.05.001

Tietze, R., Zaloga, J., Unterweger, H., Lyer, S., Friedrich, R. P., Janko, C., et al. (2015). Magnetic nanoparticle-based drug delivery for cancer therapy. *Biochem. Biophys. Res. Commun.* 468, 463–470. doi: 10.1016/j.bbrc.2015.08.022

Tong, R. T., Boucher, Y., Kozin, S. V., Winkler, F., Hicklin, D. J., and Jain, R. K. (2004). Vascular normalization by vascular endothelial growth factor receptor 2 blockade induces a pressure gradient across the vasculature and improves drug penetration in tumors. *Cancer Res.* 64, 3731–3736. doi: 10.1158/0008-5472.CAN-04-0074

Tsukigawa, K., Liao, L., Nakamura, H., Fang, J., Greish, K., Otagiri, M., et al. (2015). Synthesis and therapeutic effect of styrene–maleic acid copolymer-conjugated pirarubicin. *Cancer Sci.* 106, 270–278. doi: 10.1111/cas.12592

Udhrain, A., Skubitz, K. M., and Northfelt, D. W. (2007). Pegylated liposomal doxorubicin in the treatment of AIDS-related Kaposi's sarcoma. *Int. J. Nanomed.* 2, 345–352. Available online at: https://www.dovepress.com/pegylated-liposomal-doxorubicin-in-the-treatment-of-aids-related-kapos-peer-reviewed-article-IJN#

Ulbrich, K., Hekmatara, T., Herbert, E., and Kreuter, J. (2009). Transferrin- and transferrin-receptor-antibody-modified nanoparticles enable drug delivery across the blood–brain barrier (BBB). *Eur. J. Pharm. Biopharm.* 71, 251–256. doi: 10.1016/j.ejpb.2008.08.021

Vermeulen, L. M. P., De Smedt, S. C., Remaut, K., and Braeckmans, K. (2018). The proton sponge hypothesis: fable or fact? *Eur. J. Pharm. Biopharm.* 129, 184–190. doi: 10.1016/j.ejpb.2018.05.034

Vu, V. P., Gifford, G. B., Chen, F., Benasutti, H., Wang, G., Groman, E. V., et al. (2019). Immunoglobulin deposition on biomolecule corona determines complement opsonization efficiency of preclinical and clinical nanoparticles. *Nat. Nanotechnol.* 14, 260–268. doi: 10.1038/s41565-018-0344-3

Wan, Y., Han, J., Fan, G., Zhang, Z., Gong, T., and Sun, X. (2013). Enzyme-responsive liposomes modified adenoviral vectors for enhanced tumor cell transduction and reduced immunogenicity. *Biomaterials* 34, 3020–3030. doi: 10.1016/j.biomaterials.2012.12.051

Wang, Y., Dou, L., He, H., Zhang, Y., and Shen, Q. (2014). Multifunctional nanoparticles as nanocarrier for vincristine sulfate delivery to overcome tumor multidrug resistance. *Mol. Pharm.* 11, 885–894. doi: 10.1021/mp400547u

Wang, Y., and Kohane, D. S. (2017). External triggering and triggered targeting strategies for drug delivery. *Nat. Rev. Mater.* 2:17020. doi: 10.1038/natrevmats.2017.20

Wang-Gillam, A., Hubner, R. A., Siveke, J. T., Von Hoff, D. D., Belanger, B., de Jong, F. A., et al. (2019). NAPOLI-1 phase 3 study of liposomal irinotecan in metastatic pancreatic cancer: final overall survival analysis and characteristics of long-term survivors. *Eur. J. Cancer* 108, 78–87. doi: 10.1016/j.ejca.2018.12.007

Wang-Gillam, A., Li, C.-P., Bodoky, G., Dean, A., Shan, Y.-S., Jameson, G., et al. (2016). Nanoliposomal irinotecan with fluorouracil and folinic acid in metastatic pancreatic cancer after previous gemcitabine-based therapy (NAPOLI-1): a global, randomised, open-label, phase 3 trial. *Lancet* 387, 545–557. doi: 10.1016/S0140-6736(15)00986-1

Weber, B., Seidl, C., Schwiertz, D., Scherer, M., Bleher, S., Süss, R., et al. (2016). Polysarcosine-based lipids: from lipopolypeptoid micelles to stealth-like lipids in langmuir blodgett monolayers. *Polymers* 8:427. doi: 10.3390/polym8120427

Webster, R., Didier, E., Harris, P., Siegel, N., Stadler, J., Tilbury, L., et al. (2007). PEGylated proteins: evaluation of their safety in the absence of definitive metabolism studies. *Drug Metab. Dispos.* 35, 9–16. doi: 10.1124/dmd.106.012419

Webster, R., Elliott, V., Park, B. K., Walker, D., Hankin, M., and Taupin, P. (2009). "PEG and PEG conjugates toxicity: towards an understanding of the toxicity of PEG and its relevance to PEGylated biologicals," in *PEGylated Protein Drugs: Basic Science and Clinical Applications, Milestones in Drug Therapy*, ed F. M. Veronese (Basel: Birkhäuser Basel), 127–146.

Wei, X., Shamrakov, D., Nudelman, S., Peretz-Damari, S., Nativ-Roth, E., Regev, O., et al. (2018). Cardinal role of intraliposome doxorubicin-sulfate nanorod crystal in doxil properties and performance. *ACS Omega* 3, 2508–2517. doi: 10.1021/acsomega.7b01235

Wei, Y., Gu, X., Cheng, L., Meng, F., Storm, G., and Zhong, Z. (2019). Low-toxicity transferrin-guided polymersomal doxorubicin for potent chemotherapy of orthotopic hepatocellular carcinoma *in vivo*. *Acta Biomat.* 92, 196–204. doi: 10.1016/j.actbio.2019.05.034

Weiss, A. C. G., Kelly, H. G., Faria, M., Besford, Q. A., Wheatley, A. K., Ang, C.-S., et al. (2019). Link between low-fouling and stealth: a whole blood biomolecular corona and cellular association analysis on nanoengineered particles. *ACS Nano* 13, 4980–4991. doi: 10.1021/acsnano.9b00552

Wen, S., Zhou, J., Zheng, K., Bednarkiewicz, A., Liu, X., and Jin, D. (2018). Advances in highly doped upconversion nanoparticles. *Nat. Commun.* 9, 1–12. doi: 10.1038/s41467-018-04813-5

Wenande, E., and Garvey, L. H. (2016). Immediate-type hypersensitivity to polyethylene glycols: a review. *Clin. Exp. Allergy* 46, 907–922. doi: 10.1111/cea.12760

Wiley, D. T., Webster, P., Gale, A., and Davis, M. E. (2013). Transcytosis and brain uptake of transferrin-containing nanoparticles by tuning avidity to transferrin receptor. *Proc. Natl. Acad. Sci. U.S.A.* 110, 8662–8667. doi: 10.1073/pnas.1307152110

Wilhelm, S., Tavares, A. J., Dai, Q., Ohta, S., Audet, J., Dvorak, H. F., et al. (2016). Analysis of nanoparticle delivery to tumours. *Nat. Rev. Mater.* 1:16014. doi: 10.1038/natrevmats.2016.14

Wu, J., Akaike, T., and Maeda, H. (1998). Modulation of enhanced vascular permeability in tumors by a Bradykinin antagonist, a cyclooxygenase inhibitor, and a nitric oxide scavenger. *Cancer Res.* 58, 159–165. Available online at: https://cancerres.aacrjournals.org/content/58/1/159.long

Xia, Y., Schlapschy, M., Morath, V., Roeder, N., Vogt, E. I., Stadler, D., et al. (2019). PASylated interferon α efficiently suppresses hepatitis B virus and induces anti-HBs seroconversion in HBV-transgenic mice. *Antiviral Res.* 161, 134–143. doi: 10.1016/j.antiviral.2018.11.003

Xu, S., Zhu, X., Zhang, C., Huang, W., Zhou, Y., and Yan, D. (2018). Oxygen and Pt(II) self-generating conjugate for synergistic photo-chemo therapy of hypoxic tumor. *Nat. Commun.* 9, 1–9. doi: 10.1038/s41467-018-04318-1

Yankai, Z., Rong, Y., Yi, H., Wentao, L., Rongyue, C., Ming, Y., et al. (2006). Ten tandem repeats of beta-hCG 109-118 enhance immunogenicity and anti-tumor effects of beta-hCG C-terminal peptide carried by mycobacterial heat-shock protein HSP65. *Biochem. Biophys. Res. Commun.* 345, 1365–1371. doi: 10.1016/j.bbrc.2006.05.022

Yin, H., Kanasty, R. L., Eltoukhy, A. A., Vegas, A. J., Dorkin, J. R., and Anderson, D. G. (2014). Non-viral vectors for gene-based therapy. *Nat. Rev. Gen.* 15, 541–555. doi: 10.1038/nrg3763

Yu, M., Wu, J., Shi, J., and Farokhzad, O. C. (2016). Nanotechnology for protein delivery: overview and perspectives. *J. Control. Release* 240, 24–37. doi: 10.1016/j.jconrel.2015.10.012

Yuan, F., Dellian, M., Fukumura, D., Leunig, M., Berk, D. A., Torchilin, V. P., et al. (1995). Vascular permeability in a human tumor xenograft: molecular size dependence and cutoff size. *Cancer Res.* 55, 3752–3756. Available online at: https://cancerres.aacrjournals.org/content/55/17/3752.long

Zhang, C.-G., Zhu, W.-J., Liu, Y., Yuan, Z.-Q., Yang, S.-D., Chen, W.-L., et al. (2016). Novel polymer micelle mediated co-delivery of doxorubicin and P-glycoprotein siRNA for reversal of multidrug resistance and synergistic tumor therapy. *Sci. Rep.* 6:23859. doi: 10.1038/srep23859

Zhang, S., Gao, H., and Bao, G. (2015). Physical principles of nanoparticle cellular endocytosis. *ACS Nano* 9, 8655–8671. doi: 10.1021/acsnano.5b03184

Zhang, X., Dong, Y., Zeng, X., Liang, X., Li, X., Tao, W., et al. (2014). The effect of autophagy inhibitors on drug delivery using biodegradable polymer nanoparticles in cancer treatment. *Biomaterials* 35, 1932–1943. doi: 10.1016/j.biomaterials.2013.10.034

Zhao, W., Zhuang, S., and Qi, X.-R. (2011). Comparative study of the *in vitro* and *in vivo* characteristics of cationic and neutral liposomes. *Int. J. Nanomed.* 6, 3087–3098. doi: 10.2147/IJN.S25399

Zhou, M., Huang, H., Wang, D., Lu, H., Chen, J., Chai, Z., et al. (2019). Light-triggered PEGylation/dePEGylation of the nanocarriers for enhanced tumor penetration. *Nano Lett.* 19, 3671–3675. doi: 10.1021/acs.nanolett.9b00737

Zhu, L., and Torchilin, V. P. (2013). Stimulus-responsive nanopreparations for tumor targeting. *Integr. Biol.* 5, 96–107. doi: 10.1039/c2ib20135f

Zinger, A., Koren, L., Adir, O., Poley, M., Alyan, M., Yaari, Z., et al. (2019). Collagenase nanoparticles enhance the penetration of drugs into pancreatic tumors. *ACS Nano*. 13, 11008–11021. doi: 10.1021/acsnano.9b02395

Conflict of Interest: The authors declare that the research was conducted in the absence of any commercial or financial relationships that could be construed as a potential conflict of interest.

frontiers in Bioengineering and Biotechnology

MINI REVIEW
published: 21 January 2020
doi: 10.3389/fbioe.2019.00469

Growth Factor Engineering Strategies for Regenerative Medicine Applications

Xiaochen Ren[1], *Moyuan Zhao*[1], *Blake Lash*[1,2], *Mikaël M. Martino*[1]* *and Ziad Julier*[1]*

[1] European Molecular Biology Laboratory Australia, Australian Regenerative Medicine Institute, Monash University, Melbourne, VIC, Australia, [2] Department of Biological Engineering, Massachusetts Institute of Technology, Cambridge, MA, United States

Growth factors are critical molecules for tissue repair and regeneration. Therefore, recombinant growth factors have raised a lot of hope for regenerative medicine applications. While using growth factors to promote tissue healing has widely shown promising results in pre-clinical settings, their success in the clinic is not a forgone conclusion. Indeed, translation of growth factors is often limited by their short half-life, rapid diffusion from the delivery site, and low cost-effectiveness. Trying to circumvent those limitations by the use of supraphysiological doses has led to serious side-effects in many cases and therefore innovative technologies are required to improve growth factor-based regenerative strategies. In this review, we present protein engineering approaches seeking to improve growth factor delivery and efficacy while reducing doses and side effects. We focus on engineering strategies seeking to improve affinity of growth factors for biomaterials or the endogenous extracellular matrix. Then, we discuss some examples of increasing growth factor stability and bioactivity, and propose new lines of research that the field of growth factor engineering for regenerative medicine may adopt in the future.

Keywords: growth factors, protein engineering, regenerative medicine, biomaterials, extracellular matrix

OPEN ACCESS

Edited by:
Francesco Cellesi, Politecnico di Milano, Italy

Reviewed by:
Stephanie K. Seidlits, University of California, Los Angeles, United States
Ketul C. Popat, Colorado State University, United States

***Correspondence:**
Mikaël M. Martino
mikael.martino@monash.edu
Ziad Julier
ziad.julier@monash.edu

Specialty section:
This article was submitted to Nanobiotechnology, a section of the journal Frontiers in Bioengineering and Biotechnology

Received: *31 October 2019*
Accepted: *23 December 2019*
Published: *21 January 2020*

Citation:
Ren X, Zhao M, Lash B, Martino MM and Julier Z (2020) Growth Factor Engineering Strategies for Regenerative Medicine Applications. Front. Bioeng. Biotechnol. 7:469. doi: 10.3389/fbioe.2019.00469

INTRODUCTION

Growth factors (GFs) are molecules capable of stimulating a variety of cellular processes including cell proliferation, migration, differentiation and multicellular morphogenesis during development and tissue healing. Therefore, they have raised a lot of hope for regenerative medicine applications and several products based on growth factors have been developed (**Table 1A**). Nevertheless, GF-based therapies present limitations. For example, high levels of proteolytic activity *in vivo* leads to poor GF stability and short half-life (Mitchell et al., 2016). Thus, multiple administrations and/or supraphysiological doses are often necessary to sustain an effective concentration of GFs at the delivery site, resulting in high cost and adverse effects (**Table 1B**). Side effects and poor effectiveness are mainly linked to sub-optimal delivery systems and lack of control over GF signaling. These issues in clinically available products emphasize the need to design new strategies allowing the use of lower and localized doses of GFs where delivery and signaling are tightly controlled.

Numerous strategies have been explored, in particular with the design of biomaterial-based delivery systems, focusing on engineering biomaterials instead of modifying GFs (Wang et al., 2017). In addition, interesting approaches have emerged to enhance the stability and bioactivity of GFs (Niu et al., 2018). In this review, we will focus on strategies aiming at engineering the GF

TABLE 1A | Recombinant GF-based products for regenerative medicine applications.

Product	GF	Delivery system	Target tissue/disease	Approved authority	References
Augment® Bone Graft	PDGF-BB	Beta-tricalcium phosphate	Ankle fusion, hindfoot	FDA	FDA, 2015a
Increlex®	IGF-1	Subcutaneous Injection	Primary IGF-1 deficiency	FDA	FDA, 2005; National Drug Strategy, 2006
Infuse® Bone Graft	BMP-2	Collagen sponge	Spinal fusion, bone regeneration	FDA	James et al., 2016
Kepivance®	FGF-7 (KGF)	i.v. injection	Gastrointestinal injury	FDA	FDA, 2015b
OP-1® Putty	BMP-7	Bovine bone-derived collagen	Spinal fusion, bone regeneration	FDA	Okabe et al., 2013
PELNAC®	FGF-2 (bFGF)	Collagen sponge	Bedsores, cutaneous ulcers	Pharmaceuticals and Medical Devices Agency (Japan)	Kakudo et al., 2019
REGEN-D®	EGF	Cellulose gel	Foot ulcer	Ministry of Food and Drug Safety (South Korea)	Frew et al., 2007
Regranex®	PDGF-BB	Sodium carboxymethylcellulose-based topical gel	Chronic diabetic wound	FDA	FDA, 2008
Citrix® CRS	TGF-β1	Topical	Aged skin		Aldag et al., 2016

BMP, bone morphogenetic protein; EGF, epidermal growth factor; FGF, fibroblast growth factor; HGF, hepatocyte growth factor; IGF, insulin-like growth factor; PDGF, platelet-derived growth factor; TGF, transforming growth factor; FDA, U.S. Food Drug Administration.

TABLE 1B | Common GFs in regenerative medicine.

GFs	Desired function(s)	Half-life in blood	Side-effect(s) in humans	References
BMP-2	Osteogenic factor	1–4 h	Ectopic bone formation, abnormal osteogenesis, inflammatory complications, urogenital events, wound complications, increase cancer risk	Carragee et al., 2013; Carreira et al., 2014; James et al., 2016
BMP-7	Osteogenic factor, regulate proliferation of neural progenitor cells	1–4 h	Not reported	Calori et al., 2009; Carreira et al., 2014; Kowtharapu et al., 2018
EGF	Stimulates proliferation and differentiation of epithelial cells	<1 min	Not reported	Mitchell et al., 2016
FGF-2	Stimulates proliferation and differentiation of various cell types, angiogenesis	7.6 h	Not reported	Beenken and Mohammadi, 2009; Maddaluno et al., 2017
HGF	Stimulates epithelial cell proliferation and morphogenesis, angiogenesis	3–5 min	Not reported	Yu et al., 2007; Nakamura et al., 2019
IGF-1	Enhances neuronal growth, myelination, endometrial epithelial cell proliferation, inhibition of cell apoptosis	3–5 h	Not reported	Leroith et al., 1992; Wang et al., 2018
PDGF-BB	Proliferation of various cell types, extracellular matrix synthesis, vascularization	30 min	Increase cancer risk	Jin et al., 2008; Saika et al., 2011; Mao and Mooney, 2015; Yamakawa and Hayashida, 2019
FGF-7 (KGF)	Epithelium morphogenesis, re-epithelialization	4–6 h	Enhance epithelial tumor cell growth	FDA, 2004a,b; Yamakawa and Hayashida, 2019
TGF-β1	Differentiation of bone-forming cells, antiproliferative factor for epithelial cells	>100 min (latent form) 2–3 min (active form)	Not reported	Hermonat et al., 2007; Lee et al., 2011; Tian et al., 2011
VEGF-A	Angiogenic factor	30 min	Edema, systemic hypotension	Simons and Ware, 2003; Stefanini et al., 2008; Yamakawa and Hayashida, 2019

BMP, bone morphogenetic protein; EGF, epidermal growth factor; FGF, fibroblast growth factor; HGF, hepatocyte growth factor; IGF, insulin-like growth factor; PDGF, platelet-derived growth factor; TGF, transforming growth factor; VEGF, vascular endothelial growth factor.

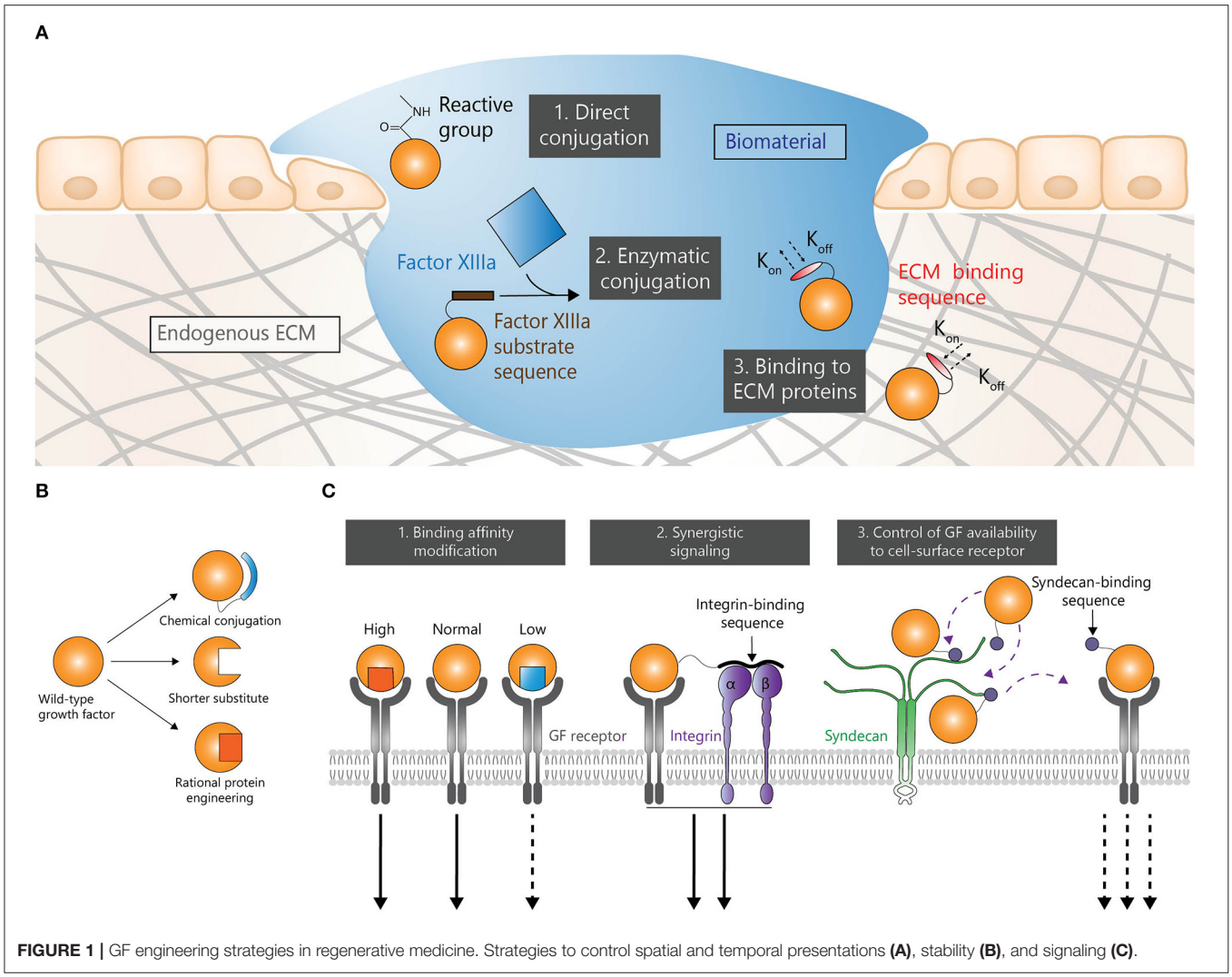

FIGURE 1 | GF engineering strategies in regenerative medicine. Strategies to control spatial and temporal presentations **(A)**, stability **(B)**, and signaling **(C)**.

itself. We first describe approaches to control GF half-life as well as spatial and temporal release. Then, we discuss various strategies to modulate GF signaling at the receptor level.

ENGINEERING GFs TO CONTROL SPATIAL AND TEMPORAL PRESENTATION

Biomaterial-based delivery is a common strategy to efficiently deliver GFs. Immobilizing GFs within a biomaterial (**Figure 1A**) gives the possibility to achieve a sustained release and a localized delivery. Such approaches may considerably reduce the need for multiple doses and potentially reduce adverse effects. Therefore, various methods have been explored to enhance interactions between GFs and biomaterials.

Engineering GFs to Be Covalently Bound to Biomaterials

Covalent conjugation is a common strategy to immobilize GFs in biomaterials. In that setting, GF release depends on biomaterial degradation and/or cleavage (hydrolytic and enzymatic) of the bond between GFs and biomaterials. Additionally, this strategy can also address low stability problems as it may reduce the exposure of GFs to a proteolytic microenvironment at the delivery site. Strategies to bind GFs to biomaterials via reactive chemical groups have been widely used (Cabanas-Danés et al., 2014). For instance, crosslinking via 1-ethyl-3-(3-dimethyl aminopropyl) carbodiimide (EDC) and N-hydroxy-succinimide (NHS) has been extensively used, due to its simplicity, low cost, mild reaction conditions, and biocompatibility (approved by the USFDA) (Grabarek and Gergely, 1990; Masters, 2011). For example, EDC-mediated immobilization of bone morphogenetic protein-2 (BMP-2) onto a polyelectrolyte multilayer film successfully promoted bone regeneration in critical-size rat femoral defect (Bouyer et al., 2016). Although EDC/NHS has extensive merits, this chemistry links primary amines with carboxylic acids in an inherently random fashion, and not necessarily always at the terminal reactive groups. The inability of this approach to recognize the difference between terminal reactive groups and reactive groups within the protein backbone may hinder the recognition of GFs by their receptors

and extracellular matrix (ECM) components (Mitchell et al., 2016).

Enzymatic conjugation is another interesting method to bind GFs to biomaterials. For example, GFs have been engineered with a transglutaminase substrate sequence derived from α_2-plasmin inhibitor (α_2PI_{1-8}) (Schense and Hubbell, 1999). This strategy allows the engineered GFs to react with lysine residues via the transglutaminase factor XIIIa. GFs such as BMP-2, vascular endothelial growth factor A (VEGF-A), platelet derived growth factor AB (PDGF-AB) and insulin-like growth factor 1 (IGF-1) have been cross-linked to fibrin using this approach (Schmoekel et al., 2005; Sacchi et al., 2014; Mittermayr et al., 2016; Vardar et al., 2018). For instance, BMP-2 with α_2PI_{1-8} fused at its N-terminus was delivered in fibrin matrices in critical-size craniotomy in rats (Schmoekel et al., 2005). Here, the engineered BMP-2 induced significantly higher bone formation compared to wild type BMP-2 after 3 weeks. Similarly, a fusion protein consisting of α_2PI_{1-8} and VEGF-A delivered in fibrin induced a functional angiogenesis and promoted regeneration in ischemic hind limb wound models in rodents (Sacchi et al., 2014). Aberrant vessel formation and vascular hyperpermeability are adverse effects associated with the uncontrolled delivery of VEGF-A which induces a burst signaling. However, it was demonstrated that low doses (0.01– 5 μg/mL) of α_2PI_{1-8}-VEGF-A promotes normal angiogenesis. Following the same approach an α_2PI_{1-8}-VEGF-C fusion was engineered to stimulate local lymphangiogenesis upon delivery in a fibrin matrix (Güç et al., 2017). The lymphangiogenesis induced by the fibrin-binding VEGF-C promoted wound healing in diabetic model as shown by extracellular matrix deposition and granulation tissue thickening. The same strategy can be used to cross-link GFs to polyethylene glycol (PEG) hydrogel as multiarm PEG molecules can be functionalized with factor XIIIa substrates to drive its crosslinking and incorporation of α_2PI_{1-8}-bearing proteins (Ehrbar et al., 2007).

Another approach to combine GFs and biomaterials is to directly create fusion proteins consisting of GFs with ECM proteins. For example, a biopolymer based on the ECM protein elastin was fused to VEGF-A (ELP-VEGF) with the objective to treat preeclampsia, a hypertensive syndrome that originates from an improperly vascularized and ischemic placenta (Logue et al., 2017). Here, ELP-VEGF reduced hypertension in a placental ischemia rat model and did not cross the placental barrier, reducing the risk of adverse effects on fetal development. Although covalent binding of GFs to biomaterial has proved to be an effective strategy it is nevertheless dependent on the biocompatibility of the used biomaterials. In addition, as the system requires both a biomaterial and an engineering protein it may complicate the pathway to approval or increase the cost.

Engineering GFs for Non-covalent Interaction to Biomaterials and Endogenous ECM

GFs can be immobilized to the ECM or ECM-derived biomaterials through affinity binding by the introduction of an ECM-binding sequence or domain at either terminus of the GF. The strategy presents the advantage of giving modified GFs the ability to bind the endogenous ECM where the GF is delivered, in some cases allowing to forgo the use of exogenous biomaterials altogether. Such approach allows GFs to be more readily available for resident cells by being immobilized in the local ECM instead of having to be released by biomaterials. In addition, the simplicity of biomaterial-free delivery systems could lead to a higher cost-effectiveness. However, the effectiveness of these strategies may depend on the local ECM composition.

As one of the most abundant ECM proteins, collagens represent good binding targets for engineering GFs for delivery to collagen-rich tissues. For example, a bacterial collagen-binding domain (CBD), was fused to fibroblast growth factor-2 (FGF-2), allowing improved bone formation in a spinal fusion model (Inoue et al., 2017). In another study, CBD-fused FGF-2 showed the ability to induce significantly higher mesenchymal cell proliferation and callus formation in a mice fracture model compared to wild-type FGF-2 (Sekiguchi et al., 2018). Similarly, a CBD-fused hepatocyte growth factor (HGF) delivered via hydrogel improved recovery after spinal cord injury in mice compared to wild-type HGF (Yamane et al., 2018).

In order to engineer GFs with stronger binding to collagen, a library of random sequences was conjugated to VEGF-A and selected *in vitro* for their binding affinity to collagen (Park et al., 2018). This method presents the advantage of identifying CBDs tailor-made for a specific GF as large GFs may affect the binding of generic CBDs to collagen. The resulting engineered collagen-binding VEGF-A stimulated angiogenesis in skin wounds and infarcted myocardiums in mice.

Natural interactions between the ECM and GFs are crucial for tissue healing (Schultz and Wysocki, 2009) as many GFs have the ability to bind ECM proteins to some extent (Macri et al., 2007; Sawicka et al., 2015). These interactions often occur between the heparin-binding domains of ECM proteins and heparin-binding GFs (Martino et al., 2013). For example, PIGF-$2_{123-144}$, a placental growth factor-2 (PlGF-2)-derived ECM-binding domain, promiscuously binds multiple ECM proteins with high affinity (Martino et al., 2014). The sequence was fused to VEGF-A, PDGF-BB, and BMP-2, and the engineered variants showed the ability to bind several ECM proteins with much higher affinity (i.e. super-affinity) compared to their wild-type counterparts. Super-affinity GFs contributed to improved therapeutic efficacy in murine models of chronic wounds and bone regeneration (Martino et al., 2014). Moreover, this approach significantly reduced the vascular hyperpermeability induced by VEGF-A.

In hard bone tissues, the ECM exists in the form of either a collagen-rich organic phase, or a calcium-phosphate (Ca-P) mineral phase (mainly hydroxyapatite) (Boonrungsiman et al., 2012). However, most GFs do not express mineral-binding domains, limiting natural interactions between the bone ECM and GFs. To overcome this limitation, several studies have explored the introduction of mineral-binding domains into GFs. Indeed, some bone ECM proteins such as osteocalcin (OC) can bind to hydroxyapatite (HA) minerals, the major inorganic component of bone tissue, through a C-terminal sequence (Dowd et al., 2003). For instance, a FGF-2-OC fusion protein displayed

a significantly stronger HA-binding affinity than wild-type FGF-2 and retained its bone repair and regeneration properties (Jeon and Jang, 2009).

STABILITY ENHANCEMENT

As mentioned earlier, some of the major limitations of GFs are their poor stability in physiological environment and rapid enzymatic degradation. The following section focuses on modifying the thermal stability and protease-resistance of GFs (**Figure 1B**), although other factors not detailed here can also reduce the stability of GFs. It is however noteworthy that decreasing the natural clearance rate of GFs from the body may requires additional side-effects monitoring.

Improving Thermal Stability

A common method to improve thermal stability of GFs is attaching a stable polypeptide or molecule, such as PEG, onto either terminal of the protein. The addition of PEG to GFs, or PEGylation, has been successfully applied clinically as the method of choice for extending protein half-life due to its flexibility, hydrophilicity, and low toxicity. To date, the USFDA has approved more than 15 PEGylated protein therapeutic products, and more are under development (Ramos-de-la-Peña and Aguilar, 2019). For instance, IGF-I is a mitogenic GF capable of stimulating anabolic processes in tissue repair and regeneration but is limited by its short half-life. Thus, a modified IGF-I was engineered through site-specific PEGylation and remained stable up to 8 h when exposed to 10% human serum. Moreover, this engineered IGF-1 showed a 3-fold increase in serum stability after 18 h incubation compared to wild-type IGF-I (Braun et al., 2018). Additionally, although PEGylated molecules often show a reduced bioactivity (Simone Fishburn, 2008; Braun et al., 2018), the site-specific nature of the modification allowed the preservation of IGF-I activity. Other molecules can also enhance the half-life of GFs. For example, conjugation of apolipoprotein A-I to the C-terminus of FGF-19 led to a 10-fold increase in circulating half-life (Alvarez-Sola et al., 2017).

Genetic modification is another effective approach to reinforce thermal stability of GFs. Indeed, the amino acid sequence of GFs can be edited to reinforce the local conformation and strengthen their tertiary structure. For instance, by introducing a triple mutation to FGF-1 increasing van der Waals forces and steric strains, a 21.5°C increase in denaturation temperature compared to wild-type FGF-1 was observed (Zakrzewska et al., 2005; Szlachcic et al., 2009). In addition, disulphide bonds are critical components of the protein structure which can greatly enhance its stability, thereby promoting bioactivity (Wedemeyer et al., 2000). In that regard, FGF-1 contains an unpaired cysteine at position 83 contributing to its poor stability. Therefore, by applying site-specific mutagenesis, Ala66 was replaced by a cysteine to introduce a disulphide bond between position 66 and 83. This variant showed a 14-fold increase in half-life and 10-fold increase in mitogenic activity (Kobielak et al., 2014).

Reducing Extracellular Proteolytic Degradation

As an indispensable element during wound healing and regeneration, proteases regulate the clearance of damaged proteins and matrix and facilitate cell infiltration (Schultz and Wysocki, 2009). However, in some cases, proteases impair tissue repair through excessive tissue degradation. Especially in chronic wounds, stimuli such as bacteria, foreign material, and impaired tissue lead to elevated and prolonged presence of proteases at the wound site. This aberrant expression of tissue-degrading enzymes results not only in poor healing outcomes, but in the degradation of pro-regenerative growth factors (Schultz and Wysocki, 2009; Harding et al., 2011; McCarty and Percival, 2013). Therefore, altering the protease-sensitive sites that naturally occurs within GFs can be an efficient method to enhance their activity. For instance, two mutations introduced at a known cleavage site in FGF-1, has demonstrated to significantly increase the proteolytic resistance of the protein up to 100-fold (Schultz and Wysocki, 2009). A similar strategy has been used for VEGF-A (Lauer et al., 2002; Traub et al., 2013).

MODIFYING GFs SIGNALING AND FUNCTIONALITY

The signaling properties of GFs can be modified to enhance their regenerative activity. The next section focuses on different approaches that attempt to modify the sequence or the structure of GFs to promote their function (**Figure 1C**), thereby effecting similar or altogether different responses at lower doses. Although those strategies have the potential to produce highly effective modified GFs, they may require longer development as the effects of modified signaling may be less predictable than those of improved delivery or stability.

Binding Affinity Modification

Binding affinities between GFs and their receptors can be modified to induce alternative signaling (Spangler et al., 2015). Whether higher or lower binding affinity is required is highly dependent on the receptor-ligand system and can lead to enhancement or abrogation of signaling in either case. For instance, site-directed mutagenesis to the residues Ile 38, Glu 51 and Leu 52 of epidermal growth factor (EGF) produced mutants with up to 30 fold higher affinity for EGF receptor (EGFR) (Cochran et al., 2006; Lahti et al., 2011). However, high affinity ligands may trigger a fast receptor internalization and degradation abrogating their signaling. Inversely, low affinity ligands may preserve the receptor leading to a longer lasting signaling (Zaiss et al., 2015).

In the EGF-EGFR signaling pathway, ligands which dissociate from the receptor within the endosome preferentially sort toward recycling rather than lysosomal fusion. Ligands that remain bound are degraded with the receptor, leading not only to receptor downregulation, but ligand depletion. Therefore, the

sustained signaling response from EGF mutant with lower binding affinity, may elicit greater cell proliferation (Reddy et al., 1996; Zaiss et al., 2015).

Synergistic Signaling

Although protein engineering allows numerous ways to engineer delivery mechanisms and systemic or local degradation kinetics, perhaps the most unique aspect of this field is the ability to confer non-canonical functionality to GFs for the purposes of promoting regeneration. In terms of circumventing the clinical limitations of GFs, there are several stages in the process that can be modified. GFs can be engineered to engage alternative signaling pathways through the creation of hybrid proteins. For example, there is significant crosstalk between integrin signaling and growth factor receptors such as VEGFR-2 and EGFR (Mahabeleshwar et al., 2008; Brizzi et al., 2012). The integrin-binding type III 10^{th} repeat of fibronectin (FNIII10) was fused to VEGF-A to create a bi-functional engineered protein (FNIII10-VEGF-A) with the ability to bind both VEGFR-2 and integrin αvβ3 (Traub et al., 2013). Surfaces coated with FNIII10-VEGF induced a significantly higher cell attachment and spreading of endothelial cells compared to FNIII10 or VEGF-A_{165}. However, even though FNIII10-VEGF immobilized in a fibrin matrix enhanced angiogenesis in a diabetic mouse skin wound model compared to soluble VEGF-A, the angiogenic response was reduced compared to the one induced by fibrin-immobilized VEGF-A. This suggests that although the crosstalk that exist between integrins and GF receptors could be used to induce improved regeneration, balancing the contribution of each signal is critical to optimize the desired effect.

Control of GFs Availability to Cell-Surface Receptor

Although the affinity of a GF for its receptor is critical in defining its effects, GF signaling can be controlled upstream of the GF-receptor interaction. Indeed, the availability of a GF for its receptor can be modulated not only by the ECM (Briquez et al., 2016) but also on the cell surface through binding to heparin sulfate proteoglycans (Rogers and Schier, 2011) such as syndecans (Kwon et al., 2012). In order to use the ability of syndecans to modulate GFs signaling, a syndecan-binding domain (SB) from laminin subunit α1 was fused to PDGF-BB (PDGF-BB-SB) and VEGF-A (VEGF-A-SB) to create syndecan-binding variants (Mochizuki et al., 2019). The controlled availability of PDGF-BB-SB and VEGF-A-SB for their cognate receptor on mesenchymal stem cells and endothelial cells, respectively, led to a long-lasting tonic signal as opposed to the short-lived burst signal induced by their wild type counterparts. Moreover, PDGF-BB-SB induced a significantly improved bone regeneration in a mouse bone defect model compared to PDGF-BB while VEGF-A-SB successfully improved skin wound healing in diabetic mice compared to wild-type VEGF-A. Interestingly, the engineered GFs abrogated common side-effects associated with clinical use of PDGF-BB and VEGF-A, respectively cancer risks and vascular permeability.

CONCLUSION AND PERSPECTIVES

Due to their critical role in tissue development and healing, GFs are ideal candidates for developing regenerative medicine therapies, but examples of successful clinical applications of GFs are still scarce. Throughout evolution, GFs have been selected to carry out specific tasks in specific environments, while being produced as needed by cells. However, their use in regenerative medicine requires to push the boundaries of their natural functions and is therefore met with limitations, such as instability or rapid diffusion from the delivery site. Trying to circumvent those limitations by delivering multiple supraphysiological doses has proven unsafe and thus highlights the need for the development of novel delivery systems (Niu et al., 2018).

The GF engineering approach is promising and generally aims at modulating the bioactivity and stability of GFs or controlling their interaction with biomaterials and the endogenous ECM. These different approaches present the advantage of being compatible with one another. It would be indeed possible to increase the bioactivity and stability of a GF while simultaneously increasing its affinity for the ECM or a biomaterial, opening the door to numerous new technologies. It is however important to note that as promising as these new technologies are, none of them are likely to represent a universal solution. Most GFs have their particular set of limitations and will require the development of new approaches for regenerative medicine to fully tap in their potential.

Future strategies in GF-based regenerative therapies may benefit by embracing a more comprehensive approach to tissue repair, as it is now evident that the immune system plays a critical role in the regenerative process (Julier et al., 2017; Larouche et al., 2018). Thus, future strategies may benefit from the co-delivery of GFs and immunomodulators or the development of multifunctional fusion proteins, with the ability of promoting morphogenesis while modulating the immune system. Moreover, most of the delivery strategies that we covered here aimed at improving the GF release and stability at the delivery site. However, several conditions, in particular ischemic injuries such as stroke or myocardial infarcts, occur at sites that are difficult to reach without invasive surgical procedures. Therefore, one of the main challenges that lies ahead is the development of engineered GFs with the ability to target distant sites.

AUTHOR CONTRIBUTIONS

XR, MZ, BL, MM, and ZJ wrote the manuscript. XR, MM, and ZJ made the tables and figure. MM and ZJ supervised the writing.

FUNDING

This work was supported in part by the Australian Research Council (DE170100398), the National Health and Medical Research Council (APP1140229) to MM and the Swiss National Science Foundation (P400PM_183891) to ZJ.

REFERENCES

Aldag, C., Nogueira Teixeira, D., and Leventhal, P. S. (2016). Skin rejuvenation using cosmetic products containing growth factors, cytokines, and matrikines: a review of the literature. *Clin. Cosmet. Investig. Dermatol.* 9, 411–419. doi: 10.2147/CCID.S116158

Alvarez-Sola, G., Uriarte, I., Latasa, M. U., Fernandez-Barrena, M. G., Urtasun, R., Elizalde, M., et al. (2017). Fibroblast growth factor 15/19 (FGF15/19) protects from diet-induced hepatic steatosis: development of an FGF19-based chimeric molecule to promote fatty liver regeneration. *Gut* 66, 1818–1828. doi: 10.1136/gutjnl-2016-312975

Beenken, A., and Mohammadi, M. (2009). The FGF family: biology, pathophysiology and therapy. *Nat. Rev. Drug Discov.* 8, 235–253. doi: 10.1038/nrd2792

Boonrungsiman, S., Gentleman, E., Carzaniga, R., Evans, N. D., McComb, D. W., Porter, A. E., et al. (2012). The role of intracellular calcium phosphate in osteoblast-mediated bone apatite formation. *Proc. Natl. Acad. Sci. U.S.A.* 109, 14170–14175. doi: 10.1073/pnas.1208916109

Bouyer, M., Guillot, R., Lavaud, J., Plettinx, C., Olivier, C., Curry, V., et al. (2016). Surface delivery of tunable doses of BMP-2 from an adaptable polymeric scaffold induces volumetric bone regeneration. *Biomaterials* 104, 168–181. doi: 10.1016/j.biomaterials.2016.06.001

Braun, A. C., Gutmann, M., Mueller, T. D., Lühmann, T., and Meinel, L. (2018). Bioresponsive release of insulin-like growth factor-I from its PEGylated conjugate. *J. Control. Release* 279, 17–28. doi: 10.1016/j.jconrel.2018.04.009

Briquez, P. S., Clegg, L. E., Martino, M. M., Gabhann, F., Mac, and Hubbell, J. A. (2016). Design principles for therapeutic angiogenic materials. *Nat. Rev. Mater.* 1, 1–15. doi: 10.1038/natrevmats.2015.6

Brizzi, M. F., Tarone, G., and Defilippi, P. (2012). Extracellular matrix, integrins, and growth factors as tailors of the stem cell niche. *Curr. Opin. Cell Biol.* 24, 645–651. doi: 10.1016/j.ceb.2012.07.001

Cabanas-Danés, J., Huskens, J., and Jonkheijm, P. (2014). Chemical strategies for the presentation and delivery of growth factors. *J. Mater. Chem. B.* doi: 10.1039/C3TB20853B

Calori, G. M., Donati, D., Di Bella, C., and Tagliabue, L. (2009). Bone morphogenetic proteins and tissue engineering: future directions. *Injury* 40 (Suppl. 3), S67–S76. doi: 10.1016/S0020-1383(09)70015-4

Carragee, E. J., Chu, G., Rohatgi, R., Hurwitz, E. L., Weiner, B. K., Yoon, S. T., et al. (2013). Cancer risk after use of recombinant bone morphogenetic protein-2 for spinal arthrodesis. *J. Bone Jt. Surgery-American Vol.* 95, 1537–1545. doi: 10.2106/JBJS.L.01483

Carreira, A. C., Alves, G. G., Zambuzzi, W. F., Sogayar, M. C., and Granjeiro, J. M. (2014). Bone morphogenetic proteins: structure, biological function and therapeutic applications. *Arch. Biochem. Biophys.* 561, 64–73. doi: 10.1016/j.abb.2014.07.011

Cochran, J. R., Kim, Y. S., Lippow, S. M., Rao, B., and Wittrup, K. D. (2006). Improved mutants from directed evolution are biased to orthologous substitutions. *Protein Eng. Des. Sel.* 19, 245–253. doi: 10.1093/protein/gzl006

Dowd, T. L., Rosen, J. F., Li, L., and Gundberg, C. M. (2003). The three-dimensional structure of bovine calcium ion-bound osteocalcin using1H NMR spectroscopy. *Biochemistry* 42, 7769–7779. doi: 10.1021/bi034470s

Ehrbar, M., Rizzi, S. C., Schoenmakers, R. G., San Miguel, B., Hubbell, J. A., Weber, F. E., et al. (2007). Biomolecular hydrogels formed and degraded via site-specific enzymatic reactions. *Biomacromolecules* 8, 3000–3007. doi: 10.1021/bm070228f

FDA (2004a). *Clinical Pharmacology and Biopharmaceutics Review*. FDA.

FDA (2004b). *Kepivance^{TM} (palifermin)*. FDA.

FDA (2005). Increlex (Mecasermin [rDNA origin]) *Injection*.

FDA (2008). *Safety Warning on Becaplermin in Regranex®*. FDA.

FDA (2015a). *Augment® Bone Graft SSED*. FDA.

FDA (2015b). *Palifermin (marketed as Kepivance)*. FDA.

Frew, S. E., Rezaie, R., Sammut, S. M., Ray, M., Daar, A. S., and Singer, P. A. (2007). India's health biotech sector at a crossroads. *Nat. Biotechnol.* 25, 403–417. doi: 10.1038/nbt0407-403

Grabarek, Z., and Gergely, J. (1990). Zero-length crosslinking procedure with the use of active esters. *Anal. Biochem.* 185, 131–135. doi: 10.1016/0003-2697(90)90267-D

Güç, E., Briquez, P. S., Foretay, D., Fankhauser, M. A., Hubbell, J. A., Kilarski, W. W., et al. (2017). Local induction of lymphangiogenesis with engineered fibrin-binding VEGF-C promotes wound healing by increasing immune cell trafficking and matrix remodeling. *Biomaterials* 131, 160–175. doi: 10.1016/j.biomaterials.2017.03.033

Harding, K., Armstrong, D. G., Barrett, S., Kaufman, H., Lazaro-Martinez, J. L., Mayer, D., et al. (2011). *The Role of Proteases in Wound Diagnostics*. Wounds International.

Hermonat, P. L., Li, D., Yang, B., and Mehta, J. L. (2007). Mechanism of action and delivery possibilities for TGFβ1 in the treatment of myocardial ischemia. *Cardiovasc. Res.*74, 235–243. doi: 10.1016/j.cardiores.2007.01.016

Inoue, G., Uchida, K., Matsushita, O., Fujimaki, H., Saito, W., Miyagi, M., et al. (2017). Effect of freeze-dried allograft bone with human basic fibroblast growth factor containing a collagen-binding domain from clostridium histolyticum collagenase on bone formation after lumbar posterolateral fusion surgery in rats. *Spine* 42, E995–E1001. doi: 10.1097/BRS.0000000000002074

James, A. W., LaChaud, G., Shen, J., Asatrian, G., Nguyen, V., Zhang, X., et al. (2016). A review of the clinical side effects of bone morphogenetic protein-2. *Tissue Eng. Part B Rev.* 22, 284–297. doi: 10.1089/ten.teb.2015.0357

Jeon, E., and Jang, J. H. (2009). Protein engineering of a fibroblast growth factor 2 protein for targeting to bone mineral hydroxyapatite. *Protein Pept. Lett.* 16, 664–667. doi: 10.2174/092986609788490267

Jin, Q., Wei, G., Lin, Z., Sugai, J. V., Lynch, S. E., Ma, P. X., et al. (2008). Nanofibrous scaffolds incorporating PDGF-BB microspheres induce chemokine expression and tissue neogenesis *in vivo*. *PLoS ONE* 3:e1729. doi: 10.1371/journal.pone.0001729

Julier, Z., Park, A. J., Briquez, P. S., and Martino, M. M. (2017). Promoting tissue regeneration by modulating the immune system. *Acta Biomater.* 53, 13–28. doi: 10.1016/j.actbio.2017.01.056

Kakudo, N., Morimoto, N., Ogawa, T., Taketani, S., and Kusumoto, K. (2019). FGF-2 combined with bilayer artificial dermis composed of collagen matrix prompts generation of fat pad in subcutis of mice. *Med. Mol. Morphol.* 52, 73–81. doi: 10.1007/s00795-018-0203-1

Kobielak, A., Zakrzewska, M., Kostas, M., Jakimowicz, P., Otlewski, J., and Krowarsch, D. (2014). Protease resistant variants of FGF1 with prolonged biological activity. *Protein Pept. Lett.* 21, 434–443. doi: 10.2174/0929866520666131203102315

Kowtharapu, B. S., Prakasam, R. K., Murín, R., Koczan, D., Stahnke, T., Wree, A., et al. (2018). Role of bone morphogenetic protein 7 (BMP7) in the modulation of corneal stromal and epithelial cell functions. *Int. J. Mol. Sci.* 19:E1415. doi: 10.3390/ijms19051415

Kwon, M. J., Jang, B., Yi, J. Y., Han, I. O., and Oh, E. S. (2012). Syndecans play dual roles as cell adhesion receptors and docking receptors. *FEBS Lett.* 586, 2207–2211. doi: 10.1016/j.febslet.2012.05.037

Lahti, J. L., Lui, B. H., Beck, S. E., Lee, S. S., Ly, D. P., Longaker, M. T., et al. (2011). Engineered epidermal growth factor mutants with faster binding on-rates correlate with enhanced receptor activation. *FEBS Lett.* 585, 1135–1139. doi: 10.1016/j.febslet.2011.03.044

Larouche, J., Sheoran, S., Maruyama, K., and Martino, M. M. (2018). Immune regulation of skin wound healing: mechanisms and novel therapeutic targets. *Adv. Wound Care* 7, 209–231. doi: 10.1089/wound.2017.0761

Lauer, G., Sollberg, S., Cole, M., Krieg, T., and Eming, S. A. (2002). Generation of a novel proteolysis resistant vascular endothelial growth factor165 variant by a site-directed mutation at the plasmin sensitive cleavage site. *FEBS Lett.* 531, 309–313. doi: 10.1016/S0014-5793(02)03545-7

Lee, K., Silva, E. A., and Mooney, D. J. (2011). Growth factor delivery-based tissue engineering: general approaches and a review of recent developments. *J. R. Soc. Interface.* 8, 153–170. doi: 10.1098/rsif.2010.0223

Leroith, D., McGuinness, M., Shemer, J., Stannard, B., Lanau, F., Faria, T. N., et al. (1992). Insulin-like growth factors. *Neurosignals* 1, 173–181. doi: 10.1159/000109323

Logue, O. C., Mahdi, F., Chapman, H., George, E. M., and Bidwell, G. L. (2017). A maternally sequestered, biopolymer-stabilized Vascular Endothelial Growth Factor (VEGF) chimera for treatment of preeclampsia. *J. Am. Heart Assoc.* 6:e007216. doi: 10.1161/JAHA.117.007216

Macri, L., Silverstein, D., and Clark, R. A. F. (2007). Growth factor binding to the pericellular matrix and its importance in tissue engineering. *Adv. Drug Deliv. Rev.* 59, 1366–1381. doi: 10.1016/j.addr.2007.08.015

Maddaluno, L., Urwyler, C., and Werner, S. (2017). Fibroblast growth factors: key players in regeneration and tissue repair. *Development* 144, 4047–4060. doi: 10.1242/dev.152587

Mahabeleshwar, G. H., Chen, J., Feng, W., Somanath, P. R., Razorenova, O. V., and Byzova, T. V. (2008). Integrin affinity modulation in angiogenesis. *Cell Cycle* 7, 335–347. doi: 10.4161/cc.7.3.5234

Mao, A. S., and Mooney, D. J. (2015). Regenerative medicine: current therapies and future directions. *Proc. Natl. Acad. Sci. U.S.A.* 112, 14452–14459. doi: 10.1073/pnas.1508520112

Martino, M. M., Briquez, P. S., Güç, E., Tortelli, F., Kilarski, W. W., Metzger, S., et al. (2014). Growth factors engineered for super-affinity to the extracellular matrix enhance tissue healing. *Science* 343, 885–888. doi: 10.1126/science.1247663

Martino, M. M., Briquez, P. S., Ranga, A., Lutolf, M. P., and Hubbell, J., a (2013). Heparin-binding domain of fibrin(ogen) binds growth factors and promotes tissue repair when incorporated within a synthetic matrix. *Proc. Natl. Acad. Sci. U.S.A.* 110, 4563–4568. doi: 10.1073/pnas.1221602110

Masters, K. S. (2011). Covalent Growth Factor Immobilization Strategies for tissue repair and regeneration. *Macromol. Biosci.* 11, 1149–1163. doi: 10.1002/mabi.201000505

McCarty, S. M., and Percival, S. L. (2013). Proteases and delayed wound healing. *Adv. Wound Care* 2, 438–447. doi: 10.1089/wound.2012.0370

Mitchell, A. C., Briquez, P. S., Hubbell, J. A., and Cochran, J. R. (2016). Engineering growth factors for regenerative medicine applications. *Acta Biomater.* 30, 1–12. doi: 10.1016/j.actbio.2015.11.007

Mittermayr, R., Slezak, P., Haffner, N., Smolen, D., Hartinger, J., Hofmann, A., et al. (2016). Controlled release of fibrin matrix-conjugated platelet derived growth factor improves ischemic tissue regeneration by functional angiogenesis. *Acta Biomater.* 29, 11–20. doi: 10.1016/j.actbio.2015.10.028

Mochizuki, M., Güç, E., Park, A. J., Julier, Z., Briquez, P. S., A., et al. (2019). Growth factors with enhanced syndecan binding generate tonic signalling and promote tissue healing. *Nat. Biomed. Eng.* doi: 10.1038/s41551-019-0469-1. [Epub ahead of print].

Nakamura, R., Katsuno, T., Kitamura, M., Yamashita, M., Tsuji, T., Suzuki, R., et al. (2019). Collagen sponge scaffolds containing growth factors for the functional regeneration of tracheal epithelium. *J. Tissue Eng. Regen. Med.* 13, 835–845. doi: 10.1002/term.2835

National Drug Strategy (2006). *Performance and Image Enhancing Grugs - What is Insulin-life Growth Factor(IGF-1).* National Drug Strategy.

Niu, Y., Li, Q., Ding, Y., Dong, L., and Wang, C. (2018). Engineered delivery strategies for enhanced control of growth factor activities in wound healing. *Adv. Drug Deliv. Rev.* 146, 190–208. doi: 10.1016/j.addr.2018.06.002

Okabe, K., Hayashi, R., Aramaki-Hattori, N., Sakamoto, Y., and Kishi, K. (2013). Wound treatment using growth factors. *Mod. Plast. Surg.* 3, 108–112. doi: 10.4236/mps.2013.33022

Park, S. H., Uzawa, T., Hattori, F., Ogino, S., Morimoto, N., Tsuneda, S., et al. (2018). "All-in-one" *in vitro* selection of collagen-binding vascular endothelial growth factor. *Biomaterials* 161, 270–278. doi: 10.1016/j.biomaterials.2018.01.055

Ramos-de-la-Peña, A. M., and Aguilar, O. (2019). Progress and challenges in PEGylated proteins downstream processing: a review of the last 8 years. *Int. J. Pept. Res. Ther.* 1–16. doi: 10.1007/s10989-019-09840-4

Reddy, C. C., Niyog, S. K., Wells, A., Wiley, H. S., and Lauffenburger, D. A. (1996). Engineering epidermal growth factor for enhanced mitogenic potency. *Nat. Biotechnol.* 14, 1696–1699. doi: 10.1038/nbt1296-1696

Rogers, K. W., and Schier, A. F. (2011). Morphogen gradients: from generation to interpretation. *Annu. Rev. Cell Dev. Biol.* 27, 377–407. doi: 10.1146/annurev-cellbio-092910-154148

Sacchi, V., Mittermayr, R., Hartinger, J., Martino, M. M., Lorentz, K. M., Wolbank, S., et al. (2014). Long-lasting fibrin matrices ensure stable and functional angiogenesis by highly tunable, sustained delivery of recombinant VEGF164. *Proc. Natl. Acad. Sci. U.S.A.* 111, 6952–6957. doi: 10.1073/pnas.1404605111

Saika, J. E., Gould, D. J., Watkins, E. M., Dickinson, M. E., and West, J. L. (2011). Covalently immobilized platelet-derived growth factor-BB promotes angiogenesis in biomimetic poly(ethylene glycol) hydrogels. *Acta Biomater.* 7, 133–143. doi: 10.1016/j.actbio.2010.08.018

Sawicka, K. M., Seeliger, M., Musaev, T., Macri, L. K., and Clark, R. A. F. (2015). Fibronectin interaction and enhancement of growth factors: importance for wound healing. *Adv. Wound Care* 4, 469–478. doi: 10.1089/wound.2014.0616

Schense, J. C., and Hubbell, J. A. (1999). Cross-linking exogenous bifunctional peptides into fibrin gels with factor XIIIa. *Bioconjug. Chem.* 10, 75–81. doi: 10.1021/bc9800769

Schmoekel, H. G., Weber, F. E., Schense, J. C., Grätz, K. W., Schawalder, P., and Hubbell, J. A. (2005). Bone repair with a form of BMP-2 engineered for incorporation into fibrin cell ingrowth matrices. *Biotechnol. Bioeng.* 89, 253–262. doi: 10.1002/bit.20168

Schultz, G. S., and Wysocki, A. (2009). Interactions between extracellular matrix and growth factors in wound healing. *Wound Repair Regen.* doi: 10.1111/j.1524-475X.2009.00466.x

Sekiguchi, H., Uchida, K., Matsushita, O., Inoue, G., Nishi, N., Masuda, R., et al. (2018). Basic fibroblast growth factor fused with tandem collagen-binding domains from clostridium histolyticum collagenase colg increases bone formation. *Biomed Res. Int.* 2018, 1-8. doi: 10.1155/2018/8393194

Simone Fishburn, C. (2008). The pharmacology of PEGylation: balancing PD with PK to generate novel therapeutics. *J. Pharm. Sci.* 17, 153–162. doi: 10.1002/jps.21278

Simons, M., and Ware, J. A. (2003). Therapeutic angiogenesis in cardiovascular disease. *Nat. Rev. Drug Discov.* 2, 863–871. doi: 10.1038/nrd1226

Spangler, J. B., Moraga, I., Mendoza, J. L., and Garcia, K. C. (2015). Insights into cytokine–receptor interactions from cytokine engineering. *Annu. Rev. Immunol.* 33, 139–167. doi: 10.1146/annurev-immunol-032713-120211

Stefanini, M. O., Wu, F. T. H., Mac Gabhann, F., and Popel, A. S. (2008). A compartment model of VEGF distribution in blood, healthy and diseased tissues. *BMC Syst. Biol.* 2:77. doi: 10.1186/1752-0509-2-77

Szlachcic, A., Zakrzewska, M., Krowarsch, D., Os, V., Helland, R., Smalås, A. O., et al. (2009). Structure of a highly stable mutant of human fibroblast growth factor 1. *Acta Crystallogr. Sect. D Biol. Crystallogr.* D65, 67–73. doi: 10.1107/S0907444908039486

Tian, M., Neil, J. R., and Schiemann, W. P. (2011). Transforming growth factor-β and the hallmarks of cancer. *Cell. Signal.* 23, 951–962. doi: 10.1016/j.cellsig.2010.10.015

Traub, S., Morgner, J., Martino, M. M., Höning, S., Swartz, M. A., Wickström, S. A., et al. (2013). The promotion of endothelial cell attachment and spreading using FNIII10 fused to VEGF-A165. *Biomaterials* 34, 5958–5968. doi: 10.1016/j.biomaterials.2013.04.050

Vardar, E., Larsson, H. M., Allazetta, S., Engelhardt, E. M., Pinnagoda, K., Vythilingam, G., et al. (2018). Microfluidic production of bioactive fibrin micro-beads embedded in crosslinked collagen used as an injectable bulking agent for urinary incontinence treatment. *Acta Biomater.* 67, 156–166. doi: 10.1016/j.actbio.2017.11.034

Wang, L., Yang, M., Jin, M., Wu, Y., Zheng, T., Gu, S., et al. (2018). Transplant of insulin-like growth factor-1 expressing bone marrow stem cells improves functional regeneration of injured rat uterus by NF-κB pathway. *J. Cell. Mol. Med.* 22, 2815–2825. doi: 10.1111/jcmm.13574

Wang, Z., Wang, Z., Lu, W. W., Zhen, W., Yang, D., and Peng, S. (2017). Novel biomaterial strategies for controlled growth factor delivery for biomedical applications. *NPG Asia Mater.* 9: e435. doi: 10.1038/am.2017.171

Wedemeyer, W. J., Welker, E., Narayan, M., and Scheraga, H. A. (2000). Disulfide bonds and protein folding. *Biochemistry* 39, 4207–4216. doi: 10.1021/bi992922o

Yamakawa, S., and Hayashida, K. (2019). Advances in surgical applications of growth factors for wound healing. *Burn. Trauma* 7, 1–14. doi: 10.1186/s41038-019-0148-1

Yamane, K., Mazaki, T., Shiozaki, Y., Yoshida, A., Shinohara, K., Nakamura, M., et al. (2018). Collagen-binding Hepatocyte Growth Factor (HGF) alone or with a gelatin-furfurylamine hydrogel enhances functional recovery in mice after spinal cord injury. *Sci. Rep.* 8, 1–12. doi: 10.1038/s41598-018-19316-y

Yu, Y., Yao, A. H., Chen, N., Pu, L. Y., Fan, Y., Lv, L., et al. (2007). Mesenchymal stem cells over-expressing hepatocyte growth factor improve small-for-size liver grafts regeneration. *Mol. Ther.* 15, 1382–1389. doi: 10.1038/sj.mt.6300202

Zaiss, D. M. W., Gause, W. C., Osborne, L. C., and Artis, D. (2015). Emerging functions of amphiregulin in orchestrating immunity, inflammation, and tissue repair. *Immunity* 42, 216–226. doi: 10.1016/j.immuni.2015.01.020

Zakrzewska, M., Krowarsch, D., Wiedlocha, A., Olsnes, S., and Otlewski, J. (2005). Highly stable mutants of human fibroblast growth factor-1 exhibit prolonged biological action. *J. Mol. Biol.* 352, 860–875. doi: 10.1016/j.jmb.2005.07.066

Conflict of Interest: The authors declare that the research was conducted in the absence of any commercial or financial relationships that could be construed as a potential conflict of interest.

frontiers in Bioengineering and Biotechnology

ORIGINAL RESEARCH
published: 24 January 2020
doi: 10.3389/fbioe.2020.00004

Stable Chitosan-Based Nanoparticles Using Polyphosphoric Acid or Hexametaphosphate for Tandem Ionotropic/Covalent Crosslinking and Subsequent Investigation as Novel Vehicles for Drug Delivery

Ramzi Mukred Saeed[1], *Isra Dmour*[2] *and Mutasem O. Taha*[1,3]*

[1] Department of Pharmaceutical Sciences, Faculty of Pharmacy, University of Jordan, Amman, Jordan, [2] Faculty of Pharmacy and Medical Sciences, Al-Ahliyya Amman University, Amman, Jordan, [3] Department of Pharmaceutical Chemistry and Pharmacognosy, Faculty of Pharmacy, Applied Science Private University, Amman, Jordan

OPEN ACCESS

Edited by:
Filippo Rossi,
Politecnico di Milano, Italy

Reviewed by:
Emanuele Mauri,
Campus Bio-Medico University, Italy
Mattia Sponchioni,
ETH Zürich, Switzerland

***Correspondence:**
Mutasem O. Taha
mutasem@ju.edu.jo

Specialty section:
This article was submitted to Nanobiotechnology, a section of the journal Frontiers in Bioengineering and Biotechnology

Received: 26 August 2019
Accepted: 06 January 2020
Published: 24 January 2020

Citation:
Saeed RM, Dmour I and Taha MO (2020) Stable Chitosan-Based Nanoparticles Using Polyphosphoric Acid or Hexametaphosphate for Tandem Ionotropic/Covalent Crosslinking and Subsequent Investigation as Novel Vehicles for Drug Delivery. Front. Bioeng. Biotechnol. 8:4. doi: 10.3389/fbioe.2020.00004

Chitosan nanoparticles (NPs) are widely studied as vehicles for drug, protein, and gene delivery. However, lack of sufficient stability, particularly under physiological conditions, render chitosan NPs of limited pharmaceutical utility. The aim of this study is to produce stable chitosan NPs suitable for drug delivery applications. Chitosan was first grafted to phthalic or phenylsuccinic acids. Subsequently, polyphosphoric acid (PPA), hexametaphosphate (HMP), or tripolyphosphate (TPP) were used to achieve tandem ionotropic/covalently crosslinked chitosan NPs in the presence of 1-ethyl-3-(3-dimethylaminopropyl)-carbodiimide (EDC). Thermal and infrared traits confirmed phosphoramide bonds formation tying chitosan with the polyphosphate crosslinkers within NPs matrices. DLS and TEM size analysis indicated spherical NPs with size range of 120 to 350 nm. The generated NPs exhibited excellent stabilities under harsh pH, $CaCl_2$, and 10% FBS conditions. Interestingly, DLS, NPs stability and infrared data suggest HMP to reside within NPs cores, while TPP and PPA to act mainly as NPs surface crosslinkers. Drug loading and release studies using methylene blue (MB) and doxorubicin (DOX) drug models showed covalent PPA- and HMP-based NPs to have superior loading capacities compared to NPs based on unmodified chitosan, generated by ionotropic crosslinking only or covalently crosslinked by TPP. Doxorubicin-loaded NPs were of superior cytotoxic properties against MCF-7 cells compared to free doxorubicin. Specifically, DOX-loaded chitosan-phthalate polyphosphoric acid-crosslinked NPs exhibited 10-folds cytotoxicity enhancement compared to free DOX. The use of PPA and HMP to produce covalently-stabilized chitosan NPs is completely novel.

Keywords: chitosan, ionotropic gelation, polyphosphoric acid, hexametaphosphate, phosphoramide bond, doxorubicin

INTRODUCTION

Chitosan (C) is a semisynthetic polyaminosaccharide obtained by N-deacetylation of chitin. Chitosan has attracted attention in various biomedical, pharmaceutical, food, and environmental fields due to its safe profile, biodegradability, and biocompatibility, in addition to its bacteriostatic and mucoadhesive properties (Alves and Mano, 2008; Riva et al., 2011; Miola et al., 2015; Silva et al., 2017; Bracharz et al., 2018; Dmour and Taha, 2018; Jiang and Wu, 2019; Savin et al., 2019).

Chitosan nanoparticles (NPs) are widely studied as nanocarriers for drug, protein, and gene delivery systems (Almaaytah et al., 2018; Baghdan et al., 2018). Ionotropic gelation is the most studied formulation method for preparing chitosan NPs. It is based on electrostatic interaction between the positively-charged aminosugar monomeric units of chitosan and negatively-charged polyanions, e.g., tripolyphosphate (TPP, **Figure 1A**) or hexametaphosphate (HMP, **Figure 1B**), or dextran sulfate (Katas et al., 2013; Kiilll et al., 2017; Rassu et al., 2019). Although ionotropic chitosan NPs have many benefits as drug delivery systems, there are still many barriers to be resolved to realize their clinical potential. These include inadequate oral bioavailability, instability in blood circulation, and toxicity (Du et al., 2014).

NPs sizes and surface charges have significant implications on their biological properties such as cellular uptake and biodistribution *in vivo*. Nanoparticles of diameters ranging from 10 to 300 nm have been reported to cross the gaps in blood vessels supplying tumor cells without significant penetration to healthy tissues (Grossman and McNeil, 2012; Yan et al., 2015). Similarly, NPs with slight negative charges, i.e., under physiological pH, tend to accumulate in tumor cells more efficiently (Honary and Zahir, 2013).

HMP is non-toxic substance, widely used in food industry as a sequestering agent and food additive (Baig et al., 2005; Parab et al., 2011). HMP was also used as stabilizer of $BaSO_4$ (Gupta et al., 2010) and ZnCdS (Wang et al., 2011b) nanoparticles. Additionally, TPP and HMP have been reported as ionotropic crosslinking agents for the preparation of chitosan NPs for drug delivery purposes (Nair et al., 2019; Rassu et al., 2019; Su et al., 2019).

On the other hand, although polyphosphoric acid (PPA, **Figure 1C**) was never used as ionotropic crosslinking agent for the preparation of NPs, chitosan-PPA beads (microspheres) have been used as a delivery system for proteins and peptides (Yuan et al., 2018). PPA-coated NPs were also used for blood pool imaging *in vivo* (Peng et al., 2013).

Carbodiimide coupling agents, in particular, EDC (**Figure 1D**), have been utilized to immobilize enzymes on chitosan NPs to enhance enzymatic stability in solution (Sun et al., 2017). Additionally, EDC is useful for surface crosslinking/immobilization of medicinal compounds onto NPs to enhance their stabilities to variable pH or temperature conditions (Shen et al., 2009; Chaiyasan et al., 2015; Esfandiarpour-Boroujeni et al., 2016; Song et al., 2018). EDC was also used for covalent crosslinking and stabilization of doxorubicin-loaded chitosan-TPP NPs (Dmour and Taha, 2017), lutein-loaded chitosan-dextran NPs (Chaiyasan et al., 2015) and doxorubicin-loaded PEG-PLGA nanoparticles (Luo et al., 2019).

In this investigation, we describe the use of polyphosphoric acid (PPA) and sodium hexametaphosphate (HMP), for the first time, as tandem ionotropic/covalent crosslinkers for stabilizing chitosan-phthalate- and chitosan-phenylsuccinate based NPs in the presence of EDC.

HMP and PPA provide more anionic charges per molecule compared to TPP, as in **Figure 1**, which should offer more interaction sites for ionotropic crosslinking with chitosan's cationic ammonium groups. Moreover, HMP and PPA are non-toxic, and therefore, superior to covalent crosslinkers such as glutaraldehyde, genipin, and glyoxal, which tend to exhibit significant toxicities (Dmour and Taha, 2018). The resulting NPs were characterized vis-à-vis their size ranges, surface charges, and physical stabilities under harsh pH, $CaCl_2$, and FBS conditions. The generated NPs exhibited excellent stabilities under such conditions. Drug loading and release studies using methylene blue (MB, **Figure 1E**) and doxorubicin (DOX, **Figure 1F**) model drugs showed covalent PPA- and HMP-based NPs to have superior loading capacities and release profiles. DOX-loaded NPs showed enhanced cytotoxic properties compared to free doxorubicin.

MATERIALS AND METHODS

Materials

All chemicals were purchased from respective companies (in brackets) and were used without pretreatment or purification. Pyridine, absolute ethanol, and acetone of analytical grades (Carlo Erba France, and Labchem, USA). Medium molecular weight chitosan, phenylsuccinic anhydride, and sodium hexametaphosphate (HMP) (Sigma-Aldrich, USA). Polyphosphoric Acid (PPA) and phthalic anhydride (Fluka, Switzerland). Ultrapure water (conductivity = 0.05 μs/cm) for DLS size analysis (Millipore, USA).

Penta basic sodium tripolyphosphate (Sigma-Aldrich, Germany), N-ethyl-N′-(3-dimethylaminopropyl) carbodiimide hydrochlorides (EDC) (Sigma- Aldrich, USA), hydrochloric acid (37%) (Carlo Erba, Spain) and sodium hydroxide (Rasayan Laboratory, India). Dialysis tubing (molecular weight cutoff = 14 kDa, Sigma-Aldrich, USA), Tris base buffer (Bio Basic Inc., Canada), Methylene blue (Seelze, Germany), and Doxorubicin HCl (Ebwe Pharma, Austria). CellTiter Non-Radioactive Cell Proliferation Assay Kit from Promega (USA). RPMI 1640 medium and fetal bovine serum (FBS) were purchased from (Caissan, USA), L-glutamine, penicillin–streptomycin and trypsin-EDTA were purchased from (EURO Clone, Italy). 4′,6-Diamidino-2-phenylindole (DAPI) stain was purchased from Invitrogen (Thermo Fisher Scientific, USA). Poly-L-lysine obtained from (Sigma- Aldrich, Germany).

Synthesis of Chitosan-Dicarboxylic Acid Derivatives and Preparation of Corresponding NPs

Chitosan-dicarboxylic acid derivatives (chitosan-phthalate and chitosan phenyl succinate) were prepared as described earlier

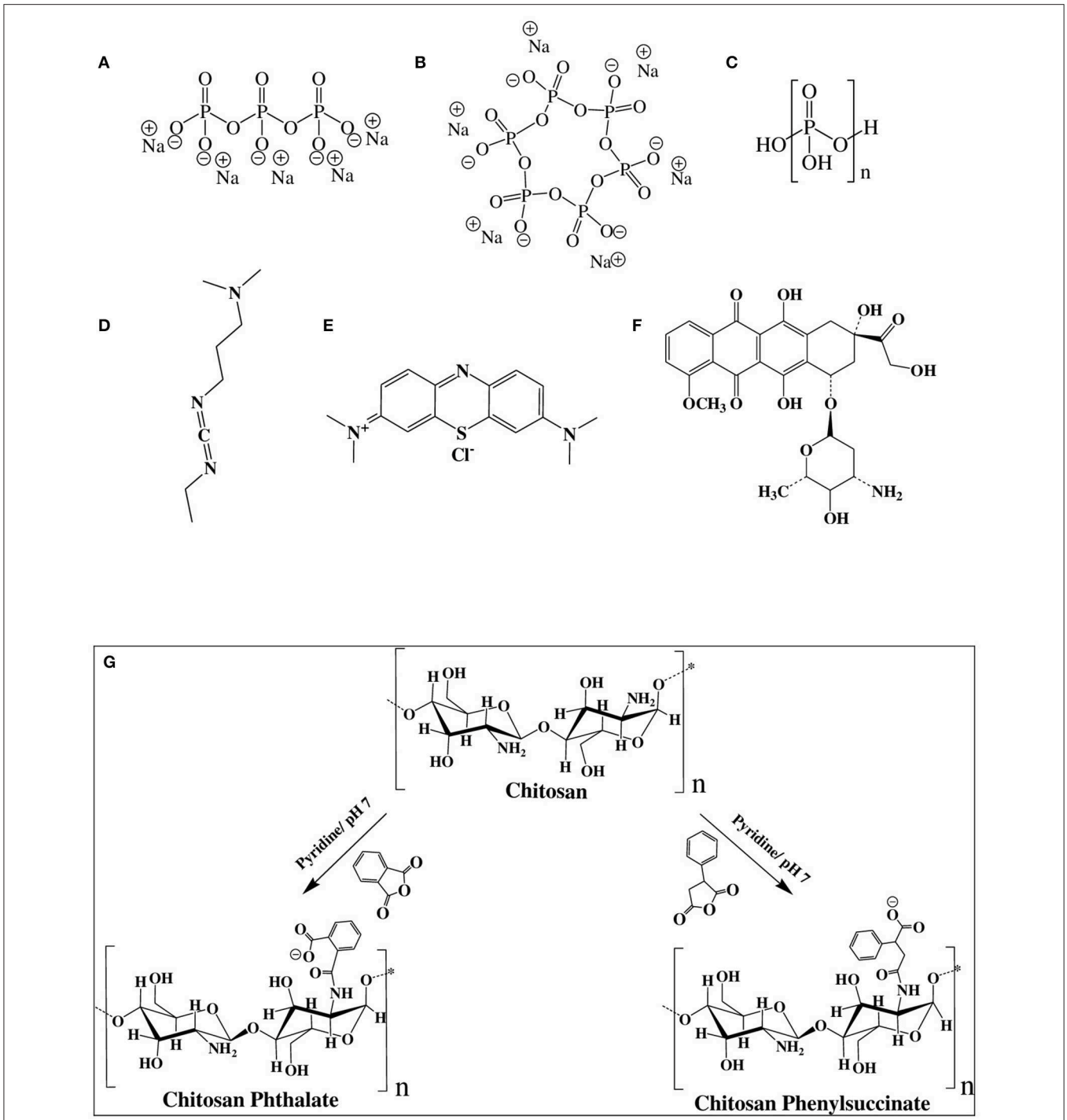

FIGURE 1 | Chemical structures of **(A)** sodium tripolyphosphate (TPP), **(B)** sodium hexametaphosphate (HMP), **(C)** polyphosphoric acid (PPA), **(D)** 1-ethyl-3-(3-dimethylaminopropyl) carbodiimide (EDC), **(E)** methylene blue (MB), **(F)** doxorubicin (DOX), and **(G)** Chemistry of grafting chitosan to phthalic and phenylsuccinic acids.

(Aiedeh and Taha, 1999) with slight modifications. Briefly, chitosan (1.00 g, corresponding to 5.58 mmol glucosamine) was dissolved in (50 ml) HCl (0.37% v/v) aqueous solution at ambient temperature. The particular anhydride (phthalic or phenylsuccinic acids, 2.5 or 5.0 mmol, respectively) was dissolved in (5 ml) pyridine and added dropwise to chitosan solution with vigorous stirring. NaOH (1.0 M) solution was added dropwise to the reaction mixture to maintain reaction pH at 7.0. The

reaction was allowed to continue for 40 min. Subsequently, the resulting chitosan derivative was precipitated by gradual addition of acetone under continuous stirring. The resulting precipitate was filtered, washed three times with absolute ethanol (100 ml), and finally with acetone (100 ml), and dried for 48 h in hot air oven at 35°C. The products were stored in airtight bottles.

Chitosan- and chitosan-carboxylate-based NPs were prepared using "syringe method" as described earlier (Calvo et al., 1997). Briefly, chitosan, or chitosan derivative, was dissolved by stirring for 48 h in aqueous HCl (4.8 mM) to produce 0.1%w/v solution. Wherever needed, the resulting solution was filtered or centrifuged at 4,000 rpm for 10 min at 25°C to remove any insoluble polymer residues. Subsequently, freshly prepared crosslinker aqueous solution, namely TPP (0.4%w/v), PPA (0.2%w/v activated by heating at 100°C for 1.5 h), or HMP (0.1% w/v) was added gradually, using syringe, to prepared chitosan, or chitosan-carboxylate solutions (5 ml) under vigorous magnetic stirring at 25°C until visual appearance of opalescent hazy dispersion (representing NPs formation). The resulting NPs were used for size and zeta potential analysis (i.e., dynamic light scattering, DLS) purposes without further processing.

The prepared NPs were covalently crosslinked using EDC as described earlier (Dmour and Taha, 2017). Briefly, EDC (25 mg) was added to NPs dispersions (5 ml) prepared from chitosan or its derivatives by ionotropic gelation method. The reaction mixture was stirred vigorously over 1 min, and then it was allowed to stand for 1 h. Subsequently, the reaction was terminated by one of the following ways: (1) For size, zeta potential and stability analysis purposes (which require minute amounts -μgs/ml- of NPs) the NPs dispersions (5 ml) were dialyzed against vigorously stirred deionized water (250 ml) for 1 min using dialysis tubing (molecular weight cutoff = 14 kDa) to remove EDC-urea byproduct and directly used for DLS. This should minimize any potential artifacts in NPs sizes or charges due separation methods (e.g., lyophilization or centrifugation) (Zhang et al., 2018) other than the influence of studied variables, i.e., pH, Ca^{2+}, and FBS. (2) For dissolution, *in vitro* release studies, and cell lines cytotoxicity studies (which require significantly more amounts of NPs – *ca.* mg/ml): Blank and loaded NPs were separated from the dispersion by centrifugation at 4,000 rpm for 45 min, washed gently by distilled water and lyophilized using Operon Freeze-Dryer - (Korea) at vacuum pressure of 0.05 mbar. The condenser surface was maintained at 55°C. Lyophilized samples were stored in light-protected containers at −20°C for later use.

Characterization of Semi-synthetic Polymers and Corresponding NPs

Infrared spectrums (Fourier-transform Infrared-FTIR or Attenuated Total Reflection-ATR) were collected using Shimadzu-FTIR-8400S (Japan) and Thermo DS spectrometer (Germany). Ionotropically- or covalently- crosslinked NPs for infrared analysis were prepared as were previously described. However, the resulting NPs dispersion was precipitated using acetone (150 ml), washed three times with absolute ethanol (100 ml), and finally with acetone (100 ml) then dried overnight at 35°C.

Crosslinked matrices (ionotropically- or covalently-crosslinked) or polymer samples (chitosan and semi-synthetic derivatives) were crushed using mortar and pestle and mixed with potassium bromide at 1:100 ratios and compressed to a 2 mm semitransparent disk over 2 min for FTIR analysis. For ATR analysis, the powdered samples were placed directly into the diamond crystal of the instrument. The spectrums were recorded over wavelength range of 4,000–400 cm^{-1}.

Thermal analysis using Differential Scanning Calorimetry (DSC) using a DSC 823^e Mettler Toledo (Thermo Electron Scientific Instruments Corp., Madison, WI). Samples were prepared by weighing (3–7 mg) of each polymer in aluminum sample pans and sealing them using the Toledo sample encapsulation press. Each sample was heated from 25 to 350°C at 10°C/min heating rate under N_2 purge using an empty sealed pan as a reference. Calibration with the standard (indium) was undertaken prior to subjecting the samples for study.

Although acetone precipitation is rather drastic method vis-à-vis NP sizes and charges, it is harmless to NPs properties monitored by IR and DSC, namely, covalent and strong reversible interactions within NPs polymeric matrices. Moreover, acetone precipitation yields large enough NPs amounts suitable for IR and DSC studies.

NPs Size Analysis, Surface Charge Measurement, and Stability Studies Under Variable pH, $CaCl_2$ Conditions and 10% FBS Solution

Aliquots of crosslinked NPs (ionotropic or covalent) dispersions (2 ml) were evaluated by dynamic light scattering (DLS) either directly (at preparation pH), or after being subjected to variable pH conditions (1.2, 6.8, 7.4, and 12.0) $CaCl_2$ concentrations (0.1, 0.2, 0.3, 0.4, and 0.5 M), or fetal bovine serum (10% FBS in PBS at 7.4 pH). pH adjustments were achieved by aqueous NaOH (0.1 M) or HCl (1.0 M) and monitored using pH-meter (Trans Instruments, Singapore). Each sample was vigorously stirred for 1 min at room temperature to ensure homogenous dispersion and was then macroscopically inspected for haziness (Tyndall effect) or aggregate formation. Only samples with hazy appearance were analyzed by DLS while those showing aggregates were discarded. Samples were evaluated by DLS after 2 h exposure to variable pH, $CaCl_2$ concentrations, or 10% FBS solution. Particle size, polydispersity index (PDI), and zeta potential were calculated by determining the electrophoretic mobility of NPs dispersions followed by applying the Stokes-Einstein and Henry equations. The following parameters were assumed in the calculations: Media viscosity = 0.8872 cP, dielectric constant = 78.5, temperature = 25°C. The measurements were performed using Zetasizer Nano ZS (4.0 mW He-Ne laser, 632.8 nm, Malvern Instruments, UK) while the respective calculations were performed using Zetasizer software version 7.11. The measurements were done in triplicates at 25°C and the average size and zeta potential were recorded.

The morphological characteristics of NPs were studied by transmission electron microscope (TEM) (Morgagni (TM) FEI 268, Holland) using Mega-View Camera. The samples were

immobilized on copper grids for 10 min and dried at room temperature prior to investigation by TEM.

Loading Capacities and *in vitro* Release Studies

To aqueous solutions of the particular chitosan or chitosan derivative (0.1% w/v, 100 ml) in HCl (4.8 mM) MB or DOX (10 or 100 mg to prepare 1:10 or 1:1 polymer to drug ratios, respectively) were added and stirred for 30 min. The resulting solutions were separated into (5 ml) fractions and the appropriate crosslinker (0.1%w/v HMP, 0.2%v/v PPA, or 0.4% w/v TPP) was added dropwise to selected fractions until the development of hazy dispersions. Then, EDC (25 mg) was added to each fraction for covalent crosslinking. The reaction mixtures were stirred vigorously over 1 min and allowed to stand over 1 h. The reactions were terminated by centrifugation (Megafuge 8R, Thermo Scientific-Slovenia) at 4,000 rpm for 45 min at 4°C, then NPs pellets were retained and the supernatant discarded. NPs pellets were gently washed with deionized water and placed overnight in deep freezer (−80°C, Polar 530 V, Italy) then lyophilized as mentioned earlier. Lyophilized samples were stored in light-protected containers at −20°C for later use (stable over 8-months period).

The release profiles and loading capacities of loaded NPs were determined using the dialysis bag method. An exactly weighed amounts of drug-loaded lyophilized NPs were re-dispersed in HCl (3 ml, 4.8 mM) in a dialysis sac and was subsequently put in an amber-glassed bottle containing TRIS base buffer (17 ml, pH 7.4). The assembly was placed in a shaking incubator (DAIKI -Scientific Co, Korea) at 100 rpm and 37°C. Samples (2 ml) were withdrawn from TRIS buffer at specified time intervals and immediately replaced with an equivalent volume of fresh buffer. For MB quantification, samples absorbances were measured using UV-Visible spectrophotometer (Thermo Fisher Scientific model B40-210600, China) at $\lambda_{max} = 666$ nm. For DOX, samples were measured using Shimadzu spectrofluorometer (model RF-5301PC, Japan) at excitation wavelength λ_{max} 485 and emission λ_{max} 558 nm. Slit widths were adjusted to 5 for excitation and emission. Unloaded NPs were used as blanks.

The released amounts were calculated from properly drawn calibration curves. The release profiles were repeated in triplicates and expressed as average cumulative amounts of released drug per mg NPs. The standard deviation (SD) was used as variability descriptor.

To determine the amounts of loaded drugs (i.e., MB or DOX) in covalently crosslinked NPs: The cumulative amounts of each drug released over 24 h upon dissolution (see above) were added to amounts released upon degrading the respective loaded NPs (core loading). NPs degradation was performed as follows: Remaining nanoparticles within dialysis bags (after drug releasing studies) were collected by centrifugation at 4,000 RPM over 10 min and washed gently with distilled water, then suspended in HCl (2.0 M) at 72°C for 3 h in case of MB loaded NPs and ultrasonicated using ultrasonic processor (Cole-Parmer, USA) for DOX loaded NPs (at 50% amplitude for 10 min) (Tang et al., 2003).

The released amounts were calculated from properly drawn calibration curves (Cabrera and Van Cutsem, 2005). The loading capacity is calculated as in the following equation:

$$Loading\ Capacity = \frac{Amount\ of\ drug\ in\ mg\ of\ NPs}{Weight\ of\ NPs\ (mg)} \times 100\%$$

Cytotoxicity Studies

The cytotoxicity of (drug-free or DOX loaded NPs) was performed using the CellTiter Non-Radioactive Cell Proliferation Assay Kit® (Promega, USA). Free DOX was used as a positive control. A stock solution of 50 μM free DOX or its equivalent amount of DOX- loaded NPs was used to prepare serial dilutions from 0.05 to 50 μM in fresh media. The culture of MCF-7 cell line was maintained in RPMI 1640 medium, supplemented with 10% (v/v) heat-inactivated fetal bovine serum (FBS), 2 mM l-glutamine, 100 U/ml and 100 μg/ml penicillin–streptomycin (EURO Clone, Italy). The cells were trypsinized by trypsin-EDTA (EURO Clone, Italy) and centrifuged to form a pellet of the cells. The supernatant was discarded. The cell pellet was then re-suspended in its growth medium. The cell stock was diluted to the desired concentration (7×10^4 cells/ml). The cell suspension was transferred to 96 well-plates by adding 100 μl of the cell suspension to each well. The plates were incubated in a humidified atmosphere at 37°C and 5% CO_2 for 24 h to allow the cells to be in their exponential growth phase at the time that NPs suspension or free DOX were added. It is important to mention that ultrasonication (30% amplitude for 2 min) was used to find fine NPs suspension and the same condition was applied for free DOX. The spent medium (deprived of nutrients) was discarded and replaced by fresh medium with an appropriate concentration of the NPs suspension or free DOX. After 72 h of incubation, MTT assay solution was added. The plates were incubated for 4 h in the absence of light at 37°C then the stop solution was added. The number of live cells was identified after 30 min of stop solution addition by measuring the absorbance at 570 nm using a 96-well plate reader (BioTek Instruments, U.S.A). The following equation was used to calculate cell viability.

$$\left[Cell\ viability\% = \frac{Absorbance\ (570\ nm)\ of\ Doxorubicin\ treated\ sample}{Absorbance\ (570\ nm)\ of\ control\ sample} \times\ 100\%\right]$$

The results of the MTT cell proliferation assay were analyzed using excel. The inhibitory concentration (IC_{50}) values, which are the drug concentration at which 50% of cells are viable, were calculated from the logarithmic trend line of the cytotoxicity graph. The cellular morphological changes related to NPs-induced cytotoxicities were monitored using inverted light microscope (Vert. A1, AX10, Carl Ziess, Germany) of MCF-7 cells after exposure to DOX-loaded NPs and free DOX (10.0 μM) over 72 h incubation. Unloaded NPs and untreated cells were used as controls.

Assessment of NPs Cellular Uptake Using Confocal Microscopy

MCF-7 cells were seeded onto poly-L-lysine coated round coverslips (prepared by incubation in poly-L-lysine aqueous solution (0.01% w/v) over 1 h at room temperature) in a 12-well plate at 5×10^4 cells/well in RPMI culture medium and left

over 24 h. DOX-loaded NPs or free DOX (1.0 μM), suspended in tissue culture media, were directly applied to coverslips adhered cells and incubated over 4 h at 37°C Subsequently, the culture media were removed and wells were washed two times with PBS. Cells were then fixed by paraformaldehyde solution (4%) at room temperature over 20 min then washed two times with PBS. Subsequently, triton-x solution (0.5% v/v) was added to wells and incubated for 10 min then washed two times with PBS. Thereafter, the coverslips were removed and slowly flipped over clean glass slides covered with 50.0 μL DAPI stain (Prolong™ Diamond Antifade Mountant with DAPI) and left overnight at room temperature under dark conditions. Fixed cells were imaged at laser/detector wavelengths of 488 nm/614–742 nm for DOX and of 405 nm/410–585 nm for DAPI using confocal laser scanning microscope (LSM 780, Carl Ziess, Germany) by 63×/1.4 oil lens. Untreated cells (i.e., with DOX-loaded NPs or free DOX) were assessed as controls. NPs uptake was also evaluated using wide-field fluorescence microscopy (Axio Imager Z2, Carl Ziess, Germany).

Statistical Analysis

All experimental data were presented as mean and standard deviation (SD). Microsoft Excel Software 2007 (Microsoft Corp., Redmont, WA, USA) was used to calculate means, standard deviations of the size, zeta potential, loading and cumulative amount released, and to create graphs. Excel was also used to calculate *t*-test and *p-values*. Microscopic images were labeled using ZEN software (version 2012, SP5).

RESULTS AND DISCUSSION

Synthesis of Chitosan-Dicarboxylic Acid Conjugates

Chitosan-phthalate (CP) and chitosan-phenylsuccinic (CPS) were recently reported to yield TPP-based NPs of optimal properties for drug delivery (Dmour and Taha, 2017) prompting us to select them for our current NPs and drug release studies.

CP and CPS were synthesized by the reaction of chitosan with phthalic or phenylsuccinic anhydride in neutral pH. Catalytic amount of pyridine was added to push the anhydride/amine acylation chemistry (Aiedeh and Taha, 1999; Dmour and Taha, 2017). **Figure 1G** summarizes the conjugation reactions. The resulting polymers were characterized by NMR spectroscopy. **Figure S29** shows the ^{1}H NMR spectra of the grafted polymers.

NPs Formulation

Initially, chitosan and conjugation derivatives (CP and CPS) were used to prepare NPs by ionotropic gelation with three polyphosphates crosslinkers, namely TPP, PPA, and HMP. **Table 1** summarizes the prepared NPs and their abbreviated names. **Figure 2** summarizes the formulation of CP-PPA NPs as example.

Ionotropic gelation proceeds via attraction between protonated amine groups of chitosan (or chitosan's derivatives) and phosphate anions of TPP, HMP, or PPA. These interactions weaken the surface charge of chitosan and therefore reduce chitosan's aqueous solubility leading to spontaneous NPs formation (**Figure 2**). Ionotropic crosslinking was practically performed by titrating solutions of chitosan (or its derivatives, pH values as in **Table 2**) with aqueous polyphosphate crosslinkers until the appearance of hazy (opalescent) dispersions. Chitosan conjugates (i.e., CP and CPS) tended to consume significantly lesser amounts of PPA and HMP crosslinkers to form NPs compared to unmodified chitosan, as in **Table 2**. However, this trend is not observed with TPP, i.e., unmodified chitosan and chitosan conjugates required the same levels of TPP to form ionotropic NPs. We believe this trend is because conjugated chitosans fold in acidic aqueous conditions in such way to keep hydrophobic acidic conjugates (unionized phthalic and phenylsuccinic acids under acidic NPs preparation conditions) confined within the interior of newly formed NPs. Apparently, TPP acts at NPs surfaces (i.e., surface crosslinker) and thus being far from core carboxylic acid-substituted amines, the amount of TPP needed for NPs formation is independent of chitosan conjugation. In comparison, HMP (and to a lesser extent PPA) seem to act as core crosslinker in direct proximity to conjugated amines (i.e., with phthalic and phenylsuccinic acids) within newly formed NPs cores, such that carboxylic acid conjugation reduces the number of core cationic amines exposed to HMP with the concomitant reduction in the required HMP phosphate counter-ions necessary to weaken chitosan's charge leading to spontaneous NPs formation. This conclusion is supported by the significantly higher positive surface charges of HMP-based NPs compared to TPP-based NPs (see section NPs Behavior under Variable pH/Calcium Ion Conditions, NPs Sizes and Surface Charges and **Table 4**).

Another interesting observation in **Table 2** is related to the change in pH profiles of chitosan dispersions upon grafting to phthalic and phenylsuccinic acids. Clearly from **Table 2**, the pH of the polymeric dispersions became more acidic upon conjugation to dicarboxylic acids, which is not surprising due to the fact conjugation consumes basic amines groups within chitosan and converts them into neutral amidic linkages. However, pH shifts accompanying conjugation to phthalic and phenylsuccinic acids (CP and CPS, respectively) were identical (from pH 4.32 to pH 2.5) suggesting identical substitution

TABLE 1 | Prepared ionotropically-crosslinked chitosan NPs, their corresponding crosslinkers, and abbreviated names.

Polymer		Ionotropic NPs	
Derivative	**Abbreviation**	**Cross-linker**	**Abbreviation**
Unmodified chitosan	C	Tripolyphosphate	C-TPP
		Polyphosphoric acid	C-PPA
		Hexametaphosphate	C-HMP
Chitosan phthalate	CP	Tripolyphosphate	CP-TPP
		Polyphosphoric acid	CP-PPA
		Hexametaphosphate	CP-HMP
Chitosan phenylsuccinate	CPS	Tripolyphosphate	CPS-TPP
		Polyphosphoric acid	CPS-PPA
		Hexametaphosphate	CPS-HMP

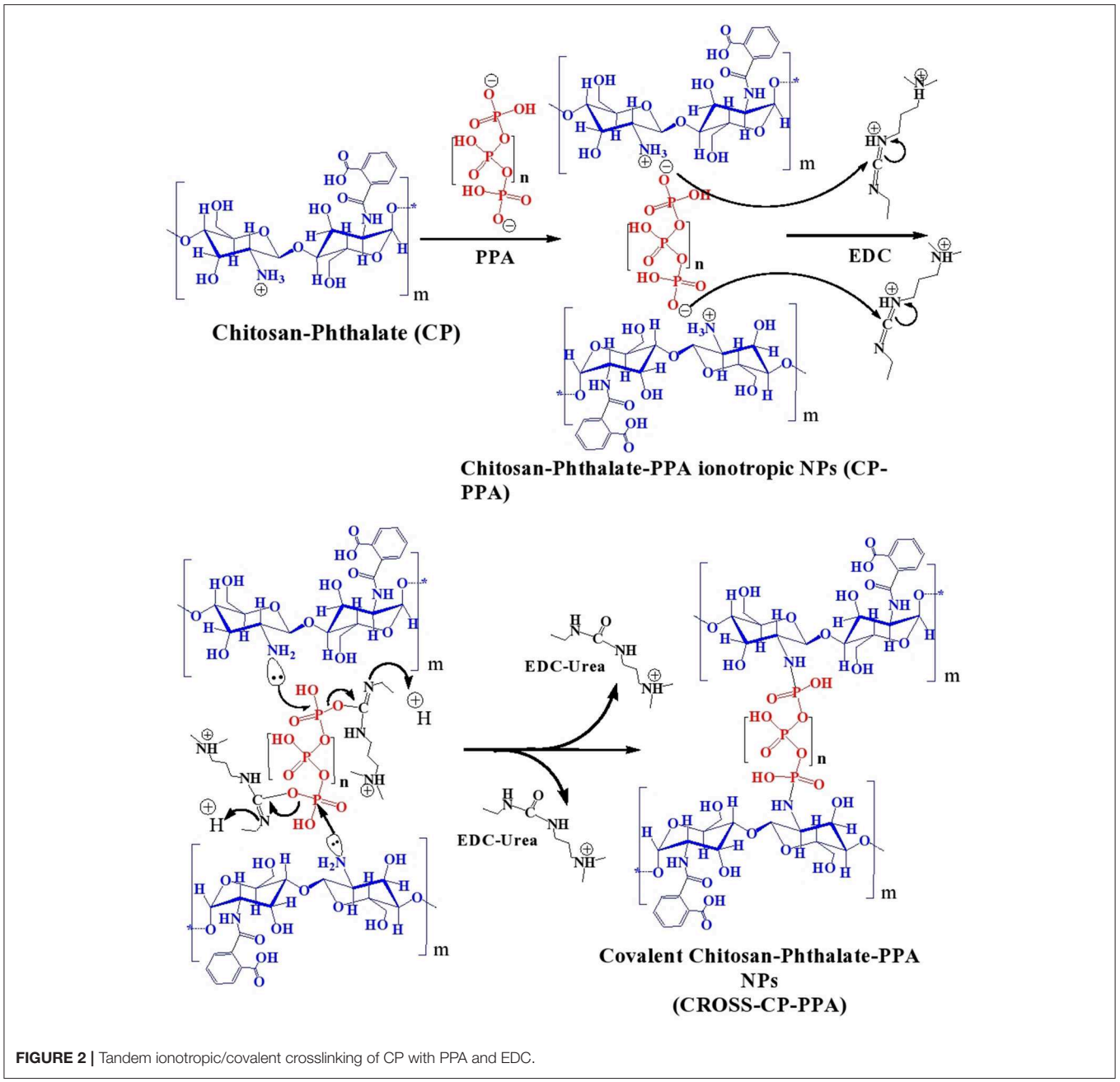

FIGURE 2 | Tandem ionotropic/covalent crosslinking of CP with PPA and EDC.

degrees in both cases (CP and CPS). In fact, we could calculate the degrees of phthalic and phenylsuccinic acids substitution on chitosan to be 43%. The calculation is based on subtracting hydrogen ion concentration before and after dissolving each chitosan derivative in certain predetermined volume of HCl (4.8 mM).

EDC was added to the generated ionotropic NPs for covalent crosslinking (**Figure 2**). Acidic conditions are necessary to protonate EDC's imino-nitrogen atoms and enhance its reactivity. The coupling chemistry was performed by excess EDC to ensure reaction completion, particularly under the sterically hindering environment of the polymer. Both EDC and EDC-urea byproduct are water soluble and allow easy subsequent polymer purification by dialysis in aqueous conditions.

Table 2 shows another interesting observation: Successful EDC-mediated covalent crosslinking (i.e., CP-TPP, CP-PPA, and CPS-HMP) significantly shifted the pH of corresponding NPs dispersions toward more basic values, while those that failed EDC crosslinking maintained the same pH values prior to EDC addition. In fact, success of EDC crosslinking can be easily monitored by observing the pH shifts of corresponding NPs dispersions upon adding EDC. Transition of EDC to EDC-urea (upon covalent crosslinking) consumes acidic protons causing the observed basic shifts, as in **Figure 2**. Failure of the

TABLE 2 | Crosslinking conditions of ionotropic and covalent NPs together with their corresponding abbreviated names.

Ionotropic NPs	Amount of ionotropic Crosslinker (mg) per polymer (mg)[a]	pH of			Abbreviations of covalent NPs
		Polymeric dispersion[b]	Ionotropic NPs dispersions[b]	NPs dispersions after EDC addition[b]	
C-TPP	0.35 ± 0.05	4.32 ± 0.05	5.53 ± 0.03	5.59 ± 0.34	—[c]
C-PPA	0.20 ± 0.07		2.04 ± 0.01	2.05 ± 0.03	—[c]
C-HMP	0.16 ± 0.04		4.69 ± 0.17	4.95 ± 0.16	—[c]
CP-TPP	0.38 ± 0.02	2.56 ± 0.04	3.00 ± 0.03	5.18 ± 0.19	CROSS-CP-TPP
CP-PPA	0.09 ± 0.02		1.87 ± 0.012	3.14 ± 0.05	CROSS-CP-PPA
CP-HMP	0.10 ± 0.03		2.62 ± 0.15	2.80 ± 0.075	—[c]
CPS-TPP	0.32 ± 0.02	2.54 ± 0.04	3.55 ± 0.27	3.79 ± 0.015	—[c]
CPS-PPA	0.09 ± 0.01		2.08 ± 0.06	2.12 ± 0.078	—[c]
CPS-HMP	0.06 ± 0.02		2.55 ± 0.01	3.08 ± 0.15	CROSS-CPS-HMP

[a] *Amounts of phosphate crosslinkers necessary for optimal mono-dispersed ionotropic NPs. Lesser or greater amounts lead to either loss of NPs, larger particles, or aggregates.*
[b] *Means were recorded for triplicate measurements ± standard deviation.*
[c] *Addition of EDC failed to produce stable NPs under variable pH and $CaCl_2$ conditions.*

conjugation reaction means EDC fails to convert into EDC-urea and thus fails to abstract protons from the medium (as in the cases of C-TPP, C-PPA, C-HMP, CP-HMP, CPS-TPP, and CPS-PPA NPs, **Table 2**). Subsequent probing with infrared, thermal and NPs stability profiles (see next) unequivocally supported our conclusions, i.e., success of EDC-induced covalent crosslinking in CP-TPP, CP-PPA, and CPS-HMP NPs cases (via forming phosphoramide crosslinks) and failure of covalent crosslinking in C-TPP, C-PPA, C-HMP, CP-HMP, CPS-TPP, and CPS-PPA NPs cases (see section NPs Behavior under variable pH/calcium ion conditions, NPs sizes and surface charges).

Characterization of Polymeric Intermediates and NPs

Infrared Spectroscopy (IR)

To probe chemical conjugation of chitosan and subsequent NPs formation, we opted to use IR and differential scanning calorimetry (DSC). **Figure 3** shows the infrared spectra of parent chitosan, corresponding derivatives, and selected NPs (ionotropically and covalently crosslinked). As in **Figure 3**, chitosan's IR spectrum exhibits NH/OH stretching and N-H bending vibrations (at 3,400 and 1,645 cm^{-1}, respectively) (Brugnerotto et al., 2001). However, it lacks stretching amide I carbonyl band at 1,655 cm^{-1} indicating considerable deacetylation (Khan et al., 2002; de Alvarenga, 2011), which agrees with the deacetylation degree reported by the manufacturing company (*ca.* 85%, Sigma Aldrich, USA).

Grafting chitosan with carboxylic acid anhydrides was evidenced in the corresponding infrared spectra by new stretching bands within 1,549–1,553 cm^{-1} range (clear in CPS and CP spectra in **Figure 3**) corresponding to carboxylate and amide II stretching vibrations accompanying the conjugation to phthalic and phenylsuccinic acids. It's noteworthy to mention that amide I stretching bands seem to be concealed by N-H bending vibrations of remaining chitosan amines at 1,640 cm^{-1}.

Although IR is blind to electrostatic interactions, and therefore, is not able to probe ionotropic phosphate-ammonium interactions, the acidic pH required for ionotropic gelling (**Table 2**) protonated amine and carboxylate residues of the polymers causing considerable change in the respective infrared spectra: In unmodified chitosan (C, **Figure 3**), acidification and treatment with polyphosphate crosslinkers lead to appearance of a new band at 1,535 cm^{-1} in C-PPA and C-HMP NPs, corresponding to bending vibrations of ammonium groups, alongside the original band at 1,641 cm^{-1} which correspond to bending vibrations of the amine groups. Conversely, acidification/phosphate treatment of anhydride-grafted chitosan derivatives significantly protonated the carboxylate residues into carboxylic acids with the concomitant emergence of new shoulder bands in CPS-HMP NPs and CP-PPA NPs spectra at *ca.* 1,710 cm^{-1} related to carboxylic acid carbonyl stretching. Additionally, ionotropically-crosslinked NPs exhibited new distinct band at 1,247 cm^{-1} corresponding to P=O stretching vibrations of the phosphate crosslinkers (Nyquist et al., 1967; Nishi et al., 1986; Dmour and Taha, 2017).

Infrared spectroscopy was also used to investigate covalent crosslinking reactions resulting from treating ionotropic NPs with EDC. From **Figure 3**, treating CP-PPA, and CPS-HMP NPs with EDC (i.e., to yield CROSS-CP-PPA, and CROSS-CPS-HMP, respectively) was accompanied by new significant band at *ca.* 980 cm^{-1} corresponding phosphoramide bond formation within NPs (Nyquist et al., 1967; Nishi et al., 1986; Dmour and Taha, 2017). This band is absent from infrared spectrums of NPs that failed covalent crosslinking despite exposure to EDC, e.g., C-PPA-EDC, C-HMP-EDC, CP-HMP-EDC, and CPS-PPA-EDC, as in **Figure 3**.

Intriguingly, carboxylic acid bands seen upon acidification/polyphosphate crosslinking (C=O stretching band at $\approx$ 1,710 cm^{-1} seen in CP-PPA and CPS-HMP) remained after treatment with EDC in CROSS-CP-PPA as well as in TPP-based NPs (Dmour and Taha, 2017), which

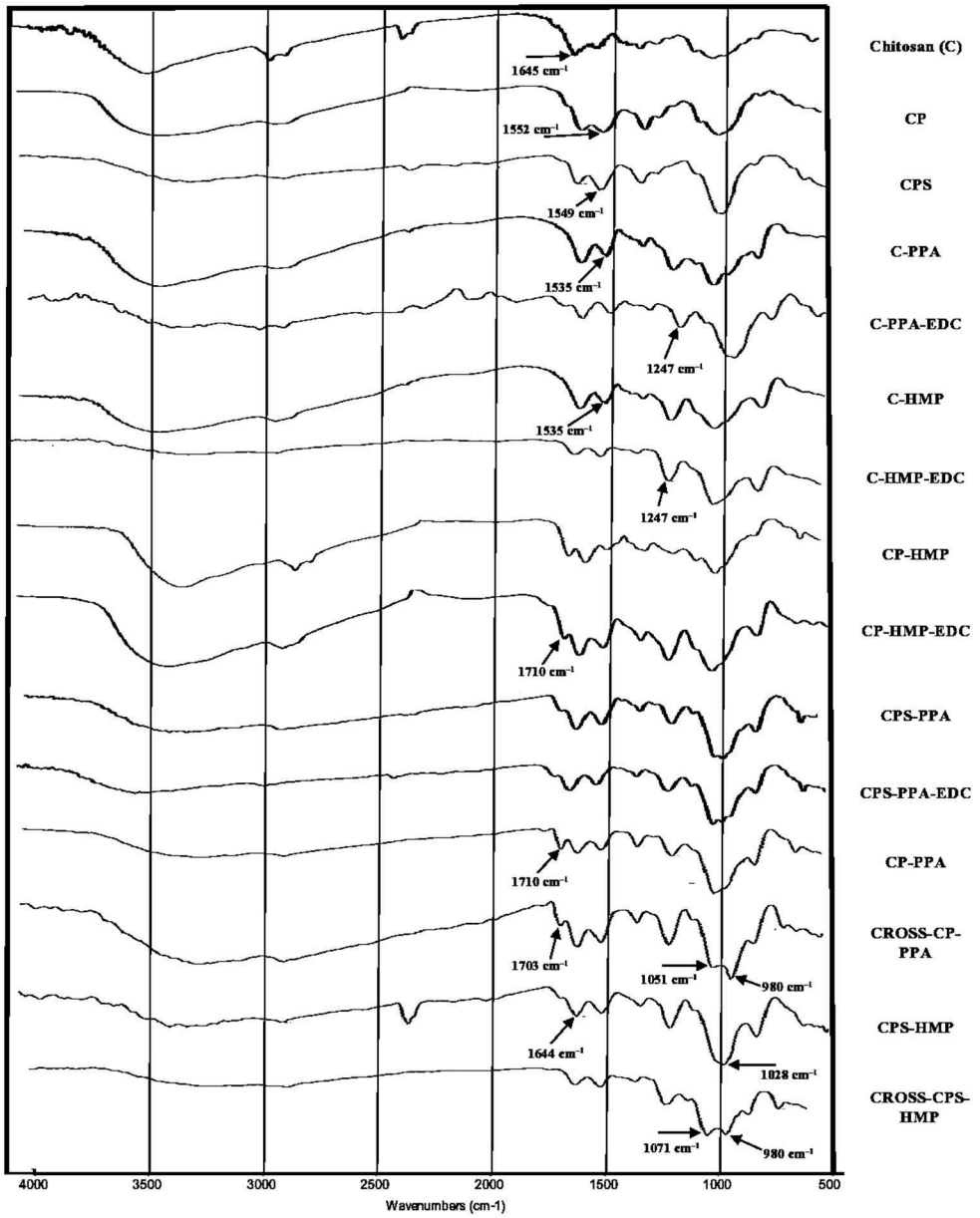

FIGURE 3 | IR spectrums of unmodified parent chitosan, corresponding derivatives, and NPs (ionotropically and covalently crosslinked). Individual infrared spectrums are shown in **Figures S2**–**S16**.

indicate that the polymeric carboxylic acid moieties were not involved (or minimally involved) in covalent crosslinking within NPs matrices. However, this band (i.e., at 1,710 cm^{-1}) disappeared totally in CROSS-CPS-HMP NPs spectrum despite acidic conditions (pH 3.08, which should protonate remaining carboxylates into carboxylic acids). This suggests that carboxylic acid moieties in CROSS-CPS-HMP NPs were consumed in EDC-mediated amide bond forming reaction additional to the phosphoramide formation reaction mentioned earlier. We believe this extra-crosslinking reaction is due to the fact that HMP is primarily core-crosslinking agent (see section NPs behavior under variable pH/calcium ion conditions, NPs sizes and surface charges) with little abundance at the outer NPs surface, thus leaving the chance for slower amide forming crosslinking (coupling free carboxylic acids of grafted anhydrides with chitosan amines) to take place at the NPs surfaces.

It remains to be mentioned that grafted carboxylic acid moieties are essential for successful formation of phosphoramide bonds as they catalyze coupling of polyphosphates with polymeric amine groups (Dmour and Taha, 2017). This explains EDC failure to achieve phosphoramide bonds in the lack of grafted carboxylic acid groups, as seen in the IR

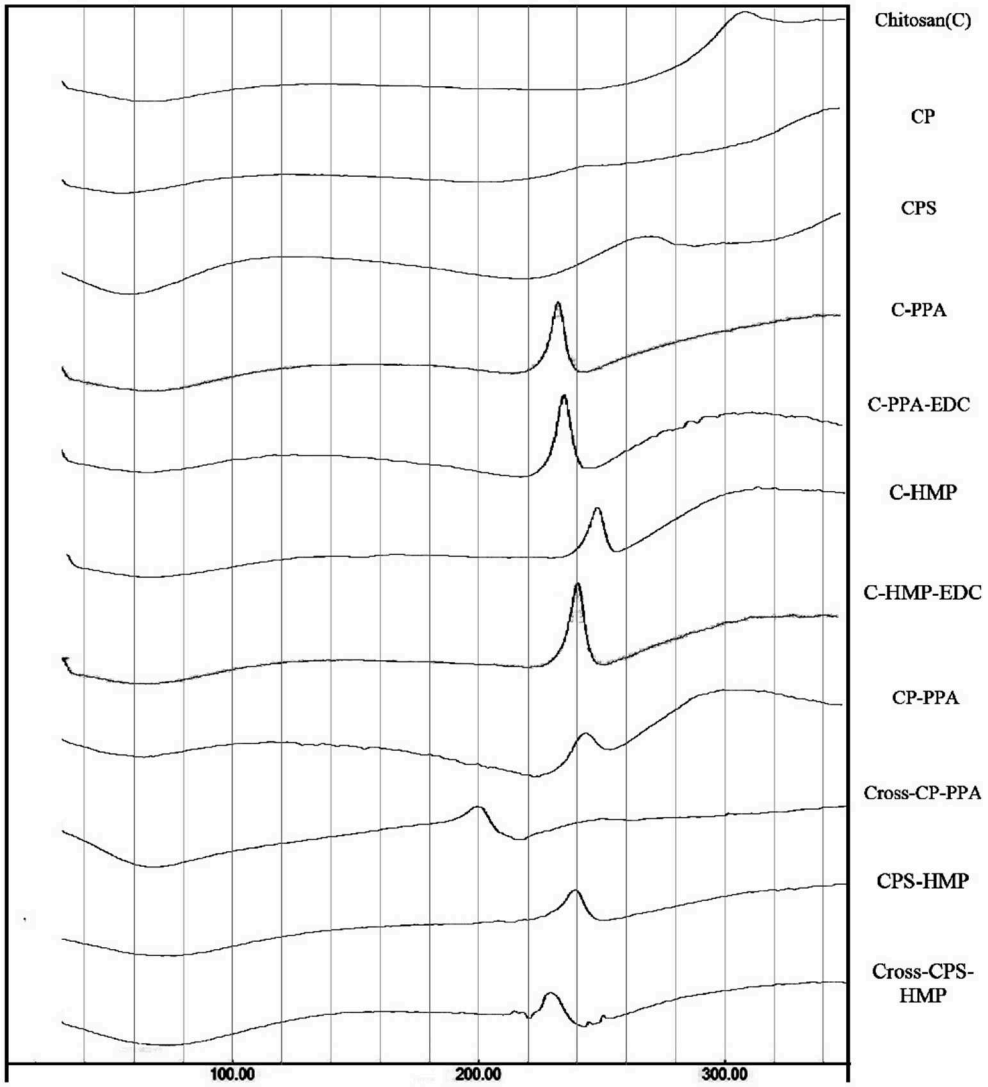

FIGURE 4 | DSC thermograms for unmodified chitosan (C), chitosan phthalate (CP), chitosan phenylsuccinate (CPS), and their ionotropic/covalent corresponded nanoparticles. The individual thermal DSC traits are shown in **Figures S17–S27**.

spectra of EDC-treated C-PPA and C-HMP NPs (absence of phosphoramide bands at *ca.* 980 cm^{-1} as in **Figure 3**). Strangely, however, all our attempts to crosslink chitosan (unmodified) NPs with polyphosphates (TPP, HMP, or PPA) in acetic acid were futile, suggesting that the carboxylic acid catalyst need to be covalently attached to NPs matrix to catalyze the EDC coupling chemistry successfully.

Thermal Analysis

DSC thermograms of chitosan, carboxylic acid derivatives, and NPs (both ionotropic and covalent) are shown in **Figure 4**. Chitosan shows typical polysaccharide thermal trait characterized with two bands. The first is endothermic wide band that extends from 40° to 100°C corresponding to polymeric dehydration. The second thermal event is exothermic band extending from 280 to 320°C corresponding to polymeric degradation. The thermal trait of CP is rather flat, while CPS shows shallow exothermic band extending from *ca.* 220–274°C probably linked to thermally-mediated amide forming reaction linking phenylsuccinic acid moieties and adjacent chitosan's amine groups in CPS. Similar exothermic feature was evidenced upon attaching phthalic anhydride to chitosan-lactate (Al Bakain et al., 2015). Probing the thermal characteristics of ionotropic NPs demonstrates intriguing exothermic peaks (extending from 225° to 247°C for CP-PPA NPs and from 220° to 240°C in CPS-HMP NPs) resulting from certain heating-induced exothermic incident within NP matrices. The most likely explanation for these peaks is heat-induced phosphoramide forming reaction linking chitosan's amine groups with polyphosphate crosslinkers (see **Figure S1**) (Dmour and Taha, 2017). We excluded the

prospect that these peaks are due to amide bond formation between carboxylic acids (phenylsuccinic or phthalic acids) and chitosan's aminosugar monomers because the same peaks emerged in the thermograms of C-PPA and C-HMP NPs (both are based on unmodified chitosan), as in **Figure 4**.

EDC coupling was also manifested in the DSC traits. EDC coupling weakened the exothermic peaks and moved them to lower temperatures (from 245 to 200°C in CP-PPA and from 240 to 230°C in CPS-HMP). The most logical reason for the observed EDC-induced decrease of exothermic bands is that EDC crosslinking depleted a considerable fraction of phosphate crosslinker molecules, and consequently, eliminated them from the thermally-induced reaction with aminosugar monomers of chitosan (or acid-grafted chitosan derivatives). Accordingly, the fact that CROSS-CP-PPA exhibited the most drastic attenuation in the exothermic peak implies that EDC crosslinking was most efficient in this case. In contrast, the DSC traits of C-PPA and C-HMP remained unchanged after EDC addition (i.e., C-PPA-EDC and C-HMP-EDC, in **Figure 4**) which further supports the notion that the presence of conjugated carboxylic acids is essential for EDC mediated formation of phosphoramide covalent bonds.

NPs Behavior Under Variable pH/Calcium Ion Conditions, NPs Sizes and Surface Charges

Table 3 summarizes NPs size information and how they behave under variable pH, calcium ions concentrations, and 10% FBS. **Figure 5A** shows how CP-PPA and CROSS-CP-PPA NPs respond to variable pH, and calcium chloride conditions, while **Figure 5B** shows how CP-TPP, CP-PPA, CPS-HMP NPs dispersions and their corresponding covalently crosslinking analogs behave in 10% FBS solution. Ionotropic NPs were stable over pH range of 2.0–6.0. However, they immediately (within seconds) dissolved in acidic pH (1.2) to form clear solutions, while at pH values $\geq$ 6.8, with or without FBS, they created macroscopical aggregates, as seen in **Figures 5A,B**.

Acidic conditions hydrolyze polyphosphate crosslinkers (Lind, 1948) and impair their abilities to electrostatically attract chitosan's ammonium moieties leading to observed dissolution of NPs. However, although all ionotropic NPs formulas lost their integrities upon exposure to acidic pH (1.2), C-HMP and CPS-HMP NPs retained their integrities under such conditions, as in **Table 3**. Resistance of HMP-based ionotropic NPs to drastic acidic pH conforms to our proposition that HMP is core crosslinker and stays within the confinement of NPs cores protected from hydrolysis by the external acidic solution.

Conversely, basic conditions deprotonate chitosan's ammonium residues resulting in loss of significant fraction of chitosan's positive charge, thus undermining its ability to electrostatically interact with negatively charged phosphates crosslinkers. Additionally, the positive surfaces of chitosan NPs serve as deflocculants adding further stability to the NPs dispersion. Losing these charges flocculates NPs suspension and forces them to aggregate into macroscopical particulate clusters.

Similarly, **Table 3** and **Figure 5** show ionotropic NPs to dissolve completely and immediately in $CaCl_2$ solutions regardless of concentration. Calcium ions form stable chelates with phosphate ions (Rehfeld et al., 1977) and therefore sequester phosphate from being electrostatically complexed to chitosan. This leads to complete dissolution of ionotropic NPs under the influence of calcium ions as in **Table 3** and **Figure 5A**.

The most notable observation in **Table 3** and **Figure 5** is that covalently crosslinked NPs maintained their opalescent appearance, nano-sizes and resisted extreme pH environment, FBS conditions, and increasing $CaCl_2$ levels over at least 2 h exposure periods. This is not unexpected because covalent crosslinking decouples the stabilities of crosslinked polymeric matrices from solution pH or calcium ions. We reported similar findings for TPP-covalently-crosslinked NPs based on modified chitosan (Dmour and Taha, 2017).

Interestingly, however, EDC failed to covalently crosslink CP-HMP, CPS-PPA, and CPS-TPP NPs as evident from their total lack of stability under variable pH and $CaCl_2$ conditions (and lack of phosphoramide IR stretching vibrations in CP-HMP-EDC and CPS-PPA-EDC in **Figure 3**).

Table 3 shows HMP to yield significantly larger ionotropic NPs compared to PPA and TPP, e.g., C-HMP NPs were of 459 nm average size, while C-PPA NPs and C-TPP NPs were of 118 and 205 nm average sizes, respectively. Similarly, CP-HMP NPs (415 nm) and CPS-HMP NPs (331 nm) significantly outsized their TPP and PPA counterparts: CP-TPP NPs (148 nm), CPS-TPP (156 nm), CP-PPA (133 nm), and CPS-PPA (120 nm). Moreover, HMP-based NPs remained larger than their TPP and PPA analogs after covalent crosslinking albeit at lesser size differences, e.g., CROSS-CPS-HMP NPs scored 254 nm average size at preparation pH, while CROSS-CP-TTP and CROSS-CP-PPA NPs scored 160 and 158 nm, respectively. We believe this trend is also related to our proposition that HMP is mainly core-ionotropic crosslinker, while TPP acts as surface (shell) crosslinker. Apparently, being surface crosslinker, TPP exerts electrostatic attraction against loose cationic chitosan layers directly beneath NPs surfaces leading to NPs size collapse, while core chitosan layers tend to be denser and harder to compress under the electrostatic influence of core HMP thus yielding larger NPs. PPA seems to act as both core/shell crosslinker, which also explains the smaller sizes of its corresponding NPs.

Table 3 shows lack of any trend connecting the pH with sizes or size distributions of covalent NPs. A similar conclusion can be drawn regarding the effect $CaCl_2$ on covalent NPs sizes. However, PPA-based covalent NPs are a noticeable exception: CROSS-CP-PPA NPs increased in size from 158 to 471 nm upon exposure to $CaCl_2$ (0.5 M). We believe the long chains of covalently attached surface PPA allow polyphosphate strands to be involved in electrostatic attraction with surface chitosan ammonium groups (extra to those involved in covalent crosslinking). These strands are readily cleavable from their PPA mother chains under the acidic aqueous conditions experienced during NPs preparation leaving them electrostatically anchored to NPs surfaces. Higher calcium concentrations are expected to sequester these ionotropic polyphosphate strands leaving their covalently attached mother chains as sole crosslinking anchors thus relaxing the crosslinker strain at NPs surfaces and allow water diffusion into NPs interior leading to NPs size enlargement.

TABLE 3 | Size properties of ionotropic and covalent NPs under varying pH, calcium chloride conditions, and 10% FBS solution.

		Ionotropic NPs	NPs After EDC addition									
NPs	**NP Property[a]**	**At Preparation Conditions**	**pH**					**$CaCl_2$ (M)[f]**				
			1.2[f]	**6.8[f]**	**7.4**		**12.0[f]**	**0.1**	**0.2**	**0.3**	**0.4**	**0.5**
					Aqueous conditions	**FBS (10%) v/v)**						
C-TPP	Size (nm)	205.4 ± 3.8	—[c]	Clear	Aggregate	Aggregate	—[e]	Aggregate	Clear	Clear	Clear	Clear	Clear
	PDI[b]	0.42 ± 0.02	—[c]	—	—	—	—[e]		—	—	—	—	—
C-PPA	Size (nm)	118.0 ± 2.4	—[c]	Clear	Aggregate	Aggregate	—[e]	Aggregate	Clear	Clear	Clear	Clear	Clear
	PDI[b]	0.35 ± 0.03	—[c]	—	—	—	—[e]		—	—	—	—	—
C-HMP	Size (nm)	458.8 ± 21.5	—[c]	933 ± 151[d]	Aggregate	Aggregate	—[e]	Aggregate	Clear	Clear	Clear	Clear	Clear
	PDI[b]	0.52 ± 0.11	—[c]	0.55 ± 0.1[d]	—	—	—[e]		—	—	—	—	—
CP-TPP	Size (nm)	148.3 ± 11.2	159.8 ± 10.3	195.9 ± 5.4	249.9 ± 6.7	319.4 ± 40.3	173.5 ± 3.71	334.9 ± 8.7	230.4 ± 4.4	269.5 ± 11.6	232.7 ± 31.3	234.6 ± 4.7	256.8 ± 11.2
	PDI[b]	0.16 ± 0.02	0.16 ± 0.18	0.17 ± 0.02	0.26 ± 0.03	0.35 ± 0.05	0.31 ± 0.05	0.35 ± 0.7	0.21 ± 0.01	0.25 ± 0.03	0.19 ± 0.028	0.19 ± 0.02	0.23 ± 0.01
CP-PPA	Size (nm)	133.5 ± 8.0	158.1 ± 6.5	189.5 ± 10.0	171.3 ± 12.2	199.1 ± 2.7	263.8 ± 12.8	228.9 ± 6.0	193.6 ± 4.0	274.5 ± 19.8	374.5 ± 30.7	260.8 ± 34.5	471.6 ± 26.4
	PDI[b]	0.28 ± 0.04	0.31 ± 0.04	0.29 ± 0.02	0.23 ± 0.01	0.29 ± 0.04	0.44 ± 0.05	0.30 ± 0.03	0.19 ± 0.03	0.29 ± 0.07	0.41 ± 0.06	0.29. ± 0.07	0.29 ± 0.05
CP-HMP	Size (nm)	415.4 ± 16.7	—[c]	259.4 ± 10.5[d]	Aggregate	Aggregate	—[c]	Aggregate	Clear	Clear	Clear	Clear	Clear
	PDI[b]	0.43 ± 0.06	—[c]	0.37 ± 0.05[d]	—	—	— [c]	—	—	—	—	—	—
CPS-TPP	Size (nm)	156.6 ± 3.3	—[c]	Clear	Aggregate	Aggregate	— [c]	Aggregate	Clear	Clear	Clear	Clear	Clear
	PDI[b]	0.09 ± 0.01	—[c]	—	—	—	— [c]	—	—	—	—	—	—
CPS-PPA	Size (nm)	120.6 ± 3.3	—[c]	Clear	Aggregate	Aggregate	— [c]	Aggregate	Clear	Clear	Clear	Clear	Clear
	PDI[b]	0.23 ± 0.01	—[c]	—	—	—	—[c]	—	—	—	—	—	—
CPS-HMP	Size (nm)	331.7 ± 10	254.0 ± 30.0	299.9 ± 13.0	200.1 ± 4.0	258.2 ± 44	335 ± 49.2	349.8 ± 39	283.8 ± 8.0	265.5 ± 10.0	247.1 ± 5.8	248.6 ± 7.6	254.8 ± 11.0
	PDI[b]	0.39 ± 0.03	0.26 ± 0.02	0.27 ± 0.01	0.26 ± 0.03	0.38 ± 0.09	0.58 ± 0.10	0.49 ± 0.09	0.29 ± 0.03	0.31 ± 0.03	0.33 ± 0.04	0.34 ± 0.05	0.30 ± 0.04

[a] *Each value represents the average of triplicate measurements ± standard deviation. DLS graphs showing the average sizes of example NPs are shown in* ***Figure S28****.*

[b] *Polydispersity index.*

[c] *Covalent crosslinking failed (EDC failed to covalently crosslink NPs based on infrared and DSC evidence, see text).*

[d] *Shown data are for ionotropic NPs (as EDC failed to covalently crosslink NPs based on infrared and DSC evidence, see text).*

[e] *Not tested.*

[f] *Aqueous conditions (no FBS).*

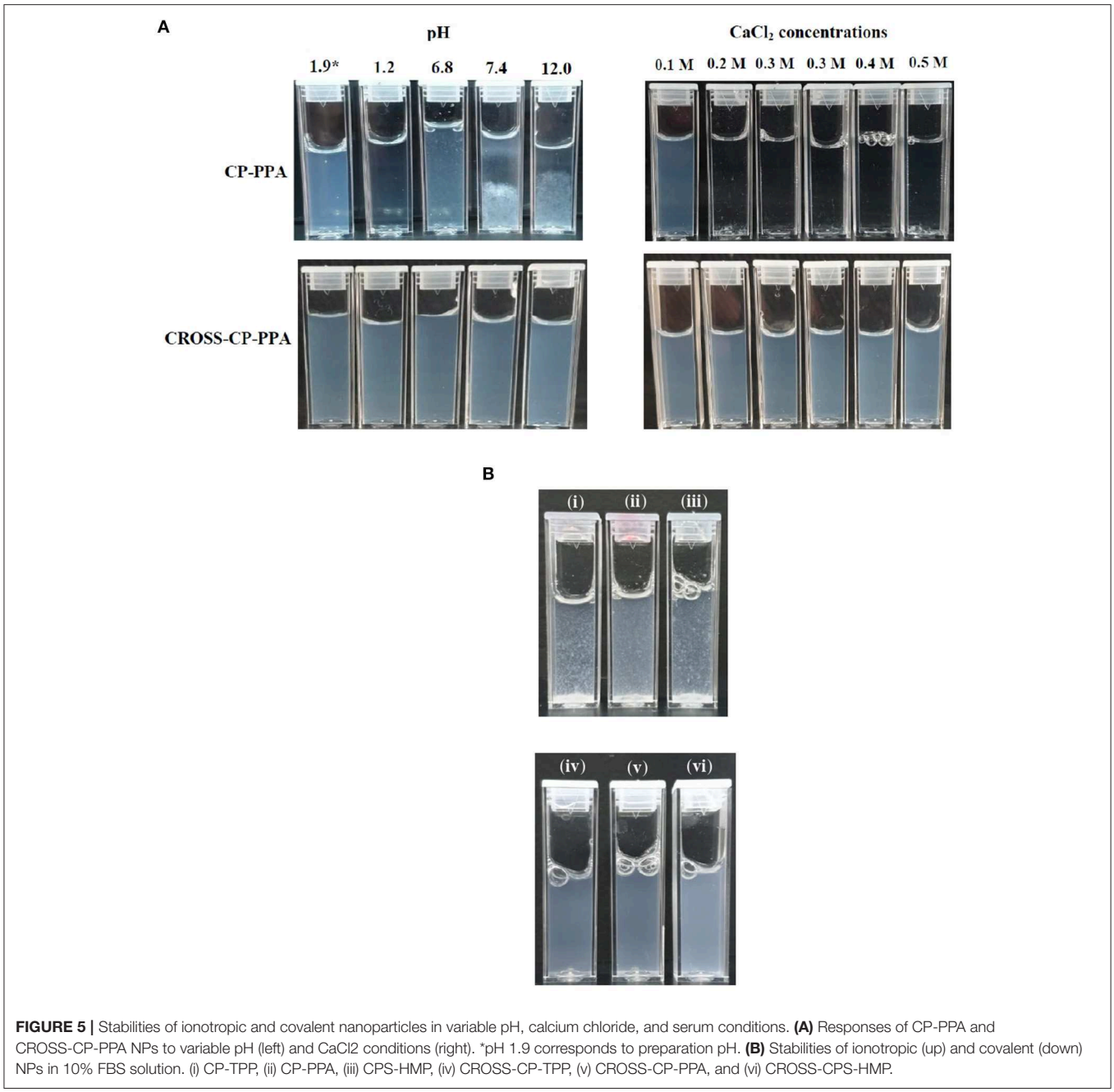

FIGURE 5 | Stabilities of ionotropic and covalent nanoparticles in variable pH, calcium chloride, and serum conditions. **(A)** Responses of CP-PPA and CROSS-CP-PPA NPs to variable pH (left) and CaCl2 conditions (right). *pH 1.9 corresponds to preparation pH. **(B)** Stabilities of ionotropic (up) and covalent (down) NPs in 10% FBS solution. (i) CP-TPP, (ii) CP-PPA, (iii) CPS-HMP, (iv) CROSS-CP-TPP, (v) CROSS-CP-PPA, and (vi) CROSS-CPS-HMP.

Table 4 shows NPs' zeta potentials and how they respond to ionotropic/covalent crosslinking and varying pH conditions. Clearly from the table, all ionotropically crosslinked NPs exhibit positive surface charges albeit significantly greater positive values are observed for NPs derived from unmodified chitosan. This is not surprising since grafting with anhydrides converts part of chitosan's surface cationic ammonium residues into neutral amides. Similar observations were reported previously (Yan et al., 2006; Dmour and Taha, 2017).

Interestingly though, HMP-based NPs (ionotropic and covalent) were accompanied with significantly higher positive surface charges (e.g., mean zeta potential for C-HMP NPs = +51 Mv) compared to their TPP- and PPA-based analogs (e.g., mean zeta potential of C-PPA NPs and C-TPP = +25.5 and 29 Mv, respectively).

This trend further proves our proposition that HMP is mainly core crosslinker with minimal influence on chitosan's cationic surface charge, while TPP, and partially PPA, act as surface crosslinkers that effectively neutralize positively charged chitosan's ammonium moieties by electrostatic attraction at NPs surfaces.

Table 4 points to another interesting observation by comparing zeta potentials of HMP-based ionotropic NPs, namely, CPS-HMP NPs and CP-HMP NPs. Clearly, CPS-HMP

TABLE 4 | Change of NPs zeta potentials upon covalent crosslinking and varying pH conditions.

NPs [a,b]	Zeta potential (mV)					
	Preparation pH[d]	pH 1.2[d]	pH 6.8[d]	pH 7.4		pH 12.0[d]
				Aqueous conditions	FBS (10% v/v)	
C-TPP	+29.0 ± 1.31	Clear	Aggregate	Aggregate	—[e]	Aggregate
C-PPA	+25.5 ± 0.92	Clear	Aggregate	Aggregate	—[e]	Aggregate
C-HMP	+51.5 ± 1.08	+7.6 ± 0.73[c]	Aggregate	Aggregate	—[e]	Aggregate
CP-TPP	+14.7 ± 1.92	clear	Aggregate	Aggregate	Aggregate	Aggregate
CP-PPA	+11.0 ± 1.31	clear	Aggregate	Aggregate	Aggregate	Aggregate
CP-HMP	+36.8 ± 1.45	+19.0 ± 1.95[c]	Aggregate	Aggregate	Aggregate	Aggregate
CPS-TPP	+13.5 ± 0.72	Clear	Aggregate	Aggregate	Aggregate	Aggregate
CPS-PPA	+11.4 ± 1.05	Clear	Aggregate	Aggregate	Aggregate	Aggregate
CPS-HMP	+26.8 ± 1.57	Aggregate	Aggregate	Aggregate	Aggregate	Aggregate
CROSS-CP-TPP	+9.4 ± 0.41	+14.9 ± 2.90	+1.4 ± 0.16	−4.5 ± 0.47	−3.14 ± 0.58	−14.3 ± 0.50
CROSS-CP-PPA	+8.2 ± 1.19	+12.0 ± 0.80	−2.9 ± 0.80	−5.9 ± 0.95	−1.64 ± 0.36	−15.9 ± 0.80
CROSS-CPS-HMP	+20.0 ± 1.64	+16.0 ± 0.76	+2.2 ± 0.50	−5.1 ± 0.47	−7.07 ± 0.37	−12.0 ± 0.69

[a] *See **Table 2** for pH value at preparation conditions.*
[b] *Each value represents the average of triplicate measurements ± standard deviation.*
[c] *NPs are stable without EDC.*
[d] *Aqueous conditions (no FBS).*
[e] *Not tested.*

NPs exhibited significantly lesser surface charge (+26 Mv) compared to CP-HMP NPs (+36 Mv). Since both NPs formulations were crosslinked by the same core crosslinking agent (HMP) and they have virtually identical degrees of carboxylic acid substitution (as deduced from pH shifts upon ionotropic gelling, see **Table 2**), it can be firmly concluded that the difference in their surface charges is related to the relative distribution of carboxylic acid substituents (phthalic and phenylsuccinic acids) on NPs surfaces vs. cores. The lower positive surface charge of CPS-HMP NPs suggests higher concentration of phenylsuccinic acid substituents at NPs surfaces compared to phthalic acid residues in CP-HMP NPs, which seem to concentrate within NPs cores leaving NPs surfaces with more intense positive charge. Probably, this behavior is because phenylsuccinic acid substituents are more hydrophilic and prefer interaction with water molecules at NPs surfaces; while hydrophobic phthalic acid residues prefer NPs cores to minimize their interactions with aqueous surroundings.

This trend is not obvious in TPP and PPA-crosslinked NPs (i.e., CPS-TPP and CPS-PPA vs. CP-TPP and CP-PPA) because of the significant neutralization of surface charge affected by these shell crosslinkers (particularly TPP) leaving little opportunity for the subtle effects of carboxylic acid substituents on surface charge to be clearly evident.

Interestingly, **Tables 3**, **4** show covalent NPs to exhibit moderate size and surface charge changes upon exposure to FBS (i.e., compared to equivalent aqueous pH 7.4).

Success to achieve covalent crosslinking with certain ionotropic NPs (i.e., CP-TPP, CP-PPA, and CPS-HMP) and failure with others (i.e., CP-HMP, CPS-TPP, and CPS-PPA) prompted us to hypothesize that EDC coupling is dependent on the shell/core complementarity of phosphate crosslinker and grafted carboxylic acid: Covalent crosslinking succeeds only if the phosphate crosslinker and grafted carboxylic acid are of opposing core/shell distribution, while it fails if the polyphosphate/carboxylic acid combination exhibit similar core/shell distribution properties. For example, in the unsuccessful case of CP-HMP NPs both grafted phthalic acid residues and HMP reside mainly within NPs cores. It appears that the steric bulk of core phthalic acid residues hinder EDC-mediated coupling of chitosan amines with core HMP phosphate groups. Similarly, CPS-TPP and CPS-PPA failed the EDC crosslinking reaction because PPA, TPP, and the attached phenylsuccinic acid units concentrate at NPs surfaces causing the steric bulk of phenylsuccinic acid moieties to interfere with EDC-mediated phosphoramide formation reaction.

On the other hand, crosslinker/carboxylic, acid combinations of orthogonal core/shell distribution minimize any negative interference in EDC coupling reaction and thus lead to better chances of covalent crosslinking. For example, success in covalent crosslinking of CPS-HMP NPs (i.e., CROSS-CPS-HMP NPs) is because HMP molecules remain within NPs cores far from the steric influence of the surface phenylsuccinic acid residues leading to effective EDC-mediated coupling of core HMP with nearby chitosan amine moieties. In contrast, TPP and PPA in CP-TPP and CP-PPA NPs reside at NPs surfaces (shell crosslinkers) far from core phthalic acid residues allowing facile EDC-mediated phosphoramide coupling at NPs surfaces to give CROSS-CP-TPP and CROSS-CP-PPA.

Finally, **Table 4** shows reduction in positive surface charges upon covalent crosslinking (from *ca.* +11 Mv for CP-PPA to +8 Mv for CROSS-CP-PPA; from *ca.* +14 Mv for CP-TPP to

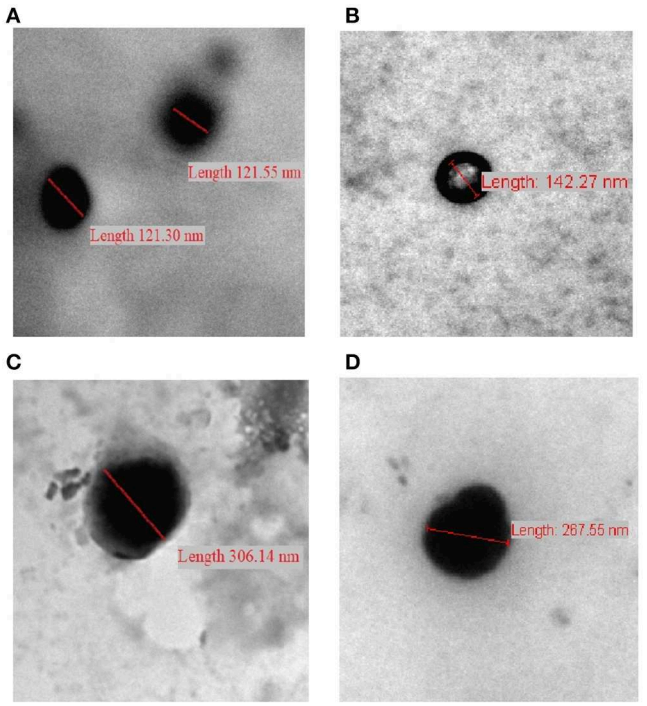

FIGURE 6 | TEM images of **(A)** CP-PPA NPs, **(B)** CROSS-CP-PPA NPs, **(C)** CPS-HMP NPs, and **(D)** CROSS-CPS-HMP NPs.

+9 Mv for CROSS-CP-TPP and from *ca.* +26 Mv for CPS-HMP NPs to +20 Mv for CROSS-CPS-HMP NPs) indicating that covalent crosslinking converted some surface chitosan ammonium moieties into neutral phosphoramides [and amides in CROSS-CPS-HMP NPs, see section Infrared spectroscopy (IR)] with loss of some positive surface charge.

NPs Morphology

We opted to use transmission electron microscopy (TEM) to assess the morphological properties of some representative NPs, as in **Figure 6**. The evaluated NPs have spherical shapes with sizes within the ranges identified by DLS. Covalent crosslinking did not change the morphology (i.e., spherical shapes) of the resulting NPs.

DRUG LOADING AND RELEASE PROFILES

Drug loading capacities (LCs) of ionotropic chitosan NPs depend on polyphosphate crosslinker content, chitosan-to-drug loading ratios (Wang et al., 2011a) and electrostatic interactions between the loaded drug(s) and the polymeric matrix of the NPs (Katas et al., 2013).

Methylene Blue Loading Into NPs

Methylene blue (MB, **Figure 1**) was used as model drug to study the LCs of prepared NPs. Two polymer-to-MB loading ratios were studied, namely, 10:1 and 1:1. The LCs were determined by measuring the amounts of released MB following shaking MB-loaded NPs in TRIS buffer (pH 7.4) over 24 h at 100 rpm and 37°C. Core MB loadings that resisted release under these conditions were determined following acid-degradation of NPs. The resulting LCs are summarized in **Table 5**.

Evidently from **Table 5**, MB loading increased significantly upon grafting chitosan with phthalic and phenylsuccinic acids. This trend is observed in ionotropic and covalent NPs alike. This behavior is not unexpected since the conjugated aromatic acids limit the cationic charge of chitosan, and therefore reduce electrostatic repulsion of cationic MB. Moreover, the aromatic rings of phthalic and phenylsuccinic conjugates provide viable flat surfaces for π-stacking interactions with MB thus promoting further NPs loading (Dmour and Taha, 2017). Additionally, grafted carboxylic acids act as hydrophobic barriers (being unionized under acidic conditions of NPs preparation) that limit free water exchange across NPs' surfaces thus hinder MB leaching from NPs during post loading processing (in particular centrifugation, see section Synthesis of chitosan-dicarboxylic acid derivatives and preparation of corresponding NPs).

Table 5 also shows another trend: Covalent crosslinking of CP NPs enhanced their LCs (i.e., in CP-TPP NPs from 18.3 to 27.3 mg/g, and in CP-PPA NPs from 37.2 to 62.1 mg/g). This is rather anticipated trend since covalent crosslinking makes NPs matrices stronger and more resistant to erosion, aqueous penetration and MB escape during processing steps performed after loading (Saboktakin et al., 2011; Dmour and Taha, 2017).

Nevertheless, ionotropic CPS-HMP NPs exhibited comparable LCs to their covalent counterparts CROSS-CPS-HMP NPs. Moreover, ionotropic and covalent CPS-HMP NPs illustrated the highest LCs amongst prepared NPs (at 1:1 loading ratios). We believe this behavior is because HMP attracts cationic MB molecules deeper into NPs cores during ionotropic NPs formation thus protecting loaded MB molecules from leaching into the medium during post loading processing. This mechanism seems to limit MB leaching from covalent CROSS-CPS-HMP NPs as well.

Interestingly, TPP-based NPs showed significantly lesser LCs compared to PPA and HMP-based counterparts. This is probably because PPA and HMP have more phosphate anions per molecule compared with TPP, which increase the efficiency of ionotropic binding with chitosan causing lesser leaching during NPs post loading processing.

DOX NPs Loading, Release Profiles, and Cytotoxicities

DOX-loaded CP-PPA, CPS-HMP, CROSS-CP-PPA, and CROSS-CPS-HMP NPs were recruited to study NPs LCs, DOX release profiles, and cytotoxicities. These particular NPs formulas were selected to study DOX loading and release profiles because they achieved the best MB LCs (see **Table 5**). **Table 6** shows their DOX LCs, average sizes and polydispersities.

Obviously, comparing NPs sizes in **Tables 3**, **6** shows DOX-loaded NPs to have larger sizes compared to their unloaded counterparts. Unsurprisingly, **Table 6** shows enhanced DOX LCs upon covalent crosslinking. Moreover, the tested NPs were able to load greater amounts of DOX compared to MB

TABLE 5 | LCs of MB-loaded NPs (mg/g).

NPs		Total LC (mg MB per g polymer)[a]			
Crosslinker	**Polymer**	**At 10:1 Polymer to MB ratio**		**At 1:1 Polymer to MB ratio**	
TPP	C	0.39 ± 0.05		7.33 ± 0.05	
	CP	1.97 ± 0.11	$p = 0.0002$[b]	18.31 ± 1.20	$p = 0.0001$[b]
	CROSS-CP[c]	4.57 ± 0.18		27.31 ± 0.62 (2.5 ± 0.05)[d]	
PPA	C	1.08 ± 0.02		10.87 ± 1.75	
	CP	2.02 ± 0.07	$p = 0.0010$[b]	37.19 ± 0.67	$p = 0.030$[b]
	CROSS-CP[c]	8.55 ± 0.35		62.05 ± 6.28 (3.9 ± 0.09)[d]	
HMP	C	1.33 ± 0.16		10.94 ± 0.96	
	CPS	4.63 ± 0.33	$p = 0.9080$[b]	100.30 ± 2.24	$p = 0.022$[b]
	CROSS-CPS[c]	4.66 ± 0.75		111.40 ± 1.58 (8.1 ± 0.02)[d]	

[a] *Each value represents the average of triplicate measurements± standard deviation.*
[b] *p-value Calculated using t-test with 5% significance for LC difference between covalent and corresponding ionotropic nanoparticles.*
[c] *EDC covalently stabilized NPs.*
[d] *NPs core loading determined through acid degradation (HCl, 2.0 M) of covalent NPs.*

TABLE 6 | LCs and size properties of DOX-loaded NPs prepared by 1:1 polymer-to-DOX loading ratios.

Ionotropic NPs				Covalent NPs			
NPs	**Loaded Doxorubicin (mg/g NPs)[a]**	**Size (nm)[a]**	**PDI[a,b]**	**NPs**	**Loaded Doxorubicin (mg/g NPs)[a]**	**Size (nm)[a]**	**PDI[a,b]**
CP-PPA	149.20 ± 2.55	212.1 ± 4.71	0.33 ± 0.04	CROSS-CP-PPA	220.07 ± 1.38	314.8 ± 19.4	0.42 ± 0.16
CPS-HMP	143.70 ± 2.80	471.1 ± 15.9	0.48 ± 0.18	CROSS-CPS-HMP	174.67 ± 3.70	357.7 ± 12.3	0.44 ± 0.10

[a] *Each point represents at least duplicate measurements ± standard deviation.*
[b] *Polydispersity index.*

(**Table 5**) probably because MB is of higher water solubility [43.6 and 20 mg/ml for MB (Peters and Freeman, 1996) and DOX, respectively] leading to more MB loss during post loading processing.

DOX release profiles from CP-PPA, CPS-HMP, CROSS-CP-PPA, and CROSS-CPS-HMP NPs are shown in **Figures 7A,B**. Three release phases can be recognized in the figure (seen in all tested NPs formulations): An initial fast phase (burst release) during the first 45 min resulting from quick dissolution of DOX molecules loosely adsorbed at NPs surfaces. A second slower subsequent phase, extending over 2–3 h, probably associated with water penetration through NPs matrices. A third phase, after ∼4–6 h, believed to be due to the degradation of polyphosphate crosslinkers (PPA and HMP) releasing DOX molecules deeply entrenched within NPs matrices.

The anticancer properties of DOX-loaded CP-PPA, CPS-HMP, CROSS-CP-PPA, and CROSS-CPS-HMP NPs were evaluated against breast cancer MCF-7 cells, which are widely used for assessing DOX drug delivery systems (Naruphontjirakul and Viravaidya-Pasuwat, 2019; Zhong et al., 2019). Unloaded NPs were virtually non-cytotoxic with cell viabilities exceeding 97% after exposure over 72 h. On the other hand, unloaded C-PPA and C-HMP NPs show significant cytotoxic properties with cell viabilities of *ca.* 80% upon exposure over the same time interval. Chitosan cytotoxicity is related to its cationic nature which disrupts the architecture of intercellular junctions between cancer cells (Loh et al., 2010; Fröhlich, 2012; Chokradjaroen et al., 2018; Morovati et al., 2019). Grafting chitosan with phthalic or phenylsuccinic acid reduce the cationic nature of chitosan and thus minimize the cytotoxicities of corresponding NPs.

Table 7 and **Figures 7C,D** show the anticancer profiles of DOX-loaded NPs compared to free DOX. The anticancer IC_{50} of DOX was enhanced by factors of 10 and 3.3 times upon loading in CP-PPA and CROSS-CP-PPA NPs, respectively (**Table 7**). This result suggests that loaded NPs are more efficiently up-taken by cancer cells compared to free DOX thus leading to higher intracellular DOX concentrations and cell death at lesser IC_{50} values. We believe this cytotoxic enhancement is due to the favorable sizes of loaded CP-PPA and CROSS-CP-PPA NPs (**Table 6**). Nevertheless, ionotropic CP-PPA performed better than their covalent counterparts (CROSS-CP-PPA) probably because they dissolve upon entry into cancer cells releasing all their DOX content, while their covalent siblings resist complete breakdown within cancer cells causing lesser intracellular release of DOX.

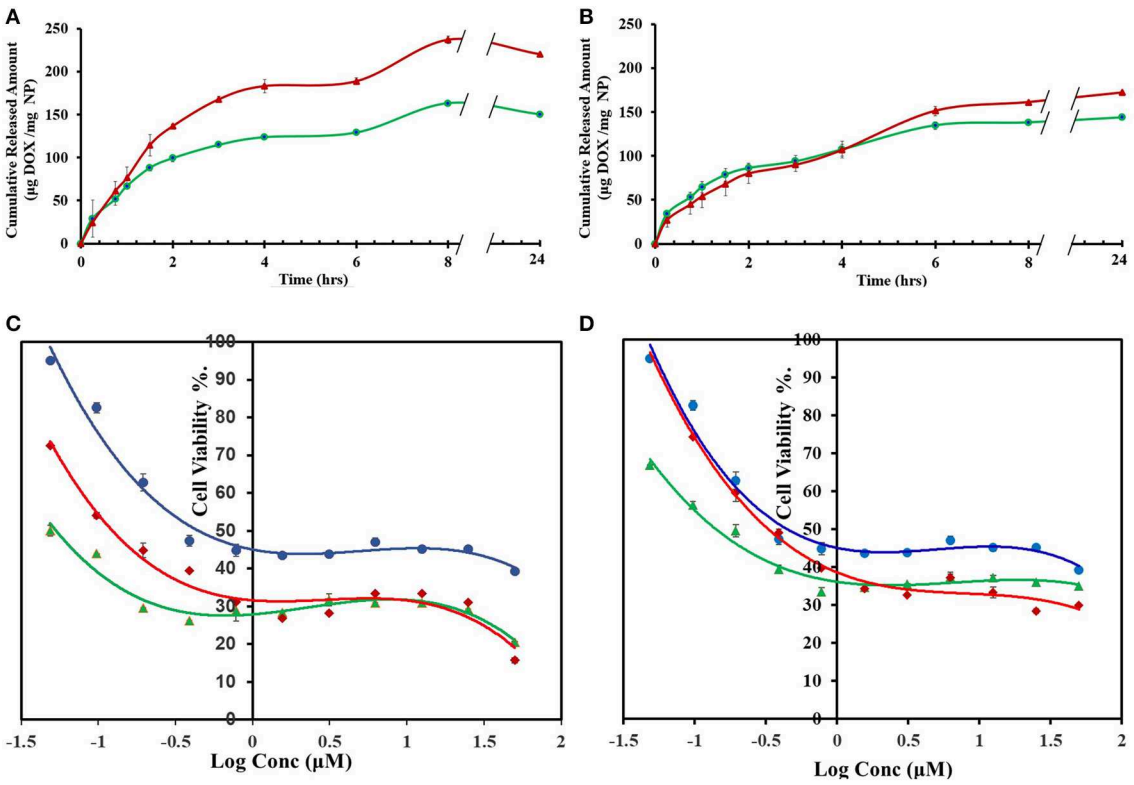

FIGURE 7 | DOX release and cytotoxic properties of DOX-loaded NPs (formulated at 1:1 polymer to DOX ratios) **(A)** Cumulative amounts of DOX released from CP-PPA (green line, ●) and CROSS-CP-PPA (red line, ▲). **(B)** Cumulative amounts of DOX released from CPS-HMP (green line, ●) and CROSS-CPS-HMP (red line, ▲). Dissolution studies were performed at 37°C and pH 7.4 TRIS buffer (100 rpm over 24 h) using 1:1 polymer to doxorubicin loading ratio. **(C)** MCF-7 cell viability after 72 h exposure to free DOX (blue line, ●), DOX-loaded ionotropic CP-PPA NPs (green line, ▲) and DOX-loaded CROSS-CP-PPA NPs (red line, ♦). **(D)** MCF-7 cell viability after 72 h exposures to free DOX (blue line, ●), DOX-loaded ionotropic CPS-HMP NPs (green line, ▲) and DOX-loaded CROSS-CPS-HMP NPs (red line, ♦). Each point represents the average of duplicate measurements. Error bars represent standard error of measurements.

TABLE 7 | IC_{50} of free DOX and DOX-loaded NPs against MCF-7 cell line.

Treatment	IC^{a}_{50} (µM)
Free DOX	0.457 ± 0.039
DOX loaded CP-PPA NPs	0.048 ± 0.001
DOX loaded CROSS-CP-PPA NPs	0.139 ± 0.014
DOX loaded CPS-HMP NPs	0.124 ± 0.005
DOX loaded CROSS-CPS-HMP NPs	0.360 ± 0.028

[a]*Each value represents the average of duplicate measurements ± standard deviation.* ***Figure S30*** *shows the cytotoxic effects of DOX and DOX-loaded NPs on tested cells.*

Regarding CPS-HMP NPs and their covalent progenies (CROSS-CPS-HMP NPs), they seem to have inferior anticancer performances compared to their ionotropic and covalent CP-PPA NPs analogs. We believe this difference in performance is related to the lesser LCs and enhanced physical and chemical stabilities of CPS-HMP NPs (ionotropic and covalent) compared to their CP-PPA analogs, which seem to reduce the rate of DOX release inside cancer cells.

To investigate NPs uptake by MCF-7 cells we used confocal laser scanning microscopy and wide-field fluorescence microscopy as means to compare cellular uptake of DOX-loaded NPs compared to free DOX. Untreated cells were evaluated as controls.

Figure 8 shows wide-field fluorescence microscopy images of MCF-7 cells treated with CROSS-CP-PPA and CROSS-CPS-HMP NPs compared to free DOX. The images clearly demonstrate the internalization of DOX-loaded NPs within cellular cytoplasm. **Figure 8** further illustrates the cellular uptake of loaded NPs with crystal-clear resolution using confocal fluorescence microscopy, particularly upon staining with DAPI to distinguish cellular nuclei from cytoplasms. In contrast to untreated cells, DOX-loaded NPs and free DOX caused cellular nuclei to fluoresce indicating nuclear uptake of DOX. However, cells treated with DOX-loaded NPs exhibited significantly more intense fluorescence compared to free DOX-treated cells indicating more efficient DOX cellular uptake via NPs. This is not unexpected since MCF-7 cells are known to exhibit DOX resistance via P-glycoprotein efflux pump (Wu et al., 2011). On the other hand, DOX-loaded NPs are not appropriate substrates for the efflux pump process (due to excessive large size), allowing efficient entry of NPs with their DOX cargos. This conclusion is supported by the appearance of numerous fluorescent aggregates within cellular cytoplasm after exposure to DOX-loaded NPs, as in **Figure 8**. These observations

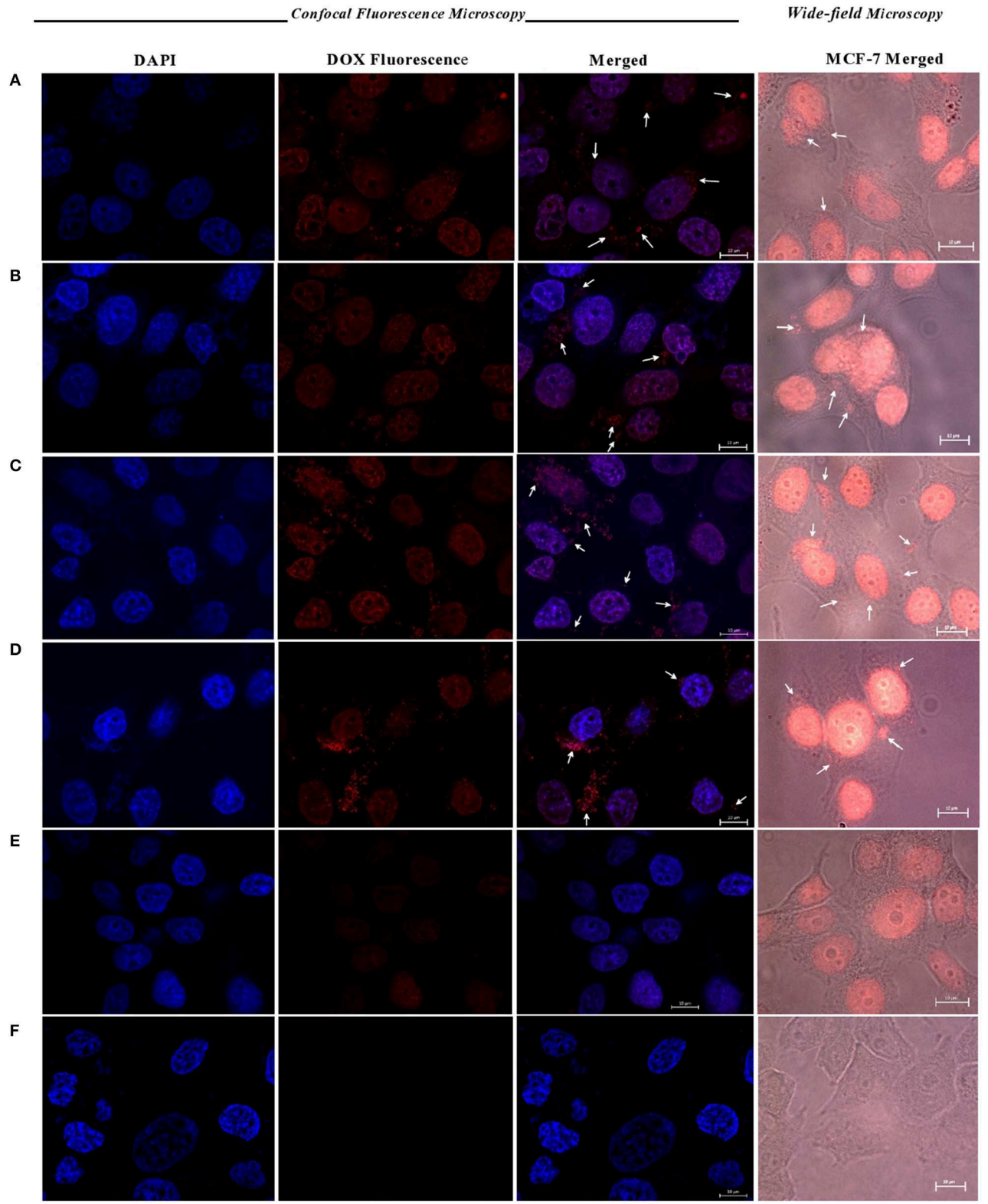

FIGURE 8 | Confocal and wide-field fluorescence microscopy images showing MCF-7 cells treated with DOX-loaded **(A)** CP-PPA NPs, **(B)** CROSS-CP-PPA NPs, **(C)** CPS-HMP NPs, **(D)** CROSS-CPS-HMP NPs, **(E)** MCF-7 cells treated with free DOX, and **(F)** untreated cells (control). All treatments are equivalent to 1.0 μM doxorubicin over 4 h periods. White arrows point nanoparticles up taken into cellular cytoplasm. Scale: 10 μm.

support our cytotoxicity results in **Table 7** and **Figures 7C,D**, suggesting that our NPs allow efficient entry of DOX into MCF-7 cells leading to improvement in DOX IC_{50} values (**Table 7**).

CONCLUSIONS

Lack of sufficient stability of chitosan NPs prompted us to produce novel stable chitosan NPs suitable for drug delivery applications. Chitosan was first grafted to phthalic or phenylsuccinic acids. Subsequently, PPA, HMP, or TPP were used to achieve tandem ionotropic/covalently crosslinked chitosan NPs in the presence of EDC. Infrared and DSC analysis confirmed the formation of phosphoramide bonds between chitosan and polyphosphate crosslinkers within NPs matrices. DLS and TEM size analysis indicated spherical NPs with size range below 350 nm. The generated NPs exhibited excellent stabilities under variable pH and $CaCl_2$ concentrations.

DLS, NPs stability and IR data suggest HMP to reside within NPs cores, while TPP and PPA act mainly as surface crosslinkers. However, we cannot exclude the possibility of certain degree of surface crosslinking by HMP and/or bulk crosslinking in TPP and PPA cases.

Drug loading and release studies using methylene blue (MB) and doxorubicin (DOX) drug models showed covalent PPA- and HMP-based NPs to have superior loading capacities compared to NPs based on unmodified chitosan, generated by ionotropic crosslinking only or covalently crosslinked by TPP. DOX-loaded CP-PPA NPs exhibited 10-fold cytotoxicity enhancement compared to free DOX.

Despite their success in delivering DOX into cancer cells, our new chitosan-based NPs need to be fully investigated with regard to biodegradability and elimination to be successfully implemented within clinical settings. We are currently researching these issues.

DATA AVAILABILITY STATEMENT

The datasets generated for this study are available on request to the corresponding author.

AUTHOR CONTRIBUTIONS

MT: study conception and administration. MT, RS, and ID: methodology and validation. RS: experimental work and manuscript drafting. MT and RS: manuscript review and editing.

FUNDING

This work was supported by the grant of the Deanship of Scientific Research, The University of Jordan. The authors express their gratitude to the generous financial support provided by the German Academic Exchange Service (DAAD) for supporting RS's master studies at The University of Jordan.

SUPPLEMENTARY MATERIAL

The Supplementary Material for this article can be found online at: https://www.frontiersin.org/articles/10.3389/fbioe.2020.00004/full#supplementary-material

REFERENCES

Aiedeh, K., and Taha, M. O. (1999). Synthesis of chitosan succinate and chitosan phthalate and their evaluation as suggested matrices in orally administered, colon-specific drug delivery systems. *Archiv der Pharmazie* 332, 103–107.

Al Bakain, R. Z., Abulateefeh, S. R., and Taha, M. O. (2015). Synthesis and characterization of chitosan-lactate–phthalate and evaluation of the corresponding zinc-and aluminum-crosslinked beads as potential controlled release matrices. *Eur. Polym. J.* 73, 402–412. doi: 10.1016/j.eurpolymj.2015.11.004

Almaaytah, A., Qaoud, M., Khalil Mohammed, G., Abualhaijaa, A., Knappe, D., Hoffmann, R., et al. (2018). Antimicrobial and antibiofilm activity of UP-5, an ultrashort antimicrobial peptide designed using only arginine and biphenylalanine. *Pharmaceuticals* 11:3. doi: 10.3390/ph11010003

Alves, N., and Mano, J. (2008). Chitosan derivatives obtained by chemical modifications for biomedical and environmental applications. *Int. J. Biol. Macromol.* 43, 401–414. doi: 10.1016/j.ijbiomac.2008.09.007

Baghdan, E., Pinnapireddy, S. R., Strehlow, B., Engelhardt, K. H., Schäfer, J., and Bakowsky, U. (2018). Lipid coated chitosan-DNA nanoparticles for enhanced gene delivery. *Int. J. Pharmaceut.* 535, 473–479. doi: 10.1016/j.ijpharm.2017.11.045

Baig, A., He, T., Buisson, J., Sagel, L., Suszcynsky-Meister, E., and White, D. (2005). Extrinsic whitening effects of sodium hexametaphosphate–a review including a dentifrice with stabilized stannous fluoride. *Compend. Contin. Educ. Dentistry* 26(9 Suppl 1):47–53.

Bracharz, F., Helmdach, D., Aschenbrenner, I., Funck, N., Wibberg, D., Winkler, A., et al. (2018). Harvest of the oleaginous microalgae Scenedesmus obtusiusculus by flocculation from culture based on natural water sources. *Front. Bioeng. Biotechnol.* 6:200. doi: 10.3389/fbioe.2018.00200

Brugnerotto, J., Lizardi, J., Goycoolea, F., Argüelles-Monal, W., Desbrieres, J., and Rinaudo, M. (2001). An infrared investigation in relation with chitin and chitosan characterization. *Polymer* 42, 3569–3580. doi: 10.1016/S0032-3861(00)00713-8

Cabrera, J. C., and Van Cutsem, P. (2005). Preparation of chitooligosaccharides with degree of polymerization higher than 6 by acid or enzymatic degradation of chitosan. *Biochem. Eng. J.* 25, 165–172. doi: 10.1016/j.bej.2005.04.025

Calvo, P., Remunan-Lopez, C., Vila-Jato, J. L., and Alonso, M. J. (1997). Chitosan and chitosan/ethylene oxide-propylene oxide block copolymer nanoparticles as novel carriers for proteins and vaccines. *Pharm Res* 14, 1431–1436. doi: 10.1023/A:1012128907225

Chaiyasan, W., Srinivas, S. P., and Tiyaboonchai, W. (2015). Crosslinked chitosan-dextran sulfate nanoparticle for improved topical ocular drug delivery. *Mol. Vision* 21:1224.

Chokradjaroen, C., Theeramunkong, S., Yui, H., Saito, N., and Rujiravanit, R. (2018). Cytotoxicity against cancer cells of chitosan oligosaccharides prepared from chitosan powder degraded by electrical discharge plasma. *Carbohydr. Polymers* 201, 20–30. doi: 10.1016/j.carbpol.2018.08.037

de Alvarenga, E. S. (2011). Characterization and properties of chitosan. *Biotechnol. Biopolym.* 91, 48–53. doi: 10.5772/17020

Dmour, I., and Taha, M. O. (2017). Novel nanoparticles based on chitosan-dicarboxylate conjugates via tandem ionotropic/covalent crosslinking with tripolyphosphate and subsequent evaluation as drug delivery vehicles. *Int. J. Pharmaceut.* 529, 15–31. doi: 10.1016/j.ijpharm.2017.06.061

Dmour, I., and Taha, M. O. (2018). "Natural and semisynthetic polymers in pharmaceutical nanotechnology," in *Organic Materials as Smart Nanocarriers for Drug Delivery,* ed A. M. Grumezescu (Elsevier; William Andrew), 35–100. doi: 10.1016/B978-0-12-813663-8.00002-6

Du, H., Yang, X., Pang, X., and Zhai, G. (2014). The synthesis, self-assembling, and biocompatibility of a novel O-carboxymethyl chitosan cholate decorated with glycyrrhetinic acid. *Carbohydr. Polym.* 111, 753–761. doi: 10.1016/j.carbpol.2014.04.095

Esfandiarpour-Boroujeni, S., Bagheri-Khoulenjani, S., and Mirzadeh, H. (2016). Modeling and optimization of degree of folate grafted on chitosan and carboxymethyl-chitosan. *Progr. Biomater.* 5, 1–8. doi: 10.1007/s40204-015-0044-0

Fröhlich, E. (2012). The role of surface charge in cellular uptake and cytotoxicity of medical nanoparticles. *Int. J. Nanomed.* 7:5577. doi: 10.2147/IJN.S36111

Grossman, J. H., and McNeil, S. E. (2012). Nanotechnology in cancer medicine. *Phys. Today* 65:38. doi: 10.1063/PT.3.1678

Gupta, A., Singh, P., and Shivakumara, C. (2010). Synthesis of BaSO4 nanoparticles by precipitation method using sodium hexa metaphosphate as a stabilizer. *Solid State Commun.* 150, 386–388. doi: 10.1016/j.ssc.2009.11.039

Honary, S., and Zahir, F. (2013). Effect of zeta potential on the properties of nano-drug delivery systems-a review (Part 1). *Trop. J. Pharmaceut. Res.* 12, 255–264. doi: 10.4314/tjpr.v12i2.19

Jiang, Y., and Wu, J. (2019). Recent development in chitosan nanocomposites for surface-based biosensor applications. *Electrophoresis* 40, 2084–2097. doi: 10.1002/elps.201900066

Katas, H., Raja, M. A. G., and Lam, K. L. (2013). Development of chitosan nanoparticles as a stable drug delivery system for protein/siRNA. *Int. J. Biomater.* 2013:146320. doi: 10.1155/2013/146320

Khan, T. A., Peh, K. K., and Ch'ng, H. S. (2002). Reporting degree of deacetylation values of chitosan: the influence of analytical methods. *J. Pharm. Pharmaceut. Sci.* 5, 205–212.

Kiilll, C. P., Barud, H. D. S., Santagneli, S. H., Ribeiro, S. J. L., Silva, A. M., Tercjak, A., et al. (2017). Synthesis and factorial design applied to a novel chitosan/sodium polyphosphate nanoparticles via ionotropic gelation as an RGD delivery system. *Carbohydr. Polym.* 157, 1695–1702. doi: 10.1016/j.carbpol.2016.11.053

Lind, S. C. (1948). Encyclopedia of Chemical Technology. Edited by Raymond E. Kirk and Donald F. Othmer. *J. Phys. Colloid Chem.* 52, 762–762. doi: 10.1021/j150460a013

Loh, J. W., Yeoh, G., Saunders, M., and Lim, L.-Y. (2010). Uptake and cytotoxicity of chitosan nanoparticles in human liver cells. *Toxicol. Appl. Pharmacol.* 249, 148–157. doi: 10.1016/j.taap.2010.08.029

Luo, X., Yang, Y., Kong, F., Zhang, L., and Wei, K. (2019). CD30 aptamer-functionalized PEG-PLGA nanoparticles for the superior delivery of doxorubicin to anaplastic large cell lymphoma cells. *Int. J. Pharmaceut.* 564, 340–349. doi: 10.1016/j.ijpharm.2019.04.013

Miola, M., Verné, E., Ciraldo, F. E., Cordero-Arias, L., and Boccaccini, A. R. (2015). Electrophoretic deposition of chitosan/45S5 bioactive glass composite coatings doped with Zn and Sr. *Front. Bioeng. Biotechnol.* 3:159. doi: 10.3389/fbioe.2015.00159

Morovati, A., Ahmadian, S., and Jafary, H. (2019). Cytotoxic effects and apoptosis induction of cisplatin-loaded iron oxide nanoparticles modified with chitosan in human breast cancer cells. *Mol. Biol. Rep.* 46:5033–5039. doi: 10.1007/s11033-019-04954-w

Nair, R. S., Morris, A., Billa, N., and Leong, C.-O. (2019). An evaluation of curcumin-encapsulated chitosan nanoparticles for transdermal delivery. *AAPS Pharm. Sci. Tech.* 20:69. doi: 10.1208/s12249-018-1279-6

Naruphontjirakul, P., and Viravaidya-Pasuwat, K. (2019). Development of anti-HER2-targeted doxorubicin–core-shell chitosan nanoparticles for the treatment of human breast cancer. *Int. J. Nanomed.* 14, 4105–4121. doi: 10.2147/IJN.S198552

Nishi, N., Ebina, A., Nishimura, S.-,i., Tsutsumi, A., Hasegawa, O., and Tokura, S. (1986). Highly phosphorylated derivatives of chitin, partially deacetylated chitin and chitosan as new functional polymers: preparation and characterization. *Int. J. Biol. Macromol.* 8, 311–317. doi: 10.1016/0141-8130(86)90046-2

Nyquist, R., Blair, E., and Osborne, D. (1967). Correlations between infrared spectra and structure: phosphoramides and related compounds—II. *Spectrochim. Acta Part A* 23, 2505–2521. doi: 10.1016/0584-8539(67)80145-4

Parab, H. J., Huang, J.-H., Lai, T.-C., Jan, Y.-H., Liu, R.-S., Wang, J.-L., et al. (2011). Biocompatible transferrin-conjugated sodium hexametaphosphate-stabilized gold nanoparticles: synthesis, characterization, cytotoxicity and cellular uptake. *Nanotechnology* 22:395706. doi: 10.1088/0957-4484/22/39/395706

Peng, J., Sun, Y., Zhao, L., Wu, Y., Feng, W., Gao, Y., et al. (2013). Polyphosphoric acid capping radioactive/upconverting NaLuF4: Yb, Tm, 153Sm nanoparticles for blood pool imaging *in vivo*. *Biomaterials* 34, 9535–9544. doi: 10.1016/j.biomaterials.2013.07.098

Peters, A. T., and Freeman, H. S. (1996). *Physico-Chemical Principles of Color Chemistry.* Springer. doi: 10.1007/978-94-009-0091-2

Rassu, G., Porcu, E. P., Fancello, S., Obinu, A., Senes, N., and Galleri, G. (2019). Intranasal delivery of genistein-loaded nanoparticles as a potential preventive system against neurodegenerative *Disorders* 11:E8. doi: 10.3390/pharmaceutics11010008

Rehfeld, S. J., Loken, H. F., and Eatough, D. J. (1977). Interaction of calcium ion with sodium triphosphate determined by potentiometric and calorimetric techniques. *Thermochim. Acta* 18, 265–271. doi: 10.1016/0040-6031(77)85060-0

Riva, R., Ragelle, H., des Rieux, A., Duhem, N., Jérôme, C., and Préat, V. (2011). "Chitosan and chitosan derivatives in drug delivery and tissue engineering," in *Chitosan for Biomaterials II. Advances in Polymer Science*, Vol. 244, eds R. Jayakumar, M. Prabaharan, and R. Muzzarelli (Berlin; Heidelberg: Springer), 19–44. doi: 10.1007/12_2011_137

Saboktakin, M., Tabatabaie, R., Maharramov, A., and Ramazanov, M. (2011). Synthesis and characterization of biodegradable thiolated chitosan nanoparticles as targeted drug delivery system. *J. Nanomed. Nanotechnol. S* 4:2. doi: 10.4172/2157-7439.S4-001

Savin, C.-L., Popa, M., Delaite, C., Costuleanu, M., Costin, D., and Peptu, C. A. (2019). Chitosan grafted-poly (ethylene glycol) methacrylate nanoparticles as carrier for controlled release of bevacizumab. *Mater. Sci. Eng.* 98, 843–860. doi: 10.1016/j.msec.2019.01.036

Shen, H., Jawaid, A. M., and Snee, P. T. (2009). Poly (ethylene glycol) carbodiimide coupling reagents for the biological and chemical functionalization of water-soluble nanoparticles. *Acs Nano* 3, 915–923. doi: 10.1021/nn800870r

Silva, M., Calado, R., Marto, J., Bettencourt, A., Almeida, A., and Gonçalves, L. (2017). Chitosan nanoparticles as a mucoadhesive drug delivery system for ocular administration. *Marine Drugs* 15:370. doi: 10.3390/md15120370

Song, M., Wang, H., Chen, K., Zhang, S., Yu, L., Elshazly, E. H., et al. (2018). Oral insulin delivery by carboxymethyl-β-cyclodextrin-grafted chitosan nanoparticles for improving diabetic treatment. *Artif. Cells Nanomed. Biotechnol.* 46, S774–S782. doi: 10.1080/21691401.2018.1511575

Su, T., Wu, Q.-X., Chen, Y., Zhao, J., Cheng, X.-D., and Chen, J. (2019). Fabrication of the polyphosphates patched cellulose sulfate-chitosan hydrochloride microcapsules and as vehicles for sustained drug release. *Int. J. Pharmaceut.* 555, 291–302. doi: 10.1016/j.ijpharm.2018.11.058

Sun, J., Yang, L., Jiang, M., and Xu, B. (2017). Stability and activity of immobilized trypsin on carboxymethyl chitosan-functionalized magnetic nanoparticles cross-linked with carbodiimide and glutaraldehyde. *J. Chromatogr. B* 1054, 57–63. doi: 10.1016/j.jchromb.2017.04.016

Tang, E., Huang, M., and Lim, L. (2003). Ultrasonication of chitosan and chitosan nanoparticles. *Int. J. Pharmaceut.* 265, 103–114. doi: 10.1016/S0378-5173(03)00408-3

Wang, J. J., Zeng, Z. W., Xiao, R. Z., Xie, T., Zhou, G. L., Zhan, X. R., et al. (2011a). Recent advances of chitosan nanoparticles as drug carriers. *Int. J. Nanomed.* 6:765. doi: 10.2147/IJN.S17296

Wang, N.-X., Wang, Y.-Q., He, X.-W., and Li, W.-Y. (2011b). One-step and rapid synthesis of composition-tunable and water-soluble ZnCdS quantum dots. *J. Nanosci. Nanotechnol.* 11, 4039–4045. doi: 10.1166/jnn.2011.3878

Wu, C.-P., Hsieh, C.-H., and Wu, Y.-S. (2011). The emergence of drug transporter-mediated multidrug resistance to cancer chemotherapy. *Mol. Pharmaceut.* 8, 1996–2011. doi: 10.1021/mp200261n

Yan, C., Chen, D., Gu, J., and Qin, J. (2006). Nanoparticles of 5-fluorouracil (5-FU) loaded N-succinyl-chitosan (Suc-Chi) for cancer chemotherapy: preparation,

characterization—*in-vitro* drug release and anti-tumour activity. *J. Pharmacy Pharmacol.* 58, 1177–1181. doi: 10.1211/jpp.58.9.0003

Yan, C., Jie, L., Yongqi, W., Weiming, X., Juqun, X., Yanbing, D., et al. (2015). Delivery of human NKG2D-IL-15 fusion gene by chitosan nanoparticles to enhance antitumor immunity. *Biochem. Biophys. Res. Commun.* 463, 336–343. doi: 10.1016/j.bbrc.2015.05.065

Yuan, D., Jacquier, J. C., and O'Riordan, E. D. (2018). Entrapment of proteins and peptides in chitosan-polyphosphoric acid hydrogel beads: a new approach to achieve both high entrapment efficiency and controlled *in vitro* release. *Food Chem.* 239, 1200–1209. doi: 10.1016/j.foodchem.2017.07.021

Zhang, J., Zhu, C., Hu, L., Liu, H., and Pan, H. C. (2018). Effect of freeze-drying process on the physical stability and properties of Voriconazole complex system. *Drying Technol.* 36, 871–878. doi: 10.1080/07373937.2017.1362648

Zhong, X.-C., Xu, W.-H., Wang, Z.-T., Guo, W.-W., Chen, J. J., Guo, N. N., et al. (2019). Doxorubicin derivative loaded Acetal-PEG-PCCL micelles for overcoming multidrug resistance in MCF-7/ADR cells. *Drug Dev Industr Pharmacy* 45, 1556–1564. doi: 10.1080/03639045.2019.1640721

Conflict of Interest: The authors declare that the research was conducted in the absence of any commercial or financial relationships that could be construed as a potential conflict of interest.

frontiers in Bioengineering and Biotechnology

REVIEW
published: 11 February 2020
doi: 10.3389/fbioe.2020.00019

Engineering Targeting Materials for Therapeutic Cancer Vaccines

Priscilla S. Briquez[1†], Sylvie Hauert[1†], Alexandre de Titta[2†], Laura T. Gray[1], Aaron T. Alpar[1], Melody A. Swartz[1,3,4] and Jeffrey A. Hubbell[1,4*]*

[1] Pritzker School of Molecular Engineering, The University of Chicago, Chicago, IL, United States, [2] Agap2 Zürich, Zurich, Switzerland, [3] Ben May Department of Cancer Research, The University of Chicago, Chicago, IL, United States, [4] Committee on Immunology, The University of Chicago, Chicago, IL, United States

OPEN ACCESS

Edited by:
Filippo Rossi, Politecnico di Milano, Italy

Reviewed by:
Benoit Frisch, UMR 7199 Laboratoire de Conception et Application de Molécules Bioactives, France
Pradipta Ranjan Rauta, University of Texas MD Anderson Cancer Center, United States

***Correspondence:**
Priscilla S. Briquez
pbriquez@uchicago.edu
Jeffrey A. Hubbell
jhubbell@uchicago.edu

[†] These authors have contributed equally to this work and share first authorship

Specialty section:
This article was submitted to Nanobiotechnology, a section of the journal Frontiers in Bioengineering and Biotechnology

Received: *10 October 2019*
Accepted: *10 January 2020*
Published: *11 February 2020*

Citation:
Briquez PS, Hauert S, de Titta A, Gray LT, Alpar AT, Swartz MA and Hubbell JA (2020) Engineering Targeting Materials for Therapeutic Cancer Vaccines. Front. Bioeng. Biotechnol. 8:19. doi: 10.3389/fbioe.2020.00019

Therapeutic cancer vaccines constitute a valuable tool to educate the immune system to fight tumors and prevent cancer relapse. Nevertheless, the number of cancer vaccines in the clinic remains very limited to date, highlighting the need for further technology development. Recently, cancer vaccines have been improved by the use of materials, which can strongly enhance their intrinsic properties and biodistribution profile. Moreover, vaccine efficacy and safety can be substantially modulated through selection of the site at which they are delivered, which fosters the engineering of materials capable of targeting cancer vaccines to specific relevant sites, such as within the tumor or within lymphoid organs, to further optimize their immunotherapeutic effects. In this review, we aim to give the reader an overview of principles and current strategies to engineer therapeutic cancer vaccines, with a particular focus on the use of site-specific targeting materials. We will first recall the goal of therapeutic cancer vaccination and the type of immune responses sought upon vaccination, before detailing key components of cancer vaccines. We will then present how materials can be engineered to enhance the vaccine's pharmacokinetic and pharmacodynamic properties. Finally, we will discuss the rationale for site-specific targeting of cancer vaccines and provide examples of current targeting technologies.

Keywords: cancer, vaccines, material engineering, targeting strategies, immunoengineering, immunotherapy

INTRODUCTION

Cancer ranks as the second leading cause of global deaths, according to the World Health Organization, with nearly 15% of people dying from it (World Health Organization, 2018). More alarmingly, the rate of cancer incidence is increasing and is expected to reach more than 20 million newly diagnosed cases per year and 13 million cancer-related deaths in 2030 (American Cancer Society, 2018; World Health Organization, 2018). Among the various types of cancer, the most prevalent are lung, liver, colorectal, stomach and breast cancers. While cancer can affect any part of the body and is very heterogeneous between patients, most malignant tumors share biological similarities – defined as the "hallmarks of cancer" (Hanahan and Weinberg, 2011) – which

help researchers break down the disease complexity and subsequently guide them toward the development of effective cancer therapies.

Currently, surgery, radiotherapy and chemotherapy remain the first-lines of cancer treatments that are prescribed as a single therapy or in combination, in a patient-tailored fashion that depends on the tumor characteristics (e.g., type, stage, aggressiveness and accessibility), as well as the patient's symptoms and health conditions (National Institutes of Health of the USA, 2019). In recent years, immunotherapies have emerged as highly promising treatments to educate the patient's immune system to efficiently fight its own cancer cells. The most successful clinical cancer immunotherapies that have received United States FDA approval to date include adoptive T cells therapies, immunomodulatory therapies, targeted cancer therapies, oncolytic virus therapies and cancer vaccines, as detailed in **Table 1**. Some of these treatments are currently being established as first-line treatments in cases of advanced cancers (Peters et al., 2019), highlighting the strong clinical potential of such immunotherapies. Furthermore, a multitude of novel immunotherapeutic compounds are currently being tested in clinical trials, foreseeing a fast evolution of the cancer therapy landscape in upcoming years.

Among these immunotherapies, vaccines aim at reducing cancer occurrence by preventing cancer-causing infections, in the case of prophylactic vaccines, or at developing strong host immune reactions and subsequent immune memory to efficiently eradicate primary tumor cells and metastasis, in the case of therapeutic vaccines. Therapeutic vaccines hold great promises for long-term remission in patients, in that they can install immunological memory directed against the tumor. Unfortunately, despite extensive research, only four cancer vaccines have made it into the clinic to date: two prophylactic ones, the human papilloma virus vaccine and the hepatitis B virus vaccine for prevention of cervical and liver cancer respectively, and two therapeutic ones, namely the Bacillus Calmette-Guérin (BCG) vaccine, which reduces relapse and metastasis of early stage bladder cancers, and Sipuleucel-T, a cell-based vaccine for advanced prostate cancer (DeMaria and Bilusic, 2019). Therefore, important additional efforts are required to achieve the high expectations of especially therapeutic cancer vaccines at the bedside.

Indeed, the next generation of therapeutic cancer vaccines will necessitate improvements both in terms of vaccine compositions and delivery strategies. In this review, we will discuss how such improvements could be achieved via materials engineering. Furthermore, while vaccination can lead to toxicity concerns due to strong systemic activation of the patient's immune system, we will present how engineering of targeting materials can enhance the safety profile of vaccines by localizing their effects to specific sites. Therefore, here we aim at providing the reader with design considerations, current challenges and lines of thoughts for the development of potent and safe site-specific targeting therapeutic cancer vaccines. Because very few of these vaccines have been developed to date, this review will take selected examples of targeting cancer immunotherapies – not only vaccines – to highlight possible engineering strategies that can be further applied to vaccination.

WHICH TYPE OF IMMUNE REACTIONS SHOULD THERAPEUTIC CANCER VACCINES INDUCE?

Engineering an optimal therapeutic cancer vaccine requires a good understanding of the type of immune reactions needed to eradicate tumors. Ideally, the vaccine should elicit potent immune responses that specifically recognize and eliminate all tumor cells present in the body, including those in the primary tumor, in circulation and in metastatic lesions. These immune responses should therefore be cancer cell antigen-specific to limit unwanted systemic side effects and prevent adverse autoimmune reactions. In addition, the vaccine should induce a strong immune memory against the cancer cells, able to efficiently reactivate anti-tumor immunity upon detection of cancer relapse, which is necessary to achieve long-term disease remission. In fact, cancer mortality has been largely imputed to relapses rather than to the primary tumor (Mehlen and Puisieux, 2006). As specificity and memory are hallmarks of the adaptive immune system, therapeutic cancer vaccines aim at activating endogenous cellular or humoral mechanisms of adaptive immunity against tumors.

The most common strategy exploited for the development of therapeutic cancer vaccines relies on the generation of endogenous cancer-specific cytotoxic $CD8^+$ T cells (cytotoxic T lymphocytes, CTLs), due to their unique ability to kill cancer cells upon specific recognition (Farhood et al., 2018). This recognition is mediated by the T cell receptor (TCR) of CTLs that can bind to cancer antigen epitopes mounted on the major histocompatibility complex class I (MHCI) displayed at the cancer cell surface. TCR-signaled CTLs can then induce cancer cell death via multiple pathways, including by degranulation, which releases perforin (PRF)/granzyme B (GZMB), or by upregulation of FasL or TRAIL that signal cancer cell apoptotic pathways (**Figure 1A**).

To become effective, CTLs need to be educated by antigen-presenting cells (APCs) prior to cancer cell recognition, the most professional APCs being dendritic cells (DCs) and especially $CD103^+$ migratory DCs. APCs provide CTLs with three required activation signals, namely (1) the cancer antigen epitope mounted on MHCI, (2) co-stimulatory molecules such as CD80/86 and CD40, and (3) pro-inflammatory cytokines such as IL-12, IFNβ and TNFα (Locy et al., 2018). In addition, activation and survival of CTLs is further supported by activated $CD4^+$ T helper (Th) cells via the secretion of additional cytokines, as well as via a process known as "DC licensing," by which a $CD4^+$ Th cell activates a DC through interaction with CD40, and subsequently supports CTLs that come in contact with the same DC (Ridge et al., 1998; Laidlaw et al., 2016). $CD4^+$ Th cells are activated by APCs similarly to $CD8^+$ T cells, with the exception that the cancer antigen epitope is presented on MHCII instead of MHCI.

Upon activation, CTLs and $CD4^+$ Th cells acquire particular phenotypes, which strongly determine the subsequent efficacy of CTL cytotoxic responses (Thorsson et al., 2018). Commonly, phenotypes of CTLs are defined by the cocktail of cytokines they

TABLE 1 | Current approved United States FDA immunotherapies.

Type of immunotherapy	Immunotherapy	Drugs	Cancer types
Adoptive cell therapy	CD19-targeting CAR T cells	Tisangenlecleucel (Kymriah) Axicabtagene ciloleucel (Yescarta)	Leukemia, lymphoma, pediatric cancer
Oncolytic virus therapy	Herpes simplex virus	T-VEC (Imlygic)	Melanoma
Cancer vaccine	Bacillus Calmette-Guérin (BCG) vaccine *(therapeutic)*	BCG vaccine	Bladder cancer
	Human papilloma virus (HPV) vaccine *(preventive)*	Cervarix, Gardasil, Gardasil-9	Cervical cancer
	Hepatitis B virus vaccine *(preventive)*	Heplisav-B	Liver cancer
	Patient immune cells stimulated with PAP (prostatic acid phosphatase) (*therapeutic*)	Sipuleucel-T (Provenge)	Prostate cancer
Immunomodulator	Anti-PD-1/PDL-1	Atezolizumab (Tecentriq) Avelumab (Bavencio) Cemiplimab (Libtayo) Durvalumab (Imfinzi) Nivolumab (Opdivo) Pembrolizumab (Keytruda)	Bladder cancer, breast cancer, cervical cancer, Colorectal cancer, esophageal cancer, head and neck cancer, kidney cancer, liver cancer, lung cancer, lymphoma, melanoma, pediatric cancer, skin cancer, stomach cancer
	Anti-CTLA-4	Ipilimumab (Yervoy)	Melanoma, pediatric cancer
	Combination anti-PD-1 and anti-CTLA-4	Nivolumab (Opdivo) + Ipilimumab (Yervoy)	Kidney cancer, melanoma
	IL-2	Aldesleukin (Proleukin)	Kidney cancer, melanoma
	Interferon alfa-2a	Roferin-A	Leukemia
	Interferon alfa-2b	Intron A, Sylatron/PEG-Intron	Leukemia, lymphoma, melanoma
Other targeted therapies	Anti-GD2	Dinutuximab (Unituxin)	Brain cancer, pediatric cancer
	Anti-VEGF-R	Bevacizumab (Avastin) Ramucirumab (Cyramza)	Brain cancer, cervical cancer, colorectal cancer, esophageal cancer, kidney cancer, lung cancer, ovarian cancer, stomach cancer
	Anti-HER2	Pertuzumab (Perjeta) Tratuzumab (Herceptin)	Esophageal cancer, breast cancer, stomach cancer
	Anti-HER2-drug conjugates	Tratuzumab emtansine (Kadcyla)	
	Anti-EGFR	Cetuximab (Erbitux) Necitumumab (Protrazza)	Colorectal cancer, head and neck cancer, lung cancer
	CD19-CD3 bispecific antibody	Blinatumomab (Blincyto)	Leukemia
	Anti-CD20	Obinutuzumab (Gazyva), Ofatumumab (Arzerra), Rituximab (Rituxan)	Leukemia, lymphoma
	Anti-CD20-drug conjugates	Ibritumomab tiuxetan (Zevalin)	
	Anti-CD22-drug conjugates	Inotuzumab ozogamicin (Besponsa)	Leukemia
	Anti-CD33-drug conjugates	Gemtuzumab ozogamicin (MyloTarg)	
	Anti-CD52	Alemtuzumab (Campath)	Leukemia
	Anti-CD30-drug conjugates	Brentuximab vedotin (Adcetris)	Lymphoma
	Anti-CD79b-drug conjugates	Polatuzumab vedotin (Polivy)	
	Anti-CD38	Daratumumab (Darzalex)	Multiple myeloma
	Anti-SLAMF7	Elotuzumab (Empliciti)	
	Anti-RANKL	Denosumab (Xgeva)	Sarcoma

Immunotherapies are currently emerging in the landscape of treatments for most type of cancers. Among them, a few cancer vaccines are approved, and many more are currently under assessment in clinical trials. List taken from the Cancer Research Institute (CRI) website on July 2019 (www.cancerresearch.org/immunotherapy).

produce, as well as by the cytotoxic pathway they use to induce cell death. Many studies have shown that the production of IFNγ and TNFα by CTLs correlates with better control of tumor burden and enhanced patient survival (Matsushita et al., 2015; Bhat et al., 2017). In parallel, other studies have demonstrated an increased patient survival when $CD4^+$ Th cells acquire a Th1 phenotype, characterized by the secretion of IFNγ, TNFα and IL-2. Although more controversial (Chen and Gao, 2019), it has been shown that combination of the Th1 response with a Th17 orientation, characterized by IL-17 production, can be further beneficial (Punt et al., 2015; Thorsson et al., 2018). Noteworthily, not only the type of secreted cytokine matters, but also their variety and amount. Indeed, T cells that secrete multiple cytokines are known to be more efficient than those expressing a

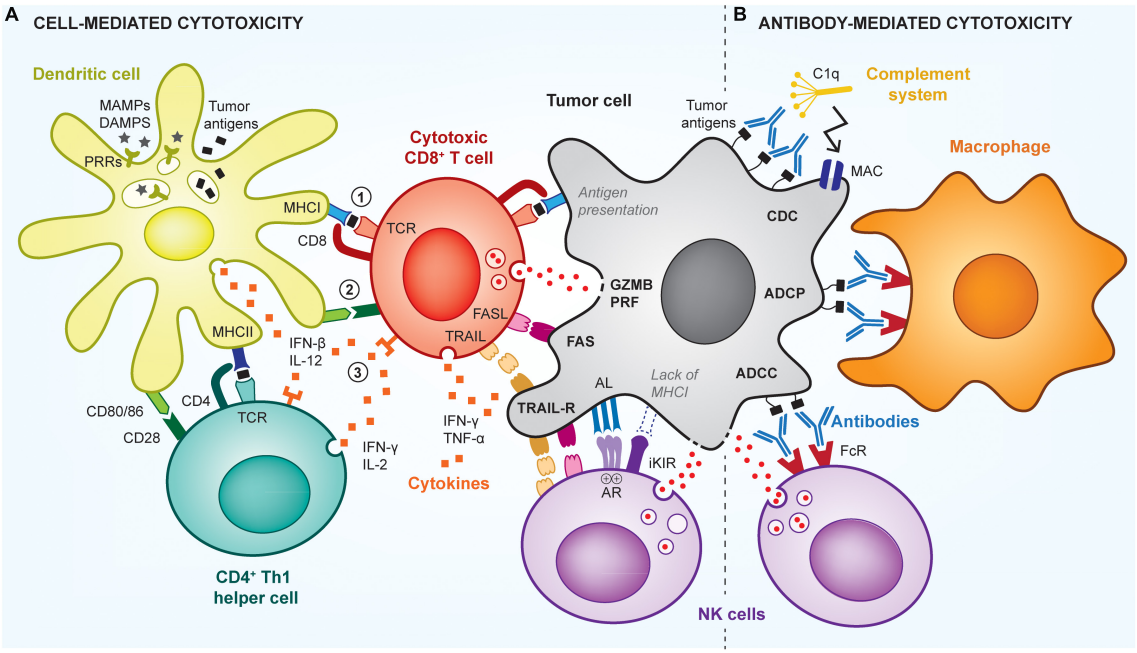

FIGURE 1 | Cell- and antibody-mediated cytotoxic mechanisms of anti-tumor immunity. The immune system uses multiple mechanisms to efficiently kill tumor cells, via cytotoxic CD8$^+$ T cells (CTLs), NK cells, or antibody-mediated mechanisms. **(A)** To be activated, T cells need 3 signals from antigen-presenting cells (APCs; e.g., dendritic cell): signal (1) is the presentation of cancer antigens (black squares) via MHC complexes; signal (2) is the signaling induced by co-stimulatory receptors (e.g., CD80/86), which are expressed by the APCs in the presence of adjuvants (e.g., MAMPs/DAMPs); and signal (3) is the stimulation by pro-inflammatory cytokines. Such cytokines are produced by APCs as well as by CD4$^+$ Th1 helper cells that further enhance activation of CTLs. Upon activation and recognition of tumor cells, CTLs can induce their death via various pathways, including perforin (PRF)/granzyme B (GZMB), FasL-Fas, TRAIL or inflammatory cytokines. Using similar pathways, NK cells can kill cancer cells that have downregulated their MHCI expression and fail to signal through the inhibitory killer immunoglobulin-like receptor (iKIR), or that overstimulate NK activating receptors (AR). **(B)** Tumors cells can also be targeted by antibodies that induce direct killing via the activation of the complement cascade, through a mechanism called complement-dependent cytotoxicity (CDC), which leads to the formation of membrane attack complexes (MAC) perforating the tumor cell membrane. In addition, antibodies can signal via Fc receptors (FcR) on innate immune cells, to induce antibody-dependent cell phagocytosis (ADCP) of tumor cells by macrophages, or antibody-dependent cell cytotoxicity (ADCC) by NK cells or neutrophils.

single one (Seder et al., 2008). In addition, because each T cell has a unique TCR able to recognize only a single antigenic epitope, immune responses that generate a broad clonality of anti-tumor T cells (i.e., multiple T cells clones) are more robust (Thorsson et al., 2018). All that being said, the ideal type of immune response sought upon vaccination might vary between cancers.

In addition, antibody-mediated cytotoxic mechanisms can also efficiently control tumor growth (Zahavi et al., 2018) and be harnessed by cancer vaccination (**Figure 1B**). Particularly, antibodies that specifically bind to cancer cells can trigger their elimination by antibody-mediated cellular cytotoxicity (ADCC), antibody-mediated cellular phagocytosis (ADCP) or complement-dependent cytotoxicity (CDC) (Almagro et al., 2018). To date, such mechanisms have been mostly exploited in passive cancer immunotherapies via the infusion of therapeutic antibodies in patients, rather than in the context of humoral-based cancer vaccines, which aim to activate endogenous host anti-cancer antibody responses (Huijbers and Griffioen, 2017). In both cases, antibodies recognize short conformational or linear epitopes exposed on the cancer cell surface (Bayrami et al., 2016; Tarek et al., 2018). Then, innate immune cells, mostly natural killer (NK) cells, macrophages and neutrophils, can detect bound antibodies via their Fc receptors and subsequently induce cell lysis, in case of ADCC, or phagocytosis, in case of ADCP. In contrast, CDC is independent of immune cells and can directly activate the complement pathway to form cytolytic pores in cancer cell membranes, inducing their death. Such antibody-mediated anti-tumor responses are antigen-specific and can provide immune memory if the tumor-specific antibodies are produced endogenously.

Finally, the anti-cancer adaptive immune response sought by cancer vaccination can be further supported by co-activation of other mechanisms of innate immunity. For example, innate lymphoid cells (ILCs), such as NK cells or invariant NK T cells (iNKT), have the ability to control cancer cells in complementary ways to CTLs (Nair and Dhodapkar, 2017; Souza-Fonseca-Guimaraes et al., 2019). For example, NK cells possess cytotoxic capabilities and can lyse cancer cells that downregulate MHCI to avoid T cell recognition or that overstimulate activating receptors on NK cells (e.g., NKG2D, 4-1BB) (Souza-Fonseca-Guimaraes et al., 2019). On the other hand, activation of iNKT cells can result in secretion of Th1 or Th2 cytokines in the microenvironment and increase their CD40L expression. Therefore, iNKT cells can strongly stimulate DC and B cell maturation and indirectly promote T cell responses, thus illustrating a pivotal role in modulating adaptive immune responses (Cerundolo et al., 2009).

Nevertheless, because NK or iNKT cells are not antigen-specific and do not establish immune memory, they are often not the primary targets of cancer vaccines.

WHAT SHOULD THERAPEUTIC CANCER VACCINES BE COMPOSED OF?

The composition of therapeutic cancer vaccines directly relates to their anticipated biological outcomes. Commonly, cancer vaccines are made of antigens that define what is recognized on or within cancer cells, as well as adjuvants that determine the type of immune response that will be induced.

Cancer Antigens

Including cancer antigens in vaccines is essential to induce targeted cancer cell death as well as to avoid toxic, non-specific immune reactions. Determining the appropriate immunogenic antigen to incorporate in therapeutic cancer vaccines, however, remains extremely challenging. Indeed, the self-origin of cancer cells makes them hard to discriminate from healthy cells, as they carry most of the host proteome, which is naturally immune tolerized to prevent autoimmune reactions. Nevertheless, different types of cancer antigens have been successfully used in cancer vaccines, as detailed below (Vigneron, 2015; Finn, 2017).

First, cancer vaccines often use tumor-associated antigens (TAAs) as targets, which are molecules largely overexpressed in tumor cells (e.g., 10–1000 fold increase in some cases) as compared to healthy cells (Vigneron, 2015). Notably, TAAs can be proteins involved in tumor cell survival and proliferation, such as HER2, EGFR, p53, telomerase, survivin, and Ras, in tumor metabolism, such as folate-related proteins and glucose receptors (e.g., GLUT1), or other proteins such as MUC-1 and mesothelin (Vigneron, 2015). However, the main drawbacks of TAAs reside in the difficulty of inducing strong immunity against them, which must break endogenous immune tolerance mechanisms, while preventing autoimmune reactions against healthy cells.

As an alternative, vaccines can use tumor-specific antigens, which are absent in healthy cells or expressed in limited areas. Particularly, cancer cells can re-express MAGE antigens, NY-ESO-1, 5T4 or the carcinoembryonic antigen (CEA), which are only present during the developmental stage or in very specific tissues (e.g., placenta, testis) in the body (Vigneron, 2015). The restricted expression of such tumor-specific antigens provides the advantage of limiting off-target reactions. Interestingly, it has been shown that some of these antigens are naturally immunogenic and able to raise specific T cell responses in spite of their endogenous origin. Additionally, some types of cancer exhibit specific mutations that can be conserved across patients, such as the BRAF mutation in melanoma, which can constitute good antigenic targets as they are exclusively present in cancerous tissues (Mandalà and Voit, 2013).

Similarly, most tumors contain specific mutated antigens, called neoantigens, due to the higher mutational rate of cancer cells as compared to healthy ones (Schumacher and Schreiber, 2015). These antigens constitute a subclass of tumor-specific antigens, and can be similarly targeted by cancer vaccines. However, the use of neoantigens implies more personalized therapies, as they are different between patients, tumors or even tumor cell subsets. Nevertheless, recent technological advances and ease in genome sequencing allow the fast emergence of such therapies. Neoantigens have been proven to be immunogenic, and their restricted expression in cancer cells highly limits the risk of T cell reactions against healthy self cells. Neoantigens are being widely addressed, with many researchers focusing on understanding how to select, design and deliver the most relevant neoepitopes to incorporate into vaccines (Schumacher et al., 2019).

Furthermore, other strategies use whole cancer cells or cancer cell-derived materials as antigenic components in vaccines, instead of selecting single or combinations of defined antigens (Vermaelen, 2019). Such approaches are particularly interesting as they allow vaccination against multiple cancer antigens, while bypassing the need of identifying them. For example, lethally irradiated cancer cells derived from the primary tumor have been used to induce effective polyantigenic anti-tumor immune responses (Vermaelen, 2019). In addition, tumor cells can be prepared as lysates (González et al., 2014). In such cases, it is expected that the immunogenic responses will be mainly directed against cancer-specific antigens rather than against co-delivered endogenous proteins, since immune tolerance mechanisms would dampen responses to self-antigens. Lastly, cancer antigens have been shown to be present on tumor-derived extracellular vesicles, such as exosomes, as well as on tumor apoptotic debris, which can then also serve as antigenic materials (André et al., 2002). Importantly, targeting multiple antigens provides the advantage of reducing the risk of tumor immune escape, a mechanism by which cancer cells downregulate targeted antigens, mutate them or limit their presentation on MHC to avoid recognition and killing by CTLs.

Finally, cancer vaccines could also be rationally designed to target the tumor *in vivo* and use it as an *in situ* source of cancer antigens, as further discussed in the section "Rationale for Site-Specific Targeting of Therapeutic Cancer Vaccines". Because these tumor-targeting vaccines can be composed of only adjuvants (i.e., without added antigens), whether it is classified as a therapeutic vaccine or as another type of immunotherapy is arguable.

Immune Adjuvants

The delivery of antigens alone may induce immune tolerance rather than activation. As a consequence, vaccines need to combine antigens with adjuvants, which are immunostimulatory molecules able to skew immune cells toward the desired type of immune response. Adjuvants can be derived from microbes, so called microbial-associated molecular patterns (MAMPs) or pathogen-associated molecular patterns (PAMPs), from endogenous danger signals released upon cell damage or immunogenic cell death, known as damage-associated molecular patterns (DAMPs), or can simply be cytokines that are naturally secreted to support endogenous immune responses (Tovey and Lallemand, 2010; Tang et al., 2012).

Both MAMPs and DAMPs are able to generate Th1 and CTL immune responses, as mostly intended in cancer vaccines, via the activation of pattern-recognizing receptors (PRRs) on APCs (Tang et al., 2012). Among these PRRs, Toll-Like receptors (TLRs) have been the most studied, with 6 gathering a significant interest in cancer vaccines, namely TLR-2, -3, -4, -7/-8, and -9 (Gay and Gangloff, 2007). These receptors are located in the endosomal compartment of APCs, except for TLR-2 and -4 which are on the cell surface. Consistent with their subcellular location, TLR-3, -7/-8, and -9 primarily recognize nucleic acid ligands from viruses or bacteria, double-stranded RNA, single-stranded RNA and unmethylated CpG oligodinucleotides (ODN), respectively, whereas TLR-2 recognizes bacterial lipoproteins (Lpp) upon dimerization with TLR-1 or -6, and TLR-4 recognizes lipopolysaccharides (LPS) from bacterial outer membranes. Examples of well-known TLR ligands that have been assessed in cancer vaccines are Pam3CSK4 (Zom et al., 2018) and Pam2Cys (Zhou et al., 2019) for TLR-2/1 and -2/6 respectively, poly(I:C) for TLR-3 (Ammi et al., 2015), LPS and monophosphoryl lipid A (MPLA) for TLR-4 (Cluff, 2010), imiquimod and other imidazoquinolines for TLR-7/-8 (Dowling, 2018), and CpG-B for TLR-9 (Shirota et al., 2015). Although these TLR agonists are very potent in activating immune responses, they can be associated with toxicity, which affects their clinical translation. Interestingly, some endogenous extracellular proteins have also been identified as TLR agonists and might be potentially safer considering their endogenous origin. For instance, the extra domain A (EDA) of fibronectin, a matrix protein, can bind to TLR-4 upon proteolytic cleavage and has showed some promises as adjuvant in cancer vaccines in pre-clinical models (Lasarte et al., 2007; Julier et al., 2015).

In addition to TLRs, other PRRs can be targeted by cancer vaccines. For example, the cytosolic DNA sensor cGAS detects aberrant concentrations of DNA in the cytosol and triggers the simulator of interferon genes (STING) pathway (Li et al., 2019). Another example is the cytosolic RNA sensor RIG-I that detects particular viral dsRNA (Tang et al., 2012; Elion and Cook, 2018). Stimulators of these cytosolic nucleic-acid sensor pathways are currently being explored as adjuvants for cancer immunotherapies.

Upon PRR signaling, APCs undergo maturation, which results in increased antigen presentation, expression of co-stimulatory receptors and secretion of cytokines, thus providing the three signals necessary for T cell activation, as previously detailed. Additionally, the nature of the co-stimulatory receptors and cytokine expression by APCs depends on the type of delivered adjuvants. Interestingly, it has been shown that secretion of IFNα and IFNβ by APCs upon maturation can induce direct inhibitory effects on tumor cell proliferation and activate their apoptotic pathways, inducing cancer cell death (Apelbaum et al., 2013).

Since cytokines themselves can strongly support immune responses, they have also been considered as adjuvants in cancer vaccines. Particularly, cytokines can be delivered to promote activation of immune cells, recruit them at specific sites, or induce their proliferation. For instance, IL-2, IL-12, IFNα, and IFNβ have been used to increase survival and activation of T cells, NK cells and APCs. Despite being very effective in boosting anti-tumor immune responses, these cytokines suffer from toxicity-related issues, similarly to TLR agonists, and require further development of appropriate delivery systems to harness their potential in the clinic. On the other hand, chemokines – a subset of cytokines – have been used to attract APCs at the vaccine site, thus enhancing overall antigen presentation and subsequent immune cell activation. While some chemokines induce the recruitment of multiple types of APC (e.g., DCs, macrophages), such as CCL3 and CCL4 (Nguyen-Hoai et al., 2016; Allen et al., 2018), some others recruit specific APC subsets. For example, the delivery of XCL1 specifically attracts the $CD103^+$ DCs (Russell et al., 2007; Sánchez-Paulete et al., 2018), known to express the cognate receptor XCR1 and be highly efficient in generating CTLs. Moreover, chemokines can also be used to recruit T cells, rather than APCs. Notably, CXCL10 and CXCL11 have been delivered to increase infiltration of activated T cells in tumors (Groom and Luster, 2011). Lastly, as an alternative to recruitment, *in situ* proliferation of immune cells can be promoted by the delivery of growth factors. Particularly, granulocyte-macrophage colony-stimulating factor (GM-CSF) has been used to expand DC populations in a therapy called GVAX (Simons and Sacks, 2006).

Interestingly, the secretion of multiple cytokines by activated iNKT cells can also be exploited as an adjuvant in cancer immunotherapies, including vaccines (Wolf et al., 2018; Fujii and Shimizu, 2019). Upon activation by CD1d-bound α-Galactosylceramide (α-GalCer; KRN7000) on APCs, iNKT cells secrete large amounts of IFNγ and IL-4 that enhance DC maturation and subsequent antigen-specific T cell responses.

Finally, in addition to exogenous adjuvant delivery, another important strategy in cancer vaccines is to exploit the release of endogenous DAMPs by the tumor itself to self-adjuvant vaccines (Hernandez et al., 2016). Indeed, induction of immunogenic cancer cell death by current therapies, such as chemotherapy, radiotherapy, and/or immunotherapy, can substantially increase the release of DAMPs from dying tumor cells, such as heat-shock proteins (HSPs), adenosine-triphosphate (ATP) or the high mobility group protein B1 (HMGB1) (Tang et al., 2012). Along with endogenous DAMPs, immunogenic cancer cell death co-releases cancer antigens, together promoting antigen spreading, a complex mechanism by which immune reactions are mounted against antigens that were not originally targeted by a therapy (Gulley et al., 2017). As a consequence, any method capable of killing cancer cells in an immunogenic way can potentially boost the effects of cancer vaccines and broaden the anti-cancer immune response to multiple antigens.

HOW TO ENGINEER TARGETING MATERIALS FOR THERAPEUTIC CANCER VACCINE DELIVERY?

Once the cancer vaccine components have been defined, the way they are delivered will significantly impact overall efficacy and safety. As a consequence, the vaccine delivery needs to be rationally designed from the entry into the patient to its terminal

effect; this includes the administration route into the patient, the targeting to correct tissues, cell types, subcellular locations and specific receptors, and ultimately the onset of appropriate immune responses. All together, these steps constitute the pharmacokinetic and pharmacodynamic profiles of the vaccine and can be fine-tuned by the use of materials. Here, we will discuss how materials can be engineered to optimally deliver its components and target them into relevant sites.

Where to Target Therapeutic Cancer Vaccines?

Possible Delivery Routes for Therapeutic Cancer Vaccines

From a clinical point of view, cancer vaccines can be conveniently administered to patients via intradermal, subcutaneous, intramuscular, intravenous or intratumoral routes, if the tumor is easily accessible at the body surface, as in skin cancers. However, intratumoral administration can become challenging depending on the tumor size, location, the number of tumors to inject, as well as on the intrinsic heterogeneity of tumor structures that can lead to non-homogenous drug distribution (Marabelle et al., 2018). Similarly, intralymphatic, intranodal and intrasplenic delivery routes are relatively complex, although they may be relevant from a biological point of view, as discussed below. Other routes, such as topical, oral or intranasal, are often less utilized yet might be appropriate in specific types of cancer.

The choice of the vaccine delivery route should be based on the anticipated biological mechanisms of action, since its efficacy depends on its bioavailability at the targeted sites. In the case of therapeutic cancer vaccines, tumor tissues and lymphoid organs are generally considered as the most interesting sites to target, and many direct or indirect strategies have been explored to deliver drugs at these locations.

Rationale for Site-Specific Targeting of Therapeutic Cancer Vaccines

Tumors are the primary location where therapeutic efficacy is sought, when they cannot be fully removed by surgery. Accordingly, targeting cancer vaccines into tumors is an appealing strategy to induce direct *in situ* cytotoxic effects and promote potent antigen-specific adaptive immune responses (Marabelle et al., 2014). Of particular importance, the tumor is the main source of cancer antigens, and thus can be used in place of or in combination with antigens from the vaccine (**Figure 2A**). Because the tumor gathers high concentrations of all cancer antigens at the same location, it theoretically constitutes an ideal target to promote broad polyantigenic immune responses. Interestingly, targeting the vaccine into tumors may also allow induction of immune reactions against antigens expressed only by small subpopulations of cancer cells, such as cancer stem cells, which are particularly important to eradicate (Saygin et al., 2019). Another advantage of targeting tumors *in vivo* is provided by the local release of antigens and DAMPs upon intratumoral cytotoxicity, which can enhance antigen spreading and thus the vaccine's effects, as discussed in the section "Immune Adjuvants" (Hernandez et al., 2016; Gulley et al., 2017). Finally, some inflamed tumors are the battlefield of pre-existing anti-tumor immune reactions, which can be further supported or re-activated *in situ* by tumor-targeting vaccines.

On the other hand, tumor-targeting strategies also present some important limitations for vaccination. First, although intratumoral activation of immune cells has been demonstrated, tumors are not physiologically optimized to mount strong immune responses, as opposed to lymphoid tissues (Thompson et al., 2010). Secondly, the high heterogeneity of tumor compositions may strongly affect the efficacy of the vaccines, possibly requiring tailoring per tumor characteristics (Binnewies et al., 2018). In particular, vaccines targeted to tumors that are known as immune deserts (i.e., lack of immune infiltrates) are likely to be poorly effective as compared to targeting into inflamed tumors. Thirdly, the tumor microenvironment is known to be strongly immunosuppressive, which would undeniably prevent potent anti-tumor immune reactions to be mounted upon vaccination.

To overcome these limitations, other sites might be interesting to target by cancer vaccines, notably lymphoid organs, including lymph nodes and the spleen, which are physiologically optimized to build potent immune responses and might be exposed to tumor antigens (Thomas et al., 2014; Rotman et al., 2019; **Figure 2B**). Indeed, tumor interstitial fluid and debris are drained from the tumor to the lymph nodes through lymphatic vessels, and then to the blood systemic circulation. In addition to lymphatic routes, some debris can directly enter the blood circulation via tumor venous drainage. Eventually, they are filtered by the spleen, liver and kidneys (**Figure 2C**). Recently, it has been highlighted that tertiary lymphoid structures (TLS) can form in proximity of tumors, which might constitute another relevant site to target, although our current knowledge on these structures remain limited to date (Sautès-Fridman et al., 2019).

Targeting the tumor-draining lymph nodes (TdLNs) might therefore constitute a good alternative to direct tumor-targeting, considering their high exposure to cancer antigens, optimal content and organization of immune cell populations and conserved structures, which would permit the development of more generic (i.e., less tumor-specific) cancer vaccines (Jeanbart et al., 2014). Nevertheless, TdLNs can also be affected by tumor-derived immunosuppression, as they drain immunosuppressive factors from the tumor. In addition, tumor-draining lymph nodes are sometimes surgically removed for diagnosis purposes, to establish the metastatic and aggressiveness profile of cancers.

Should this be the case, targeting cancer vaccines to the spleen or to non-tumor draining lymph nodes (nTdLNs) remain other relevant options (Jeanbart et al., 2014). Since those are located downstream in the circulatory system, they are less exposed to the tumor immunosuppression, although also less supplied with tumor antigens. As a consequence, adding exogenous tumor antigens in vaccines targeting these sites might be necessary to achieve proper efficacy.

Practically, tumors can be directly targeted via intratumoral delivery or indirectly by the use of tumor-targeting technologies. On the other hand, lymph nodes can be indirectly targeted by delivering the vaccine in the tissues they drain, via topical, intradermal, subcutaneous or intramuscular routes, for example,

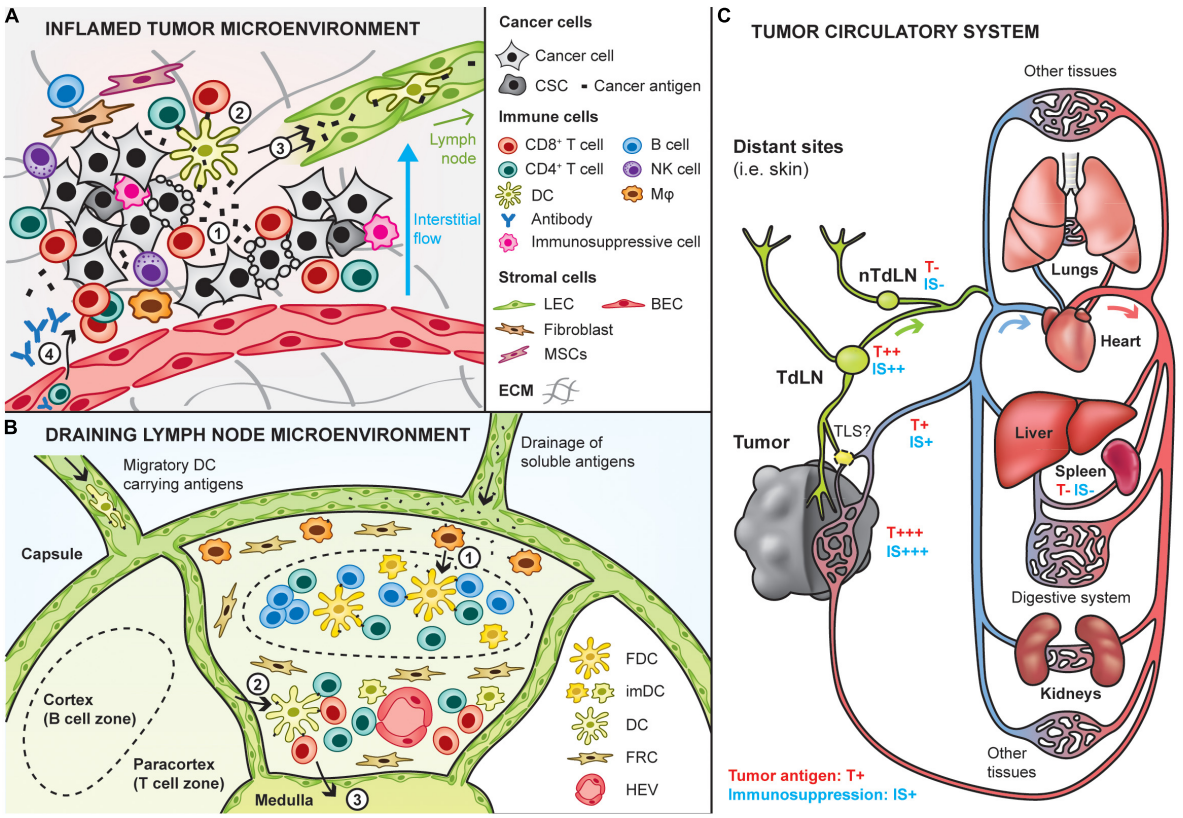

FIGURE 2 | Site-specific targeting of therapeutic cancer vaccines. Cancer vaccines can be designed to specifically target sites that are potent for inducing anti-tumor immunity, including the tumor and lymphoid tissues. **(A)** Interactions between the tumor and immune infiltrates in the inflamed tumor microenvironment. Upon cancer cell death (e.g., T cell-mediated), cancer antigens are released in the local environment (1) and can be taken up by dendritic cells (DCs) to induce *in situ* activation of cancer-specific T cells (2). In addition, cancer antigens are either passively drained by lymphatic vessels or actively transported by immune cells trafficking to the draining lymph node (3), where potent immune responses can be induced. Then, T cells activated in the lymph nodes can home into the tumor to kill tumor cells (4). In addition, humoral immune responses may be triggered in the lymph node and can lead to the production of cancer-targeting antibodies that enter the tumor bed to induce antibody-mediated cytotoxic mechanisms (4). It is important to note here that the depicted tumor-immune interactions do not take place in tumors that are known as immune deserts (i.e., non-inflamed). CSC: cancer stem cells, Mφ: macrophage, LEC/BEC: lymphatic/blood endothelial cell, MSC: mesenchymal stem cells, ECM extracellular matrix. **(B)** Lymph nodes are relevant to target by therapeutic cancer vaccines as they are naturally optimized to induce strong immune responses, due to their high content in immature DCs, and naive T and B cells. Naive lymphocytes enter the lymph node via the high endothelial venules (HEV). Antigens and adjuvants can enter lymph nodes in soluble form and be further transported by subcapsular macrophages to follicular DCs to induce B cell responses (1). In addition, migratory DCs loaded with cancer antigens can go into the paracortical zone (2), where they activate antigen-specific $CD4^+$ and $CD8^+$ T cells. Activated T cells exit the lymph node via the medulla (3). FDC: follicular dendritic cell, imDC: immature dendritic cell, FRC: fibroblastic reticular cells. **(C)** Overview of the tumor circulatory system and tumor antigen biodistribution. Tumors are connected to the blood circulatory system by blood vessels (arterial system in red, venous system in blue) and lymphatic routes (in green). The tumor is a relevant site to target by cancer vaccines as it has the highest concentration of tumor antigens (high exposure: T+++), although its high immunosuppression (IS+++) might impair vaccine efficacy. Alternative sites to target can be the tumor-draining lymph node (TdLN) also relatively highly exposed to tumor antigens. As they are less immunosuppressed, targeting non-tumor-draining lymph nodes (nTdLN) and the spleen might lead to better immune activation upon vaccination, yet their poor exposure to tumor antigens might require the use of exogenous cancer antigens.

which might be more convenient than via intranodal or intralymphatic injections. Lastly, the spleen can be efficiently targeted via intravenous perfusion, or less commonly via an intrasplenic route.

Passive Targeting Using Material Engineering

Establishing the vaccine delivery route and strategy will inform on the intrinsic properties required for the vaccine to be efficient, notably providing criteria on the components' half-life, stability, solubility, toxicity or biodistribution. Modulation of these parameters has been widely achieved by the use of materials. In addition, some materials can act themselves as immunostimulants (Sun et al., 2017), as targeting tools (Weissleder and Pittet, 2008), or have direct cytotoxic effects on cancer cells (Zou et al., 2016), further enhancing the vaccine outcomes.

Choice of Material Physicochemical Properties

When developing a new material for cancer vaccines, or using an already existing one, the choice of material primarily depends on its physicochemical properties, such as its size, shape, charge, solubility and elasticity. These parameters will affect the

vaccine by modifying its biodistribution, cell internalization and activation capabilities, as well as its half-life and release kinetics. Thus, the material needs to be chosen according to both the delivery route into the patient and its ability to target and get metabolized by the correct cell types.

Size

First, the size of a material, or particle, can range from a few nanometers up to several microns and will influence its drainage, biodistribution, which cells internalize it as well as its retention time. It has been demonstrated that intradermal injection of nanoparticles ranging from 20 to 200 nm can enter the lymphatic system and drain to the lymph node, with a preference for particles ranging around 40 nm, whereas larger ones will be retained at the injection site and internalized by APCs before being transported to the lymph node via cellular trafficking (Swartz, 2001; Reddy et al., 2006; Irvine et al., 2013). On the other hand, if the formulation is injected intravenously, carriers smaller than 5 nm will not only be filtered by the kidney in less than 5 min but will also escape the vessels to diffuse in the neighboring tissues, whereas larger particles have a longer half-life in the blood (Choi et al., 2011; Hoshyar et al., 2016). Interestingly, compared to the tight junction of the endothelium of blood vessels in healthy tissues (5–10 nm), fast growing cancer vessels have looser junctions with pores ranging from 200 to 1200 nm, allowing particle extravasation within that range (Chauhan et al., 2012). Upon extravasation, particles can additionally be retained in the tumor for extended time, as a result of impaired tissue drainage. This is a process known as the enhanced permeability and retention (EPR) effect that has been widely exploited in cancer animal models for the development of tumor targeting nanosystems, but that remains controversial for use in humans (Danhier, 2016; Golombek et al., 2018). Unfortunately, although larger particles have several advantages when injected directly in the bloodstream, their penetration efficiency in the tumor is reduced compared to smaller particles (Hauert and Bhatia, 2014).

At a cellular level, the size of the carrier influences endocytosis by specific cell types. Indeed, it has been demonstrated that particles of 20–600 nm are preferentially taken up by DCs, whereas particles from 0.5 to 5 μm are rather taken up by macrophages (Xiang et al., 2006; Kanchan and Panda, 2007). Finally, the material fate upon intracellular trafficking will directly affect the efficacy of the vaccine itself since the payload has to reach the correct subcellular compartment to activate the cognate receptors or signaling cascade. Briefly, particles ranging from 250 nm up to 3 μm are preferentially taken up by phagocytosis whereas smaller particles enter the cell through pino- or macro-pinocytosis (Rivolta et al., 2012). Several uptake studies on cancer cells have demonstrated that the highest uptake was observed for particles around 50 nm (Chithrani et al., 2006).

Shape

Second, the shape of the material also affects its systemic biodistribution, circulation in blood, cellular uptake and interactions. For example, it has been shown that for some materials, such as gold nanoparticles, rod-shape structures tend to accumulate more in the spleen and less in the liver than their spherical counterparts (Arnida et al., 2011; Black et al., 2014); although not a general rule, this exemplifies how material shape can influence biodistribution. In addition, non-spherical particles in the bloodstream tend to marginate more and escape the blood flow (Toy et al., 2014). Microscopically, it has been demonstrated that the rate of cellular internalization of non-spherical particles depends on their angular orientation relative to the cell membrane (Sharma et al., 2010; Behzadi et al., 2017). Furthermore, spherical particles are favorably internalized by monocytes/macrophages compared to particles with a high aspect ratio, which will marginate and target the endothelial cell and evade macrophage uptake (Peiris et al., 2012). Finally, an interesting study has highlighted that T cell activation is enhanced when using ellipsoidal synthetic APCs rather than spherical ones, due to an increased contact interactions with the immune cell membrane (Meyer et al., 2015).

Elasticity

Thirdly, it is hypothesized that the elasticity of particles influences cellular uptake and tumor accumulation properties. Generally, quantum dots, gold or magnetic particles are considered hard particles, whereas hydrogels, liposomes or polymersomes are described as soft particles. Overall, harder particles are better internalized than soft materials (Beningo and Wang, 2002; Anselmo et al., 2015). Anselmo et al. (2015) also showed that soft particles circulate at a higher concentration in the blood at early times after intravenous delivery and were slower and less endocytosed compared to hard particles. In addition, it was demonstrated that soft nanolipogels accumulated more in tumors compared to hard ones (Guo et al., 2018).

Charge, hydrophobicity and other chemical properties

Lastly, compared to the parameters discussed above, the chemical properties are based on intrinsic characteristics of the material, such as its charge, hydrophobicity and functional groups. Indeed, the material charge – cationic, anionic or neutral – influences cell internalization, immune activation and blood half-life. Since cell membranes are negatively charged, they will take up positively charged molecules much faster due to electrostatic interactions compared to other particles (Foged et al., 2005). However, the uptake of positively charged particles can disrupt cell membranes, leading to increased cell toxicity (Fröhlich, 2012). Furthermore, several studies have demonstrated that changing the charge of a material from negative to positive can induce a higher immune response (Wen et al., 2016). Finally it has been demonstrated that neutral particles have a slower internalization rate than charged ones (Owens and Peppas, 2006).

With regard to hydrophobic materials, a shorter half-life in the bloodstream is observed compared to their hydrophilic counterparts due to the reticulo-endothelial system recognizing them as foreign and removing them in the liver or the spleen (Owens and Peppas, 2006). In addition, a positive correlation has been demonstrated between hydrophobicity and immune activation (Moyano et al., 2012). However, hydrophobic materials can be "masked" to prevent removal and reduce intrinsic immune activation by coating them with a hydrophilic material such as polyethylene glycol (PEG), for

example. Such a strategy is useful to improve the delivery of vaccines with hydrophobic compounds in the particle core (Maiti et al., 2019). Nevertheless, surface modification of particles additionally modulates their half-life and distribution profile in the body.

The interplay of all these parameters and how they affect treatment outcomes shows the importance of thoroughly characterizing new materials and their intrinsic properties *in vitro* and *in vivo*. Beyond that, core material properties can be further tuned by modifying the material with particular molecules, ligands or polymers, to fulfill specific criteria and needs.

Selected Examples of Different Types of Material

The extensive research on material engineering for drug delivery has provided a tremendous amount of available materials and technologies that could be used for the development of cancer vaccines. Here, we present a few examples of different types of materials to illustrate possible designs and structures (**Figure 3**).

Materials can be organic or inorganic, each having specific properties, advantages and limitations that should guide the choice of a material. Furthermore, organic material can either be synthetic, such as poly(D,L-lactide-co-glycolide) (PLGA), poly(γ-carboxyglutamic acid) (γ-PGA), and PEG, or natural, such as dextran, alginate, lipids and chitosan (**Figure 3A**). Similarly, they can be synthetically produced or derived from biological origin (**Figure 3B**). They can form a broad range of structures, including solid core particles, vesicles, micelles, emulsions, dendrimers or hydrogels. On the other hand, inorganic particles have the advantage of having rigid structure, controllable synthesis, with a size range of 2 to 150 nm, as well as low toxicity, although most are not biodegradable. Examples of inorganic particles include silica-based and magnetic particles (**Figure 3C**).

Solid core nanoparticles (NPs)

Nanoparticles are spherical particles with solid cores in the nanoscale size and have been extensively used for drug delivery over the past decades (de Titta et al., 2013; Tran et al., 2017; Ankita et al., 2019). Apart from their spherical shape, most of their parameters and characteristics can be tuned, such as their charges, hydrophobicity or surface properties (i.e., by conjugation of specific moieties), to give a few examples (van der Vlies et al., 2010).

Liposomes and polymersomes

Liposomes and polymersomes are 50–500 nm often spherical bilayered vesicles composed of phospholipids or block copolymers, respectively. They can incorporate hydrophobic or viral envelope glycoproteins on their bilayer as well as encapsulate hydrophilic molecule in their core (Senapati et al., 2018). Similarly, to NPs, these vesicles are highly versatile since it is possible to modify most of their parameters, by modifying their surface charge (Mo et al., 2012) or conjugating targeting ligands (Noble et al., 2014), for instance. Interestingly, they can be designed to release their payload in specific subcellular compartments (Jiang et al., 2012).

Micelles

Micelles are self-assembled spherical materials composed of amphiphilic block copolymers with a hydrophobic core and a hydrophilic corona (Hanafy et al., 2018). These colloids will spontaneously form at a specific concentration, called the critical micelle concentration (CMC), and temperature. Hydrophobic molecules can be encapsulated into micelles through physical, chemical or electrostatic interactions (Park et al., 2008).

Dendrimers

Dendrimers are spherical macromolecules composed of many branches originating from a central point forming a star-like structure. The advantages of these particles are their highly tunable properties since their molecular weight, size, flexibility, branching density, and solubility can be modulated (Tran et al., 2017; Sherje et al., 2018). Interestingly, it is possible to both conjugate dendrimers with several different drugs using different chemistry and "encapsulate" poorly water-soluble molecules into them (Wang et al., 2011). Furthermore, if the polymer used in the dendrimer is positively charged, DNA or RNA can be complexed to it for delivery into cells (Shan et al., 2012). The main drawback of this material is its potential toxicity, and bio-incompatibility, depending on its surface physico-chemical properties (Palmerston Mendes et al., 2017).

Immunostimulating complex (ISCOM)

Immunostimulating complexes are cage like particles of 40 nm composed of phospholipids, cholesterol, saponin adjuvant Quil A and protein antigens (Homhuan et al., 2004). Usually the antigen is not directly conjugated to the particle but rather interacts by hydrophobicity (Peek et al., 2008). In addition, they naturally induce an immune response, thus acting as immunostimulant materials.

Hydrogels

Hydrogels are a three-dimensional network of hydrophilic polymers cross-linked together. They have the capacity to retain large quantities of fluids and can be chemically modified to insert enzymatic, hydrolytic or stimuli-responsive components to ensure their biodegradability (Peppas et al., 2000). The main advantage of hydrogels is their high water-content similar to biological tissues, thus reducing surface tension induced by the material. In addition, the drug loading and release rate can be tightly controlled by modifying the quantity of gel cross-linking (Lin and Metters, 2006). An interesting feature of hydrogels is the possibility to induce their gelation *in situ* with a specific stimuli such as pH, temperature or light (Van Tomme et al., 2008).

Drug-conjugates

These materials simply consist of a drug conjugated to a polymer, or a protein via a linker, which can be cleavable or not. This delivery system has the advantage of reducing treatment toxicity and adverse side effects, solubilizing the drug as well as an easy synthesis (Dan et al., 2018). Cleavable linkers are either acid-sensitive, glutathione-sensitive, lysosomal protease-sensitive or β-glucuronide-sensitive, whereas non-cleavable linkers usually have thioether bonds, which do not have the risk of releasing the drug at the wrong time (Dan et al., 2018).

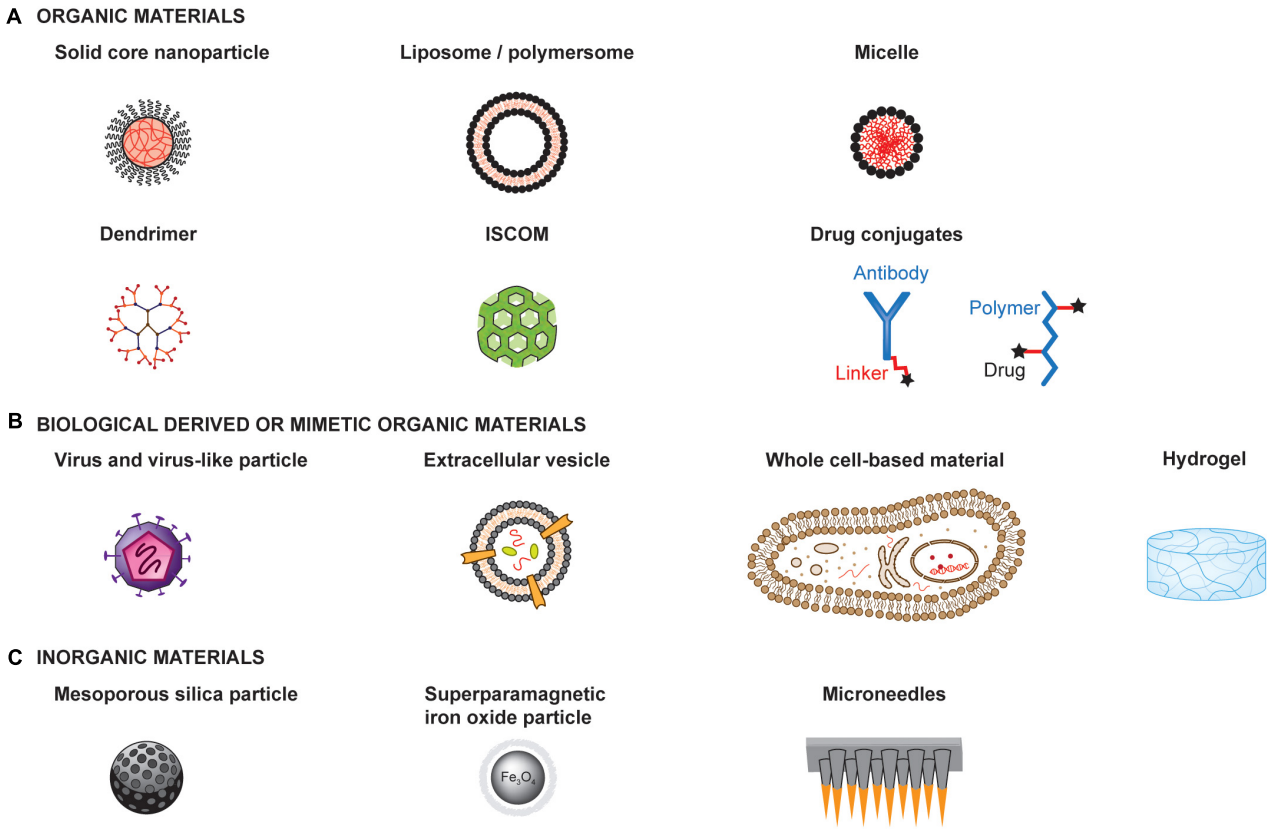

FIGURE 3 | Examples of materials for the development of therapeutic cancer vaccines. Materials can be engineered to enhance the therapeutic efficacy and safety profiles of cancer vaccines. Materials with very different structures and physicochemical properties can be used as a basis for engineering the delivery of adjuvants and antigens to optimize immune activation. Such materials can be organic materials **(A)**, including those derived from or mimicking biological materials **(B)**, or inorganic materials **(C)** ISCOM: Immunostimulatory complex.

Viruses and virus-like particles

Viruses and virus-like particles both have the advantage of naturally inducing a strong immune response due to their envelope (Zhang et al., 2000). In addition, they can be used as a delivery system for genes, antigens or drugs into tumor cells (Chulpanova et al., 2018). The choice of virus for a treatment will depend on the virus tropism, size and longevity of the desired gene that has to be delivered, as well as on its safety profile. The most common viruses currently tested in clinical trials as oncolytic viruses for cancer therapies are adenoviruses, herpes viruses, measles viruses, retroviruses, vaccinia viruses, and vesicular stomatitis viruses. Despite their relative success with inducing tumor regression, a major drawback of viruses is that they are strongly neutralized by host antibody responses upon re-injection. In addition, the immune response can be diverted from tumor antigens to viral antigens (Cawood et al., 2012). Another option is to use only highly immunogenic virus-like particles (VLP) to induce a strong immune response against tumor antigens without having the issue of self-replication and safety concerns caused by viruses (Cubas et al., 2011; Li et al., 2013; Palladini et al., 2018; Thong et al., 2019). These particles can usually range between 20 and 800 nm (Pushko et al., 2013).

Extracellular vesicles (EVs)

Extracellular vesicles are biological materials naturally secreted by cells and delimited by a lipid bilayer, commonly found with a size of 20–500 nm, although some can reach several microns (van Niel et al., 2018). They can be derived from the cell plasma membrane in case of microvesicles or from endosomal origin in case of exosomes. As important mediators of intercellular communication, extracellular vesicles can carry proteins, nucleic acid, metabolites and lipids from one cell to another. As such, they have raised interest for possible use as drug delivery systems (Vader et al., 2016). Interestingly, it has been shown that the composition of extracellular vesicles can be modified by engineering either the producing cells or the vesicles after isolation. Although EVs are considered poorly immunogenic carriers (Saleh et al., 2019), they play a role in mediating immunostimulating or immunosuppressive responses (Robbins and Morelli, 2014).

Whole cell-based materials

Mammalian cells are living materials also delimited by a lipid bilayer, with a typical size of 10–50 μm of various shapes, that can be used as carriers to deliver drugs or as therapeutic agents *per se* when administered into patients

(Cheng et al., 2019; Gong et al., 2019). To prevent cell rejection upon delivery, cells for clinical use are often derived from autologous sources, processed *ex vivo* and re-administered into the patient. One key advantage of using living cells as delivery materials is their ability to actively migrate to specific sites and to dynamically interact with endogenous cells and tissues (Leibacher and Henschler, 2016). Nevertheless, controlling the fate of living materials upon delivery can be challenging due to their high complexity.

Silica-based nanoparticles

Silica-based nanoparticles (SiNPs), especially porous SiNPs such as mesoporous silica nanoparticles (MSN), are used for drug delivery due to their high loading capacity and the possibility to control the release and encapsulation of different molecular weight drugs (Lai et al., 2003). In addition, MSN can be functionalized with targeting ligands, antibodies, peptides and even magnetic particles (Mamaeva et al., 2009).

Superparamagnetic iron oxide nanoparticles

Superparamagnetic iron oxide nanoparticles (SPIONs) are receiving increasing attention due to their broad applications in chemotherapy, hypothermia, magnetic resonance imaging (MRI), cell and tissue targeting, to mention a few (Quinto et al., 2015; Senapati et al., 2018). They are composed of an inner magnetic core and a hydrophilic coating polymer, such as PEG, polysaccharide and poly(vinyl alcohol), which can be used to deliver drugs or conjugate targeting ligand (Laurent et al., 2014). Due to their magnetic properties, studies showed the possibility to use an external magnetic field to localize them in the correct tissue and/or heat them to kill cancer cells.

Microneedles

Microneedles are sharp protrusions measuring from 100 μm to less than 1 mm, and are used as topical materials for local drug delivery. They are minimally painful for the patient and can be self-administered. The needle tips can be coated with protein, viruses, drugs or immunotherapy and will release the payload in a controlled slow manner (Ingrole and Gill, 2019). In the context of melanoma, for instance, transdermal delivery of immunotherapies with microneedles has demonstrated promising efficacy (Ye et al., 2017).

Engineering Tumor-Targeting Materials

In addition to their intrinsic physicochemical properties, materials can be further engineered to preferentially or specifically target tumors. Until recently, tumor-targeting materials have been primarily developed to deliver immunotherapeutic or chemotherapeutic drugs, or for diagnostic purposes, rather than for cancer vaccination. Therefore, we here focus on the different targeting technologies used by cancer immunotherapies in a broader scope, considering that they could inspire the design of future cancer vaccines. Particularly, we detail how tumors can be targeted at different levels, including macroscopic targeting of the tumor environment and microscopic targeting of cancer cells, tumor-associated stromal cells and the tumor extracellular matrix (ECM).

Targeting the Tumor Biochemical Environment

Due to unusual metabolism, the tumor environment has unique biochemical properties that differ from those of healthy tissues, and that can be used to activate or release drugs in a stimuli-responsive fashion, for example based on pH, oxygenation, protease contents, and chemokine secretion. Using stimuli-responsive materials, it may be possible to improve drug safety by limiting activity in off-target sites.

pH-responsive materials

Due to a high metabolism, the tumor environment is at a pH of 6.5 compared to the physiological one at 7.4 (Tian and Bae, 2012). This decrease in pH is caused by an increase in lactate and hydrogen ions produced to permit the substantial and rapid tumor growth. This pH difference has been exploited to develop materials capable of shrinking, aggregating or even enhancing cellular uptake upon tumor microenvironment entry (Wu et al., 2018). For example, particles coated with a zwitterionic monolayer change charge on their surface from negative to positive upon entering the tumor thus enhancing cell uptake and aggregation (Mizuhara et al., 2015). Another option to induce aggregation or release would be to have acid-labile amide bond breakage (Wu et al., 2018). Such strategies have been used to deliver chemotherapy (Yang et al., 2017), thermal therapy (Liu et al., 2017) or for tumor imaging (Hoffmann et al., 2012).

Hypoxia-responsive materials

A well-known characteristic of tumors is their low content of oxygen (Shannon et al., 2003; Bennewith and Dedhar, 2011). Based on this property, engineers have developed materials that incorporate bioreductive linkers, such as nitroimidazole analogs, thiol groups, and azobenzene moieties to deliver drugs upon entry into tumors (Guise et al., 2014; Ahmad et al., 2016; Kulkarni et al., 2016). For example, hypoxia-responsive nanoparticles have been developed to release doxorubicin in squamous carcinomas (Thambi et al., 2014). Similarly, prodrugs have been engineered to be activated in low-oxygen environments (Hunter et al., 2016). However, as hypoxia increases with tumor growth, hypoxia-sensitive drugs may have limited efficacy for early stage tumor targeting.

Protease-responsive materials

Many tumors exhibit abnormal enzymatic activity (Anderson and Cui, 2017; Yao et al., 2018), including the overexpression of matrix-metalloproteinases (MMPs) (Gialeli et al., 2010), caspases (Nejadnik et al., 2015), urokinase-type plasminogen activators (uPA) and cathepsins (Joyce et al., 2004). Therefore, including protease substrate sequences in materials and prodrugs has been exploited to specifically release drugs into tumors and limit their side-effects. Furthermore, some materials can change size and shape upon protease exposure, for example forming nanostructures (Hu et al., 2014; Anderson and Cui, 2017). As an example, Tanaka et al. designed a gelator precursor that self-assembles into nanofibers upon exposure to MMP-7 in tumor cells, inducing their death (Tanaka et al., 2015). Another study used caspase-sensitive gold NPs (AuNPs) as an apoptosis-inducing imaging probe (Sun et al., 2010).

Chemotaxis-based cellular tumor targeting

Tumor inflammation induces the secretion of chemokines, such as CXCL12, which are able to recruit specific cell types. Based on this mechanism, active tumor targeting can be achieved by the delivery of cells capable of sensing these chemokine gradients and actively migrating into tumor-inflamed regions (Cheng et al., 2019), such as myeloid cells, T cells, neural stem cells and mesenchymal stem cells (MSCs) for example (Leibacher and Henschler, 2016; Combes et al., 2018). Furthermore, these cells can be engineered to deliver anti-cancer drugs; for example, MSCs have been genetically modified to overexpress IFNβ or to carry paclitaxel into tumors (Ling et al., 2010; Sadhukha et al., 2014).

Targeting Tumor Cells

As cancer cells are the ones to eradicate, they constitute the ultimate target of cancer immunotherapies, including vaccines. Currently, many clinical treatments use targeted therapies to directly kill tumor cells. Coupling such targeting strategies with immune adjuvants would be valuable to turn them into therapeutic cancer vaccines, thus colocalizing tumor cell antigens and immunostimulatory molecules. Cancer cells can be targeted at multiple levels, including cell surface, intracellular or genomic levels, or by other approaches that use infectious materials (**Figure 4**).

Targeting the cancer cell surface (Figure 4A)

One of the most common approaches to target cancer cells relies on affinity-based interactions of surface tumor-associated antigens with antibodies or antibody derivatives (e.g., Fab, scFv). As a clinical example, HER2-positive tumor cells can be targeted by intravenous or subcutaneous injection of anti-HER2 antibodies, which accumulate at the cancer cell surface due to their high specific affinity for the receptor, in both the primary tumor and metastases. Such antibodies can display intrinsic activities to affect tumor cell growth, notably by blocking the surface protein functions and by triggering antibody-mediated cytotoxicity. They can additionally be modified with anti-cancer drugs or adjuvants for the development of cancer vaccines (Hong et al., 2011). For example, Sharma et al. (2008) have chemically conjugated anti-HER2 to CpG, which has led to tumor eradication and induction of protective memory when combined with anti-GITR immunotherapy. In addition, tumor-targeting antibodies have been conjugated to material surfaces, such as nanoparticles (Kubota et al., 2018) or liposomes (Espelin et al., 2016), to confer them the ability to target tumors. Interestingly, biological cell-based materials can be similarly engineered; for instance, in the context of chimeric antigen receptor (CAR)-T cell therapies, patient-derived T lymphocytes are transduced with a modified TCR that comprises a scFv fragment recognizing a specific cancer antigen (Jackson et al., 2016). Although not a cancer vaccine, CAR-T cell therapies strongly mimic their purpose, by both delivering tumor-specific cytotoxic T cells and having the potential to establish anti-tumor memory (McLellan and Ali Hosseini Rad, 2019).

In addition to antibodies, cell surface receptors can be targeted using receptor ligands, peptides, or small molecules. Indeed, ligand/receptor interactions have been exploited to target the epidermal growth factor receptor (EGFR) on urinary bladder cancer, by delivering an EGF-diphteria toxin fusion protein, for example (Yang et al., 2013). Alternatively, cancer-targeting peptides can be found by phage display screening (Zhang et al., 2001), and have the advantages of being smaller and potentially easier to synthesize than antibodies. Lastly, small molecules have been used to functionalize materials to target cancer cell receptors. Particularly, materials conjugated to folate can successfully bind to cancer cell folate receptors with very high affinity (Xia and Low, 2010; Tao et al., 2015).

Not only proteins can be targeted at the cancer cell surface, but also glycans or lipids. Particularly, cancer cells express specific glycans or overexpress others as compared to healthy cells (Dube and Bertozzi, 2005), which can be targeted using glycan-binding proteins, notably lectins. For example, the conjugation of the specific rBC2LC-N lectin to bacterial exotoxin has shown successful targeting and therapeutic effects in pancreatic cancer (Shimomura et al., 2018). Interestingly, lectins themselves can induce autophagy or apoptosis of cancer cells (Yau et al., 2015). Similarly, cancer cells lack the ability to maintain the natural lipid asymmetry in cell membranes, thus exposing phosphatidylserine (PS) and phosphatydilethanolamine (PE) on the outer leaflet of their membranes, has encouraged the development PS/PE-targeting drug delivery systems (De et al., 2018).

Finally, differences have been found in the physicochemical properties of cancer cell membranes, which are more negative and more fluid, as compared to healthy cells (Bernardes and Fialho, 2018). Approaches targeting such differences have been attempted (Chen et al., 2016a), but are likely to be less efficient than those relying on specific interactions for drug delivery purposes.

Targeting the cancer cell cytosol (Figure 4B)

Some strategies have been developed to target the cancer cell cytoplasm, for example by using molecular transport via specific channel receptors. Particularly, many cancer cells overexpress the GLUT1 glucose channel receptor to increase their glucose metabolism. Conjugation of glucose to small molecules enables their transport through GLUT1 into the cytoplasm, as exemplified by Glucosfamid or glucose-conjugated paclitaxel (Liu et al., 2007; Calvaresi and Hergenrother, 2013). Interestingly, conjugation of glucose to larger moieties, such as nanoparticles, has allowed an increase of their uptake by cancer cells, yet via clathrin-dependent endocytosis (Dreifuss et al., 2018).

Another approach that can be considered as cytoplasmic targeting is the delivery of small molecules that passively diffuse through cell membranes, but that mostly display activity in cancer cells upon binding to their cytoplasmic target. For example, BRAF inhibitors selectively target the $BRAF^{V600E}$ mutated protein present in melanoma cells but not in healthy ones (Sharma et al., 2012; Karoulia et al., 2017). Similarly, prodrugs can be engineered to be activated in the cytosol of cancer cells specifically (Zhang et al., 2017b).

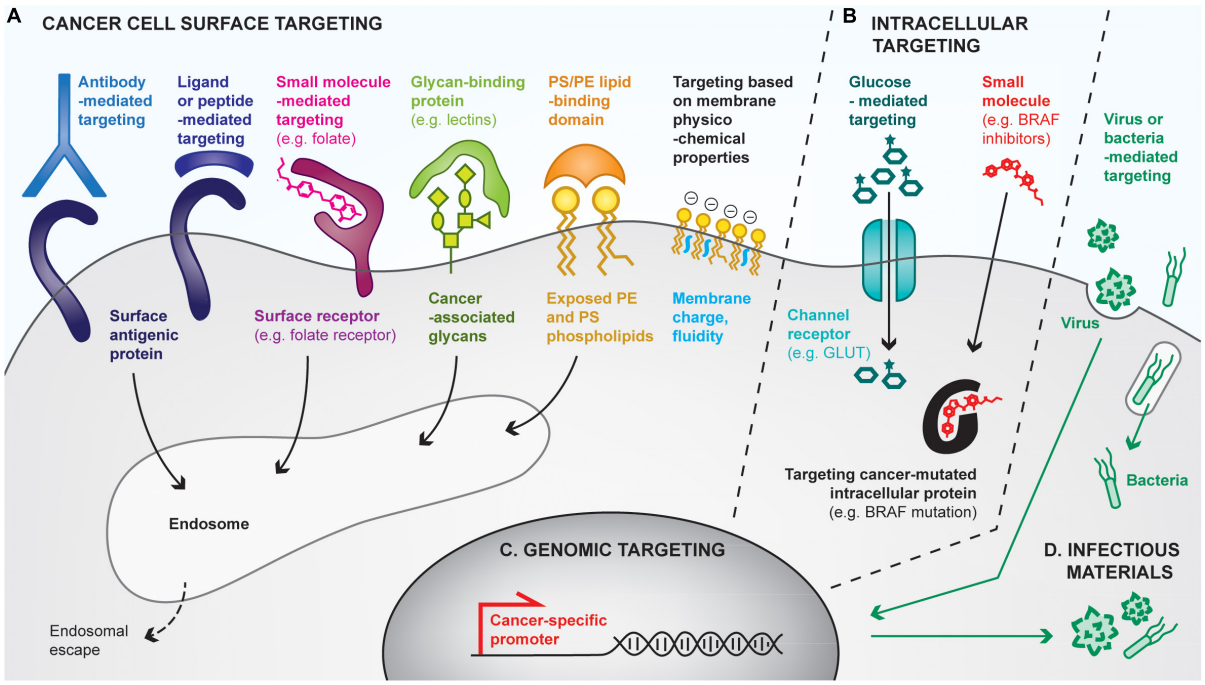

FIGURE 4 | Overview of strategies for cancer cell targeting. Biomolecular engineering can be used to preferentially target the cancer cell at multiple levels, using differences between cancer cells and healthy ones to discriminate between them. **(A)** Cancer cells can be targeted with cell surface-binding moieties, based on specific affinities with cell-surface antigens, receptors, glycans, lipids or based on physicochemical properties (e.g., membrane charges). Most cell surface targeting strategies will lead to endocytosis of the targeting moiety. **(B)** The cancer cell cytoplasm can be directly targeted by using channel receptors that transport small molecules, or by using small molecules capable of crossing cell membranes. **(C)** Cancer cells reactivate specific promoters that are silenced in healthy cells, allowing cancer cell targeting by the delivery of genes placed under cancer specific promoters. **(D)** Finally, some pathogens (e.g., oncolytic viruses, bacteria) favorably infect and replicate in cancer cells, often leading to their death, thus providing additional means for preferential cancer cell targeting.

Targeting the cancer cell genome (Figure 4C)

Cancer cells additionally upregulate some specific promoters that can be targeted for gene delivery. For example, the telomerase hTERT promoter has been shown to be re-activated in 90% of human cancers while being silenced in healthy cells (Jafri et al., 2016). Delivering genes under the control of such promoters allows restriction of their expression to cancer cells (Zarogoulidis et al., 2013). Such approaches have mostly been used to deliver cytotoxic genes, such as suicide genes inducing cancer cell death (Xu and Goldkorn, 2016). Interestingly, multiple cancer-specific promoters can be used in combination to further enhance cancer-targeting specificity (Li et al., 2005).

Targeting the cancer cell with infectious materials (Figure 4D)

It has been demonstrated that cancer cells are more prone to infection than healthy cells, and that some pathogens tend to favorably infect cancer cells (Marelli et al., 2018; Zhou et al., 2018). As a consequence, strategies targeting cancer cells with infectious materials have been developed. As an example of choice, one of the two approved therapeutic cancer vaccines uses the BCG bacteria as a tumor-killing agent. Currently, most of the infectious-based cancer therapies under development focus on the use of oncolytic viruses, which naturally infect, replicate inside and lyse cancer cells, thus releasing additional viruses in the tumor. Viruses can be engineered at multiple levels to improve their specificity to cancer cells. First, their capsid or envelope can be modified to enhance tropism to cancer cell surfaces (Büning and Srivastava, 2019). For instance, Münch et al. (2013) have modified the capsid of an adeno-associated virus to specifically target HER2-positive tumors upon systemic delivery. Secondly, the virus genome can be manipulated to incorporate cancer-specific promoters, as described above. Similarly, bacteria have been engineered for enhanced cancer-targeting. For instance, *Salmonella typhimurium* decorated with anti-CEA scFv have efficiently targeted CEA-expressing MC38 colon cancer models (Bereta et al., 2007). In cancer vaccines, the use of pathogens as delivery tools is particularly interesting as they naturally contain multiple MAMPs that act as adjuvants.

Targeting Tumor-Associated Stromal Cells

Tumors are not only composed of cancer cells, but also of tumor-associated stromal cells (TASCs), including endothelial cells and fibroblasts. Since stromal cells are less heterogenous populations than cancer cells, their markers are more conserved across cancers and patients, possibly enabling the development of less personalized targeting therapies. To date, most strategies that target TASCs focus on the use of antibodies, peptides and small molecules, although gene therapy remains a feasible option.

Since TASCs often support tumor development, progression and dissemination, most therapies aim at blocking or killing them to stop tumor nurturing.

Targeting tumor-associated blood endothelial cells (BECs)

Because tumors get nutrients and oxygen from blood vessels, many strategies have been developed to prevent tumor angiogenesis and subsequently starve the tumor. Clinically, tumor angiogenesis has been mostly inhibited by blocking the vascular endothelial growth factor-A (VEGF-A), using either blocking antibodies against it or against its receptor VEGF-R2, or tyrosine kinase inhibitors that block VEGF-R2 downstream signaling (Zirlik and Duyster, 2018). Furthermore, tumoral BECs express some surface proteins that are not commonly present in healthy vasculature, such as VEGF-R3 or endoglin, which can be used to preferentially target them (Laakkonen et al., 2007; Dallas et al., 2008). Importantly, it has been shown that modulating tumor vasculature strongly impacts the outcomes of immunotherapies, since blood vessels directly control immune cell trafficking into tumors. Indeed, some anti-angiogenic therapies have been shown to enhance intratumoral trafficking of lymphocytes in some cancers, notably by increasing the expression of adhesion molecules involved in T cell homing and by increased chemokine expression (Tartour et al., 2011; Wu et al., 2016). Alternatively, several strategies have been explored to normalize tumor vasculature rather than blocking it to relieve hypoxia, which has been shown to impair T cell cytotoxic activities (Huang et al., 2013; Uldry et al., 2017).

Targeting tumor-associated lymphatic endothelial cells (LECs)

The presence of lymphatic vessels in tumors has been associated with increased metastasis and overall poor diagnosis. Nevertheless, when combined with immunotherapies, lymphatic vessels can instead promote anti-tumor responses by increasing immune infiltrates into tumors, as it has been demonstrated in mouse melanoma models and positively correlated in human melanoma (Fankhauser et al., 2017). By draining tumor interstitial fluid and debris, lymphatic capillaries of LECs are strongly exposed to tumor antigens, which they scavenge and present on their MHCs to further modulate immune responses (Hirosue et al., 2014; Kimura et al., 2015). Due to their endocytic capability, targeting LECs has been achieved passively by injecting drugs upstream to their draining route, using liposomes for instance (Oussoren et al., 1997), although such passive approaches can side-target other phagocytic cells. In contrast, preferential targeting of LECs has been achieved by using anti-VEGF-R3 antibodies (Saif et al., 2016). More recently, a dual targeting approach using anti-Lyve-1 combined with anti-Podoplanin antibodies coated on magnetic nanoparticles has been engineered, although the specificity of this last approach remains to be demonstrated *in vivo* (Wu et al., 2019). Noteworthily, LECs can not only be targeted in the tumor and lymphatic vessels, but also in the lymph nodes where they strongly interact with immune cells.

Targeting tumor-associated fibroblasts (TAFs)

Tumor-associated fibroblasts, which constitute a preponderant population in solid tumors, have been shown to promote cancer progression, mediate tumor immunosuppression and affect T cell infiltration (Shiga et al., 2015; Liu et al., 2019), and have therefore been chosen as targets for direct killing. For example, TAFs have been preferentially targeted using lipid-protamine-DNA nanoparticles displaying aminoethylanisamide (AEAA) ligands at their surface, which can bind to their cognate sigma receptors highly expressed by TAFs (Liu et al., 2019). Another interesting approach for the therapeutic use of TAFs in cancer immunotherapy has been proposed by Müller et al. (2008) who have engineered a bispecific antibody-derived fusion protein that targets on one side the Fibroblast Activation Protein (FAP) receptors on TAFs, and on the other side display the extracellular portion of 4-1BBL, a co-stimulatory molecule that promotes T cell activation. This approach of rendering TAFs immunostimulatory could be highly relevant in the context of therapeutic vaccines, to increase intratumoral immunogenicity and endogenous T cell stimulation.

Targeting other stromal cells

Other stromal cells present in the tumor microenvironment could be used as potential targets to localize vaccines in the tumor, for example, stromal stem cells such as MSCs (Poggi et al., 2018). Interestingly, MSCs can actively migrate from the systemic circulation into the tumor microenvironment via chemokine gradient sensing, as seen before in the section "Targeting the Tumor Biochemical Environment."

Targeting Tumor Extracellular Matrix (ECM)

In addition to cell targeting, the tumoral ECM has been exploited for the delivery of anti-cancer or immunomodulatory drugs. During tumorigenesis, the ECM is remodeled and dysregulated, leading to changes in composition as compared to healthy ECMs. Such differences in tumor ECM composition make it amenable to targeting of cancer therapeutics. Targeting the tumoral ECM is particularly relevant for the delivery of cytokines or similar signaling molecules, considering the important physiological roles of the ECM in regulating cytokine spatiotemporal release and activity *in vivo* (Frantz et al., 2010; Martino et al., 2014; Briquez et al., 2016). Various components of the ECM have been targeted within tumors, particularly glycoproteins, fibrous scaffold proteins (e.g., collagen), and glycosaminoglycans.

Glycoprotein targeting

Some glycoproteins are differently spliced or overexpressed in tumors; for example, the EDA and EDB domains of fibronectin are present in tumors and wounded tissues, but absent in normal matrices. Both of these domains have served as targets for the delivery of cytokines and small molecules into tumoral ECMs (Kaspar et al., 2005; Hutmacher and Neri, 2019). Particularly, the anti-EDB antibody fused to IL-2 and TNF have shown promising results in enhancing anti-tumor immunity and are currently being tested in clinical trials (Hutmacher and Neri, 2019). Other glycoproteins can be similarly targeted, such as tenascin-C or the G45 domain of laminin-332 that are respectively, absent and degraded in physiological ECMs, but often expressed in

tumoral matrices. Interestingly, functionalization of drug-loaded nanoliposomes with tenascin-C-binding peptides or sulfatide – a tenascin-C-binding glycosphingolipid – showed successful tumor targeting and reduction of drug side-effects (Lin et al., 2014; Chen et al., 2016b).

Collagen targeting

Collagen is another ECM component that can be targeted, as it is present at higher levels in many types of tumors compared to normal tissue (Provenzano et al., 2008; Zhou et al., 2017). Consequently, engineering drugs for collagen targeting can increase *in situ* retention within the tumor. Indeed, intratumoral delivery of IL-2 and IL-12 fused with lumican, a collagen VI-binding protein, has led to increased sustainability, efficacy and safety of these cytokines (Momin et al., 2019). Additionally, collagen is not naturally exposed to the blood stream in healthy tissues, but is accessible upon increase of vessel permeability during inflammation and in cancer. As such, drugs conjugated to appropriate collagen-binding moieties can accumulate in the tumor microenvironment upon systemic delivery (e.g., intravenous). As an example, the fusion of an anti-EGFR Fab to a collagen-binding peptide exhibited localization to A431 xenografts and enhanced retention time compared to untargeted anti-EGFR Fab when injected intraperitoneally (Liang et al., 2016). In addition, a recent study by Ishihara et al. used a collagen I and III-binding domain derived from von Willebrand factor to target checkpoint blockade antibodies and IL-2 to various tumors, which resulted in tumor growth suppression and lowered drug toxicity (Ishihara et al., 2019).

Proteoglycan and glycosaminoglycan (GAG) targeting

Similarly to other ECM components, GAGs are also dysregulated in cancers, and many of them, such as hyaluronan (HA) or chondroitin sulfate (CS) are overexpressed by tumor cells (Toole, 2004; Vallen et al., 2014). Accordingly, GAG-binding peptides have been used to target materials into tumors. For instance, silver nanoparticles functionalized with the IP3 HA-binding peptide have successfully localized into peritoneal tumors (Ikemoto et al., 2017). In addition to being overexpressed, some tumoral GAGs also display differences in sulfation patterns, which can be further exploited to enhance targeting specificity (Vallen et al., 2014). As an example, Salanti et al. targeted a specific sulfated form of CS, called CSA, in melanoma and prostate tumors by using a peptide derived from the *Plasmodium falciparum* VAR2CSA protein (Salanti et al., 2015). Other approaches to target CS have used antibody fragments (van der Steen et al., 2017) or liposomes containing a cationic lipid TRX-20 (Lee et al., 2002). Lastly, other GAGs can be used as tumoral ECM targets, notably heparan sulfates and aggrecans (Raavé et al., 2018).

Promiscuous ECM Targeting

Finally, a more versatile approach for cancer ECM targeting is to target multiple ECM components at the same time rather than just a single component at a time. For example, this strategy has been exploited by conjugating materials to the heparin-binding domain (HBD) of placenta growth factor-2 (PlGF-$2_{123-144}$), which has been shown to display a super-affinity for multiple ECM components (Martino et al., 2014). In one study, PlGF-$2_{123-144}$ successfully allowed the retention of checkpoint blockade antibodies within the tumor environment, improving efficacy and safety of these antibodies (Ishihara et al., 2017). However, such an approach is limited to local delivery as it also targets fibrinogen in the blood. Another multi-targeting strategy used a bispecific peptide (PL1) that binds to both fibronectin EDB and tenascin-C. Lingasamy et al. used PL1 to target iron oxide nanoworms loaded with proapoptotic peptides into glioblastoma and prostate carcinoma tumors (Lingasamy et al., 2019).

Engineering Immune Cell-Targeting Materials

Immune cells are the main actors to mediate tumor cell killing and establish anti-cancer memory. As such, the main challenge of cancer vaccines is to leverage their potential by targeting and stimulating the correct set of immune cells with the appropriate signals. Immune cells can be targeted at various places including in the tumor (depending on the presence of immune infiltrates), in lymphoid organs or in distant tissues, from where they can migrate to the lymphoid organs. As immune cells are dynamically migrating between the different sites, we here classified targeting strategies per cell type rather than by site. We focus on strategies targeting DCs, T cells, B cells, and NK cells as being the most studied targeted cell types for cancer vaccines. However, all immune cells and mechanisms able to mediate or enhance cytotoxicity and memory could play a significant role in the development of future strategies. In particular, macrophages and neutrophils, capable of ADCP, or the complement system are of emerging interests in cancer immunotherapies (Gul and van Egmond, 2015; Reis et al., 2017). Whether their potential could be harnessed to enhance cancer vaccination, however, remains unclear.

Targeting Dendritic Cells (DCs)

Dendritic Cells are considered as the most potent APCs and play a pivotal role in triggering adaptive immune responses, due to their ability to promote T and B cell maturation. Consequently, targeting antigens and adjuvants to DCs is an important strategy pursued in cancer vaccines, and has been primarily explored *ex vivo* and more recently *in vivo*.

Ex vivo DC vaccines

The development of DC-targeting therapies has been made possible by the technical advances in DC isolation and *in vitro* culture. Modifying DCs *ex vivo* has the unique advantage of avoiding the influence of the tumor immunosuppression, which has been shown to impair DCs functions *in vivo* (Pinzon-Charry et al., 2005). Conventional DCs can be isolated from the patient peripheral blood and targeted *in vitro* with both cancer-associated antigens and adjuvants to stimulate their maturation. Delivery of tumor-associated antigens to DCs has been tested in the form of mRNA transfection (Borch et al., 2016), tumor lysates (Yu et al., 2004), co-culture with tumor cells or even fusion of tumor cells with DCs (Yu et al., 2004). Similarly, many adjuvants have been used to mature the DCs, notably exposure to TLR-3, -4, -7/-8, and -9 ligands and co-stimulatory receptor

ligands such as CD40L or cytokines (Saxena and Bhardwaj, 2018). Following *in vitro* antigen loading and maturation, DCs are re-administered to the patient via intradermal, intravenous, intranodal or intralymphatic, or intratumoral injection (Shang et al., 2017). Noteworthily, the currently approved therapeutic cancer vaccine Sipuleucel-T for prostate cancer treatment is an *ex vivo* DC-based vaccine.

In vivo DC-targeting vaccines

While delivered nanomaterials are taken up by DCs *in vivo*, more specific targeting has been achieved by the use of antibodies against DC-specific receptors, such as anti-DEC205, anti-CLEC9A or anti-DC-SIGN (Bonifaz et al., 2004; Hesse et al., 2013; Tullett et al., 2016). Interestingly, it has been shown that targeting different regions on the DC-SIGN receptor can modulate the internalization pathway and influence the extent of antigen presentation on MHCI by DCs (Tacken et al., 2011). In this study, Tacken et al. additionally highlighted that co-targeting of the antigen and adjuvants at the same time using PLGA nanoparticles enhances DC maturation (Tacken et al., 2011; Zitvogel and Palucka, 2011). In addition to antibodies, DCs have been targeted by materials conjugated to mannose or TLR-ligands, the latter being used as targeting tools in addition to being adjuvants (Thomann et al., 2011; Wilson et al., 2019). Upon *in vivo* targeting, DCs migrate to lymph nodes wherein they can efficiently educate T cells. Interestingly, it has been shown that pre-conditioning the vaccine site with pro-inflammatory cytokines enhances DC migration to lymphoid organs (Mitchell et al., 2015).

Targeting T Lymphocytes

T lymphocytes are the main actors in anti-tumor cell-mediated cytotoxicity, and their presence in the tumor correlates with good prognosis (Gooden et al., 2011). Currently, the most widely used T cell-targeting strategy relies on antibodies that bind to T cell surface receptors, such as PD1, CTLA4 or LAG3, and has been developed in the context of checkpoint blockade immunotherapies (Grywalska et al., 2018; Havel et al., 2019). In cancer vaccination, however, T cells have been mainly targeted by materials that mimic the role of APCs, aiming at promoting endogenous cancer-specific T cell responses.

DC-derived exosomes

One major challenge of DC vaccine remains the control of DC fates upon delivery, which has fostered the development of cell-free alternative strategies. In particular, DCs secrete exosomes that carry antigen-MHC complexes, both MHCI and MHCII, as well as co-stimulatory receptors, which make them capable of activating T cell responses (Zitvogel et al., 1998). DC-derived exosomes have been tested in clinical trials with encouraging outcomes (Morse et al., 2005; Tian and Li, 2017).

Artificial APCs (aAPCs)

Similar to the use of exosomes, synthetic materials have been developed to bypass APCs and directly activate T cells *ex vivo* and *in vivo*. Indeed, aAPCs are composed of a biomaterial (lipid-, polymeric- or inorganic-based) with all three signals required for T-cell activation, including MHC-antigen complex, co-stimulatory molecules and cytokines. Generally the co-stimulatory moieties are the antibodies anti-CD3 or anti-CD28 and the cytokines can be any T cell stimulating cytokines, such as IL-2, IL-7, IL-15, or IL-23 (Steenblock et al., 2011; Eggermont et al., 2014; Wang et al., 2017). Interestingly, it has been demonstrated that microparticles are more suited for the design of aAPCs than smaller sized ones as they provide increased interaction with T cells, due to their lower curvature. Particularly, ellipsoidal nanoworm particles induce higher activation efficacy compared to spherical ones (Mandal et al., 2013; Sunshine et al., 2014). In this context, it has been additionally shown that more sustained release of cytokines elicits a stronger immune response. Lastly, these aAPC platforms have also been used to deliver immunosuppressive blocking antibodies and showed promising results in delayed tumor growth (Eggermont et al., 2014; Zhang et al., 2017a).

Targeting B Cells

B cells have the dual role of serving as APCs and mediating humoral immune responses. Although the first role has taken more attention in the development of therapeutic cancer vaccines, new strategies are being explored to induce potent anti-tumor immunity relying on humoral responses.

B cells as APCs in cancer vaccines

B cells can be turned into potent APCs upon stimulation of their CD40 receptors, using soluble CD40L recombinant proteins, CD40 agonist antibodies or co-culturing them with CD40L-expressing feeder cells (Wennhold et al., 2019). CD40-activated B cells have been then shown to present antigens on both MHCI and MHCII to trigger $CD8^+$ and $CD4^+$ T cell responses respectively, upon adoptive transfer in humans (Schultze et al., 1997; Lapointe et al., 2003; Wennhold et al., 2019). As a consequence, B cells are being considered as an alternative source of APCs to DCs in cancer vaccines, as they are easier to isolate in sufficient number from patient peripheral blood, even from cancer patients, and are less sensitive to tumor immunosuppression, among other advantages (von Bergwelt-Baildon et al., 2002; Shimabukuro-Vornhagen et al., 2012). In addition, B cells can be targeted *in vivo* for antigen presentation, notably using anti-CD19 antibody as a targeting tool, as exemplified by Ding et al. (2008).

Humoral-based cancer vaccines

Another interesting approach relying on B cells is the vaccination against B-cell cancer epitopes, which generates large amounts of endogenous antibodies able to target the cancer cell surface and induce their death via antibody-mediated cytotoxicity (Kaumaya, 2015). As an example, HER2-Vaxx (developed by Imugene) induces polyclonal antibody responses against a specific epitope of HER2 and is being tested in patients with HER2-positive gastric, esophageal, and breast cancers. In the current vaccine, the HER2 peptide is formulated using the carrier protein CRM197, a non-toxic mutant of diphtheria toxin, combined with an adjuvant, whereas the previous formulation used virosome-based materials. This therapy has successfully passed a Phase I safety trial and is under evaluation in a Phase II trial. In addition to direct cytotoxicity, such a B-cell epitope peptide vaccine

could provide immune protection against cancer relapse, via the presence of long-term circulating antibodies and memory B cells.

Targeting NK Cells

Although NK cells are not the primary targeted cell type in cancer vaccines, they are generating substantial interest due to their cytotoxic ability as well as their strong cooperation with T and B cells. The role of NK cells in cancer immunotherapy is particularly important as they can detect cancer cells that avoid T cell recognition by downregulating their MHC and can mediate antigen-specific ADCC via recognition of cancer cell membrane-bound antibodies (Collins et al., 2011).

Because NK cells are innate immune cells, they do not have, according to our traditional understanding, the ability to mediate direct antigen-specific recognition and immunologic memory, which are central criteria for vaccines. Nevertheless, new roles for NK cells have been unveiled recently, notably in the context of viral infections, suggesting some features of antigen specificity and long-term memory in mouse and primate NK cells (Paust et al., 2010; Reeves et al., 2015; Pahl et al., 2018). Particularly in mice, it has been shown that NK cells can develop specific memory against antigens from murine cytomegalovirus (MCMV), influenza, and vesicular stomatitis virus (VSV) and human immunodeficient virus-1 (HIV), which can be effectively recalled upon antigen re-encounter (Sun et al., 2009; Paust et al., 2010). Currently, researchers are exploring whether such NK memory cells can be harnessed for vaccination purposes in cancer (Sun and Lanier, 2018; Capuano et al., 2019). For example, a study by Romee et al. (2016) has shown that adoptive transfer of cytokine-induced memory-like NK cells reduce leukemia burden in humans.

Post-targeting Fate of Materials

Targeting the material to the appropriate cells is not sufficient to ensure the therapeutic effect of a cancer vaccine. Indeed, upon targeting, the drugs – antigens and/or adjuvants – remain to be delivered in the appropriate subcellular compartments (i.e., where their targets or receptors are located), which can be the endosomes, cytoplasm, nucleus or other cell organelles. Interestingly, most cell-surface targeting strategies will result in drug internalization in endosomes, yet via multiple pathways (Elkin et al., 2016; Owens et al., 2016). Particularly, from the endosomes, drugs can travel to late endosomes and lysosomes, escape into the cytosol, be recycled at the cell surface or be transported to other organelles such as in the endoplasmic reticulum (Cullen and Steinberg, 2018). Upon escape in the cytosol, drugs can further be directed to the nucleus or to other specific sites, for example targeting mitochondria (Battogtokh et al., 2018). Importantly, the material itself (e.g., size, shapes, ligands, etc.) can influence which internalization pathway will be favored (Gratton et al., 2008).

As a consequence, the type of drug to deliver should be rationally chosen; for example, antigens can be in the form of protein, peptides, RNA or DNA. Importantly, proteinaceous antigens delivered from the extracellular space can be presented on MHCII but less so on MHCI, which is generally restricted to presentation of intracellular antigens. As a consequence, extracellularly-delivered proteins should undergo endosomal escape and reach the cytoplasm to trigger $CD8^+$ T cell responses. Accordingly, materials can be engineered to promote endosomal escape (Selby et al., 2017), for example by being pH-sensitive, redox-sensitive, or osmotic change-sensitive to burst the endosomes (Phillips and Gibson, 2014; Kongkatigumjorn et al., 2018; Rangasamy et al., 2018). In addition, some antigenic peptides can be designed to bind to MHCI from the extracellular space, thus bypassing this challenge (Ilca et al., 2018). Interestingly, some APCs subsets (e.g., $CD103^+$ DCs) (Joffre et al., 2012) are known to be naturally capable of mounting extracellular antigens onto MHCI, through a mechanism called antigen cross-presentation, and have therefore raised particular attention in vaccination (Fehres et al., 2014). As an alternative to protein forms, antigens can be delivered as DNA or RNA, which are directly translated into the cytosol. This particular advantage has encouraged the development of DNA vaccines to enhance CTL responses (Tiptiri-Kourpeti et al., 2016).

As to adjuvants, their receptors can be similarly located at the cell surface, in the endosomes or intracellularly. Therefore, materials that aim at co-delivering antigens and adjuvants need to be carefully designed in an integrated way.

COMBINATION OF THERAPEUTIC CANCER VACCINES WITH OTHER CANCER THERAPIES

While potent cancer vaccines will strongly activate the immune system to recognize and fight tumors, the activated immune cells still have to infiltrate the tumor and be locally effective to achieve therapeutic effects. These final steps constitute additional challenges, which could be partly overcome by the combination of the vaccine with other cancer therapies.

First, immune cells need to be in contact with the tumor cells to induce their death. The migration of immune cells into tumors is highly dependent on the tumor structure, and can be further dampened through impaired chemokine expression and downregulation of adhesion molecules on endothelial cells (Lanitis et al., 2015; Harjunpää et al., 2019). Consequently, combining cancer vaccines with therapies that ameliorate intratumoral immune infiltrations, such as those modulating local angiogenesis (Wu et al., 2016; Calcinotto et al., 2012) and lymphangiogenesis (Fankhauser et al., 2017), might be highly beneficial.

Secondly, upon reaching the tumor, the immune cells will face an immunosuppressive environment hampering their cytotoxic activity. Indeed, multiple mechanisms are at play in the tumor to prevent tumor cell killing by immune cells, via myeloid-derived suppressive cells, regulatory T cells or the secretion of immunosuppressive factors (e.g., IL-10, TGFβ, IDO) (Binnewies et al., 2018). Nevertheless, the reduction of tumor immunosuppression can potentially be achieved using immune checkpoint blockade, pro-inflammatory cytokines or IDO inhibitors, to mention a few examples.

Lastly, in the tumor, the immune cells still need to detect their targeted antigens in sufficient amount on cancer

cells. Particularly, cancer cells that downregulate expression of the antigens or of MHCs will avoid immune recognition and subsequent killing, leading to cancer relapse. Therefore, diversifying antigen targets and immune-mediated cytotoxic mechanisms is essential to reduce the risk of tumor escape. To do so, cancer vaccines can be combined with other therapies that enhance cancer antigen spreading and local DAMPs release from the tumor, such as chemo-, radio- or other immunotherapies (Wang et al., 2018; Joshi and Durden, 2019).

CONCLUSION AND PERSPECTIVES

In conclusion, cancer vaccines hold the promises of eradicating tumors and preventing relapse by inducing strong antigen-specific immune responses and long-term memory. Nevertheless, despite the extensive efforts invested in their development over the last decades, very few have thus far been approved in the clinic. However, lessons from successes, developments-in-progress and failures have increased our knowledge on the design of cancer vaccines, providing some rules to rationally engineer materials that enhance their therapeutic outcomes. Overall, we here proposed that the development of potent vaccines requires careful considerations of their (1) intrinsic composition, i.e., antigens and adjuvants, (2) formulation with materials, (3) delivery route and subsequent targeting to specific relevant sites and cell types, (4) subcellular targeting of their receptors and downstream biological pathways, and (5) combination with other cancer treatments. Although not discussed in this review, the optimal dosing and delivery regimen of the vaccine would also need to be precisely determined, which includes the number of doses to be administered and the delay between repeated delivery.

Defining all these parameters constitutes a major challenge as their combined effects remain poorly predictable, thus requiring thorough investigations *in vitro* and *in vivo*. Therefore, improvement of cancer models for better translatability would be beneficial to select the most relevant formulations and strategies to move forward in the clinic. In addition, establishing which tumor types/subtypes and subset of patients would be the most responsive to a cancer vaccine remains difficult to date, despite advances in diagnostic tools and immunological tests. In that perspective, clinical data collection, standardization and availability are essential to allow meta-analyses that help researchers and clinicians to draw criteria for the vaccine efficacy. Overall, improving the predictability of vaccines' outcomes would permit to reduce their cost and the time required for their development.

Finally, the vaccine would also need to be manufactured at scale and to comply with the regulatory authorities. The multitude of available materials and engineering strategies could lead to highly complex formulations, optimized for biological efficacy yet challenging to produce and become approved therapies. Therefore, a good compromise between efficacy and feasibility is essential to accelerate clinical translation of therapeutic cancer vaccines in the near future.

AUTHOR CONTRIBUTIONS

All authors have contributed in writing of the manuscript. MS and JH have supervised the work and contributed in writing and corrections.

ACKNOWLEDGMENTS

The authors would like to thank Dr. Renata Mezyk-Kopec for her advice and corrections on the manuscript.

REFERENCES

Ahmad, Z., Lv, S., Tang, Z., Shah, A., and Chen, X. (2016). Methoxy poly (ethylene glycol)-block-poly (glutamic acid)-graft-6-(2-nitroimidazole) hexyl amine nanoparticles for potential hypoxia-responsive delivery of doxorubicin. *J. Biomater. Sci. Polym. Ed.* 27, 40–54. doi: 10.1080/09205063.2015.1107707

Allen, F., Bobanga, I. D., Rauhe, P., Barkauskas, D., Teich, N., Tong, C. et al. (2018). CCL3 augments tumor rejection and enhances CD8+ T cell infiltration through NK and CD103+ dendritic cell recruitment via IFNγ. *OncoImmunology* 7:e1393598. doi: 10.1080/2162402X.2017.1393598

Almagro, J. C., Daniels-Wells, T. R., Perez-Tapia, S. M., and Penichet, M. L. (2018). Progress and challenges in the design and clinical development of antibodies for cancer therapy. *Front. Immunol.* 8, 495–19. doi: 10.3389/fimmu.2017.01751

American Cancer Society (2018). *Cancer Facts and Figures 2018*. Atlanta, GA: American Cancer Society.

Ammi, R., De Waele, J., Willemen, Y., Van Brussel, I., Schrijvers, D. M., Lion, E. et al. (2015). Poly(I:C) as cancer vaccine adjuvant: knocking on the door of medical breakthroughs. *Pharmacol. Ther.* 146, 120–131. doi: 10.1016/j.pharmthera.2014.09.010

Anderson, C. F., and Cui, H. (2017). Protease-sensitive nanomaterials for cancer therapeutics and imaging. *Ind. Eng. Chem. Res.* 56, 5761–5777. doi: 10.1021/acs.iecr.7b00990

André, F., Schartz, N. E. C., Chaput, N., Flament, C., Raposo, G., Amigorena, S., et al. (2002). Tumor-derived exosomes: a new source of tumor rejection antigens. *Vaccine* 20 (Suppl 4), A28–A31.

Ankita, D., Ashish, B., and Raj, K. N. (2019). Nanoparticles as carriers for drug delivery in cancer. *Artif. Cells Nanomed. Biotechnol.* 46, S295–S305. doi: 10.1080/21691401.2018.1457039

Anselmo, A. C., Zhang, M., Kumar, S., Vogus, D. R., Menegatti, S., Helgeson, M. E., et al. (2015). Elasticity of nanoparticles influences their blood circulation, phagocytosis, endocytosis, and targeting. *ACS Nano* 9, 3169–3177. doi: 10.1021/acsnano.5b00147.

Apelbaum, A., Yarden, G., Warszawski, S., Harari, D., and Schreiber, G. (2013). Type I interferons induce apoptosis by balancing cFLIP and caspase-8 independent of death ligands. *Mol. Cell. Biol.* 33, 800–814. doi: 10.1128/MCB.01430-1412

Arnida Janát-Amsbury, M. M., Ray, A., Peterson, C. M., and Ghandehari, H. (2011). Geometry and surface characteristics of gold nanoparticles influence their biodistribution and uptake by macrophages. *Eur. J. Pharm. Biopharm.* 77, 417–423. doi: 10.1016/j.ejpb.2010.11.010

Battogtokh, G., Cho, Y. Y., Lee, J. Y., Lee, H. S., and Kang, H. C. (2018). Mitochondrial-targeting anticancer agent conjugates and nanocarrier systems for cancer treatment. *Front. Pharmacol.* 9, 17450–20. doi: 10.3389/fphar.2018.00922.

Bayrami, V., Keyhanfar, M., Mohabatkar, H., Mahdavi, M., and Moreau, V. (2016). In silico prediction of B cell epitopes of the extracellular domain of insulin-like growth factor-1 receptor. *Mol. Biol. Res. Commun.* 5, 201–214.

Behzadi, S., Serpooshan, V., Tao, W., Hamaly, M. A., Alkawareek, M. Y., Dreaden, E. C., et al. (2017). Cellular uptake of nanoparticles: journey inside the cell. *Chem. Soc. Rev.* 46, 4218–4244. doi: 10.1039/C6CS00636A

Beningo, K. A., and Wang, Y. L. (2002). Fc-receptor-mediated phagocytosis is regulated by mechanical properties of the target. *J. Cell Sci.* 115, 849–856.

Bennewith, K. L., and Dedhar, S. (2011). Targeting hypoxic tumour cells to overcome metastasis. *BMC Cancer* 11:504. doi: 10.1186/1471-2407-11-504

Bereta, M., Hayhurst, A., Gajda, M., Chorobik, P., Targosz, M., Marcinkiewicz, J., et al. (2007). Improving tumor targeting and therapeutic potential of *Salmonella* VNP20009 by displaying cell surface CEA-specific antibodies. *Vaccine*. 25, 4183–4192. doi: 10.1016/j.vaccine.2007.03.008

Bernardes, N., and Fialho, A. (2018). Perturbing the dynamics and organization of cell membrane components: a new paradigm for cancer-targeted therapies. *IJMS* 19, 3871–19. doi: 10.3390/ijms19123871

Bhat, P., Leggatt, G., Waterhouse, N., and Frazer, I. H. (2017). Interferon-γ derived from cytotoxic lymphocytes directly enhances their motility and cytotoxicity. *Cell Death Dis.* 8:e2836. doi: 10.1038/cddis.2017.67.

Binnewies, M., Roberts, E. W., Kersten, K., Chan, V., Fearon, D. F., Merad, M., et al. (2018). Understanding the tumor immune microenvironment (TIME) for effective therapy. *Nat. Med.* 24, 541–550. doi: 10.1038/s41591-018-0014-x

Black, K. C. L., Wang, Y., Luehmann, H. P., Cai, X., Xing, W., Pang, B., et al. (2014). Radioactive 198Au-doped nanostructures with different shapes for in vivo analyses of their biodistribution, tumor uptake, and intratumoral distribution. *ACS Nano* 8, 4385–4394. doi: 10.1021/nn406258m

Bonifaz, L. C., Bonnyay, D. P., Charalambous, A., Darguste, D. I., Fujii, S.-I., Soares, H. et al. (2004). In vivo targeting of antigens to maturing dendritic cells via the DEC-205 receptor improves T cell vaccination. *J. Exp. Med.* 199, 815–824. doi: 10.1084/jem.20032220

Borch, T. H., Engell-Noerregaard, L., Iversen, T. Z., Ellebaek, E., Met, Ö., Hansen, M., et al. (2016). mRNA-transfected dendritic cell vaccine in combination with metronomic cyclophosphamide as treatment for patients with advanced malignant melanoma. *OncoImmunology* 5, 1–12. doi: 10.1080/2162402X.2016.1207842

Briquez, P. S., Clegg, L. E., Martino, M. M., Gabhann, F. M., and Hubbell, J. A. (2016). Design principles for therapeutic angiogenic materials. *Nat. Rev. Mater.* 1, 15006–15. doi: 10.1038/natrevmats.2015.6

Büning, H., and Srivastava, A. (2019). Capsid modifications for targeting and improving the efficacy of AAV vectors. *Mol. Ther. Methods Clin. Dev.* 12, 248–265. doi: 10.1016/j.omtm.2019.01.008

Calcinotto, A., Grioni, M., Jachetti, E., Curnis, F., Mondino, A., Parmiani, G., et al. (2012). Targeting TNF-α to neoangiogenic vessels enhances lymphocyte infiltration in tumors and increases the therapeutic potential of immunotherapy. *J. Immunol.* 188, 2687–2694. doi: 10.4049/jimmunol.1101877

Calvaresi, E. C., and Hergenrother, P. J. (2013). Glucose conjugation for the specific targeting and treatment of Cancer. *Chem. Sci.* 4, 2319–30. doi: 10.1039/c3sc22205e

Capuano, C., Pighi, C., Battella, S., Santoni, A., Palmieri, G., and Galandrini, R. (2019). Memory NK cell features exploitable in anticancer immunotherapy. *J. Immunol. Res.* 2019, 1–8. doi: 10.1155/2019/8795673

Cawood, R., Hills, T., Wong, S. L., Alamoudi, A. A., Beadle, S., Fisher, K. D., et al. (2012). Recombinant viral vaccines for cancer. *Trends Mol. Med.* 18, 564–574. doi: 10.1016/j.molmed.2012.07.007

Cerundolo, V., Silk, J. D., Masri, S. H., and Salio, M. (2009). Harnessing invariant NKT cells in vaccination strategies. *Nat. Rev. Immunol.* 9, 28–38. doi: 10.1038/nri2451.

Chauhan, V. P., Stylianopoulos, T., Martin, J. D., Popoviæ, Z., Chen, O., Kamoun, W. S., et al. (2012). Normalization of tumour blood vessels improves the delivery of nanomedicines in a size-dependent manner. *Nat. Nanotechnol.* 7, 383–388. doi: 10.1038/nnano.2012.45

Chen, B., Le, W., Wang, Y., Li, Z., Wang, D., Lin, L., et al. (2016a). Targeting negative surface charges of cancer cells by multifunctional nanoprobes. *Theranostics* 6, 1887–1898. doi: 10.7150/thno.16358

Chen, B., Wang, Z., Sun, J., Song, Q., He, B., Zhang, H., et al. (2016b). A tenascin C targeted nanoliposome with navitoclax for specifically eradicating of cancer-associated fibroblasts. *Nanomedicine* 12, 131–141. doi: 10.1016/j.nano.2015.10.001

Chen, C., and Gao, F. -H. (2019). Th17 Cells paradoxical roles in melanoma and potential application in immunotherapy. *Front. Immunol.* 10:187. doi: 10.3389/fimmu.2019.00187.

Cheng, S., Nethi, S. K., Rathi, S., Layek, B., and Prabha, S. (2019). Engineered mesenchymal stem cells for targeting solid tumors: therapeutic potential beyond regenerative therapy. *J. Pharmacol. Exp. Ther.* 370, 231–241. doi: 10.1124/jpet.119.259796

Chithrani, B. D., Ghazani, A. A., and Chan, W. C. W. (2006). Determining the size and shape dependence of gold nanoparticle uptake into mammalian cells. *Nano Lett.* 6, 662–668. doi: 10.1021/nl052396o

Choi, C. H. J., Zuckerman, J. E., Webster, P., and Davis, M. E. (2011). Targeting kidney mesangium by nanoparticles of defined size. *Proc. Natl. Acad. Sci. U.S.A.* 108, 6656–6661. doi: 10.1073/pnas.1103573108

Chulpanova, D., Solovyeva, V., Kitaeva, K., Dunham, S., Khaiboullina, S., and Rizvanov, A. (2018). Recombinant viruses for cancer therapy. *Biomedicines* 6, 94–14. doi: 10.3390/biomedicines6040094.

Cluff, C. W. (2010). Monophosphoryl lipid A (MPL) as an adjuvant for anti-cancer vaccines: clinical results. *Adv. Exp. Med. Biol.* 667, 111–123. doi: 10.1007/978-1-4419-1603-7-10

Collins, D. M., O'Donovan, N., McGowan, P. M., O'Sullivan, F., Duffy, M. J., and Crown, J. (2011). Trastuzumab induces antibody-dependent cell-mediated cytotoxicity (ADCC) in HER-2-non-amplified breast cancer cell lines. *Ann. Oncol.* 23, 1788–1795. doi: 10.1093/annonc/mdr484

Combes, F., Cafferty, S. M., Meyer, E., and Sanders, N. N. (2018). Off-target and tumor-specific accumulation of monocytes, macrophages and myeloid-derived suppressor cells after systemic injection. *Neoplasia* 20, 848–856. doi: 10.1016/j.neo.2018.06.005.

Cubas, R., Zhang, S., Li, M., Chen, C., and Yao, Q. (2011). Chimeric Trop2 virus-like particles: a potential immunotherapeutic approach against pancreatic cancer. *J. Immunother.* 34, 251–263. doi: 10.1097/CJI.0b013e318209ee72

Cullen, P. J., and Steinberg, F. (2018). To degrade or not to degrade: mechanisms and significance of endocytic recycling. *Nat. Rev. Mol. Cell Biol.* 19, 679–696. doi: 10.1038/s41580-018-0053-57

Dallas, N. A., Samuel, S., Xia, L., Fan, F., Gray, M. J., Lim, S. J., et al. (2008). Endoglin (CD105): a marker of tumor vasculature and potential target for therapy. *Clin. Cancer Res.* 14, 1931–1937. doi: 10.1158/1078-0432.CCR-07-4478

Dan, N., Setua, S., Kashyap, V., Khan, S., Jaggi, M., Yallapu, M., et al. (2018). Antibody-drug conjugates for cancer therapy: chemistry to clinical implications. *Pharmaceuticals* 11:32. doi: 10.3390/ph11020032

Danhier, F. (2016). To exploit the tumor microenvironment: since the EPR effect fails in the clinic, what is the future of nanomedicine? *J. Control. Release* 244, 108–121. doi: 10.1016/j.jconrel.2016.11.015

de Titta, A., Ballester, M., Julier, Z., Nembrini, C., Jeanbart, L., van der Vlies, A. J., et al. (2013). Nanoparticle conjugation of CpG enhances adjuvancy for cellular immunity and memory recall at low dose. *Proc. Natl. Acad. Sci. U.S.A.* 110, 19902–19907. doi: 10.1073/pnas.1313152110

De, M., Ghosh, S., Sen, T., Shadab, M., Banerjee, I., Basu, S. et al. (2018). A novel therapeutic strategy for cancer using phosphatidylserine targeting stearylamine-bearing cationic liposomes. *Mol. Ther. Nucleic Acid* 10, 9–27. doi: 10.1016/j.omtn.2017.10.019

DeMaria, P. J., and Bilusic, M. (2019). Cancer vaccines. *Hematol. Oncol. Clin. North Am.* 33, 199–214. doi: 10.1016/j.hoc.2018.12.001

Ding, C., Wang, L., Marroquin, J., and Yan, J. (2008). Targeting of antigens to B cells augments antigen-specific T-cell responses and breaks immune tolerance to tumor-associated antigen MUC1. *Blood* 112, 2817–2825. doi: 10.1182/blood-2008-05-157396

Dowling, D. J. (2018). Recent advances in the discovery and delivery of tlr7/8 agonists as vaccine adjuvants. *Immunohorizons* 2, 185–197. doi: 10.4049/immunohorizons.1700063

Dreifuss, T., Ben-Gal, T. -S., Shamalov, K., Weiss, A., Jacob, A., Sadan, T., et al. (2018). Uptake mechanism of metabolic-targeted gold nanoparticles. *Nanomedicine* 13, 1535–1549. doi: 10.2217/nnm-2018-2022

Dube, D. H., and Bertozzi, C. R. (2005). Glycans in cancer and inflammation — potential for therapeutics and diagnostics. *Nat. Rev. Drug Discov.* 4, 477–488. doi: 10.1038/nrd1751

Eggermont, L. J., Paulis, L. E., Tel, J., and Figdor, C. G. (2014). Towards efficient cancer immunotherapy: advances in developing artificial antigen-presenting cells. *Trends Biotechnol.* 32, 456–465. doi: 10.1016/j.tibtech.2014.06.007

Elion, D. L., and Cook, R. S. (2018). Harnessing RIG-I and intrinsic immunity in the tumor microenvironment for therapeutic cancer treatment. *Oncotarget* 9, 29007–29017. doi: 10.18632/oncotarget.25626

Elkin, S. R., Lakoduk, A. M., and Schmid, S. L. (2016). Endocytic pathways and endosomal trafficking: a primer. *Wien. Med. Wochenschr.* 166, 196–204. doi: 10.1007/s10354-016-0432-437

Espelin, C. W., Leonard, S. C., Geretti, E., Wickham, T. J., and Hendriks, B. S. (2016). Dual HER2 targeting with trastuzumab and liposomal-encapsulated doxorubicin (MM-302) demonstrates synergistic antitumor activity in breast and gastric cancer. *Cancer Res.* 76, 1517–1527. doi: 10.1158/0008-5472.CAN-15-1518

Fankhauser, M., Broggi, M. A. S., Potin, L., Bordry, N., Jeanbart, L., Lund, A. W., et al. (2017). Tumor lymphangiogenesis promotes T cell infiltration and potentiates immunotherapy in melanoma. *Sci. Transl. Med.* 9:eaal4712. doi: 10.1126/scitranslmed.aal4712

Farhood, B., Najafi, M., and Mortezaee, K. (2018). CD8 +cytotoxic T lymphocytes in cancer immunotherapy: a review. *J. Cell. Physiol.* 234, 8509–8521. doi: 10.1002/jcp.27782

Fehres, C. M., Unger, W. W. J., Garcia-Vallejo, J. J., and van Kooyk, Y. (2014). Understanding the biology of antigen cross-presentation for the design of vaccines against cancer. *Front. Immunol.* 5:149. doi: 10.3389/fimmu.2014.00149.

Finn, O. J. (2017). Human tumor antigens yesterday, today, and tomorrow. *Cancer Immunol. Res.* 5, 347–354. doi: 10.1158/2326-6066.CIR-17-0112

Foged, C., Brodin, B., Frokjaer, S., and Sundblad, A. (2005). Particle size and surface charge affect particle uptake by human dendritic cells in an in vitro model. *Int. J. Pharm.* 298, 315–322. doi: 10.1016/j.ijpharm.2005.03.035

Frantz, C., Stewart, K. M., and Weaver, V. M. (2010). The extracellular matrix at a glance. *J. Cell Sci.* 123, 4195–4200. doi: 10.1242/jcs.023820.

Fröhlich, E. (2012). The role of surface charge in cellular uptake and cytotoxicity of medical nanoparticles. *Int. J. Nanomed.* 19, 5577–15. doi: 10.2147/IJN.S36111

Fujii, S. -I., and Shimizu, K. (2019). Immune networks and therapeutic targeting of inkt cells in cancer. *Trends Immunol.* 40, 984–997. doi: 10.1016/j.it.2019.09.008

Gay, N. J., and Gangloff, M. (2007). Structure and function of toll receptors and their ligands. *Annu. Rev. Biochem.* 76, 141–165. doi: 10.1146/annurev.biochem.76.060305.151318

Gialeli, C., Theocharis, A. D., and Karamanos, N. K. (2010). Roles of matrix metalloproteinases in cancer progression and their pharmacological targeting. *FEBS J.* 278, 16–27. doi: 10.1111/j.1742-4658.2010.07919.x

Golombek, S. K., May, J. -N., Theek, B., Appold, L., Drude, N., Kiessling, F., et al. (2018). Tumor targeting via EPR: strategies to enhance patient responses. *Adv. Drug Del. Rev.* 130, 17–38. doi: 10.1016/j.addr.2018.07.007

Gong, X., Li, J., Tan, T., Wang, Z., Wang, H., Wang, Y., et al. (2019). Emerging approaches of cell-based nanosystems to target cancer metastasis. *Adv. Funct. Mater.* 29, 1903441–36. doi: 10.1002/adfm.201903441

González, F. E., Gleisner, A., Falcón-Beas, F., Osorio, F., López, M. N., and Salazar-Onfray, F. (2014). Tumor cell lysates as immunogenic sources for cancer vaccine design. *Hum. Vaccin. Immunother.* 10, 3261–3269. doi: 10.4161/21645515.2014.982996

Gooden, M. J. M., de Bock, G. H., Leffers, N., Daemen, T., and Nijman, H. W. (2011). The prognostic influence of tumour-infiltrating lymphocytes in cancer: a systematic review with meta-analysis. *Br. J. Cancer* 105, 93–103. doi: 10.1038/bjc.2011.189

Gratton, S. E. A., Ropp, P. A., Pohlhaus, P. D., Luft, J. C., Madden, V. J., Napier, M. E., et al. (2008). The effect of particle design on cellular internalization pathways. *Proc. Natl. Acad. Sci. U.S.A.* 105, 11613–11618. doi: 10.1073/pnas.0801763105

Groom, J. R., and Luster, A. D. (2011). CXCR3 in T cell function. *Exp. Cell Res.* 317, 620–631. doi: 10.1016/j.yexcr.2010.12.017

Grywalska, E., Pasiarski, M., Góźdź, S., and Roliński, J. (2018). Immune-checkpoint inhibitors for combating T-cell dysfunction in cancer. *OTT Vol.* 11, 6505–6524. doi: 10.2147/OTT.S150817

Guise, C. P., Mowday, A. M., Ashoorzadeh, A., Yuan, R., Lin, W. -H., Wu, D. -H., et al. (2014). Bioreductive prodrugs as cancer therapeutics: targeting tumor hypoxia. *Chin. J. Cancer* 33, 80–86. doi: 10.5732/cjc.012.10285

Gul, N., and van Egmond, M. (2015). Antibody-dependent phagocytosis of tumor cells by macrophages: a potent effector mechanism of monoclonal antibody therapy of cancer. *Cancer Res.* 75, 5008–5013. doi: 10.1158/0008-5472.CAN-15-1330

Gulley, J. L., Madan, R. A., Pachynski, R., Mulders, P., Sheikh, N. A., Trager, J., et al. (2017). Role of antigen spread and distinctive characteristics of immunotherapy in cancer treatment. *J. Natl. Cancer Inst.* 109:djw261 doi: 10.1093/jnci/djw261.

Guo, P., Liu, D., Subramanyam, K., Wang, B., Yang, J., Huang, J., et al. (2018). Nanoparticle elasticity directs tumor uptake. *Nat. Commun.* 9:130. doi: 10.1038/s41467-017-02588-2589

Hanafy, N., El-Kemary, M., and Leporatti, S. (2018). Micelles structure development as a strategy to improve smart cancer therapy. *Cancers* 10, 238–14. doi: 10.3390/cancers10070238

Hanahan, D., and Weinberg, R. A. (2011). Hallmarks of cancer: the next generation. *Cell* 144, 646–674. doi: 10.1016/j.cell.2011.02.013

Harjunpää, H., Llort Asens, M., Guenther, C., and Fagerholm, S. C. (2019). Cell adhesion molecules and their roles and regulation in the immune and tumor microenvironment. *Front. Immunol.* 10, 883–24. doi: 10.3389/fimmu.2019.01078

Hauert, S., and Bhatia, S. N. (2014). Mechanisms of cooperation in cancer nanomedicine: towards systems nanotechnology. *Trends Biotechnol.* 32, 448–455. doi: 10.1016/j.tibtech.2014.06.010

Havel, J. J., Chowell, D., and Chan, T. A. (2019). The evolving landscape of biomarkers for checkpoint inhibitor immunotherapy. *Nat. Rev. Cancer* 19, 133–150. doi: 10.1038/s41568-019-0116-x

Hernandez, C., Huebener, P., and Schwabe, R. F. (2016). Damage-associated molecular patterns in cancer: a double-edged sword. *Oncogene* 35, 5931–5941. doi: 10.1038/onc.2016.104

Hesse, C., Ginter, W., Förg, T., Mayer, C. T., Baru, A. M., Arnold-Schrauf, C., et al. (2013). In vivo targeting of human DC-SIGN drastically enhances CD8 +T-cell-mediated protective immunity. *Eur. J. Immunol.* 43, 2543–2553. doi: 10.1002/eji.201343429

Hirosue, S., Vokali, E., Raghavan, V. R., Rincon-Restrepo, M., Lund, A. W., Corthésy-Henrioud, P., et al. (2014). Steady-state antigen scavenging, cross-presentation, and CD8+ T cell priming: a new role for lymphatic endothelial cells. *J. Immunol.* 192, 5002–5011. doi: 10.4049/jimmunol.1302492

Hoffmann, S., Vystrèilová, L., Ulbrich, K., Etrych, T., Caysa, H., Mueller, T., et al. (2012). Dual fluorescent HPMA copolymers for passive tumor targeting with pH-sensitive drug release: synthesis and characterization of distribution and tumor accumulation in mice by noninvasive multispectral optical imaging. *Biomacromolecules* 13, 652–663. doi: 10.1021/bm2015027

Homhuan, A., Prakongpan, S., Poomvises, P., Maas, R. A., Crommelin, D. J. A., Kersten, G. F. A., et al. (2004). Virosome and ISCOM vaccines against Newcastle disease: preparation, characterization and immunogenicity. *Eur. J. Pharm. Sci.* 22, 459–468. doi: 10.1016/j.ejps.2004.05.005

Hong, L. P. T., Scoble, J. A., Doughty, L., Coia, G., and Williams, C. C. (2011). Cancer-targeting antibody–drug conjugates: site-specific conjugation of doxorubicin to anti-EGFR 528 fab' through a polyethylene glycol linker. *Aust. J. Chem.* 64, 779–11. doi: 10.1071/CH11071

Hoshyar, N., Gray, S., Han, H., and Bao, G. (2016). The effect of nanoparticle size on in vivopharmacokinetics and cellular interaction. *Nanomedicine* 11, 673–692. doi: 10.2217/nnm.16.5

Hu, Q., Katti, P. S., and Gu, Z. (2014). Enzyme-responsive nanomaterials for controlled drug delivery. *Nanoscale* 6, 12273–12286. doi: 10.1039/C4NR04249B.

Huang, Y., Goel, S., Duda, D. G., Fukumura, D., and Jain, R. K. (2013). Vascular normalization as an emerging strategy to enhance cancer immunotherapy. *Cancer Res.* 73, 2943–2948. doi: 10.1158/0008-5472.CAN-12-4354

Huijbers, E. J. M., and Griffioen, A. W. (2017). The revival of cancer vaccines - the eminent need to activate humoral immunity. *Hum. Vaccin. Immunother.* 13, 1112–1114. doi: 10.1080/21645515.2016.1276140

Hunter, F. W., Wouters, B. G., and Wilson, W. R. (2016). Hypoxia-activated prodrugs: paths forward in the era of personalised medicine. *Br. J. Cancer* 114, 1071–1077. doi: 10.1038/bjc.2016.79

Hutmacher, C., and Neri, D. (2019). Antibody-cytokine fusion proteins: biopharmaceuticals with immunomodulatory properties for cancer therapy. *Adv. Drug Del. Rev.* 141, 67–91. doi: 10.1016/j.addr.2018.09.002

Ikemoto, H., Lingasamy, P., Anton Willmore, A. -M., Hunt, H., Kurm, K., Tammik, O., et al. (2017). Hyaluronan-binding peptide for targeting peritoneal carcinomatosis. *Tumour Biol.* 39:1010428317701628. doi: 10.1177/1010428317701628

Ilca, F. T., Neerincx, A., Wills, M. R., de la Roche, M., and Boyle, L. H. (2018). Utilizing TAPBPR to promote exogenous peptide loading onto cell surface MHC I molecules. *Proc. Natl. Acad. Sci. U.S.A.* 115, E9353–E9361. doi: 10.1073/pnas.1809465115

Ingrole, R. S. J., and Gill, H. S. (2019). Microneedle coating methods: a review with a Perspective. *J. Pharmacol. Exp. Ther.* 370, 555–569. doi: 10.1124/jpet.119.258707.

Irvine, D. J., Swartz, M. A., and Szeto, G. L. (2013). Engineering synthetic vaccines using cues from natural immunity. *Nat. Mater.* 12, 978–990. doi: 10.1038/nmat3775

Ishihara, J., Fukunaga, K., Ishihara, A., Larsson, H. M., Potin, L., Hosseinchi, P., et al. (2017). Matrix-binding checkpoint immunotherapies enhance antitumor efficacy and reduce adverse events. *Sci. Transl. Med.* 9:eaan0401. doi: 10.1126/scitranslmed.aan0401

Ishihara, J., Ishihara, A., Sasaki, K., Lee, S. S.-Y., Williford, J.-M., Yasui, M., et al. (2019). Targeted antibody and cytokine cancer immunotherapies through collagen affinity. *Sci. Transl. Med.* 11:eaau3259. doi: 10.1126/scitranslmed.aau3259

Jackson, H. J., Rafiq, S., and Brentjens, R. J. (2016). Driving CAR T-cells forward. *Nat. Rev. Clin. Oncol.* 13, 370–383. doi: 10.1038/nrclinonc.2016.36

Jafri, M. A., Ansari, S. A., Alqahtani, M. H., and Shay, J. W. (2016). Roles of telomeres and telomerase in cancer, and advances in telomerase- targeted therapies. *Genome Med.* 8:69. doi: 10.1186/s13073-016-0324-x

Jeanbart, L., Ballester, M., de Titta, A., Corthésy, P., Romero, P., Hubbell, J. A., et al. (2014). Enhancing efficacy of anticancer vaccines by targeted delivery to tumor-draining lymph nodes. *Cancer Immunol. Res.* 2, 436–447. doi: 10.1158/2326-6066.CIR-14-0019-T

Jiang, T., Zhang, Z., Zhang, Y., Lv, H., Zhou, J., Li, C., et al. (2012). Dual-functional liposomes based on pH-responsive cell-penetrating peptide and hyaluronic acid for tumor-targeted anticancer drug delivery. *Biomaterials* 33, 9246–9258. doi: 10.1016/j.biomaterials.2012.09.027

Joffre, O. P., Segura, E., Savina, A., and Amigorena, S. (2012). Cross-presentation by dendritic cells. Nat Rev Immunol. 12, 557–69. doi: 10.1038/nri3254

Joshi, S., and Durden, D. L. (2019). Combinatorial approach to improve cancer immunotherapy: rational drug design strategy to simultaneously hit multiple targets to kill tumor cells and to activate the immune system. *J. Oncol.* 2019, 1–18. doi: 10.1155/2019/5245034

Joyce, J. A., Baruch, A., Chehade, K., Meyer-Morse, N., Giraudo, E., Tsai, F. -Y., et al. (2004). Cathepsin cysteine proteases are effectors of invasive growth and angiogenesis during multistage tumorigenesis. *Cancer Cell* 5, 443–453. doi: 10.1038/nrc1396

Julier, Z., Martino, M. M., de Titta, A., Jeanbart, L., and Hubbell, J. A. (2015). The TLR4 agonist fibronectin extra domain a is circulation, phagocytosis, endocytosis, and targeting. *Sci. Rep.* 5:8569. doi: 10.1038/srep08569

Kanchan, V., and Panda, A. K. (2007). Interactions of antigen-loaded polylactide particles with macrophages and their correlation with the immune response. *Biomaterials* 28, 5344–5357. doi: 10.1016/j.biomaterials.2007.08.015

Karoulia, Z., Gavathiotis, E., and Poulikakos, P. I. (2017). New perspectives for targeting RAF kinase in human cancer. *Nat. Rev. Cancer* 17, 676–691. doi: 10.1038/nrc.2017.79

Kaspar, M., Zardi, L., and Neri, D. (2005). Fibronectin as target for tumor therapy. *Int. J. Cancer* 118, 1331–1339. doi: 10.1002/ijc.21677

Kaumaya, P. T. (2015). A paradigm shift: cancer therapy with peptide-based B-cell epitopes and peptide immunotherapeutics targeting multiple solid tumor types: emerging concepts and validation of combination immunotherapy. *Hum. Vaccin. Immunother.* 11, 1368–1386. doi: 10.1080/21645515.2015.1026495

Kimura, T., Sugaya, M., Oka, T., Blauvelt, A., Okochi, H., and Sato, S. (2015). Lymphatic dysfunction attenuates tumor immunity through impaired antigen presentation. *Oncotarget* 6, 18081–18093. doi: 10.18632/oncotarget.4018

Kongkatigumjorn, N., Smith, S. A., Chen, M., Fang, K., Yang, S., Gillies, E. R., et al. (2018). Controlling endosomal escape using pH-responsive nanoparticles with tunable disassembly. *ACS Appl. Nano Mater.* 1, 3164–3173. doi: 10.1021/acsanm.8b00338

Kubota, T., Kuroda, S., Kanaya, N., Morihiro, T., Aoyama, K., Kakiuchi, Y., et al. (2018). HER2-targeted gold nanoparticles potentially overcome resistance to trastuzumab in gastric cancer. *Nanomedicine* 14, 1919–1929. doi: 10.1016/j.nano.2018.05.019

Kulkarni, P., Haldar, M. K., You, S., Choi, Y., and Mallik, S. (2016). Hypoxia-responsive polymersomes for drug delivery to hypoxic pancreatic cancer cells. *Biomacromolecules* 17, 2507–2513. doi: 10.1021/acs.biomac.6b00350

Laakkonen, P., Waltari, M., Holopainen, T., Takahashi, T., Pytowski, B., Steiner, P., et al. (2007). Vascular endothelial growth factor receptor 3 is involved in tumor angiogenesis and growth. *Cancer Res.* 67, 593–599. doi: 10.1158/0008-5472.CAN-06-3567

Lai, C.-Y., Trewyn, B. G., Jeftinija, D. M., Jeftinija, K., Xu, S., Jeftinija, S., et al. (2003). A mesoporous silica nanosphere-based carrier system with chemically removable CdS nanoparticle caps for stimuli-responsive controlled release of neurotransmitters and drug molecules. *J. Am. Chem. Soc.* 125, 4451–4459. doi: 10.1021/ja028650l

Laidlaw, B. J., Craft, J. E., and Kaech, S. M. (2016). The multifaceted role of CD4(+) T cells in CD8(+) T cell memory. *Nat. Rev. Immunol.* 16, 102–111. doi: 10.1038/nri.2015.10

Lanitis, E., Irving, M., and Coukos, G. (2015). Targeting the tumor vasculature to enhance T cell activity. *Curr. Opin. Immunol.* 33, 55–63. doi: 10.1016/j.coi.2015.01.011

Lapointe, R., Bellemare-Pelletier, A., Housseau, F., Thibodeau, J., and Hwu, P. (2003). CD40-stimulated B lymphocytes pulsed with tumor antigens are effective antigen-presenting cells that can generate specific T cells. *Cancer Res.* 63, 2836–2843.

Lasarte, J. J., Casares, N., Gorraiz, M., Hervás-Stubbs, S., Arribillaga, L., Mansilla, C., et al. (2007). The extra domain A from fibronectin targets antigens to TLR4-expressing cells and induces cytotoxic T cell responses in vivo. *J. Immunol.* 178, 748–756. doi: 10.4049/jimmunol.178.2.748

Laurent, S., Saei, A. A., Behzadi, S., Panahifar, A., and Mahmoudi, M. (2014). Superparamagnetic iron oxide nanoparticles for delivery of therapeutic agents: opportunities and challenges. *Expert. Opin. Drug Deliv.* 11, 1449–1470. doi: 10.1517/17425247.2014.924501

Lee, C. M., Tanaka, T., Murai, T., Kondo, M., Kimura, J., Su, W., et al. (2002). Novel chondroitin sulfate-binding cationic liposomes loaded with cisplatin efficiently suppress the local growth and liver metastasis of tumor cells in vivo. *Cancer Res.* 62, 4282–4288.

Leibacher, J., and Henschler, R. (2016). Biodistribution, migration and homing of systemically applied mesenchymal stem/ stromal cells. *Stem Cell Res. Ther.* 7:7. doi: 10.1186/s13287-015-0271-272

Li, A., Yi, M., Qin, S., Song, Y., Chu, Q., and Wu, K. (2019). Activating cGAS-STING pathway for the optimal effect of cancer immunotherapy. *J. Hematol. Oncol.* 12:35. doi: 10.1186/s13045-019-0721-x

Li, K., Peers-Adams, A., Win, S. J., Scullion, S., Wilson, M., Young, V. L., et al. (2013). Antigen incorporated in virus-like particles is delivered to specific dendritic cell subsets that induce an effective antitumor immune response in vivo. *J. Immunother.* 36, 11–19. doi: 10.1097/CJI.0b013e3182787f5e

Li, Y., Idamakanti, N., Arroyo, T., Thorne, S., Reid, T., Nichols, S., et al. (2005). Dual promoter-controlled oncolytic adenovirus CG5757 has strong tumor selectivity and significant antitumor efficacy in preclinical models. *Clin. Cancer Res.* 11, 8845–8855. doi: 10.1158/1078-0432.CCR-05-1757

Liang, H., Li, X., Bin, W., Chen, B., Zhao, Y., Sun, J., et al. (2016). A collagen-binding EGFR antibody fragment targeting tumors with a collagen-rich extracellular matrix. *Sci. Rep.* 6:18205. doi: 10.1038/srep18205

Lin, C.-C., and Metters, A. T. (2006). Hydrogels in controlled release formulations: Network design and mathematical modeling. *Adv. Drug Deliv. Rev.* 58, 1379–1408. doi: 10.1016/j.addr.2006.09.004

Lin, J., Shigdar, S., Fang, D. Z., Xiang, D., Wei, M. Q., Danks, A., et al. (2014). Improved efficacy and reduced toxicity of doxorubicin encapsulated in sulfatide-containing nanoliposome in a glioma model. *PLoS One* 9:e103736. doi: 10.1371/journal.pone.0103736

Ling, X., Marini, F., Konopleva, M., Schober, W., Shi, Y., Burks, J., et al. (2010). Mesenchymal stem cells overexpressing IFN-β inhibit breast cancer growth and metastases through stat3 signaling in a syngeneic tumor model. *Cancer Microenviron.* 3, 83–95. doi: 10.1007/s12307-010-0041-48

Lingasamy, P., Tobi, A., Haugas, M., Hunt, H., Paiste, P., Asser, T., et al. (2019). Bi-specific tenascin-C and fibronectin targeted peptide for solid tumor delivery. *Biomaterials* 219:119373. doi: 10.1016/j.biomaterials.2019.119373

Liu, D.-Z., Sinchaikul, S., Reddy, P. V. G., Chang, M.-Y., and Chen, S.-T. (2007). Synthesis of 2'-paclitaxel methyl 2-glucopyranosyl succinate for specific targeted delivery to cancer cells. *Bioorg. Med. Chem. Lett.* 17, 617–620. doi: 10.1016/j.bmcl.2006.11.008

Liu, M., Song, W., and Huang, L. (2019). Drug delivery systems targeting tumor-associated fibroblasts for cancer immunotherapy. *Cancer Lett.* 448, 31–39. doi: 10.1016/j.canlet.2019.01.032

Liu, Y., Zhi, X., Yang, M., Zhang, J., Lin, L., Zhao, X., et al. (2017). Tumor-triggered drug release from calcium carbonate-encapsulated gold nanostars for near-infrared photodynamic/photothermal combination antitumor therapy. *Theranostics* 7, 1650–1662. doi: 10.7150/thno.17602

Locy, H., Melhaoui, S., Maenhout, S. K., and Thielemans, K. (2018). "Dendritic cells: the tools for cancer treatment," in *Dendritic Cells*, ed. S. P. Chapoval, (London: InTech), 1–29. doi: 10.5772/intechopen.79273

Maiti, S., Manna, S., Shen, J., Esser-Kahn, A. P., and Du, W. (2019). Mitigation of hydrophobicity-induced immunotoxicity by sugar poly(orthoesters). *J. Am. Chem. Soc.* 141, 4510–4514. doi: 10.1021/jacs.8b12205

Mamaeva, V., Rosenholm, J. M., Bate-Eya, L. T., Bergman, L., Peuhu, E., Duchanoy, A., et al. (2009). *Mesoporous silica* nanoparticles as drug delivery systems for targeted inhibition of notch signaling in cancer. *Mol. Ther.* 19, 1538–1546. doi: 10.1038/mt.2011.105

Mandal, S., Eksteen-Akeroyd, Z. H., Jacobs, M. J., Hammink, R., Koepf, M., Lambeck, A. J. A., et al. (2013). Therapeutic nanoworms: towards novel synthetic dendritic cells for immunotherapy. *Chem. Sci.* 4:4168. doi: 10.1039/c3sc51399h

Mandalà, M., and Voit, C. (2013). Targeting BRAF in melanoma: biological and clinical challenges. *Crit. Rev. Oncol.* 87, 239–255. doi: 10.1016/j.critrevonc.2013.01.003

Marabelle, A., Andtbacka, R., Harrington, K., Melero, I., Leidner, R., de Baere, T., et al. (2018). Starting the fight in the tumor: expert recommendations for the development of human intratumoral immunotherapy (HIT-IT). *Ann. Oncol.* 29, 2163–2174. doi: 10.1093/annonc/mdy423

Marabelle, A., Kohrt, H., Caux, C., and Levy, R. (2014). Intratumoral immunization: a new paradigm for cancer therapy. *Clin. Cancer Res.* 20, 1747–1756. doi: 10.1158/1078-0432.CCR-13-2116

Marelli, G., Howells, A., Lemoine, N. R., and Wang, Y. (2018). Oncolytic Viral Therapy and the Immune System: A Double-Edged Sword Against Cancer. *Front. Immunol.* 9:866. doi: 10.3389/fimmu.2018.00866

Martino, M. M., Briquez, P. S., Guc, E., Tortelli, F., Kilarski, W. W., Metzger, S., et al. (2014). Growth factors engineered for super-affinity to the extracellular matrix enhance tissue healing. *Science* 343, 885–888. doi: 10.1126/science.1247663

Matsushita, H., Hosoi, A., Ueha, S., Abe, J., Fujieda, N., Tomura, M., et al. (2015). Cytotoxic T lymphocytes block tumor growth both by lytic activity and IFNγ-dependent cell-cycle arrest. *Cancer Immunol. Res.* 3, 26–36. doi: 10.1158/2326-6066.CIR-14-0098

McLellan, A. D., and Ali Hosseini Rad, S. M. (2019). Chimeric antigen receptor T cell persistence and memory cell formation. *Immunol. Cell Biol.* 129, 664–674. doi: 10.1111/imcb.12254

Mehlen, P., and Puisieux, A. (2006). Metastasis: a question of life or death. *Nat. Rev. Cancer* 6, 449–458. doi: 10.1038/nrc1886

Meyer, R. A., Sunshine, J. C., Perica, K., Kosmides, A. K., Aje, K., Schneck, J. P., et al. (2015). Biodegradable nanoellipsoidal artificial antigen presenting cells for antigen specific T-Cell activation. *Small* 11, 1519–1525. doi: 10.1002/smll.201402369

Mitchell, D. A., Batich, K. A., Gunn, M. D., Huang, M.-N., Sanchez-Perez, L., Nair, S. K., et al. (2015). Tetanus toxoid and CCL3 improve dendritic cell vaccines in mice and glioblastoma patients. *Nature* 519, 366–369. doi: 10.1038/nature14320

Mizuhara, T., Saha, K., Moyano, D. F., Kim, C. S., Yan, B., Kim, Y.-K., et al. (2015). Acylsulfonamide-functionalized zwitterionic gold nanoparticles for enhanced cellular uptake at tumor pH. *Angew. Chem. Int. Ed.* 54, 6567–6570. doi: 10.1002/anie.201411615

Mo, R., Sun, Q., Xue, J., Li, N., Li, W., Zhang, C., et al. (2012). Multistage pH-Responsive liposomes for mitochondrial-targeted anticancer drug delivery. *Adv. Mater.* 24, 3659–3665. doi: 10.1002/adma.201201498

Momin, N., Mehta, N. K., Bennett, N. R., Ma, L., Palmeri, J. R., Chinn, M. M., et al. (2019). Anchoring of intratumorally administered cytokines to collagen safely potentiates systemic cancer immunotherapy. *Sci. Transl. Med.* 11:eaaw2614. doi: 10.1126/scitranslmed.aaw2614

Morse, M. A., Garst, J., Osada, T., Khan, S., Hobeika, A., Clay, T. M., et al. (2005). A phase I study of dexosome immunotherapy in patients with advanced non-small cell lung cancer. *J. Transl. Med.* 3:9. doi: 10.1186/1479-5876-3-9

Moyano, D. F., Goldsmith, M., Solfiell, D. J., Landesman-Milo, D., Miranda, O. R., Peer, D., et al. (2012). Nanoparticle hydrophobicity dictates immune response. *J. Am. Chem. Soc.* 134, 3965–3967. doi: 10.1021/ja2108905

Müller, D., Frey, K., and Kontermann, R. E. (2008). A novel antibody-4-1BBL fusion protein for targeted costimulation in cancer immunotherapy. *J. Immunother.* 31, 714–722. doi: 10.1097/CJI.0b013e31818353e9

Münch, R. C., Janicki, H., Völker, I., Rasbach, A., Hallek, M., Büning, H., et al. (2013). Displaying high-affinity ligands on adeno-associated viral vectors enables tumor cell-specific and safe gene transfer. *Mol. Ther.* 21, 109–118. doi: 10.1038/mt.2012.186

Nair, S., and Dhodapkar, M. V. (2017). Natural killer T cells in cancer immunotherapy. *Front. Immunol.* 8:1178. doi: 10.3389/fimmu.2017.01178

National Institutes of Health of the USA (2019). *Type of Cancer Treatments*. Available at: www.cancer.gov/about-cancer/treatment/types (accessed 2019).

Nejadnik, H., Ye, D., Lenkov, O. D., Donig, J. S., Martin, J. E., Castillo, R., et al. (2015). Magnetic resonance imaging of stem cell apoptosis in arthritic joints with a caspase activatable contrast agent. *ACS Nano* 9, 1150–1160. doi: 10.1021/nn504494c

Nguyen-Hoai, T., Pham-Duc, M., Gries, M., Dörken, B., Pezzutto, A., and Westermann, J. (2016). CCL4 as an adjuvant for DNA vaccination in a Her2/neu mouse tumor model. *Cancer Gene Ther.* 23, 162–167. doi: 10.1038/cgt.2016.9

Noble, G. T., Stefanick, J. F., Ashley, J. D., Kiziltepe, T., and Bilgicer, B. (2014). Ligand-targeted liposome design: challenges and fundamental considerations. *Trends Biotechnol.* 32, 32–45. doi: 10.1016/j.tibtech.2013.09.007

Oussoren, C., Zuidema, J., Crommelin, D. J., and Storm, G. (1997). Lymphatic uptake and biodistribution of liposomes after subcutaneous injection. II. Influence of liposomal size, lipid compostion and lipid dose. *Biochim. Biophys. Acta* 1328, 261–272. doi: 10.1016/s0005-2736(97)00122-123

Owens, D. E., and Peppas, N. A. (2006). Opsonization, biodistribution, and pharmacokinetics of polymeric nanoparticles. *Int. J. Pharm.* 307, 93–102. doi: 10.1016/j.ijpharm.2005.10.010

Owens, G. J., Singh, R. K., Foroutan, F., Alqaysi, M., Han, C.-M., Mahapatra, C., et al. (2016). Sol-gel based materials for biomedical applications. *Prog. Mater. Sci.* 77, 1–79. doi: 10.1016/j.pmatsci.2015.12.001

Pahl, J. H. W., Cerwenka, A., and Ni, J. (2018). Memory-like NK cells: remembering a previous activation by cytokines and NK cell receptors. *Front. Immunol.* 9:2796. doi: 10.3389/fimmu.2018.02796

Palladini, A., Thrane, S., Janitzek, C. M., Pihl, J., Clemmensen, S. B., de Jongh, W. A., et al. (2018). Virus-like particle display of HER2 induces potent anti-cancer responses. *Oncoimmunology* 7:e1408749. doi: 10.1080/2162402X.2017.1408749

Palmerston Mendes, L., Pan, J., and Torchilin, V. (2017). Dendrimers as nanocarriers for nucleic acid and drug delivery in cancer therapy. *Molecules* 22, 1401–1421. doi: 10.3390/molecules22091401

Park, J. H., Lee, S., Kim, J.-H., Park, K., Kim, K., and Kwon, I. C. (2008). Polymeric nanomedicine for cancer therapy. *Prog. Polym. Sci.* 33, 113–137. doi: 10.1016/j.progpolymsci.2007.09.003

Paust, S., Gill, H. S., Wang, B.-Z., Flynn, M. P., Moseman, E. A., Senman, B., et al. (2010). Critical role for the chemokine receptor CXCR6 in NK cell–mediated antigen-specific memory of haptens and viruses. *Nat. Immunol.* 11, 1127–1135. doi: 10.1038/ni.1953

Peek, L. J., Middaugh, C. R., and Berkland, C. (2008). Nanotechnology in vaccine delivery. *Adv. Drug Deliv. Rev.* 60, 915–928. doi: 10.1016/j.addr.2007.05.017

Peiris, P. M., Bauer, L., Toy, R., Tran, E., Pansky, J., Doolittle, E., et al. (2012). Enhanced delivery of chemotherapy to tumors using a multicomponent nanochain with radio-frequency-tunable drug release. *ACS Nano* 6, 4157–4168. doi: 10.1021/nn300652p

Peppas, N. A., Bures, P., Leobandung, W., and Ichikawa, H. (2000). Hydrogels in pharmaceutical formulations. *Eur. J. Pharm. Biopharm.* 50, 27–46.

Peters, S., Reck, M., Smit, E. F., Mok, T., and Hellmann, M. D. (2019). How to make the best use of immunotherapy as first-line treatment of advanced/metastatic non-small-cell lung cancer. *Ann. Oncol.* 30, 884–896. doi: 10.1093/annonc/mdz109

Phillips, D. J., and Gibson, M. I. (2014). Redox-sensitive materials for drug delivery: targeting the correct intracellular environment, tuning release rates, and appropriate predictive systems. *Antioxid. Redox Signal.* 21, 786–803. doi: 10.1089/ars.2013.5728

Pinzon-Charry, A., Maxwell, T., and López, J. A. (2005). Dendritic cell dysfunction in cancer: a mechanism for immunosuppression. *Immunol. Cell Biol.* 83, 451–461. doi: 10.1111/j.1440-1711.2005.01371.x

Poggi, A., Varesano, S., and Zocchi, M. R. (2018). How to hit mesenchymal stromal cells and make the tumor microenvironment immunostimulant rather than immunosuppressive. *Front. Immunol.* 9:262. doi: 10.3389/fimmu.2018.00262

Provenzano, P. P., Inman, D. R., Eliceiri, K. W., Knittel, J. G., Yan, L., Rueden, C. T., et al. (2008). Collagen density promotes mammary tumor initiation and progression. *BMC Med.* 6:11. doi: 10.1186/1741-7015-6-11

Punt, S., Langenhoff, J. M., Putter, H., Fleuren, G. J., Gorter, A., and Jordanova, E. S. (2015). The correlations between IL-17 vs. *Th*17 cells and cancer patient survival: a systematic review. *OncoImmunology* 4:e984547. doi: 10.4161/2162402X.2014.984547

Pushko, P., Pumpens, P., and Grens, E. (2013). Development of virus-like particle technology from small highly symmetric to large complex virus-like particle structures. *Intervirology* 56, 141–165. doi: 10.1159/000346773

Quinto, C. A., Mohindra, P., Tong, S., and Bao, G. (2015). Multifunctional superparamagnetic iron oxide nanoparticles for combined chemotherapy and hyperthermia cancer treatment. *Nanoscale* 7, 12728–12736. doi: 10.1039/C5NR02718G

Raavé, R., van Kuppevelt, T. H., and Daamen, W. F. (2018). Chemotherapeutic drug delivery by tumoral extracellular matrix targeting. *J. Control. Rel.* 274, 1–8. doi: 10.1016/j.jconrel.2018.01.029

Rangasamy, L., Chelvam, V., Kanduluru, A. K., Srinivasarao, M., Bandara, N. A., You, F., et al. (2018). New mechanism for release of endosomal contents: osmotic lysis via Nigericin-Mediated K+/H+ exchange. *Bioconjugate Chem.* 29, 1047–1059. doi: 10.1021/acs.bioconjchem.7b00714

Reddy, S. T., Rehor, A., Schmoekel, H. G., Hubbell, J. A., and Swartz, M. A. (2006). In vivo targeting of dendritic cells in lymph nodes with poly(propylene sulfide) nanoparticles. *J. Control. Rel.* 112, 26–34. doi: 10.1016/j.jconrel.2006.01.006

Reeves, R. K., Li, H., Jost, S., Blass, E., Li, H., Schafer, J. L., et al. (2015). Antigen-specific NK cell memory in rhesus macaques. *Nat. Immunol.* 16, 927–932. doi: 10.1038/ni.3227

Reis, E. S., Mastellos, D. C., Ricklin, D., Mantovani, A., and Lambris, J. D. (2017). Complement in cancer: untangling an intricate relationship. *Nat. Publ. Group* 18, 5–18. doi: 10.1038/nri.2017.97

Ridge, J. P., Di Rosa, F., and Matzinger, P. (1998). A conditioned dendritic cell can be a temporal bridge between a CD4+ T-helper and a T-killer cell. *Nature* 393, 474–478. doi: 10.1038/30989

Rivolta, I., Panariti, A., and Miserocchi, G. (2012). The effect of nanoparticle uptake on cellular behavior: disrupting or enabling functions? *NSA* 5:87. doi: 10.2147/NSA.S25515

Robbins, P. D., and Morelli, A. E. (2014). Regulation of immune responses by extracellular vesicles. *Nat. Rev. Immunol.* 14, 195–208. doi: 10.1038/nri3622

Romee, R., Rosario, M., Berrien-Elliott, M. M., Wagner, J. A., Jewell, B. A., Schappe, T., et al. (2016). Cytokine-induced memory-like natural killer cells exhibit enhanced responses against myeloid leukemia. *Sci. Transl. Med.* 8:357ra123. doi: 10.1126/scitranslmed.aaf2341

Rotman, J., Koster, B. D., Jordanova, E. S., Heeren, A. M., and de Gruijl, T. D. (2019). Unlocking the therapeutic potential of primary tumor-draining lymph nodes. *Cancer Immunol. Immunother.* 68, 1681–1688. doi: 10.1007/s00262-019-02330-y

Russell, H. V., Strother, D., Mei, Z., Rill, D., Popek, E., Biagi, E., et al. (2007). Phase I trial of vaccination with autologous neuroblastoma tumor cells genetically modified to secrete IL-2 and lymphotactin. *J. Immunother.* 30, 227–233. doi: 10.1097/01.cji.0000211335.14385.57

Sadhukha, T., O'Brien, T. D., and Prabha, S. (2014). Nano-engineered mesenchymal stem cells as targeted therapeutic carriers. *J. Control. Rel.* 196, 243–251. doi: 10.1016/j.jconrel.2014.10.015

Saif, M. W., Knost, J. A., Chiorean, E. G., Kambhampati, S. R. P., Yu, D., Pytowski, B., et al. (2016). Phase 1 study of the anti-vascular endothelial growth factor receptor 3 monoclonal antibody LY3022856/IMC-3C5 in patients with advanced and refractory solid tumors and advanced colorectal cancer. *Cancer Chemother. Pharmacol.* 78, 815–824. doi: 10.1007/s00280-016-3134-3133

Salanti, A., Clausen, T. M., Agerbæk, M. Ø, Nakouzi, A. N. I, Dahlbäck, M., Oo, H. Z., et al. (2015). Targeting human cancer by a Glycosaminoglycan binding malaria protein. *Cancer Cell* 28, 500–514. doi: 10.1016/j.ccell.2015.09.003

Saleh, A. F., Lázaro-Ibáñez, E., Forsgard, M. A. M., Shatnyeva, O., Osteikoetxea, X., Karlsson, F., et al. (2019). Extracellular vesicles induce minimal hepatotoxicity and immunogenicity. *Nanoscale* 11, 6990–7001. doi: 10.1039/C8NR08720B

Sánchez-Paulete, A. R., Teijeira, Á, Quetglas, J. I, Rodríguez-Ruiz, M. E., Sánchez-Arráez, Á, Labiano, S., et al. (2018). Intratumoral immunotherapy with XCL1 and sFlt3L Encoded in recombinant semliki forest virus-derived vectors fosters dendritic cell-mediated t-cell cross-priming. *Cancer Res.* 78, 6643–6654. doi: 10.1158/0008-5472.CAN-18-0933

Sautès-Fridman, C., Petitprez, F., Calderaro, J., and Fridman, W. H. (2019). Tertiary lymphoid structures in the era of cancer immunotherapy. *Nat. Rev. Cancer* 19, 307–325. doi: 10.1038/s41568-019-0144-146

Saxena, M., and Bhardwaj, N. (2018). Re-emergence of dendritic cell vaccines for cancer treatment. *Trends Cancer* 4, 119–137. doi: 10.1016/j.trecan.2017.12.007

Saygin, C., Matei, D., Majeti, R., Reizes, O., and Lathia, J. D. (2019). Targeting cancer stemness in the clinic: from hype to hope. *Cell Stem Cell* 24, 25–40. doi: 10.1016/j.stem.2018.11.017

Schultze, J. L., Michalak, S., Seamon, M. J., Dranoff, G., Jung, K., Daley, J., et al. (1997). CD40-activated human B cells: an alternative source of highly efficient antigen presenting cells to generate autologous antigen-specific T cells for adoptive immunotherapy. *J. Clin. Invest.* 100, 2757–2765. doi: 10.1172/JCI119822

Schumacher, T. N., and Schreiber, R. D. (2015). Neoantigens in cancer immunotherapy. *Science* 348, 69–74. doi: 10.1126/science.aaa4971

Schumacher, T. N., Scheper, W., and Kvistborg, P. (2019). Cancer neoantigens. *Annu. Rev. Immunol.* 37, 173–200. doi: 10.1146/annurev-immunol-042617-053402

Seder, R. A., Darrah, P. A., and Roederer, M. (2008). T-cell quality in memory and protection: implications for vaccine design. *Nat. Rev. Immunol.* 8, 247–258. doi: 10.1038/nri2274

Selby, L. I., Cortez-Jugo, C. M., Such, G. K., and Johnston, A. P. R. (2017). Nanoescapology: progress toward understanding the endosomal escape of polymeric nanoparticles. *WIREs Nanomed. Nanobiotechno.l* 9:e1452. doi: 10.1002/wnan.1452

Senapati, S., Mahanta, A. K., Kumar, S., and Maiti, P. (2018). Controlled drug delivery vehicles for cancer treatment and their performance. *Signal. Transduct. Target Ther.* 3, 7–19. doi: 10.1038/s41392-017-0004-3

Shan, Y., Luo, T., Peng, C., Sheng, R., Cao, A., Cao, X., et al. (2012). Gene delivery using dendrimer-entrapped gold nanoparticles as nonviral vectors. *Biomaterials* 33, 3025–3035. doi: 10.1016/j.biomaterials.2011.12.045

Shang, N., Figini, M., Shangguan, J., Wang, B., Sun, C., Pan, L., et al. (2017). Dendritic cells based immunotherapy. *Am. J. Cancer Res.* 7, 2091–2102.

Shannon, A. M., Bouchier-Hayes, D. J., Condron, C. M., and Toomey, D. (2003). Tumour hypoxia, chemotherapeutic resistance and hypoxia-related therapies. *Cancer Treatment Rev.* 29, 297–307. doi: 10.1016/S0305-7372(03)00003-3

Sharma, A., Shah, S. R., Illum, H., and Dowell, J. (2012). Vemurafenib: targeted inhibition of mutated BRAF for treatment of advanced melanoma and its potential in other malignancies. *Drugs* 72, 2207–2222. doi: 10.2165/11640870-000000000-00000

Sharma, G., Valenta, D. T., Altman, Y., Harvey, S., Xie, H., Mitragotri, S., et al. (2010). Polymer particle shape independently influences binding and internalization by macrophages. *J. Control. Rel.* 147, 408–412. doi: 10.1016/j.jconrel.2010.07.116

Sharma, S., Dominguez, A. L., Manrique, S. Z., Cavallo, F., Sakaguchi, S., and Lustgarten, J. (2008). Systemic targeting of CpG-ODN to the tumor microenvironment with anti-neu-CpG hybrid molecule and T regulatory cell depletion induces memory responses in BALB-neuT tolerant mice. *Cancer Res.* 68, 7530–7540. doi: 10.1158/0008-5472.CAN-08-1635

Sherje, A. P., Jadhav, M., Dravyakar, B. R., and Kadam, D. (2018). Dendrimers_A versatile nanocarrier for drug delivery and targeting. *Int. J. Pharm.* 548, 707–720. doi: 10.1016/j.ijpharm.2018.07.030

Shiga, K., Hara, M., Nagasaki, T., Sato, T., Takahashi, H., and Takeyama, H. (2015). Cancer-associated fibroblasts: their characteristics and their roles in tumor growth. *Cancers* 7, 2443–2458. doi: 10.3390/cancers7040902

Shimabukuro-Vornhagen, A., Draube, A., Liebig, T. M., Rothe, A., Kochanek, M., Bergwelt-Baildon, et al. (2012). The immunosuppressive factors IL-10, TGF-β, and VEGF do not affect the antigen-presenting function of CD40-activated B cells. *J. Exp. Clin. Cancer Res.* 31, 47–47. doi: 10.1186/1756-9966-31-47

Shimomura, O., Oda, T., Tateno, H., Ozawa, Y., Kimura, S., Sakashita, S., et al. (2018). A Novel therapeutic strategy for pancreatic cancer: targeting cell surface glycan using rBC2LC-N Lectin-Drug Conjugate (LDC). *Mol. Cancer Ther.* 17, 183–195. doi: 10.1158/1535-7163.MCT-17-0232

Shirota, H., Tross, D., and Klinman, D. (2015). CpG oligonucleotides as cancer vaccine adjuvants. *Vaccines* 3, 390–407. doi: 10.3390/vaccines3020390

Simons, J. W., and Sacks, N. (2006). Granulocyte-macrophage colony-stimulating factor-transduced allogeneic cancer cellular immunotherapy: the GVAX vaccine for prostate cancer. *Urol. Oncol.* 24, 419–424. doi: 10.1016/j.urolonc.2005.08.021

Souza-Fonseca-Guimaraes, F., Cursons, J., and Huntington, N. D. (2019). The emergence of natural killer cells as a major target in cancer immunotherapy. *Trends Immunol.* 40, 142–158. doi: 10.1016/j.it.2018.12.003

Steenblock, E. R., Fadel, T., Labowsky, M., Pober, J. S., and Fahmy, T. M. (2011). An artificial antigen-presenting cell with paracrine delivery of IL-2 impacts the magnitude and direction of the T cell response. *J. Biol. Chem.* 286, 34883–34892. doi: 10.1074/jbc.M111.276329

Sun, I.-C., Lee, S., Koo, H., Kwon, I. C., Choi, K., Ahn, C.-H., et al. (2010). Caspase sensitive gold nanoparticle for apoptosis imaging in live cells. *Bioconjugate Chem.* 21, 1939–1942. doi: 10.1021/bc1003026

Sun, J. C., and Lanier, L. L. (2018). Is there natural killer cell memory and can it be harnessed by vaccination? *Cold Spring Harb. Perspect. Biol.* 10, a29538–a29539. doi: 10.1101/cshperspect.a029538

Sun, J. C., Beilke, J. N., and Lanier, L. L. (2009). Adaptive immune features of natural killer cells. *Nature* 457, 557–561. doi: 10.1038/nature07665

Sun, Z.-Y., Chen, P.-G., Liu, Y.-F., Shi, L., Zhang, B.-D., Wu, J.-J., et al. (2017). Self-assembled nano-immunostimulant for synergistic immune activation. *ChemBioChem* 18, 1721–1729. doi: 10.1002/cbic.201700246

Sunshine, J. C., Perica, K., Schneck, J. P., and Green, J. J. (2014). Particle shape dependence of CD8+ T cell activation by artificial antigen presenting cells. *Biomaterials* 35, 269–277. doi: 10.1016/j.biomaterials.2013.09.050

Swartz, M. A. (2001). The physiology of the lymphatic system. *Adv. Drug Deliv. Rev.* 50, 3–20.

Tacken, P. J., Ginter, W., Berod, L., Cruz, L. J., Joosten, B., Sparwasser, T., et al. (2011). Targeting DC-SIGN via its neck region leads to prolonged antigen residence in early endosomes, delayed lysosomal degradation, and cross-presentation. *Blood* 118, 4111–4119. doi: 10.1182/blood-2011-04-346957

Tanaka, A., Fukuoka, Y., Morimoto, Y., Honjo, T., Koda, D., Goto, M., et al. (2015). Cancer cell death induced by the intracellular self-assembly of an enzyme-responsive supramolecular gelator. *J. Am. Chem. Soc.* 137, 770–775. doi: 10.1021/ja510156v

Tang, D., Kang, R., Coyne, C. B., Zeh, H. J., and Lotze, M. T. (2012). PAMPs and DAMPs: signal 0s that spur autophagy and immunity. *Immunol. Rev.* 249, 158–175. doi: 10.1111/j.1600-065X.2012.01146.x

Tao, W., Zhang, J., Zeng, X., Liu, D., Liu, G., Zhu, X., et al. (2015). Blended nanoparticle system based on miscible structurally similar polymers: a safe, simple, targeted, and surprisingly high efficiency vehicle for cancer therapy. *Adv. Healthc. Mater.* 4, 1203–1214. doi: 10.1002/adhm.201400751

Tarek, M. M., Shafei, A. E., Ali, M. A., and Mansour, M. M. (2018). Computational prediction of vaccine potential epitopes and 3-dimensional structure of XAGE-1b for non-small cell lung cancer immunotherapy. *Biomed. J.* 41, 118–128. doi: 10.1016/j.bj.2018.04.002

Tartour, E., Pere, H., Maillere, B., Terme, M., Merillon, N., Taieb, J., et al. (2011). Angiogenesis and immunity: a bidirectional link potentially relevant for the monitoring of antiangiogenic therapy and the development of novel therapeutic combination with immunotherapy. *Cancer Metastasis. Rev.* 30, 83–95. doi: 10.1007/s10555-011-9281-9284

Thambi, T., Deepagan, V. G., Yoon, H. Y., Han, H. S., Kim, S.-H., Son, S., et al. (2014). Hypoxia-responsive polymeric nanoparticles for tumor-targeted drug delivery. *Biomaterials* 35, 1735–1743. doi: 10.1016/j.biomaterials.2013.11.022

Thomann, J.-S., Heurtault, B., Weidner, S., Brayé, M., Beyrath, J., Fournel, S., et al. (2011). Antitumor activity of liposomal ErbB2/HER2 epitope peptide-based vaccine constructs incorporating TLR agonists and mannose receptor targeting. *Biomaterials* 32, 4574–4583. doi: 10.1016/j.biomaterials.2011.03.015

Thomas, S. N., Vokali, E., Lund, A. W., Hubbell, J. A., and Swartz, M. A. (2014). Targeting the tumor-draining lymph node with adjuvanted nanoparticles reshapes the anti-tumor immune response. *Biomaterials* 35, 814–824. doi: 10.1016/j.biomaterials.2013.10.003

Thompson, E. D., Enriquez, H. L., Fu, Y.-X., and Engelhard, V. H. (2010). Tumor masses support naive T cell infiltration, activation, and differentiation into effectors. *J. Exp. Med.* 207, 1791–1804. doi: 10.1084/jem.20092454

Thong, Q. X., Biabanikhankahdani, R., Ho, K. L., Alitheen, N. B., and Tan, W. S. (2019). Thermally-responsive virus-like particle for targeted delivery of cancer drug. *Sci. Rep.* 9:3945. doi: 10.1038/s41598-019-40388-x

Thorsson, V., Gibbs, D. L., Brown, S. D., Wolf, D., Bortone, D. S., Ou Yang, T.-H., et al. (2018). The immune landscape of cancer. *Immunity* 48, 812.e–830.e. doi: 10.1016/j.immuni.2018.03.023

Tian, H., and Li, W. (2017). Dendritic cell-derived exosomes for cancer immunotherapy: hope and challenges. *Ann. Transl. Med.* 5, 221–221. doi: 10.21037/atm.2017.02.23

Tian, L., and Bae, Y. H. (2012). Cancer nanomedicines targeting tumor extracellular pH. *Colloids Surf. B* 99, 116–126. doi: 10.1016/j.colsurfb.2011.10.039

Tiptiri-Kourpeti, A., Spyridopoulou, K., Pappa, A., and Chlichlia, K. (2016). DNA vaccines to attack cancer: Strategies for improving immunogenicity and efficacy. *Pharmacol. Ther.* 165, 32–49. doi: 10.1016/j.pharmthera.2016.05.004

Toole, B. P. (2004). Hyaluronan: from extracellular glue to pericellular cue. *Nat. Rev. Cancer* 4, 528–539. doi: 10.1038/nrc1391

Tovey, M. G., and Lallemand, C. (2010). Adjuvant activity of cytokines. *Methods Mol. Biol.* 626, 287–309. doi: 10.1007/978-1-60761-585-9_19

Toy, R., Peiris, P. M., Ghaghada, K. B., and Karathanasis, E. (2014). Shaping cancer nanomedicine: the effect of particle shape on the in vivojourney of nanoparticles. *Nanomedicine* 9, 121–134. doi: 10.2217/nnm.13.191

Tran, S., DeGiovanni, P.-J., Piel, B., and Rai, P. (2017). Cancer nanomedicine: a review of recent success in drug delivery. *Clin. Transl. Med.* 6:44. doi: 10.1186/s40169-017-0175-170

Tullett, K. M., Leal Rojas, I. M., Minoda, Y., Tan, P. S., Zhang, J.-G., Smith, C., et al. (2016). Targeting CLEC9A delivers antigen to human CD141+ DC for CD4+ and CD8+T cell recognition. *JCI Insight* 1:e87102. doi: 10.1172/jci.insight.87102

Uldry, E., Faes, S., Demartines, N., and Dormond, O. (2017). Fine-tuning tumor endothelial cells to selectively kill cancer. *IJMS* 18, 1401–1416. doi: 10.3390/ijms18071401

Vader, P., Mol, E. A., Pasterkamp, G., and Schiffelers, R. M. (2016). Extracellular vesicles for drug delivery. *Adv. Drug Deliv. Rev.* 106, 148–156. doi: 10.1016/j.addr.2016.02.006

Vallen, M. J. E., van der Steen, S. C. H. A., van Tilborg, A. A. G., Massuger, L. F. A. G., and van Kuppevelt, T. H. (2014). Sulfated sugars in the extracellular matrix orchestrate ovarian cancer development: "When sweet turns sour. *Gynecol. Oncol.* 135, 371–381. doi: 10.1016/j.ygyno.2014.08.023

van der Steen, S. C. H. A., Raavé, R., Langerak, S., van Houdt, L., van Duijnhoven, S. M. J., van Lith, S. A. M., et al. (2017). Targeting the extracellular matrix of ovarian cancer using functionalized, drug loaded lyophilisomes. *Eur. J. Pharm. Biopharm.* 113, 229–239. doi: 10.1016/j.ejpb.2016.12.010

van der Vlies, A. J., O'Neil, C. P., Hasegawa, U., Hammond, N., and Hubbell, J. A. (2010). Synthesis of Pyridyl disulfide-functionalized nanoparticles for conjugating thiol-containing small molecules. Peptides, and Proteins. *Bioconjugate Chem.* 21, 653–662. doi: 10.1021/bc9004443

van Niel, G., D'Angelo, G., and Raposo, G. (2018). Shedding light on the cell biology of extracellular vesicles. *Nat. Publ. Group* 19, 213–228. doi: 10.1038/nrm.2017.125

Van Tomme, S. R., Storm, G., and Hennink, W. E. (2008). In situ gelling hydrogels for pharmaceutical and biomedical applications. *Int. J. Pharm.* 355, 1–18. doi: 10.1016/j.ijpharm.2008.01.057

Vermaelen, K. (2019). Vaccine strategies to improve anti-cancer cellular immune responses. *Front. Immunol.* 10:8. doi: 10.3389/fimmu.2019.00008

Vigneron, N. (2015). Human tumor antigens and cancer immunotherapy. *BioMed. Res. Int.* 2015:948501. doi: 10.1155/2015/948501

von Bergwelt-Baildon, M. S., Vonderheide, R. H., Maecker, B., Hirano, N., Anderson, K. S., Butler, M. O., et al. (2002). Human primary and memory cytotoxic T lymphocyte responses are efficiently induced by means of CD40-activated B cells as antigen-presenting cells: potential for clinical application. *Blood* 99, 3319–3325. doi: 10.1182/blood.v99.9.3319.

Wang, C., Sun, W., Ye, Y., Bomba, H. N., and Gu, Z. (2017). Bioengineering of artificial antigen presenting cells and lymphoid organs. *Theranostics* 7, 3504–3516. doi: 10.7150/thno.19017

Wang, Y., Deng, W., Li, N., Neri, S., Sharma, A., Jiang, W., et al. (2018). Combining immunotherapy and radiotherapy for cancer treatment: current challenges and future directions. *Front. Pharmacol.* 9:185. doi: 10.3389/fphar.2018.00185

Wang, Y., Guo, R., Cao, X., Shen, M., and Shi, X. (2011). Encapsulation of 2-methoxyestradiol within multifunctional poly(amidoamine) dendrimers for targeted cancer therapy. *Biomaterials* 32, 3322–3329. doi: 10.1016/j.biomaterials.2010.12.060

Weissleder, R., and Pittet, M. J. (2008). Imaging in the era of molecular oncology. *Nature* 452, 580–589. doi: 10.1038/nature06917

Wen, Y., Waltman, A., Han, H., and Collier, J. H. (2016). Switching the immunogenicity of peptide assemblies using surface properties. *ACS Nano* 10, 9274–9286. doi: 10.1021/acsnano.6b03409

Wennhold, K., Shimabukuro-Vornhagen, A., and von Bergwelt-Baildon, M. (2019). B Cell-based cancer immunotherapy. *Transfus. Med. Hemother.* 46, 36–46. doi: 10.1159/000496166

Wilson, D. S., Hirosue, S., Raczy, M. M., Bonilla-Ramirez, L., Jeanbart, L., Wang, R., et al. (2019). Antigens reversibly conjugated to a polymeric glyco-adjuvant induce protective humoral and cellular immunity. *Nat. Mater.* 18, 175–185. doi: 10.1038/s41563-018-0256-255

Wolf, B. J., Choi, J. E., and Exley, M. A. (2018). Novel approaches to exploiting invariant NKT cells in cancer immunotherapy. *Front. Immunol.* 9:384. doi: 10.3389/fimmu.2018.00384

World Health Organization, (2018). *Cancer: Key Facts*. Available at: www.who.int/en/news-room/fact-sheets/detail/cancer (accessed 2019).

Wu, S., Liu, X., He, J., Wang, H., Luo, Y., Gong, W., et al. (2019). A dual targeting magnetic nanoparticle for human cancer detection. *Nanosc. Res. Lett.* 14:228. doi: 10.1186/s11671-019-3049-3040

Wu, W., Luo, L., Wang, Y., Wu, Q., Dai, H.-B., Li, J.-S., et al. (2018). Endogenous pH-responsive nanoparticles with programmable size changes for targeted tumor therapy and imaging applications. *Theranostics* 8, 3038–3058. doi: 10.7150/thno.23459

Wu, X., Giobbie-Hurder, A., Liao, X., Lawrence, D., McDermott, D., Zhou, J., et al. (2016). VEGF neutralization plus CTLA-4 blockade alters soluble and cellular factors associated with enhancing lymphocyte infiltration and humoral recognition in melanoma. *Cancer Immunol. Res.* 4, 858–868. doi: 10.1158/2326-6066.CIR-16-0084

Xia, W., and Low, P. S. (2010). Folate-targeted therapies for cancer. *J. Med. Chem.* 53, 6811–6824. doi: 10.1021/jm100509v

Xiang, S. D., Scholzen, A., Minigo, G., David, C., Apostolopoulos, V., Mottram, P. L., et al. (2006). Pathogen recognition and development of particulate vaccines: does size matter? *Methods* 40, 1–9. doi: 10.1016/j.ymeth.2006.05.016

Xu, Y., and Goldkorn, A. (2016). Telomere and telomerase therapeutics in cancer. *Genes* 7:22. doi: 10.3390/genes7060022

Yang, G., Wang, X., Fu, S., Tang, R., and Wang, J. (2017). pH-triggered chitosan nanogels via an ortho ester-based linkage for efficient chemotherapy. *Acta Biomaterialia* 60, 232–243. doi: 10.1016/j.actbio.2017.05.003

Yang, X., Kessler, E., Su, L.-J., Thorburn, A., Frankel, A. E., Li, Y., et al. (2013). Diphtheria toxin-epidermal growth factor fusion protein DAB389EGF for the treatment of bladder cancer. *Clin. Cancer Res.* 19, 148–157. doi: 10.1158/1078-0432.CCR-12-1258

Yao, Q., Kou, L., Tu, Y., and Zhu, L. (2018). MMP-responsive "Smart" drug delivery and tumor targeting. *Trends Pharmacol. Sci.* 39, 766–781. doi: 10.1016/j.tips.2018.06.003

Yau, T., Dan, X., Ng, C., and Ng, T. (2015). Lectins with potential for anti-cancer therapy. *Molecules* 20, 3791–3810. doi: 10.3390/molecules20033791

Ye, Y., Wang, C., Zhang, X., Hu, Q., Zhang, Y., Liu, Q., et al. (2017). A melanin-mediated cancer immunotherapy patch. *Sci. Immunol.* 2:eaan5692. doi: 10.1126/sciimmunol.aan5692

Yu, J. S., Liu, G., Ying, H., Yong, W. H., Black, K. L., and Wheeler, C. J. (2004). Vaccination with tumor lysate-pulsed dendritic cells elicits antigen-specific, cytotoxic T-cells in patients with malignant glioma. *Cancer Res.* 64, 4973–4979. doi: 10.1158/0008-5472.CAN-03-3505

Zahavi, D., AlDeghaither, D., O'Connell, A., and Weiner, L. M. (2018). Enhancing antibody-dependent cell-mediated cytotoxicity: a strategy for improving antibody-based immunotherapy. *Antibody Therapeutics* 1, 7–12. doi: 10.1093/abt/tby002

Zarogoulidis, P., Darwiche, K., Sakkas, A., Yarmus, L., Huang, H., Li, Q., et al. (2013). Suicide gene therapy for cancer - current strategies. *J. Genet. Syndr. Gene Ther.* 4:16849. doi: 10.4172/2157-7412.1000139

Zhang, J., Spring, H., and Schwab, M. (2001). Neuroblastoma tumor cell-binding peptides identified through random peptide phage display. *Cancer Lett.* 171, 153–164. doi: 10.1016/s0304-3835(01)00575-574

Zhang, L. F., Zhou, J., Chen, S., Cai, L. L., Bao, Q. Y., Zheng, F. Y., et al. (2000). HPV6b virus like particles are potent immunogens without adjuvant in man. *Vaccine* 18, 1051–1058. doi: 10.1016/s0264-410x(99)00351-355

Zhang, L., Wang, L., Shahzad, K. A., Xu, T., Wan, X., Pei, W., et al. (2017a). Paracrine release of IL-2 and anti-CTLA-4 enhances the ability of artificial polymer antigen-presenting cells to expand antigen-specific T cells and inhibit tumor growth in a mouse model. *Cancer Immunol. Immunother.* 66, 1229–1241. doi: 10.1007/s00262-017-2016-2019

Zhang, X., Li, X., You, Q., and Zhang, X. (2017b). Prodrug strategy for cancer cell-specific targeting: A recent overview. *Eur. J. Med. Chem.* 139, 542–563. doi: 10.1016/j.ejmech.2017.08.010

Zhou, S., Gravekamp, C., Bermudes, D., and Liu, K. (2018). Tumour-targeting bacteria engineered to fight cancer. *Nat. Rev. Cancer* 18, 727–743. doi: 10.1038/s41568-018-0070-z

Zhou, Y., Banday, A. H., Hruby, V. J., and Cai, M. (2019). Development of N-Acetylated dipalmitoyl-s-glyceryl cysteine analogs as efficient TLR2/TLR6 agonists. *Molecules* 24:3512. doi: 10.3390/molecules24193512

Zhou, Z.-H., Ji, C.-D., Xiao, H.-L., Zhao, H.-B., Cui, Y.-H., and Bian, X.-W. (2017). Reorganized collagen in the tumor microenvironment of gastric cancer and its association with prognosis. *J. Cancer* 8, 1466–1476. doi: 10.7150/jca.18466

Zirlik, K., and Duyster, J. (2018). Anti-angiogenics: current situation and future perspectives. *Oncol. Res. Treat.* 41, 166–171. doi: 10.1159/000488087

Zitvogel, L., and Palucka, K. (2011). Antibody co-targeting of DCs. *Blood* 118, 6726–6727. doi: 10.1182/blood-2011-10-384552

Zitvogel, L., Regnault, A., Lozier, A., Wolfers, J., Flament, C., Tenza, D., et al. (1998). Eradication of established murine tumors using a novel cell-free vaccine: dendritic cell-derived exosomes. *Nat. Med.* 4, 594–600.

Zom, G. G., Willems, M. M. J. H. P., Khan, S., van der Sluis, T. C., Kleinovink, J. W., Camps, M. G. M., et al. (2018). Novel TLR2-binding adjuvant induces enhanced T cell responses and tumor eradication. *J. Immunol. Ther. Cancer* 6:146. doi: 10.1186/s40425-018-0455-452

Zou, L., Wang, H., He, B., Zeng, L., Tan, T., Cao, H., et al. (2016). Current approaches of photothermal therapy in treating cancer metastasis with nanotherapeutics. *Theranostics* 6, 762–772. doi: 10.7150/thno.14988

Conflict of Interest: AT was employed by the company Agap2 Zürich, Switzerland.

The remaining authors declare that the research was conducted in the absence of any commercial or financial relationships that could be construed as a potential conflict of interest.

frontiers in Bioengineering and Biotechnology

REVIEW
published: 14 February 2020
doi: 10.3389/fbioe.2020.00089

Nanosized Delivery Systems for Therapeutic Proteins: Clinically Validated Technologies and Advanced Development Strategies

*Filippo Moncalvo, Maria Isabel Martinez Espinoza† and Francesco Cellesi**

Dipartimento di Chimica, Materiali e Ingegneria Chimica "G. Natta", Politecnico di Milano, Milan, Italy

The impact of protein therapeutics in healthcare is steadily increasing, due to advancements in the field of biotechnology and a deeper understanding of several pathologies. However, their safety and efficacy are often limited by instability, short half-life and immunogenicity. Nanodelivery systems are currently being investigated for overcoming these limitations and include covalent attachment of biocompatible polymers (PEG and other synthetic or naturally derived macromolecules) as well as protein nanoencapsulation in colloidal systems (liposomes and other lipid or polymeric nanocarriers). Such strategies have the potential to develop next-generation protein therapeutics. Herein, we review recent research progresses on these nanodelivery approaches, as well as future directions and challenges.

Keywords: therapeutic proteins, protein delivery, polymer conjugates, PEGylation, liposomes, nanocarriers

OPEN ACCESS

Edited by:
Maria Rosa Antognazza, Centro per la Scienza e la Tecnologia Nano, IIT, Italy

Reviewed by:
Zuben E. Sauna, United States Food and Drug Administration, United States
Loredana Latterini, University of Perugia, Italy

****Correspondence:***
Francesco Cellesi
francesco.cellesi@polimi.it

†ORCID:
Maria Isabel Martinez Espinoza
orcid.org/0000-0003-3823-1069

Specialty section:
This article was submitted to Nanobiotechnology, a section of the journal Frontiers in Bioengineering and Biotechnology

Received: *06 September 2019*
Accepted: *30 January 2020*
Published: *14 February 2020*

Citation:
Moncalvo F, Martinez Espinoza MI and Cellesi F (2020) Nanosized Delivery Systems for Therapeutic Proteins: Clinically Validated Technologies and Advanced Development Strategies. Front. Bioeng. Biotechnol. 8:89. doi: 10.3389/fbioe.2020.00089

INTRODUCTION

Over the last few years, several therapeutic proteins have been approved for clinical usage, and others are in the process of development (Leader et al., 2008; Walsh, 2018). Nowadays, approximately 40% of the 6,000 or more products wordwide currently in clinical development are biopharmaceuticals, in which the predominance of protein-based products is likely to remain an industry reality for the next years (Walsh, 2018).

From a therapeutic perspective, the success of therapeutic protein products is related to their increased specificity and high potency, longer duration of their effect due to the slower clearance from the body, and reduced intrinsic toxicity (Yin et al., 2015). These characteristics provide a clear advantage over low molecular weight drugs, which are generally associated with off-target effects and harmful metabolites. With the use of recombinant DNA technology, therapeutic proteins have been developed to treat a wide variety of disease, including cancers, autoimmunity/inflammation, exposure to infectious agents, and genetic disorders (Leader et al., 2008).

Despite these advantages, these products must overcome the typical drawbacks of short half-life, instability, and immunogenicity, and limited permeability through the biological barriers, due to their high molecular weight (Kintzing et al., 2016). Several strategies have been evaluated in order to improve these limitations and develop a next generation protein therapeutics (Kintzing et al., 2016; Lagassé et al., 2017).

Most efforts have been devoted to the modification of the protein structure, either by mutation or by covalent attachment of moieties, including Fc-fusion (Levin et al., 2015), albumin-fusion (Lagassé et al., 2017), synthetic polypeptide (XTEN) fusion (Schellenberger et al., 2009),

the conjugation of polymers such as poly(ethylene glycol) (PEG) or alternative non-degradable/biodegradable macromolecules. A change in drug formulation, introducing liposomes and other lipid-based or polymeric nanocarriers, has also been used to overcome the current limitations of protein therapeutics.

The intent of this review is to highlight the recent advances in developing nanosized delivery systems to improve safety and efficacy of protein therapeutics. This includes the areas of polymer conjugates (such as PEGylation and more recent technologies), liposomes, as well as alternative strategies based on protein nanoencapsulation in lipid-based and polymer-based nanocarriers. The advantages and limitations of systems that have reached the clinical stage are discussed, and advanced delivery strategies are also examined, aiming to provide useful insights for future development.

PROTEIN-POLYMER CONJUGATES

Protein-polymer conjugates are widely used as therapeutics, since these nanosystems display a unique combination of properties derived from both materials (i.e., the protein and the polymer), which can be individually tuned to obtain the desired effects (Pelegri-O'Day et al., 2014). Polymer conjugates that display enhanced pharmacokinetic properties along with improved stability and/or degradability will be presented hereafter.

PEGylation

Poly(ethylene glycol) (PEG) is a synthetic, hydrophilic and FDA-approved polymer, typically synthesized using a ring-opening polymerization of ethylene oxide to produce a broad range of polymers with targeted molecular weight, narrow molecular weight distribution, and desired terminal functional groups (Zalipsky, 1995). Due to its biocompatibility and protein-repellent properties, PEG is frequently used in many biomedical applications including bioconjugation and drug delivery (Veronese and Pasut, 2005; Cheng et al., 2007; Bruni et al., 2017). Bioconjugation with PEG, also known as PEGylation, is the formation of a covalent bond between therapeutic molecules and PEG in order to extend circulation half-life of therapeutics, thus reducing the frequency of dosing while maintaining the pharmaceutical effects (Grigoletto et al., 2016).

PEG is well-known as "stealth" molecule; due to its protein-repellent properties, it exhibits low opsonization, and this allows PEG conjugates to avoid phagocytosis and fast removal from the bloodstream (Owens and Peppas, 2006). Additionally, PEGylation also limits the interaction with enzymes, thus inhibiting the breakdown of the therapeutic (bio)molecules *in vivo* (Harris and Chess, 2003).

In case of small proteins or peptides, the right choice of PEG molecular weight may further prolong the circulation time of the biomolecules by enhancing their hydrodynamic radii, up to a size which prevents excretion through the kidney filtration barrier (Xue et al., 2013). Narrow molecular weight distributions (low dispersity) are generally favored for approval by the regulatory authorities, as they guarantee uniformity in the final physico-chemical properties of the product (Jevsevar et al., 2010). In some cases, polymer branching may also be useful in reducing the viscosity of the protein suspension to be injected, and mimicking the glycosylation patterns on native proteins (Pelegri-O'Day et al., 2014). Since the first PEGylated protein approved by the FDA in 1990, PEG bioconjugation has been extensively used for proteins modification, leading to several PEGylated-proteins approved for clinical use (**Table 1**).

Conjugation Strategies

PEG reagents are functionalised PEG-based polymers which allow stable bond formation with specific functional groups from the amino acid sequence of the protein. Different sites can be targeted for PEGylation (**Figure 1**). Many PEG functionalised with activated esters [succinimidyl succinate (PEG-SS), *N*-hydroxysuccinimide esters (PEG-NHS)] and carbonates (PEG p-nitrophenyl carbonate) target the ε-amino groups of lysines, due to their abundance on the protein surface. This conjugation is generally non-selective, and other groups (N-terminal amines, histidine, tyrosine) can also be modified to a minor degree (Turecek et al., 2016). Random conjugation of lysine units often leads to a complex mixture of proteins with different number and position of PEG chains, which may also interfere with the receptor/substrate binding (Zaghmi et al., 2019). Although homogenous products can be obtained with purification processes such as chromatography techniques (Pfister and Morbidelli, 2014), a site-specific PEGylation reaction is often preferred.

N-terminal PEGylation is a site-specific reaction based on pKa differences between the ε-amino group of lysine residues (9.3–10.5) and the N-terminal α-amino group of proteins (7.6 to 8) (Dozier and Distefano, 2015). At optimal pH values (generally comprised between 5.5 and 6.5) the N-terminal is unprotonated while lysine residues are predominantly protonated and unable to react (Lee et al., 2003; Gao et al., 2009; Chen et al., 2017). A reductive alkylation with aldehyde derivatives (PEG-aldehyde) proceeds through formation of a Shiff base, and the addition of a reducing agent stabilizes the linkage producing a secondary amine (Hamley, 2014).

Another functional group used for PEGylation is the thiol of cysteine residues. In this case, PEG functionalised with electron-poor olefins (mainly maleimide, but also acrylate, vinyl sulfone) are frequently used to form a thioether bond by Michael-type addition. In order to avoid non-selective coupling with amines, the reaction pH should be carried out at range of 6.5–7.5, values below lysine residues pKa (Dozier and Distefano, 2015; Ravasco et al., 2019). A method related to labeling a disulfide bond between two cysteines was also proposed. The disulfide can be reduced under mild conditions and both the resulting free cysteines react with a bridging PEG-based reagent (Balan et al., 2007; Badescu et al., 2014). Covalent re-bridging of the disulfide bond has the advantage of leaving the protein structurally intact after conjugation.

O-glycosylation is a post-translational modification which occurs when a saccharide is covalently bound to a protein through a hydroxyl group of a serine or threonine. *O*-glycosylated proteins can be conjugated to sialic acid-functionalised PEG by sialyltransferase (DeFrees et al., 2006;

TABLE 1 | List of approved PEGylated proteins of therapeutic use.

Generic name	Brand name	PEGylated protein	PEGylation	Therapeutic indication	Year	References
(A) Proteins with non-specific PEGylation.						
Pegadamase	Adagen®	Bovine adenosine deaminase	Random amine PEGylation multiple linear 5 kDa PEG	Severe combined immunodeficiency disease	1990	Levy et al., 1988
Pegaspargase	Oncaspar®	L-asparaginase	Random amine PEGylation multiple linear 5 kDa PEG	Acute lymphoblastic leukemia	1994	Graham, 2003
Peginterferon-α2b	PegIntron®	IFN-α2b	Random amine PEGylation linear 12 kDa PEG	Hepatitis C	2000	Wang et al., 2002
Peginterferon-α2a	Pegasys®	IFN-α2a	Random amine PEGylation branched 40 kDa PEG	Hepatitis C	2001	Foser et al., 2003
Pegvisomant	Somavert®	Genetically engineered hGH	Random amine PEGylation multiple linear 5 kDa PEG	Acromegaly	2002	Pradhananga et al., 2002
CERA	Mircera®	Epoetin-β	Random amine PEGylation linear 30 kDa PEG	Anemia associated with kidney disease	2007	Macdougall and Eckardt, 2006
Pegloticase	Krystexxa®	Uricase	Random amine PEGylation 10 kDa PEG	Chronic gout	2010	Schlesinger et al., 2010
Peginterferon-α2b	Sylatron	INF-α2b	Random PEGylation at different site with linear 12 kDa PEG	Melanoma	2011	Patel and Walko, 2012
Rurioctocog alfa pegol	Adynovi®/Adynovate®	Coagulation factor VIII	Random amine PEGylation branched 20 kDa PEG	Hemophilia A	2015	Dunn et al., 2018
Pegvaliase	Palynziq®	Phenylalanine ammonia lyase	Random amine PEGylation 20 kDa PEG	Phenylketonuria	2018	Levy et al., 2018
(B) Site-directed PEGylated products.						
Pegfilgrastim	Neulasta®	G-CSF	N-terminal PEGylation linear 20kDa PEG	Neutropenia during chemotherapy	2002	Piedmonte and Treuheit, 2008
Certolizumab Pegol	Cimzia®	Fab' antibody fragment	Site specific thiol PEGylation branched 40 kDa PEG	Rheumatoid arthritis and Crohn's disease	2008	Blick and Curran, 2007
Lipegfilgrastim	Lonquez®	G-CSF	Site specific single 20-kDa via carbohydrate linker	Neutropenia	2013	Mahlert et al., 2013
Peginterferon-β1a	Plegridy®	INF-β1a	N-terminal PEGylation Linear 20 kDa PEG	Multiple sclerosis	2014	Chaplin and Gnanapavan, 2015
Nonacog beta pegol	Refixia®	Coagulation factor IX	A 40 kDa PEG attached to the FIX activation peptide by site-directed glycoPEGylation	Hemophilia B	2017	Ezban et al., 2019
Damoctocog alfa pegol	Jivi®	Coagulation factor VIII	Site specific 60 kDa branched PEG (two 30 kDa chains)	Hemophilia A	2018	Paik and Deeks, 2019
Turoctocog alfa pegol	Esperoct®	Coagulation factor VIII	40 kDa PEG bound by a unique O-linked glycan on the residual 21 amino acid B-domain region	Hemophilia A	2019	Novo-Nordisk, 2019

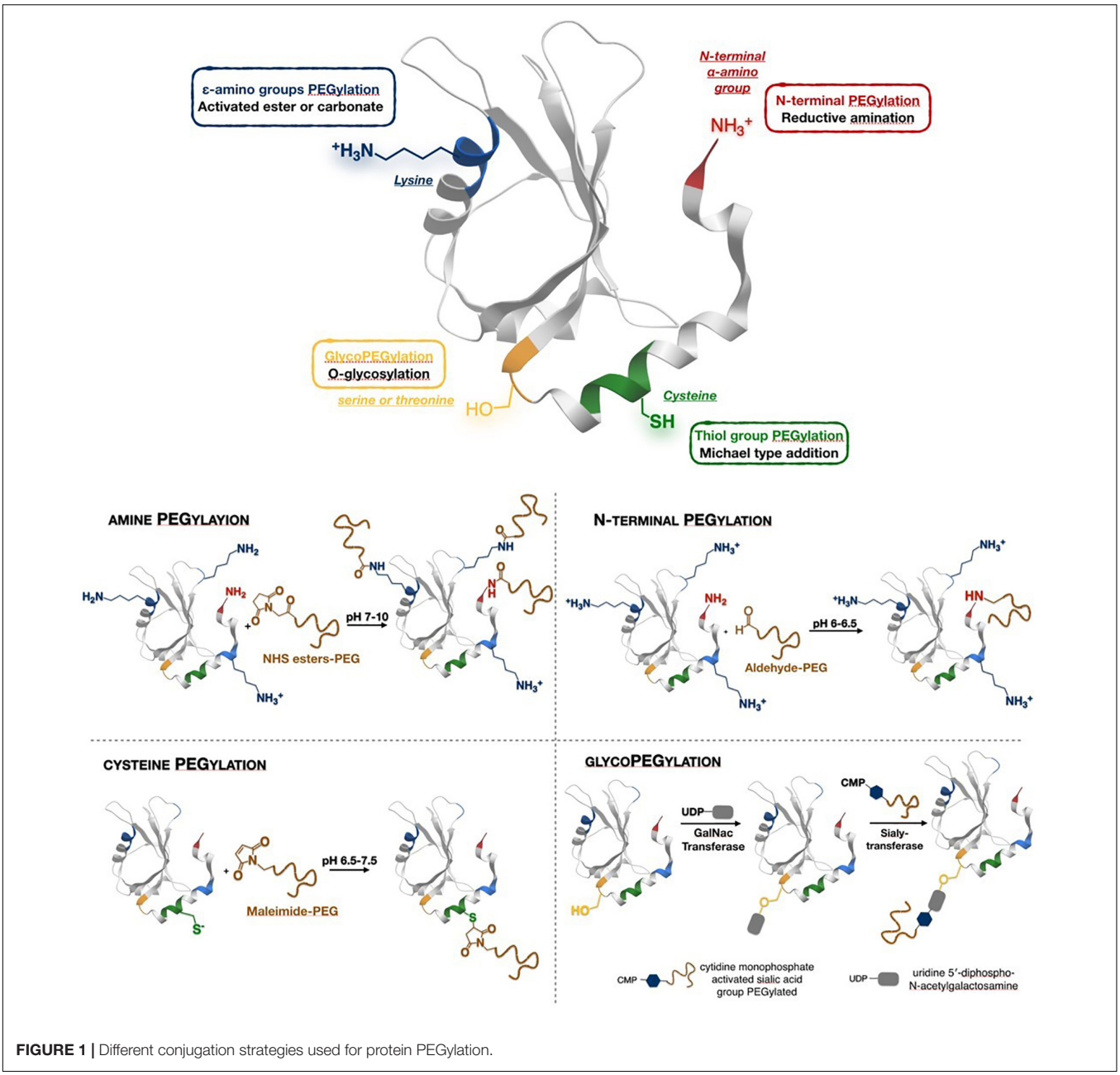

FIGURE 1 | Different conjugation strategies used for protein PEGylation.

Dozier and Distefano, 2015). This site-selective modification is therefore obtained at the position that is normally modified with a glycan *in vivo*, and therefore the effect of PEGylation on protein activity is minimized.

PEGylated Proteins in the Clinic

PEGylated-proteins which have been approved for clinical use or reached the clinical stage are summarized in **Table 1**. They can be classified as non-specific or site-specific PEGylated proteins.

Non-specific PEGylated Proteins

The first PEGylated pharmaceuticals **Adagen**® (pegademase) and **Oncaspar**® (pegaspargase) are actually complex mixtures of various PEGylated species for the treatment of severe combined immunodeficiency, and adequate asparagine depletion in leukemia patients, respectively (Levy et al., 1988; Graham, 2003). In Adagen, the adenosine deaminase was modified with 11–17 molecules of 5 kDa PEG-SS. In Oncaspar, L-asparaginase is covalently conjugated to 69–82 molecules of 5 kDa PEG-SS.

PegIntron® is a product based on linear 12-kDa succinimidyl carbonate PEG chains is covalently linked to different sites of Interferon-α 2b (IFN-α2b), via an unstable urethane bond that slowly releases the free protein (Wang et al., 2002; Youngster et al., 2002). In **Pegasys**®, a branched 40 kDa PEG-NHS yielded a stable amide bond mainly to four lysine residues of IFN-α2a (Foser et al., 2003).

Somavert® (pegvisomant), was approved in 2003 for the treatment of acromegaly (Pradhananga et al., 2002; Parkinson et al., 2003) and it is obtained by nonspecific conjugation of an analog of human growth hormone (hGH) with 4–6 equivalents of PEG-NHS (5kDa). It guarantees an elevated stability to esterase hydrolysis and a half-life approximately 70 h higher than the native protein.

Mircera® is an FDA approved (2007) PEGylated erythropoietin with an extended half-life (Macdougall and Eckardt, 2006; Banerjee et al., 2012). It is a mono-PEGylation of a 30-kDa succinimidyl PEG, predominately at lysine or at the N terminus of the protein.

Krystexxa® is a hyper-PEGylated product derived by non-human uricase and used to treat gout (Schlesinger et al., 2010; Shannon and Cole, 2012). The conjugation is obtained from PEG *p*-Nitrophenyl carbonate ester, and is necessary to reduce immunogenicity of the non-human enzyme and increase its half-life (Sherman et al., 2008).

Sylatron® (peginterferon alfa-2b) was FDA approved in 2011 as adjuvant treatment of melanoma (Herndon et al., 2012; Patel and Walko, 2012) and it is a IFN-α2b conjugate with 12 kDa succinimidyl carbonate PEG (31 kDa).

Adynovate® is a PEGylated recombinant factor VIII (rFVIII) approved for hemophilia A and characterized by the prolonged circulatory half-life (Dunn et al., 2018). PEGylation is obtained from lysine residues and optimized to occur in the B-domain which is not required for activity of the protein, thus resulting in an improved pharmacokinetic profile (Konkle et al., 2015).

Palynziq® (Pegvaliase) is a phenylalanine ammonia-lyase (rAvPAL) conjugated with linear 20 kDa PEG-NHS. It was recently used in the clinic to treat phenylketonuria, a genetic disorder caused by a lack of phenylalanine hydroxylase causing neurotoxic phenylalanine accumulation (Levy et al., 2018).

PEGylation diminishes immunogenicity and improves pharmacodynamic stability (Longo et al., 2014).

ADI-PEG 20 is a arginine deiminase (rhArg) conjugate with 10–12 chains of 20 kDa SS-PEG, which has been used against glioblastoma tumor (GBM). Preliminary tests showed that ADI-PEG20 efficiently depleted blood arginine and significantly reduces the growth of GBM in mice, with the advantage that this approach does not require overcoming the blood brain barrier. Although ADI-PEG20 is still under development and not in the market, it is in phase III clinical trials for the treatment of hepatocellular carcinoma, and in phase II studies for acute myeloid leukemia/non-Hodgkin's lymphoma and for the treatment of metastatic melanoma and some other tumors (Cheng et al., 2007; Tsai et al., 2017).

Site-Specific PEGylated Proteins

Filgrastim is an unglycosylated recombinant methionyl human granulocyte colony-stimulating factor (G-CSF), which regulates the production and release of functional neutrophils from the bone marrow.

Two similar products (**Lonquez**® and **Neulasta**®) have been recently approved against neutropenia (Piedmonte and Treuheit, 2008; Mahlert et al., 2013). In Lonquez (lipegfilgrastim), the selective addition of PEG in guaranteed through *O*-glycosylation (Mahlert et al., 2013). In Neulasta (pegfilgrastim), methoxy-PEG-propionaldehyde (PEG-aldehyde) is used to obtain selective bioconjugation at the N-terminus via reductive alkylation (Kinstler et al., 2002; Molineux, 2004).

Cimzia® (certolizumab pegol) is a PEGylated anti tumor necrosis factor (TNF) recombinant antibody Fab fragment approved for the treatment of rheumatoid arthritis, Crohn's disease, and axial spondyloarthritis (Blick and Curran, 2007; Nesbitt et al., 2009). The antibody fragment is covalently bound through Michael type addition of PEG2MAL40K moiety which comprises two 20 kDA PEG chains linked to a maleimide group (Chapman et al., 1999). The reactive cysteine is located at three amino acids from the C-terminus of the heavy chain antibody fragment. Due to this site-specific PEG attachment, Cimzia® maintains full binding activity, elevated circulation time and low immunogenicity (Jevševar et al., 2012).

Plegridy® is a PEGylated form of IFN β-1a, approved for the treatment of relapsing multiple sclerosis (Chaplin and Gnanapavan, 2015). Glycosylated recombinant IFN β-1a is conjugated with a single linear 20 kDa methoxy PEG-*O*-2-methyl propionaldehyde (44 kDa) moiety at the N-terminus via reductive amination (Baker et al., 2006).

Refixia® (nonacog beta pegol), a PEGylated factor IX (rFIX), is used against hemophilia B. The protein is modified by a selective glycoPEGylation (DeFrees et al., 2006; Ezban et al., 2019). Release of the activation peptide by physiologic activators converted the PEGylated recombinant factor IX to recombinant native factor IX and proceeded normal kinetics for factor IX (Østergaard et al., 2011).

Jivi® (Damoctocog alfa pegol) and **Esperoct**® (Turoctocog alfa pegol) are site-specific PEGylated (rFVIII) approved for the treatment of hemophilia A (2019; Paik and Deeks, 2019). In Jivi, a single dual-branched 60 kDa PEG molecule is attached to an engineered cysteine residue on the A3 domain of the protein (Castaman and Linari, 2018). The A3 domain was selected to provide a consistent coagulation activity as well as high PEGylation efficiency (Shah et al., 2014). Esperoct is being developed for prophylaxis and treatment of bleeds in hemophilia A patients (Meunier et al., 2017). It is an another B-domain truncated FVIII with a 40 kDa PEG bound by a unique O-linked glycan on the residual 21 amino acid B-domain region (Tiede, 2015; Wynn and Gumuscu, 2016).

Limits of PEGylation

Despite the widespread clinical use of PEGylated proteins, some important limitations have emerged for clinical applications, which are mainly related to PEG immunogenicity hypersensitivity and non-degradability (Knop et al., 2010; Garay et al., 2012). Here, we critically review the drawbacks associated with pre-existing and induced anti-PEG antibodies, the activation of the complement system and PEG-related cellular vacuolation.

PEG Immunogenicity

PEG is generally considered a "stealth" polymer in drug delivery because of its protein-repellent properties, which make conjugated proteins and nanoparticles mostly inert to the

biological environment (Yang and Lai, 2015). Steric repulsion and water barrier models are used to explain these characteristics (Zheng et al., 2005). Steric repulsion is mainly attributed to conformational entropy loss due to chain compression as the protein approaches a long PEG chain (McPherson et al., 1998), while water barrier mechanism arises from the large number of water molecules tightly bound (through hydrogen bonds) to the ethylene glycol repeating units, which generate repulsive forces against protein adsorption (Zheng et al., 2004). In these models, chain length, conformation and grafting density are important factors for limiting protein binding (Yang and Lai, 2015). These protein-repellent features should suppress interactions between PEGylated systems and the biological environment, thus PEG conjugation is used to decrease enzymatic degradation, opsonization, and immunogenicity of the protein conjugates.

In contrast to this general assumption, animal studies clearly showed that some PEGylated proteins, particularly ovalbumin and uricase, can elicit antibody formation against PEG (Garay et al., 2012).

In humans, pre-existing and induced antibodies against PEG (anti-PEG) cause an unexpected immunogenic response, also known as the "accelerated blood clearance (ABC) phenomenon (Cheng et al., 1999; Armstrong et al., 2007; Schellekens et al., 2013; Lipsky et al., 2014; Mima et al., 2015). The presence of anti-PEG was correlated with the fast clearance of PEG-asparaginase in patients with acute lymphoblastic leukemia (Armstrong et al., 2007). In a clinical study on the effects of PEG uricase on chronic refractory gout, 40% of patients developed anti-PEG, which was strongly correlated with loss of responsiveness to this protein conjugate (Lipsky et al., 2014).

In a recent study, pre-existing anti-PEG was identified in over 25% of healthy blood donors (Armstrong, 2009), in contrasts with only 0.2% occurrence reported over 20 years ago by Richter and Åkerblom (1984). This increase may be explained as a result of the large amount of PEG that is present nowadays in cosmetics, pharmaceuticals and processed foods. The continuous exposure to these products may induce anti-PEG antibodies in humans (Garay et al., 2012), although the constant analytical improvements of antibody detection over the years may also explain some discrepancies among different tests.

Different studies have shown that pre-existing and induced anti-PEG may bind to the PEG backbone (Richter and Åkerblom, 1984; Armstrong, 2009). However, since PEGylated therapeutic proteins generally contain methoxy-terminated PEG (mPEG), it has been hypothesized that antibodies with high affinity for methoxy groups may also be involved (Garay et al., 2012). Using hydroxy-PEG (HO-PEG) instead of mPEG in preparing conjugates of albumin, human interferon-α, and porcine uricase, a reduced immunogenicity was found in rabbits (Sherman et al., 2012). On the other hand, *in vitro* studies demonstrated that OH-PEG is a stronger complement activator than mPEG, since the hydroxyl group is able to covalently bind to the complement component C3 (Reddy et al., 2007). PEG-induced complement activation requires further investigation. Anti-PEG binding can trigger opsonization of complement factors, which subsequently promote phagocytosis by the mononuclear phagocyte system (Verhoef et al., 2014). Moreover, other studies on PEGylated therapeutics reported non-antibody-mediated complement activation, either by the mannose-binding lectin pathway or the alternative pathway (Verhoef et al., 2014).

Further studies are therefore required to determine the specificity of anti-PEGs, how these antibodies can influence the pharmacokinetics of PEGylated proteins, and how the complement activation by the polymer may cause severe hypersensitivity reactions.

Safety of PEGylation

The molecular weight of the conjugated PEG is typically selected to avoid renal clearance, and therefore to obtain an elevated half-life of the therapeutic proteins (Verhoef et al., 2014). However, the non-degradability of PEG in systemic circulation may lead to polymer accumulation *in vivo*. After repeated administration of some approved PEGylated biopharmaceuticals, cellular vacuolation were histologically observed in certain organs and tissues (Ivens et al., 2015). Vacuolation is considered a normal physiological process by which various cell types attempt to remove foreign materials (Stidl et al., 2018). In mammalian cells, vacuoles are formed in different cellular compartments (e.g., endosomes, lysosomes, endothelial reticulum), and this phenomenon can be transient or irreversible (Stidl et al., 2018).

PEG-associated vacuolization in macrophages, predominantly within the reticuloendothelial system, is well documented with no detectable toxicological relevance (Kronenberg et al., 2013). However, several preclinical toxicology studies on approved PEGylated therapeutics provided evidence of vacuolation in renal tubule cells and epithelial cells of the choroid plexus (Stidl et al., 2016; Stidl et al., 2018). In one study, high doses of tumor necrosis factor binding protein (TNF-bp) conjugated with a 20 kDa PEG caused vacuolation of renal cortical tubular epithelium cells in rats, over a period of 3 months (Bendele et al., 1998). Tubular vacuolation caused distortion of tubular profiles and compression of nuclei, without leading to necrosis (Bendele et al., 1998; Stidl et al., 2016). Renal tubular cell vacuoles and splenic vacuolated macrophages were also reported for hemoglobin (Hb) conjugated to a 5 kDa PEG administered in rats (Conover et al., 1996). A serious concern is the vacuolation in the epithelial cells of the choroid plexus, which is the main source of cerebrospinal fluid and a key component of the blood-cerebrospinal fluid barrier (Stidl et al., 2018). Recently, a correlation between the molecular weight of unconjugated linear PEG (from 10 to 40 kDa) and vacuolation in rats was reported after repeated injections for 3 months (Rudmann et al., 2013). It was observed that the highest molecular weight PEG (40 kDa) triggered vacuolation in macrophages, choroid plexus epithelial cells and renal tubular epithelial cells. Immune-historeactivity to PEG decreased in renal tubule cells, but increased in splenic macrophages and choroid plexus epithelial cells (Rudmann et al., 2013).

Due to the diversity of marketed PEGylated proteins and new conjugates under development, nonclinical toxicology studies are therefore important to determine tissue location, reversibility, and severity of vacuolation with its possible functional consequences, in order to evaluate potential patient safety risks (Ivens et al., 2015).

Non-degradable PEG Alternatives

Although PEGylated proteins are the only protein-polymer conjugates approved for clinical use, many other biocompatible polymers have been recently investigated as an alternative to PEG, which showed promising results *in vitro* and *in vivo*.

Poly(vinyl pyrrolidone) (PVP) and **Poly(N-(2-hydroxypropyl) methacrylamide) (PHPMA)** are non-biodegradable, nonionic and non-immunogenic polymers, well-established as biocompatible drug carriers. They have been recently synthesized via Reversible Addition Fragmentation Chain Transfer (RAFT) to obtain narrow molecular weight distributions, which are ideal for bioconjugation (Scales et al., 2005; Zelikin et al., 2007). PVP- conjugated TNF-α provided longer circulation than PEG-TNF-α at the same molecular weight (Kaneda et al., 2004). HPMA copolymer–insulin and HPMA copolymer–chymotrypsin conjugates were also investigated (Kopecek and Kopecková, 2010).

Polyglycerol (PG) showed similar characteristics to PEG in terms of non-degradability, protein repellence, and superior biocompatibility and toxicity profile (Kainthan and Brooks, 2007; Imran ul-haq et al., 2012). Linear and hyperbranched PG were conjugated to model proteins (bovine serum albumin (BSA) and lysozyme) to assess their effect on conjugate activity (Wurm et al., 2012).

Polyoxazolines (POZs) are biocompatible polymers with 'stealth' properties and easy renal clearance (Zalipsky et al., 1996; Gaertner et al., 2007). Bioconjugation between poly(2-ethyl-2-oxazoline) and G-CSF, a hemopoietic cytokine, through reductive amination or enzyme-mediated acyl transfer, resulted in bioactive conjugates *in vivo* (Mero et al., 2012). POZs with methyl, ethyl and propyl side chains were synthesized by living cationic polymerisation and conjugated to BSA and insulin (Viegas et al., 2011) obtaining low immunogenicity and longer blood glucose control than native insulin in rats.

Poly(*N*-acryloylmorpholine) (PNAM) is a biocompatible water-soluble acrylamide derivative which can be synthesized via RAFT polymerisation and modified for attachment to enzymes in order to reduce immunogenicity. Monovalent lysozyme-PNAM conjugates with relatively low molar mass polymers displayed equal or even higher activity than the native protein, while all conjugates showed an improved protein solubility (Morgenstern et al., 2018).

Degradable PEG Alternatives

Polysialic acid (PSA), also known as columinic acid, is a linear small polysaccharide containing α-2,8-linked sialic acid (neurominic acid) with (n = 8 to >100) residues. PSA-conjugated L-asparaginase, obtained by reductive amination, reduced the antigenicity of asparaginase and prolongs the circulation half-life in mice (Fernandes and Gregoriadis, 2001). PSA conjugated to insulin on the N-terminus and lysine residues improved pharmacological properties and provided a more accurate long-term control of blood glucose levels (Jain et al., 2003).

Trehalose glycopolymers enhance *in vivo* plasma half-life and enhance stability on storage. Insulin-trehalose glycopolymer conjugate showed similar insulin-PEG prolonged plasma circulation in mice and low toxic effects (Liu et al., 2017; Mansfield and Maynard, 2018).

Biodegradable polysaccharides, such as **alginate** (Mondal et al., 2006) and **hyaluronic acid (HA)** (Mero and Campisi, 2014), have been explored for protein conjugation. As for SS-PEG, random lysines conjugation showed critical purification, reproducibility drawbacks, and lost in activity (Ferguson et al., 2010). The partial periodate oxidation of some saccharide repeating units generates aldehyde groups which allows selective N-terminal reductive amination. This approach was used to selectively modify insulin, hGH and INFα (Yang et al., 2011, 2012). A site selective conjugation of insulin and IFNα was also obtained by introducing an aldehyde group in the polymer backbone without altering the HA integrity (Mero and Campisi, 2014). In diabetic rats, HA-insulin conjugates maintained a glucose lowering effect up to 6 h, while free insulin was inactive after 1 h. Unexpectedly, when an elevated amount of insulin was conjugated, its effect on blood glucose level decreased, probably because of a steric entanglement affecting the receptor/protein recognition (Mero and Campisi, 2014).

Hydroxyethyl starch (HES) is a biodegradable FDA approved polymer, whose non-immunogenicity is possibly attributed to structural similarities with glycogen (Paleos et al., 2017). HES is degraded by α-amylase in the plasma, which can be controlled by modifying the molar mass and the degree of hydroxyethylation. Its conjugates have been extensively investigated for therapeutic uses (Ko and Maynard, 2018). The HESylation of erythropoietin (EPO) had comparable *in vitro* and *in vivo* activities to PEGylated-EPO (Mircera) (Hey et al., 2012; Pelegri-O'Day et al., 2014). The conjugation of HES to G-CSF and INF-α have also shown comparable results (Hey et al., 2012). Furthermore HESylation® sharply improved the storage stability over PEGylation by remaining totally amorphous during lyophilisation, with and without lyoprotectants (Liebner et al., 2015).

Protein conjugation with biodegradable **poly(ethyl ethylene phosphate) (PEEP)** was also reported (Steinbach et al., 2017). PPEylated BSA and catalase showed comparable activity to their PEG-equivalent.

Recombinant synthetic polypeptides, are biomimetic polymers with tunable degradability, versatile side chain functionalities, and self-assembly behaviors. They can be conjugated with proteins either by chemical coupling or by genetic engineering approach. The hGH fused with the synthetic polypeptide XTEN™ (Schellenberger et al., 2009) (hGH-XTEN) is undergoing a Phase II clinical trial as monthly administration for the treatment of hGH deficiency. Elastin-like polypeptide (ELP) fused with IFN-α was able to prolong the circulating half-life of the protein (Hu et al., 2015). A randomized sequence of proline, alanine and serine (PAS) guaranteed properties remarkably similar to PEG when they were fused to therapeutic proteins, including GF, hGH, Leptin (Schlapschy et al., 2013; Gebauer and Skerra, 2018). PASylated-hGH exhibited 94-fold longer plasma half-life in mice than the native protein (Gebauer and Skerra, 2018), and it led to a 2.8-fold higher IGF-1 plasma concentration compared with the mice treated with hGH

(Schlapschy et al., 2013). Kidney, liver, and spleen showed no histological changes after the treatment, and repeated dose administration confirmed the absence of immune reactivity toward the PAS moiety (Schlapschy et al., 2013). Artificial gelatin-like peptidic sequence (GLK) was fused to granulocyte-colony-stimulating factor (G-CSF) in order to generate a chimeric GLK/G-CSF fusion protein with enhanced plasma half-life (Huang et al., 2010). The polypeptoid Polysarcosine (PSar) has been recently considered an emerging "stealth" biodegradable polymer for many biomedical applications (Chan et al., 2018). A N-terminal specific polysarcosine-interferon conjugate (PSar-IFN) showed significantly more potency in inhibiting tumor growth, and elicited considerably less anti-IFN antibodies in mouse than its PEGylated counterpart (Hu et al., 2018).

Grafting Methods

In all the materials discussed above, end-functionalised polymers are firstly synthesized and then attached to the protein via a conjugation reaction. This strategy is generally called 'grafting to,' and it is generally characterized by low conversion, due to the steric hindrance and the low concentration of the reactive groups (Francis et al., 1998). An excess of reactive polymer is generally needed, therefore an efficient purification step to remove the unbound polymer is required (Wallat et al., 2014). Recently, an alternative 'grafting from' approach has been proposed to overcome these drawbacks. This method consists of initiating the polymerization directly from the surface of proteins, obtaining finely controlled products (Magnusson et al., 2010) (**Figure 2**). A low molecular weight initiator is firstly attached to the protein via bioconjugation. Due to the small size of this molecule, the steric hindrance that occurred between two 'giant' macromolecules during the "grafting to" method is avoided, and an excellent yield of protein-polymer conjugates can be obtained (Salmaso and Caliceti, 2011). The purification process of high molecular weight conjugates from the unreacted small molecular monomers and catalyst is easier and faster (Pelegri-O'Day and Maynard, 2016; Kovaliov et al., 2018).

Controlled-living polymerisation techniques such as Atom transfer radical polymerization (ATRP) and RAFT have been recently explored for site-specific polymer growth in aqueous solvent, ambient temperature, and physiological pH, i.e., conditions that are well tolerated by biomolecules (Averick et al., 2011). The main drawbacks are related to the challenges in controlling the polymerisation process under bio-relevant conditions. Activator Generated by Electron Transfer (AGET) ATRP has been recently developed to synthesize polymer-protein conjugates through polymerization of PEG methacrylate (PEGMA) macromonomers, from initiator-functionalized recombinant hGH (Magnusson et al., 2010) and trypsin (Yaşayan et al., 2011). Activator ReGenerated by Electron Transfer (ARGET) ATRP in aqueous media, has shown promising results for conjugation of therapeutic proteins (Simakova et al., 2012) achieving narrow molecular weight distributions (Mw/Mn < 1.3).

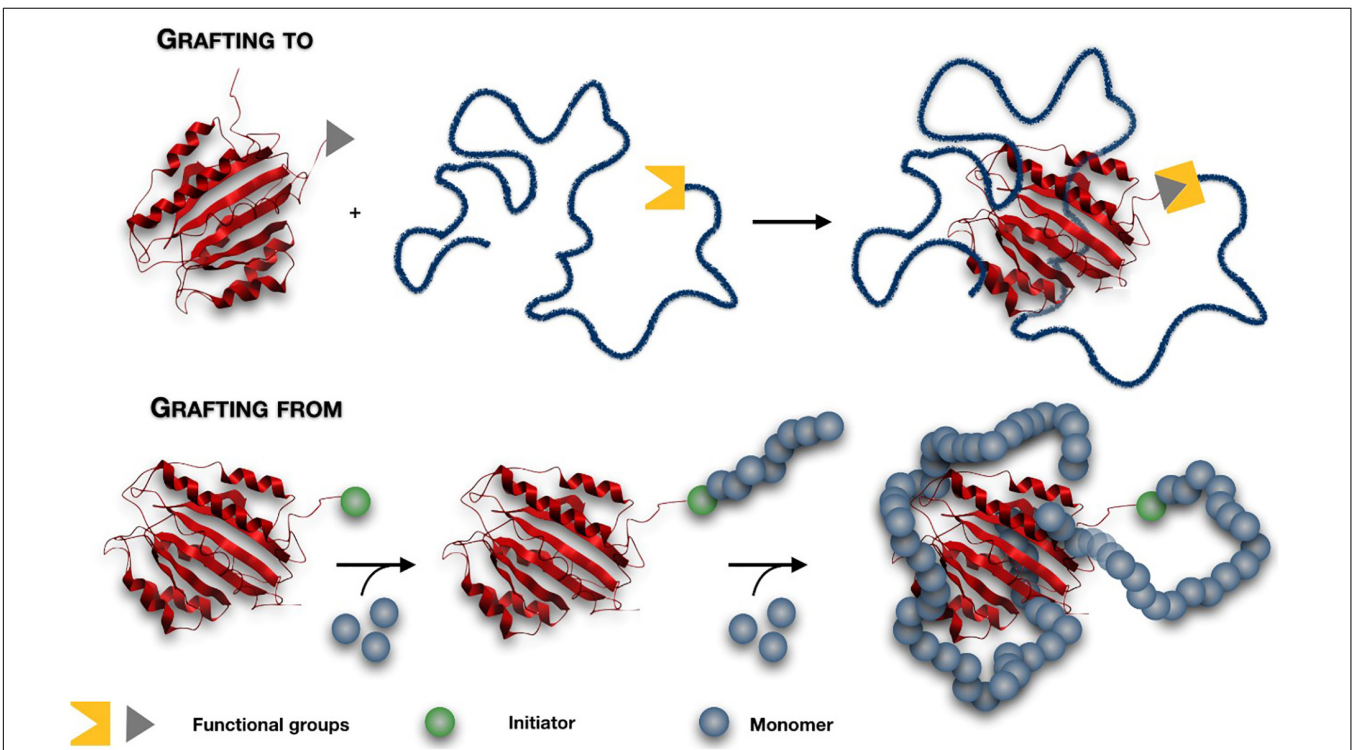

FIGURE 2 | The 'grafting to' and 'grafting from' conjugation strategies. In a 'grafting to' method, end-functionalised polymers are firstly synthesized and then attached to the protein via a conjugation reaction. In a 'grafting from' method, a low molecular weight initiator is firstly attached to the protein and then the polymerization is initiated directly from the protein.

A PEG-based polymer grafted from the C-terminus of INFα, obtained by ATRP of poly(oligo(ethylene glycol) methyl ether methacrylate) (POEGMA), was used to treat a murine cancer model. The POEGMA-INFα conjugate completely inhibited and eradicated tumors of 75% mice without appreciable systemic toxicity, whereas at the same dose, no mice treated with the PEGASYS® survived for over 58 days (Hu et al., 2016).

TL lipase was modified with ATRP initiators either at the amine side chain of lysine or acid residues of aspartic and glutamic amino acids, and *N*-[3-(*N,N*-dimethylamino)propyl] acrylamide (DMAPA) was grafted-from by Continuous Activator Regeneration (ICAR) ATRP (Kovaliov et al., 2018). The activity was higher for both conjugates compare to native protein.

Alternatively, photoinduced electron transfer reversible addition-fragmentation chain transfer (PET-RAFT) polymerisation of DMAPA was successfully used on TL lipase without affecting its activity (Kovaliov et al., 2018). RAFT polymerisation allowed to obtain well-defined poly(*N*-isopropylacrylamide) linked with BSA (Li et al., 2011a) and lysozyme–poly(*N*-isopropylacrylamide)-*b*-poly(*N,N*-dimethylacrylamide) block copolymer conjugates (Li et al., 2011b).

LIPOSOMES

Liposomes are phospholipid vesicles which consist of at least one lipid bilayer enclosing a discrete aqueous domain. While hydrophobic compounds can be inserted into the lipid membrane, hydrophilic molecules can be entrapped in the aqueous core, and this characteristic enables low and high molecular weight biomolecules to be encapsulated and later released at the targeted site (Sercombe et al., 2015; Huang et al., 2017). Liposomes represent the first nanosized drug delivery system which made the transition from bench to clinical application, and provide ideal characteristics of biocompatibility, biodegradability, variable compositions (Allen and Cullis, 2013; Sercombe et al., 2015). Among their advantages, liposomal formulations can be administered through several different routes such as parenteral (the most studied), oral (He et al., 2019), pulmonary (Khanna et al., 1997b), nasal (Luo et al., 2018), ocular (Agarwal et al., 2016), and topical (Yarosh et al., 2001).

Liposome surfaces can be easily functionalised with an appropriate ligand for targeted delivery and also decorated with protein-repellent polymers, such as PEG, to inhibit opsonization and clearance by the mononuclear phagocytic system (Immordino et al., 2006; Hwang et al., 2012; Pattni et al., 2015). Due to the fast development of nanomedicine, several protein delivery formulations based on liposomes have been developed for therapeutic use. Once entrapped in liposomes, a therapeutic protein may increase its stability, as the lipid bilayer provides protection from degradation (**Figure 3**) (Tan et al., 2010). Liposomes can be PEGylated to prolong circulation *in vivo*, and may be conjugated with active ligands to provide active targeting (Hatakeyama et al., 2013). Some protein-loaded liposomes reached the clinical trials and some products are already on the market. However, compared with protein-polymer conjugates, a limited quantity of protein-loaded liposomes has been approved for marketing, and the majority of current liposomal protein formulations are still in preclinical stages (**Table 2**). In fact, although liposomes are good candidates for *in vivo* delivery of high molecular weight compounds (such as protein/peptide drugs and nucleic acids), their nanoencapsulation is often hindered by instability issues during the liposome preparative process and storage, as well as by the low encapsulation efficiencies (Xu et al., 2012; Huang et al., 2017), as discussed hereafter.

Protein-Loaded Liposomes in the Clinic

The first protein-liposome systems accepted for clinical use were virosomes, i.e., drug/vaccine delivery systems based on unilamellar phospholipid membrane which incorporate virus-derived proteins. **Epaxal®** was the first commercially available liposomal vaccine, which consists of particles of ∼150 nm composed of phosphatidylcholine and phosphatidylethanolamine lipids, neuraminidase, hemagglutinin and inactivated hepatitis A virus. The hemagglutinin and the neuraminidase bind strongly to the lipid layer by a non-covalent bond, stabilize the liposomal structure, and target the liposome to immune-competent cells (Cryz, 1999; Bovier, 2008). Epaxal has demonstrated safety and efficacy in clinical studies, and is licensed in several countries. **Inflexal-V®** is present on the market since 1997 in many countries (with different commercial names) as a therapy against flu. It is similar to Epaxal as it consists of unilamellar bilayer liposomes of about 150 nm, made of phosphatidylcholine, and the mixture of three monovalent virosome pools, each formed with one influenza strain- specific hemagglutinin and neuraminidase glycoproteins (Herzog et al., 2009).

Curosurf® (poractant alfa) is a product (FDA approved in the '90s) composed by sterile suspension for endotracheobronchial instillation of animal-derived lipids used for the treatment of neonatal respiratory distress syndrome. This product is composed of phosphatidylcholine, dipalmitoylphosphatidylcholine and the small hydrophobic surfactant proteins SP-B (8.7 kDa) and SP-C (3.7 kDa). Through a reorganization of the lipids present in the fluid that covers the lung, the alveoli can swell more easily, thus preventing the alveolar collapse. The two proteins are essential to reduce the surface tension at the air-water interface by the formation of a surface-active film highly enriched in dipalmitoylphosphatidylcholine (Walther et al., 2000). The particle size is variable and different studies reported values between 35 μm to 50 nm (uni- and multilamellar vesicles) (Waisman et al., 2007).

T4N5 liposome lotion (Dimericine) is based on T4 endonuclease V enzyme loaded into egg lecithin liposomes. The T4 endonuclease V enzyme repairs the damaged DNA preventing the first stage of skin cancer (Bulbake et al., 2017; Jeter et al., 2019). Phase I/II trials indicated effective prevention of skin cancer in Xeroderma pigmentosum patients. However, phase III trials were terminated in 2009 with lack of expected clinical outcomes (Bulbake et al., 2017).

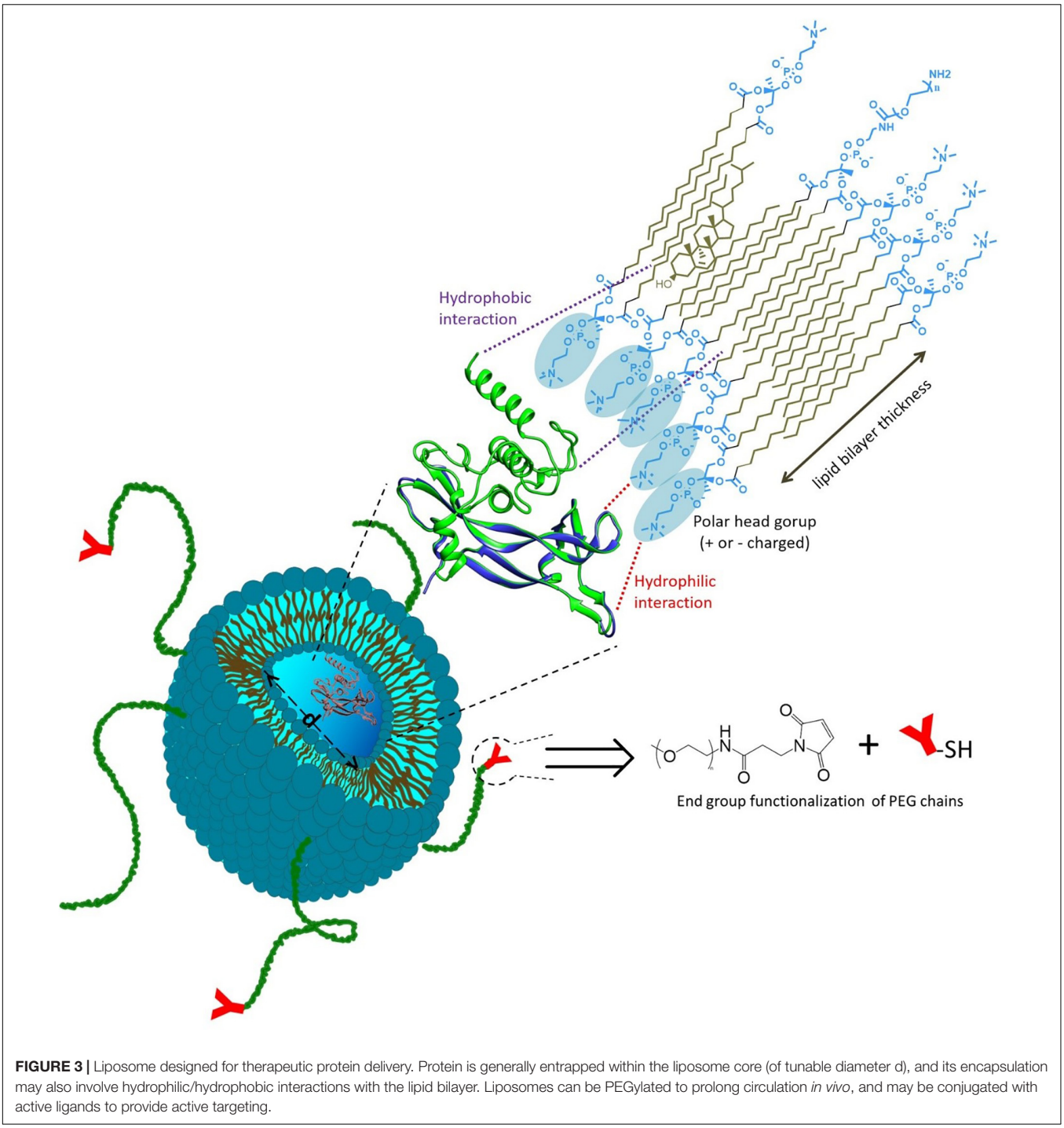

FIGURE 3 | Liposome designed for therapeutic protein delivery. Protein is generally entrapped within the liposome core (of tunable diameter d), and its encapsulation may also involve hydrophilic/hydrophobic interactions with the lipid bilayer. Liposomes can be PEGylated to prolong circulation *in vivo*, and may be conjugated with active ligands to provide active targeting.

Hepatic-directed vesicles-insulin (HDV-1) is a liposomal delivery system for diabetes treatment via oral and subcutaneous routes, which have been tested in phase II clinical trials (Diasome_Pharmaceuticals, 2019). These insulin-loaded liposomes (size < 150 nm), contain the proprietary hepatocyte-targeting molecule (HTM) and biotin-phosphatidylethanolamine lipids. In diabetic animal models, it was an effective insulin-replacement treatment as it showed very low toxicity and successfully targeted the hepatocytes in the liver (Geho et al., 2009).

Biphasix^{TM} is a topical formulation that is intended to be easily self-applied to human papillomavirus (HPV) - infected tissues, to deliver IFN-α into the skin and mucosal tissues. It regards with the encapsulation of the therapeutic protein in multilayered, lipid-based submicronvesicles (Altum_Pharmaceuticals_Inc.; Roohnikan et al., 2019). These

TABLE 2 | List of protein-loaded liposomes in clinical use.

Commercial name	Active protein	Treatment	Company	Status	Year	References
Epaxal	Hepatitis A virus proteins	Hepatitis-A	Crucell (former Berna Biotech Ltd.)	On market	1994	Cryz, 1999
Inflexal-V	Influenza virus proteins	Trivalent influenza vaccine	Crucell (former Berna Biotech Ltd.)	On market	1997	Herzog et al., 2009
Curosurf	SP-B and SP-C proteins	Lung activator for stress disorder	Chiesi Farmaceutici	On market	1999	Walther et al., 2000
T4N5 liposome lotion	T4 endonuclease V (T4N5) enzyme	Skin cancer	AGI Dermatics Inc.	Phase III	2007	Bulbake et al., 2017
Hepatic-directed vesicles-insulin (HDV-I)	Insulin	Diabetes	Diasome Pharmaceuticals	Phase II	2019	Diasome_Pharmaceuticals, 2019
Biphasix	INF-α	Genital warts and cervical dysplasia	Altum Pharmaceuticals	Phase I/II	2011	Altum_Pharmaceuticals_Inc, 2019
IL-2 liposomes	IL-2	Pulmonary metastases	Biomira United States	Phase I	2000	Skubitz and Anderson, 2000

vesicles have complex structures that include a variety of compartments into which drug molecules can be integrated, and the emulsion is completed with other excipients typical of a topic formulation. It has completed phase I and II clinical trials, where it was shown to be active (in cervical neoplasia regression) with no systemic or local side effects (Altum_Pharmaceuticals_Inc.).

IL-2 liposomes are interleukin-2 loaded liposomes which have been tested in phase I clinical trials (Skubitz and Anderson, 2000). This liposome preparation contains a synthetic lipid, dimyristoylphosphatidyl choline (DMPC), human serum albumin and human recombinant IL-2 (Khanna et al., 1997a). Administration by inhalation showed a significant increase in bronchoalveolar lavage leukocytes in the lung compared to free IL-2 administered via conventional routes due to a high concentration of the drug at the specific site of action (Khanna et al., 1997b).

Liposome Composition for Protein Delivery

In general, the liposome composition includes lipids of natural origin (e.g., egg lecithin, cholesterol), synthetic, or semi-synthetic [e.g., lipids manufactured by modification of naturally occurring precursors such as dipalmitoylphosphatidylcholine (DPPC), distearoylphosphatidylcholine (DSPC), or dimyristoyl-phosphatidylcholine (DMPC)] (Olusanya et al., 2018).

Conventional liposomes have a short circulation time *in vivo*, since they are quickly uptaken and eliminated by mononuclear phagocyte system. PEGylation is also used in liposomes to inhibit the opsonization, thus extending blood-circulation. This effect can be modulated by the molecular weight of the PEG chains and the grafting density at the liposome surface (Wang et al., 2016).

PEGylated (stealth) liposomal formulations have been studied for protein delivery, for instance as safe and effective means to deliver protein antigens (tetanus toxoid (TT), ovalbumin) to potent antigen-presenting dendritic cells for the induction of CD4+ and CD8+ T-cell response *in vivo* (Ignatius et al., 2000). Hemoglobin (LEH)-loaded liposomes, prepared with anionic lipid hexadecylcarbamoylmethyl-hexadecanoate (HDAS), cholesterol and HDAS-conjugated PEG2000, were tested as oxygen nanocarriers, and succeed in preventing systemic inflammation and multi-organ injuries caused by hemorrhagic shock in mice (Yadav et al., 2016).

Similarly to PEG-protein conjugates, PEGylation also presents undesirable effects in liposomes. For example, PEG steric effects reduce the interaction of liposomes with the cell membrane or tissue extracellular matrix when specific targeting is required (Hatakeyama et al., 2013). Ligands such as antibodies, protein fragments, peptides and aptamers are often conjugated to the terminal group of the PEG chains which are attached to the liposome surface, in order to respond to the extracellular or intracellular environment, thus obtaining active targeting (Hatakeyama et al., 2013; Fang et al., 2017). Several papers have been dedicated to PEG-ligand conjugation of liposomes for the release of low molecular weight drugs (Eloy et al., 2014; Noble et al., 2014; Belfiore et al., 2018) and this approach has also been used for protein nanoencapsulation (e.g., trypsin and chymotrypsin inhibitor into PEGylated liposomes conjugated with transferrin) (Joanitti et al., 2018). However, it is worth noting that functionalization of liposomes with various targeting ligands has resulted in enhanced detection by the immune-system, and that targeting capability may be compromised by the interaction between serum-protein and ligands (Riaz et al., 2018).

Methods for Preparing Liposomes

Different methods of liposomes preparation have been reported to optimize the drug encapsulation and to obtain a homogenous particle population, such as mechanical dispersion methods, solvent dispersion methods, and detergent removal methods (Vemuri and Rhodes, 1995; Akbarzadeh et al., 2013). The poor protein stability during preparation, especially when organic solvents and detergents are used, generally limit the preparative

choice to the mechanical dispersion methods (Xu et al., 2012). In most cases, the procedure to prepare protein-loaded liposomes is based on the following steps (as summarized in **Figure 4**): firstly, a thin lipid film is formed or dried from organic solvents, then the film/solid is hydrated with dispersed-protein aqueous media. In this step, liposomes of different sizes and/or uni-, bi- and multi-lamellar vesicles are obtained. A further step is dedicated to the size homogenisation (mainly by extrusion or sonication) and improvement of drug loading (typically by freeze-thawing), then the liposomes are purified and characterized (Xu et al., 2012; Akbarzadeh et al., 2013).

Compared with low molecular weight drugs, the encapsulation of large biomolecules such as proteins and peptides generally lead to several drawbacks, such as low encapsulation efficiency, irregular particle size distributions, the presence of organic solvent residues or metal ions, which can affect the protein stability and the safety of the clinical treatment. The purification also represents a critical step; size exclusion or dialysis are the most used methods, and possible liposome interaction with the stationary phases or membranes should not be excluded. When centrifugation is used, the right choice of the centrifugal speed is necessary to avoid the formation of agglomerates or liposome destruction. The sterilization of liposomal preparations is also a critical issue (Meyer et al., 1994; Heeremans et al., 1995), as well as storage conditions. Liposome suspensions should be stored in a refrigerator, as a freezer will lead to formation of ice crystals that may rupture the phospholipid membrane (Riaz et al., 2018). Different preparative methods have been reported in literature for *in vivo* applications, with results showing significant differences in terms of size distribution and encapsulation efficiency (**Table 3**).

The encapsulation of granulocyte colony-stimulating factor (rhG-CSF) was obtained by using three different preparative methods (lipid film hydration- microfluidisation- centrifugation, lipid powder hydration- microfluidisation- dialysis, and lipid film hydration- sonication- freeze-thawing- dialysis). Results showed that encapsulation efficiency increased with the size of the nanocarriers, and that these liposomes were successful in releasing rhG-CSF in rats (Meyer et al., 1994). In this work, a rapid protein release (100% within 24 h) or a much slower release (50% in 4 days) was obtained *in vivo* by varying the lipid composition (DPPC or DSPC:cholesterol, respectively).

The encapsulation of ovalbumin (OVA), tetanus toxoid (TT), bovine serum albumin (BSA), glutathione S-transferase (GST), human gamma-globulin (hIgG) by different techniques also showed marked differences in size distribution and encapsulation

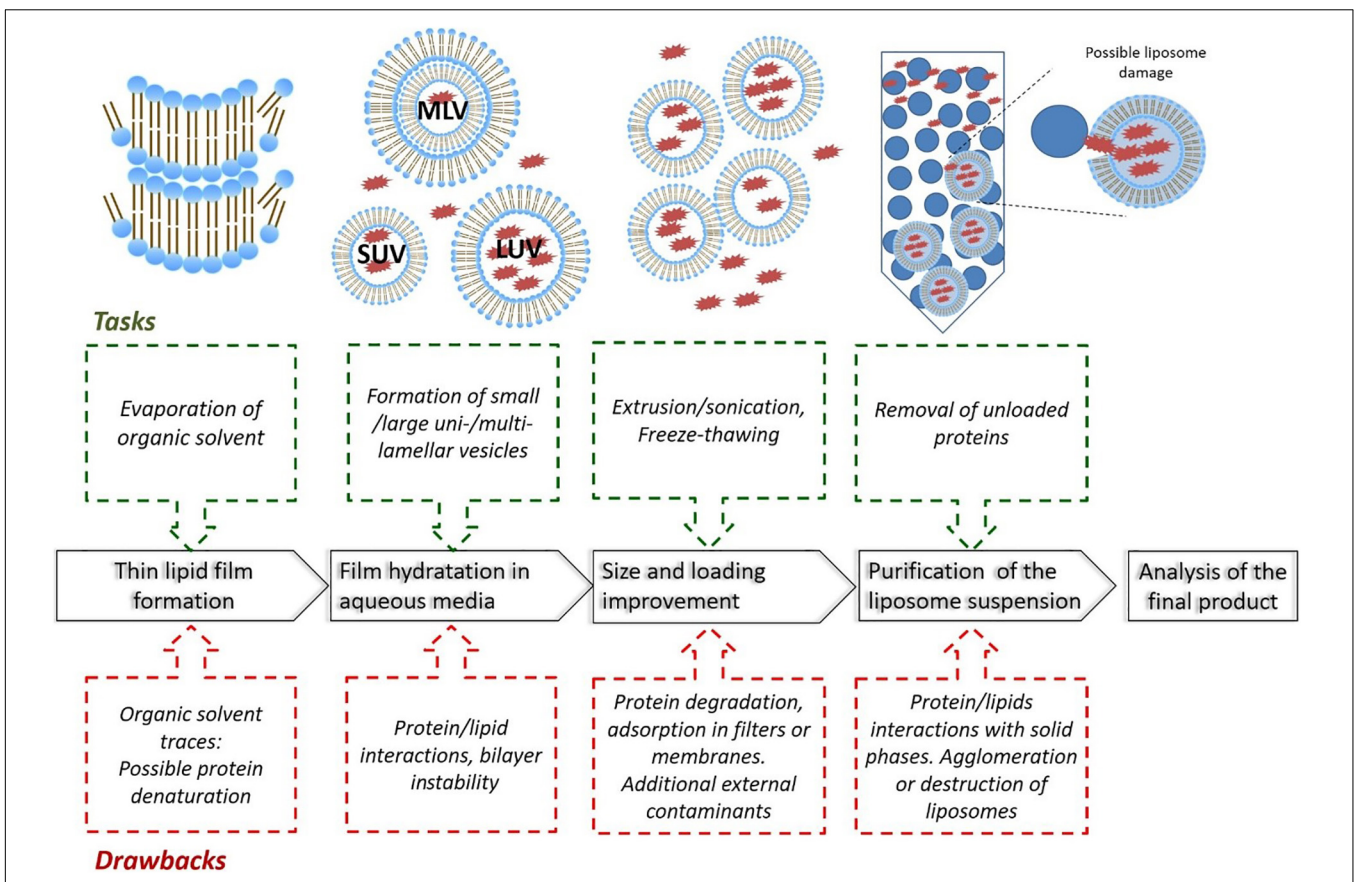

FIGURE 4 | Main steps involved with the preparation of protein-loaded liposomes, including typical tasks and drawbacks (MLV: Multilamellar Vesicles, LUV: Large unilamellar vesicles, SUV: small unilamellar vesicles).

TABLE 3 | Lipid formulations, preparative methods and characterisation of protein-loaded liposomes for *in vivo* applications.

Protein	Formulation*	Method	Size <d> [nm]	Encap. Efficiency (%)	*In vivo* study	References
rhG-CSF	DMPG:DSPC:Chol	Lipid film hydration/ microfluidisation /centrifugation Lipid powder hydration/ microfluidisation/dialysis Lipid film hydration/sonication/ freeze-thawing/dialysis	250 340 760–780	2 30 80–90	Subcutaneous injections in rats	Meyer et al., 1994
OVA and TT	Chol:POPC:PE-PEG2k	Thin film hydration and extrusion	∼100	–	Immunization of mice	Ignatius et al., 2000
bFGF	PC/Chol	pH gradient method Ammonium sulfate gradient method Reverse-phase evaporation method Thin film method	∼120	81.6 65.7 69.5 58.6	Wound healing in rats	Xiang et al., 2011
NGF	PC/Chol DSPE-PEG2k-RMP-7/DSPE-PEG2k	Reverse phase evaporation	64–73	24–34	Transport across BBB in rats	Xie et al., 2005
(FTIC-) BSA	PC/Chol/DSPE-PEG2k/S-PEG-polySDM/Rh-DHPE	Thin layer rehydration and extrusion	167–287	18–20	Bladder epithelium targeting in mice	Vila-Caballer et al., 2016
BSA	PC:Chol:DSPE-PEG.	Thin film hydration, Freezing-thawing and extrusion	208–346	41–45	Safety and pharmacokinetic studies in mice	Okamoto et al., 2018
hIgG	PC/Chol	Dehydration-rehydration	219–230	30–31	Biodistribution in mice	García-Santana et al., 2006
Hb	HDAS:Chol:HDAS-PEG2k	High pressure homogenization method	216	<5	Hemorrhagic shock in rats	Yadav et al., 2016

**1,2-dimyristoyl sn-glycero-3-phosphocholine (DMPG); 1,2-Distearoyl-sn-glycero-3-phosphocholine (DSPC); cholesterol (Chol); 1-Palmitoyl-2-oleoyl-sn-glycero-3-phosphocholine (POPC); 1,2-dipalmitoyl-sn-glycero-3-phosphoethanolamine-N-[methoxy(polyethylene glycol)-2000] (PE-PEG2k),* L-α-*phosphatidylcholine (PC); RMP-7-conjugated- 1,2-dioleoyl-sn-glycero-3-phosphoethanolamine-n-[poly(ethyleneglycol)]-hydroxy succinamide (DSPE-PEG2k-RMP-7); 1,2-distearoyl-sn-glycero-3-phosphoethanol-amine-N-[methoxy-poly(ethyleneglycol) 2000], (DSPE-PEG2k); stearoyl-poly(ethylene glycol)-poly(methacryloyl sulfadimethoxine) copolymer, (S-PEG-polySDM); N-(Lissamine Rhodamine B sulfonyl)-1, 2-dihexadecanoyl-sn-glycero-3-phosphoethanolamine triethylammonium salt, (rh-DHPE); hexadecylcarbamoylmethylhexadecanoate, (HDAS); Hexadecylcarbamoylmethylhexadecanoate-PEG2000 conjugated, (HDAS-PEG2k).*

efficiency (Ignatius et al., 2000; García-Santana et al., 2006; Ahn et al., 2009; Vila-Caballer et al., 2016; Okamoto et al., 2018; Forbes et al., 2019; Hussain et al., 2019). More specific therapeutic proteins have been encapsulated in liposomal formulations to improve release at a specific site. Basic fibroblast growth factor (bFGF), nerve growth factor (NGF), hemoglobin (Hb) are some of the biomolecules examined (Xie et al., 2005; Xiang et al., 2011; Yadav et al., 2016). It was observed that by using either a pH gradient method or freeze-thawing followed by extrusion, similar bFGF encapsulation yield (∼80%) were obtained (Xiang et al., 2011).

Nowadays, new methods have emerged with the aim of improving the encapsulation degree without affecting the integrity of the biomacromolecules. The use of supercritical carbon dioxide ($ScCO_2$) as a non-toxic substitute for organic solvents have led to some potential applications in the pharmaceutical industry for the micro- and nano-encapsulation of drugs (Santo et al., 2014; Trucillo et al., 2019). The encapsulation in liposomes of several payloads including antibodies and albumin was obtained using a $ScCO_2$-assisted process (Santo et al., 2014) with high encapsulation efficiency (>90%) (Trucillo et al., 2019).

The microfluidic-based system is a promising method to prepare protein-loaded liposomes for a rapid and scale-independent manufacture, which incorporated in-line purification and particle size monitoring. A range of neutral and anionic protein-loaded liposomes was obtained with protein efficiency (20–35%) higher than conventional methods (sonication or extrusion, <5%) and presented smaller and homogenous particle size between 60 and 100 nm (Forbes et al., 2019).

Protein Encapsulation Efficiency

The low encapsulation efficiency in small-sized liposomes represents a major challenge in the development of liposomal drug delivery systems for therapeutic proteins (Xu et al., 2012).

The nanoencapsulation of large macromolecules is predominately limited by the low entrapment volume (which depends on particle size), however, other factors are also crucial for the protein encapsulation efficiency, such as lipid composition and molar ratio, concentrations, buffer solution pH and ionic strength, preparative method, as well as the protein nature, its hydrodynamic diameter and concentration. In studies carried out with phosphatidylcholine and tissue-type Plasminogen activator (t-PA), higher encapsulation yields were obtained at higher lipids concentration, lower ionic strength larger liposome size (Heeremans et al., 1995). The effects of lipid composition concentration, buffer pH, ionic strength, protein size, liposome size and surface charge were evaluated on trypsin, horseradish peroxidase, enterokinase and hyaluronidase as model enzymes with different molecular weights and isoelectric points (Hwang et al., 2012). Results confirmed the behavior reported by Heeremans on the effect of lipid concentration and the particle size, and also showed that the encapsulation yield did not depend of the protein molecular weight, it was relatively low in any case (approximately 5–20%), and that basic pH and lower ionic strength favored the encapsulation of all proteins (Hwang et al., 2012).

The effect of protein interactions with the lipid membrane on the encapsulation efficiency is still a point of discussion among scientists. In fact, the protein may be surrounded by the lipid membrane or occupy the hydrophobic transmembrane region, depending on the nature of the proteins and the lipids involved, which are capable of forming electrostatic and hydrophobic interactions, hydrogen bonds, due to the polar and hydrophobic groups present in their complex structure (Lee, 2004; McClements, 2018). Computational simulations have also been used for a deeper understanding of protein-lipid interaction (Khan et al., 2016; van't Hag et al., 2016).

Stimuli-Responsive Liposomes

In liposomes, the release of proteins is generally controlled by physicochemical mechanisms such as lipid dissociations and simple diffusion (Lu et al., 2014). Recently, stimulus-responsive liposomes have been studied for the release of conventional drugs, and more recently for large biomolecules such as proteins and peptides. Different activation methods (temperature, pH, enzyme, redox, and light) have been used to confer stimuli-responsive properties. pH-responsive liposomes can be used for targeted release when the pathological site presents altered pH compared with normal tissues. The slightly pH change can trigger deformations in the permeability of the liposomal membrane due to the presence of pH-sensitive moieties which produce morphological changes of the lipid bilayers and consequent release of the payload. Lipids such as oleic and hyaluronic acid, derivatives of succinic acid, and other pH-sensitive phospholipids can be used for the release of therapeutic proteins, for the release in solid tumors or in the bladder cavity (Vila-Caballer et al., 2016).

Thermosensitive liposomes (TSL) are another example of "smart" nanocarriers as temperature changes can be used as "trigger" at the diseased site. Such liposomes are composed of phospholipids that present a gel-to-liquid crystalline phase transition temperature (Tm) slightly above the physiological temperature. When mild hyperthermia (a local increase of temperature up to 42°C) is applied, the lipid bilayer will 'melt' to a fluid state upon arrival in the heated targeted area, and in that process liposomes rapidly release their payloads (Al-Ahmady and Kostarelos, 2016). Several lipids present a low-temperature transition, DPPC is the most common thermosensitive lipid which presents a Tm close to 41°C (Mazzotta et al., 2018). DSPE-PEG2000 also helped to stabilize the lipid membrane at physiological temperature and to enhance the kinetics release at 40–41°C (from 10 to 40% after 2 h incubation) (Huang et al., 2017). Listeriolysin *O*-loaded thermosensitive immunoliposomes were developed to release the payload when heated slightly above body temperature (Kullberg et al., 2005). Small unilamellar LTSL loaded with mistletoe lectin-1 (ML1), a ribosome-inactivating protein with potent cytotoxic activity in tumor cells, showed protein release (15–46%) after a 15-min heating period at 41–42°C (de Matos et al., 2018).

ALTERNATIVE NANOCARRIERS FOR PROTEIN DELIVERY

Beside protein-polymer conjugates and liposomes, alternative nanosized systems are under development for the delivery for therapeutic proteins (**Figure 5**). Advanced lipid-based and polymer-based nanocarriers show several advantages over current clinically validated systems, with the potential to overcome most of their limitations. However, the translation of nanotechnology from the bench to the market imposes several challenges (Soares et al., 2018), and many of these systems are at a development stage of proof-of-principle studies.

Lipid-based micro- and nanocarriers such as emulsions, exosomes, non-ionic surfactant vesicles, solid lipid particles and micelles and have been studied for nanoencapsulation and transport of therapeutic proteins (McClements, 2018; Liu et al., 2019).

Emulsions are colloidal dispersions composed of oil, water and surfactants. Depending on the formulation and manufacturing conditions, the oil-in-water or water-in-oil droplets can be small in size (microemulsion and nanoemulsions) and employed for the delivery of proteins by non-parenteral routes, such as oral and transdermal delivery (Pachioni-Vasconcelos et al., 2016; Shukla et al., 2018). They generally present high encapsulation efficiency, the manufacturing process is relatively cheap and it can easily be scaled up. However, the harsh manufacturing conditions (the use of organic phases, high mechanical forces, pressure and temperatures) may expose to the proteins to stresses and affect their activity (Tan and Danquah, 2012).

Exosomes are neutral extracellular vesicles (cell-derived vesicles) with a native membrane composition. These natural vesicles are involved in cell-to-cell communication and play an important role in the biomolecule transfer pathways. The similarities between exosomes and liposomes include the presence of the lipid bilayer (rich in cholesterol and diacylglycerol), the minimal toxicity, biocompatibility, the

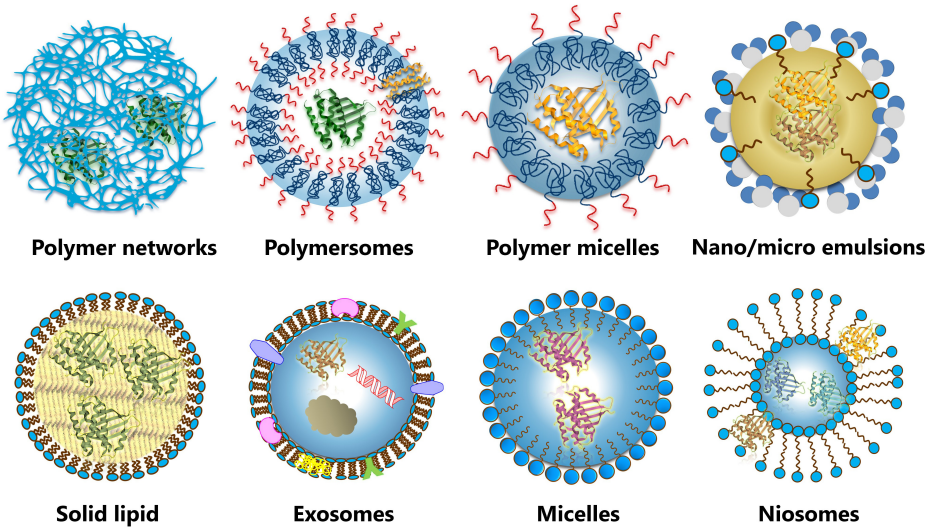

FIGURE 5 | Different types of nanosized systems for protein delivery, including lipid-based, and polymer-based nanocarriers.

nanometric size and the internal volume where several biomolecules can be entrapped (Antimisiaris et al., 2018). The principal advantages of these nanoparticles are the high and specific organotropism and the immunocompatibility, thus representing promising vehicles for protein delivery (Hong et al., 2018). For instance, an exosomal-based delivery system for a potent antioxidant, catalase, was developed to treat Parkinson's disease (Haney et al., 2015). Catalase was successfully encapsulated with a loading efficiency up to 26% and a sustained release was obtained *in vitro* (less that 40% in 24 h) (Haney et al., 2015). The complex preparative and purification methods and the very low isolation yields represent serious hinders to overcome (De Toro et al., 2015; Antimisiaris et al., 2018; Bunggulawa et al., 2018).

Niosomes are non-ionic surfactant vesicles principally composed of non-ionic surfactants and cholesterol. The particle size (from 10 nm to 20 μm) depends on the preparation method and the composition (Kaur and Kumar, 2018). Niosomes present similar advantages of liposomes in terms of ease preparation, biocompatibility, low toxicity (Kaur and Kumar, 2018; Samed et al., 2018). The main disadvantages are related to physical instability, as niosomes tend to form aggregates or fuse between themselves (Moghassemi and Hadjizadeh, 2014). However, these lipid-based carriers are in continuous development. Surfactants such as terpenoids (squalene), polysorbates, spans, alkyl oxyethylenes (usually from C12 to C18), polyoxyethylene alkyl ether and several neutral lipids have been used to obtain niosomes as nanocarriers for insulin, and peptides (Ge et al., 2019). Niosomes with sorbitan monoester were developed for vaginal delivery of insulin and tested in rats (Ning et al., 2005). These nanosystems (size 220–300 nm) were able to achieve a maximum entrapment efficiency of ∼29% and insulin release of approximately 30% in simulated vaginal fluid (Ning et al., 2005).

Solid lipid nanoparticles are composed of a solid lipid nucleus stabilized with a monolayer of phospholipids or surfactants. They are prepared using various lipids such as mono-, di- and triglycerides, phospholipids, fatty acids, waxes and steroids, and amphiphiles such as poloxamers and polysorbates (Geszke-Moritz and Moritz, 2016). Solid lipid nanoparticles have been extensively used for drug encapsulation, although their use for encapsulation of large biomolecules such as proteins and peptides is less conventional. A fair amount of proteins such as albumin, insulin, lysozyme, gonadorelin, antide and CyA have been encapsulated in these nanocarriers (Martins et al., 2007; Li et al., 2012). Recently, insulin-loaded solid lipid nanoparticles designed for oral delivery, formulated with an endosomal escape agent (HA2 peptides) to facilitate release, increased the absorption while maintaining the biological activity of the protein (Xu et al., 2018). Compared with subcutaneously administered free insulin, SLN administration showed a relatively slower increase in the serum insulin concentration and a significant higher relative bioavailability (3.2-fold higher than free insulin) (Xu et al., 2018).

Amphiphilic block copolymers can self-assemble into a wide range of morphologies, including micelles and polymersomes. **Polymeric micelles** are significantly more stable than surfactant-based micelles, due to their remarkably low critical micellar concentrations (10^{-6} - 10^{-7} M) and slow kinetics of dissociation, they do not undergo immediate dissolution after extreme dilution after intravenous injection (La et al., 1996). However, the encapsulation of therapeutic proteins is generally limited by the presence of the hydrophobic micellar core (Pachioni-Vasconcelos et al., 2016). Ionic-hydrophilic block copolymers have been used for the preparation of polyionic complex micelles, which may encapsulate proteins via electrostatic interactions (Insua et al., 2016).

Recently, uniform core–shell self-assembled particles, based on poly(ethylene glycol)-b-poly(l-glutamic acid) (PEG-PLE), were proposed to stabilize and to improve BDNF delivery throughout the brain (Jiang et al., 2018).

Polymersomes composed of block or graft amphiphilic copolymers have properties similar to those of liposomes, with the advantage of a higher membrane stability. The hydrophobic domain of the polymeric membrane can incorporate hydrophobic proteins/drugs, whereas the aqueous core can encapsulate hydrophilic proteins (Letchford and Burt, 2007). By varying block-copolymer composition, molecular weight and architecture, it is possible to tune the size, shape, membrane thickness, mechanical strength, permeability and surface chemistry for optimizing drug loading and delivery (Liu et al., 2019). Although polymerosomes are promising for protein encapsulation, further developments are required to overcome the poor encapsulation efficiency (<5% for BSA and Hb) (Lee et al., 2001). In fact, their large membrane thickness (d ≈ 8–21 nm) compared to liposomes (d ≈ 3–5 nm), represents a thermodynamic and kinetic barrier to permeability (Lee et al., 2001).

Recently, a formulation of poly(ethylene glycol)-poly(propylene sulfide) block copolymers and low molecular weight PEG was used to obtain polymersomes by a direct hydration method (O'Neil et al., 2009). Encapsulation efficiencies for ovalbumin at 37%, BSA at 19%, and bovine γ-globulin at 15%, were obtained when the proteins were included in the hydration solution (O'Neil et al., 2009).

Polymer networks may be used to encapsulate hydrophilic proteins within their matrix (Vermonden et al., 2012). Hydrogel nanoparticles are three-dimensional polymer networks containing a large amount of water; swelling and degradability of the hydrogel can be tuned through the choice of the type of polymer and the crosslinking density, in order to achieve an efficient protein loading and release. The polymer composition can be selected to provide stealth character, to guarantee extended plasma half-life, and to enhance targeting. For example, insulin-loaded chitosan-based hydrogel nanoparticles showed promising results for the intestinal absorption of insulin *in vivo* (Pan et al., 2002; Ma et al., 2005). Nanosized dendrimers and hyperbranched polymers have also been proposed as protein nanocarriers. Negatively charged proteins can be easily entrapped within positively charged dendrimers such as PAMAM (He et al., 2018). Dendrimer-based carriers with a hydrophobic membrane-disruptive region (aromatic motif), and a multivalent protein binding surface (guanidyl-based) was developed for the delivery of BSA, R- phycoerythrin, p53, saporin, β-galactosidase, and peptides into the cytosol of living cells (Chang et al., 2017; Liu et al., 2019). Recently, an innovative delivery system named single-protein nanocapsules (SPN) was proposed (Yan et al., 2009). In this case, polymerisable groups are covalently linked to the protein and the polymerisation occurs in an aqueous solution containing monomers and a crosslinker, resulting in each protein enfolded in a thin polymer shell. By varying the chemistry of monomers and crosslinker, it is also possible to obtain a degradable shell as well as a stimuli-responsive delivery (Lu et al., 2014; Pachioni-Vasconcelos et al., 2016). Similarly to PEGylation, limitations of SPN regards with the interference of the polymer with protein activity, because of its steric hindrance and possible conjugation of amino acids directly involved with substrate/receptor binding (Pachioni-Vasconcelos et al., 2016). Self-assembled nanostructures based on complexation with polyester nanoparticles (Choi et al., 2014; Wu et al., 2014), and layer-by-layer structures (Gu et al., 2013) have also been proposed for encapsulation and release of therapeutic proteins.

CONCLUSION

Nanomedicine has already demonstrated its ability to overcome some critical limitations of protein therapeutics, and we expect to provide more examples of clinically validated technologies in the upcoming years. While protein-polymer conjugates and liposomes are well-established nanosystems with a list of therapeutically approved products, various forms of protein-loaded nanocarriers of different sizes, shapes, and compositions have been explored. The use of different nanodelivery methods and the design of nanomaterials of tunable physicochemical properties, release mechanisms and targeting strategies make these alternatives very attractive. Each of these technologies has its own advantages and disadvantages. Although some of them have successfully reached the market, the delivery of therapeutic proteins at the right concentration to the right site of action, without provoking adverse side effects, still remains a major challenge. Moreover, the development of more sophisticated nanomaterials needs a deeper understanding of their physicochemical and biological properties, and of their pharmacokinetic and pharmacodynamic effects. All these requirements, together with the need of a higher control of the manufacturing process, scale-reproducibility, and the final quality of the product, pose additional challenges in regulatory terms, which need to be addressed to achieve the maximal impact in healthcare.

AUTHOR CONTRIBUTIONS

All authors listed have made a substantial, direct and intellectual contribution to the work, and approved it for publication.

FUNDING

Financial support from Regione Lombardia (POR FESR 2014 – 2020) within the framework of the NeOn project (ID 239047), is gratefully acknowledged.

REFERENCES

Agarwal, R., Iezhitsa, I., Agarwal, P., Abdul Nasir, N. A., Razali, N., Alyautdin, R., et al. (2016). Liposomes in topical ophthalmic drug delivery: an update. *Drug Deliv.* 23, 1075–1091. doi: 10.3109/10717544.2014.943336

Ahn, T., Chi, Y. T., and Yun, C. H. (2009). Effect of nonlamellar-prone lipids on protein encapsulation in liposomes. *Macromol. Res.*17, 956–962. doi: 10.1007/bf03218642

Akbarzadeh, A., Rezaei-Sadabady, R., Davaran, S., Joo, S. W., Zarghami, N., Hanifehpour, Y., et al. (2013). Liposome: classification, preparation,

and applications. *Nanoscale Res Lett.*8:102. doi: 10.1186/1556-276 x-8-102

Al-Ahmady, Z., and Kostarelos, K. (2016). Chemical components for the design of temperature-responsive vesicles as cancer therapeutics. *Chem. Rev.* 116, 3883–3918. doi: 10.1021/acs.chemrev.5b00578

Allen, T. M., and Cullis, P. R. (2013). Liposomal drug delivery systems: from concept to clinical applications. *Adv. Drug Deliv. Rev.* 65, 36–48. doi: 10.1016/j. addr.2012.09.037

Altum_Pharmaceuticals_Inc, (2019). *Altum_Pharmaceuticals_Inc.* Available: https://www.altumpharma.com/pipeline/ap-001/ (accessed 1 September 2019).

Antimisiaris, S. G., Mourtas, S., and Marazioti, A. (2018). Exosomes and exosome-inspired vesicles for targeted drug delivery. *Pharmaceutics* 10:218. doi: 10.3390/ pharmaceutics10040218

Armstrong, J. K. (2009). "The occurrence, induction, specificity and potential effect of antibodies against poly(ethylene glycol)," in *PEGylated Protein Drugs: Basic Science and Clinical Applications*, ed. F.M. Veronese. (Basel: Birkhäuser Basel), 147–168. doi: 10.1007/978-3-7643-8679-5_9

Armstrong, J. K., Hempel, G., Koling, S., Chan, L. S., Fisher, T., Meiselman, H. J., et al. (2007). Antibody against poly (ethylene glycol) adversely affects PEG-asparaginase therapy in acute lymphoblastic leukemia patients. *Cancer* 110, 103–111. doi: 10.1002/cncr.22739

Averick, S., Simakova, A., Park, S., Konkolewicz, D., Magenau, A. J., Mehl, R. A., et al. (2011). ATRP under biologically relevant conditions: grafting from a protein. *Acs Macro Lett.* 1, 6–10. doi: 10.1021/mz200020c

Badescu, G., Bryant, P., Bird, M., Henseleit, K., Swierkosz, J., Parekh, V., et al. (2014). Bridging disulfides for stable and defined antibody drug conjugates. *Bioconjug. Chem.* 25, 1124–1136. doi: 10.1021/bc500148x

Baker, D. P., Lin, E. Y., Lin, K., Pellegrini, M., Petter, R. C., Chen, L. L., et al. (2006). N-Terminally PEGylated human interferon-β-1a with improved pharmacokinetic properties and in vivo efficacy in a melanoma angiogenesis model. *Bioconjug. Chem.* 17, 179–188. doi: 10.1021/bc050237q

Balan, S., Choi, J. -W., Godwin, A., Teo, I., Laborde, C. M., Heidelberger, S., et al. (2007). Site-Specific pegylation of protein disulfide bonds using a three-carbon bridge. *Bioconjug. Chem.* 18, 61–76. doi: 10.1021/bc0601471

Banerjee, S. S., Aher, N., Patil, R., and Khandare, J. (2012). Poly (ethylene glycol)-prodrug conjugates: concept, design, and applications. *J. Drug Deliv.* 2012:103973

Belfiore, L., Saunders, D. N., Ranson, M., Thurecht, K. J., Storm, G., and Vine, K. L. (2018). Towards clinical translation of ligand-functionalized liposomes in targeted cancer therapy: challenges and opportunities. *J. Control. Release* 277, 1–13. doi: 10.1016/j.jconrel.2018.02.040

Bendele, A., Seely, J., Richey, C., Sennello, G., and Shopp, G. (1998). Short communication: renal tubular vacuolation in animals treated with polyethylene-glycol-conjugated proteins. *Toxicol. Sci.* 42, 152–157. doi: 10. 1093/toxsci/42.2.152

Blick, S. K. A., and Curran, M. P. (2007). Certolizumab pegol. *BioDrugs* 21, 195–201. doi: 10.2165/00063030-200721030-00006

Bovier, P. A. (2008). Epaxal®: a virosomal vaccine to prevent hepatitis A infection. *Exp. Rev. Vaccines* 7, 1141–1150. doi: 10.1586/14760584.7.8.1141

Bruni, R., Possenti, P., Bordignon, C., Li, M., Ordanini, S., Messa, P., et al. (2017). Ultrasmall polymeric nanocarriers for drug delivery to podocytes in kidney glomerulus. *J. Control. Release* 255, 94–107. doi: 10.1016/j.jconrel.2017.04.005

Bulbake, U., Doppalapudi, S., Kommineni, N., and Khan, W. (2017). Liposomal formulations in clinical use: an updated review. *Pharmaceutics* 9:E12. doi: 10. 3390/pharmaceutics9020012

Bunggulawa, E. J., Wang, W., Yin, T., Wang, N., Durkan, C., Wang, Y., et al. (2018). Recent advancements in the use of exosomes as drug delivery systems. *J. Nanobiotechnol.* 16:81. doi: 10.1186/s12951-018-0403-9

Castaman, G., and Linari, S. (2018). Pharmacokinetic drug evaluation of recombinant factor VIII for the treatment of hemophilia A. *Exp. Opin. Drug Metabol. Toxicol.* 14, 143–151. doi: 10.1080/17425255.2018.1420161

Chan, B. A., Xuan, S., Li, A., Simpson, J. M., Sternhagen, G. L., Yu, T., et al. (2018). Polypeptoid polymers: synthesis, characterization, and properties. *Biopolymers* 109:e23070. doi: 10.1002/bip.23070

Chang, H., Lv, J., Gao, X., Wang, X., Wang, H., Chen, H., et al. (2017). Rational design of a polymer with robust efficacy for intracellular protein and peptide delivery. *Nano lett.* 17, 1678–1684. doi: 10.1021/acs.nanolett.6b0 4955

Chaplin, S., and Gnanapavan, S. (2015). Plegridy for the treatment of RRMS in adults. *Prescriber* 26, 29–31. doi: 10.1002/psb.1349

Chapman, A. P., Antoniw, P., Spitali, M., West, S., Stephens, S., and King, D. J. (1999). Therapeutic antibody fragments with prolonged in vivo half-lives. *Nat. Biotechnol.* 17, 780. doi: 10.1038/11717

Chen, D., Disotuar, M. M., Xiong, X., Wang, Y., and Chou, D. H. -C. (2017). Selective N-terminal functionalization of native peptides and proteins. *Chem. Sci.* 8, 2717–2722. doi: 10.1039/C6SC04744K

Cheng, P. N. -M., Lam, T. -L., Lam, W. -M., Tsui, S. -M., Cheng, A. W. -M., Lo, W. -H., et al. (2007). Pegylated recombinant human arginase (rhArg-peg5, 000mw) inhibits the in vitro and in vivo proliferation of human hepatocellular carcinoma through arginine depletion. *Cancer Res.* 67, 309–317. doi: 10.1158/ 0008-5472.CAN-06-1945

Cheng, T. -L., Wu, P. -Y., Wu, M. -F., Chern, J. -W., and Roffler, S. R. (1999). Accelerated clearance of polyethylene glycol-modified proteins by anti-polyethylene glycol IgM. *Bioconjug Chem.* 10, 520–528. doi: 10.1021/bc980143z

Choi, W. I., Kamaly, N., Riol-Blanco, L., Lee, I. -H., Wu, J., Swami, A., et al. (2014). A Solvent-free thermosponge nanoparticle platform for efficient delivery of labile proteins. *Nano Lett.* 14, 6449–6455. doi: 10.1021/nl502994y

Conover, C., Lejeune, L., Linberg, R., Shum, K., and Shorr, R. G. L. (1996). Transitional vacuole formation following a bolus infusion of peg-hemoglobin in the rat. *Artif. Cells Blood Substi. Biotechnol.* 24, 599–611. doi: 10.3109/ 10731199609118885

Cryz, S. J. (1999). BERNA: a century of immunobiological innovation. *Vaccine* 17, S1-S5. doi: 10.1016/S0264-410X(99)00228-5

de Matos, M. B. C., Beztsinna, N., Heyder, C., Fens, M. H. A. M., Mastrobattista, E., Schiffelers, R. M., et al. (2018). Thermosensitive liposomes for triggered release of cytotoxic proteins. *Eur. J. Pharm. Biopharm.* 132, 211–221. doi: 10.1016/j. ejpb.2018.09.010

De Toro, J., Herschlik, L., Waldner, C., and Mongini, C. (2015). Emerging Roles of Exosomes in normal and pathological conditions: new insights for diagnosis and therapeutic applications. *Front. Immunol.* 6:203. doi: 10.3389/fimmu.2015. 00203

DeFrees, S., Wang, Z. -G., Xing, R., Scott, A. E., Wang, J., Zopf, D., et al. (2006). GlycoPEGylation of recombinant therapeutic proteins produced in *Escherichia coli*. *Glycobiology* 16, 833–843. doi: 10.1093/glycob/cwl004

Diasome_Pharmaceuticals, (2019). *Breakthrough HDV Technology.* Diasome: Diasome Pharmaceuticals, Inc.

Dozier, J. K., and Distefano, M. D. (2015). Site-Specific PEGylation of therapeutic proteins. *Int. J. Mol Sci.* 16, 25831–25864. doi: 10.3390/ijms161025831

Dunn, A. L., Ahuja, S. P., and Mullins, E. S. (2018). Real-world experience with use of antihemophilic factor (Recombinant), PEGylated for prophylaxis in severe haemophilia A. *Haemophilia* 24, e84-e92. doi: 10.1111/hae.13403

Eloy, J. O., Claro, de Souza, M., Petrilli, R., Barcellos, J. P. A., Lee, R. J., and Marchetti, J. M. (2014). Liposomes as carriers of hydrophilic small molecule drugs: strategies to enhance encapsulation and delivery. *Coll. Surfa. B Biointerf.* 123, 345–363. doi: 10.1016/j.colsurfb.2014.09.029

Ezban, M., Hermit, M. B., and Persson, E. (2019). FIXing postinfusion monitoring: assay experiences with N9-GP (nonacog beta pegol; Refixia®; Rebinyn®). *Haemophilia* 25, 154–161. doi: 10.1111/hae.13671

Fang, Y., Xue, J., Gao, S., Lu, A., Yang, D., Jiang, H., et al. (2017). Cleavable PEGylation: a strategy for overcoming the "PEG dilemma" in efficient drug delivery. *Drug Deliv.* 24, 22–32. doi: 10.1080/10717544.2017.1388451

Ferguson, E. L., Alshame, A. M., and Thomas, D. W. (2010). Evaluation of hyaluronic acid–protein conjugates for polymer masked–unmasked protein therapy. *Int. J. Pharm.* 402, 95–102. doi: 10.1016/j.ijpharm.2010.09.029

Fernandes, A. I., and Gregoriadis, G. (2001). The effect of polysialylation on the immunogenicity and antigenicity of asparaginase: implication in its pharmacokinetics. *Int. J. Pharm.* 217, 215–224. doi: 10.1016/S0378-5173(01) 00603-2

Forbes, N., Hussain, M. T., Briuglia, M. L., Edwards, D. P., Horst, J. H. T., Szita, N., et al. (2019). Rapid and scale-independent microfluidic manufacture of liposomes entrapping protein incorporating in-line purification and at-line size monitoring. Int. J. Pharm. 556, 68–81. doi: 10.1016/j.ijpharm.2018.11.060

Foser, S., Schacher, A., Weyer, K. A., Brugger, D., Dietel, E., Marti, S., et al. (2003). Isolation, structural characterization, and antiviral activity of positional isomers of monopegylated interferon α-2a (PEGASYS). *Protein Exp. Purif.* 30, 78–87. doi: 10.1016/S1046-5928(03)00055-X

Francis, G., Fisher, D., Delgado, C., Malik, F., Gardiner, A., and Neale, D. (1998). PEGylation of cytokines and other therapeutic proteins and peptides: the importance of biological optimisation of coupling techniques. *Int. J. Hematol.* 68, 1–18. doi: 10.1016/S0925-5710(98)00039-5

Gaertner, F. C., Luxenhofer, R., Blechert, B., Jordan, R., and Essler, M. (2007). Synthesis, biodistribution and excretion of radiolabeled poly (2-alkyl-2-oxazoline) s. *J. Control. Release* 119, 291–300. doi: 10.1016/j.jconrel.2007.02.015

Gao, W., Liu, W., Mackay, J. A., Zalutsky, M. R., Toone, E. J., and Chilkoti, A. (2009). In situ growth of a stoichiometric PEG-like conjugate at a protein's N-terminus with significantly improved pharmacokinetics. *Proc. Natl. Acad. Sci. U.S.A.* 106, 15231–15236. doi: 10.1073/pnas.0904378106

Garay, R. P., El-Gewely, R., Armstrong, J. K., Garratty, G., and Richette, P. (2012). Antibodies against polyethylene glycol in healthy subjects and in patients treated with PEG-conjugated agents. *Exp. Opin. Drug Deliv.* 9, 1319–1323. doi: 10.1517/17425247.2012.720969

García-Santana, M. A., Duconge, J., Sarmiento, M. E., Lanio-Ruíz, M. E., Becquer, M. A., Izquierdo, L., et al. (2006). Biodistribution of liposome-entrapped human gamma-globulin. *Biopharm. Drug Dispos.* 27, 275–283. doi: 10.1002/bdd.511

Ge, X., Wei, M., He, S., and Yuan, W. -E. (2019). Advances of non-ionic surfactant vesicles (niosomes) and their application in drug delivery. *Pharmaceutics* 11:55. doi: 10.3390/pharmaceutics11020055

Gebauer, M., and Skerra, A. (2018). Prospects of PASylation® for the design of protein and peptide therapeutics with extended half-life and enhanced action. *Bioorg. Med. Chem.* 26, 2882–2887. doi: 10.1016/j.bmc.2017.09.016

Geho, W. B., Geho, H. C., Lau, J. R., and Gana, T. J. (2009). Hepatic-directed vesicle insulin: a review of formulation development and preclinical evaluation. *J. Diabetes Sci. Technol.* 3, 1451–1459. doi: 10.1177/193229680900300627

Geszke-Moritz, M., and Moritz, M. (2016). Solid lipid nanoparticles as attractive drug vehicles: composition, properties and therapeutic strategies. *Mater. Sci. Eng.C* 68, 982–994. doi: 10.1016/j.msec.2016.05.119

Graham, M. L. (2003). Pegaspargase: a review of clinical studies. *Adv. Drug Deliv. Rev.* 55, 1293–1302. doi: 10.1016/S0169-409X(03)00110-8

Grigoletto, A., Maso, K., Mero, A., Rosato, A., Schiavon, O., and Pasut, G. (2016). Drug and protein delivery by polymer conjugation. *J. Drug Deliv. Sci. Technol.* 32, 132–141. doi: 10.1016/j.jddst.2015.08.006

Gu, X., Wang, J., Wang, Y., Wang, Y., Gao, H., and Wu, G. (2013). Layer-by-layer assembled polyaspartamide nanocapsules for pH-responsive protein delivery. *Coll. Surf. BBiointerf.* 108, 205–211. doi: 10.1016/j.colsurfb.2013.03.007

Hamley, I. W. (2014). PEG–Peptide Conjugates. *Biomacromolecules* 15, 1543–1559. doi: 10.1021/bm500246w

Haney, M. J., Klyachko, N. L., Zhao, Y., Gupta, R., Plotnikova, E. G., He, Z., et al. (2015). Exosomes as drug delivery vehicles for Parkinson's disease therapy. *J. Control. Release* 207, 18–30. doi: 10.1016/j.jconrel.2015.03.033

Harris, J. M., and Chess, R. B. (2003). Effect of pegylation on pharmaceuticals. *Nat. Rev. Drug Discov.* 2, 214–221. doi: 10.1038/nrd1033

Hatakeyama, H., Akita, H., and Harashima, H. (2013). The polyethyleneglycol dilemma: advantage and disadvantage of pegylation of liposomes for systemic genes and nucleic acids delivery to tumors. *Biol Pharm. Bull.* 36, 892–899. doi: 10.1248/bpb.b13-00059

He, H., Chen, Y., Li, Y., Song, Z., Zhong, Y., Zhu, R., et al. (2018). Effective and selective anti-cancer protein delivery via all-functions-in-one nanocarriers coupled with visible light-responsive, reversible protein engineering. *Adv. Func. Mater.* 28, 1706710. doi: 10.1002/adfm.201706710

He, H., Lu, Y., Qi, J., Zhu, Q., Chen, Z., and Wu, W. (2019). Adapting liposomes for oral drug delivery. *Acta Pharm. Sin. B* 9, 36–48. doi: 10.1016/j.apsb.2018.06.005

Heeremans, J. L. M., Gerrttsen, H. R., Meusen, S. P., Mijnheer, F. W., Gangaram Panday, R. S., Prevost, R., et al. (1995). The preparation of tissue-type plasminogen activator (t-PA) containing liposomes: entrapment efficiency and ultracentrifugation damage. *J. Drug Target.* 3, 301–310. doi: 10.3109/10611869509015959

Herndon, T. M., Demko, S. G., Jiang, X., He, K., Gootenberg, J. E., Cohen, M. H., et al. (2012). US food and drug administration approval: peginterferon-alfa-2b for the adjuvant treatment of patients with melanoma. *Oncol.* 17, 1323–1328. doi: 10.1634/theoncologist.2012-0123

Herzog, C., Hartmann, K., Künzi, V., Kürsteiner, O., Mischler, R., Lazar, H., et al. (2009). Eleven years of Inflexal® V—a virosomal adjuvanted influenza vaccine. *Vaccine* 27, 4381–4387. doi: 10.1016/j.vaccine.2009.05.029

Hey, T., Knoller, H., and Vorstheim, P. (2012). "Half-life extension through HESylation," in *Therapeutic Proteins*, ed. R. Kontermann, (Hoboken, NJ: John Wiley and Sons), 117–140. doi: 10.1002/9783527644827.ch7

Hong, Y., Nam, G.-H., Koh, E., Jeon, S., Kim, G. B., Jeong, C., et al. (2018). Exosome as a vehicle for delivery of membrane protein therapeutics, ph20, for enhanced tumor penetration and antitumor efficacy. *Adv. Func. Mater.* 28, 1703074. doi: 10.1002/adfm.201703074

Hu, J., Wang, G., Liu, X., and Gao, W. (2015). Enhancing pharmacokinetics, tumor accumulation, and antitumor efficacy by elastin-like polypeptide fusion of interferon alpha. *Adv. Mater.* 27, 7320–7324. doi: 10.1002/adma.201503440

Hu, J., Wang, G., Zhao, W., Liu, X., Zhang, L., and Gao, W. (2016). Site-specific in situ growth of an interferon-polymer conjugate that outperforms PEGASYS in cancer therapy. *Biomaterials* 96, 84–92. doi: 10.1016/j.biomaterials.2016.04.035

Hu, Y., Hou, Y., Wang, H., and Lu, H. (2018). Polysarcosine as an alternative to PEG for therapeutic protein conjugation. *Bioconjug. Chem.* 29, 2232–2238. doi: 10.1021/acs.bioconjchem.8b00237

Huang, X. Y., Li, M., Bruni, R., Messa, P., and Cellesi, F. (2017). The effect of thermosensitive liposomal formulations on loading and release of high molecular weight biomolecules. *Int. J. Pharm.* 524, 279–289. doi: 10.1016/j.ijpharm.2017.03.090

Huang, Y.-S., Wen, X.-F., Wu, Y.-L., Wang, Y.-F., Fan, M., Yang, Z.-Y., et al. (2010). Engineering a pharmacologically superior form of granulocyte-colony-stimulating factor by fusion with gelatin-like-protein polymer. *Eur. J. Pharm. Biopharm.* 74, 435–441. doi: 10.1016/j.ejpb.2009.12.002

Hussain, M. T., Forbes, N., and Perrie, Y. (2019). Comparative analysis of protein quantification methods for the rapid determination of protein loading in liposomal formulations. *Pharmaceutics* 11, 39. doi: 10.3390/pharmaceutics11010039

Hwang, S. Y., Kim, H. K., Choo, J., Seong, G. H., Hien, T. B. D., and Lee, E. K. (2012). Effects of operating parameters on the efficiency of liposomal encapsulation of enzymes. *Coll. Surf. BBiointerf.* 94, 296–303. doi: 10.1016/j.colsurfb.2012.02.008

Ignatius, R., Mahnke, K., Rivera, M., Hong, K., Isdell, F., Steinman, R. M., et al. (2000). Presentation of proteins encapsulated in sterically stabilized liposomes by dendritic cells initiates CD8+ T-cell responses in vivo. *Blood* 96, 3505–3513. doi: 10.1182/blood.v96.10.3505.h8003505_3505_3513

Immordino, M. L., Dosio, F., and Cattel, L. (2006). Stealth liposomes: review of the basic science, rationale, and clinical applications, existing and potential. *Int. J. Nanomed.* 1, 297–315. doi: 10.2217/17435889.1.3.297

Imran ul-haq, M., Lai, B. F., Chapanian, R., and Kizhakkedathu, J. N. (2012). Influence of architecture of high molecular weight linear and branched polyglycerols on their biocompatibility and biodistribution. *Biomaterials* 33, 9135–9147. doi: 10.1016/j.biomaterials.2012.09.007

Insua, I., Wilkinson, A., and Fernandez-Trillo, F. (2016). Polyion complex (PIC) particles: preparation and biomedical applications. *Eur. Polym. J.* 81, 198–215. doi: 10.1016/j.eurpolymj.2016.06.003

Ivens, I. A., Achanzar, W., Baumann, A., Braendli-Baiocco, A., Cavagnaro, J., Dempster, M., et al. (2015). PEGylated biopharmaceuticals: current experience and considerations for nonclinical development. *Toxicol. Pathol.* 43, 959–983. doi: 10.1177/0192623315591171

Jain, S., Hreczuk-Hirst, D. H., McCormack, B., Mital, M., Epenetos, A., Laing, P., et al. (2003). Polysialylated insulin: synthesis, characterization and biological activity in vivo. Biochim. *Biophys. Acta Gen. Subjects* 1622, 42–49. doi: 10.1016/S0304-4165(03)00116-118

Jeter, J. M., Bowles, T. L., Curiel-Lewandrowski, C., Swetter, S. M., Filipp, F. V., Abdel-Malek, Z. A., et al. (2019). Chemoprevention agents for melanoma: a path forward into phase 3 clinical trials. *Cancer* 125, 18–44. doi: 10.1002/cncr.31719

Jevsevar, S., Kunstelj, M., and Porekar, V. G. (2010). PEGylation of therapeutic proteins. *Biotechnol. J.* 5, 113–128. doi: 10.1002/biot.200900218

Jevševar, S., Kusterle, M., and Kenig, M. (2012). ""PEGylation of antibody fragments for half-life extension,"," in *Antibody Methods and Protocols*, eds G. Proetzel, and H. Ebersbach, (Berlin: Springer), 233–246. doi: 10.1007/978-1-61779-931-0_15

Jiang, Y., Fay, J. M., Poon, C.-D., Vinod, N., Zhao, Y., Bullock, K., et al. (2018). Nanoformulation of brain-derived neurotrophic factor with target receptor-triggered-release in the central nervous system. *Adv. Func. Mater.* 28, 1703982. doi: 10.1002/adfm.201703982

Joanitti, G. A., Sawant, R. S., Torchilin, V. P., Freitas, S. M. D., and Azevedo, R. B. (2018). Optimizing liposomes for delivery of bowman-birk protease inhibitors — platforms for multiple biomedical applications. *Coll.o Surf. BBiointerf.* 167, 474–482. doi: 10.1016/j.colsurfb.2018.04.033

Kainthan, R. K., and Brooks, D. E. (2007). In vivo biological evaluation of high molecular weight hyperbranched polyglycerols. *Biomaterials* 28, 4779–4787. doi: 10.1016/j.biomaterials.2007.07.046

Kaneda, Y., Tsutsumi, Y., Yoshioka, Y., Kamada, H., Yamamoto, Y., Kodaira, H., et al. (2004). The use of PVP as a polymeric carrier to improve the plasma half-life of drugs. *Biomaterials* 25, 3259–3266. doi: 0.1016/j.biomaterials.2003.10.003

Kaur, D., and Kumar, S. (2018). Niosomes: present scenario and future aspects. *J. Drug Deliv. Ther.* 8, 35–43. doi: 10.22270/jddt.v8i5.1886

Khan, H. M., He, T., Fuglebakk, E., Grauffel, C., Yang, B., Roberts, M. F., et al. (2016). A role for weak electrostatic interactions in peripheral membrane protein binding. *Biophys. J.* 110, 1367–1378. doi: 10.1016/j.bpj.2016.02.020

Khanna, C., Anderson, P. M., Hasz, D. E., Katsanis, E., Neville, M., and Klausner, J. S. (1997a). Interleukin-2 liposome inhalation therapy is safe and effective for dogs with spontaneous pulmonary metastases. *Cancer* 79, 1409–1421. doi: 10.1002/(sici)1097-0142(19970401)79:7<1409::aid-cncr19>3.0.co;2-3

Khanna, C., Waldrep, J. C., Anderson, P. M., Weischelbaum, R. W., Hasz, D. E., Katsanis, E., et al. (1997b). Nebulized Interleukin 2 Liposomes: aerosol Characteristics and Biodistribution. *J. Pharm. Pharmacol.* 49, 960–971. doi: 10.1111/j.2042-7158.1997.tb06024.x

Kinstler, O., Molineux, G., Treuheit, M., Ladd, D., and Gegg, C. (2002). Mono-N-terminal poly (ethylene glycol)–protein conjugates. *Adv. Drug Deliv. Rev.* 54, 477–485. doi: 10.1016/S0169-409X(02)00023-6

Kintzing, J. R., Filsinger Interrante, M. V., and Cochran, J. R. (2016). Emerging strategies for developing next-generation protein therapeutics for cancer treatment. *Trends Pharmacol. Sci.* 37, 993–1008. doi: 10.1016/j.tips.2016.10.005

Knop, K., Hoogenboom, R., Fischer, D., and Schubert, U. S. (2010). Poly (ethylene glycol) in drug delivery: pros and cons as well as potential alternatives. *Angew. Chem. Int. Ed.* 49, 6288–6308. doi: 10.1002/anie.200902672

Ko, J. H., and Maynard, H. D. (2018). A guide to maximizing the therapeutic potential of protein-polymer conjugates by rational design. *Chem. Soc. Rev.* 47, 8998–9014. doi: 10.1039/c8cs00606g

Konkle, B. A., Stasyshyn, O., Chowdary, P., Bevan, D. H., Mant, T., Shima, M., et al. (2015). Pegylated, full-length, recombinant factor VIII for prophylactic and on-demand treatment of severe hemophilia A. *Blood* 126, 1078–1085. doi: 10.1182/blood-2015-03-630897

Kopecek, J., and Kopecková, P. (2010). HPMA copolymers: origins, early developments, present, and future. *Adv. Drug Deliv. Rev.* 62, 122–149. doi: 10.1016/j.addr.2009.10.004

Kovaliov, M., Allegrezza, M. L., Richter, B., Konkolewicz, D., and Averick, S. (2018). Synthesis of lipase polymer hybrids with retained or enhanced activity using the grafting-from strategy. *Polymer* 137, 338–345. doi: 10.1016/j.polymer.2018.01.026

Kronenberg, S., Baumann, A., de Haan, L., Hinton, H. J., Moggs, J., Theil, F.-P., et al. (2013). Current challenges and opportunities in nonclinical safety testing of biologics. *Drug Discov. Today* 18, 1138–1143. doi: 10.1016/j.drudis.2013.08.003

Kullberg, M., Mann, K., and Owens, J. L. (2005). Improved drug delivery to cancer cells: a method using magnetoliposomes that target epidermal growth factor receptors. *Med. Hypotheses* 64, 468–470. doi: 10.1016/j.mehy.2004.07.033

La, S. B., Okano, T., and Kataoka, K. (1996). Preparation and characterization of the micelle-forming polymeric drug indomethacin-lncorporated polyfethylene oxide)-Poly (β-benzyl L-aspartate) block copolymer micelles. *J. Pharm. Scie.* 85, 85–90. doi: 10.1021/js950204r

Lagassé, H., Alexaki, A., Simhadri, V., Katagiri, N., Jankowski, W., Sauna, Z., et al. (2017). Recent advances in (therapeutic protein) drug development. *F1000Res.* 6, 113. doi: 10.12688/f1000research.9970.1

Leader, B., Baca, Q. J., and Golan, D. E. (2008). Protein therapeutics: a summary and pharmacological classification. *Nat. Rev. Drug Discov.* 7, 21. doi: 10.1038/nrd2399

Lee, A. G. (2004). How lipids affect the activities of integral membrane proteins. *Biochim. Biophys. Acta Biomem.* 1666, 62–87. doi: 10.1016/j.bbamem.2004.05.012

Lee, H., Jang, I. H., Ryu, S. H., and Park, T. G. (2003). N-terminal site-specific mono-PEGylation of epidermal growth factor. *Pharm. Res.* 20, 818–825. doi: 10.1023/A:1023402123119

Lee, J. C. M., Bermudez, H., Discher, B. M., Sheehan, M. A., Won, Y. Y., Bates, F. S., et al. (2001). Preparation, stability, and in vitro performance of vesicles made with diblock copolymers. *Biotechnol. Bioengin.* 73, 135–145. doi: 10.1002/bit.1045

Letchford, K., and Burt, H. (2007). A review of the formation and classification of amphiphilic block copolymer nanoparticulate structures: micelles, nanospheres, nanocapsules and polymersomes. *Eur. J. Pharm. Biopharm.* 65, 259–269. doi: 10.1016/j.ejpb.2006.11.009

Levin, D., Golding, B., Strome, S. E., and Sauna, Z. E. (2015). Fc fusion as a platform technology: potential for modulating immunogenicity. *Trends Biotechnol.* 33, 27–34. doi: 10.1016/j.tibtech.2014.11.001

Levy, H. L., Sarkissian, C. N., and Scriver, C. R. (2018). Phenylalanine ammonia lyase (PAL): from discovery to enzyme substitution therapy for phenylketonuria. *Mol. Genet. Metabol.* 124, 223–229. doi: 10.1016/j.ymgme.2018.06.002

Levy, Y., Hershfield, M. S., Fernandez-Mejia, C., Polmar, S. H., Scudiery, D., Berger, M., et al. (1988). Adenosine deaminase deficiency with late onset of recurrent infections: response to treatment with polyethylene glycol-modified adenosine deaminase. *J. Pediatr.* 113, 312–317. doi: 10.1016/S0022-3476(88)80271-3

Li, H., Li, M., Yu, X., Bapat, A. P., and Sumerlin, B. S. (2011a). Block copolymer conjugates prepared by sequentially grafting from proteins via RAFT. *Polym. Chem.* 2, 1531–1535. doi: 10.1039/C1PY00031D

Li, M., Li, H., De, P., and Sumerlin, B. S. (2011b). Thermoresponsive block copolymer–protein conjugates prepared by grafting-from via RAFT polymerization. *Macromol. Rapid Commun.* 32, 354–359. doi: 10.1002/marc.201000619

Li, P., Nielsen, H. M., and Mullertz, A. (2012). Oral delivery of peptides and proteins using lipid-based drug delivery systems. *Exp. Opin. Drug Deliv.* 9, 1289–1304. doi: 10.1517/17425247.2012.717068

Liebner, R., Bergmann, S., Hey, T., Winter, G., and Besheer, A. (2015). Freeze-drying of HESylated IFNα-2b: effect of HESylation on storage stability in comparison to PEGylation. *Int. J. Pharm.* 495, 608–611. doi: 10.1016/j.ijpharm.2015.09.031

Lipsky, P. E., Calabrese, L. H., Kavanaugh, A., Sundy, J. S., Wright, D., Wolfson, M., et al. (2014). Pegloticase immunogenicity: the relationship between efficacy and antibody development in patients treated for refractory chronic gout. *Arthritis Res. Ther.* 16, R60. doi: 10.1186/ar4497

Liu, X., Wu, F., Ji, Y., and Yin, L. (2019). Recent advances in anti-cancer protein/peptide delivery. *Bioconjug. Chem.* 30, 305–324. doi: 10.1021/acs.bioconjchem.8b00750

Liu, Y., Lee, J., Mansfield, K. M., Ko, J. H., Sallam, S., Wesderniotis, C., et al. (2017). Trehalose glycopolymer enhances both solution stability and pharmacokinetics of a therapeutic protein. *Bioconjug. Chem.* 28, 836–845. doi: 10.1021/acs.bioconjchem.6b00659

Longo, N., Harding, C. O., Burton, B. K., Grange, D. K., Vockley, J., Wasserstein, M., et al. (2014). Single-dose, subcutaneous recombinant phenylalanine ammonia lyase conjugated with polyethylene glycol in adult patients with phenylketonuria: an open-label, multicentre, phase 1 dose-escalation trial. *Lancet* 384, 37–44. doi: 10.1016/S0140-6736(13)61841-3

Lu, Y., Sun, W., and Gu, Z. (2014). Stimuli-responsive nanomaterials for therapeutic protein delivery. *J. Control. Release* 194, 1–19. doi: 10.1016/j.jconrel.2014.08.015

Luo, J., Yang, Y., Zhang, T., Su, Z., Yu, D., Lin, Q., et al. (2018). Nasal delivery of nerve growth factor rescue hypogonadism by up-regulating GnRH and testosterone in aging male mice. *EBioMed.* 35, 295–306. doi: 10.1016/j.ebiom.2018.08.021

Ma, Z., Lim, T. M., and Lim, L.-Y. (2005). Pharmacological activity of peroral chitosan–insulin nanoparticles in diabetic rats. *Int. J. Pharma.* 293, 271–280. doi: 10.1016/j.ijpharm.2004.12.025

Macdougall, I. C., and Eckardt, K.-U. (2006). Novel strategies for stimulating erythropoiesis and potential new treatments for anaemia. *Lancet* 368, 947–953. doi: 10.1016/S0140-6736(06)69120-4

Magnusson, J. P., Bersani, S., Salmaso, S., Alexander, C., and Caliceti, P. (2010). In situ growth of side-chain PEG polymers from functionalized human growth hormone? a new technique for preparation of enhanced protein- polymer conjugates. *Bioconjug. Chem.* 21, 671–678. doi: 10.1021/bc900468v

Mahlert, F., Schmidt, K., Allgaier, H., Liu, P., and Shen, W. D. (2013). Rational development of lipegfilgrastim, a novel long-acting granulocyte colony-stimulating factor, using glycopegylation Technology. *Blood* 122, 4853. doi: 10.1182/blood.v122.21.4853.4853

Mansfield, K. M., and Maynard, H. D. (2018). Site-specific insulin-trehalose glycopolymer conjugate by grafting from strategy improves bioactivity. *Acs Macro Lett.* 7, 324–329. doi: 10.1021/acsmacrolett.7b00974

Martins, S., Sarmento, B., Ferreira, D. C., and Souto, E. B. (2007). Lipid-based colloidal carriers for peptide and protein delivery - liposomes versus lipid nanoparticles. *Int. J. Nanomed.* 2, 595–607.

Mazzotta, E., Tavano, L., and Muzzalupo, R. (2018). Thermo-sensitive vesicles in controlled drug delivery for chemotherapy. *Pharmaceutics* 10, 150. doi: 10.3390/pharmaceutics10030150

McClements, D. J. (2018). Encapsulation, protection, and delivery of bioactive proteins and peptides using nanoparticle and microparticle systems: a review. *Adv. Coll. Interface Sci.* 253, 1–22. doi: 10.1016/j.cis.2018.02.002

McPherson, T., Kidane, A., Szleifer, I., and Park, K. (1998). Prevention of protein adsorption by tethered poly(ethylene oxide) layers: experiments and single-chain mean-field analysis. *Langmuir* 14, 176–186. doi: 10.1021/la9706781

Mero, A., and Campisi, M. (2014). Hyaluronic acid bioconjugates for the delivery of bioactive molecules. *Polymers* 6, 346–369. doi: 10.3390/polym6020346

Mero, A., Fang, Z., Pasut, G., Veronese, F. M., and Viegas, T. X. (2012). Selective conjugation of poly (2-ethyl 2-oxazoline) to granulocyte colony stimulating factor. *J. Control. Release* 159, 353–361. doi: 10.1016/j.jconrel.2012.02.025

Meunier, S., Alamelu, J., Ehrenforth, S., Hanabusa, H., Karim, F. A., Kavakli, K., et al. (2017). Safety and efficacy of a glycoPEGylated rFVIII (turoctocog alpha pegol, N8-GP) in paediatric patients with severe haemophilia A. *Thromb. Haemost.* 117, 1705–1713. doi: 10.1160/TH17-03-0166

Meyer, J., Whitcomb, L., and Collins, D. (1994). Efficient encapsulation of proteins within liposomes for slow release in vivo. *Biochemi. Biophys. Res. Commun.* 199, 433–438. doi: 10.1006/bbrc.1994.1247

Mima, Y., Hashimoto, Y., Shimizu, T., Kiwada, H., and Ishida, T. (2015). Anti-PEG IgM Is a major contributor to the accelerated blood clearance of polyethylene glycol-conjugated protein. *Mol. Pharm.* 12, 2429–2435. doi: 10.1021/acs.molpharmaceut.5b00144

Moghassemi, S., and Hadjizadeh, A. (2014). Nano-niosomes as nanoscale drug delivery systems: an illustrated review. *J. Contr. Release* 185, 22–36. doi: 10.1016/j.jconrel.2014.04.015

Molineux, G. (2004). The design and development of pegfilgrastim (PEG-rmetHuG-CSF, Neulasta®). *Curr. Pharm. Design* 10, 1235–1244. doi: 10.2174/1381612043452613

Mondal, K., Mehta, P., Mehta, B. R., Varandani, D., and Gupta, M. N. (2006). A bioconjugate of *Pseudomonas* cepacia lipase with alginate with enhanced catalytic efficiency. *Biochim. Biophys. Acta Proteins Proteom.* 1764, 1080–1086. doi: 10.1016/j.bbapap.2006.04.008

Morgenstern, J., Gil Alvaradejo, G., Bluthardt, N., Beloqui, A., Delaittre, G., and Hubbuch, J. (2018). Impact of polymer bioconjugation on protein stability and activity investigated with discrete conjugates: alternatives to PEGylation. *Biomacromolecules* 19, 4250–4262. doi: 10.1021/acs.biomac.8b01020

Nesbitt, A. M., Stephens, S., and Chartash, E. K. (2009). "Certolizumab pegol: a PEGylated anti-tumour necrosis factor alpha biological agent," in *PEGylated Protein Drugs: Basic Science and Clinical Applications*, ed. F. M. Veronese, (Berlin: Springer), 229–254. doi: 10.1007/978-3-7643-8679-5_14

Ning, M., Guo, Y., Pan, H., Yu, H., and Gu, Z. (2005). Niosomes with sorbitan monoester as a carrier for vaginal delivery of insulin: studies in rats. *Drug Deliv.* 12, 399–407. doi: 10.1080/10717540590968891

Noble, G. T., Stefanick, J. F., Ashley, J. D., Kiziltepe, T., and Bilgicer, B. (2014). Ligand-targeted liposome design: challenges and fundamental considerations. *Trends Biotechnol.* 32, 32–45. doi: 10.1016/j.tibtech.2013.09.007

Novo-Nordisk. (2019). Drug and Device News. *P T* 44, 170–202.

Okamoto, Y., Taguchi, K., Yamasaki, K., Sakuragi, M., Kuroda, S. I., and Otagiri, M. (2018). Albumin-encapsulated liposomes: a novel drug delivery carrier with hydrophobic drugs encapsulated in the inner aqueous core. *J. Pharm. Sci.* 107, 436–445. doi: 10.1016/j.xphs.2017.08.003

Olusanya, T. O. B., Haj Ahmad, R. R., Ibegbu, D. M., Smith, J. R., and Elkordy, A. A. (2018). Liposomal drug delivery systems and anticancer drugs. *Molecules* 23, 907. doi: 10.3390/molecules23040907

O'Neil, C. P., Suzuki, T., Demurtas, D., Finka, A., and Hubbell, J. A. (2009). A novel method for the encapsulation of biomolecules into polymersomes via direct hydration. *Langmuir* 25, 9025–9029. doi: 10.1021/la900779t

Østergaard, H., Bjelke, J. R., Hansen, L., Petersen, L. C., Pedersen, A. A., Elm, T., et al. (2011). Prolonged half-life and preserved enzymatic properties of factor IX selectively PEGylated on native N-glycans in the activation peptide. *Blood* 118, 2333–2341. doi: 10.1182/blood-2011-02-336172

Owens, D. E., and Peppas, N. A. (2006). Opsonization, biodistribution, and pharmacokinetics of polymeric nanoparticles. *Int. J. Pharm.* 307, 93–102. doi: 10.1016/j.ijpharm.2005.10.010

Pachioni-Vasconcelos, J. D. A., Lopes, A. M., Apolinário, A. C., Valenzuela-Oses, J. K., Costa, J. S. R., Nascimento, L. D. O., et al. (2016). Nanostructures for protein drug delivery. *Biomater. Sci.* 4, 205–218. doi: 10.1039/c5bm00360a

Paik, J., and Deeks, E. D. (2019). damoctocog alfa pegol: a review in haemophilia A. *Drugs* 79, 1147–1156. doi: 10.1007/s40265-019-011527

Paleos, C. M., Sideratou, Z., and Tsiourvas, D. (2017). Drug delivery systems based on hydroxyethyl starch. *Bioconjug. Chem.* 28, 1611–1624. doi: 10.1021/acs.bioconjchem.7b00186

Pan, Y., Li, Y.-J., Zhao, H.-Y., Zheng, J.-M., Xu, H., Wei, G., et al. (2002). Bioadhesive polysaccharide in protein delivery system: chitosan nanoparticles improve the intestinal absorption of insulin in vivo. *Int. J. Pharm.* 249, 139–147. doi: 10.1016/S0378-5173(02)00486-6

Parkinson, C., Scarlett, J., and Trainer, P. J. (2003). Pegvisomant in the treatment of acromegaly. *Adv. Drug Deliv. Rev* 55, 1303–1314. doi: 10.1159/000381644

Patel, J. N., and Walko, C. M. (2012). Sylatron: a pegylated interferon for use in melanoma. *Ann. Pharm.* 46, 830–838. doi: 10.1345/aph.1Q791

Pattni, B. S., Chupin, V. V., and Torchilin, V. P. (2015). New developments in liposomal drug delivery. *Chem. Rev.* 115, 10938–10966. doi: 10.1021/acs.chemrev.5b00046

Pelegri-O'Day, E. M., Lin, E.-W., and Maynard, H. D. (2014). Therapeutic protein–polymer conjugates: advancing beyond PEGylation. *J. Am. Chem. Soc.* 136, 14323–14332. doi: 10.1021/ja504390x

Pelegri-O'Day, E. M., and Maynard, H. D. (2016). Controlled radical polymerization as an enabling approach for the next generation of protein–polymer conjugates. *Acc. Chem. Res.* 49, 1777–1785. doi: 10.1021/acs.accounts.6b00258

Pfister, D., and Morbidelli, M. (2014). Process for protein PEGylation. *J. Control. Rel.* 180, 134–149. doi: 10.1016/j.jconrel.2014.02.002

Piedmonte, D. M., and Treuheit, M. J. (2008). Formulation of Neulasta® (pegfilgrastim). *Adv. Drug Deliv. Rev.* 60, 50–58. doi: 10.1016/j.addr.2007.04.017

Pradhananga, S., Wilkinson, I., and Ross, R. J. (2002). Pegvisomant: structure and function. *J. f Mol. Endocrinol.* 29, 11–14. doi: 10.1677/jme.0.0290011

Ravasco, J. M. J. M., Faustino, H., Trindade, A., and Gois, P. M. P. (2019). Bioconjugation with maleimides: a useful tool for chemical biology. *Chem.A Eur. J.* 25, 43–59. doi: 10.1002/chem.201803174

Reddy, S. T., van der Vlies, A. J., Simeoni, E., Angeli, V., Randolph, G. J., O'Neil, C. P., et al. (2007). exploiting lymphatic transport and complement activation in nanoparticle vaccines. *Nat. Biotechnol.* 25, 1159–1164. doi: 10.1038/nbt1332

Riaz, M. K., Riaz, M. A., Zhang, X., Lin, C., Wong, K. H., Chen, X., et al. (2018). Surface functionalization and targeting strategies of liposomes in solid tumor therapy: a review. *Int. J. Mol. Sci.* 19, 195. doi: 10.3390/ijms19010195

Richter, A. W., and Åkerblom, E. (1984). Polyethylene glycol reactive antibodies in man: titer distribution in allergic patients treated with monomethoxy polyethylene glycol modified allergens or placebo, and in healthy blood donors. *Int. Arch. Allergy Immunol.* 74, 36–39. doi: 10.1159/000233512

Roohnikan, M., Laszlo, E., Babity, S., and Brambilla, D. (2019). A snapshot of transdermal and topical drug delivery research in Canada. *Pharmaceutics* 11, E256. doi: 10.3390/pharmaceutics11060256

Rudmann, D. G., Alston, J. T., Hanson, J. C., and Heidel, S. (2013). High molecular weight polyethylene glycol cellular distribution and peg-associated cytoplasmic vacuolation is molecular weight dependent and does not require conjugation to proteins. *Toxicol. Pathol.* 41, 970–983. doi: 10.1177/0192623312474726

Salmaso, S., and Caliceti, P. (2011). "Peptide and protein bioconjugation: a useful tool to improve the biological performance of biotech drugs," in *Peptide and*

Protein Delivery, ed. C. Van Der Walle, (Amsterdam: Elsevier), 247–290. doi: 10.1016/b978-0-12-384935-9.10011-2

Samed, N., Sharma, V., and Sundaramurthy, A. (2018). Hydrogen bonded niosomes for encapsulation and release of hydrophilic and hydrophobic anti-diabetic drugs: an efficient system for oral anti-diabetic formulation. *Appl. Surface Sci.* 449, 567–573. doi: 10.1016/j.apsusc.2017.11.055

Santo, I. E., Campardelli, R., Albuquerque, E. C., de Melo, S. V., Della Porta, G., and Reverchon, E. (2014). Liposomes preparation using a supercritical fluid assisted continuous process. *Chem. Eng. J.* 249, 153–159. doi: 10.1016/j.cej.2014.03.099

Scales, C. W., Vasilieva, Y. A., Convertine, A. J., Lowe, A. B., and McCormick, C. L. (2005). Direct, controlled synthesis of the nonimmunogenic, hydrophilic polymer, poly (N-(2-hydroxypropyl) methacrylamide) via RAFT in aqueous media. *Biomacromolecules* 6, 1846–1850. doi: 10.1021/bm0503017

Schellekens, H., Hennink, W. E., and Brinks, V. (2013). The immunogenicity of polyethylene glycol: facts and fiction. *Pharm. Res.* 30, 1729–1734. doi: 10.1007/s11095-013-1067-7

Schellenberger, V., Wang, C.-W., Geething, N. C., Spink, B. J., Campbell, A., To, W., et al. (2009). A recombinant polypeptide extends the in vivo half-life of peptides and proteins in a tunable manner. *Nat. Biotechno.* 27, 1186. doi: 10.1038/nbt.1588

Schlapschy, M., Binder, U., Börger, C., Theobald, I., Wachinger, K., Kisling, S., et al. (2013). PASylation: a biological alternative to PEGylation for extending the plasma half-life of pharmaceutically active proteins. *Protein Eng., Des. Sel.* 26, 489–501. doi: 10.1093/protein/gzt023

Schlesinger, N., Yasothan, U., and Kirkpatrick, P. (2010). Pegloticase. *Nat. Rev. Drug Discov.* 10, 17. doi: 10.1038/nrd3349

Sercombe, L., Veerati, T., Moheimani, F., Wu, S. Y., Sood, A. K., and Hua, S. (2015). Advances and challenges of liposome assisted drug delivery. *Front. Pharmacol.* 6:286. doi: 10.3389/fphar.2015.00286

Shah, A., Coyle, T., Lalezari, S., Kohlstaedde, B., and Michaels, L. (2014). pharmacokinetics of Bay 94-9027, a Pegylated B-domain-deleted recombinant factor Viii with an extended half-life, in patients with severe hemophilia A. *Haemophilia* 20, 22. doi: 10.1111/hae.12980

Shannon, J. A., and Cole, S. W. (2012). Pegloticase: a novel agent for treatment-refractory gout. *Ann. Pharm.* 46, 368–376. doi: 10.1345/aph.1Q593

Sherman, M. R., Saifer, M. G., and Perez-Ruiz, F. (2008). PEG-uricase in the management of treatment-resistant gout and hyperuricemia. *Adv. Drug Deliv. Rev.* 60, 59–68. doi: 10.1016/j.addr.2007.06.011

Sherman, M. R., Williams, L. D., Sobczyk, M. A., Michaels, S. J., and Saifer, M. G. P. (2012). Role of the Methoxy Group in Immune Responses to mPEG-Protein Conjugates. *Bioconjug.te Chem.* 23, 485–499. doi: 10.1021/bc200551b

Shukla, T., Upmanyu, N., Agrawal, M., Saraf, S., Saraf, S., and Alexander, A. (2018). Biomedical applications of microemulsion through dermal and transdermal route. *Biomed. Pharm.* 108, 1477–1494. doi: 10.1016/j.biopha.2018.10.021

Simakova, A., Averick, S. E., Konkolewicz, D., and Matyjaszewski, K. (2012). Aqueous arget atrp. *Macromolecules* 45, 6371–6379. doi: 10.1021/ma301303b

Skubitz, K. M., and Anderson, P. M. (2000). Inhalational interleukin-2 liposomes for pulmonary metastases: a phase I clinical trial. *Anticancer Drugs* 11, 555–563. doi: 10.1097/00001813-200008000-00006

Soares, S., Sousa, J., Pais, A., and Vitorino, C. (2018). Nanomedicine: principles, properties, and regulatory issues. *Front. Chem.* 6:360. doi: 10.3389/fchem.2018.00360

Steinbach, T., Becker, G., Spiegel, A., Figueiredo, T., Russo, D., and Wurm, F. R. (2017). Reversible bioconjugation: biodegradable poly(phosphate)-protein conjugates. *Macrom. Biosci.* 17, 9. doi: 10.1002/mabi.201600377

Stidl, R., Denne, M., Goldstine, J., Kadish, B., Korakas, I. K., and Turecek, L. P. (2018). Polyethylene glycol exposure with antihemophilic factor (Recombinant), PEGylated (rurioctocog alfa pegol) and other therapies indicated for the pediatric population: history and safety. *Pharmaceuticals* 11, E75. doi: 10.3390/ph11030075

Stidl, R., Fuchs, S., Bossard, M., Siekmann, J., Turecek, P. L., and Putz, M. (2016). Safety of PEGylated recombinant human full-length coagulation factor VIII (BAX 855) in the overall context of PEG and PEG conjugates. *Haemophilia* 22, 54–64. doi: 10.1111/hae.12762

Tan, M. L., Choong, P. F. M., and Dass, C. R. (2010). Recent developments in liposomes, microparticles and nanoparticles for protein and peptide drug delivery. *Peptides* 31, 184–193. doi: 10.1016/j.peptides.2009.10.002

Tan, M. X. L., and Danquah, M. K. (2012). Drug and protein encapsulation by emulsification: technology enhancement using foam formulations. *Chem. Eng. Technol.* 35, 618626. doi: 10.1002/ceat.201100358

Tiede, A. (2015). Half-life extended factor VIII for the treatment of hemophilia A. *J. Thromb. Haemost.* 13, S176–S179. doi: 10.1111/jth.12929

Trucillo, P., Campardelli, R., and Reverchon, E. (2019). A versatile supercritical assisted process for the one-shot production of liposomes. *J. Supercrit. Fluids* 146, 136–143. doi: 10.1016/j.supflu.2019.01.015

Tsai, H. J., Jiang, S. S., Hung, W. C., Borthakur, G., Lin, S. F., Pemmaraju, N., et al. (2017). A phase II study of arginine deiminase (ADI-PEG20) in relapsed/refractory or poor-risk acute myeloid leukemia patients. *Sci. Rep.* 7, 11253. doi: 10.1038/s41598-017-10542-4

Turecek, P. L., Bossard, M. J., Schoetens, F., and Ivens, I. A. (2016). PEGylation of biopharmaceuticals: a review of chemistry and nonclinical safety information of approved drugs. *J.Pharm. Sci.* 105, 460–475. doi: 10.1016/j.xphs.2015.11.015

van't Hag, L., Shen, H.-H., Lin, T.-W., Gras, S. L., Drummond, C. J., and Conn, C. E. (2016). Effect of lipid-based nanostructure on protein encapsulation within the membrane bilayer mimetic lipidic cubic phase using transmembrane and lipoproteins from the beta-barrel assembly machinery. *Langmuir* 32, 12442–12452. doi: 10.1021/acs.langmuir.6b01800

Vemuri, S., and Rhodes, C. T. (1995). Preparation and characterization of liposomes as therapeutic delivery systems: a review. *Pharm. Acta Helv.* 70, 95–111. doi: 10.1016/0031-6865(95)00010-7

Verhoef, J. J. F., Carpenter, J. F., Anchordoquy, T. J., and Schellekens, H. (2014). Potential induction of anti-PEG antibodies and complement activation toward PEGylated therapeutics. *Drug Discov. Today* 19, 1945–1952. doi: 10.1016/j.drudis.2014.08.015

Vermonden, T., Censi, R., and Hennink, W. E. (2012). Hydrogels for protein delivery. *Chem. Rev.* 112, 2853–2888. doi: 10.1021/cr200157d

Veronese, F. M., and Pasut, G. (2005). PEGylation, successful approach to drug delivery. *Drug Discov. Today* 10, 1451–1458. doi: 10.1016/S1359-6446(05)03575-0

Viegas, T. X., Bentley, M. D., Harris, J. M., Fang, Z., Yoon, K., Dizman, B., et al. (2011). Polyoxazoline: chemistry, properties, and applications in drug delivery. *Bioconjug. Chem.* 22, 976–986. doi: 10.1021/acs.bioconjchem.9b00236

Vila-Caballer, M., Codolo, G., Munari, F., Malfanti, A., Fassan, M., Rugge, M., et al. (2016). A pH-sensitive stearoyl-PEG-poly(methacryloyl sulfadimethoxine)-decorated liposome system for protein delivery: an application for bladder cancer treatment. *J. Control. Release* 238, 31–42. doi: 10.1016/j.jconrel.2016.07.024

Waisman, D., Danino, D., Weintraub, Z., Schmidt, J., and Talmon, Y. (2007). Nanostructure of the aqueous form of lung surfactant of different species visualized by cryo-transmission electron microscopy. *Clin. Phys. Func. Imaging* 27, 375–380. doi: 10.1111/j.1475-097X.2007.00763.x

Wallat, J. D., Rose, K. A., and Pokorski, J. K. (2014). Proteins as substrates for controlled radical polymerization. *Polym. Chem.* 5, 1545–1558. doi: 10.1039/C3PY01193C

Walsh, G. (2018). Biopharmaceutical benchmarks 2018. *Nat. Biotechnol.* 36, 1136. doi: 10.1038/nbt.4305

Walther, F. J., Gordon, L. M., Zasadzinski, J. A., Sherman, M. A., and Waring, A. J. (2000). Surfactant protein B and C analogues. *Mol. Genet. Metabol.* 71, 342–351. doi: 10.1006/mgme.2000.3053

Wang, X., Song, Y., Su, Y., Tian, Q., Li, B., Quan, J., et al. (2016). Are PEGylated liposomes better than conventional liposomes? A special case for vincristine. *Drug Deliv.* 23, 1092–1100. doi: 10.3109/10717544.2015.1027015

Wang, Y.-S., Youngster, S., Grace, M., Bausch, J., Bordens, R., and Wyss, D. F. (2002). Structural and biological characterization of pegylated recombinant interferon alpha-2b and its therapeutic implications. *Adv. Drug Deliv. Rev.* 54, 547–570. doi: 10.1016/S0169-409X(02)00027-3

Wu, J., Kamaly, N., Shi, J., Zhao, L., Xiao, Z., Hollett, G., et al. (2014). Development of multinuclear polymeric nanoparticles as robust protein nanocarriers. *Angew. Chem. Int. Ed.* 53, 8975–8979. doi: 10.1002/anie.201404766

Wurm, F., Dingels, C., Frey, H., and Klok, H.-A. (2012). Squaric acid mediated synthesis and biological activity of a library of linear and hyperbranched poly(Glycerol)–protein conjugates. *Biomacromolecules* 13, 1161–1171. doi: 10.1021/bm300103u

Wynn, T. T., and Gumuscu, B. (2016). Potential role of a new PEGylated recombinant factor VIII for hemophilia A. *J.Blood Med.* 7, 121. doi: 10.2147/JBM

Xiang, Q., Xiao, J., Zhang, H., Zhang, X., Lu, M., Zhang, H., et al. (2011). Preparation and characterisation of bFGF-encapsulated liposomes and evaluation of wound-healing activities in the rat. *Burns* 37, 886–895. doi: 10.1016/j.burns.2011.01.018

Xie, Y., Ye, L., Zhang, X., Cui, W., Lou, J., Nagai, T., et al. (2005). Transport of nerve growth factor encapsulated into liposomes across the blood–brain barrier: in vitro and in vivo studies. *J. Control. Release* 105, 106–119. doi: 10.1016/j.jconrel.2005.03.005

Xu, X., Costa, A., and Burgess, D. J. (2012). Protein Encapsulation in unilamellar liposomes: high encapsulation efficiency and a novel technique to assess lipid-protein interaction. *Pharm. Res.* 29, 1919–1931. doi: 10.1007/s11095-012-0720-x

Xu, Y., Zheng, Y., Wu, L., Zhu, X., Zhang, Z., and Huang, Y. (2018). Novel solid lipid nanoparticle with endosomal escape function for oral delivery of insulin. *ACS Appl. Mat. Interfaces* 10, 9315–9324. doi: 10.1021/acsami.8b00507

Xue, X., Li, D., Yu, J., Ma, G., Su, Z., and Hu, T. (2013). Phenyl linker-induced dense PEG conformation improves the efficacy of C-terminally monoPEGylated staphylokinase. *Biomacromolecules* 14, 331–341. doi: 10.1021/bm301511w

Yadav, V. R., Rao, G., Houson, H., Hedrick, A., Awasthi, S., Roberts, P. R., et al. (2016). Nanovesicular liposome-encapsulated hemoglobin (LEH) prevents multi-organ injuries in a rat model of hemorrhagic shock. *Eur. J. Pharm. Sci* 93, 97–106. doi: 10.1016/j.ejps.2016.08.010

Yan, M., Du, J., Gu, Z., Liang, M., Hu, Y., Zhang, W., et al. (2009). A novel intracellular protein delivery platform based on single-protein nanocapsules. *Nat. Nanotechnol.* 5, 48. doi: 10.1038/nnano.2009.341

Yang, J.-A., Kim, E.-S., Kwon, J. H., Kim, H., Shin, J. H., Yun, S. H., et al. (2012). Transdermal delivery of hyaluronic acid–human growth hormone conjugate. *Biomaterials* 33, 5947–5954. doi: 10.1016/j.biomaterials.2012.05.003

Yang, J.-A., Park, K., Jung, H., Kim, H., Hong, S. W., Yoon, S. K., et al. (2011). Target specific hyaluronic acid–interferon alpha conjugate for the treatment of hepatitis C virus infection. *Biomaterials* 32, 8722–8729. doi: 10.1016/j.biomaterials.2011.07.088

Yang, Q., and Lai, S. K. (2015). Anti-PEG immunity: emergence, characteristics, and unaddressed questions. *Wiley Interdiscip. Rev. Nanomed. Nanobiotechnol.* 7, 655–677. doi: 10.1002/wnan.1339

Yarosh, D., Klein, J., O'Connor, A., Hawk, J., Rafal, E., and Wolf, P. (2001). Effect of topically applied T4 endonuclease V in liposomes on skin cancer in xeroderma pigmentosum: a randomised study. *Lancet* 357, 926–929. doi: 10.1016/S0140-6736(00)04214-8

Yaşayan, G., Saeed, A. O., Fernández-Trillo, F., Allen, S., Davies, M. C., Jangher, A., et al. (2011). Responsive hybrid block co-polymer conjugates of proteins–controlled architecture to modulate substrate specificity and solution behaviour. *Polym. Chem.* 2, 1567–1578. doi: 10.1039/C1PY00128K

Yin, L., Chen, X., Vicini, P., Rup, B., and Hickling, T. P. (2015). Therapeutic outcomes, assessments, risk factors and mitigation efforts of immunogenicity of therapeutic protein products. *Cell. Immunol.* 295, 118–126. doi: 10.1016/j.cellimm.2015.03.002

Youngster, S., Wang, Y.-S., Grace, M., Bausch, J., Bordens, R., and Wyss, D. F. (2002). Structure, biology, and therapeutic implications of pegylated interferon alpha-2b. *Curr. Pharm. De.* 8, 2139–2157. doi: 10.2174/1381612023393242

Zaghmi, A., Mendez-Villuendas, E., Greschner, A. A., Liu, J. Y., de Haan, H. W., and Gauthier, M. A. (2019). Mechanisms of activity loss for a multi-PEGylated protein by experiment and simulation. *Mater.Today Chem.* 12, 121–131. doi: 10.1016/j.mtchem.2018.12.007

Zalipsky, S. (1995). Functionalized poly (ethylene glycols) for preparation of biologically relevant conjugates. *Bioconjug. Chem.* 6, 150–165. doi: 10.1021/bc00032a002

Zalipsky, S., Hansen, C. B., Oaks, J. M., and Allen, T. M. (1996). Evaluation of blood clearance rates and biodistribution of poly (2 oxazoline) grafted liposomes. *J. Pharm. Sci.* 85, 133–137. doi: 10.1021/js9504043

Zelikin, A. N., Such, G. K., Postma, A., and Caruso, F. (2007). Poly (vinylpyrrolidone) for bioconjugation and surface ligand immobilization. *Biomacromolecules* 8, 2950–2953. doi: 10.1021/bm700498j

Zheng, J., Li, L., Chen, S., and Jiang, S. (2004). Molecular simulation study of water interactions with oligo (ethylene glycol)-terminated alkanethiol self-assembled monolayers. *Langmuir* 20, 8931–8938. doi: 10.1021/la036345n

Zheng, J., Li, L., Tsao, H.-K., Sheng, Y.-J., Chen, S., and Jiang, S. (2005). Strong repulsive forces between protein and oligo (ethylene glycol) self-assembled monolayers: a molecular simulation study. *Biophys. J.* 89, 158–166. doi: 10.1529/biophysj.105.059428

Conflict of Interest: The authors declare that the research was conducted in the absence of any commercial or financial relationships that could be construed as a potential conflict of interest.

frontiers in Bioengineering and Biotechnology

REVIEW
published: 18 February 2020
doi: 10.3389/fbioe.2020.00079

Nanoscale Drug Delivery Systems: From Medicine to Agriculture

Pablo Vega-Vásquez[1], *Nathan S. Mosier*[1] *and Joseph Irudayaraj*[2,3]*

[1] *Laboratory of Renewable Resources Engineering, Department of Agricultural and Biological Engineering, Purdue University, West Lafayette, IN, United States,* [2] *Department of Agricultural and Biological Engineering, Purdue University, West Lafayette, IL, United States,* [3] *Department of Bioengineering, University of Illinois at Urbana-Champaign, Champaign, IL, United States*

The main challenges in drug delivery systems are to protect, transport and release biologically active compounds at the right time in a safe and reproducible manner, usually at a specific target site. In the past, drug nano-carriers have contributed to the development of precision medicine and to a lesser extent have focused on its inroads in agriculture. The concept of engineered nano-carriers may be a promising route to address confounding challenges in agriculture that could perhaps lead to an increase in crop production while reducing the environmental impact associated with crop protection and food production. The main objective of this review is to contrast the advantages and disadvantages of different types of nanoparticles and nano-carriers currently used in the biomedical field along with their fabrication methods to discuss the potential use of these technologies at a larger scale in agriculture. Here we explain what is the problem that nano-delivery systems intent to solve as a technological platform and describe the benefits this technology has brought to medicine. Also here we highlight the potential drawbacks that this technology may face during its translation to agricultural applications, based on the lessons learned so far from its use for biomedical purposes. We discuss not only the characteristics of an ideal nano-delivery system, but also the potential constraints regarding the fabrication including technical, environmental, and legal aspects. A key motivation is to evaluate the potential use of these systems in agriculture, especially in the area of plant breeding, growth promotion, disease control, and post-harvest quality control. Further, we highlight the importance of a rational design of nano-carriers and identify current research gaps to enable scale-up relevant to applications in the treatment of plant diseases, controlled release of fertilizers, and plant breeding.

Keywords: drug delivery systems, nanotechnology, agriculture, encapsulation, phytonanotechnology

OPEN ACCESS

Edited by:
Filippo Rossi,
Politecnico di Milano, Italy

Reviewed by:
Madhuri Sharon,
Walchand Centre for Research in Nanotechnology & Bionanotechnology, India
Umberto Capasso Palmiero,
ETH Zürich, Switzerland

***Correspondence:**
Joseph Irudayaraj
jirudaya@illinois.edu

Specialty section:
This article was submitted to Nanobiotechnology, a section of the journal Frontiers in Bioengineering and Biotechnology

Received: *24 October 2019*
Accepted: *29 January 2020*
Published: *18 February 2020*

Citation:
Vega-Vásquez P, Mosier NS and Irudayaraj J (2020) Nanoscale Drug Delivery Systems: From Medicine to Agriculture. Front. Bioeng. Biotechnol. 8:79. doi: 10.3389/fbioe.2020.00079

INTRODUCTION

The potency and efficacy of an exogenously administrated bioactive molecule heavily depend on the extent of its prolonged availability in the intended final site of action. In turn, its availability depends on the intrinsic factors related to the nature of the molecule itself, such as its solubility (Savjani et al., 2012), pKa (Manallack, 2007), affinity for the receptor (Rang, 2006), molecular weight (Lajiness et al., 2004), among others. These characteristics largely influence the membrane permeability of the molecules and therefore, its capability to ingress to the target cell and produce its biological activity in it. On the other hand, some extrinsic factors such as the physiological stage of the receptor organism, enzymatic machinery, and external pH in

the surrounding environment, make the drug prone to inactivation or degradation. Moreover, some other substances encountered throughout the organisms during the distribution process may interact with the drug in different ways resulting in either inactivation by the formation of molecular complexes, or either synergistic or antagonistic interactions (Foucquier and Guedj, 2015) which may modulate the potency of the drug or generate unexpected responses (FDA, 2012). After its administration, the processes of absorption, distribution throughout the circulatory system and subsequent metabolism may lead to physicochemical modifications due to the dynamic interaction with its new surrounding environment.

In order to successfully execute its therapeutic effect, a bioactive molecule must overcome every unfavorable physiological condition to reach its target in such a way that, a proper amount of active compound (i.e., adjusted within its therapeutic window) enters the target cell at a proper time. The challenge of drug delivery is to accomplish the release of the drug agents at the right time in a safe and reproducible manner, usually to a specific target site.

Drug delivery systems are engineered devices used to transport a pharmaceutical compound throughout the body in order to release its therapeutic cargo in a controlled manner (NIH, 2016). By encapsulating the molecules within a protective shell-like structure, potential physical-chemical or enzymatic disruptions of the active compound are diminished. In turn, not only the bioavailability of the active compound is increased but also undesirable side effects resulting from unspecific systemic distribution are reduced (Felice et al., 2014). Nano-encapsulation of bioactive compounds helps to reduce the frequency of dosing needed during treatment and also may confer physical protection to the drug during storage prior to its use for controlled release of cargo (Choudhury et al., 2017).

One of the most notable advantages offered by nano-delivery systems for drug therapy is the controlled drug release not only at a specific location level but in a time-dependent manner via passive or active targeting. Passive targeting drug nano-carrier is designed based on pathophysiological features from the targeted tissue that allow the accumulation of the nano-sized delivery system on it. On the other hand, active targeting refers to the coupling or assembly of surface-active ligands onto the surface of the drug delivery systems, which are able to recognize and interact with a receptor in the target cell. As a result of the interaction between ligands and receptors, the drug delivery specificity and nanoparticle up-take is enhanced (Felice et al., 2014). Different types of ligands have been successfully tested *in vitro* such as engineered antibodies, growth factors (Lee et al., 2010), vitamins (Chen et al., 2010), and aptamers (Colombo et al., 2015). Describing the complete pathway which had to take the controlled drug delivery systems from their very origins to their current state is not within the scope of this review. However, a highly detailed review describing the evolution of controlled drug delivery systems from their non-biodegradable macro-scaled state, up to the more updated biocompatible nano-carriers used in therapeutics is available (Hoffman, 2008).

The challenge of drug delivery is to accomplish the release of the drug agents at the right time in a safe and reproducible manner, usually to a specific target site. In this sense, medicine and agriculture share similar challenges and final goals. Similarly, nano delivery systems that have contributed to the development of precision medicine by delivering therapeutic molecules in a controlled manner have potential applications in agriculture. For instance, the use of encapsulated agrochemicals into nano-carriers to deliver pesticides to the desired crop to provide a focused delivery of the required dose (i.e., diminished application dosages), time-controlled release, and less eco-toxicity is not only an expanding area of research but a potential growth market (Slattery et al., 2019). Other areas within agriculture that could benefit from nano-encapsulation approaches include plant breeding (Kim et al., 2015), plant nutrition (Rai et al., 2015), growth promotion (Siddiqui and Al-Whaibi, 2015), disease control (Nuruzzaman et al., 2016), and post-harvest quality control (Yadollahi et al., 2010) to name a few. Conversely, agricultural materials such as cellulose (Bhandari et al., 2017, 2018) and chitosan (Cai and Lapitsky, 2019) have been used as base materials to develop drug delivery systems.

Nano-carriers intended for drug delivery can be prepared from a variety of materials such as proteins, polysaccharides, synthetic polymers and inorganic metallic salts (Panchapakesan et al., 2011; Wang et al., 2012). The selection of matrix materials depends on many factors such as the size of nanoparticles required; the physical properties of the drug (e.g., aqueous solubility and stability); the surface characteristics such as charge and permeability; the degree of biodegradability, biocompatibility and toxicity; drug release characteristics of the final product; and challenges involved in regulatory approvals. Scalability and approval from regulatory governmental entities are two other major concerns when the intention is to release a product to the market, which are closely related to the formulation and fabrication. The main objective of this review is to contrast the advantages and disadvantages of different types of nanoparticles and nano-carriers currently used in the biomedical field along with their fabrication methods to discuss the potential use of these technologies at a larger scale in agriculture. We also aim to highlight and discuss the applications of nano-encapsulation technology in agriculture and its potential drawbacks. Specifically, we address the use of nano-delivery systems as a non-viral vector for gene delivery in plant cells, and for the delivery of nutrients during plant growth promotion and crop protection.

NANO-DRUG DELIVERY SYSTEMS FROM THE ENGINEERING PERSPECTIVE

Ideally, nano delivery systems should fulfill certain technical and economical requirements. **Table 1** presents a summary of the characteristics of an ideal nano-carrier for biomedical and agricultural purposes. First, the materials used as carriers should not trigger any adverse response in the recipient organism. Also, not only the matrix material should be biocompatible, but its degradation products. Second, the mechanical properties of the polymer must provide prolonged protection to its cargo allowing chemical stability over time. Third, the scalability of

TABLE 1 | Characteristics of an ideal nano-carrier for agricultural purposes.

Fabrication conditions	Encapsulation properties	Release profile
✓ Mild conditions ✓ Scalable ✓ Low-cost ✓ Reproducible ✓ Low batch-to-batch variability	✓Stable ✓ No early cargo release/leakage ✓ Non-toxic ✓ Biodegradable ✓ Eco-compatible Water soluble	✓Controlled ✓ Targeted ✓ Stimuli sensitive (pH, light, temperature)

the fabrication process should be technologically feasible and economically viable. Accordingly, the processes employed for the elaboration of nano-carriers should yield consistent results in a batch to batch basis, in terms of size, polydispersity, encapsulation efficiency, and stability. Finally, the materials to act as nano-carriers should be carefully selected since they not only must meet the technical criteria to address mandatory regulations prior to being commercialized (Tinkle et al., 2014), but they also must display good performance in terms of cost/benefit and eco-compatibility.

Table 2 presents a summary of the advantages and disadvantages of drug delivery nano-carriers with potential use in agriculture. In general, drug nano-encapsulation depends on the physicochemical nature of the encapsulation matrix, the cargo, and the method to carry out the process. However, regardless of the encapsulation matrix and cargo nature; or the method used to fabricate the drug-loaded nano-carriers, a plethora of reports confirm that some processes to elaborate them have the potential to be standardized since their reproducibility is fairly consistent.

NANOPARTICLES AND NANO-CARRIERS FOR AGRICULTURE: ADVANTAGES AND DISADVANTAGES

Metallic Nanoparticles

Due to their chemical nature, metallic nanoparticles such as gold and silver display enhanced physicochemical properties when presented as nanometric particles. Taking advantage of these properties, major efforts on research has focused on the development of devices, predominantly in the biomedical field, for detection and treatment. Chemical sensors are one of the most prominent biomedical applications of metallic nanoparticles (Guo and Irudayaraj, 2011). For instance, gold nanoparticles conjugated with specific oligonucleotides can sense complementary deoxyribonucleic acid (DNA) strands, detectable by color changes (Kouassi and Irudayaraj, 2006). Furthermore, gold nanoparticles can be readily functionalized with antibodies and oligonucleotides (Orendorff et al., 2006; Yu and Irudayaraj, 2007; Sun and Irudayaraj, 2009a,b; Wang et al., 2010; Wang and Irudayaraj, 2013;), enzymes (Majouga et al., 2015). These hybrid nanostructures are also active elements of a number of biosensor assays to detect gene products in plants (Kadam et al., 2014, 2017), drug and gene delivery systems (Ding et al., 2014). Although metallic nanoparticles are widely used in detection, these have limited applications as delivery systems.

Mesoporous Silicon-Based Nano-Carriers (MPSNPs)

Silicon-based mesoporous materials belong to the group of inorganic nano-carriers widely used as drug delivery systems. This approach takes advantage of the highly stable porous surface of silicon mesoporous materials to fill with bioactive cargo. Ideally, loaded pores are capped and the cargo is released intracellularly (Xu et al., 2019). One of the main advantages of MPSNPs is their stability, which confers the ability to cope with physical stress such as temperature and pH variations in their surrounding environment. Moreover, their tunable and uniform pore size (3–50 nm) allows them not only to load relatively high amounts of drug cargo due to their high surface area and large pore volume but to selectively functionalize candidate molecules onto its surface (Perez et al., 2017; See **Figure 1**). Different synthesis protocols to obtain fine-tuned large-pore mesoporous nano-carriers and their suitability in the delivery of proteins, enzymes, antibodies, and nucleic acids were explored (Knezevic, 2015).

The extended use of silicon-based mesoporous nano-carriers in clinical applications has been delayed due to the lack of pharmacokinetic-pharmacodynamic studies concerning biodistribution, clearance, therapeutic efficacy, and safety are important parameters that need further attention in the quest of providing competent porous nanoparticles (Shahbazi et al., 2012) For instance, it has been demonstrated that mesoporous silica nanoparticles is not completely hemo-compatible; such phenomena have been attributed to the surface density of silanol groups interacting with the surface of phospholipids or the red blood cell membranes resulting in hemolysis (Zhao et al., 2011). One of the potential drawbacks of the use of MPSNPs in agriculture is its non-biodegradability and lack of data on bioaccumulation to meet regulatory standards.

However, due to their intrinsic physico-chemical properties, the scope of use of MPSNPs include a wide range of applications such as: (i) water decontamination through adsorption of radioactive pollutants (Iqbal and Yun, 2018), separation of dyes (Shinde et al., 2017); (ii) catalysis (Verho et al., 2014; Munz et al., 2016); (iii) delivery of agrochemicals (Yi et al., 2015); (iv) chromatography (Ahmed et al., 2014) to mention a few.

Solid Lipid Nanoparticles (SLN)

Solid lipid nanoparticles (SLN) (**Figure 2**) are spherical nanoparticles, which makes these ideal candidates for the encapsulation of lipophilic bioactive compounds. The main advantage of SLN relies on their relatively low fabrication cost with the potential for scaling-up of production (Pallerla and Prabhakar, 2013). However, potential disadvantages for its use in agriculture include poor cargo loading capacity and early cargo expulsion after polymorphic transition during storage (Singhal et al., 2011; Pardeshi et al., 2012).

SLN have been successfully implemented in a wide range of applications. In the biomedical field, for instance, it has been used to increase both the solubility of several poorly soluble

TABLE 2 | Summary of advantages and disadvantages of drug delivery nano-carriers with potential use in agriculture.

Type of nano-carrier	Advantages	Disadvantages
Mesoporous silicon-based materials	Stable structure	Inorganic
	Tunable and uniform pore size	Non-biodegradable
	Controlled release of cargo	Potential cell lysis caused by silanol groups interacting with membrane lipids
Solid lipidic nanoparticles (SLNs)	Improves solubility in water of hydrophobic cargo	Low load capacity
	Hydrophilic cargo possible	Low Encapsulation efficiency
	Relatively inexpensive production	High water content in dispersions (70–99.9%)
	Biocompatible/biodegradable	Premature cargo release during storage
	Feasible production scaling-up	
Nano-emulsions	- Highly stable to gravitational separation and aggregation - Improves solubility in water of hydrophobic cargo - Biocompatible/biodegradable - Relatively inexpensive production - Suitable for incorporating lipophilic cargo - Increase efficacy of antimicrobial agents	- High amounts of surfactant needed to achieve oil droplets of nanometric sizes
Dendrimers	Functionalization of peripheral groups determines solubilization and enables targeted delivery of cargo	Cytotoxicity reported on cationic dendrimers
	Suitable for incorporating lipophilic or lipophobic cargo	Toxicity correlated with the number of surface amine groups
	PAMAM dendrimers are reported to be relatively resistant to hydrolysis	Pharmacokinetics, biodistribution, biodegradation, and chronic toxicity of PAMAM dendrimers are not yet clearly understood
Nanocrystals	Carrier-free (i.e., they are almost 100% drug)	Difficult to control morphology and crystallinity of final product
	Improves bioavailability of water-insoluble compounds Improves drug adhesiveness to surface cell membranes	Highly time/money/energy demanding. Need for large amounts of organic solvents (Bottom-up approach)
	Enhances particle stability in suspension	Residual presence of surfactants, solvents or stabilizers (top-down approach)
	Increase drug dissolution velocity	Specialized equipment is needed
Hydrogels	Complete bio and eco-compatibility Relatively inexpensive production Easy to fabricate	Batch to batch variation due to the heterogeneity of the polymer Fine tuning formulation required to achieve stable particles

drugs, (Patel et al., 2012; Padhye and Nagarsenker, 2013) just to mention some. In the cosmetic industry, they have been used to encapsulate UV blockers such as 3,4,5-trimethoxybenzoylchitin (TMBC), 2-hydroxy-4-methoxybenzophenone and vitamin E for use as sunscreen (Wissing and Müller, 2001; Song and Liu, 2005). In the food industry, SLNs have been used to encapsulate antioxidant molecules such as ferulic acid and tocopherol (Oehlke et al., 2017), natural antimicrobial compounds (Piran et al., 2017), and hydrophobic flavoring agents (Eltayeb et al., 2013).

Nano-Capsules

Nano-capsules are nano-vesicular systems in which drugs are enclosed in an inner cavity created by a unique polymeric membrane (see **Figure 3**). Nano-encapsulation enhances drug delivery and efficacy, but the different methods used for the preparation of nano-capsules frequently produce dispersions with low drug loading. This is a serious disadvantage when the aim is to obtain therapeutic concentrations (Mora-Huertas et al., 2010). Similar to NLPs, the application of nano-capsules also extends from the pharmaceutical sector for the encapsulation and delivery of drugs, to the food industry and agriculture, as well as application in cosmetics and personal care in the form of cosmeceuticals.

Drug loaded nano-capsules are especially useful for skincare and dermatological treatments because of their enhanced bioavailability in dermal cells. Ebselen (Eb) is an example of a repurposed drug with poor aqueous solubility which requires a sophisticated delivery system such as nano-encapsulation for topical application as a promising, safe and complementary alternative to the treatment of cutaneous candidiasis (Jaromin et al., 2018). Examples of commercially available cosmeceutical products are "Hydra flash bronzer" a facial skin moisturizer, "Soleil soft-touch anti-wrinkle sunscreen," "Soleil instant cooling sun" and "primordiale optimum lip" produced by Lancôme®. These products claim to contain nano-capsules of vitamin E and antioxidant agents as active ingredient. A more comprehensive list of readily available cosmeceuticals products containing nano-capsules and SLN is available in the literature (Lohani et al., 2014).

The food industry is taking advantage of the benefits of nano-encapsulating essential oils to enhance their antimicrobial activity against food borne-pathogens to increase their solubility when loaded into polymeric nano-capsules (Granata et al., 2018).

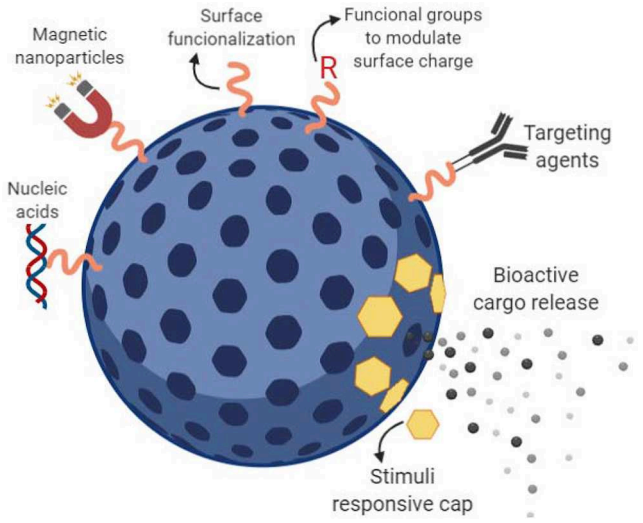

FIGURE 1 | Mesoporous silicon-based nano-carriers (MPSNPs). Schematic representation of a mesoporous silicon-based nanocarrier. The bioactive cargo can be loaded into the porous spaces via passive adsorption or active anchoring. Stimuli responsive caps can be design to prevent early cargo release and detach from its pore allowing controlled release. Targeted cargo delivery can be performed by attachment of targeting agents onto previously functionalized particle surface.

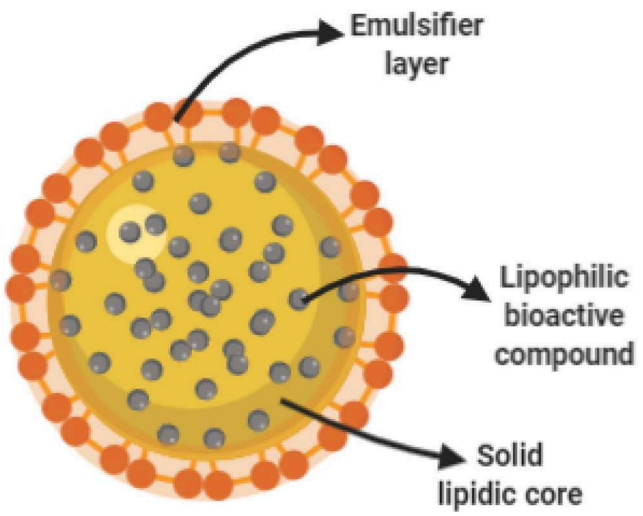

FIGURE 2 | Schematic representation of a solid lipidic nanoparticle. During SLN fabrication, a lipophilic bioactive cargo is dissolved in a liquid hot lipid matrix. Under proper formulation and operational conditions, nanoparticles are formed assisted by an emulsifier as the lipidic core solidifies at room temperature.

In agriculture, nano-encapsulation technology has been used for the delivery of currently available pesticide molecules (Yin et al., 2012). However, the increased water solubility, which is desirable for pesticide efficiency, brings environmental and in turn, regulatory concerns. By studying a commercially available insecticide with an encapsulated active ingredient,

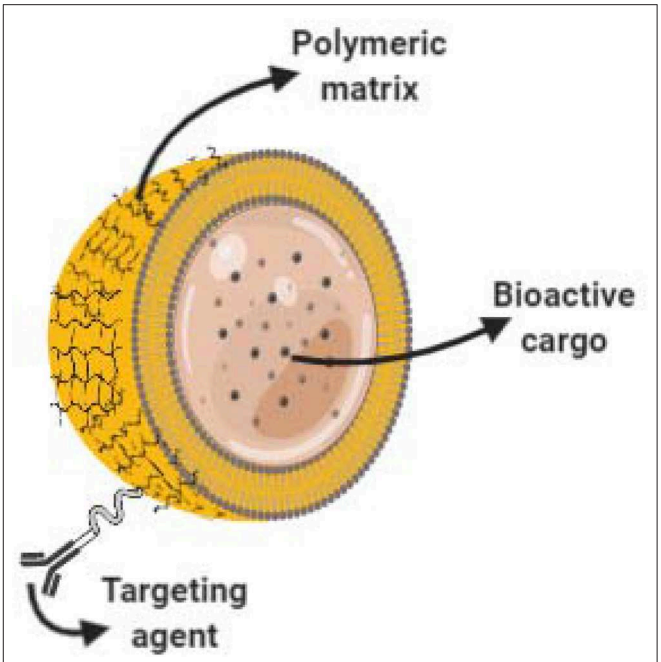

FIGURE 3 | Core shell nano-capsules for drug delivery. Schematic representation of a nanocapsule. Bioactive cargo is encapsulated into a core-shell polymeric matrix. Polymer surface can be functionalized and decorated with targeting agents enabling targeted delivery.

Slattery et al. demonstrated that by encapsulating the in nano-sized carriers, the active ingredient's water solubility increases. Enhanced water solubility disrupts foundational assumptions on its chemical behavior of the pesticide, such as its hydrophobicity (KOW) and soil sorption (Kd). The hydrophobicity (KOW) and soil sorption (Kd) values are numerical descriptors used to predict the environmental fate of a molecule (pesticide) and its toxicity. By encapsulating the pesticide molecules into nano-sized carriers, these indexes may not adjust to the prediction models once built based on their free un-encapsulated forms. Thus, complicating the use of hydrophobicity metrics to predict their fate and toxicity. Determining how carrier size influences the hydrophobicity (KOW) and soil sorption (Kd) of a given pesticide, and thus its mobility through soil and water, is important to our understanding of whether the current pesticide's toxicity risk assessments are sufficient to protect against products that incorporate nano-encapsulation technology (Meredith et al., 2016; Slattery et al., 2019).

Micelles, Liposomes, and Nano-Emulsions

Micelles are spontaneously self-arranged spherical aggregates made of surfactant molecules. Liposomes are spherical vesicles with at least one lipid bilayer, and nano-emulsions are surfactant-assisted homogeneous suspensions of nano-sized droplets of a dispersed phase in a continuous phase. They all display spherical shape (Pavlic et al., 2009) and facilitated a controlled release of cargo (Godfroy, 2009; Joo et al., 2013). Besides their inherent biocompatibility, their surface can be modified and functionalized for conjugation with targeting moieties which

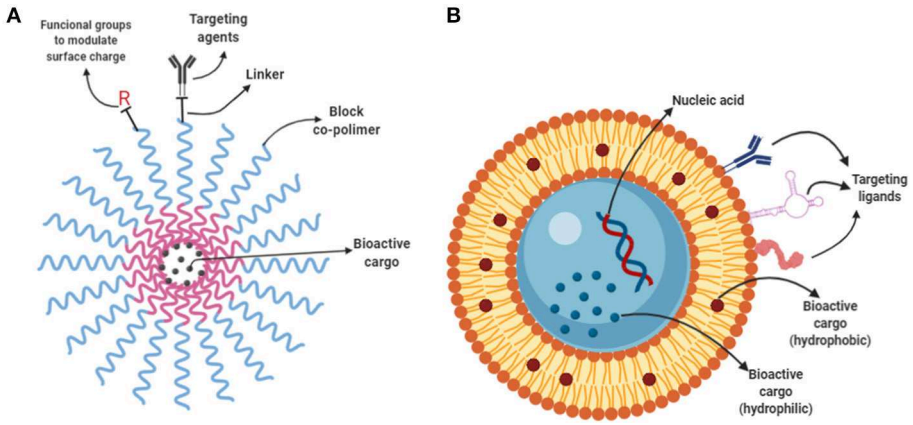

FIGURE 4 | Polymeric micelles and liposomes. **(A)** Schematic representation of a polymeric micelles composed by a co-block polymer (red and blue wavy lines). The core shell is formed encapsulating the bioactive cargo inside. The surface can be functionalized with linker molecules and further decorated with targeting ligands to enable targeted delivery. **(B)** Depiction of a liposome containing hydrophilic cargo in its core a hydrophobic cargo allocated in the bilayer. Surface functionalization can be achieved by anchoring of targeting ligands such as antibodies, proteins and aptamers.

enable targeting to specific sites, improving efficacy and potency (Vabbilisetty and Sun, 2014).

In general, liposomes (**Figure 4B**) are used to encapsulate water-soluble compounds because they are comprised of a lipid bilayer separating an aqueous internal compartment from the bulk aqueous phase. Whereas, oil in water (O/W) nano-emulsions are used to encapsulate hydrophobic compounds. In contrast, polymeric micelles (**Figure 4A**) are used to encapsulate both hydrophobic and hydrophilic compounds depending on the design. Block copolymers have a hydrophilic and a lipophilic block. Block-copolymers can easily reach NP size higher than 20 nm and close the liposomes.

The applications of micelles, liposomes, and nano-emulsions include the encapsulation of poorly water-soluble bioactive molecules to be further incorporated into aqueous products. For instance, for biomedical purposes, a plethora of different types of drug-loaded nano-emulsions is available including oral, topical, intranasal and ocular administration (Yukuyama et al., 2017). In the food industry, several types of different nano-emulsions have also been used as carriers of natural occurring, but poorly soluble flavors, colors, preservatives and antioxidant agents (Donsì, 2018). Increased attention has been focused on the nano-emulsification of essential oils because it has been proven that when presented on a nanometric scale, their antimicrobial activity is enhanced. Moreover, its long-term stability is also enhanced (**Figure 5**). In a recent work D-limonene was used to prevent the formation of biofilms on *E.coli* O157:H7 at sub-lethal doses, by blocking the quorum sensing mediated autoinducer-2 (AI-2) communication and curli-related gene expression (Wang et al., 2018).

Dendrimers

Dendrimer structures are comprised of three components (**Figure 6**): a focal core, dendrons, and cavities formed between dendrons (Safari and Zarnegar, 2014). Some of the desirable characteristics of dendrimers are their uniform molecular weight and their three-dimensional structure with peripheral groups that determine solubility, making them relatively easy to design upon specific demands. Further, their smaller hydrodynamic volume and lower molecular volume compared with linear polymers of similar molecular weight (Markowicz-Piasecka and Mikiciuk-Olasik, 2016). Exposed terminal groups in dendrimeric particles mostly control their chemical interactions with the molecular environment. Their properties such as nanometer size range, ease of preparation and functionalization, also their multiple copies of surface groups displaying stability, make them an attractive system for drug delivery. However, despite their initial popularity in drug delivery, at present, serious concerns exist on the cytotoxicity of cationic dendrimers, which has led to further investigation of alternatives to overcome this issue. The toxicity of dendrimers mainly comes from the high cationic charge density in the periphery, where charges interact with the biological cell membrane and then result in membrane disruption (Tsai and Imae, 2011).

Dendrimer-based non-viral vectors for gene delivery have gained traction over the past two decades, especially in the field of biomedicine for cancer treatment. In plants, the use of cationic polyamidoamine (PAMAM) vector assisted by ultrasound has been used for DNA delivery. Amani et al. (2018) demonstrated in alfalfa cells, that single and double-stranded DNA transfection efficiency can be significantly improved when PAMAM dendrimers are used assisted by sonication (Amani et al., 2018). Production of dendrimers can be approached in two different ways: convergent approach and divergent approach, each with its own limitations (Gupta and Nayak, 2015). Although the main applications of dendrimers are in drug/gene delivery for biomedical applications (Palmerston Mendes et al., 2017), several other applications exist (Abbasi et al., 2014).

Dendrimers are also useful for agricultural purposes. They may improve the delivery of agrochemicals intended to either promote growth or discourage diseases. For instance, in 2016, a crop protection company (Adama) licensed Starpharma's

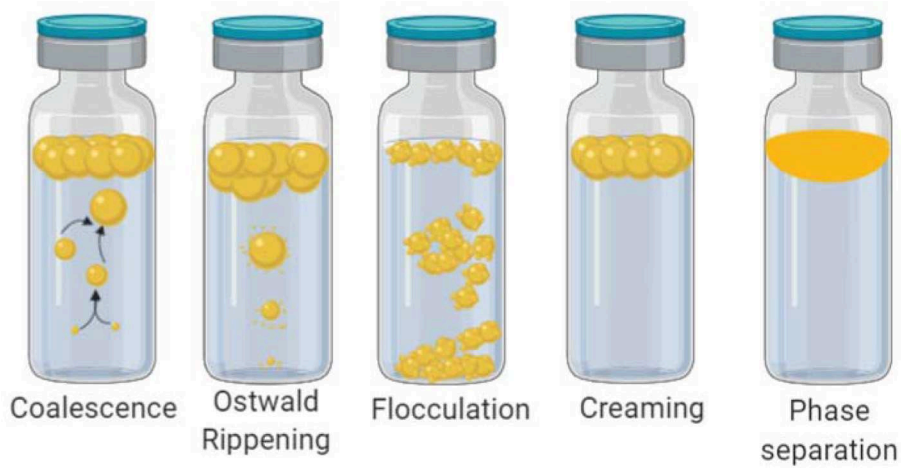

FIGURE 5 | Types of emulsion destabilization. Schematic depiction of how emulsions naturally tend to separate its phases. (i) Coalescence occur when two separate oil droplets merge into a single larger oil droplet because surfactant monolayers fuse together. (ii) Ostwald ripening is the most common way of nano-emulsion failure. Larger oil droplets become larger at expense of smaller oil droplets driven by the pressure difference between to oil droplets of different diameters. The process accelerates as the diameter difference increases. (iii) Flocculation occurs when oil droplets collide, but instead of coalescence, they remain as independent droplets. Co-joined droplets form clusters that precipitate with enough time, the before mentioned processes produce (iv) creaming and later on they lead to complete (v) phase separation.

(ASX:SPL) Priostar dendrimer technology for the development of an enhanced 2,4-D herbicide for the US market. According to the manufacturer, some of the potential benefits from the use of dendrimer technology in crop protection include improved efficacy, more concentrated formulations to reduce transport costs, reduction in solvent requirements and increased adhesion. Stapharma's lysine dendrimer based Vivagel® managed to achieve clinical approval (Moura et al., 2019) which indicates the technological feasibility of mass-production. However, the technical details regarding up-scaled production are not publicly available.

The use of dendrimers for crop protection faces the challenge impose by mass-production. The main challenge relies on preserving their purity and monodispersity upon up-scaled manufacture. Technical details with respect to improved reaction conditions and purification of half- and full-generation PAMAM dendrimers to overcome the critical limitations for upscaling this class of polymers are available elsewhere (Ficker et al., 2017).

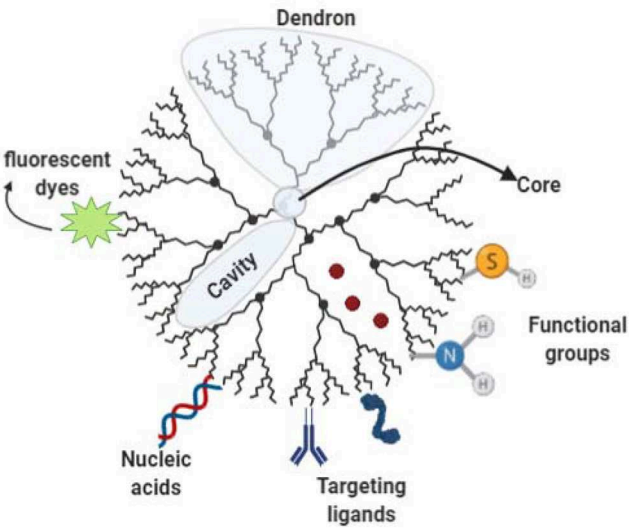

FIGURE 6 | Dendrimer structure and functionalization Schematic representation of a Dendron comprising Dendron units branching out of a focal core interspaced by cavities. Bioactive cargo can be encapsulated into cavities. Dendron ends can be functionalized allowing targeting ligand attachment, fluorophore molecules, nucleic acids among other molecules of interest.

Nanocrystals

Nanocrystals are another nanotechnological approach to deliver poorly soluble drugs. In contrast to the prior mentioned drug delivery system platforms, nanocrystals have several unique traits. Drug delivery nanocrystals are carrier-free colloidal delivery systems (i.e., they are almost 100% drug). Thus, drug nanocrystals possess the merits of improving the oral bioavailability of water-insoluble compounds, reducing administered dose, avoiding abnormal absorption thus minimizing utilization of large excipients, increasing dissolution velocity, increasing adhesiveness to surface cell membranes, and increasing particle stability (Wang et al., 2011). Conventionally, drug nanocrystals can be produced whether from a top-down or a bottom-up approach. The demand for energy, time and money is high for top-down approaches such as milling or high-pressure homogenization. For instance, high-pressure methods require specialized equipment able to deliver up to 1,700 bar for over 100 homogenization cycles, and the milling method requires hours if not days to achieve the desired particle size, depending on the drug properties (Lu et al., 2016). Moreover, the grinding process

may contaminate or denature labile drugs which may lead to unexpected side effects on the recipient patient. Further concerns exist on the potential loss of bioactivity and molecular integrity due to severe thermogenesis derived from the milling process. Other disadvantages for the top-down methods are: The lack of complete control of the morphology and crystallinity of the final product; particle aggregation/agglomeration issues; losses of the product due to drug adherence to equipment surfaces and residual presence of surfactants, solvents or stabilizers (Padrela et al., 2018).

In comparison, bottom-up processes are achieved through nucleation and subsequent crystallization. One way to achieve nucleation is by mixing the drug with an antisolvent by simple stirring. Another way is to remove the solvent via spray and freeze-drying. Subsequent crystallization does require high energy methods such as sonication or intense micro-stirring (Lu et al., 2016). Another approach to producing drug nanocrystals is based on supercritical carbon dioxide ($ssCO_2$). The details on the roles of $ssCO_2$ as solvent, co-solvent and as an additive for the production of drug nanocrystals are comprehensively reviewed elsewhere (Padrela et al., 2018). Amongst the main disadvantages of the bottom-up methods to produce drug nano-crystals are: (i) the difficulty to control the particle size, nucleation, and growth of crystals that may lead to both, undesired morphologies or amorphous crystallinities and subsequent particle agglomeration; (ii) the need for large amounts of organic solvents; (iii) fine-tuning solvent/antisolvent formulation is time-consuming; (iv) need for solvent removal; (v) labile drugs may denature during heating solvent removal; (vi) need for specialized equipment for $ssCO_2$-based nanocrystals (Padrela et al., 2018).

The use of nanocrystals in agriculture has enormous potential for sustained and efficient nutrient delivery into crops. For instance, nitrogen can be applied in the form of Urea-Hydroxyapatite nanohybrids. When tested in rice fields, urea-hydroxyapatite nanohybrids significantly enhanced nitrogen bioavailability, resulting in higher crop yields, while reducing the nitrogen input up to 50%, when compared to granular urea (Kottegoda et al., 2017). The efficacy of hydroxyapatite nanoparticles as Phosphorus fertilizer has also been studied in andisols and oxisols. Montalvo et al. showed that the effect of phosphorus in the form of hydroxyapatite nanoparticles, in the wheat dry matter production significantly depends on the type of soil these particles are applied on. Nano-Hydroxyapatite in strongly phosphorous sorbing soils had more effect on shoot dry matter production and plant phosphorous uptake than bulk-HAP but less than the water-soluble triple superphosphate. This is maybe due to the propensity of nano-hydroxyapatite to aggregate, thus reducing both the mobility and the dissolution rate of the particles (Montalvo et al., 2015). Since nano-nutrient/soil particle interaction is strongly affected by the intrinsic heterogeneity of the soil, it is reasonable to study alternative nano-nutrient up-take pathways in plants. In a recent study, Avellan et al. analyzed how nano-crystals move throughout the plant, from the leaves to the roots, using gold nanoparticles as a model in wheat. They found that "regardless of their coating and sizes, the majority of the transported AuNPs accumulated in younger shoots (10–30%) and in roots (10–25%), and 5–15% of the NPs <50 nm were exuded into the rhizosphere soil. A greater fraction of larger sizes AuNPs (presenting lower ζ potentials) was transported to the roots" (Avellan et al., 2019).

Accounting for these disadvantages, scaling up of its production has been a challenge. It is also worth noting that there is a lack of cytotoxicity studies, and the details of the intracellular fate of the nanocrystals are not well-understood (Junyaprasert and Morakul, 2015).

Nanogels

Nanogels are hydrophilic cross-linked networks forming polymer chains that absorb substantial amounts of aqueous solutions. Due to their conformational tridimensional structure, hydrogels are capable of imbibing bioactive molecules solubilized in water or aqueous fluids. The presence of chemical crosslinks (tie-points or junctions) or physical crosslinks, such as entanglements or crystallites, are responsible for their characteristic conformational structure and size (Himi and Maurya, 2013), which can be fine-tuned via chemical control of the formulation and the process to obtain the hydrogel nanoparticles. The main advantages of hydrogels, when used as drug delivery systems, is their complete biocompatibility due to their high content of water (Caló and Khutoryanskiy, 2015). On the other hand, one of the major drawbacks of these types of particles is the batch-to-batch variation due to the heterogeneity of the polymer itself, such as the case for chitosan-based drug delivery systems.

Coacervation or ionic gelation method is one of the most common processes carried out to produce this type of nanoparticles because it is easy to implement and requires un-expensive materials. In general, the process involves the mixture of two aqueous phases, where one of which is the polymer and the other is the dissolved cross-linker. It is common to use an oil/water emulsion as one of the aqueous phases containing the bioactive hydrophobic molecule or drug of interest to be encapsulated within the forming capsule. The method is relatively easy to perform since it does not require sophisticated equipment, which is imperative for the scaling up. However, the final characteristics of the produced nanoparticles, such as size, polydispersity, and stability, are highly sensitive to changes in the fabrication conditions, such as pH, ionic strength, stirring speed, addition rate, and type and concentration of polymers and cross-linkers. Chitosan-based nano-carriers are of special interest in agriculture. However, the literature regarding both, nanoparticle formation via ionic gelation and cargo release profile, is overwhelmingly inconsistent (Huang et al., 2015; Cai and Lapitsky, 2019). An example is illustrated in **Figure 7** showing factors that influence chitosan nanoparticles' formation and stability.

Typical applications of hydrogels revolve around the biomedical field, including drug encapsulation, transport and delivery; tissue engineering for wound-healing treatment; and 3-D cell culture. Nonetheless, hydrogels can also be used as antimicrobial agents. Chitosan, for instance, is a polymer commonly used to fabricate nano-carriers, naturally displays antimicrobial activity. Metal ions, such as $Ti3^{+}$, $Fe3^{+}$, Ag^{+}, $Cu2^{+}$, and Zn2 can also be incorporated into

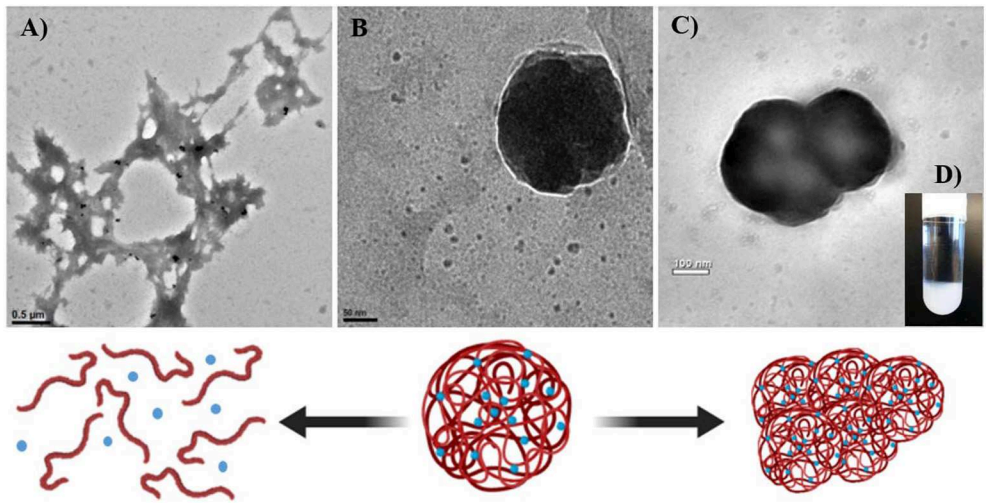

FIGURE 7 | Factors influencing formation and stability of chitosan-based nanoparticles mediated by the cross-linker tripolyphosphate (TPP). Formation and stability of chitosan-based nanoparticles are sensitive to formulation and preparation conditions. **(A)** When the amount (per mole) of cross-linker (TPP) is insufficient relative to the amount (per mole of NH_3^+ from chitosan), chitosan particles **(B)** rapidly dissolve at pH levels below its pKa. When the pH of the solution is not acid enough, amino groups from chitosan deprotonate preventing chitosan to dissolve and then failing to form electrostatic interactions with the crosslinker, resulting in particle dissolution and ulterior precipitation. **(C)** Excess of crosslinker in the solution result in particle aggregation and **(D)** further precipitation.

non-antimicrobial hydrogels in order to confer antimicrobial properties. Incorporation of some metallic ions can also confer catalytic, photo-responsive, photochemical, redox, and conductive properties to hydrogels (Wahid et al., 2017). In agriculture, the use of chitosan nanoparticles are of special interest due to its immune-modulatory activity elicited in plants. Chitin is a pathogen-associated molecular pattern (PAMP), detected by a transmembrane chitin receptor (LysM/CERK1) in plant cells. Sensing chitosan triggers an intracellular defense immune response (i.e., PTI—Pathogen triggered immunity) involving the activation of kinases and up-regulation of defense-related genes, such as plant defensin PDF1.2, resulting in jasmonic acid and ethylene accumulation associated with immunity to necrotrophs (Mengiste, 2012; Malerba and Cerana, 2016).

DRUG DELIVERY SYSTEMS IN THE AGRICULTURE

According to the United Nations, the estimated world population projected for 2050 will be 9.7 billion people. The increasing world population brings challenges that may imbalance the food production chain at various levels such as social, economic, technologic and environmental. Efforts to find new strategies that will allow improving the quantity and quality of food supply under a scheme of sustainability are imperative to meet the demands of the incoming population. The application of engineered nano-carrier devices, intended for the delivery of encapsulated molecules, could be a promising alternative to meet the future agriculture needs of increased productivity. Phytonanotechnology (i.e., the application of nanotechnology in plants) may improve the way we grow crops. Nano-delivery systems enable the controlled release of agrochemicals (e.g., fertilizers, pesticides, and herbicides) and target-specific delivery of biomolecules (e.g., nucleotides, proteins, and activators; Wang et al., 2016; see **Figure 8**, **Table 3**).

Nano-encapsulated pesticides offer enhanced controlled release of cargo and enhanced efficacy. Regarding the development of nano-pesticides is worth noting that a common practice in this industry is to focus on the modification of already registered existing molecules, rather than discovering new molecules. This is due to the costs associated with the development and further registration which is a process often measured in years. A commercially available capsule suspension insecticide (Environmental Protection Agency (EPA) Reg. No. 67760-104-53883) with 5.9% γ-cyhalothrin; and an EPA registered capsule suspension insecticide with 22.8% λ-cyhalothrin (EPA Reg. Number 100–1,295, Greensboro, NC, USA) are two examples of nano-pesticides currently available in the market under this reformulation scheme (Meredith et al., 2016; Slattery et al., 2019).

Nano-Carriers as a Non-viral Vector for Gene Delivery in Plant Cells

In order to obtain higher crop production yields, it is necessary to develop new plant varieties by introducing traits that ideally enables them to better resist different environmental-derived abiotic stresses or pathogen-mediated diseases along with the generation of higher biomass under limited resources. The transfer of genes to the target plant cells is challenging due to the rigid plant cell wall which prevents the exogenous particle movement from the outside to the cytoplasm (Abd-Elsalam and Alghuthaymi, 2015). There is evidence that the plant's nano-particle uptake is strongly dependent on the cell wall pore

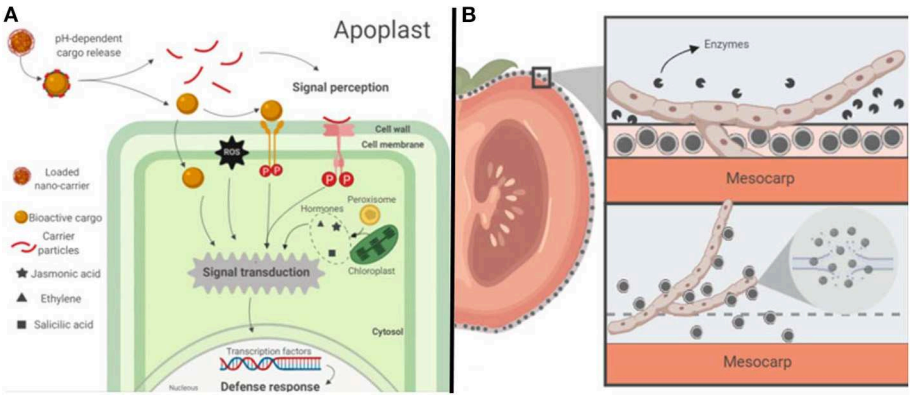

FIGURE 8 | Schematic representation of the potential mode of action of drug-nanocarriers applied in the agriculture: **(A)** Example of a potential mode of action of drug nano-carriers for systemic protection of plants: A pH-sensitive polymeric loaded nano-carrier enters the plant apoplast and releases its cargo. The bioactive payload may enter to the plant cell cytosol or Activate a signaling cascade upon recognition by a transmembrane receptor triggering the plant defense immune response. Carrier molecules (e.g., chitosan) can also elicit an immune response in plants upon recognition by receptors. **(B)** Example of a potential mode of action of drug nano-carriers for post-harvest produce protection: (a) Fungal extracellular enzymes degrade an edible coating with embedded nano-carriers. (b) Drug nano-carriers loaded with antimicrobial compounds are released from the coating. Fungal membrane is disrupted by direct contact with antimicrobial compounds.

diameter (i.e., exclusion size limit), which may vary amongst different tissues and organs. In general, the plant cell wall's exclusion size limit is up to 50 nm (Cunningham et al., 2018). Due to its small size, nanoparticle-enabled gene delivery into plant cells pose a promising option for genetic engineering for agriculture. The first reported example of this was done by Torney et al. who managed to develop a 3-nanometer pore mesoporous nanoparticle (MSN) able to transport DNA and chemicals into isolated plant cells that interact with leaves. MSN were designed in such way that gold nanoparticles capped the pores in order to avoid cargo leakage and release the content in the intended target to trigger gene expression under controlled-release conditions (Torney et al., 2007).

For plant genetic recombination purposes, exogenous gene delivery into plant cells is required. In animal models, nanoparticle penetration into cells is often reported to be improved when mediated with ultrasound. Ultrasound-assisted gene delivery is in use for plants because of its easier operation, lower cost and no plant specificity constraints among others (Liu et al., 2005). Nevertheless, the main disadvantage of ultrasound-mediated technique is that naked DNA is highly sensitive to external high energy sources and as a result, it may suffer damage, especially when increasing ultrasonic strength and time to achieve high transfection efficiency; so the ultrasound-mediated transgenic method has been largely restricted in practice (Yu-qin et al., 2012). Interestingly, DNA-nanoparticle complexes can protect DNA from ultrasound damage as well as from enzymatic degradation (Liu et al., 2005). DNA-nanoparticle complexes that have been studied before included Zinc and Calcium phosphate (Naqvi et al., 2012; Yu-qin et al., 2012).

Foreign particle uptake in plants can naturally occur either via endocytosis or by direct penetration. In plants, different engineered nanomaterials can be used for nanoparticle-mediated DNA transfer using gene-nanoparticle (NP) anchoring using zinc, calcium phosphate, silica, gold, magnetite, strontium phosphate, magnesium phosphate, and manganese phosphate (Sokolova and Epple, 2008; Mahendra et al., 2012) and carbon-based materials such as starch (Sun et al., 2009) fullerenes, single-walled carbon nanohorns (SWCNHs), single-walled carbon nanotubes (SWCNTs), multi-walled carbon nanotubes (MWCNTs) (Burlaka et al., 2015) and dendrimers. However, it has been reported that nanoparticle uptake by plant cells undergoes faster when positively charged nanoparticles are used rather than negatively charged nanoparticles, perhaps due to the preference of the negatively charged cell wall for cations (Cunningham et al., 2018).

Chitosan-based nano-carriers are a promising platform for cargo delivery into plant cells because it is positively charged, amongst other advantages it has. A recent study demonstrated organelle-targeted delivery and transient expression of genetic material via chitosan-complexed single-walled carbon nanotube carriers. Successful transformation of chloroplasts was achieved in mature *Eruca sativa, Nasturtium officinale, Nicotiana tabacum,* and *Spinacia oleracea* plants and in isolated *Arabidopsis thaliana* mesophyll protoplasts.

Since the plastid genome is maternally inherited in most plants, organelle-specific gene delivery is important because it can prevent the potential proliferation of genes to weedy relatives (Kwak et al., 2019). In this specific study, the authors showed that chitosan-complexed single-walled carbon nanotubes (SWNTs) uptake mechanism was described by the lipid exchange envelope penetration (LEEP) model, whereby the ability of nanoparticles to penetrate the cell membrane and the chloroplast envelope is governed primarily by the nanoparticle size and surface charge (Kwak et al., 2019)

In conclusion, nanoparticle assisted gene delivery systems initially developed for medical purposes has been shown to display the same delivery function in plant cells. It is worth noting that the individual performance of DNA delivery into plant

TABLE 3 | Some commercial product of nanofertilizers.

Commercial product	Content	Company
Nano-Gro™	Plant growth regulator and immunity enhancer	Agro Nanotechnology Corp., FL, United States
Nano green	Extracts of corn, grain, soybeans, potatoes, coconut, and palm	Nano Green Sciences, Inc., India
Nano-Ag answer®	Microorganism, sea kelp, and mineral electrolyte	Urth Agriculture, CA, United States
Biozar nano-fertilizer	Combination of organic materials, micronutrients, and macromolecules	Fanavar Nano-Pazhoohesh Markazi Company, Iran
Nano max NPK fertilizer	Multiple organic acids chelated with major nutrients, amino acids, organic carbon, organic micro nutrients/trace elements, vitamins, and probiotic	JU Agri Sciences Pvt. Ltd, Janakpuri, New Delhi, India
Master nano chitosan organic fertilizer	Water soluble liquid chitosan, organic acid, and salicylic acids, phenolic compounds	Pannaraj Intertrade, Thailand
TAG NANO (NPK, PhoS, Zinc, Cal, etc.) fertilizers	Proteino-lacto-gluconate chelated with micronutrients, vitamins, probiotics, seaweed extracts, humic acid	Tropical Agrosystem India (P) Ltd, India

Source: Ram Prasad, Atanu Bhattacharyya et al. Frontiers in Microbiology, 8, JUN, 6 2017 (creativecommons.org/licenses/by/4.0).

cells must be evaluated on a case to case basis since the results presented in literature has several inconsistencies related to the transformation efficiencies achieved by different materials on different plant models. However, the evidence suggests that the concept of non-viral gene delivery into plant cells is promising. The specific design of nanoparticles should respond to the specific demands of the plant model/gene to be transferred, therefore no universal or generic delivery system for gene delivery into plants has been developed.

Nano-Delivery Systems for Nutrition and Growth Promotion in Plants

Commercial fertilizers play a critical role in improving crop yields, however, inherent inefficiencies derived from the nature of the soil, plant health, environmental conditions, or the fertilization method among other factors, can lead to dire negative economic and environmental consequences that may endure in the long term. Not all the nutrient ions in fertilizer applied to a field soil are uptaken by the growing crop. At least three things can happen to the remaining residues from chemical fertilization: They may persist in the soil or, washed away by water leaching through the soil either downwards or throughout the surface or, lost to the atmosphere by volatilization.

In particular, higher than optimum nitrogen, phosphorus and potassium levels can lead to excessive plant and algal growth in waterways that can degrade potable water, fisheries, and recreational areas; leach nitrates into underground or sea waters and release nitrogen-oxides into the atmosphere. Phosphorous losses are also a major environmental concern derived from excessive fertilization in agriculture. It is estimated that the overall efficiency of applied phosphorus to the soil is <20% (Balemi and Negisho, 2012). Nutrient depletion leads to a variety of plant symptoms which affects the overall yield of a crop. Similarly, over-fertilization leads to an ecological imbalance which is hard to restore. Excessive soluble salts from fertilizers alter soil salinity, which in turn alters the soil pH; lower pH values diminish the availability of nutrients to plants by causing an imbalance in the soil native microbial ecology, responsible for nutrient solubilization.

Excessive fertilization is common due to soil nutrient heterogeneity. Overfertilization releases to the environment nutrients that cause, for instance, eutrophication of water bodies. Estimated losses of nitrogen, phosphorus and potassium are around 40–70%, 80–90%, and 50–90%, respectively. In a practical scenario, very less concentration (much below to minimum desired concentration) reaches the targeted site due to leaching of chemicals, drift, runoff, evaporation, hydrolysis by soil moisture, and photolytic and microbial degradation losses. Thus, nano-delivery systems for controlled release emerge as a highly valuable technology with the potential to strengthen the responsive capabilities of a sustainable food chain supply.

The application of nanotechnology for fertilizer delivery is encouraging. Patent applications related to nano-fertilizers are growing consistently according to the world intellectual property organization database. a 10% increment in patent filings related to nano-fertilizers from China, in a period of fewer than 3 years (01/2014–11/2016). This is consistent with data reported by Mastronardi et al. (2015) who noted a 10x (c.a) increase in patent results (Ref. SciFinder) over a 10 year period from 2002 to 2012 (Mastronardi et al., 2015). Current applications of nanotechnology in fertilization and plant protection can be divided into three different categories: (1) Nanoscale fertilizer inputs, which describes examples of nano-sized reformulation of fertilizer input in such a way that the size of the fertilizer or supplement is reduced down to nano-scale. (2) Nanoscale additives, which include the additives presented as nanoparticles and added to bulk materials, and (3) nanoscale coatings or host materials for fertilizers, which includes nano-thin films or nanoporous materials used to encapsulate fertilizers for the controlled release of nutrients in crops (Mastronardi et al., 2015).

Current applications of nanotechnology in fertilization and plant protection can be divided into three different categories (1) Nanoscale fertilizer inputs, which describe examples of nano-sized reformulation of fertilizer input in such a way that the size of the fertilizer or supplement is reduced down to the nano-scale. (2) Nanoscale additives, which include the

additives presented as nanoparticles and added to bull materials. And 3, nanoscale coatings or host materials for fertilizers, which include nano-thin films or nanoporous materials used to encapsulate fertilizers for the controlled release of nutrients in crops (Mastronardi et al., 2015). Gao et al. working with spinach, have shown an enhancement of plant growth when titanium dioxide nanoparticles (TiO2-NPs) were administered to the seeds or when they were sprayed onto the leaves. TiO_2-NPs were shown to increase the activity of several enzymes and promote the adsorption of nitrate, which accelerated the transformation of inorganic nitrogen into organic nitrogen (Gao et al., 2008). The current understanding of the mechanisms involved in nanoparticle uptake and translocation from leaves to roots were discussed earlier in this document (see section Nanocrystals).

The Importance of Nano-Delivery Systems for Disease and Pests Control in Crops

In 1985, Pimentel and Levitan reported that approximately 500 million kilograms of pesticides were applied to plants in the United States (U.S) each year, but only 0.1% of this reach its desired target to effectively eliminate pests (Pimentel and Levitan, 1986). Over 25 years later, in 2011, Pimentel and Burgess reinforced this statement, stating that 545 million kilograms of pesticides were applied to crops in the United States each year, and several applications show that <0.1% of these pesticides reach their target (Pimentel and Burgess, 2012). The use of pesticides including herbicides, insecticides, and fungicides is consistently increasing worldwide, but nowadays, we do not know exactly by how much. According to the United States Department of Agriculture (USDA), the total pesticide expenditures in U.S. agriculture reached close to $12 billion in 2008, a 5-fold increase in real terms (adjusted for inflation) since 1960, but well-below the $15.4-billion peak reached in 1998 (Fernandez-Cornejo et al., 2014). The most recent report about pesticide usage dates to 2017 covering data from 2008 to 2012. According to the report, by 2012 over an estimated 380,000 tons were used in the US, from which 282,000 tons were herbicides, with a total expenditure over 9 billion $US (Atwood and Paisley-Jones, 2017). The lack of up-dated data reports in this regard makes it difficult to enable an informed pesticide policy debate, as well as sway science-based decisions in the right direction.

It is conceivable that improving the targeting and accuracy of pesticides could substantially reduce the amount of toxic chemicals that are applied to crops and improve the yield and safety of agriculture. Ideally, a pesticide should be able to remain active regardless of the environmental conditions in order to perform its intended biocide action. Correspondingly, it should also overcome the defense mechanisms from the pest it must target, it should also be harmless to the surrounding flora and fauna, and be engineered in such a way that it can be mass-produced at the lowest possible cost in order to guarantee economic returns to farmers. Current pesticides fail to completely fulfill these requirements, which results in more frequent and higher doses application schemes, and therefore, higher economic, and environmental costs. Nanomaterials used as a pesticide or as a carrier material have exhibited functional properties such as stiffness, permeability, crystallinity, thermal stability, and biodegradability over commonly used pesticides (Bordes et al., 2009).

Increasing wealth of knowledge in the literature regarding the development and use of pesticide-loaded nano-carriers intended for crop protection supports the importance of this technology toward sustainable agriculture by increasing the potency and bioavailability of pesticides, thus reducing the total amount of agrochemicals released in the environment. Pesticides such as β-cypermethrin (an insecticide; Wang et al., 2007), tebuconazole (a fungicide; Díaz-Blancas et al., 2016), and atrazine (a herbicide; Oliveira et al., 2015) presented as nano-encapsulated formulations are some examples of the potential use of nano-carriers to enhance the biological activity of active ingredients and also increase their stability over time. Zhao et al. (2017) demonstrated that it is feasible to develop a nano-emulsified pesticide displaying not only high stability over time (90 days) but also stronger absorption on negatively charged surfaces, which are desirable characteristics for spray-based foliar applications of pesticides in crops (Zhao et al., 2017).

PROSPECTS OF NANO-DELIVERY SYSTEM TECHNOLOGY IN AGRICULTURE

Based on the data collected from the literature, we expect at least two main positive impacts of the extended, prolonged and improved use of nano-delivery technology translocated into the food production chain. The first is related to the technical aspects of pesticide usage. Similar to the role they play in the medical field, nano-delivery systems can increase the controlled-release properties of the pesticide, increased solubility of active ingredients, protection against premature degradation and increase the stability of active ingredients. Another advantage is that non-target surrounding or distant flora and fauna will be less affected as a result of reducing exposure to toxic chemical compounds. In addition, the technical constraints concerning the massive production of nano-carriers for use in agriculture should be correlated with the economical boundaries which limit the production costs and configures the potential revenues for producers. Additional studies are required to assess, not only the fate of nano-encapsulation materials and payloads, and the resulting physical-chemical and biological performance, but the long-term environmental risks and economic viability.

CONCLUSIONS

It is clear that there is an immense need to develop methods or technologies that allow us to cope with the contrasting challenges of the food supply chain. For instance, the toxicity threshold of materials used in the delivery system is species-dependent and responses to these are driven by a series of factors including not only the nanomaterial itself but the environmental and physiological conditions on which they are applied. Another noteworthy factor is the broader impact of

the delivery system to the environment, while in the medical systems, it is localized to the individual receiving the treatment. Impacts on plant growth, and therefore on product yield and food quality, have been reported. However, several gaps exist in understanding the dynamics of interactions between plants and engineered nanomaterials (ENMs). Given the lack of experimental standardization and the divergent responses, even within similar plant species, it is challenging to foresee the challenges on the use of ENMs in plants (Zuverza-Mena et al., 2016). Finally, there is an imperative need to standardize and validate protocols to assess the positive and negative impact of nano-carriers in an experimental setting, and scale-up of testing can yet be another challenge. Most of the currently available information stems from experiments under controlled conditions, making it difficult to predict the real potential of functional prototypes. Research efforts could focus on controlled release, particle stability, and environmental fate and toxicity to make this a fully-embedded technology.

AUTHOR CONTRIBUTIONS

The initial framework and idea were conceptualized by PV-V and JI. All authors contributed toward the writing of this article.

FUNDING

Partial funding from the Colombian Ministry of Science, Technology, and Innovation (Colciencias 728/2015) in the form of fellowship to PV-V was appreciated. Support provided under the USDA-ARS project number 1935-42000-049-00D with the Center for Food Safety Engineering at Purdue University is appreciated.

REFERENCES

Abbasi, E., Aval, S. F., Akbarzadeh, A., Milani, M., Nasrabadi, H. T., Joo, S. W., et al. (2014). Dendrimers: synthesis, applications, and properties. *Nanoscale Res. Lett.* 9:247. doi: 10.1186/1556-276X-9-247

Abd-Elsalam, K. A., and Alghuthaymi, M. A. (2015). Nanobiofungicides: are they the next generation of fungicides? *J. Nanotechnol. Mater. Sci.* 2, 1–2. doi: 10.15436/2377-1372.15.013

Ahmed, A., Myers, P., and Zhang, H. (2014). Synthesis of nanospheres-on-microsphere silica with tunable shell morphology and mesoporosity for improved HPLC. *Langmuir* 30, 12190–12199. doi: 10.1021/la503015x

Amani, A., Zare, N., Asadi, A., and Asghari-Zakaria, R. (2018). Ultrasound-enhanced gene delivery to alfalfa cells by hPAMAM dendrimer nanoparticles. *Turk. J. Biol.* 42, 63–75. doi: 10.3906/biy-1706-6

Atwood, D., and Paisley-Jones, C. (2017). *Pesticides Industry Sales and Usage*. United States Environmental Protection Agency, 24. Available online at: https://www.epa.gov/sites/production/files/2017-01/documents/pesticides-industry-sales-usage-2016_0.pdf (accessed November 20, 2019).

Avellan, A., Yun, J., Zhang, Y., Spielman-Sun, E., Unrine, J. M., Thieme, J., et al. (2019). Nanoparticle size and coating chemistry control foliar uptake pathways, translocation, and leaf-to-rhizosphere transport in wheat. *ACS Nano* 13, 5291–5305. doi: 10.1021/acsnano.8b09781

Balemi, T., and Negisho, K. (2012). Management of soil phosphorus and plant adaptation mechanisms to phosphorus stress for sustainable crop production: a review. *J. Soil Sci. Plant Nutr.* 12, 547–561. doi: 10.4067/S0718-95162012005000015

Bhandari, P., Novikova, G., Goergen, C. J., and Irudayaraj, J. (2018). Ultrasound beam steering of oxygen nanobubbles for enhanced bladder cancer therapy. *Sci. Rep.* 8:3112. doi: 10.1038/s41598-018-20363-8

Bhandari, P. N., Cui, Y., Elzey, B. D., Goergen, C. J., Long, C. M., and Irudayaraj, J. (2017). Oxygen nanobubbles revert hypoxia by methylation programming. *Sci. Rep.* 7:9268. doi: 10.1038/s41598-017-08988-7

Bordes, P., Pollet, E., and Avérous, L. (2009). Nano-biocomposites: biodegradable polyester/nanoclay systems. *Prog. Polym. Sci.* 34, 125–155. doi: 10.1016/j.progpolymsci.2008.10.002

Burlaka, O. M., Pirko, Y. V., Yemets, A. I., and Blume, Y. B. (2015). Plant genetic transformation using carbon nanotubes for DNA delivery. *Cytol. Genet.* 49, 349–357. doi: 10.3103/S009545271506002X

Cai, Y., and Lapitsky, Y. (2019). Pitfalls in analyzing release from chitosan/tripolyphosphate micro- and nanoparticles. *Eur. J. Pharm. Biopharm.* 142, 204–215. doi: 10.1016/j.ejpb.2019.06.020

Caló, E., and Khutoryanskiy, V. V. (2015). Biomedical applications of hydrogels: a review of patents and commercial products. *Eur. Polym. J.* 65, 252–267. doi: 10.1016/j.eurpolymj.2014.11.024

Chen, S., Zhao, X., Chen, J., Chen, J., Kuznetsova, L., Wong, S. S., et al. (2010). Mechanism-based tumor-targeting drug delivery system. Validation of efficient vitamin receptor-mediated endocytosis and drug release. *Bioconjug. Chem.* 21, 979–987. doi: 10.1021/bc9005656

Choudhury, S. R., Ordaz, J., Lo, C. L., Damayanti, N. P., Zhou, F., and Irudayaraj, J. (2017). Zinc oxide nanoparticles-induced reactive oxygen species promotes multimodal cyto- and epigenetic toxicity. *Toxicol. Sci.* 156, 261–274. doi: 10.1093/toxsci/kfw252

Colombo, M., Mizzotti, C., Masiero, S., Kater, M. M., and Pesaresi, P. (2015). Peptide aptamers: the versatile role of specific protein function inhibitors in plant biotechnology. *J. Integr. Plant Biol.* 57, 892–901. doi: 10.1111/jipb.12368

Cunningham, F. J., Goh, N. S., Demirer, G. S., Matos, J. L., and Landry, M. P. (2018). Nanoparticle-mediated delivery towards advancing plant genetic engineering. *Trends Biotechnol.* 36, 882–897. doi: 10.1016/j.tibtech.2018.03.009

Díaz-Blancas, V., Medina, D., Padilla-Ortega, E., Bortolini-Zavala, R., Olvera-Romero, M., Luna-Bárcenas, G., et al. (2016). Nanoemulsion formulations of fungicide tebuconazole for agricultural applications. *Molecules* 21:1271. doi: 10.3390/molecules21101271

Ding, Y., Jiang, Z., Saha, K., Kim, C. S., Kim, S. T., Landis, R. F., et al. (2014). Gold nanoparticles for nucleic acid delivery. *Mol. Ther.* 22, 1075–1083. doi: 10.1038/mt.2014.30

Donsì, F. (2018). Applications of nanoemulsions in foods. *Nanoemulsions* 2018, 349–377. doi: 10.1016/B978-0-12-811838-2.00011-4

Eltayeb, M., Bakhshi, P. K., Stride, E., and Edirisinghe, M. (2013). Preparation of solid lipid nanoparticles containing active compound by electrohydrodynamic spraying. *Food Res. Int.* 53, 88–95. doi: 10.1016/j.foodres.2013.03.047

FDA (2012). *Guidance for Industry. Drug Interaction Studies Study Design, Data Analysis, Implications for Dosing, and Labeling Recommendations. Guidance Document 79*. Silver Spring, MD: FDA.

Felice, B., Prabhakaran, M. P., Rodríguez, A. P., and Ramakrishna, S. (2014). Drug delivery vehicles on a nano-engineering perspective. *Mater. Sci. Eng. C* 41, 178–195. doi: 10.1016/j.msec.2014.04.049

Fernandez-Cornejo, J., Nehring, R., Osteen, C., Wechsler, S., Martin, A., and Vialou, A. (2014). *Pesticide Use in US Agriculture: 21 Selected Crops, 1960–2008*. Washington, DC: United States Department of Agriculture. doi: 10.2139/ssrn.2502986

Ficker, M., Paolucci, V., and Christensen, J. B. (2017). Improved large-scale synthesis and characterization of small and medium generation PAMAM dendrimers. *Can. J. Chem.* 95, 954–964. doi: 10.1139/cjc-2017-0108

Foucquier, J., and Guedj, M. (2015). Analysis of drug combinations: current methodological landscape. *Pharmacol. Res. Perspect.* 3:e00149. doi: 10.1002/prp2.149

Gao, F., Liu, C., Qu, C., Zheng, L., Yang, F., Su, M., et al. (2008). Was improvement of spinach growth by nano-TiO_2 treatment related to the changes of Rubisco activase? *BioMetals* 21, 211–217. doi: 10.1007/s10534-007-9110-y

Godfroy, I. (2009). Polymeric micelles – the future of oral drug delivery. *J. Biomater. Appl. Rev.* 3, 216–232. doi: 10.1351/pac200476071321

Granata, G., Stracquadanio, S., Leonardi, M., Napoli, E., Consoli, G. M. L., Cafiso, V., et al. (2018). Essential oils encapsulated in polymer-based nanocapsules as potential candidates for application in food preservation. *Food Chem.* 269, 286–292. doi: 10.1016/j.foodchem.2018.06.140

Guo, C., and Irudayaraj, J. (2011). Fluorescent Ag clusters via a protein-directed approach as a Hg(II) Ion sensor. *Anal. Chem.* 83, 2883–2889. doi: 10.1021/ac1032403

Gupta, V., and Nayak, S. K. (2015). Dendrimers: a review on synthetic approaches. *J. Appl. Pharm. Sci.* 5, 117–122. doi: 10.7324/JAPS.2015.50321

Himi, M., and Maurya, S. D. (2013). Review article preparation and evaluation of stomach specific ipn hydrogels for oral drug delivery: a review. *J. Drug Deliv. Ther.* 3, 131–140. doi: 10.22270/jddt.v3i2.400

Hoffman, A. S. (2008). The origins and evolution of "controlled" drug delivery systems. *J. Control. Release* 132, 153–163. doi: 10.1016/j.jconrel.2008.08.012

Huang, Y., Cai, Y., and Lapitsky, Y. (2015). Factors affecting the stability of chitosan/tripolyphosphate micro- and nanogels: resolving the opposing findings. *J. Mater. Chem. B* 3, 5957–5970. doi: 10.1039/C5TB00431D

Iqbal, S., and Yun, J. I. (2018). Decontamination of radionuclides by functionalized mesoporous silica under gamma irradiation. *RSC Adv.* 8, 32211–32220. doi: 10.1039/C8RA05939J

Jaromin, A., Zarnowski, R., Pi, M., Etka-Ottlik, Andes, D. R., and Gubernator, J. (2018). Topical delivery of ebselen encapsulated in biopolymeric nanocapsules: drug repurposing enhanced antifungal activity. *Nanomedicine* 13, 1139–1155. doi: 10.2217/nnm-2017-0337

Joo, K. I., Xiao, L., Liu, S., Liu, Y., Lee, C. L., Conti, P. S. et al. (2013). Crosslinked multilamellar liposomes for controlled delivery of anticancer drugs. *Biomaterials* 34, 3098–3109. doi: 10.1016/j.biomaterials.2013.01.039

Junyaprasert, V. B., and Morakul, B. (2015). Nanocrystals for enhancement of oral bioavailability of poorly water-soluble drugs. *Asian J. Pharm. Sci.* 10, 13–23. doi: 10.1016/j.ajps.2014.08.005

Kadam, U., Moeller, C. A., Irudayaraj, J., and Schulz, B. (2014). Effect of T-DNA insertions on mRNA transcript copy numbers upstream and downstream of the insertion site in arabidopsis thaliana explored by surface enhanced raman spectroscopy. *Plant Biotechnol. J.* 12, 568–577. doi: 10.1111/pbi.12161

Kadam, U. S., Schulz, B., and Irudayaraj, J. M. K. (2017). Multiplex single-cell quantification of rare RNA transcripts from protoplasts in a model plant system. *Plant J.* 90, 1187–1195. doi: 10.1111/tpj.13537

Kim, H., Kim, S. T., Kim, S. G., and Kim, J. S. (2015). Targeted genome editing for crop improvement. *Plant Breed. Biotechnol.* 3, 283–290. doi: 10.9787/PBB.2015.3.4.283

Knezevic, N. (2015). Large pore mesoporous silica nanomaterials for application in delivery of biomolecules. *Nanoscale* 7, 2199–2209. doi: 10.1039/C4NR06114D

Kottegoda, N., Sandaruwan, C., Priyadarshana, G., Siriwardhana, A., Rathnayake, U. A., Berugoda Arachchige, D. M., et al. (2017). Urea-hydroxyapatite nanohybrids for slow release of nitrogen. *ACS Nano* 11, 1214–1221. doi: 10.1021/acsnano.6b07781

Kouassi, G. K., and Irudayaraj, J. (2006). Magnetic and gold-coated magnetic nanoparticles as a DNA sensor. *Anal. Chem.* 78, 3234–3241. doi: 10.1021/ac051621j

Kwak, S. Y., Lew, T. T. S., Sweeney, C. J., Koman, V. B., Wong, M. H., Bohmert-Tatarev, K., et al. (2019). Chloroplast-selective gene delivery and expression in planta using chitosan-complexed single-walled carbon nanotube carriers. *Nat. Nanotechnol.* 14, 447–455. doi: 10.1038/s41565-019-0375-4

Lajiness, M. S., Vieth, M., and Erickson, J. (2004). Molecular properties that influence oral drug-like behavior. *Curr. Opin. Drug Discov. Devel.* 7, 470–477.

Lee, K., Silva, E. A., and Mooney, D. J. (2010). Growth factor delivery-based tissue engineering: general approaches and a review of recent developments. *J. R. Soc. Interface* 8, 153–170. doi: 10.1098/rsif.2010.0223

Liu, Y., Yang, H., and Sakanishi, A. (2005). Ultrasound: mechanical gene transfer into plant cells by sonoporation. *Biotechnol. Adv.* 24, 1–16. doi: 10.1016/j.biotechadv.2005.04.002

Lohani, A., Verma, A., Joshi, H., Yadav, N., and Karki, N. (2014). Nanotechnology-based cosmeceuticals. *ISRN Dermatol.* 2014, 1–14. doi: 10.1155/2014/843687

Lu, Y., Li, Y., and Wu, W. (2016). Injected nanocrystals for targeted drug delivery. *Acta Pharm. Sin. B* 6, 106–113. doi: 10.1016/j.apsb.2015.11.005

Mahendra, R., Shivaji, D., and Mahendra, G. (2012). Strategic nanoparticles mediated gene transfer in plants and animals. *Curr. Nanosci.* 8, 170–179. doi: 10.2174/1573413711208010170

Majouga, A., Sokolsky-Papkov, M., Kuznetsov, A., Lebedev, D., Efremova, M., Beloglazkina, E., et al. (2015). Enzyme-functionalized gold-coated magnetite nanoparticles as novel hybrid nanomaterials: synthesis, purification and control of enzyme function by low-frequency magnetic field. *Colloids Surf. B Biointerfaces* 125, 104–109. doi: 10.1016/j.colsurfb.2014.11.012

Malerba, M., and Cerana, R. (2016). Chitosan effects on plant systems. *Int. J. Mol. Sci.* 17:996. doi: 10.3390/ijms17070996

Manallack, D. T. (2007). The pKa distribution of drugs: application to drug discovery. *Perspect. Medicin. Chem.* 1, 25–38. doi: 10.1177/1177391X0700100003

Markowicz-Piasecka, M., and Mikiciuk-Olasik, E. (2016). Dendrimers in drug delivery. *Molecules* 23:E938. doi: 10.1016/B978-0-323-42866-8.00002-2

Mastronardi, E., Tsaem, P., Zhang, X., Monreal, C., and DeRosa, M. C. (2015). "Strategic role of nanotechnology in fertilizers: potential and limitations," in *Nanotechnologies in Food and Agriculture*, eds M. Rai, C. Ribeiro, L. Mattoso, and N. Duran (Cham: Springer), 25–67. doi: 10.1007/978-3-319-14024-7_2

Mengiste, T. (2012). Plant immunity to necrotrophs. *Annu. Rev. Phytopathol.* 50, 267–294. doi: 10.1146/annurev-phyto-081211-172955

Meredith, A. N., Harper, B., and Harper, S. L. (2016). The influence of size on the toxicity of an encapsulated pesticide: a comparison of micron- and nano-sized capsules. *Environ. Int.* 86, 68–74. doi: 10.1016/j.envint.2015.10.012

Montalvo, D., McLaughlin, M. J., and Degryse, F. (2015). Efficacy of hydroxyapatite nanoparticles as phosphorus fertilizer in andisols and oxisols. *Soil Sci. Soc. Am. J.* 79, 551–558. doi: 10.2136/sssaj2014.09.0373

Mora-Huertas, C. E., Fessi, H., and Elaissari, A. (2010). Polymer-based nanocapsules for drug delivery. *Int. J. Pharm.* 385, 113–142. doi: 10.1016/j.ijpharm.2009.10.018

Moura, L. I. F., Malfanti, A., Peres, C., Matos, A. I., Guegain, E., Sainz, V., et al. (2019). Functionalized branched polymers: promising immunomodulatory tools for the treatment of cancer and immune disorders. *Mater. Horizons* 6, 1956–1973. doi: 10.1039/C9MH00628A

Munz, D., Wang, D., Moyer, M. M., Webster-Gardiner, M. S., Kunal, P., Watts, D., et al. (2016). Aerobic epoxidation of olefin by platinum catalysts supported on mesoporous silica nanoparticles. *ACS Catal.* 7, 4584–4593. doi: 10.1021/acscatal.6b01532

Naqvi, S., Maitraa, A. N., Abdin, M. Z., Akmal, M., Arora, I., and Samim, M. (2012). Calcium phosphate nanoparticle mediated genetic transformation in plants. *J. Mater. Chem.* 22, 3500–3507. doi: 10.1039/c2jm11739h

NIH (2016). *Drug Delivery Systems: Getting Drugs to Their Targets in a Controlled Manner | National Institute of Biomedical Imaging and Bioengineering. Science Education.* Available online at: https://www.nibib.nih.gov/science-education/science-topics/drug-delivery-systems-getting-drugs-their-targets-controlled-manner (accessed March 18, 2019).

Nuruzzaman, M., Rahman, M. M., Liu, Y., and Naidu, R. (2016). Nanoencapsulation, nano-guard for pesticides: a new window for safe application. *J. Agric. Food Chem.* 64, 1447–1483. doi: 10.1021/acs.jafc.5b05214

Oehlke, K., Behsnilian, D., Mayer-Miebach, E., Weidler, P. G., and Greiner, R. (2017). Edible solid lipid nanoparticles (SLN) as carrier system for antioxidants of different lipophilicity. *PLoS ONE* 12:e0171662. doi: 10.1371/journal.pone.0171662

Oliveira, H. C., Stolf-Moreira, R., Martinez, C. B. R., Grillo, R., de Jesus, M. B., and Fraceto, L. F. (2015). Nanoencapsulation enhances the post-emergence herbicidal activity of atrazine against mustard plants. *PLoS ONE* 10:e0132971. doi: 10.1371/journal.pone.0132971

Orendorff, C. J., Gearheart, L., Jana, N. R., and Murphy, C. J. (2006). Aspect ratio dependence on surface enhanced Raman scattering using silver and gold nanorod substrates. *Phys. Chem. Chem. Phys.* 8, 165–170. doi: 10.1039/B512573A

Padhye, S. G., and Nagarsenker, M. S. (2013). Simvastatin solid lipid nanoparticles for oral delivery: formulation development and *in vivo* evaluation. *Indian J. Pharm. Sci.* 75, 591–598. doi: 10.4103/0250-474X.122883

Padrela, L., Rodrigues, M. A., Duarte, A., Dias, A. M. A., Braga, M. E. M., and de Sousa, H. C. (2018). Supercritical carbon dioxide-based technologies for the production of drug nanoparticles/nanocrystals – a comprehensive review. *Adv. Drug Deliv. Rev.* 131, 22–78. doi: 10.1016/j.addr.2018.07.010

Pallerla, S. M., and Prabhakar, B. (2013). A review on solid lipid nanoparticles. *Int. J. Pharm. Sci. Rev. Res.* 20, 196–206.

Palmerston Mendes, L., Pan, J., and Torchilin, V. P. (2017). Dendrimers as nanocarriers for nucleic acid and drug delivery in cancer therapy. *Molecules* 22:1401. doi: 10.3390/molecules22091401

Panchapakesan, B., Book-Newell, B., Sethu, P., Rao, M., and Irudayaraj, J. (2011). Gold nanoprobes for theranostics. *Nanomedicine* 6, 1787–1811. doi: 10.2217/nnm.11.155

Pardeshi, C., Rajput, P., Belgamwar, V., Tekade, A., Patil, G., Chaudhary, K., et al. (2012). Solid lipid based nanocarriers: an overview. *Acta Pharm.* 62, 433–472. doi: 10.2478/v10007-012-0040-z

Patel, K., Padhye, S., and Nagarsenker, M. (2012). Duloxetine HCl lipid nanoparticles: preparation, characterization, and dosage form design. *AAPS PharmSciTech* 13, 125–133. doi: 10.1208/s12249-011-9727-6

Pavlic, J. I., Mares, T., Bester, J., Jansa, V., Daniel, M., and Iglic, A. (2009). Encapsulation of small spherical liposome into larger flaccid liposome induced by human plasma proteins. *Comput. Methods Biomech. Biomed. Engin.* 12, 147–150. doi: 10.1080/10255840802560326

Perez, R. A., Singh, R. K., Kim, H., and Kim, T. (2017). Silica-based multifunctional nanodelivery systems toward regenerative medicine. *Mater. Horizons* 4, 772–799. doi: 10.1039/C7MH00017K

Pimentel, D., and Burgess, M. (2012). Small amounts of pesticides reaching target insects. *Environ. Dev. Sustain.* 14, 1–2. doi: 10.1007/s10668-011-9325-5

Pimentel, D., and Levitan, L. (1986). Pesticides: amounts applied and amounts reaching pests. *Bioscience* 36, 86–91. doi: 10.2307/1310108

Piran, P., Kafil, H. S., Ghanbarzadeh, S., Safdari, R., and Hamishehkar, H. (2017). Formulation of menthol-loaded nanostructured lipid carriers to enhance its antimicrobial activity for food preservation. *Adv. Pharm. Bull.* 7, 261–268. doi: 10.15171/apb.2017.031

Rai, M., Ribeiro, C., Mattoso, L., and Duran, N. (2015). *Nanotechnologies in Food and Agriculture*. Cham: Springer. doi: 10.1007/978-3-319-14024-7

Rang, H. P. (2006). The receptor concept: pharmacology's big idea. *Br. J. Pharmacol.* 147(Suppl. 1), S9–16. doi: 10.1038/sj.bjp.0706457

Safari, J., and Zarnegar, Z. (2014). Advanced drug delivery systems: Nanotechnology of health design a review. *J. Saudi Chem. Soc.* 18, 85–99. doi: 10.1016/j.jscs.2012.12.009

Savjani, K. T., Gajjar, A. K., and Savjani, J. K. (2012). Drug solubility: importance and enhancement techniques. *ISRN Pharm.* 2012:195727. doi: 10.5402/2012/195727

Shahbazi, M. A., Herranz, B., and Santos, H. A. (2012). Nanostructured porous Si-based nanoparticles for targeted drug delivery. *Biomatter* 2, 296–312. doi: 10.4161/biom.22347

Shinde, P., Sayam, A., Gupta, S., Singh, B., Polshettiwar, V., and Prasad, B. L. V. (2017). Amphi-functional mesoporous silica nanoparticles for dye separation. *J. Mater. Chem. A* 5, 14914–14921. doi: 10.1039/C7TA03904B

Siddiqui, M. H., Al-Whaibi, F. M. (eds.). (2015). *Nanotechnology and Plant Sciences Nanoparticles and Their Impact on Plants*. Cham: Springer. doi: 10.1007/978-3-319-14502-0

Singhal, G. B., Patel, R. P., Prajapati, B. G., and Patel, N. A. (2011). Solid lipid nanoparticles and nanolipid carriers: as novel solid lipid based drug carrier. *Int. Res. J. Pharm.* 2, 40–52.

Slattery, M., Harper, B., and Harper, S. (2019). Pesticide encapsulation at the nanoscale drives changes to the hydrophobic partitioning and toxicity of an active ingredient. *Nanomaterials* 9:81. doi: 10.3390/nano9010081

Sokolova, V., and Epple, M. (2008). Inorganic nanoparticles as carriers of nucleic acids into cells. *Angew. Chem. Int. Ed. Engl.* 47, 1382–1395. doi: 10.1002/anie.200703039

Song, C., and Liu, S. (2005). A new healthy sunscreen system for human: solid lipid nannoparticles as carrier for 3,4,5-trimethoxybenzoylchitin and the improvement by adding Vitamin E. *Int. J. Biol. Macromol.* 36, 116–119. doi: 10.1016/j.ijbiomac.2005.05.003

Sun, L., and Irudayaraj, J. (2009a). PCR-free quantification of multiple splice variants in a cancer gene by surface-enhanced Raman spectroscopy. *J. Phys. Chem. B* 113, 14021–14025. doi: 10.1021/jp908225f

Sun, L., and Irudayaraj, J. (2009b). Quantitative surface-enhanced Raman for gene expression estimation. *Biophys. J.* 96, 4709–4716. doi: 10.1016/j.bpj.2009.03.021

Sun, L., Zhao, Q., Xiang, J., Shi, J., Wang, L., Hu, S., et al. (2009). Adsorption of NO and NH3 over CuO/γ-Al2O3 catalyst by DRIFTS. *Huagong Xuebao/CIESC J.* 60, 444–449. doi: 10.1007/s11771-011-0918-9

Tinkle, S., Mcneil, S. E., Mühlebach, S., Bawa, R., Borchard, G., Barenholz, Y. C., et al. (2014). Nanomedicines: addressing the scientific and regulatory gap. *Ann. N. Y. Acad. Sci.* 1313, 35–56. doi: 10.1111/nyas.12403

Torney, F., Trewyn, B. G., Lin, V. S. Y., and Wang, K. (2007). Mesoporous silica nanoparticles deliver DNA and chemicals into plants. *Nat. Nanotechnol.* 2, 295–300. doi: 10.1038/nnano.2007.108

Tsai, H. C., and Imae, T. (2011). *Fabrication of Dendrimers Toward Biological Application*, *1st Edn*. Taipei: Elsevier Inc. doi: 10.1016/B978-0-12-416020-0.00003-6

Vabbilisetty, P., and Sun, X. L. (2014). Liposome surface functionalization based on different anchoring lipids via Staudinger ligation. *Org. Biomol. Chem.* 12, 1237–1244. doi: 10.1039/c3ob41721b

Verho, O., Gao, F., Johnston, E. V., Wan, W., Nagendiran, A., Zheng, H., et al. (2014). Mesoporous silica nanoparticles applied as a support for Pd and Au nanocatalysts in cycloisomerization reactions. *APL Mater.* 2:113316. doi: 10.1063/1.4901293

Wahid, F., Zhong, C., Wang, H. S., Hu, X. H., and Chu, L. Q. (2017). Recent advances in antimicrobial hydrogels containing metal ions and metals/metal oxide nanoparticles. *Polymers* 9:636. doi: 10.3390/polym9120636

Wang, L., Li, X., Zhang, G., Dong, J., and Eastoe, J. (2007). Oil-in-water nanoemulsions for pesticide formulations. *J. Colloid Interface Sci.* 314, 230–235. doi: 10.1016/j.jcis.2007.04.079

Wang, P., Lombi, E., Zhao, F. J., and Kopittke, P. M. (2016). Nanotechnology: a new opportunity in plant sciences. *Trends Plant Sci.* 21, 699–712. doi: 10.1016/j.tplants.2016.04.005

Wang, R., Vega, P., Xu, Y., Chen, C. Y., and Irudayaraj, J. (2018). Exploring the anti-quorum sensing activity of a D-limonene nanoemulsion for Escherichia coli O157:H7. *J. Biomed. Mater. Res. A* 106, 1979–1986. doi: 10.1002/jbm.a.36404

Wang, Y., Chen, J., and Irudayaraj, J. (2011). Nuclear targeting dynamics of gold nanoclusters for enhanced therapy of $HER2^{+}$ breast cancer. *ACS Nano* 5, 9718–9725. doi: 10.1021/nn2032177

Wang, Y., and Irudayaraj, J. (2013). Surface-enhanced Raman spectroscopy at single-molecule scale and its implications in biology. *Philos. Trans. R. Soc. Lond. B Biol. Sci.* 368:20120026. doi: 10.1098/rstb.2012.0026

Wang, Y., Lee, K., and Irudayaraj, J. (2010). SERS aptasensor from nanorod–nanoparticle junction for protein detection. *Chem. Commun.* 46, 613–615. doi: 10.1039/B919607B

Wang, Y., Newell, B. B., and Irudayaraj, J. (2012). Folic acid protected silver nanocarriers for targeted drug delivery. *J. Biomed. Nanotechnol.* 8, 751–759. doi: 10.1166/jbn.2012.1437

Wissing, S. A., and Müller, R. H. (2001). Solid lipid nanoparticles (SLN)–a novel carrier for UV blockers. *Pharmazie* 56, 783–6.

Xu, C., Lei, C., and Yu, C. (2019). Mesoporous silica nanoparticles for protein protection and delivery. *Front. Chem.* 7:290. doi: 10.3389/fchem.2019.00290

Yadollahi, A., Arzani, K., and Khoshghalb, H. (2010). The role of nanotechnology in horticultural crops postharvest management. *Acta Hortic.* 875, 49–56. doi: 10.17660/ActaHortic.2010.875.4

Yi, Z., Hussain, H. I., Feng, C., Sun, D., She, F., Rookes, J. E., et al. (2015). Functionalized mesoporous silica nanoparticles with redox-responsive short-chain gatekeepers for agrochemical delivery. *ACS Appl. Mater. Interfaces* 7, 9937–9946. doi: 10.1021/acsami.5b02131

Yin, Y., Guo, Q., Han, Y., Wang, L., and Wan, S. (2012). Preparation, characterization and nematicidal activity of lansiumamide B nano-capsules. *J. Integr. Agric.* 11, 1151–1158. doi: 10.1016/S2095-3119(12)60109-9

Yu, C., and Irudayaraj, J. (2007). Multiplex biosensor using gold nanorods. *Anal. Chem.* 79, 572–579. doi: 10.1021/ac061730d

Yukuyama, M. N., Tomiko, E., Kato, M., Löbenberg, R., and Araci Bou-Chacra, N. (2017). Challenges and future prospects of nanoemulsion as drug delivery system. *Curr. Pharm. Des.* 23, 495–508. doi: 10.2174/1381612822666161027111957

Yu-qin, F. U., Lu-hua, L. I., Pi-wu, W., Jing, Q. U., Yong-ping, F. U., and Hui, W. (2012). Delivering DNA into plant cell by gene carriers of ZnS nanoparticles. *Chem. Res. Chinese Univ.* 28, 672–676.

Zhao, X., Zhu, Y., Zhang, C., Lei, J., Ma, Y., and Du, F. (2017). Positive charge pesticide nanoemulsions prepared by the phase inversion composition

method with ionic liquids. *RSC Adv.* 7, 48586–48596. doi: 10.1039/C7RA08653A

Zhao, Y., Sun, X., Zhang, G., Trewyn, B. G., Slowing, I. I., and Lin, V. S. Y. (2011). Interaction of mesoporous silica nanoparticles with human red blood cell membranes: size and surface effects. *ACS Nano* 5, 1366–1375. doi: 10.1021/nn103077k

Zuverza-Mena, N., Martínez-Fernández, D., Du, W., Hernandez-Viezcas, J. A., Bonilla-Bird, N., López-Moreno, M. L., et al. (2016). Exposure of engineered nanomaterials to plants: insights into the physiological and biochemical responses-a review. *Plant Physiol. Biochem.* 110, 236–264. doi: 10.1016/j.plaphy.2016.05.037

Conflict of Interest: The authors declare that the research was conducted in the absence of any commercial or financial relationships that could be construed as a potential conflict of interest.

frontiers in Bioengineering and Biotechnology

REVIEW
published: 18 February 2020
doi: 10.3389/fbioe.2020.00069

Targeted Drug Delivery via the Use of ECM-Mimetic Materials

Jeongmin Hwang[1], Millicent O. Sullivan[1,2] and Kristi L. Kiick[3]**

[1] Department of Biomedical Engineering, University of Delaware, Newark, DE, United States, [2] Department of Chemical and Biomolecular Engineering, University of Delaware, Newark, DE, United States, [3] Department of Materials Science and Engineering, University of Delaware, Newark, DE, United States

The use of drug delivery vehicles to improve the efficacy of drugs and to target their action at effective concentrations over desired periods of time has been an active topic of research and clinical investigation for decades. Both synthetic and natural drug delivery materials have facilitated locally controlled as well as targeted drug delivery. Extracellular matrix (ECM) molecules have generated widespread interest as drug delivery materials owing to the various biological functions of ECM. Hydrogels created using ECM molecules can provide not only biochemical and structural support to cells, but also spatial and temporal control over the release of therapeutic agents, including small molecules, biomacromolecules, and cells. In addition, the modification of drug delivery carriers with ECM fragments used as cell-binding ligands has facilitated cell-targeted delivery and improved the therapeutic efficiency of drugs through interaction with highly expressed cellular receptors for ECM. The combination of ECM-derived hydrogels and ECM-derived ligand approaches shows synergistic effects, leading to a great promise for the delivery of intracellular drugs, which require specific endocytic pathways for maximal effectiveness. In this review, we provide an overview of cellular receptors that interact with ECM molecules and discuss examples of selected ECM components that have been applied for drug delivery in both local and systemic platforms. Finally, we highlight the potential impacts of utilizing the interaction between ECM components and cellular receptors for intracellular delivery, particularly in tissue regeneration applications.

Keywords: targeted drug delivery, extracellular matrix, hydrogel, ECM ligand, ECM cell receptors

OPEN ACCESS

Edited by:
Martin Ehrbar,
University of Zurich, Switzerland

Reviewed by:
Mikaël M. Martino,
Monash University, Australia
Silvia Minardi,
Northwestern University, United States
Uwe Freudenberg,
Leibniz Institute of Polymer Research (LG), Germany

****Correspondence:***
Millicent O. Sullivan
msulliva@udel.edu
Kristi L. Kiick
kiick@udel.edu

Specialty section:
This article was submitted to Nanobiotechnology, a section of the journal Frontiers in Bioengineering and Biotechnology

Received: *05 October 2019*
Accepted: *27 January 2020*
Published: *18 February 2020*

Citation:
Hwang J, Sullivan MO and Kiick KL (2020) Targeted Drug Delivery via the Use of ECM-Mimetic Materials. Front. Bioeng. Biotechnol. 8:69. doi: 10.3389/fbioe.2020.00069

INTRODUCTION

Conventional drugs have been critical to the effective management of disease. Despite the benefits of free drugs, 118 drugs approved from 1980 to 2009 in the United States were withdrawn from the market, 22% of them due to safety reasons including hepatic toxicity, severe cardiovascular effects, gastrointestinal issues, and allergic reactions (Qureshi et al., 2011; Prasad, 2014). In addition, safety concerns and inadequate efficacy (78%) were the main reasons for the failure of 54% of the 640 therapeutics that entered phase 3 trials between 1998 and 2008, with follow-up through 2015 (Hwang et al., 2016). The pharmacokinetics of any drug compound, including its efficacy and safety, is critically affected by the route of drug entry (Tibbitt et al., 2016). For example, systemically administrated drugs are exposed to the entire circulatory system, and may access multiple tissues/organs within the body in the absence of direct targeting (Blanco et al., 2015);

for drugs with intracellular targets, additional challenges are posed by the need to navigate the intracellular landscape. The challenges are compounded for drugs that are highly toxic to healthy cells, such as cytostatic drugs for chemotherapeutics or immunosuppressants, adding an extra set of barriers during pre-clinical and clinical evaluation.

To overcome the pharmacokinetic limitations of free drugs, drug delivery systems (DDS) have been designed based on nanomaterials, polymers, and lipids, which can be attached to drugs or used to encapsulate drugs in order to better localize their delivery or control drug release over extended periods (Langer, 1998; Hu et al., 2016; Kanamala et al., 2016; Liu et al., 2016). Nanometer-scale therapeutics can extravasate from circulation and accumulate in some tissues via passive targeting effects (Allen and Cullis, 2004). Such advances were the basis of the improvements in chemotherapy efficacy using liposomal formulations of doxorubicin (Doxil), which was introduced for the treatment of Kaposi's sarcoma in 1995. In addition, over 340 DDS have been approved by the FDA and employed clinically to date (Table 3 from Zhong et al., 2018), and it is clear that nanomaterial DDS have great potential for the targeted delivery of drugs. However, passive targeting is only useful for targeting very specific organs such as tumors (Torchilin, 2014), and even in those cases, some regions of tumors exhibit variations in microvascular permeability that diminish the efficacy of passive targeting.

Local administration provides a simple strategy to enhance active targeting to specific sites, taking advantage of physical localization (Panyam and Labhasetwar, 2003). Employing DDS for localized therapy can improve drug efficacy by preventing the loss of therapeutic agent from the administration site, which minimizes necessary doses and maximizes potency. In addition, polymeric or liposomal carriers can be tailored to achieve sustained release of drugs at optimal therapeutic concentrations in a particular tissue (Sheikhpour et al., 2017; Cervadoro et al., 2018; Raave et al., 2018). As DDS for localized therapy, hydrophilic polymeric hydrogels (for hydrophilic drugs) or nanoparticles (for encapsulation of hydrophobic drugs) can be directly injected or applied to the tissue of interest to achieve sustained and controlled drug release to a particular site through diffusion (Kohane and Todd, 2008; Tibbitt et al., 2016). The tailoring of hydrogel and nanoparticle composition, structure, and porosity has been possible owing to the enormous range of polymers and crosslinking chemistries developed for these applications.

Hydrogels have been designed to exploit the mechanical and biochemical activities of the native extracellular matrix (ECM) to influence cells through cell-matrix interactions (Kharkar et al., 2013; Cai and Heilshorn, 2014; Caliari and Burdick, 2016; Ooi et al., 2017; Zhang and Khademhosseini, 2017). These cell-matrix interactions are pivotal to enhance cell infiltration into the hydrogel and promote cell responses in hydrogels that are appropriate for tissue regeneration and drug delivery applications. To create hydrogels that support cell-matrix interactions, ECM molecules are often utilized in hydrogel formulations. For example, decellularized ECM (dECM) matrices derived from tissues and organs are composed of native ECM molecules, and dECM therefore mimics the structural properties of the native matrix (Crapo et al., 2011; Saldin et al., 2017). Owing to the preservation of biochemical cues from the native tissue microenvironment, dECM matrices trigger cellular response that have been exploited clinically in tissue engineering and regenerative medicine [Tissue Mend® (Stryker Orthopaedics, United States), AlloDerm® (LifeCell Corp. United States), CutffPatch™ (Organogenesis, United States)]. In addition, the delivery of growth factors (Seif-Naraghi et al., 2012) and microRNA (Hernandez et al., 2018) using dECM has recently been explored.

Owing to the myriad cellular interactions with ECM-based materials, the surfaces of drug-loaded nanoparticles also have been modified with ECM-based materials to increase the extent of ligand-mediated, site-specific DDS. The incorporation of bio-specific ligands such as proteins, polysaccharides, peptides, aptamers, and small molecules, facilitates interaction with specific receptors that are either over-expressed or expressed only in specific tissues or cells to achieve active targeting. For example, it has been reported that $\alpha_v\beta_3$ integrin and CD44 receptors are upregulated in various tumor tissues (Danhier et al., 2010). The RGD sequence derived from multiple ECM proteins to target integrin receptors, and hyaluronic acid to target CD44 receptor on cancerous cells, have been widely employed to transport anti-tumor agents (Murphy et al., 2008; Danhier et al., 2012; Huang and Huang, 2018; Fu et al., 2019). Furthermore, target receptor-mediated siRNA delivery has been developed utilizing ligands such as peptides, GalNAc, and aptamers (Nikam and Gore, 2018). Alnylam Pharmaceuticals launched the first RNA interference (RNAi) drug, ONPATTRO®, which uses lipid nanoparticles to deliver RNAi intravenously and treat polyneuropathy caused by hereditary ATTR amyloidosis (Garber, 2018). As next-generation alternatives of ONPATTRO®, the GalNac ligand has been employed to target asialoglycoprotein receptor (ASGP-R) on the hepatocytes. ASGP-R has been shown to mediate endocytosis and degradation of wide variety of desialylated glycoproteins and neoglycoproteins which contain GalNAc residues on the their N-linked carbohydrate chains, and it recognizes specific markers of autoimmune hepatitis (Roggenbuck et al., 2012). The GalNAc conjugated RNAi systems for treatment of liver diseases are currently in phase III (Table 1 from Morrison, 2018). Thus, active targeting strategies have great potential to optimize the delivery of intracellularly active drugs such as many small molecules, as well as biomacromolecules including nucleic acids, peptides, or proteins, which require specific endocytic pathways for action.

Here, we focus on recent developments in the use of ECM components for actively targeted DDS. In particular, we briefly review ligand-receptor mediated endocytosis and cellular interactions with various ECM components as targeting strategies, and we consider the advantages afforded by each approach. We then provide examples of the use of key ECM components in DDS, either as hydrogels or as ligands applied for targeted intracellular DDS.

TABLE 1 | The extracellular matrix components and their cell surface receptors.

	Integrin	Non-integrin receptors
Collagen	$\alpha_1\beta_1$, $\alpha_2\beta_1$, $\alpha_{10}\beta_1$, $\alpha_{11}\beta_1$	Discoidin domain receptors (DDR1 and DDR2), GPVI (platelets), LAIR (immune cell), OSCAR (osteoblast), and mannose receptors (Endo180 or uPARAP), syndecan, CD44
Fibronectin	$\alpha_5\beta_1$, $\alpha_3\beta_1$, $\alpha_8\beta_1$, and $\alpha_v\beta_3$, $\alpha_4\beta_1$, $\alpha_4\beta_7$, $\alpha_9\beta_1$,	Syndecan
Laminin	$\alpha_1\beta_1$, $\alpha_2\beta_1$, $\alpha_3\beta_1$, $\alpha_6\beta_1$, $\alpha_7\beta_1$, $\alpha_{10}\beta_1$, $\alpha_6\beta_4$, $\alpha_v\beta_8$	Syndecan, α-dystroglycan CD44
Heparan sulfate		Syndecan, glypicans
Chondroitin sulfate		CD44, NG2, RPTP-σ, GPI-brevican
Hyaluronic acid		CD44, RHAMM, Toll-like receptors

ECM-CELL INTERACTION MEDIATED DRUG DELIVERY APPLICATIONS

Researchers have exploited an expanded understanding of the interactions between cells and the ECM, as well as increased knowledge about signaling pathways and molecules relevant to the treatment of disease, in designing new, more cell-specific therapeutics and DDS. Cell surface receptors are attractive pharmacological targets since they transduce signals from the extracellular environment to modulate cell responses. Integrins, a major class of transmembrane receptors whose primary role is to recognize and bind ECM, have been a target of therapeutic development for nearly 30 years in the pharmaceutical industry (Goodman and Picard, 2012; Raab-Westphal et al., 2017). However, despite some promising therapeutic advances, the complex biology of integrins has often confounded drug development. Integrins are involved in canonical processes ranging from embryonic development to mature tissue function through binding to their ligands. Therefore, it is critical to understand the mechanisms by which cell-ECM interactions enable cells to sense and respond to extracellular signals encoded in the matrix.

Each ECM molecule has an affinity to a cell surface receptor or receptors, including integrins (**Figure 1**); moreover, the specific integrins expressed by a given cell depend both on the cell type as well as on the cell's physiological state. Accordingly, DDS can be modified with ECM molecules to serve as ligands that will facilitate drug targeting. These approaches are described below for various classes of ECM that have been particularly fruitful in targeted delivery.

Types of ECM Molecules

Proteins

Extracellular matrix proteins include fibrous proteins such as collagen and elastin, and glycoproteins such as fibronectin, laminins, vitronectin, thrombospondin, chondronectin, osteonectin, and fibrin. Collagen is a major ECM component that provides mechanical support, regulates cellular behavior, and directs tissue development. Collagen fibrils, which are formed by self-assembly of triple helical collagen molecules, are cross-linked to provide mechanical strength and integrity to the ECM, and collagens strongly influence the tensile strength and elasticity of tissue. In addition, collagens interact with integrins to regulate cell adhesion, proliferation, and migration, and collagens also interact with other ECM components to direct matrix remodeling (Leitinger and Hohenester, 2007). Fibronectin also regulates a wide variety of cellular functions including cell adhesion, migration, growth and proliferation, embryonic morphogenesis, and wound healing (Pankov and Yamada, 2002; Zollinger and Smith, 2017). Fibronectin usually exists as a dimer composed two nearly identical subunits (type I, type II, and type III) linked together through disulfide bond formation at their C-termini. The type III subunit contains about 100 amino acids in two anti-parallel β-sheets, which are also present in collagens, and the type III subunit also encodes integrin binding (via the RGD motif) and heparin-binding domains. Laminins promote cell adhesion and migration, neurite outgrowth, angiogenesis. Laminins are a major component of basement membrane along with collagen type IV, with a structure that is comprised of heterotrimeric glycoproteins; three subunits, α, β, and γ, come together to form at least 19 laminin isoforms (Colognato and Yurchenco, 2000; Yao, 2017). These laminin isoforms are specifically expressed in tissues to promote biological activities, including cell differentiation, cell shape and movement, and managing tissue phenotypes and survival. The isoforms can bind to other laminins, proteoglycans, and other ECM proteins via various integrins receptors. Due to the ability of ECM proteins to influence cell fate via interactions with integrins, the biocompatible and biodegradable ECM proteins are widely used natural materials for biomedical application (Ramshaw et al., 2009; Benton et al., 2014; Hinderer et al., 2016).

Polysaccharides

Extracellular matrix polysaccharides including heparin sulfate, chondroitin sulfate, dermatan sulfate, keratin sulfate and hyaluronic acid provide largely a structural network, as most ECM polysaccharides are not directly involved in cellular interactions, but indirectly through interaction with other proteins. Heparan sulfate/heparin is a linear polysaccharide of repeating N-acetyl glucosamine (GlcNAc)-D-glucuronic acid (GlcA) disaccharide units (Meneghetti et al., 2015), and is often covalently attached to cell-associated proteins such as the syndecans (SDCs) and glypicans (GPCs) to form heparan sulfate proteoglycans (HSPGs) (Christianson and Belting, 2014). HSPGs such as syndecans and glypicans are able to modulate the cellular uptake of bound ligands; in addition, heparin interacts with various proteins to regulate biological process including growth factor or cytokine signaling, coagulation factor activity, microbe-host interactions, and lipoprotein metabolism

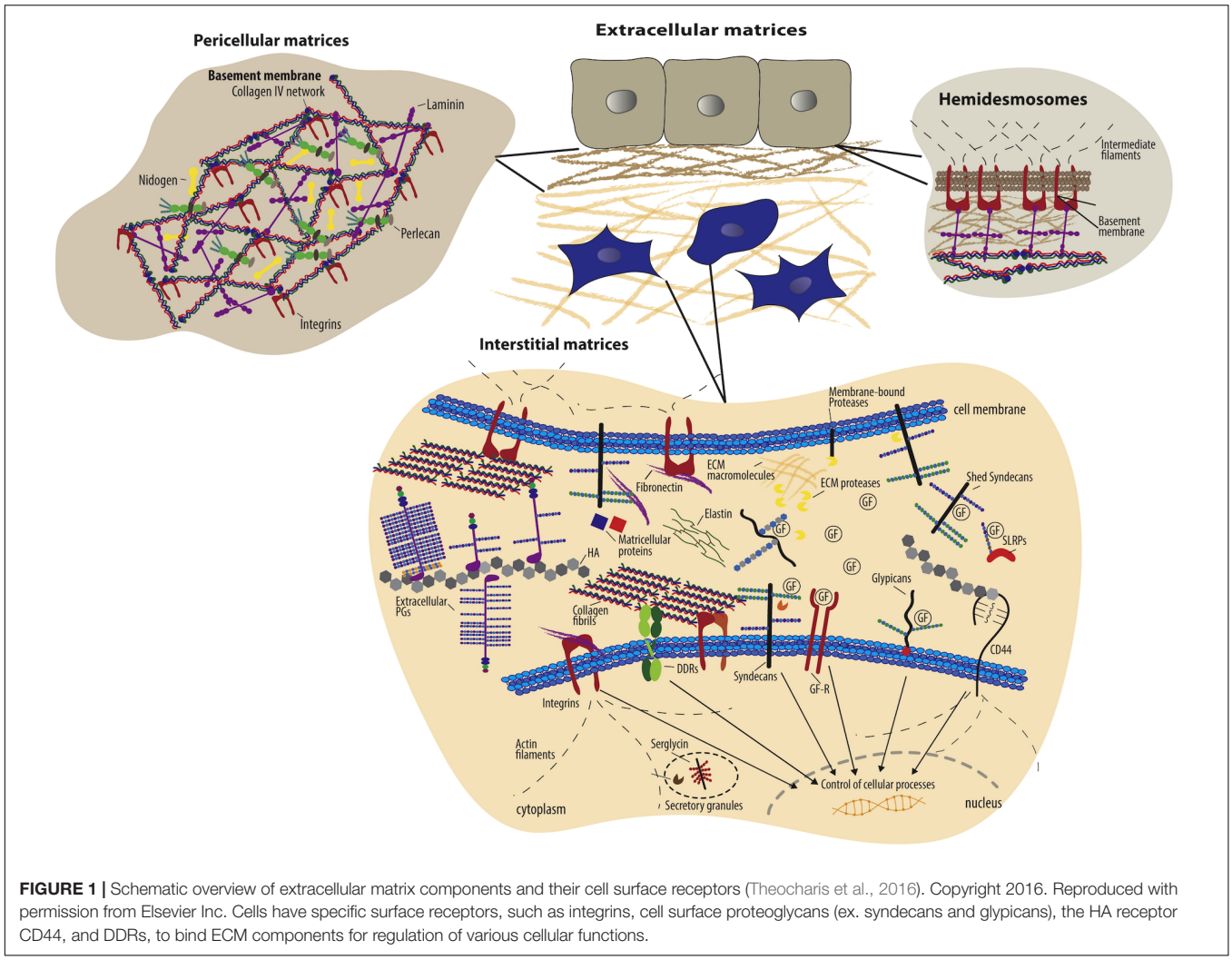

FIGURE 1 | Schematic overview of extracellular matrix components and their cell surface receptors (Theocharis et al., 2016). Copyright 2016. Reproduced with permission from Elsevier Inc. Cells have specific surface receptors, such as integrins, cell surface proteoglycans (ex. syndecans and glypicans), the HA receptor CD44, and DDRs, to bind ECM components for regulation of various cellular functions.

(Belting, 2003). The interaction is highly specific, involving electrostatic forces between the negatively charged heparin and positively charged amino acid residues (e.g., lysine and arginine), and both protects the stability of proteins and increases their affinity for cell receptors (Gospodarowicz and Cheng, 1986). Due to the ability of heparin to interact with proteins, particularly growth factors, heparin has been utilized widely in DDS, with a focus on binding of growth factors (rather than to cell-surface receptors). Heparin-based hydrogels have been widely employed as growth factor carriers for tissue regeneration (Zieris et al., 2010, 2011; Prokoph et al., 2012; Tsurkan et al., 2013; Liang and Kiick, 2014; Freudenberg et al., 2016).

On the other hand, chondroitin sulfate and hyaluronic acid have an affinity to non-integrin cell receptors such as CD44. Chondroitin sulfate is also composed of a sulfated β-1,3-linked N-acetyl galactosamine (GalNAc) and β-1,4-linked D-glucuronic acid (GlcA) disaccharide repeating units. The sulfation pattern defines the different roles of chondroitin sulfate and its selective interaction with molecules mediating such functions as regulation of signal transduction, cell division and morphogenesis, and development of the central nervous system (Zhao et al., 2015). Hyaluronic acid is a non-sulfated polysaccharide composed of disaccharide repeating units of glucuronic acid and N-acetylglucosamine. Hyaluronic acid as a major role in tissue architecture, tissue regeneration, ingrowth of blood vessels, and cellular functions such as motility, adhesion, and proliferation (Jiang et al., 2011) has been utilized in DDS to improve long-acting and target-specific delivery (Tripodo et al., 2015; Highley et al., 2016; Jiao et al., 2016). In particular, due to the highly specific cellular receptor interaction and cellular uptake of hyaluronic acid in kidney, liver, lymphatic vessels, and tumor sites, hyaluronic acid often has been employed as carriers for intracellular drugs such as anti-tumor agents, and nucleic acids (Oh et al., 2010; Dosio et al., 2016; Lallana et al., 2017; Huang and Huang, 2018; Miyazaki et al., 2018).

Interactions of ECM With Cell Receptors

Extracellular matrix molecules typically interact with cells through both integrin and non-integrin cell surface receptors (**Table 1**). The integrin receptors primarily bind the ECM proteins to connect with the cytoskeleton and to cooperate with

growth factor receptors for cell survival, cell cycle progression, and cell migration (Giancotti and Ruoslahti, 1999; Giancotti, 2003; Harburger and Calderwood, 2009). As introduced above, integrins consist of heterodimeric non-covalent association of α and β subunits which comprise a specific receptor. In particular, α subunits have a highly specific role in ligand binding for signal transduction (Rosso et al., 2004), with $\alpha_2\beta_1$, for example, binding to the collagen family, $\alpha_5\beta_1$ binding to fibronectin, and $\alpha_v\beta_3$ binding to fibronectin, vitronectin and fibrinogen as summarized in Table 1 from Alam et al. (2007). Integrin-mediated binding has been leveraged for an enormous range of applications, as multiple integrin receptors, including $\alpha_v\beta_3$, $\alpha_v\beta_5$, $\alpha_v\beta_6$, $\alpha_v\beta_8$, $\alpha_{IIb}\beta_3$, $\alpha_5\beta_1$, and $\alpha_8\beta_1$ recognize and bind to the Arg-Gly-Asp (RGD) motif which is found in multiple ECM proteins including collagens, fibronectin, laminin, tenascin, vitronectin, and thrombospondin (Ruoslahti and Pierschbacher, 1986; Kim et al., 2011). The RGD sequence as a "minimal" ligand for multiple integrins has been widely used over numerous decades in the development of targeted polymeric and nanoparticle-based therapies. The selectivity of RGD peptide for a specific integrin can be modulated by conformation of the RGD sequence and its flanking residues (Dunehoo et al., 2006). Cyclic peptides, cRGDfK, cRGDyK, and RGDC4 are selective for the integrins $\alpha_v\beta_3$ and $\alpha_v\beta_5$, which are overexpressed in vasculature of tumor tissue. Likewise, the GFOGER sequence of collagen binds to four different integrin cell receptors ($\alpha_1\beta_1$, $\alpha_2\beta_1$, $\alpha_{10}\beta_1$, and $\alpha_{11}\beta_1$) (Zeltz et al., 2014); since the $\alpha_2\beta_1$ integrin receptor is involved in osteogenesis, the GFOGER sequence has been utilized to assist in bone repair (Wojtowicz et al., 2010).

The REDV sequence from fibronectin is a cell adhesion motif to integrin $\alpha_4\beta_1$, selective for the endothelial cells (Mould et al., 1991; Massia and Hubbell, 1992). Owing to the specificity toward endothelial cells, the REDV sequence has been modified on the system to transport gene to vascular endothelial cells (Wang et al., 2015; Zhou et al., 2016) In addition, the active peptide sequences from laminin are able to interact with integrins, syndecans, α-dystroglycan, and CD44, to perform various biological activities, cell adhesion and neurite outgrowth and proliferation, and angiogenesis, such as those mediated by laminin (Farrukh et al., 2017). The YIGSR sequence and IKVAV sequence from laminin are also cell adhesion domains (Graf et al., 1987; Tashiro et al., 1989), and the RKRLQVQLSIRT (AG73) sequence derived from the mouse laminin α1 chain interacts with syndecans to promote cell adhesion, neurite outgrowth, and angiogenesis (Hoffman et al., 2001). In contrast, DFKLFAVYIKYR-GGC (C16Y), derived from the mouse laminin γ1 chain, binds to integrin $\alpha_v\beta_3$ and $\alpha_5\beta_1$ receptors (Hamano et al., 2012). Laminin-derived peptides have been incorporated into the delivery systems of anti-tumor agents to enhance their specificity to highly expressed laminin receptors on cancer cells, including YIGSR for the 32/67 kD receptor, IKVAV for the $\alpha_3\beta_1$ and $\alpha_6\beta_1$ integrin receptors, AG73 for syndecan-2 receptor and C16Y for the $\alpha_v\beta_3$ integrin receptors (Dubey et al., 2010; Negishi et al., 2011; Hamano et al., 2012; Okur et al., 2016; Negishi and Nomizu, 2019).

Short synthetic peptides derived from ECM proteins retain the integrin-binding function, thus are attractive in the design of materials. For example, the Stupp group has developed bioactive peptide amphiphiles (PA) for regenerative medicine applications (Boekhoven and Stupp, 2014; Hendricks et al., 2017; Sato et al., 2018). The RGDS sequence has been attached to PA to induce integrin-mediated adhesion, spreading or migration of fibroblasts, breast cancer cells, and bone marrow mononuclear cells *in vitro* (Storrie et al., 2007; Webber et al., 2010; Zhou et al., 2019). In addition, the IKVAV sequence has been added to PA to induce differentiation of progenitor cells into neurons (Silva et al., 2004). In addition, these ECM proteins have binding sites for both integrin and growth factors. Once ECM proteins engage integrins for adhesion, the proximity of the cell to the ECM localizes the growth factors to their cell surface receptors to induce and/or amplify the signaling for development or repair. Capitalizing on this biological cooperativity offers an enormous advantage in ECM protein-based systems for delivery of growth factors, particularly, in inflammatory diseases where the growth factors are easily degraded (Park et al., 2017). ECM protein-based DDS are able to protect growth factors while delivering them to their receptor sites to regulate cellular responses.

Non-integrin cell receptors for ECM molecules include CD36, certain laminin-binding proteins, and proteoglycans (Rosso et al., 2004) comprising glycosaminoglycan (GAG) chains such as heparan sulfate, chondroitin sulfate, dermatan sulfate and keratin sulfate (Mythreye and Blobe, 2009). Proteoglycan co-receptors (CD44, glypicans, neuropilins, syndecans, and TβRIII/betaglycan) mediate interactions with ligands, ECM proteins or other cell surface receptors to promote the formation of cell surface receptor-signaling complexes, and also to regulate cell adhesion, migration, morphogenesis, and differentiation. Among the proteoglycan co-receptors, syndecan and CD44 receptors also bind ECM molecules. Syndecan receptors bind collagens, fibronectin, and laminin and growth factors (e.g., fibroblast growth factor) to assemble signaling complexes with other receptors to control cellular differentiation and development (Yoneda and Couchman, 2003), and CD44 receptors bind to type I and IV collagens and hyaluronan to regulate cell adhesion and movement (Cichy and Pure, 2003). These ECM molecules have been exploited in the DDS not only to target cells that highly expressed those receptors in certain pathological conditions, but also to control the regulation of cellular responses.

Collagen directly interacts with four different integrin cell receptors, $\alpha_1\beta_1$, $\alpha_2\beta_1$, $\alpha_{10}\beta_1$, and $\alpha_{11}\beta_1$, depending on the type and form of collagen (Zeltz et al., 2014). $\alpha_2\beta_1$ and $\alpha_{11}\beta_1$ integrins primarily interact with the fibrillar collagen type I (e.g., $\alpha_2\beta_1$ integrin mediates collagen type I binding for phagocytosis in fibroblasts (Rainero, 2016), while $\alpha_1\beta_1$ and $\alpha_{10}\beta_1$ interact with the non-fibrillar collagens IV and VI. Collagen also binds to non-integrin receptors such as discoidin domain receptors (DDR1 and DDR2), the GPVI receptor on platelets, the LAIR receptor of immune cells, the OSCAR receptor of osteoblasts, and mannose receptors (Endo180 or uPARAP) (An and Brodsky, 2016). Under particular pathological conditions, these collagen receptors are highly expressed. Endo180/uPARAP receptor is overexpressed by malignant cells in sarcomas, glioblastomas, subsets of acute myeloid leukemia (Nielsen et al., 2017). For integrins, expression

of $\alpha_1\beta_1$ and $\alpha_2\beta_1$ was localized to scleral fibroblast focal adhesions and expression of integrin $\alpha_{11}\beta_1$ is restricted to tumor stroma or other fibrotic disease (McBrien et al., 2006; Schnittert et al., 2018). Collagen as a ligand to target these pathological conditions thus represents a powerful therapeutic strategy.

Fibronectin binds both integrin receptors and other ECM molecules. Fibronectin type III_{10} domain which includes the RGD sequence, is the binding sites for integrins, $\alpha_5\beta_1$, $\alpha_3\beta_1$, $\alpha_8\beta_1$, and $\alpha_v\beta_3$ in a broad range of cell types and tissues (Pankov and Yamada, 2002). In particular, $\alpha_5\beta_1$ integrin is required for internalization of fibronectin through caveolin-1 dependent endocytosis in myofibroblasts (Rainero, 2016). And, $\alpha_4\beta_1$ and $\alpha_4\beta_7$ integrins recognize the LDV and REDV motifs in the alternatively spliced V region, IDAPS in the III_{14} domain, and KLDAPT in the III_5 domain. In addition, $\alpha_4\beta_1$ and $\alpha_9\beta_1$ binds the EDGIHEL sequence in the alternatively spliced EDA segment. Fibronectin also contains two heparin-binding domains within its V domain to interact with heparin and chondroitin sulfate for cell adhesion, and the fibronectin I_{6-9} and $II_{1,2}$ domains recognize denatured collagens to clear them from blood and tissue. The expression of the various fibronectin integrin receptors depends on the pathological conditions, providing targets for DDS. The integrins $\alpha_5\beta_1$ and $\alpha_v\beta_3$ are upregulated in angiogenic vessels during angiogenesis (Ruoslahti, 2002); in particular, the integrin $\alpha_v\beta_3$ is not expressed in healthy adult animal tissue but overexpressed during angiogenesis in tumor tissues, allowing for the targeting of integrin $\alpha_v\beta_3$ with fibronectin-based, chemotherapeutic DDS.

Moreover, laminin binds various integrins receptors ($\alpha_1\beta_1$, $\alpha_2\beta_1$, $\alpha_3\beta_1$, $\alpha_6\beta_1$, $\alpha_7\beta_1$, $\alpha_{10}\beta_1$, $\alpha_6\beta_4$, and $\alpha_v\beta_8$) (Alam et al., 2007). Laminin-1, 2, 5, 8, 10, 11 isoforms interact with integrins $\alpha_3\beta_1$ and $\alpha_6\beta_1$ which regulate embryonic development, epithelial regeneration, and wound healing processes, and which also internalize to endosome as well (Das et al., 2017). Laminin binding cell receptors are highly expressed in various cancer cells types. For example, integrins $\alpha_3\beta_1$ and $\alpha_6\beta_1$ are overexpressed in various epithelial cancers. Amongst non-integrin receptors, laminin receptor (LAM 67R) is overexpressed on human prostate cancer cells and syndecan-2 is overexpressed in various cancer cell lines and during angiogenesis (Shukla et al., 2012). Based on expression of laminin receptors in certain pathological condition, laminin or synthetic laminin mimetic peptides as ligand are utilized as ligands to target and deliver therapeutic agents.

Chondroitin sulfate interacts with cell-surface CD44 receptors. CD44 receptors are an attractive target as they are a cancer stem cell marker which is overexpressed about four- to five-fold in metastasis and cancer progression (Goebeler et al., 1996). Owing to the interaction between chondroitin sulfate and CD44 receptor, chondroitin sulfate has been utilized in DDS to target CD44 overexpressing cancer cells and promote receptor-mediated endocytosis. The polysaccharide hyaluronic acid binds toll-like receptors, CD44, and RHAMM on cell membrane. Interactions with toll-like receptors regulate signaling in inflammatory cells and other cell types, and those with CD44 control leukocyte homing and recruitment. In addition, hyaluronic acid interactions with CD44 and RHAMM regulates tumor growth and metastasis. CD44 expression is characteristic in cells under certain pathological conditions such as infarcted myocardium, infiltrating leukocytes, wound myofibroblasts, vascular cells, and many tumor cells.

Receptor-Mediated Endocytosis

The efficacy, biomedical function, biodistribution, and toxicity of drugs with intracellular targets of action are dictated by their internalization into the cells through interaction with the exterior of the plasma membrane and their endocytic pathway (Sahay et al., 2010; Foroozandeh and Aziz, 2018). Endocytosis occurs via two primary routes – phagocytosis and pinocytosis (Yameen et al., 2014), with phagocytosis characteristic of dendritic cells, neutrophils, monocytes and macrophages (Aderem and Underhill, 1999) and pinocytosis, which occurs via clathrin-mediated endocytosis, caveolae-mediated endocytosis, clathrin/caveolae-independent endocytosis, and micropinocytosis (Sahay et al., 2010; Yameen et al., 2014), possible for all cell types. Micropinocytosis is an actin-driven endocytic process that initiates the activation of receptor tyrosine kinases (e.g., via growth factors) to polymerize actin and form macropinosomes for cell entry. Unlike micropinocytosis, receptor-mediated endocytosis (e.g., clathrin-mediated endocytosis, caveolae-mediated endocytosis, and clathrin/caveolase-independent endocytosis) is regulated by specific interactions between a receptor and an extracellular ligand or particle (Yameen et al., 2014). Physical properties of the extracellular cargo, including particle size, shape, and surface charge, all influence the cellular uptake pathway. In addition to these physical properties, very specific ligand-receptor interactions dictate the receptor-mediated endocytosis pathways of ligand-decorated cargo.

The majority of DDS are internalized into cells through the clathrin-mediated endocytosis pathway using interactions with numerous receptors on cell membrane including transferrin, asialoglycoprotein receptor, epidermal growth factor receptor, chemokine receptors, and cell adhesion receptors (Tsuji et al., 2013; Xu et al., 2013; D'Souza and Devarajan, 2015; Phuc and Taniguchi, 2017; Hu et al., 2018; Nieto Gutierrez and McDonald, 2018). In this process, particular ligands in the extracellular fluid bind to the receptors on the surface of the cell membrane, which is rich in clathrin, to form a ligand-receptor complex (Munsell et al., 2016) that forms a clathrin-coated pit and results in the formation of clathrin-coated vesicles approximately 10 to 200 nm in diameter for internalization. After internalization, the clathrin coat on the vesicles is expelled and recycled to the plasma membrane and the vesicle fuses with the early endosomes. The cargo within early endosomes will reach lysosomes and eventually be degraded by the acidic pH and digestive enzyme of the lysosome. Given the relatively large number of binding molecules, clathrin-mediated endocytosis is a primary uptake pathway for most polymeric DDS.

Polymer-mediated nucleic acid delivery systems have been reported with both clathrin-mediated endocytosis and caveolae-mediated endocytosis as their uptake pathways, depending on the size, types, and surface charge of their cargos, and cellular microenvironment (2D vs. 3D) (El-Sayed and Harashima, 2013; Truong et al., 2019). However, trafficking of cargo through

caveolae-mediated endocytosis routes enhances gene expression owing to the low or non-acidifying pathway (Rejman et al., 2005; Reilly et al., 2012). Caveolae-mediated endocytosis occurs via association of the delivery vehicle with cholesterol-rich lipid rafts in the plasma membrane for cellular entry (Sahay et al., 2010). Once cargo molecules bind to the caveolae surface rich in glycosphingolpids including GM-1 and Gb3, the caveolae engulf the cargo to form vesicles approximately 50 nm in diameter. The detached caveolar vesicles can fuse with early endosomes, but because the caveolar vesicles have neutral pH, they generally avoid fusion with lysosomes thus preventing lyososomal degradation of drug cargo.

Clathrin-and caveolae-independent endocytosis occurs without binding of the cargo to clathrin or caveolae (Yameen et al., 2014); the pathway depends instead on cell-surface molecules such as Arf-6, flotillin, Cdc42, and RhoA, involving different subtypes of internalization routes depending on the specific cell-surface molecule. Once cargo is internalized, it is usually delivered to the early endosome and trafficked though lysosomal pathways.

The ECM is constantly remodeled, via balancing of synthesis, deposition, and degradation to control tissue homeostasis, and during this process ECM molecules themselves are internalized through receptor-mediated endocytic pathways. Degradation of the ECM occurs largely through two pathways; extracellular degradation mediated by matrix metalloproteases (MMPs) and lysosomal degradation after receptor-mediated internalization (Rainero, 2016). The internalization of the most abundant component of ECM, collagen, is controlled by integrin-mediated phagocytic uptake and Endo-180 dependent clathrin mediated pathway. Fibrillar collagen type I binds to $\alpha_2\beta_1$ integrin receptor, promoting internalization of collagen to early endosomes (Arora et al., 2013). On the other hand, soluble collagen type I, IV and V fragments bind Endo180 or uPARAP to internalize to endosome via the clathrin-dependent endocytic pathway (Madsen et al., 2011).

Similar to collagens, fibronectin is degraded by lysosomal degradation after endocytosis. Endocytosis of both soluble and matrix fibronectin is mediated by $\alpha_5\beta_1$ integrin receptor via caveolin-1 dependent uptake (Shi and Sottile, 2008). Fibronectin binding to $\alpha_2\beta_1$ integrin receptor, ultimately leading to endosomal sorting and transport to the lysosome (Lobert et al., 2010). The internalization of the major component of basement membrane, laminin, is controlled by $\alpha_3\beta_1$ integrin receptor and dystroglycan for protein turnover. Interestingly, the activation of the $\alpha_3\beta_1$ integrin receptor by laminin binding results in phagocytosis of other ECM molecules as well (Coopman et al., 1996). The internalization of laminin requires dystroglycan for receptor-mediated and dynamin-dependent pathways, leading to lysosomal degradation (Leonoudakis et al., 2014). Meanwhile, degradation of hyaluronic acid is controlled by multiple events. High molecular weight hyaluronic acid is degraded to smaller fragments by the extracellular hyaluronic acid-digesting enzyme, hyaluronidase 2 (Hyal 2) (Racine and Mummert, 2012). These fragments can be endocytosed by either receptor-mediated endocytosis (10^4 Da) or micropinocytosis (10^6 Da), depending on the molecular weight of the fragment. Hyaluronic acid fragments binding to CD44 and lymphatic vessel endothelial-1 (LYVE-1) receptors promote the endocytosis of hyaluronic acid via the clathrin-mediated pathway. The wide range of different internalization mechanisms for ECM molecules can be exploited in DDS for the selective uptake of intracellularly active drugs.

ECM-TARGETED DELIVERY OF PARTICLE-BASED DDS

Extracellular matrix molecules have been successfully formulated into particles for drug delivery applications. The chondroitin-sulfate modified CD44 receptor is able to bind to triple helical sequence from collagen Type IV (Rezler et al., 2007); Fields and co-workers thus developed CD44-binding, collagen-mimetic peptides [$(GPO)_4GVKGDKGNPGWPGAP(GPO)_4$] and used them to modify liposomes as a DDS to cancer cells with highly expressed CD44 cell receptor (**Table 2**). They demonstrated that doxorubicin delivered via this DDS reduced the tumor size up to 60%, compared to untreated control in a $CD44^+$ mouse melanoma model (Ndinguri et al., 2012). Moreover, others have taken advantage of another collagen receptors, DDR2, which is highly expressed in fast-growing invasive tumors (Leitinger, 2014). The Brodsky group reported a recombinant collagen protein (VCLCL-DDRT) that binds DDR2 and could thus serve as a potential tumor treatment (An and Brodsky, 2016). They showed the delay of megakaryocyte migration as a result of the competition between the recombinant VCLCL-DDRT and animal collagen for binding to DDR2. In addition, our group recently has developed conjugates of the collagen-like peptide [$(GPO)_4GFOGER(GPO)_4GG$, CLP] and elastin-like peptide [$(VPGFG)_6$, ELP] to serve as thermoresponsive vesicles as a drug carrier (**Figure 2A**) (Luo et al., 2017). This CLP-decorated vesicle has both thermally responsive assembly behavior owing to the temperature-responsiveness of the CLP domain's triple helix formation, and a strong affinity to native collagen through collagen triple helix hybridization, and is therefore able to sequester, for at least 21 days, a hydrophobic model compound (fluorescein) in collagen type II films, with subsequent thermally triggered release. The vesicles also show high cytocompatibility with both fibroblasts and chondrocytes and essentially no activation of a macrophage cell line. The ELP-CLP conjugates have the potential to deliver intracellularly active drugs through receptor-mediated endocytosis using interactions between the GFOGER sequence on CLP and integrin receptors ($\alpha_1\beta_1$, $\alpha_2\beta_1$, $\alpha_{10}\beta_1$, and $\alpha_{11}\beta_1$) (Zeltz et al., 2014).

The use of fibronectin-based molecules has also been employed for successful targeting and increased intracellular uptake of local DDS. The Akaike group incorporated fibronectin in a calcium phosphate co-precipitated, non-viral gene delivery system (Chowdhury and Akaike, 2006); the fibronectin coating in calcium phosphate and pDNA precipitate allowed cell-surface integrin receptor binding for internalization into cells and supported 100-fold higher levels of gene expression than without the fibronectin coating. In the past, direct conjugation of the cyclic RGD peptide, RGD4C, on the anticancer agent, doxorubicin, demonstrated better efficacy in suppressing

TABLE 2 | Extracellular matrix protein-derived peptides as ligands to bind to cell surface receptors in drug delivery systems.

ECM molecules	Peptides	Cell receptor	Application	References
Collagen	GGYGGGP(GPP)$_5$GFOGER(GPP)$_5$GPC	$\alpha_2\beta_1$	Local protein delivery	Shekaran et al., 2014
	(GPO)$_4$GVKGDKGNPGWPGAP(GPO)$_4$	Chondroitin sulfate modified CD44	Anti-cancer drug delivery	Ndinguri et al., 2012
	VCLCL-DDRT (Recombinant protein)	DDRs	Block the activity of cancer cell	An and Brodsky, 2016
ECM proteins	cRGD4C	$\alpha_v\beta_3$ and $\alpha_v\beta_5$	Anti-cancer drug delivery	Arap et al., 1998
	cRGDfC	$\alpha_v\beta_3$ and $\alpha_v\beta_5$	Anti-cancer drug delivery	Bibby et al., 2005
	cACRGDMFGCA	$\alpha_v\beta_3$ and $\alpha_v\beta_5$	VEGFR2-SiRNA delivery	Schiffelers et al., 2004
Laminin	RKRLQVQLSIRT	Syndecan	Anti-cancer drug delivery	Negishi and Nomizu, 2019
	DFKLFAVYIKYR-GGC (C16Y)	Integrin $\alpha_v\beta_3$	Anti-cancer drug delivery	Hamano et al., 2012

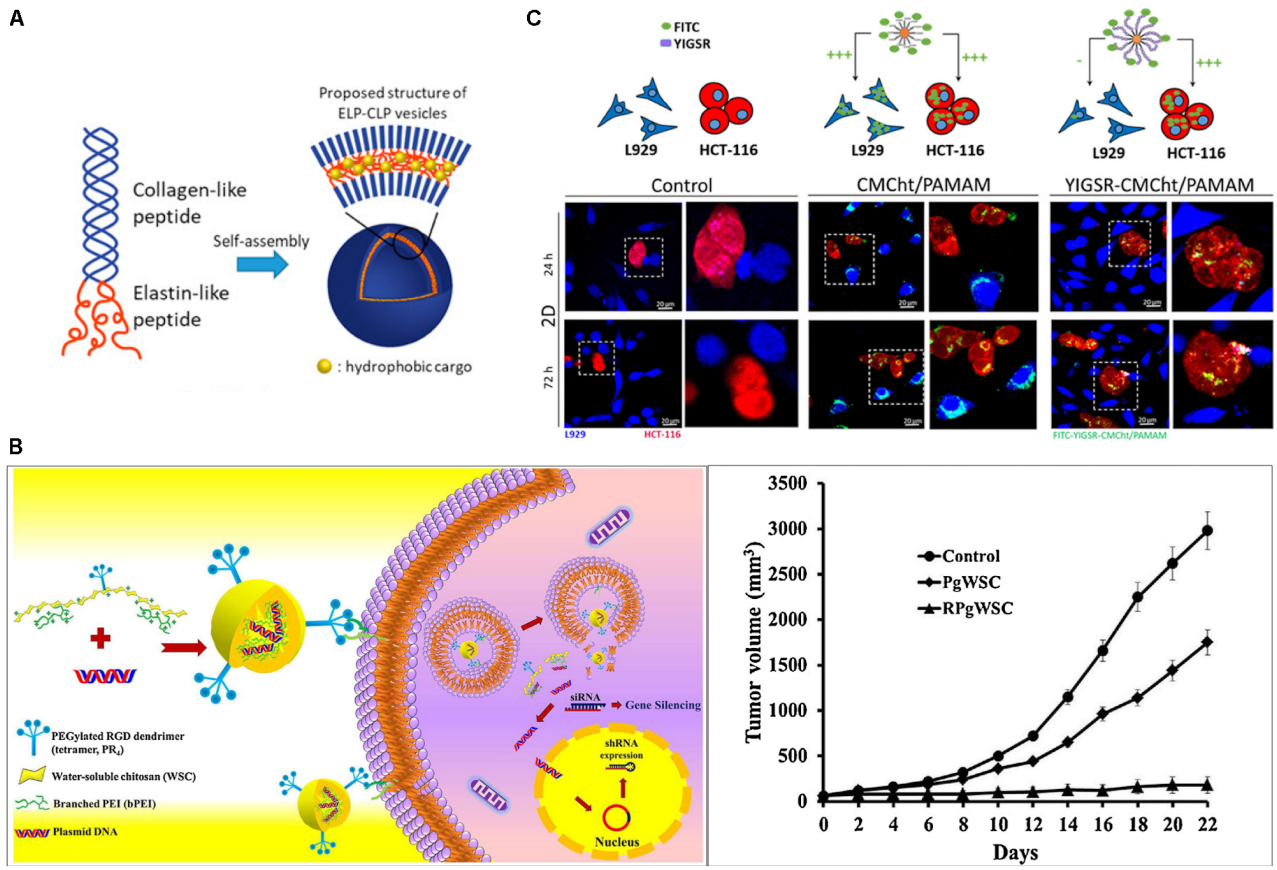

FIGURE 2 | Extracellular matrix-based targeted delivery of particle-based DDS. **(A)** Schematic of ELP-CLP conjugate-based thermoresponsive nanovesicles (Luo et al., 2017). Copyright 2017. Reproduced with permission from American chemical society. **(B)** RGD dendrimer peptide modified polyethyleneimine-grafted chitosan for siRNA delivery. *In vivo* tumor growth of treatment with non-RGD-modified system (PgWSC) and RGD-modified system (RpgWSC), and non-treatment (Y.M. Kim et al., 2017). Copyright 2017. Reproduced with permission from Elsevier Inc. **(C)** Confocal images of internalization of dendrimer particles (CMCht/PAMAM and YIGSR-CMCht/PAMAM) on HCT-116 cancer cells (red) and L929 fibroblasts (blue) (Carvalho et al., 2019). Copyright Wiley-VCH Verlag GmbH. & Co. KGaA. Reproduced with permission.

tumor progression than doxorubicin alone, in mouse models bearing human breast carcinoma cells (Arap et al., 1998). The RGD peptide-modified DDS showed improved localization and intracellular uptake into cancer cells. The Jang group investigated the dendrimeric RGD peptides modified on co-polymer, which consists of polyethyleneimine and water soluble chitosan (RpgWSC), for an siRNA delivery system to target $\alpha_v\beta_3$ integrin-overexpressing tumor cells for cancer therapy (**Figure 2B**; Kim et al., 2017). The delivery systems allow the cellular uptake of siRNA to PC3 cancer cells through microtubule-dependent micropinocytosis and clathrin-mediated endocytosis. The delivery of siRNA, via the use of their DDS with RGD (RpgWSC), for silencing the mRNA encoding the hBCL2 protein in a PC3 tumor xenograft mouse model, presented greater inhibition of tumor growth through the blocking of BCL2 protein expression, compared to a non-RGD modified delivery system

(PgWSC) (**Figure 2B**). These results are a recent illustration of the power of employing RGD in DDS for improving delivery of intracellularly active cancer therapeutics into $\alpha_v\beta_3$ integrin overexpressing tumor cells.

The active sequence peptides from laminin are able to interact with cell surface receptors, integrins, syndecans, α-dystroglycan, and CD44, to perform various biological activities like those mediated by full-length laminin. The laminin-derived RKRLQVQLSIRT (AG73) peptide was modified with PEGylated liposomes to deliver plasmid DNA in human embryonic kidney carcinoma cells, which overexpress syndecan-2 (Negishi et al., 2010; Negishi and Nomizu, 2019). On the other hand, cancer cells, including bile duct carcinoma, colorectal carcinoma, cervical cancer, and breast carcinoma, highly express the 67 KDa laminin receptor (67LR), for which the laminin-derived YIGSR sequence has high affinity. YIGSR-modified carboxylmethychitosan/poly(amidoamine) (CMCht/PAMAM) dendrimer nanoparticles were developed to drive targeted internalization into colorectal cancer cells (HCT-116 CRC cells) (Carvalho et al., 2019) via this interaction. The YIGSR-modified CMCht/PAMAM nanoparticles were more selectively internalized by HCT-116 colorectal cancer cells than by L929 fibroblasts and non-YIGSR-modified CMCht/PAMAM nanoparticles were non-selectively internalized by both types of cells (**Figure 2C**). Laminin-based material modification are a promising strategy to improve the specificity of the delivery system on the laminin receptor expressed cells such as tumor.

Heparin is incorporated in DDS to target overexpressed angiogenic growth factors in tumor tissues (Shing et al., 1984). Tae groups demonstrated heparin-coated PLGA nanoparticle to accumulate in the tumor in SCC7 tumor-bearing athymic mice (Chung et al., 2010). In addition, dendronized heparin-doxorubicin conjugate-based nanoparticle developed by Gu group represented the improvement of antitumor efficacy and anti-angiogenic effects in a mouse 4T1 breast cancer tumor model, compared to free doxorubicin (She et al., 2013). On the other hand, many studies have investigated the DDS incorporating hyaluronic acid or chondroitin sulfate as a ligand to target CD44-overexpressing cancer cells. Gupta and co-workers formulated polyehtylenimine (PEI) conjugated chondroitin sulfate to form complexes with plasmid DNA (Pathak et al., 2009). Their system, administrated by intravenous injection in Ehrlich ascites tumor (EAT)-bearing mice, accumulated in tumor mass to a significantly greater extent as compared to non-chondroitin sulfate-modified PEI/pDNA complex. The attachment of hyaluronic acid on liposomes loaded with doxorubicin resulted in the selective binding of the DDS on CD44-expressing murine melanoma cells, resulting in a substantial reduction in the IC_{50} (Eliaz and Szoka, 2001). In addition, Zhang group developed ternary complex based on hyaluronic acid, dexamethasone conjugated polyethyleneimine (PEI) and plasmid DNA to enhance CD44 receptor-mediated endocytosis (Fan et al., 2013). This ternary complex improved cellular uptake and nuclear transport of DNA in melanoma tumor cells, leading to the highest transfection efficiency and suppressed the growth of tumor in mice. Hyaluronic acid has also been utilized to target CD44 receptors overexpressed in macrophages as a strategy for the treatment of inflammatory disease. Pilehvar-Soltanahmadi and co-workers reported hyaluronic acid-conjugated polylactide nanoparticles encapsulated curcumin delivered to macrophage to achieve the modulation of macrophage polarity from the pro-inflammatory M1 phenotype to the anti-inflammatory M2 phenotype (Farajzadeh et al., 2018). The modification of ECM polysaccharides accomplishes the delivery of drugs at the target sites where their receptors are highly expressed.

ECM-BASED HYDROGEL MATRICES FOR DRUG DELIVERY

Drug transport within a hydrogel can be controlled by manipulating its mesh size and/or its interaction with drugs using chemical strategies (Merino et al., 2015; Li and Mooney, 2016; Sood et al., 2016; Oliva et al., 2017; Dimatteo et al., 2018). Hydrogels comprise crosslinked polymer networks, and drugs smaller than the network mesh size can simply diffuse through the hydrogel, whereas drugs larger than the mesh size are entrapped in the hydrogel and released upon degradation of the network. The polymer backbone and crosslinks can be degraded by either slow hydrolysis of ester bonds or peptide bonds, by the scission of thiol-based crosslinks, or by bio-responsive mechanisms such as enzyme activity (Lutolf et al., 2003; Zustiak and Leach, 2010; Wang, 2018). The degradation of hydrogels in biomedical applications can be tuned based on the local cellular environment by incorporating crosslinks comprising peptides that are degradable by different types of matrix metalloproteinases (Patterson and Hubbell, 2010). Moreover, drug release from the hydrogel can be modulated by incorporating non-covalent or covalent drug-matrix interactions (Appel et al., 2015; Li and Mooney, 2016; Ruskowitz and DeForest, 2018; Narayanaswamy and Torchilin, 2019). Non-covalent interactions include electrostatic interactions such as heparin and heparin binding proteins (Liang and Kiick, 2014; Freudenberg et al., 2016), or hydrophobic associations such as cyclodextrin and hydrophobic drugs (Mateen and Hoare, 2014). Otherwise, covalent interactions can be designed using non-cleavable and cleavable linkages between drugs and hydrogels that are incorporated via reactions such as click chemistries (e.g., copper-free click, thiol-ene, Diels-Alder reactions, and oxime and hydrazine ligation) and photochemistries (e.g., nitrobenzyl and coumarin photocleavage reactions); these reactions also are employed for hydrogel crosslinking (Christman et al., 2011; Yigit et al., 2011; Phelps et al., 2012; Ulrich et al., 2014; Kolmel and Kool, 2017; Ruskowitz and DeForest, 2018; Palmese et al., 2019). Thus, the chemical tunability of hydrogels, particularly their mesh size, crosslinking chemistry, and drug interactions, enables fine-tuned control over drug transport through the hydrogel.

Simple Diffusion

Extracellular matrix-based hydrogels for local drug delivery not only support cells biochemically and mechanically through cell-matrix interactions, but also release the drugs into infiltrated cells. Since the hydrogel is formed by the

crosslinked polymer network, the mesh space between polymer chains allows the diffusion of liquid and small molecules (Li and Mooney, 2016). Depending on the mesh size of a hydrogel, small molecule drugs can diffuse through the hydrogel and be released from the hydrogel for delivery to the surrounding cells.

Due to its structural properties, collagen is often utilized as the matrix for local drug delivery. A type I collagen matrix on the surface of polyurethane films enhanced fibroblast attachment, proliferation, and growth (Park et al., 2000). While collagen matrices provide a physiologically inspired microenvironment to cells, collagen also can control the delivery of drugs such as small molecules, proteins, and genes via simple diffusion and/or biodegradation. Collagen matrices have been loaded with a variety of small molecules such as antibiotics for wound care, cisplatin for local cancer therapy, and anti-inflammatory reagents for tissue regeneration in ophthalmology (Zilberman and Elsner, 2008; De Souza et al., 2010; Duxfield et al., 2016). Small molecule gentamicin-eluting collagen matrix [Collatamp® (Schering-Plough, Stockholm, Sweden), Sulmycin®-Implant (Schering-Plough, United States), and Septocoll® (Biomet Merck, Germany)] have been used in the clinic as wound care products to promote both granulation tissue formation and epithelialization, and to protect tissues from potential infection (de Bruin et al., 2010; Raja, 2012; Chia et al., 2014).

In addition to small molecule delivery, proteins such as growth factors can be loaded into the collagen matrix; for example the delivery of bone morphogenetic protein (BMP) from a collagen matrix has been shown to promote bone formation. Recombinant human BMP-2 (rhBMP-2)-loaded collagen matrices (INFUSE® bone graft and MASTERGRAFT®) are available in the clinic to treat bone fracture and spinal fusion (Li and Mooney, 2016). Clinical trials using INFUSE® in spinal orthopedic trauma, and oral maxillofacial applications have demonstrated the efficacy of INFUSE® to form *de novo* bone (**Figure 3A**; McKay et al., 2007). The Garcia group created a collagen mimetic peptide (GFOGER)-modified PEG synthetic hydrogel to deliver BMP-2 to murine radial critical-sized defects (Shekaran et al., 2014). The GFOGER-modified hydrogel increased osteoprogenitor localization in the defect site and sustained release of BMP-2 to enhance bone formation and healing. In addition, the Garcia group investigated RGD and GFOGER-modified PEG synthetic hydrogels for the delivery of lysostaphin to treat *Staphylococcus aureus* infections in bone fractures (**Figure 3B**; Johnson et al., 2018). Based on histological analysis, lysostaphin delivery using the RGD/GFOGER-based PEG hydrogel system (UAMS-1 + Lst) demonstrated the ability of the system to reduce bacterial infection compared to the non-treatment control (UAMS-1), and these materials were shown to promote fracture repair of femoral bone in mouse such that the resulting healed tissue was similar to sterile positive control groups. A lysostaphin solution without hydrogel (UAMS-1 + Sol.) failed both in reducing bacterial infection and in improving bone repair. ECM-based hydrogel matrices create a microenvironment conductive to supporting growth of recruited cells while also controlling drug release to enhance tissue regeneration.

ECM-Based Matrix and Drug/Carrier Interactions

Drug release from ECM-based matrix is also dependent upon drug-ECM interactions. Electrostatic and hydrophobic attractive forces between drug molecules and ECM molecules can reduce and/or prohibit drug diffusion through the network, leading to prolonged drug retention and alternate controlling parameters for release from the matrix. The electrostatic interactions between highly negative polysaccharides and drugs are employed in the sustained delivery/retention of many drugs. For example, Cool and colleagues validated the delivery efficacy of BMP-2 using thiol-modified hyaluronan (Glycosil^{TM}), and these materials were compared to collagen sponges (e.g., as a mimic of INFUSE® bone grafts) in terms of their influence on ectopic bone formation (Bhakta et al., 2013). The electrostatic interaction between BMP-2 and negatively charged hyaluronic acid hydrogels resulted in a low burst followed by sustained release of BMP-2, whereas collagen hydrogels showed high burst and sustained release of BMP-2. The low burst and sustained release of BMP-2 from hyaluronic acid hydrogels improved the bone formation to the greatest extent in a rat intramuscular ectopic model.

Moreover, due to the ability of ECM molecules to interact with growth factors, ECM molecules are utilized in DDS for the sustained release of growth factors from hydrogel matrices. In particular, heparin-based hydrogels have been widely employed as growth factor carriers for tissue regeneration (Sakiyama-Elbert and Hubbell, 2000; Tanihara et al., 2001; Jeong and Panitch, 2009; Liang and Kiick, 2014; Freudenberg et al., 2016). Netti and co-workers developed porous PEG-heparin hydrogels encapsulating the angiogenic growth factor VEGF. Because of the interaction between heparin and VEGF, VEGF was released in a controlled manner and the released VEGF promoted angiogenesis *in vivo* (Oliviero et al., 2012). Also, the Werner group investigated RGD-functionalized star PEG-heparin hydrogels with a variable degree of heparin sulfation for controlled release of angiogenic growth factors from the hydrogel and capture of inflammatory chemokines in the hydrogel for the chronic wound healing applications (Freudenberg et al., 2015; Lohmann et al., 2017). In addition, the Hubbell group developed laminin-mimetic peptides, which include heparin-binding domains, and employed them to decorate a fibrin matrix for the delivery of VEGF-A165 and platelet derived growth factor PDGF-BB in a chronic wound treatment application (Ishihara et al., 2018). Since the heparin-binding domain in laminin-mimetic peptides has a strong affinity to syndecan cell surface receptors, as well as to VEGF-A165 and PDGF-BB, the system enhanced cell adhesion through interaction with syndecan, and also enabled the sustained release of growth factors from the matrix (**Figure 4A**). This resulted in promotion of wound healing in a type-2 diabetic mouse. With a similar approach, the Christman group applied decellularized ECM-derived hydrogels in heparin-binding growth factor delivery systems for tissue regeneration in the post-myocardial infarction (Seif-Naraghi et al., 2012).

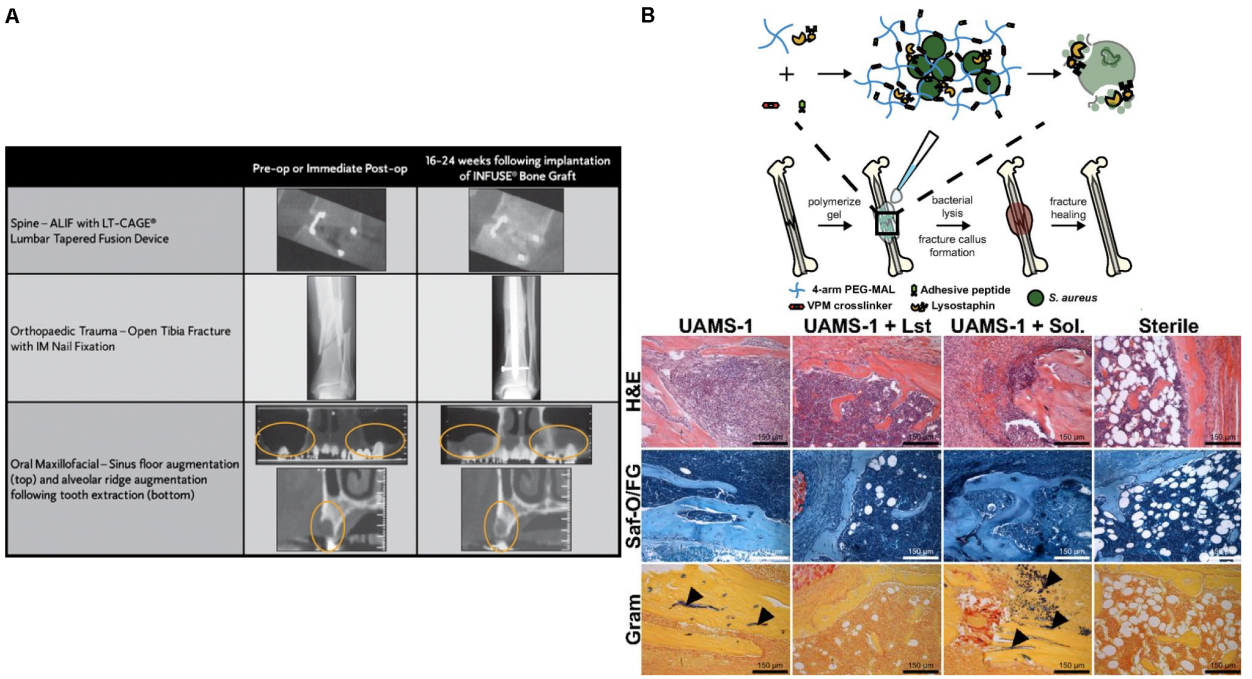

FIGURE 3 | Simple diffusion of drugs from ECM based matrices. **(A)** Computed tomography (CT) images for the efficacy of INFUSE® Bone Graft in clinical applications (McKay et al., 2007). Copyright 2007. Reproduced with permission from Springer Nature. **(B)** The scheme of overall study design. Histologic analysis using H&E, Saf-O/FG, and Gram staining of femurs after treating with hydrogel (UAMS-1), Lysostaphin-delivering hydrogel (UAMS-1 + Lst), and Lysostaphin, and sterilization (Johnson et al., 2018). Copyright 2018. Reproduced with permission from the National Academy of Sciences.

Porcine pericardia were decellularized using 1% SDS and digested with pepsin to prepare decellularized ECM-derived hydrogel with intact native sulfated glycosaminoglycans (PPM). Plasmid DNA encoding fibroblast growth factors (pFGF) in PPM injected into rats with post-myocardial infarction was still retained in the tissue after 5 days of administration, and the amount of pFGF retained was greater than the amount of bFGF retained in collagen hydrogels or in saline.

While controlled drug release via drug-ECM interactions is a powerful strategy to improve retention and sustained delivery, existing examples are mostly limited to the use of heparin-binding growth factors and charged molecules. To address this limitation, as described above, active peptide sequences from various ECM proteins have been identified and exploited in controlling the drug release from ECM-based matrices. Chemical modifications of the active sequences and their attachment to drugs or polymeric carriers enable immobilization in ECM-based hydrogel matrices for sustained drug release. Rolle and co-workers utilized a collagen-binding domain (cCBD derived from collagenase or fCBD derived from fibronectin) to tether synthetic human antimicrobial peptides, cateliciding LL37, on collagen scaffolds for treatment of wound infection (**Figure 4B**; Lozeau et al., 2017). Even after 14 days, LL37 with collagen domains (cCBD-LL37 and fCBD-LL37) was still retained on the collagen scaffold and showed similar levels of antimicrobial activity after 12 h. However, due to the burst release of LL37 from collagen scaffold, the antimicrobial activity of LL37-loaded collagen scaffolds was reduced at 14 days compared to 12 h. In another example, the Hubbell group developed strategies for the delivery and release of both immune checkpoint inhibitor antibodies (αCTLA4 + αPD-L1) and interleukin-2 (IL-2) using collagen-binding domains (CBDs) derived from the von Willebrand factor (vWF) A3 domain to immobilize drugs on collagen in the tumor stroma for cancer immunotherapy (Ishihara et al., 2019). Systemically administered CBD-tumor drug conjugates mainly accumulated in the tumor sites in murine cancer models, whereas non-CBD modified drugs did not. Drug delivery and release from the tumor collagen matrix-DDS interaction improved safety by eliminating antibody hepatotoxicity and by ameliorating pulmonary edema by IL-2, and it also improved efficacy through reducing the size of tumor. Overall, these examples demonstrate that the immobilization of therapeutic agents on the matrix using peptides prolongs the effectiveness of the therapeutic agents via controlled release from the scaffold.

ECM-Based Matrix and Carrier Interaction for Intracellular Delivery

Drug delivery systems that combine these two approaches, e.g., immobilizing a drug in an ECM-based hydrogel and exploiting ECM-mediated cell uptake, have demonstrated enhanced therapeutic efficacy. In particular, this hybrid strategy will have enormous benefit on the delivery of intracellular therapeutic agents such as nucleic acids, which require DDS to facilitate cellular internalization and prevent the degradation of nucleic acids in the extra- and intracellular environments

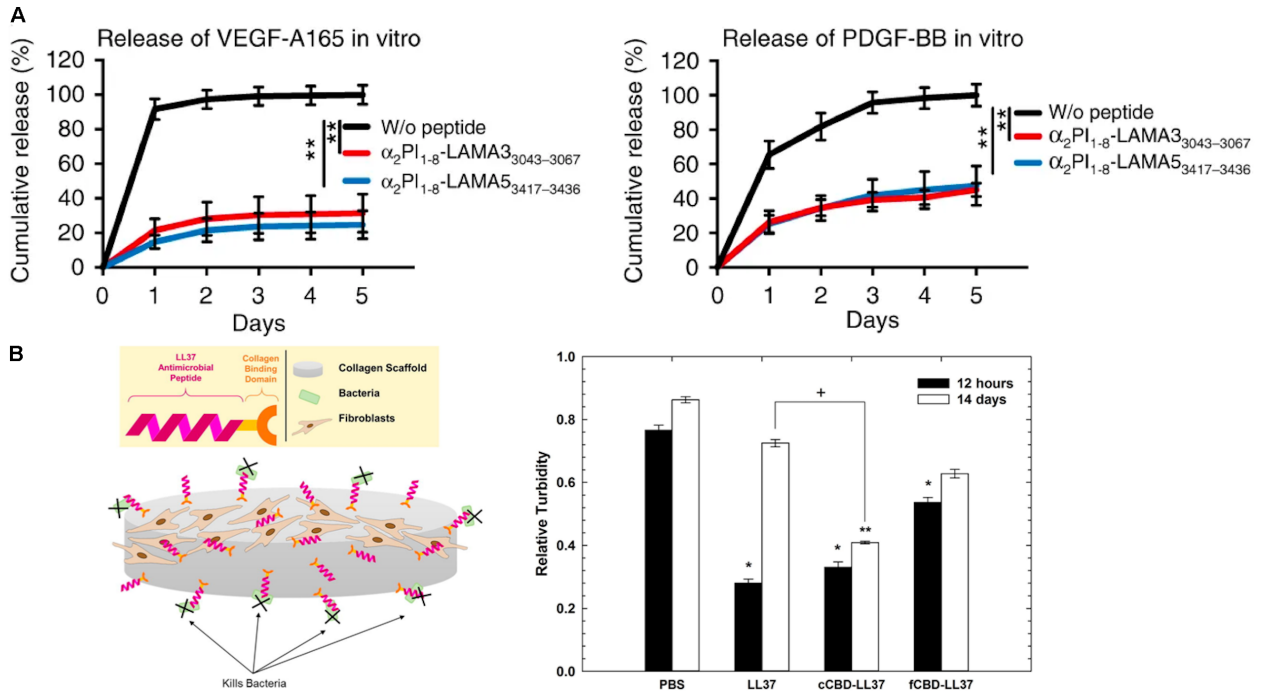

FIGURE 4 | Extracellular matrix-based matrices and drug interaction-based delivery systems. **(A)** Growth factor retention in fibrin matrices with laminin-mimetic peptides (α2PI1–8-LAMA33043–3067 or α2PI1–8-LAMA53417–3436) or without peptide (**$p < 0.01$) (Ishihara et al., 2018). Copyright 2018. Reproduced with permission from Springer Nature. **(B)** The scheme of study design. Antimicrobial activity of LL37 and with collagen-binding domains (cCBD-LL37 or fCBD-LL37) on collagen scaffold after 12 h and 14 days (*$p < 0.01$, **$p < 0.001$, $^{+}p < 0.05$) (Lozeau et al., 2017). Copyright 2017. Reproduced with permission from Elsevier Inc.

before they transfer to the appropriate cellular compartment. BMP-delivery systems using ECM-based hydrogels (INFUSE, MASTERGRAFT, OP-1) are clinically available. However, gene delivery systems often fail to meet their clinical potential due to their relative low transfection efficiency and off-target expression (Al-Dosari and Gao, 2009; Li and Mooney, 2016). The ideal gene delivery system in tissue regeneration applications should be able to sustain the delivery of active genes throughout the tissue formation process. Thus, immobilization of gene carriers in ECM-based hydrogels has the potential to achieve sustained delivery in response to cell-secreted proteases that are present during tissue repair and regeneration process, and the subsequent targeted cell uptake mediated by cell-receptor/ECM interactions.

Polymer and DNA complexes (polyplexes) have been encapsulated into scaffolds through non-specific and specific interactions between the complex and scaffold, leading to sustained DNA release from the matrix (De Laporte and Shea, 2007; Wang and Gao, 2014). Collagen-based matrix has been widely utilized to incorporate DNA complexes via non-specific interactions with the matrix to promote skin tissue repair and bone regeneration applications (Mao et al., 2009; Elangovan et al., 2014). For example, Gao and co-workers demonstrated the incorporation of cationic trimethylchitosan chloride (TMC) and DNA encoding VEGF-165 complex into the collagen-chitosan/silicone membrane bilayer dermal scaffold (TMC/pDNA-VEGF complexes loaded scaffold) to enhance angiogenesis for wound repair applications (Guo et al., 2010). Immunohistological analysis, RT-qPCR, and Western blotting analysis showed that the TMC/pDNA-VEGF complex-loaded scaffold was able to promote wound healing in incisional porcine wounds via VEGF-driven angiogenesis. The Salem group explored the delivery of polyethylenimine (PEI) and DNA encoding PDGF-B complex (Polyplex-PDGF-B) using collagen scaffolds for bone regeneration (Elangovan et al., 2014). *In vivo* studies using a calvarial defect rat model revealed that after 4 weeks of sample implantation, polyplex-PDGF-B in collagen promoted significantly higher new bone formation as compared to collagen-only scaffold, suggesting the effective approach and potential clinical translation for bone regeneration.

Polyplexes also have been incorporated into the matrix via specific interactions between polyplex and matrix. Netti et al. developed gene-activated matrices through immobilization of biotin-polyethylenimine (PEI) and DNA complexes (polyplexes) in avidin-functionalized collagen matrix (Orsi et al., 2010). The immobilized polyplexes provided higher bioavailability to NIH3T3 cells recruited into the collagen matrix. The use of avidin-biotin interactions increased the transfection efficiency by approximately two-fold as compared polyplexes in collagen matrix lacking avidin-biotin linkages (**Figure 5A**). Moreover, Segura and co-workers recently investigated electrostatically immobilized PEI/DNA complexes (polyplexes) in porous hyaluronic acid hydrogels (Truong and Segura, 2018). The hydrogel formulation approach reduced the cytotoxicity of the polyplexes in murine mesenchymal

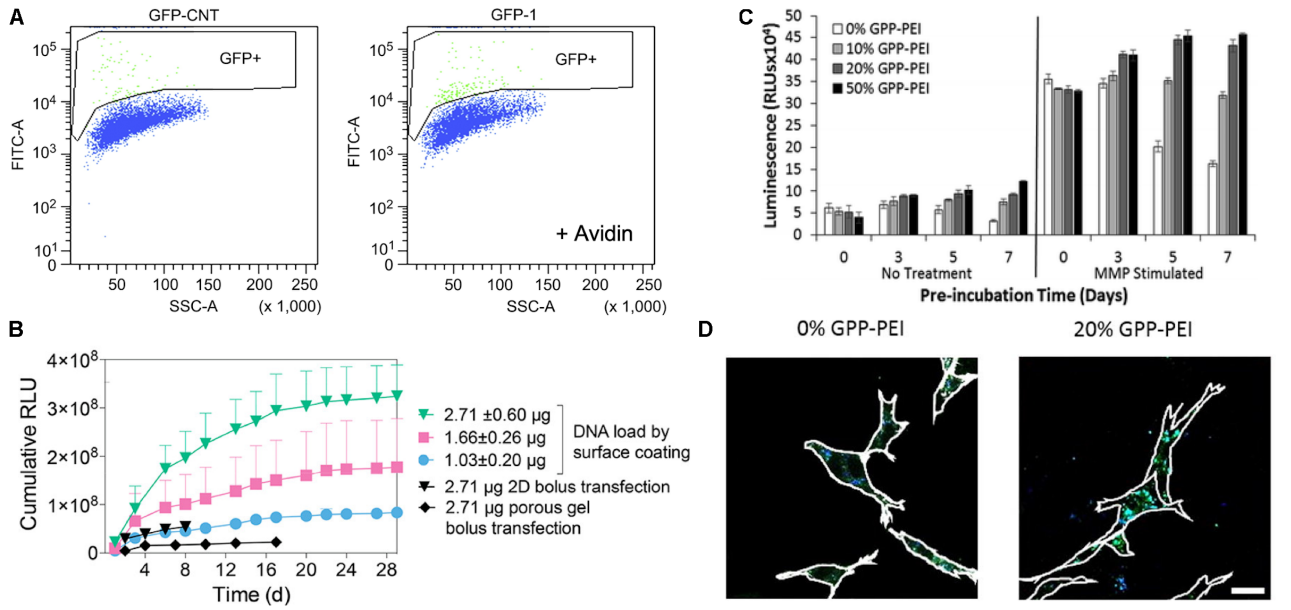

FIGURE 5 | Polyplex immobilized in an ECM-based matrix for gene delivery. **(A)** Flow-activated cell sorting (FACS) analysis of biotin-functionalized pGFP polyplex immobilized in avidin-modified collagen hydrogel through avidin-biotin interaction (right graph) and avidin-free collagen hydrogel (left) (Orsi et al., 2010). Copyright 2010. Reproduced with permission from Elsevier Inc. **(B)** pGluc expression for 30 days of cell culture in the presence of immobilized pGluc polyplex on the surface of hyaluronic acid hydrogel through electrostatic interaction, and bolus transfection controls (Truong and Segura, 2018). Copyright 2018. Reproduced with permission from the American Chemical Society. **(C)** pGluc expression of immobilized GPP-PEI in the collagen hydrogel and free GPP polyplex in hydrogel after a week of pre-incubation in media with and without the presence of metalloproteinase (Urello et al., 2014). Copyright 2014. Reproduced with permission from The Royal Society of Chemistry. **(D)** Colocalization study of FITC labeled collagen (Green) with Alexa Fluor 350 labeled GPP-PEI (Blue) in NIH3T3 cells after 5 days of pre-incubation in the media (Urello et al., 2017). The scale bar is 25 µm. Copyright 2017. Reproduced with permission from Elsevier Inc.

stem cells as compared to 2D bolus transfections with multiple doses. These observations suggested that the immobilized polyplex on the hydrogel enhanced and sustained the transgene expression over 30 days of cell culture, compared to a non-coated bolus transfection (**Figure 5B**). In addition to these two strategies for non-covalent immobilization of poyplex to ECM hydrogels, our group has developed approaches to immobilize polyplexes in collagen hydrogels through interactions with collagen-mimetic peptides [e.g., GPP: $(GPP)_3GPRGEKGERGPR(GPP)_3GPCCG$] that have affinity for native collagen through strand invasion and triple-helical binding (Urello et al., 2014, 2016, 2017). With higher amounts of GPP incorporated in the polyplex, the polyplex was retained in the hydrogel longer, with retention up to 35 days (Urello et al., 2014). In addition, GPP-modified PEI polyplexes, after a week of pre-incubation within collagen hydrogels in media, still showed greater gene expression by murine fibroblasts compared to GPP-free polyplexes. In particular, gene transfer in MMP-stimulated cells was highly robust, suggesting potential treatment options for chronic inflammatory diseases such as chronic wounds (**Figure 5C**). A collagen-polyplex colocalization study revealed that the GPP-PEI, along with collagen fragments, were internalized in cells largely via caveolar endocytosis, suggesting integrin interaction with the integrin-binding sites of collagen fragments are involved in cellular internalization (**Figure 5D**; Urello et al., 2017). GPP-PEI and collagen hydrogel interactions allowed both the controlled release and ligand-mediated efficient endocytosis into cells.

SUMMARY AND FUTURE PROSPECTS

For the past several decades, significant progress has been made in the development of targeted DDS using both local administration and ligand-based active targeting strategies. Hydrogel-based local delivery and ligand-cell interaction-mediated delivery enable drugs such as biomacromolecules (e.g., growth factors or genes) and small molecules to better localize at the target sites. Owing to the biological versatility of ECM molecules, ECM-based DDS have been applied not only to provide structural and biochemical signals to cells, but also to serve as ligands for cell receptors in specific pathological conditions to improve therapeutic efficacy of growth factor, gene, and small molecule treatments. However, despite progressive improvements, many challenges and unmet clinical needs still remain, particularly for intracellularly active drugs such as genes, which require control over cellular uptake mechanisms for optimized delivery and activity.

The innovative combination of these two targeting approaches using immobilizing drug carriers in ECM-based hydrogels has generated promising cell-responsive gene-activated matrices for

regenerative medicine and functional tissue repair. ECM scaffolds not only function as substrates for cell infiltration, organization, and differentiation, but also enable resident cells to efficiently uptake genes on demand to supply essential tissue inductive factors. However, many challenges remain in further developing this type of DDS to, for example, enable the delivery of multiple drugs from a single system, or provide mechanisms for on-demand drug release with a high level of control to a specific cell type. The sequential signaling of multiple growth factors typically regulates tissue repair and regeneration. Although researchers have demonstrated the release of multiple drugs, obtaining release of a specific molecule with optimal timing remains a challenge. Further, despite the advances in targeting, materials that localize only at or in their target cells are still difficult to design due to the lack of cell-specific gene expression relevant to a given disease physiology. Use of multiple ECM-inspired peptides in conjunction may offer a promising strategy to increase affinity to a particular cell type, using information about the cell's natural ECM receptor expression patterns, or to promote the sequential delivery of a series of drugs in a desired profile. In the future, ECM molecule-based DDS are likely to have an increasingly significant impact on disease treatment and tissue regeneration.

AUTHOR CONTRIBUTIONS

All authors conceived the layout, the rationale, and the plan of this manuscript. JH wrote the first draft of the manuscript that was iteratively improved by MS and KK.

FUNDING

Related work in the authors' laboratories was supported by the National Institutes of Health (NIH RO1 AR067247, NIH R21 AR069778, and NIH P30GM110758) and the National Science Foundation (NSF PFI1700980, NSF CBET1159466, and NSF 1605130) awarded to MS and KK. The views expressed here are the responsibility of the authors and do not necessarily reflect the position of the funding agencies.

REFERENCES

Aderem, A., and Underhill, D. M. (1999). Mechanisms of phagocytosis in macrophages. *Annu. Rev. Immunol.* 17, 593–623. doi: 10.1146/annurev.immunol.17.1.593

Alam, N., Goel, H. L., Zarif, M. J., Butterfield, J. E., Perkins, H. M., Sansoucy, B. G., et al. (2007). The integrin-growth factor receptor duet. *J. Cell Physiol.* 213, 649–653. doi: 10.1002/jcp.21278

Al-Dosari, M. S., and Gao, X. (2009). Nonviral gene delivery: principle, limitations, and recent progress. *AAPS J.* 11, 671–681. doi: 10.1208/s12248-009-9143-y

Allen, T. M., and Cullis, P. R. (2004). Drug delivery systems: entering the mainstream. *Science* 303, 1818–1822. doi: 10.1126/science.1095833

An, B., and Brodsky, B. (2016). Collagen binding to OSCAR: the odd couple. *Blood* 127, 521–522. doi: 10.1182/blood-2015-12-682476

Appel, E. A., Tibbitt, M. W., Webber, M. J., Mattix, B. A., Veiseh, O., and Langer, R. (2015). Self-assembled hydrogels utilizing polymer-nanoparticle interactions. *Nat. Commun.* 6:6295. doi: 10.1038/ncomms7295

Arap, W., Pasqualini, R., and Ruoslahti, E. (1998). Cancer treatment by targeted drug delivery to tumor vasculature in a mouse model. *Science* 279, 377–380. doi: 10.1126/science.279.5349.377

Arora, P. D., Wang, Y., Bresnick, A., Dawson, J., and Janmey, P. A. (2013). Collagen remodeling by phagocytosis is determined by collagen substrate topology and calcium-dependent interactions of gelsolin with nonmuscle myosin IIA in cell adhesions. *Mol. Biol. Cell* 24, 734–747. doi: 10.1091/mbc.E12-10-0754

Belting, M. (2003). Heparan sulfate proteoglycan as a plasma membrane carrier. *Trends Biochem. Sci.* 28, 145–151. doi: 10.1016/S0968-0004(03)00031-8

Benton, G., Arnaoutova, I., George, J., Kleinman, H. K., and Koblinski, J. (2014). Matrigel: from discovery and ECM mimicry to assays and models for cancer research. *Adv. Drug Deliv. Rev.* 7, 3–18. doi: 10.1016/j.addr.2014.06.005

Bhakta, G., Lim, Z. X., Rai, B., Lin, T., Hui, J. H., Prestwich, G. D., et al. (2013). The influence of collagen and hyaluronan matrices on the delivery and bioactivity of bone morphogenetic protein-2 and ectopic bone formation. *Acta Biomater.* 9, 9098–9106. doi: 10.1016/j.actbio.2013.07.008

Bibby, D. C., Talmadge, J. E., Dalal, M. K., Kurz, S. G., Chytil, K. M., Barry, S. E., et al., (2005). Pharmacokinetics and biodistribution of RGD-targeted doxorubicin-loaded nanoparticles in tumor-bearing mice. *Int. J. Pharm.* 293, 281–290. doi: 10.1016/j.ijpharm.2004.12.021

Blanco, E., Shen, H., and Ferrari, M. (2015). Principles of nanoparticle design for overcoming biological barriers to drug delivery. *Nat. Biotechnol.* 33, 941–951. doi: 10.1038/nbt.3330

Boekhoven, J., and Stupp, S. I. (2014). 25th anniversary article: supramolecular materials for regenerative medicine. *Adv. Mater.* 26, 1642–1659. doi: 10.1002/adma.201304606

Cai, L., and Heilshorn, S. C. (2014). Designing ECM-mimetic materials using protein engineering. *Acta Biomater.* 10, 1751–1760. doi: 10.1016/j.actbio.2013.12.028

Caliari, S. R., and Burdick, J. A. (2016). A practical guide to hydrogels for cell culture. *Nat. Methods* 13, 405–414. doi: 10.1038/nmeth.3839

Carvalho, R. M., Carvalho, R. C., Maia, R. F., Caballero, D., Kundu, C. S., Reis, L. R., et al. (2019). Peptide-modified dendrimer nanoparticles for targeted therapy of colorectal cancer. *Adv. Ther.* 2:1900132. doi: 10.1002/adtp.201900132

Cervadoro, A., Palomba, R., Vergaro, G., Cecchi, R., Menichetti, L., Decuzzi, P., et al. (2018). Targeting inflammation with nanosized drug delivery platforms in cardiovascular diseases: immune cell modulation in atherosclerosis. *Front. Bioeng. Biotechnol.* 6:177. doi: 10.3389/fbioe.2018.00177

Chia, C. L., Shelat, V. G., Low, W., George, S., and Rao, J. (2014). The use of Collatamp G, local gentamicin-collagen sponge, in reducing wound infection. *Int. Surg.* 99, 565–570. doi: 10.9738/INTSURG-D-13-00171.1

Chowdhury, E. H., and Akaike, T. (2006). Fibronectin-coated nano-precipitates of calcium-magnesium phosphate for integrin-targeted gene delivery. *J. Control Release* 116:e68–e69. doi: 10.1016/j.jconrel.2006.09.054

Christianson, H. C., and Belting, M. (2014). Heparan sulfate proteoglycan as a cell-surface endocytosis receptor. *Matrix Biol.* 35, 51–55. doi: 10.1016/j.matbio.2013.10.004

Christman, K. L., Broyer, R. M., Schopf, E., Kolodziej, C. M., Chen, Y., Maynard, H. D., et al. (2011). Protein nanopatterns by oxime bond formation. *Langmuir* 27, 1415–1418. doi: 10.1021/la103978x

Chung, Y. I., Kim, J. C., Kim, Y. H., Tae, G., Lee, S. Y., Kim, K., et al. (2010). The effect of surface functionalization of PLGA nanoparticles by heparin- or chitosan-conjugated Pluronic on tumor targeting. *J. Control Release* 143, 374–382. doi: 10.1016/j.jconrel.2010.01.017

Cichy, J., and Pure, E. (2003). The liberation of CD44. *J. Cell Biol.* 161, 839–843. doi: 10.1083/jcb.200302098

Colognato, H., and Yurchenco, P. D. (2000). Form and function: the laminin family of heterotrimers. *Dev. Dyn.* 218, 213–234.

Coopman, P. J., Thomas, D. M., Gehlsen, K. R., and Mueller, S. C. (1996). Integrin alpha 3 beta 1 participates in the phagocytosis of extracellular matrix molecules by human breast cancer cells. *Mol. Biol. Cell* 7, 1789–1804. doi: 10.1091/mbc.7.11.1789

Crapo, P. M., Gilbert, T. W., and Badylak, S. F. (2011). An overview of tissue and whole organ decellularization processes. *Biomaterials* 32, 3233–3243. doi: 10.1016/j.biomaterials.2011.01.057

Danhier, F., Feron, O., and Preat, V. (2010). To exploit the tumor microenvironment: Passive and active tumor targeting of nanocarriers for anti-cancer drug delivery. *J. Control Release* 148, 135–146. doi: 10.1016/j.jconrel.2010.08.027

Danhier, F., Le Breton, A., and Preat, V. (2012). RGD-based strategies to target alpha(v) beta(3) integrin in cancer therapy and diagnosis. *Mol. Pharm.* 9, 2961–2973. doi: 10.1021/mp3002733

Das, L., Anderson, T. A., Gard, J. M., Sroka, I. C., Strautman, S. R., Nagle, R. B., et al. (2017). Characterization of laminin binding integrin internalization in prostate cancer cells. *J. Cell Biochem.* 118, 1038–1049. doi: 10.1002/jcb.25673

de Bruin, A. F., Gosselink, M. P., van, der Harst, E., and Rutten, H. J. (2010). Local application of gentamicin collagen implants in the prophylaxis of surgical site infections following gastrointestinal surgery: a review of clinical experience. *Tech. Coloproctol.* 14, 301–310. doi: 10.1007/s10151-010-0593-0

De Laporte, L., and Shea, L. D. (2007). Matrices and scaffolds for DNA delivery in tissue engineering. *Adv. Drug Deliv. Rev.* 59, 292–307. doi: 10.1016/j.addr.2007.03.017

De Souza, R., Zahedi, P., Allen, C. J., and Piquette-Miller, M. (2010). Polymeric drug delivery systems for localized cancer chemotherapy. *Drug Deliv.* 17, 365–375. doi: 10.3109003762854

Dimatteo, R., Darling, N. J., and Segura, T. (2018). In situ forming injectable hydrogels for drug delivery and wound repair. *Adv. Drug Deliv. Rev.* 127, 167–184. doi: 10.1016/j.addr.2018.03.007

Dosio, F., Arpicco, S., Stella, B., and Fattal, E. (2016). Hyaluronic acid for anticancer drug and nucleic acid delivery. *Adv. Drug Deliv. Rev.* 97, 204–236. doi: 10.1016/j.addr.2015.11.011

D'Souza, A. A., and Devarajan, P. V. (2015). Asialoglycoprotein receptor mediated hepatocyte targeting - strategies and applications. *J. Control Release* 203, 126–139. doi: 10.1016/j.jconrel.2015.02.022

Dubey, P. K., Singodia, D., and Vyas, S. P. (2010). . Polymeric nanospheres modified with YIGSR peptide for tumor targeting. *Drug. Deliv.* 17, 541–551. doi: 10.3109.2010.490249

Dunehoo, A. L., Anderson, M., Majumdar, S., Kobayashi, N., Berkland, C., et al. (2006). Cell adhesion molecules for targeted drug delivery. *J. Pharm. Sci.* 95, 1856–1872. doi: 10.1002/jps.20676

Duxfield, L., Sultana, R., Wang, R., Englebretsen, V., Deo, S., Rupenthal, I. D., et al. (2016). . Ocular delivery systems for topical application of anti-infective agents. *Drug. Dev. Ind. Pharm.* 42, 1–11. doi: 10.3109.2015.1070171

Elangovan, S., D'Mello, S. R., Hong, L., Ross, R. D., Allamargot, C., Dawson, D. V., et al. (2014). The enhancement of bone regeneration by gene activated matrix encoding for platelet derived growth factor. *Biomaterials* 35, 737–747. doi: 10.1016/j.biomaterials.2013.10.021

Eliaz, R. E., and Szoka, F. C. Jr. (2001). Liposome-encapsulated doxorubicin targeted to CD44: a strategy to kill CD44-overexpressing tumor cells. *Cancer Res.* 61, 2592–2601.

El-Sayed, A., and Harashima, H. (2013). Endocytosis of gene delivery vectors: from clathrin-dependent to lipid raft-mediated endocytosis. *Mol. Ther.* 21, 1118–1130. doi: 10.1038/mt.2013.54

Fan, Y., Yao, J., Du, R., Hou, L., Zhou, J., Lu, Y., et al. (2013). Ternary complexes with core-shell bilayer for double level targeted gene delivery: in vitro and in vivo evaluation. *Pharm. Res.* 30, 1215–1227. doi: 10.1007/s11095-012-0960-9

Farajzadeh, R., Zarghami, N., Serati-Nouri, H., Momeni-Javid, Z., Farajzadeh, T., and Jalilzadeh-Tabrizi, S. (2018). Macrophage repolarization using CD44-targeting hyaluronic acid-polylactide nanoparticles containing curcumin. *Artif. Cells Nanomed Biotechnol.* 46, 2013–2021. doi: 10.1080.2017.1408116

Farrukh, A., Ortega, F., Fan, W., Marichal, N., Paez, J. I., Berninger, B., et al. (2017). Bifunctional hydrogels containing the laminin Motif IKVAV promote neurogenesis. *Stem Cell Rep.* 9, 1432–1440. doi: 10.1016/j.stemcr.2017.09.002

Foroozandeh, P., and Aziz, A. A. (2018). Insight into cellular uptake and intracellular trafficking of nanoparticles. *Nanoscale Res. Lett.* 13:339. doi: 10.1186/s11671-018-2728-6

Freudenberg, U., Liang, Y., Kiick, K. L., and Werner, C. (2016). Glycosaminoglycan-based biohybrid hydrogels: a sweet and smart choice for multifunctional biomaterials. *Adv. Mater.* 28, 8861–8891. doi: 10.1002/adma.201601908

Freudenberg, U., Zieris, A., Chwalek, K., Tsurkan, M. V., Maitz, M. F., Atallah, P., et al. (2015). Heparin desulfation modulates VEGF release and angiogenesis in diabetic wounds. *J. Control Release* 220(Pt A), 79–88. doi: 10.1016/j.jconrel.2015.10.028

Fu, S., Xu, X., Ma, Y., Zhang, S., and Zhang, S. (2019). RGD peptide-based non-viral gene delivery vectors targeting integrin alphavbeta3 for cancer therapy. *J. Drug. Target.* 27, 1–11. doi: 10.1080/1061186X.2018.1455841

Garber, K. (2018). Alnylam launches era of RNAi drugs. *Nat. Biotechnol.* 36, 777–778. doi: 10.1038/nbt0918-777

Giancotti, F. G. (2003). A structural view of integrin activation and signaling. *Dev. Cell* 4, 149–151.

Giancotti, F. G., and Ruoslahti, E. (1999). Integrin signaling. *Science* 285, 1028–1032. doi: 10.1126/science.285.5430.1028

Goebeler, M., Kaufmann, D., Brocker, E. B., and Klein, C. E. (1996). Migration of highly aggressive melanoma cells on hyaluronic acid is associated with functional changes, increased turnover and shedding of CD44 receptors. *J. Cell Sci.* 109(Pt 7), 1957–1964.

Goodman, S. L., and Picard, M. (2012). Integrins as therapeutic targets. *Trends Pharmacol. Sci.* 33, 405–412. doi: 10.1016/j.tips.2012.04.002

Gospodarowicz, D., and Cheng, J. (1986). Heparin protects basic and acidic FGF from inactivation. *J. Cell Physiol.* 128, 475–484. doi: 10.1002/jcp.1041280317/3528177

Graf, J., Iwamoto, Y., Sasaki, M., Martin, G. R., Kleinman, H. K., Robey, F. A., et al. (1987). Identification of an amino acid sequence in laminin mediating cell attachment, chemotaxis, and receptor binding. *Cell* 48, 989–996. doi: 10.1016/0092-8674(87)90707-0 /2951015

Guo, R., Xu, S., Ma, L., Huang, A., and Gao, C. (2010). Enhanced angiogenesis of gene-activated dermal equivalent for treatment of full thickness incisional wounds in a porcine model. *Biomaterials* 31, 7308–7320. doi: 10.1016/j.biomaterials.2010.06.013

Hamano, N., Negishi, Y., Fujisawa, A., Manandhar, M., Sato, H., Katagiri, F., et al. (2012). Modification of the C16Y peptide on nanoparticles is an effective approach to target endothelial and cancer cells via the integrin receptor. *Int. J. Pharm.* 428, 114–117. doi: 10.1016/j.ijpharm.2012.02.006

Harburger, D. S., and Calderwood, D. A. (2009). Integrin signalling at a glance. *J. Cell Sci.* 122(Pt 2), 159–163. doi: 10.1242/jcs.018093

Hendricks, M. P., Sato, K., Palmer, L. C., and Stupp, S. I. (2017). Supramolecular Assembly of Peptide Amphiphiles. *Acc. Chem. Res.* 50, 2440–2448. doi: 10.1021/acs.accounts.7b00297

Hernandez, J. M., Gaetani, R., Pieters, M. V., Ng, W. N., Chang, E. A., Martin, T. R., et al. (2018). Decellularized extracellular matrix hydrogels as a delivery platform for MicroRNA and extracellular vesicle therapeutics. *Adv. Ther.* 1: 1800032.

Highley, C. B., Prestwich, G. D., and Burdick, J. A. (2016). Recent advances in hyaluronic acid hydrogels for biomedical applications. *Curr. Opin. Biotechnol.* 40, 35–40. doi: 10.1016/j.copbio.2016.02.008

Hinderer, S., Layland, S. L., and Schenke-Layland, K. (2016). ECM and ECM-like materials - Biomaterials for applications in regenerative medicine and cancer therapy. *Adv. Drug. Deliv. Rev.* 97, 260–269. doi: 10.1016/j.addr.2015.11.019

Hoffman, M. P., Engbring, J. A., Nielsen, P. K., Vargas, J., Steinberg, Z., Karmand, A. J., et al. (2001). Cell type-specific differences in glycosaminoglycans modulate the biological activity of a heparin-binding peptide (RKRLQVQLSIRT) from the G domain of the laminin alpha1 chain. *J. Biol. Chem.* 276, 22077–22085. doi: 10.1074/jbc.M100774200

Hu, H., Wan, J., Huang, X., Tang, Y., Xiao, C., Xu, H., et al. (2018). iRGD-decorated reduction-responsive nanoclusters for targeted drug delivery. *Nanoscale* 10, 10514–10527. doi: 10.1039/c8nr02534g

Hu, Q., Sun, W., Wang, C., and Gu, Z. (2016). Recent advances of cocktail chemotherapy by combination drug delivery systems. *Adv. Drug. Deliv. Rev.* 98, 19–34. doi: 10.1016/j.addr.2015.10.022

Huang, G., and Huang, H. (2018). Hyaluronic acid-based biopharmaceutical delivery and tumor-targeted drug delivery system. *J. Control Release* 278, 122–126. doi: 10.1016/j.jconrel.2018.04.015

Hwang, T. J., Carpenter, D., Lauffenburger, J. C., Wang, B., Franklin, J. M., and Kesselheim, A. S. (2016). Failure of investigational drugs in late-stage clinical development and publication of trial results. *JAMA Intern. Med.* 176, 1826–1833. doi: 10.1001/jamainternmed.2016.6008

Ishihara, J., Ishihara, A., Fukunaga, K., Sasaki, K., White, M. J. V., Briquez, P. S., et al. (2018). Laminin heparin-binding peptides bind to several growth factors and enhance diabetic wound healing. *Nat. Commun.* 9:2163. doi: 10.1038/s41467-018-04525-w

Ishihara, J., Ishihara, A., Sasaki, K., Lee, S. S., Williford, J. M., Yasui, M., et al. (2019). Targeted antibody and cytokine cancer immunotherapies through collagen affinity. *Sci. Transl. Med.* 11:eaau3259. doi: 10.1126/scitranslmed.aau3259

Jeong, K. J., and Panitch, A. (2009). Interplay between covalent and physical interactions within environment sensitive hydrogels. *Biomacromolecules* 10, 1090–1099. doi: 10.1021/bm801270k

Jiang, D., Liang, J., and Noble, P. W. (2011). Hyaluronan as an immune regulator in human diseases. *Physiol. Rev.* 91, 221–264. doi: 10.1152/physrev.00052.2009

Jiao, Y., Pang, X., and Zhai, G. (2016). Advances in hyaluronic acid-based drug delivery systems. *Curr. Drug. Targets* 17, 720–730. doi: 10.2174166661505311552 00

Johnson, C. T., Wroe, J. A., Agarwal, R., Martin, K. E., Guldberg, R. E., Donlan, R. M., et al. (2018). Hydrogel delivery of lysostaphin eliminates orthopedic implant infection by Staphylococcus aureus and supports fracture healing. *Proc. Natl. Acad. Sci. U.S.A.* 115, E4960–E4969. doi: 10.1073/pnas.1801013115

Kanamala, M., Wilson, W. R., Yang, M., Palmer, B. D., and Wu, Z. (2016). Mechanisms and biomaterials in pH-responsive tumour targeted drug delivery: a review. *Biomaterials* 85, 152–167. doi: 10.1016/j.biomaterials.2016.01.061

Kharkar, P. M., Kiick, K. L., and Kloxin, A. M. (2013). Designing degradable hydrogels for orthogonal control of cell microenvironments. *Chem. Soc. Rev.* 42, 7335–7372. doi: 10.1039/c3cs60040h

Kim, S. H., Turnbull, J., and Guimond, S. (2011). Extracellular matrix and cell signalling: the dynamic cooperation of integrin, proteoglycan and growth factor receptor. *J. Endocrinol.* 209, 139–151. doi: 10.1530/JOE-10-0377

Kim, Y. M., Park, S. C., and Jang, M. K. (2017). Targeted gene delivery of polyethyleneimine-grafted chitosan with RGD dendrimer peptide in alphavbeta3 integrin-overexpressing tumor cells. *Carbohydr. Polym.* 174, 1059–1068. doi: 10.1016/j.carbpol.2017.07.035

Kohane, D. S., and Todd, H. R. (2008). Hydrogels in drug delivery: progress and challenges. *polymer* 49, 1993–2007.

Kolmel, D. K., and Kool, E. T. (2017). Oximes and hydrazones in bioconjugation: mechanism and catalysis. *Chem. Rev.* 117, 10358–10376. doi: 10.1021/acs.chemrev.7b00090

Lallana, E., Rios, J., de la Rosa, M., Tirella, A., Pelliccia, M., Gennari, A., et al. (2017). Chitosan/hyaluronic acid nanoparticles: rational design revisited for RNA delivery. *Mol. Pharm.* 14, 2422–2436. doi: 10.1021/acs.molpharmaceut.7b00320

Langer, R. (1998). Drug delivery and targeting. *Nature* 392(6679 Suppl.), 5–10.

Leitinger, B. (2014). Discoidin domain receptor functions in physiological and pathological conditions. *Int. Rev. Cell Mol. Biol.* 310, 39–87. doi: 10.1016/B978-0-12-800180-6.00002-5

Leitinger, B., and Hohenester, E. (2007). Mammalian collagen receptors. *Matrix. Biol.* 26, 146–155. doi: 10.1016/j.matbio.2006.10.007

Leonoudakis, D., Huang, G., Akhavan, A., Fata, J. E., Singh, M., Gray, J. W., et al. (2014). Endocytic trafficking of laminin is controlled by dystroglycan and is disrupted in cancers. *J. Cell Sci.* 127(Pt 22), 4894–4903. doi: 10.1242/jcs.152728

Li, J., and Mooney, D. J. (2016). Designing hydrogels for controlled drug delivery. *Nat. Rev. Mater.* 1, doi: 10.1038/natrevmats.2016.71

Liang, Y., and Kiick, K. L. (2014). Heparin-functionalized polymeric biomaterials in tissue engineering and drug delivery applications. *Acta Biomater.* 10, 1588–1600. doi: 10.1016/j.actbio.2013.07.031

Liu, D., Yang, F., Xiong, F., and Gu, N. (2016). The smart drug delivery system and its clinical potential. *Theranostics* 6, 1306–1323. doi: 10.7150/thno.14858

Lobert, V. H., Brech, A., Pedersen, N. M., Wesche, J., Oppelt, A., Malerod, L., et al. (2010). Ubiquitination of alpha 5 beta 1 integrin controls fibroblast migration through lysosomal degradation of fibronectin-integrin complexes. *Dev. Cell* 19, 148–159. doi: 10.1016/j.devcel.2010.06.010

Lohmann, N., Schirmer, L., Atallah, P., Wandel, E., Ferrer, R. A., Werner, C., et al. (2017). Glycosaminoglycan-based hydrogels capture inflammatory chemokines and rescue defective wound healing in mice. *Sci. Transl. Med.* 9:16071. doi: 10.1126/scitranslmed.aai9044

Lozeau, L. D., Grosha, J., Kole, D., Prifti, F., Dominko, T., Camesano, T. A., et al. (2017). Collagen tethering of synthetic human antimicrobial peptides cathelicidin LL37 and its effects on antimicrobial activity and cytotoxicity. *Acta Biomater.* 52, 9–20. doi: 10.1016/j.actbio.2016.12.047

Luo, T., David, M. A., Dunshee, L. C., Scott, R. A., Urello, M. A., Price, C., et al. (2017). Thermoresponsive Elastin-b-Collagen-Like peptide bioconjugate nanovesicles for targeted drug delivery to collagen-containing matrices. *Biomacromolecules* 18, 2539–2551. doi: 10.1021/acs.biomac.7b00686

Lutolf, M. P., Lauer-Fields, J. L., Schmoekel, H. G., Metters, A. T., Weber, F. E., Fields, G. B., et al. (2003). Synthetic matrix metalloproteinase-sensitive hydrogels for the conduction of tissue regeneration: engineering cell-invasion characteristics. *Proc. Natl. Acad. Sci. U.S.A.* 100, 5413–5418. doi: 10.1073/pnas.0737381100

Madsen, D. H., Ingvarsen, S., Jurgensen, H. J., Melander, M. C., Kjoller, L., Moyer, A., et al. (2011). The non-phagocytic route of collagen uptake: a distinct degradation pathway. *J. Biol. Chem.* 286, 26996–27010. doi: 10.1074/jbc.M110.208033

Mao, Z., Shi, H., Guo, R., Ma, L., Gao, C., Han, C., et al. (2009). Enhanced angiogenesis of porous collagen scaffolds by incorporation of TMC/DNA complexes encoding vascular endothelial growth factor. *Acta Biomater.* 5, 2983–2994. doi: 10.1016/j.actbio.2009.04.004

Massia, S. P., and Hubbell, J. A. (1992). Vascular endothelial cell adhesion and spreading promoted by the peptide REDV of the IIICS region of plasma fibronectin is mediated by integrin alpha 4 beta 1. *J. Biol. Chem.* 267, 14019–14026.

Mateen, R., and Hoare, T. (2014). Injectable, in situ gelling, cyclodextrin-dextran hydrogels for the partitioning-driven release of hydrophobic drugs. *Mater J. Chem. B* 2, 5157–5167. doi: 10.1039/C4TB00631C

McBrien, N. A., Metlapally, R., Jobling, A. I., and Gentle, A. (2006). Expression of collagen-binding integrin receptors in the mammalian sclera and their regulation during the development of myopia. *Invest. Ophthalmol. Vis. Sci.* 47, 4674–4682. doi: 10.1167/iovs.05-1150

McKay, W. F., Peckham, S. M., and Badura, J. M. (2007). A comprehensive clinical review of recombinant human bone morphogenetic protein-2 (INFUSE Bone Graft). *Int. Orthop.* 31, 729–734. doi: 10.1007/s00264-007-0418-6

Meneghetti, M. C., Hughes, A. J., Rudd, T. R., Nader, H. B., Powell, A. K., Yates, E. A., et al. (2015). Heparan sulfate and heparin interactions with proteins. *J. R. Soc. Interface* 12:0589. doi: 10.1098/rsif.2015.0589

Merino, S., Martin, C., Kostarelos, K., Prato, M., and Vazquez, E. (2015). Nanocomposite hydrogels: 3D polymer-nanoparticle synergies for on-demand drug delivery. *ACS Nano* 9, 4686–4697. doi: 10.1021/acsnano.5b01433

Miyazaki, M., Yuba, E., Hayashi, H., Harada, A., and Kono, K. (2018). Hyaluronic acid-based pH-sensitive polymer-modified liposomes for cell-specific intracellular drug delivery systems. *Bioconjug Chem.* 29, 44–55. doi: 10.1021/acs.bioconjchem.7b00551

Morrison, C. (2018). Alnylam prepares to land first RNAi drug approval. *Nat. Rev. Drug Discov.* 17, 156–157. doi: 10.1038/nrd.2018.20

Mould, A. P., Komoriya, A., Yamada, K. M., and Humphries, M. J. (1991). The CS5 peptide is a second site in the IIICS region of fibronectin recognized by the integrin alpha 4 beta 1. Inhibition of alpha 4 beta 1 function by RGD peptide homologues. *J. Biol. Chem.* 266, 3579–3585.

Munsell, E. V., Ross, N. L., and Sullivan, M. O. (2016). Journey to the Center Of The Cell: Current Nanocarrier Design Strategies Targeting Biopharmaceuticals To The Cytoplasm And Nucleus. *Curr. Pharm. Des.* 22, 1227–1244. doi: 10.21742266151216151420

Murphy, E. A., Majeti, B. K., Barnes, L. A., Makale, M., Weis, S. M., and Lutu, K. (2008). Nanoparticle-mediated drug delivery to tumor vasculature suppresses metastasis. *Proc. Natl. Acad. Sci. U.S.A.* 105, 9343–9348. doi: 10.1073/pnas.0803728105

Mythreye, K., and Blobe, G. C. (2009). Proteoglycan signaling co-receptors: roles in cell adhesion, migration and invasion. *Cell Signal.* 21, 1548–1558. doi: 10.1016/j.cellsig.2009.05.001

Narayanaswamy, R., and Torchilin, V. P. (2019). Hydrogels and their applications in targeted drug delivery. *Molecules* 24:E603. doi: 10.3390/molecules24030603

Ndinguri, M. W., Zheleznyak, A., Lauer, J. L., Anderson, C. J., and Fields, G. B. (2012). Application of collagen-model triple-helical peptide-amphiphiles for CD44-TARGETED DRUG DELIVERY SYStems. *J. Drug. Deliv.* 2012:592602. doi: 10.1155/2012/592602

Negishi, Y., Hamano, N., Omata, D., Fujisawa, A., Manandhar, M., Nomizu, M., et al. (2011). Effects of doxorubicin-encapsulating AG73 peptide-modified liposomes on tumor selectivity and cytotoxicity. *Results Pharm. Sci.* 1, 68–75. doi: 10.1016/j.rinphs.2011.10.001

Negishi, Y., and Nomizu, M. (2019). Laminin-derived peptides: applications in drug delivery systems for targeting. *Pharmacol. Ther.* 202, 91–97. doi: 10.1016/j.pharmthera.2019.05.017

Negishi, Y., Omata, D., Iijima, H., Hamano, N., Endo-Takahashi, Y., Nomizu, M., et al. (2010). Preparation and characterization of laminin-derived peptide AG73-coated liposomes as a selective gene delivery tool. *Biol. Pharm. Bull* 33, 1766–1769. doi: 10.1248/bpb.33.1766

Nielsen, C. F., van Putten, S. M., Lund, I. K., Melander, M. C., Norregaard, K. S., Jurgensen, H. J., et al. (2017). The collagen receptor uPARAP/Endo180 as a novel target for antibody-drug conjugate mediated treatment of mesenchymal and leukemic cancers. *Oncotarget* 8, 44605–44624. doi: 10.18632/oncotarget.17883

Nieto Gutierrez, A., and McDonald, P. H. (2018). GPCRs: emerging anti-cancer drug targets. *Cell Signal.* 41, 65–74. doi: 10.1016/j.cellsig.2017.09.005

Nikam, R. R., and Gore, K. R. (2018). Journey of siRNA: clinical developments and targeted delivery. *Nucleic Acid Ther.* 28, 209–224. doi: 10.1089/nat.2017.0715

Oh, E. J., Park, K., Kim, K. S., Kim, J., Yang, J. A., Kong, J. H., et al. (2010). Target specific and long-acting delivery of protein, peptide, and nucleotide therapeutics using hyaluronic acid derivatives. *J. Control Release* 141, 2–12. doi: 10.1016/j.jconrel.2009.09.010

Okur, A. C., Erkoc, P., and Kizilel, S. (2016). Targeting cancer cells via tumor-homing peptide CREKA functional PEG nanoparticles. *Coll. Surf. B Biointerf* 147, 191–200. doi: 10.1016/j.colsurfb.2016.08.005

Oliva, N., Conde, J., Wang, K., and Artzi, N. (2017). Designing hydrogels for on-demand therapy. *Acc. Chem. Res.* 50, 669–679. doi: 10.1021/acs.accounts.6b00536

Oliviero, O., Ventre, M., and Netti, P. A. (2012). Functional porous hydrogels to study angiogenesis under the effect of controlled release of vascular endothelial growth factor. *Acta Biomater.* 8, 3294–3301. doi: 10.1016/j.actbio.2012.05.019

Ooi, H. W., Hafeez, S., van, C. A., Blitterswijk, A., Moroni, L., et al. (2017). Hydrogels that listen to cells: a review of cell-responsive strategies in biomaterial design for tissue regeneration. *Mater. Horizons* 4, 1020–1040. doi: 10.1039/c7mh00373k

Orsi, S., De, A., Capua, Guarnieri, D., Marasco, D., Netti, P. A., et al. (2010). Cell recruitment and transfection in gene activated collagen matrix. *Biomaterials* 31, 570–576. doi: 10.1016/j.biomaterials.2009.09.054

Palmese, L. L., Thapa, R., Sullivan, M. O., and Kiick, K. L. (2019). Hybrid hydrogels for biomedical applications. *Curr. Opin.Chem. Eng.* 24, 143–157. doi: 10.1016/j.coche.2019.02.010

Pankov, R., and Yamada, K. M. (2002). Fibronectin at a glance. *J. Cell Sci.* 115(Pt 20), 3861–3863. doi: 10.1242/jcs.00059

Panyam, J., and Labhasetwar, V. (2003). Biodegradable nanoparticles for drug and gene delivery to cells and tissue. *Adv. Drug Deliv. Rev.* 55, 329–347.

Park, J. C., Hwang, Y. S., Lee, J. E., Park, K. D., Matsumura, K., Hyon, S. H., et al. (2000). Type I atelocollagen grafting onto ozone-treated polyurethane films: cell attachment, proliferation, and collagen synthesis. *J. Biomed Mater. Res.* 52, 669–677.

Park, J. W., Hwang, S. R., and Yoon, I. S. (2017). Advanced growth factor delivery systems in wound management and skin regeneration. *Molecules* 22:E1259. doi: 10.3390/molecules22081259

Pathak, A., Kumar, P., Chuttani, K., Jain, S., Mishra, A. K., Vyas, S. P., et al. (2009). Gene expression, biodistribution, and pharmacoscintigraphic evaluation of chondroitin sulfate-PEI nanoconstructs mediated tumor gene therapy. *ACS Nano* 3, 1493–1505. doi: 10.1021/nn900044f

Patterson, J., and Hubbell, J. A. (2010). Enhanced proteolytic degradation of molecularly engineered PEG hydrogels in response to MMP-1 and MMP-2. *Biomaterials* 31, 7836–7845. doi: 10.1016/j.biomaterials.2010.06.061

Phelps, E. A., Enemchukwu, N. O., Fiore, V. F., Sy, J. C., Murthy, N., Sulchek, T. A., et al. (2012). Maleimide cross-linked bioactive PEG hydrogel exhibits improved reaction kinetics and cross-linking for cell encapsulation and in situ delivery. *Adv. Mater.* 24, 64–70. doi: 10.1002/adma.201103574

Phuc, L. T. M., and Taniguchi, A. (2017). Epidermal growth factor enhances cellular uptake of polystyrene nanoparticles by clathrin-mediated endocytosis. *Int. J. Mol. Sci.* 18:1301. doi: 10.3390/ijms18061301

Prasad, V. (2014). The withdrawal of drugs for commercial reasons: the incomplete story of tositumomab. *JAMA Intern. Med.* 174, 1887–1888. doi: 10.1001/jamainternmed.2014.5756

Prokoph, S., Chavakis, E., Levental, K. R., Zieris, A., Freudenberg, U., Dimmeler, S., et al. (2012). Sustained delivery of SDF-1alpha from heparin-based hydrogels to attract circulating pro-angiogenic cells. *Biomaterials* 33, 4792–4800. doi: 10.1016/j.biomaterials.2012.03.039

Qureshi, Z. P., Seoane-Vazquez, E., Rodriguez-Monguio, R., Stevenson, K. B., and Szeinbach, S. L. (2011). Market withdrawal of new molecular entities approved in the United States from 1980 to 2009. *Pharmacoepidemiol. Drug Saf.* 20, 772–777. doi: 10.1002/pds.2155

Raab-Westphal, S., Marshall, J. F., and Goodman, S. L. (2017). Integrins as therapeutic targets: successes and cancers. *Cancers* 9:E110. doi: 10.3390/cancers9090110

Raave, R., van Kuppevelt, T. H., and Daamen, W. F. (2018). Chemotherapeutic drug delivery by tumoral extracellular matrix targeting. *J. Control Release* 274, 1–8. doi: 10.1016/j.jconrel.2018.01.029

Racine, R., and Mummert, E. M. (2012). "Hyaluronan endocytosis: mechanisms of uptake and biological functions," in *Molecular Regulation of Endocytosis*, ed. B. Ceresa, (London: IntechOpen), 377–390.

Rainero, E. (2016). Extracellular matrix endocytosis in controlling matrix turnover and beyond: emerging roles in cancer. *Biochem. Soc. Trans.* 44, 1347–1354. doi: 10.1042/BST20160159

Raja, S. G. (2012). Local application of gentamicin-containing collagen implant in the prophylaxis and treatment of surgical site infection following cardiac surgery. *Int. J. Surg.* 10(Suppl. 1), S10–S14. doi: 10.1016/j.ijsu.2012.05.018

Ramshaw, J. A., Peng, Y. Y., Glattauer, V., and Werkmeister, J. A. (2009). Collagens as biomaterials. *J. Mater. Sci. Mater. Med.* 20(Suppl. 1), S3–S8. doi: 10.1007/s10856-008-3415-4

Reilly, M. J., Larsen, J. D., and Sullivan, M. O. (2012). Polyplexes traffic through caveolae to the Golgi and endoplasmic reticulum en route to the nucleus. *Mol. Pharm.* 9, 1280–1290. doi: 10.1021/mp200583d

Rejman, J., Bragonzi, A., and Conese, M. (2005). Role of clathrin- and caveolae-mediated endocytosis in gene transfer mediated by lipo- and polyplexes. *Mol. Ther.* 12, 468–474. doi: 10.1016/j.ymthe.2005.03.038

Rezler, E. M., Khan, D. R., Lauer-Fields, J., Cudic, M., Baronas-Lowell, D., et al. (2007). Targeted drug delivery utilizing protein-like molecular architecture. *J. Am. Chem. Soc.* 129. doi: 10.1021/ja066929m

Roggenbuck, D., Mytilinaiou, M. G., Lapin, S. V., Reinhold, D., and Conrad, K. (2012). Asialoglycoprotein receptor (ASGPR): a peculiar target of liver-specific autoimmunity. *Auto Immun. Highlights* 3, 119–125. doi: 10.1007/s13317-012-0041-4

Rosso, F., Giordano, A., Barbarisi, M., and Barbarisi, A. (2004). From cell-ECM interactions to tissue engineering. *J. Cell Physiol.* 199, 174–180. doi: 10.1002/jcp.10471

Ruoslahti, E. (2002). Drug targeting to specific vascular sites. *Drug Discov. Today* 7, 1138–1143.

Ruoslahti, E., and Pierschbacher, M. D. (1986). Arg-Gly-Asp: a versatile cell recognition signal. *Cell* 44, 517–518. doi: 10.1016/0092-8674(86)90259-x

Ruskowitz, R. E., and DeForest, A. C. (2018). Photoresponsive biomaterials for targeted drug delivery and 4D cell culture. *Nat. Rev. Mater.* 3, 1–17. doi: 10.1038/natrevmats2017.87

Sahay, G., Alakhova, D. Y., and Kabanov, A. V. (2010). Endocytosis of nanomedicines. *J. Control Release* 145, 182–195. doi: 10.1016/j.jconrel.2010.01.036

Sakiyama-Elbert, S. E., and Hubbell, J. A. (2000). Development of fibrin derivatives for controlled release of heparin-binding growth factors. *J. Control Release* 65, 389–402. doi: 10.1016/s0168-3659(99)00221-7

Saldin, L. T., Cramer, M. C., Velankar, S. S., White, L. J., and Badylak, S. F. (2017). Extracellular matrix hydrogels from decellularized tissues: Structure and function. *Acta Biomater.* 49, 1–15. doi: 10.1016/j.actbio.2016.11.068

Sato, K., Hendricks, M. P., Palmer, L. C., and Stupp, S. I. (2018). Peptide supramolecular materials for therapeutics. *Chem. Soc. Rev.* 47, 7539–7551. doi: 10.1039/c7cs00735c

Schiffelers, R. M., Ansari, A., Xu, J., Zhou, Q., Tang, Q., Storm, G., et al., (2004). Cancer siRNA therapy by tumor selective delivery with ligand-targeted sterically stabilized nanoparticle. *Nucleic Acids Res.* 32:e149. doi: 10.1093/nar/gnh140

Schnittert, J., Bansal, R., Storm, G., and Prakash, J. (2018). Integrins in wound healing, fibrosis and tumor stroma: high potential targets for therapeutics and drug delivery. *Adv. Drug Deliv. Rev.* 129, 37–53. doi: 10.1016/j.addr.2018.01.020

Seif-Naraghi, S. B., Horn, D., Schup-Magoffin, P. J., and Christman, K. L. (2012). Injectable extracellular matrix derived hydrogel provides a platform for enhanced retention and delivery of a heparin-binding growth factor. *Acta Biomater.* 8, 3695–3703. doi: 10.1016/j.actbio.2012.06.030

She, W., Li, N., Luo, K., Guo, C., Wang, G., Geng, Y., et al. (2013). Dendronized heparin-doxorubicin conjugate based nanoparticle as pH-responsive drug delivery system for cancer therapy. *Biomaterials* 34, 2252–2264. doi: 10.1016/j.biomaterials.2012.12.017

Sheikhpour, M., Barani, L., and Kasaeian, A. (2017). Biomimetics in drug delivery systems: a critical review. *J. Control Release* 253, 97–109. doi: 10.1016/j.jconrel.2017.03.026

Shekaran, A., Garcia, J. R., Clark, A. Y., Kavanaugh, T. E., Lin, A. S., Guldberg, R. E., et al. (2014). Bone regeneration using an alpha 2 beta 1 integrin-specific hydrogel as a BMP-2 delivery vehicle. *Biomaterials* 35, 5453–5461. doi: 10.1016/j.biomaterials.2014.03.055

Shi, F., and Sottile, J. (2008). Caveolin-1-dependent beta1 integrin endocytosis is a critical regulator of fibronectin turnover. *J. Cell Sci.* 121(Pt 14), 2360–2371. doi: 10.1242/jcs.014977

Shing, Y., Folkman, J., Sullivan, R., Butterfield, C., Murray, J., Klagsbrun, M., et al. (1984). Heparin affinity: purification of a tumor-derived capillary endothelial cell growth factor. *Science* 223, 1296–1299. doi: 10.1126/science.6199844

Shukla, R., Chanda, N., Zambre, A., Upendran, A., Katti, K., Kulkarni, R. R., et al. (2012). Laminin receptor specific therapeutic gold nanoparticles (198AuNP-EGCg) show efficacy in treating prostate cancer. *Proc. Natl. Acad. Sci. U.S.A.* 109, 12426–12431. doi: 10.1073/pnas.1121174109

Silva, G. A., Czeisler, C., Niece, K. L., Beniash, E., Harrington, D. A., Kessler, J. A., et al. (2004). Selective differentiation of neural progenitor cells by high-epitope density nanofibers. *Science* 303, 1352–1355. doi: 10.1126/science.1093783

Sood, N., Bhardwaj, A., Mehta, S., and Mehta, A. (2016). Stimuli-responsive hydrogels in drug delivery and tissue engineering. *Drug Deliv.* 23, 758–780. doi: 10.3109.2014.940091

Storrie, H., Guler, M. O., Abu-Amara, S. N., Volberg, T., Rao, M., Geiger, B., et al. (2007). Supramolecular crafting of cell adhesion. *Biomaterials* 28, 4608–4618. doi: 10.1016/j.biomaterials.2007.06.026

Tanihara, M., Suzuki, Y., Yamamoto, E., Noguchi, A., Mizushima, Y., et al. (2001). Sustained release of basic fibroblast growth factor and angiogenesis in a novel covalently crosslinked gel of heparin and alginate. *J. Biomed Mater. Res.* 56, 216–221.

Tashiro, K., Sephel, G. C., Weeks, B., Sasaki, M., Martin, G. R., Kleinman, H. K., et al. (1989). A synthetic peptide containing the IKVAV sequence from the A chain of laminin mediates cell attachment, migration, and neurite outgrowth. *J. Biol. Chem.* 264, 16174–16182.

Theocharis, A. D., Skandalis, S. S., Gialeli, C., and Karamanos, N. K. (2016). Extracellular matrix structure. *Adv. Drug Deliv. Rev.* 97, 4–27. doi: 10.1016/j.addr.2015.11.001

Tibbitt, M. W., Dahlman, J. E., and Langer, R. (2016). Emerging frontiers in drug delivery. *J. Am. Chem. Soc.* 138, 704–717. doi: 10.1021/jacs.5b09974

Torchilin, V. P. (2014). Multifunctional, stimuli-sensitive nanoparticulate systems for drug delivery. *Nat. Rev. Drug Discov.* 13, 813–827. doi: 10.1038/nrd4333

Tripodo, G., Trapani, A., Torre, M. L., Giammona, G., Trapani, G., and Mandracchia, D. (2015). Hyaluronic acid and its derivatives in drug delivery and imaging: recent advances and challenges. *Eur. J. Pharm. Biopharm.* 97(Pt B), 400–416. doi: 10.1016/j.ejpb.2015.03.032

Truong, N. F., Lesher-Perez, S. C., Kurt, E., and Segura, T. (2019). Pathways governing polyethylenimine polyplex transfection in microporous annealed particle scaffolds. *Bioconjug Chem.* 30, 476–486. doi: 10.1021/acs.bioconjchem.8b00696

Truong, N. F., and Segura, T. (2018). Sustained transgene expression via hydrogel-mediated gene transfer results from multiple transfection events. *ACS Biomater. Sci. Eng* 4, 981–987. doi: ..1021/acsbiomaterials.7b00957

Tsuji, T., Yoshitomi, H., and Usukura, J. (2013). Endocytic mechanism of transferrin-conjugated nanoparticles and the effects of their size and ligand number on the efficiency of drug delivery. *Microscopy* 62, 341–352. doi: 10.1093/jmicro/dfs080

Tsurkan, M. V., Hauser, P. V., Zieris, A., Carvalhosa, R., Bussolati, B., Freudenberg, U., et al. (2013). Growth factor delivery from hydrogel particle aggregates to promote tubular regeneration after acute kidney injury. *J. Control Release* 2013, 248–255. doi: 10.1016/j.jconrel.2013.01.030

Ulrich, S., Boturyn, D., Marra, A., Renaudet, O., and Dumy, P. (2014). Oxime ligation: a chemoselective click-type reaction for accessing multifunctional biomolecular constructs. *Chemistry* 20, 34–41. doi: 10.1002/chem.201302426

Urello, M. A., Kiick, K. L., and Sullivan, M. O. (2016). Integration of growth factor gene delivery with collagen-triggered wound repair cascades using collagen-mimetic peptides. *Bioeng Transl. Med.* 1, 207–219. doi: 10.1002/btm2.10037

Urello, M. A., Kiick, K. L., and Sullivan, M. O. (2017). ECM turnover-stimulated gene delivery through collagen-mimetic peptide-plasmid integration in collagen. *Acta Biomater.* 62, 167–178. doi: 10.1016/j.actbio.2017.08.038

Urello, M. A., Kiick, K. L., and Sullivan, M. O. (2014). A CMP-based method for tunable, cell-mediated gene delivery from collagen scaffolds. *Mater. J. Chem. B* 8174–8185. doi: 10.1039/c4tb01435a

Wang, C., and Gao, C. (2014). Design of gene-activated matrix for the repair skin and cartilage. *Polym. J.* 46, 476–482. doi: 10.1038/pj.2014.50

Wang, H., Feng, Y., Yang, J., Guo, J., and Zhang, W. (2015). Targeting REDV peptide functionalized polycationic gene carrier for enhancing the transfection and migration capability of human endothelial cells. *J. Mater. Chem. B* 3, 3379–3391. doi: 10.1039/C4TB02019G

Wang, Y. (2018). Programmable hydrogels. *Biomaterials* 178, 663–680. doi: 10.1016/j.biomaterials.2018.03.008

Webber, M. J., Tongers, J., Renault, M. A., Roncalli, J. G., Losordo, D. W., et al. (2010). Development of bioactive peptide amphiphiles for therapeutic cell delivery. *Acta Biomater* 6, 3–11. doi: 10.1016/j.actbio.2009.07.031

Wojtowicz, A. M., Shekaran, A., Oest, M. E., Dupont, K. M., Templeman, K. L., Hutmacher, D. W., et al. (2010). Coating of biomaterial scaffolds with the collagen-mimetic peptide GFOGER for bone defect repair. *Biomaterials* 31, 2574–2582. doi: 10.1016/j.biomaterials.2009.12.008

Xu, S., Olenyuk, B. Z., Okamoto, C. T., and Hamm-Alvarez, S. F. (2013). Targeting receptor-mediated endocytotic pathways with nanoparticles: rationale and advances. *Adv. Drug Deliv Rev.* 65, 121–138. doi: 10.1016/j.addr.2012.09.041

Yameen, B., Choi, W. I., Vilos, C., Swami, A., Shi, J., and Farokhzad, O. C. (2014). Insight into nanoparticle cellular uptake and intracellular targeting. *J. Control Release* 190, 485–499. doi: 10.1016/j.jconrel.2014.06.038

Yao, Y. (2017). Laminin: loss-of-function studies. *Cell Mol. Life Sci.* 74, 1095–1115. doi: 10.1007/s00018-016-2381-0

Yigit, S., Sanyal, R., and Sanyal, A. (2011). Fabrication and functionalization of hydrogels through click chemistry. *Chem. Asian. J.* 6, 2648–2659. doi: 10.1002/asia.201100440

Yoneda, A., and Couchman, J. R. (2003). Regulation of cytoskeletal organization by syndecan transmembrane proteoglycans. *Matrix Biol.* 22, 25–33.

Zeltz, C., Orgel, J., and Gullberg, D. (2014). Molecular composition and function of integrin-based collagen glues-introducing COLINBRIs. *Biochim. Biophys. Acta* 1840, 2533–2548. doi: 10.1016/j.bbagen.2013.12.022

Zhang, Y. S., and Khademhosseini, A. (2017). Advances in engineering hydrogels. *Science* 356:eaaf3627. doi: 10.1126/science.aaf3627

Zhao, L., Liu, M., Wang, J., and Zhai, G. (2015). Chondroitin sulfate-based nanocarriers for drug/gene delivery. *Carbohydr. Polym.* 133, 391–399. doi: 10.1016/j.carbpol.2015.07.063

Zhong, H., Chan, G., Hu, Y., Hu, H., and Ouyang, D. (2018). A comprehensive map of FDA-approved pharmaceutical products. *Pharmaceutics* 10:E263. doi: 10.3390/pharmaceutics10040263

Zhou, F., Jia, X., Yang, Q., Yang, Y., Zhao, Y., Fan, Y., et al. (2016). Targeted delivery of microRNA-126 to vascular endothelial cells via REDV peptide modified PEG-trimethyl chitosan. *Biomater. Sci.* 4, 849–856. doi: 10.1039/c5bm00629e

Zhou, S., Hokugo, A., McClendon, M., Zhang, Z., Bakshi, R., and Wang, L. (2019). Bioactive peptide amphiphile nanofiber gels enhance burn wound healing. *Burns* 45, 1112–1121. doi: 10.1016/j.burns.2018.06.008

Zieris, A., Chwalek, K., Prokoph, S., Levental, K. R., Welzel, P. B., Freudenberg, U., et al. (2011). Dual independent delivery of pro-angiogenic growth factors from starPEG-heparin hydrogels. *J. Control Release* 156, 28–36. doi: 10.1016/j.jconrel.2011.06.042

Zieris, A., Prokoph, S., Levental, K. R., Welzel, P. B., Grimmer, M., Freudenberg, U., et al. (2010). FGF-2 and VEGF functionalization of starPEG-heparin hydrogels

to modulate biomolecular and physical cues of angiogenesis. *Biomaterials* 31, 7985–7994. doi: 10.1016/j.biomaterials.2010.07.021

Zilberman, M., and Elsner, J. J. (2008). Antibiotic-eluting medical devices for various applications. *J. Control Release* 130, 202–215. doi: 10.1016/j.jconrel.2008.05.020

Zollinger, A. J., and Smith, M. L. (2017). Fibronectin, the extracellular glue. *Matrix Biol.* 6, 27–37. doi: 10.1016/j.matbio.2016.07.011

Zustiak, S. P., and Leach, J. B. (2010). Hydrolytically degradable poly(ethylene glycol) hydrogel scaffolds with tunable degradation and mechanical properties. *Biomacromolecules* 11, 1348–1357. doi: 10.1021/bm100137q

Conflict of Interest: The authors declare that the research was conducted in the absence of any commercial or financial relationships that could be construed as a potential conflict of interest.

frontiers in Bioengineering and Biotechnology

REVIEW
published: 17 April 2020
doi: 10.3389/fbioe.2020.00240

Nanoparticles as Versatile Tools for Mechanotransduction in Tissues and Organoids

*Abdel Rahman Abdel Fattah and Adrian Ranga**

Laboratory of Bioengineering and Morphogenesis, Department of Mechanical Engineering, KU Leuven, Leuven, Belgium

Organoids are 3D multicellular constructs that rely on self-organized cell differentiation, patterning and morphogenesis to recapitulate key features of the form and function of tissues and organs of interest. Dynamic changes in these systems are orchestrated by biochemical and mechanical microenvironments, which can be engineered and manipulated to probe their role in developmental and disease mechanisms. In particular, the *in vitro* investigation of mechanical cues has been the focus of recent research, where mechanical manipulations imparting local as well as large-scale mechanical stresses aim to mimic *in vivo* tissue deformations which occur through proliferation, folding, invagination, and elongation. However, current *in vitro* approaches largely impose homogeneous mechanical changes via a host matrix and lack the required positional and directional specificity to mimic the diversity of *in vivo* scenarios. Thus, while organoids exhibit limited aspects of *in vivo* morphogenetic events, how local forces are coordinated to enable large-scale changes in tissue architecture remains a difficult question to address using current techniques. Nanoparticles, through their efficient internalization by cells and dispersion through extracellular matrices, have the ability to provide local or global, as well as passive or active modulation of mechanical stresses on organoids and tissues. In this review, we explore how nanoparticles can be used to manipulate matrix and tissue mechanics, and highlight their potential as tools for fate regulation through mechanotransduction in multicellular model systems.

Keywords: nanoparticles, organoid, hydrogel, tissue engineering, synthetic microenvironments

OPEN ACCESS

Edited by:
Francesco Cellesi, Politecnico di Milano, Italy

Reviewed by:
Nina Bono, Politecnico di Milano, Italy
Francesca Taraballi, Houston Methodist Research Institute, United States

***Correspondence:**
Adrian Ranga
adrian.ranga@kuleuven.be

Specialty section:
This article was submitted to Nanobiotechnology, a section of the journal Frontiers in Bioengineering and Biotechnology

Received: *15 November 2019*
Accepted: *09 March 2020*
Published: *17 April 2020*

Citation:
Abdel Fattah AR and Ranga A (2020) Nanoparticles as Versatile Tools for Mechanotransduction in Tissues and Organoids. Front. Bioeng. Biotechnol. 8:240. doi: 10.3389/fbioe.2020.00240

INTRODUCTION

Over the last decades advances in methods to precisely direct stem cell fate have enabled the generation of increasingly biomimetic models of human development in a dish, and the translation of these approaches to disease-specific models has led to important insights into the etiology of pathological states. Stem cell-derived organoids have enhanced our ability to mimic human physiology by providing multicellular, tissue-like organization, allowing for modeling of complex tissue functions and disease phenotypes. In particular, human induced pluripotent stem cell (iPSC)-derived organoids begin to recapitulate key features of human-specific developmental steps and pathological features which are impossible to mimic with animal models (Lancaster and Huch, 2019). The *in vitro* aspect of organoid culture, and the use of biomaterials to rationally design their surrounding microenvironment, provides the freedom to interrogate the specific role of biochemical and mechanical cues in determining cell fate

specification, morphogenesis and patterning. In particular, mechanical stresses imparted by dynamic tissue deformation during development are increasingly recognized as critical sources of timed inductive cues with important regulatory roles. To sense these cues, cells rely on their ability to receive and process external changes in the biophysical environment to activate genetic programs driving specific responses, a process known as mechanotransduction (Chan et al., 2017; Davidson, 2017). The interpretation of mechanical signals is performed by specialized mechanosensitive and mechanotransductive proteins, whose dysregulation leads to important pathologies. Vinculin is one such critical element in mechanoregulation, serving to link integrins with the cytoskeleton, and vinculin mutations in mouse embryos are associated with severe neural tube defects (Xu et al., 1998).

The *in vitro* modulation of the mechanical microenvironment can be broadly characterized as being either passive or active. Passive modulation consists of setting a mechanical milieu within which cells can interact but which cannot be changed, such as the culture of cells on or within an extracellular matrix (ECM) of specific stiffness. Landmark studies have established that substrate stiffness alone can direct stem cell fate, with, for example, mesenchymal stem cells adopting the fates of tissues whose stiffness corresponds to that of the substrates on which they were cultured (Engler et al., 2006). Active mechanical modulation of the microenvironment provides for controlled changes in the stress/strain fields, which can be actuated externally. In both cases, the entire multicellular construct is subject to a homogenous mechanical state (**Figure 1A**) which can be different from that of the *in vivo* scenario, where specific regions of the tissue may experience local and anisotropic mechanical stresses and deformations. To overcome these limitations, increasingly biomimetic *in vitro* technologies for modeling tissue mechanobiology are beginning to incorporate features of the complex and dynamic mechanical interplay between tissues. Here, we provide a brief overview on the role of mechanobiology in tissue development, review current methods to alter matrix and tissue mechanics *in vitro*, and illustrate how nanoparticles (NPs) provide additional design parameters offering unique capabilities to engineer the mechanical microenvironment in tissues and organoids with a high degree of spatial and temporal resolution.

ROLE OF MECHANICAL CUES IN DEVELOPING TISSUES

Continuous tissue deformations underlie the early development of all tissues, and are orchestrated by 3D cell rearrangements, sorting, migration and differentiation. The toolkit of morphogenesis includes mechanisms such as differential adhesion, epithelial-to-mesenchymal and mesenchymal-to-epithelial transitions, as well as apical constrictions and intercalations, which all contribute to the generation of intracellular mechanical forces. Classic *in vitro* cell reaggregation experiments have shown that cells of the same type can sort within a mixed population to give rise to an ordered construct (Steinberg, 1963), based on expression of junctional cadherins and catenins. Similarly, the minimization of free energy can help explain *in vitro* germ layers stratification based on differential surface tensions (Davis et al., 1997). Additionally, integrin-mediated interactions between cells and ECM have been shown to play a critical role in enabling large-scale tissue motions during convergent extension and somitogenesis (Bénazéraf et al., 2010). The ECM is also involved in regulating cavity and lumen formations in epithelial tissues throught its role in cytoskeletal modifications via integrin binding (Bedzhov and Zernicka-Goetz, 2014). At the scale of the single cell as well as at multicellular and tissue scales, these deformations contribute to the establishment of mechanical fields which feed back onto gene regulatory networks. The development of the embryonic gut provides an illustrative example of how differential growth rates at local scales lead to large-scale changes in morphology. Here, the, differences in growth rate between the gut tube and mesentery cause an initially straight structure to loop due to buckling forces along its long axis (Nerurkar et al., 2017).

The molecular mechanisms of mechanosensing and mechanotransduction include factors such as the Hippo pathway effector Yap (Lian et al., 2010; Dupont et al., 2011; Benham-Pyle et al., 2015) as well as the mechanically gated ion channels Piezo1/2 (Pathak et al., 2014; Hennes et al., 2019), which produce their effects either indirectly, e.g., through Yap nuclear translocation, or directly, e.g., through the nucleocytoskeleton and cytoskeleton (LINC) complex (Stewart et al., 2015). Indeed, Yap changes its localization from cytoplasmic (no mechanical stimulation/inactive form) to nuclear (under mechanical stimulation/active form) (Dupont et al., 2011) and Yap has been shown to play an important role in stem cell differentiation, with its levels gradually decreasing during the transition from pluripotency (Lian et al., 2010). Moreover, Yap, in concert with β-catenin, has been shown to initiate cell cycle reentry when active mechanical forces are present (Benham-Pyle et al., 2015). Independently of the Hippo pathway, the pressure-activated cation channels Piezo1 and Piezo2 have been shown to be direct sensors of fluid sheer stress and membrane stretch, converting applied force into electrical signals (Lin et al., 2019) in such varied contexts as vascular endothelium, pancreas and skin. Piezo1 has notably also been involved in determining lineage choice in human neural stem cells, where activation by traction forces resulted in neurogenesis, while inhibition gave rise to astrocytes and limited neuronal differentiation (Pathak et al., 2014). Another study in human endometrial epithelial cells (hEECs) demonstrated that activation of Piezo1 was a direct response to cell membrane mechanical indentation, suggesting such mechanoregulation may be important in embryo implantation (Hennes et al., 2019). Interestingly, endometrial organoids were used here as a model system which could sustain longer culture under mechanical activation compared to primary hEECs. These examples illustrate that while the elements of the cellular

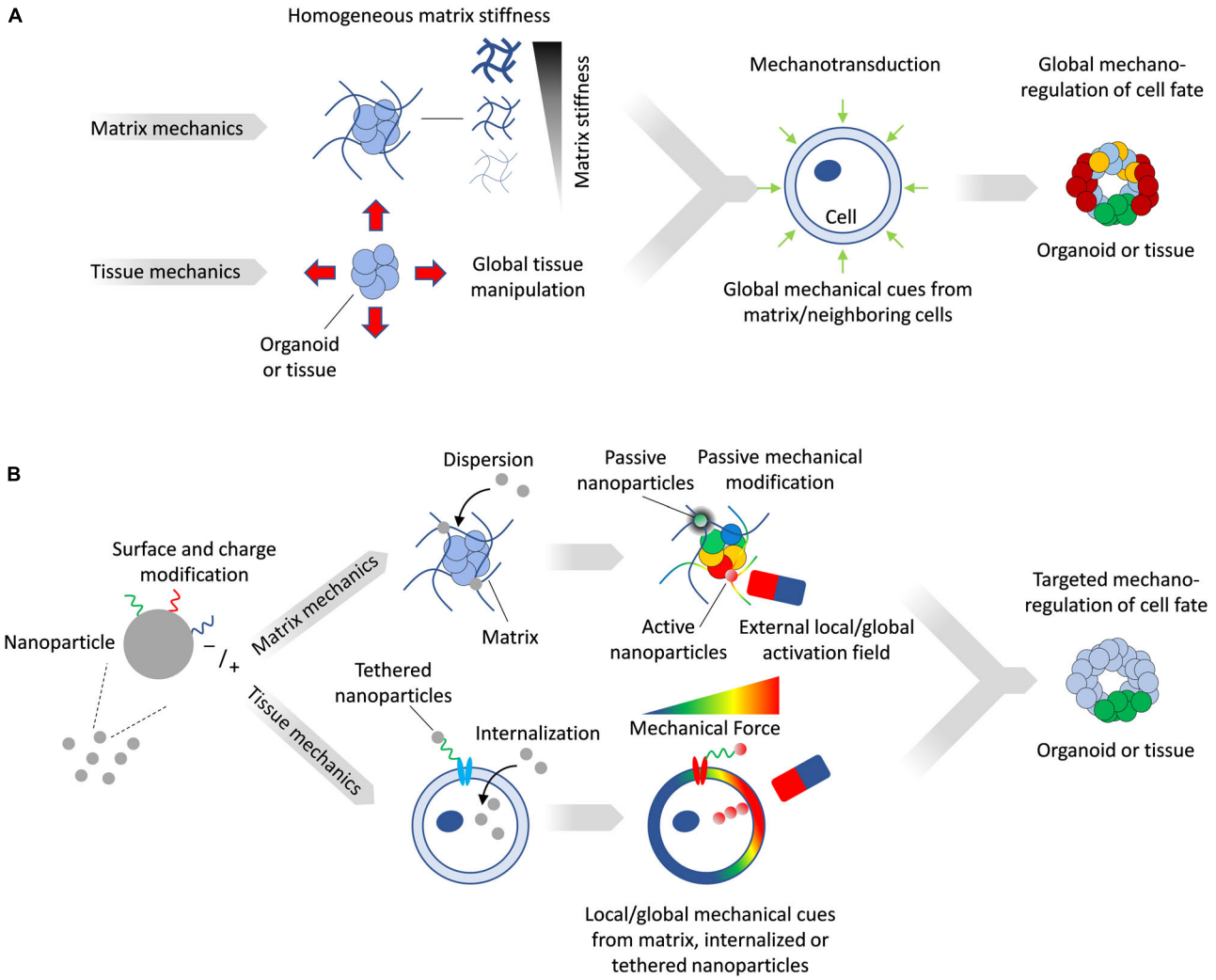

FIGURE 1 | (A) Matrix mechanics can be modulated to create stiff or soft synthetic microenvironment, while device-driven tissue manipulation can impose mechanical stresses directly on tissues. Such manipulation provides global and homogenous mechanical cues on tissues and organoids. **(B)** Magnetic NPs can be tailored to matrix or tissue mechanics applications. NPs activated by a field can generate local mechanical forces, while inactive ones can passively alter local matrix stiffness. Magnetized cells can be subjected to forces by an external field and transfer these mechanical stresses to the surrounding tissue.

mechanosensing and mechanotransducing machinery are the same in various tissues and spatial configurations, they are highly context-specific in how they are deployed and in their role.

ARTIFICIAL EXTRACELLULAR MATRICES TO ENGINEER MICROENVIRONMENTAL CONTROL

Organoids provide tractable model systems to deconvolve the complex and multifactorial interplay between mechanics and biological response. As such, matrix engineering has provided a powerful avenue to controllably modulate the mechanical microenvironment *in vitro*. Naturally derived matrices such as collagen and Matrigel have routinely fulfilled the role of supportive host matrix required for the emergence of characteristic three-dimensional organoid features. However, these materials suffer from batch-to-batch variability and lack mechanical tunability, which hinders efforts to understand the role of individual microenvironmental elements. Artificial extracellular matrices (aECM) have emerged as important alternatives to overcome these limitations by mimicking specific elements of natural ECMs in a more controllable manner. Their mesh-like or fibrillar network composition in the form of hydrogels provides mechanical support, and such aECMs can be engineered to allow for remodeling capabilities, for example by cell-secreted matrix metalloproteinases (MMPs). The high degree of control over their mechanical characteristics through changes in the density of the polymer subunits has been employed to direct cell fates, with common examples including the control of embryonic stem cell pluripotency (Li et al., 2006) or the

differentiation of human mesenchymal stem cells (hMSCs) to chondrogenic fates (Kloxin et al., 2009). As in natural ECMs such as laminin, fibronectin and collagen, aECMs can be engineered to present integrin-binding sites (e.g., RGD) which enable cell traction and migration. The modularity and orthogonality of these properties has made the multiplexing of the combinatorial experimental design space possible. This has allowed for high throughput screening of matrix characteristics such as stiffness, presence and concentration of adhesion ligands and degree of degradation by cellular proteolytic activity (Ranga et al., 2014). Such platforms have been used to uncover the role of the matrix in diverse contexts such as cytoskeleton-driven symmetry breaking in a mouse neural tube organoid model (Ranga et al., 2017) and in reprogramming of iPSCs (Caiazzo et al., 2016).

Matrices with dynamic mechanical characteristics, which can transition from stiff to soft (Gjorevski and Lutolf, 2017) or from fluid to solid (Bhattacharjee et al., 2015) in a defined manner can provide additional dynamic control. These can provide timed mechanical cues and respond to the transient mechanical needs of organoid culture. For example, PEG–based aECMs have been used to elucidate the role of dynamic mechanical forces in intestinal stem cell expansion and organoid formation (Gjorevski et al., 2016) by rendering gels degradable in a time-dependent manner though the incorporation of hydrolytically degradable moieties in an otherwise non-degradable gel. Stiff matrices were shown to create ideal conditions for intestinal organoid colony formation, but not necessarily for organoids morphogenesis, i.e., crypt budding. By rendering the matrix degradable only at a later time, the initially stiff matrices could support colony formation and, upon degradation, favored organoid growth. Such modulation, translated molecularly via Yap1 (Gjorevski and Lutolf, 2017), could not be achieved in a matrix with fixed mechanical characteristics, and is a striking example of the importance of tunable aECMs. Similar degradable hydrogels have shown promise for the growth and expansion of human intestinal organoids derived from iPSCs, as well as for the successful engraftment of organoids containing hydrogels in mice for colonic wound repair applications (Cruz-Acuña et al., 2017).

In addition to cell or hydrolysis-mediated mechanical modifications, other environmental conditions such as pH and temperature can be modulated exogenously to control matrix properties and resulting organoid characteristics. For example, glioblastoma-derived cells could be cultured as tumoroids to a specified size in thermoreversible PNIPAAM-PEG hydrogels, whereupon a rapid change in temperature to 4°C caused the matrix to liquefy and free the cells, making them available for further expansion (Li Q. et al., 2016). Compared to conventional methods, this approach yielded 20-fold higher cell density while limiting aggregation. For *in vivo* applications, pH sensitivity can be more beneficial than thermoresponsiveness, since slight changes in pH can occur between diseased and healthy tissues, offering a parameter for targeting the diseased region. For instance, cardiosphere-derived cells were embedded in hydrogels that only polymerize at a pH of 6.5 and at 37°C, resembling conditions in infarcted hearts (Li Z. et al., 2016).

A disadvantage of temperature and pH-sensitive matrices is that their property changes often involve phase changes which can disrupt cellular spatial organization. Light-sensitive photodegradable materials can provide post-gelation mechanical tuning *in situ* with more gradual property modifications. In one study, ultraviolet light has been used to reduce the stiffness of photodegradable hydrogels from 10 to 2 KPa, thereby allowing *in situ* manipulation of the mechanical cues perceived by MSCs (Yang et al., 2014). These cells we shown to retain memory of stiff microenvironments by committing to an osteogenic fate despite the substrate transition from stiff to soft, which would normally favor softer tissues. An additional advantage of photosensitive materials is that spatial control over properties can be achieved, *in situ* and post-gelation (Kloxin et al., 2009). In one example, hMSCs were embedded in hydrogels with photolabile groups and targeted gel photodegradation was performed by two-photon microscopy, forming 3D internal channels through which cell could undergo directed cell migration. Precise 3D control of photodegradation over mechanical stresses, as shown here, could open interesting avenues for investigating how precisely shaped stress fields could control organoid growth.

Optimizing matrix properties *in vitro* can also have an important *in vivo* role in therapeutic applications. For example, a PEG hydrogel with a stiffness of 350 Pa promoted differentiation of iPSCs to a cardiac fate, with the resulting hydrogel-cell bioactive tissue achieving a high degree of repair when injected in infarcted mouse hearts (Bearzi et al., 2014). Further optimization of such aECMs can also be targeted toward practical purposes such as improving material handling and delivery by enhancing injectability or by enabling on-site polymerization (Chow et al., 2017).

EXTRINSIC CONTROL OF CELLULAR FORCES THROUGH MOTORIZED DEVICES AND OPTICAL TWEEZERS

In addition to designing microenvironments with specified mechanical properties, active force modulation can also be imposed independently of matrix engineering, and can be beneficial to mimic the chronology of *in vivo* deformations. A common way to achieve this at multicellular resolution is through the use of instruments where cells are plated on elastomeric membranes which undergo mechanical stretching. By stretching the membranes, strains are transferred to the adhered cells, subjecting them to mechanical stresses. Such experiments help in understanding the role of tissue deformation in specifying cell fate in highly controlled settings, and can identify the mechanosensitive pathways involved. For example, cyclic loading of fibroblast cells have shown Zyxin to be an important mechanosensitive protein, playing a role in filamentous actin remodeling and reinforcement (Hoffman et al., 2012). In some applications, more elaborate devices are necessary to provide complex strain field modulation, such as in the case of a microfabricated pneumatic device used to provide cyclic loading via inflatable membranes to differentiating human pluripotent stem cells (hPSCs) (Xue et al., 2018). The mechanical stimulation of hPSCs, together with exogenous BMP signaling, was shown to alter neural plate border patterning, highlighting

how biophysical parameters could synergize with biochemical signals to induce neuroectoderm patterning in 2D.

Other methods such as optical tweezers have been employed to directly impose pN forces at the length scale of the single cell. This is achieved by tethering polystyrene beads to cell membranes, which can be manipulated when subjected to focused light. Using this technique, a recent study highlighted how mouse neuroblastoma cells respond to forces ranging from 5 to 20 pN by activation of Ca^{2+} ion channels at defined force thresholds (Falleroni et al., 2018). Optical tweezers have been largely applied and optimized to 2D single cell scenarios and thus may prove less attractive to mechanically stimulate more complex 3D multicellular tissues and organoids. The precision of optical stimulation could, however, be used to impart differential force modulation in larger cellular constructs, e.g., stimulating a specific region of an organoid, which could help understand how forces are communicated between stimulated and unstimulated cells.

NPs FOR MECHANICAL STRESS MODULATION

While current tissue and matrix mechanics modulation approaches provide means to globally impose forces *in vitro*, in most cases such forces lack the heterogeneity in magnitude and direction that is more familiar to *in vivo* scenarios. In contrast, NPs dispersed in a matrix impart mechanical changes within their immediate vicinity, and since their distribution can be controlled, such alterations can be local or global, as well as on demand. Importantly, due to their capacity to be internalized by cells or to be tethered to targeted cells, they can directly impose forces in tissues on a cellular level (**Figure 1B**).

NPs come in many different shapes, sizes and materials, with a common feature that their characteristic length is less than 100 nm. NP types include quantum dots (Michalet et al., 2005), spherical particles (Pankhurst et al., 2003), rod and tube shaped particles (Wong et al., 1997), 2D sheets (Saliev et al., 2019; Zhu et al., 2019), and 3D superlattices (Ji et al., 2019). In the context of biological applications, NPs have been hailed for their ability to target cells of interest, shown most strikingly in targeting cancer cells to deliver drugs (Breunig et al., 2008), improving transfections (Sokolova et al., 2019), silencing genes (Frede et al., 2016; Morgan et al., 2019), or even employing material properties to destroy target cells (Sanhaji et al., 2019), all in an effort to combat disease. NPs are now increasingly being used in theranostic applications, an emerging field in medicine that combines targeted therapies with disease monitoring (Scialabba et al., 2019). The importance of these applications has prompted the development of new platforms to screen for delivery efficiency in tissues, and organoids are playing an increasingly important role here as biomimetic disease models (Davoudi et al., 2018; Leite et al., 2019). The functions that NPs can play in a biological setting are constantly being expanded, with mechanical stimulation of matrices and tissues figuring prominently as an important new application area.

LOCAL MODULATION OF MATRIX MECHANICS

In a NP-free matrix, polymer chains crosslink through bridging sidechains. The number of bridges formed during polymerization can determine the elasticity of the material, where relatively few crosslinks allow for freedom of movement and result in more elastic or viscoelastic bulk material behavior, while more crosslinks result in a more rigid material. When NPs are dispersed in a matrix, they can enhance or degrade its mechanical integrity on a local scale. If the size of NPs added to such a polymeric matrix is sufficiently small to fit within the interchain gaps while avoiding crosslink disruption, the more rigid material properties of the NPs relative to the polymers leads to a reduction in deformation and an increase in local stiffness. The incorporation of large NPs, or of NPs that disrupt the crosslinking process, has an opposite effect, creating locally suboptimal crosslinks and leading to a reduction in the local stiffness of the material. When considering the matrix as a whole, the accumulation of local nano-variations in mechanical properties can translate to bulk stiffness enhancement (Jestin et al., 2008) or hindrance (Abdel Fattah et al., 2016). One of the main uses of NPs in tissue engineering applications thus far has been to generate composite materials with enhanced properties, often as reinforcement material to strengthen the host matrix (Compton and Lewis, 2014). For example, when added to type I collagen, polyvinyl pyrrolidone-coated titanium oxide NPs have been shown to strengthen the resultant 3D scaffold and promote skin growth compared to NP-free matrices (Li N. et al., 2016). Similarly, fibrous materials whose properties would be ideal for growth of hard tissues such as bone but suffer from mechanical weakness have benefitted from NP reinforcement; for example NP-reinforced silk fibroin scaffolds successfully supported osteoblast cell culture (Kim et al., 2014). 3D bioprinting technologies have also benefited from the inclusion of nano filler materials, such as gelatin NPs in thixotropic collagen and hyaluronic acid bioinks for the culture of Hep2G organoids (Clark et al., 2019).

ACTIVE MANIPULATION OF MATRIX MECHANICS

While the addition of NPs in matrices can modulate their properties, NPs that are responsive to exogenous fields present unique advantages due to their ability to create anisotropic changes in the mechanical field in 3D (Jestin et al., 2008), and to create heterogeneous force distributions in the host matrix (Kokkinis et al., 2015; Abdalla et al., 2016; Abdel Fattah et al., 2016), allowing organoids and tissues to experience a spatio-temporally varying mechanical environment. Indeed, engineered NPs allows for continuous modulation of the mechanical stresses imposed on tissues through the control of the external activation field, which can be electric, optical, acoustic or magnetic. Magnetic fields in particular can be engineered with high precision

within the dimensions of the culture environment using permanent magnets and high gradient magnetic fields. For example, carbonyl iron particles embedded into a polyacrylamide composite hydrogel have shown promise in reversibly modulating substrate stiffness from 0.1 to 90 KPa (Abdeen et al., 2016). When exposed to a magnetic field, the particles within the substrate align in chains, which present less deformable zones in the matrix and thus cause the substrate to become stiffer. The stiffness is reverted when the field is discontinued since the particles cannot maintain their alignment and diffuse to a homogenous distribution through Brownian motion. This physical reversibility is an important aspect of mechanically responsive matrices (Sapir-lekhovitser et al., 2016), as it allows for cyclic and variable activation with minimum material plasticity, leading to biological effects illustrated by an increase in cultured MSC spread area (**Figure 2A**). An increase in cell surface area here indicated that cells were developing higher tractions, which was accompanied by an increase in the expression of the osteogenic fate marker Runx2. In a separate study, magnetic NPs were dispersed in a PEG hydrogel to render it magnetic (Filippi et al., 2019). When subjected to an external magnetic field, cells from the stromal vasculature fraction of human adipose tissue were activated by movement of the NPs through the gel. Magnetically activated cells exhibited more metabolic activity, upregulated endothelial, pericytic and perivasculature markers, and activated pathways involved in mechanotransduction such as ERK and MAPK. These studies highlight the potential of magnetically responsive matrices to regulate cell function and fate specification; while matrices embedded with field-responsive NPs are not yet widely explored, they provide an exciting technology platform for exploring questions in mechanobiology.

GENERATING FORCES FROM WITHIN: CELLULAR INTERNALIZATION OF NPs

While mechanical modulations external to cellular bodies can be achieved by embedding NPs within 3D ECMs, in order to exert a force directly within a tissue NPs must be internalized inside target cells. Synthesized NPs are not inherently biocompatible, therefore, in order to use them in biological applications, their surface chemistry must be modified in order to limit detrimental interactions with cells. In general, NPs enter cells through endocytosis and may accumulate to toxic levels or degrade within the cell due to oxidation, releasing harmful bioactive components leading to apoptosis or necrosis (Schweiger et al., 2012). NPs can also interfere with cytoskeletal rearrangement within the target cell, which can disregulate key cellular process such as cell division or migration (Bouissou et al., 2004; Mcbeath et al., 2004; Müller et al., 2013). For example, differentiating neural stem cells exposed to high levels of silver NPs exhibit disrupted β-catenin signaling, an important modulator of the cytoskeleton, via the emergence of inclusions in F-actin filaments (Cooper et al., 2019). These disruptions have been shown to lead to morphological changes such as reduction of neurite length, highlighting the vulnerability of neural cells to NP accumulation in the brain.

To overcome such cytotoxic effects, NPs can be rendered biocompatible through feature selection or surface functionalization, which allow for internalization routes that do not adversely disrupt the cell (Hsiao et al., 2019). Several types of internalization processes may be involved depending on NP size, shape, charge, and coating. NP size is often considered the main factor in determining whether the internalization mechanism occurs via phagocytosis or pinocytosis. Phagocytosis, due to the size of phagosomes, occurs for particles that are larger than ∼250 nm, while pinocytosis, responsible for the uptake of fluid and solutes, can internalize NPs ranging below ∼100 nm (Panariti et al., 2012). NP shape can also affect cellular uptake: spherical NPs, for example, have an internalization efficiency which is several orders of magnitude higher than nanorods of comparable feature length (Chithrani and Chan, 2007). This may be attributed to the longer time and higher energy needed to internalize asymmetrically shaped particles compared to their spherical counterparts.

In addition to NP shape, the negative charge of the plasma membrane makes it difficult for neutral or negatively charged particles to be internalized. To overcome this problem, NP surface charge modification may be necessary. Cationic liposome-coated magnetite NPs can be easily internalized by cells because they adopt a positive charge, which allows them to be attracted to the negatively charged plasma membrane, and to subsequently be internalized by the cell (Ito et al., 2005). A study of chitosan-based NPs of various surface charges demonstrated this principle in a systematic study where neutral particles had the lowest internalization efficiency across several cell types, followed by those with a negative charge, with optimal cellular internalization with positively charged NPs (Yue et al., 2011). However, higher uptake of positively charged NPs does not necessarily mean better NP performance, since such particles also tend to cause more extensive cytotoxic effects by inducing reactive oxygen species (ROS) production and apoptosis (Feng et al., 2018). This effect can be remedied through additional coatings of the NPs, which increase the overall NP size, but are designed to reduce the positive charge along with cytotoxic effects (Hoskins et al., 2012).

USING NPs TO BUILD 3D SPHEROIDS AND SHAPE COMPLEX GEOMETRIES

Once NPs are internalized, they can be activated remotely using a variety of fields, including optically by infrared radiation (Liu et al., 2016). Optical tweezer approaches, for example, have been extensively used to exert forces or trap cells, often using external particles tethered to cellular membranes as conduits to convert optical power gradients into mechanical forces (Gao et al., 2017). As with the use of microbeads, NP-based optical tweezer techniques work well in planar 2D configurations, however in

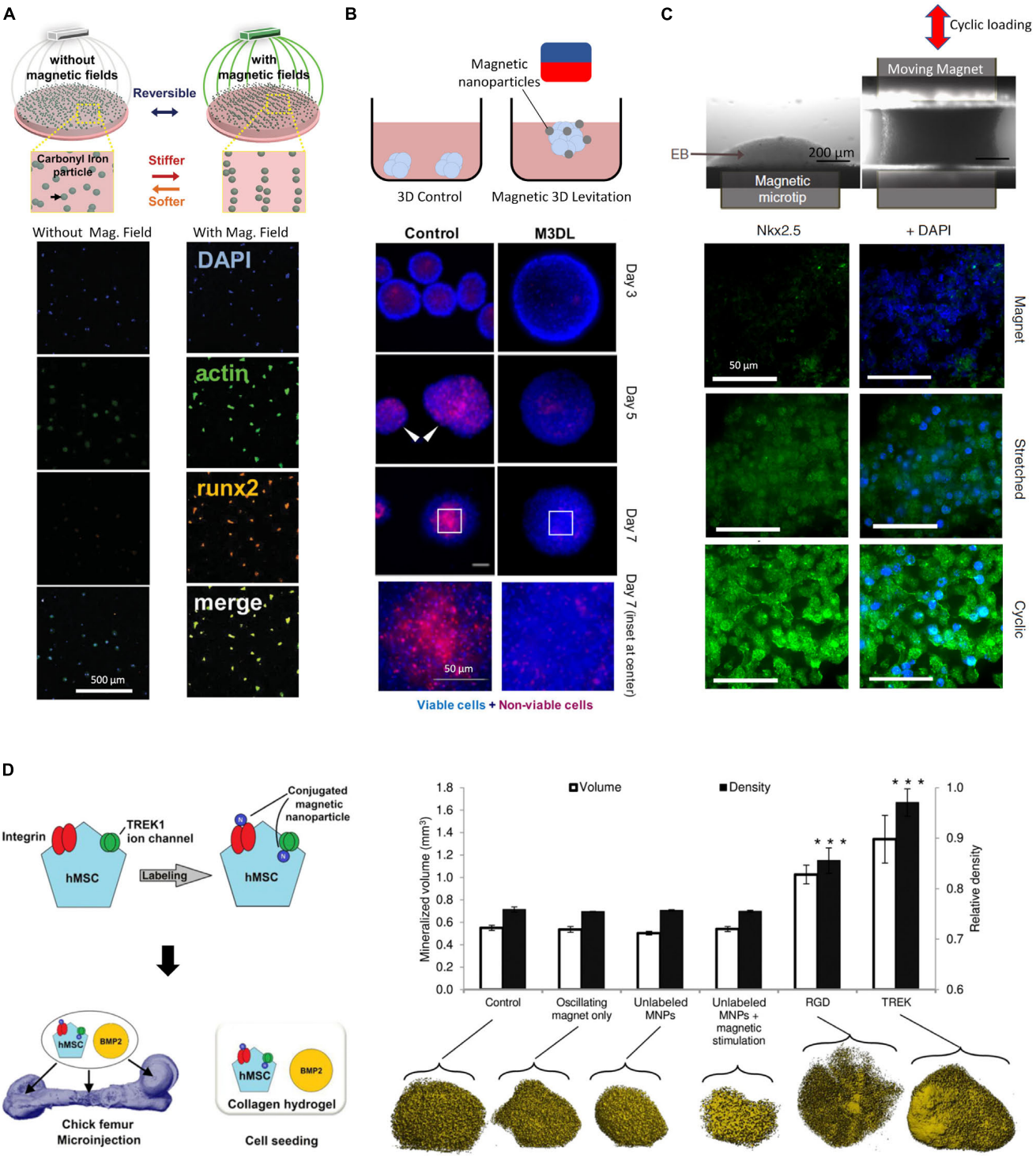

FIGURE 2 | (A) Dynamic and reversible modulation of matrix stiffness using magnetic NPs and external magnetic fields influence the activity of MSCs (adapted from Abdeen et al., 2016). A magnetic field allows for the directed assembly of magnetic particles into chains, stiffening the mechanical properties of the microenvironment, resulting in MSCs with increased area. **(B)** Internalized magnetic NPs in salivary gland-derived cells accelerate spheroid formation by an external magnetic field, yielding faster and more reproducible spheroids with lower necrosis (Ferreira et al., 2019). **(C)** Internalized magnetic NPs allow remote manipulation of embryoid bodies and direct the differentiation of embryonic stem cells toward a mesodermal cardiac identity (adapted from Du et al., 2017). A cyclic magnetic field results in highest expression of mesoderm marker Nkx2.5 compared to a static magnetic field. **(D)** Magnetic NPs conduct remote mechanotransduction by

(Continued)

FIGURE 2 | Continued
targeting mechanosensitive channels and receptors on cellular membranes (Henstock et al., 2014). Functionalized magnetic NPs designed to target the mechanosensitive TREK1 ion channel and integrins by RGD coating on hMSCs were injected in an *ex vivo* chick fetal femur. The combination of stimulation with BMP2 and oscillating magnetic field increased mineralization volume and density in targeted cells. *** indicates $p < 0.001$.

larger three-dimensional tissues, the choice of the activation field becomes limited, since such fields must penetrate the cells to reach the NPs. Magnetic fields in particular are able to penetrate biological materials with virtually no field disruption while remaining benign to tissues, which makes magnetic NPs a promising approach for remotely imparting mechanical forces directly on tissues.

Providing magnetic NPs for internalization lends cells magnetic responsiveness which can help form geometrical structures by guidance from an external magnetic field. Magnetic force generation in tissues can therefore have other applications beyond mechanotransduction, such as cell manipulation to create 3D cellular constructs. In addition to guiding cells to a specific geometry, magnetic levitation has been used to create 3D cellular spheroids (Souza et al., 2010). Magnetic fields have been used to create 3D constructs from cell cultures using paramagnetic salts (Abdel Fattah et al., 2018), however this technique provides a weak global body force which limits the effective range within which cells can be manipulated. In addition, the presence of salts means that culture durations must be limited to less than 24 hrs. In contrast, the use of magnetic NPs was shown to increase forces and effective manipulation range, which enabled the formation of highly reproducible spheroids. By applying a magnetic field, magnetized salivary gland-derived cells were guided to the air-media interface where they agglomerated to form spheroids which eventually differentiated into gland-like organoids (**Figure 2B**) (Ferreira et al., 2019). This approach provided rapid cellular assembly while foregoing the need for scaffold materials, rendering this a promising advance towards salivary gland repair. Similarly, spinal cord spheroids could be magnetically assembled with high reproducibility by magnetic NPs adhering to the membranes of dissociated primary spinal cord cells (Bowser and Moore, 2019), forming neurites upon seeding in a hydrogel matrix.

In order to create more complex geometries, experimental configurations utilizing shaped magnetic fields can be employed. In one example, urothelial, endothelial, smooth muscle, and fibroblasts cells with internalized magnetic NPs were guided into a tubular 3D multilayered cellular construct with a 5 mm lumen using a cylindrical magnet (Ito et al., 2005). This technique, also known as magnetophoresis, allows for versatile control over geometrical assembly, as demonstrated by the guidance of magnetized C2C12 myoblasts into multilayered myotube rings, thereby promoting differentiation into highly aligned skeletal muscle tissue (Yamamoto et al., 2009).

Going from bulk cell activation to targeting and mechanically stimulating specific cell populations within a tissue would represent an important advance in our ability to recapitulate the complex and heterogeneous force fields experienced *in vivo*. This level of control over spatial positioning and mechanical stimulation with high spatial resolution has been achieved in a proof-of-principle study using magnetic NPs internalized by HeLa cells plated on a magnetic array, where forces could be imposed at a resolution of less than a cell diameter (Tseng et al., 2012).

COMBINING MULTICELLULAR SHAPING AND TIMED MECHANICAL STIMULATION

In addition to creating 3D cellular constructs and designed geometries at the initiation of an experiment, magnetic NPs can provide mechanical stimulation at later time points. This two-step process was demonstrated with the initial aggregation of embryonic stem cells (ESCs) into embryoid bodies after uptake of iron oxide NPs by an external magnetic field (**Figure 2C**), followed by the re-purposing of the magnetic NPs as mechanical stimulators imparting oscillatory strains, actuated through a combination of magnetic and magneto-mechanical activation (Du et al., 2017).

Since the magnitude of exerted forces is a function of total internalized NPs, assessing their uptake is important. While chemical assays such as the potassium thiocyanate method are commonly used to assess internalization (Ito et al., 2005), other quantitative approaches have been developed. For example, pulling free-floating magnetized cells by a magnetic field through a medium and monitoring their velocities can provide a quantitative inference of the mass of the internalized NPs by balancing the forces of fluid drag under Stokes condition and that of the magnetic force. Thus, when NP internalization is sufficient, cyclic magneto-mechanical stimulation can be sufficient to direct the ESC differentiation to mesodermal cardiac fate (Du et al., 2017). Similarly, chondrogenic fate specification and collagen production can be enhanced magnetized hMSCs are subjected to cycling static and rotating external magnetic fields (Son et al., 2015). Notably, the magnetic NPs used in this study were produced by magnetospirillum sp. AMB-1 bacteria, highlighting the promise of biologically derived magnetic NPs, which are thought to be more readily internalized due to residual lipid layers surrounding the NPs.

ACHIEVING CELL SELECTIVITY AND CELL TARGETING WITH NPs

In addition to aiding in internalization, the surface coating of NPs can be bioengineered to achieve enhanced targeting

accuracy of particular cell types by mimicking specific ligands and exploiting cell-specific receptor-based endocytosis (Breunig et al., 2008; Foroozandeh and Aziz, 2018). These bioconjugation processes are often designed in conjunction with surface charge modification, as both must be optimized to avoid undesirable NP aggregation. To achieve high cell selectivity NP coatings can be designed to promote targeted interactions with the cellular membrane, becoming robustly tethered only to those cells that express receptors compatible with the coating (Hughes et al., 2007). For example, when hMSCs were treated with magnetic NPs targeting the mechanosensitive TREK1 ion channel, then injected into an *ex vivo* chick fetal femur and stimulated by an externally oscillating magnetic field, the magnetized NPs produced a 4pN force upon the receptor, initiating a remote mechanotransductive effect and leading stimulated cells to exhibit increased mineralization (Henstock et al., 2014) (**Figure 2D**). This approach was implemented in an *in vivo* pre-clinical ovine bone injury model and demonstrated the possibility of remote force induction in a large animal model to promote bone healing (Markides et al., 2018). Similar results were obtained when magnetic NPs were functionalized to target Frizzled, the receptor for Wnt (Rotherham et al., 2018), on magnetically stimulated hMSCs, suggesting that this is a versatile strategy for applications in osteogenesis. This approach is transferrable to other lineages, requiring mainly the modification of the magnetic NP functionalization to target different receptors of interest. For instance, when targeting the activin receptor type IIA on human adipose stem cells, a varying magnetic field helped activate the receptor and promoted tenogenic differentiation, providing a promising result for tendon repair applications (Gonçalves et al., 2018). Interestingly, magnetic NPs can also impose such high forces that cell death can result – in some case this may be valuable, for example to mechanically disrupt and destroy cancer cells (Shen et al., 2017) such as malignant glioma cells in- tumor-bearing mice, which could be destroyed by the application of a rotating magnetic field to internalized disk shaped permalloy magnetic NPs (Cheng et al., 2016). In the context of organoid bioengineering, targeting of specific cells through surface markers for mechanical activation could allow for selective activation of cells of specific fates within a heterogenous organoid.

OUTLOOK

The context-specific manner in which cells in tissues sense, react and in turn generate mechanical force has become an active area of research. In order to explore the relationship between mechanical forces and fate specification and morphogenetic outcomes, the development of *in vitro* multicellular model systems with local and directed force generation is critical. NPs provide unique and versatile features which enable such investigations, including control over spatial resolution, targetability as well as remote actuation which, alone or in combination with aECMs, allow for highly specific organoid manipulation. Magnetic NPs in particular are likely to see the greatest application and development in the field, as they are relatively benign and need little modification for efficient uptake by most cells. Additionally, they are also easily synthesized using straightforward benchtop fabrication techniques with simple chemistries such as co-precipitation. Magnetic NPs dispersed in a matrix can provide active mechanical stimulation in any direction, rendering them more versatile than conventional methods such as stretching devices, which are generally limited to strains along predefined orientations. While magnetic NPs are useful tools for matrix as well as tissue stimulation, magnetization of cells through NP internalization is likely to see more applications due to the ability of internalized magnetic NPs to create spheroids and organoids by magnetic guiding, and to then generate internal magnetic forces in host matrices.

Assessing the changes in mechanical state upon stimulation is critical in validating the relationship between applied force and biological outcomes. The mechanical dynamics in matrices can be interrogated using techniques such as traction force microscopy (TFM) (Jorge-Peñas et al., 2017) while those within tissues can be assessed by force inference (Veldhuis et al., 2017), fluorescence resonance energy transfer (FRET) biosensors (Grashoff et al., 2010), or dispersible and deformable hydrogel microparticles embedded within the tissue (Lee et al., 2019). Such force interrogation methods are, in principle, fully compatible with NP-mediated mechanical stimulation of the matrix or tissue. In particular, bead tracking techniques and TFM, which assess external matrix mechanics, can be beneficial for NP-mediated matrix mechanical modulation. In contrast, FRET-based sensors convey information about tissue deformations and stresses arising from direct tissue stimulation through internalized NPs.

Because NPs can be stimulated by external fields which can be engineered with high precision, such as light or magnetism, a dispersion of NPs can be homogeneous (global) while the stimulating field is highly localized. Such effects can help introduce anisotropic manipulation of organoid microenvironments. In contrast, mixing magnetized cells with non-magnetized cells in specific ratios can create cellular constructs which have specific subpopulations that are magnetically responsive. In this case a relatively local magnetic response could be obtained within the organoid using a global magnetic field, either by permanent magnets or electromagnets. Since NPs can be easily modified, they can serve multiple mechanical and biochemical purposes and can act as mechanotransducers via one field, as well as morphogen carriers released by degradation or in response to a secondary field.

As NPs are generally not in current use in organoid and tissue engineering labs, their adoption would also add a few hurdles. Since uptake and cytotoxic effects are likely to vary between different cell types and also between differentiation protocols, these will have to be tested for individual model systems. In addition, external field activation would require the acquisition and implementation of new instruments and

expertise, with consequent additional costs and complexity to experimental planning. Finally, as with current organoid culture and bioengineering approaches, reproducibility of these new and unconventional approaches will require extensive characterization to achieve robust and reproducible outcomes. Despite these current challenges, the studies we have reviewed here have demonstrated that NPs can be powerful new tools to modulate the mechanical properties of the microenvironment, and it is expected that in time, simple NP uptake, cell targeting and dispersal protocols are likely to emerge and pave the way to wider use in organoid and tissue engineering applications.

AUTHOR CONTRIBUTIONS

AA and AR wrote and edited the manuscript.

FUNDING

This work was supported by the FWO grant G087018N and FWO postdoctoral fellowship 1217220N, Interreg BIOMAT-ON-CHIP, Vlaams-Brabant and Flemish Government co-financing, KU Leuven grants C14/17/111 and C32/17/027 and King Beadouin Foundation grant J1810950-207421.

REFERENCES

Abdalla, A. M., Majdi, T., Ghosh, S., and Puri, I. K. (2016). Fabrication of nanoscale to macroscale nickel-multiwall carbon nanotube hybrid materials with tunable material properties. *Mater. Res. Express* 3:125014. doi: 10.1088/2053-1591/3/12/125014

Abdeen, A. A., Lee, J., Bharadwaj, N. A., Ewoldt, R. H., and Kilian, K. A. (2016). Temporal modulation of stem cell activity using magnetoactive hydrogels. *Adv. Healthc. Mater.* 5, 2536–2544. doi: 10.1002/adhm.201600349

Abdel Fattah, A. R., Ghosh, S., and Puri, I. K. (2016). Printing three-dimensional heterogeneities in the elastic modulus of an elastomeric matrix. *ACS Appl. Mater. Interfaces* 8, 11018–11023. doi: 10.1021/acsami.6b03091

Abdel Fattah, A. R., Mishriki, S., Kammann, T., Sahu, R. P., Geng, F., and Puri, I. K. (2018). 3D cellular structures and co-cultures formed through the contactless magnetic manipulation of cells on adherent surfaces. *Biomater. Sci.* 6, 683–694. doi: 10.1039/c7bm01050h

Bearzi, C., Gargioli, C., Baci, D., Fortunato, O., Shapira-Schweitzer, K., Kossover, O., et al. (2014). PlGFMMP9-engineered iPS cells supported on a PEGfibrinogen hydrogel scaffold possess an enhanced capacity to repair damaged myocardium. *Cell Death Dis.* 5:e1053. doi: 10.1038/cddis.2014.12

Bedzhov, I., and Zernicka-Goetz, M. (2014). Self-organizing properties of mouse pluripotent cells initiate morphogenesis upon implantation. *Cell* 156, 1032–1044. doi: 10.1016/j.cell.2014.01.023

Bénazéraf, B., Francois, P., Baker, R. E., Denans, N., Little, C. D., and Pourquié, O. (2010). A random cell motility gradient downstream of FGF controls elongation of an amniote embryo. *Nature* 466, 248–252. doi: 10.1038/nature09151

Benham-Pyle, B. W., Pruitt, B. L., and Nelson, W. J. (2015). Mechanical strain induces E-cadherin-dependent Yap1 and β-catenin activation to drive cell cycle entry. *Science* 348, 1024–1027. doi: 10.1126/science.aaa4559

Bhattacharjee, T., Zehnder, S. M., Rowe, K. G., Jain, S., Nixon, R. M., Sawyer, W. G., et al. (2015). Writing in the granular gel medium. *Sci. Adv.* 1, 4–10. doi: 10.1126/sciadv.1500655

Bouissou, C., Potter, U., Altroff, H., Mardon, H., and Van Der Walle, C. (2004). Controlled release of the fibronectin central cell binding domain from polymeric microspheres. *J. Control. Release* 95, 557–566. doi: 10.1016/j.jconrel.2003.12.016

Bowser, D. A., and Moore, M. J. (2019). Biofabrication of neural microphysiological systems using magnetic spheroid bioprinting. *Biofabrication* 12:015002. doi: 10.1088/1758-5090/ab41b4

Breunig, M., Bauer, S., and Goepferich, A. (2008). Polymers and nanoparticles: Intelligent tools for intracellular targeting? *Eur. J. Pharm. Biopharm.* 68, 112–128. doi: 10.1016/j.ejpb.2007.06.010

Caiazzo, M., Okawa, Y., Ranga, A., Piersigilli, A., Tabata, Y., and Lutolf, M. P. (2016). Defined three-dimensional microenvironments boost induction of pluripotency. *Nat. Mater.* 15, 344–352. doi: 10.1038/nmat4536

Chan, C. J., Heisenberg, C. P., and Hiiragi, T. (2017). Coordination of morphogenesis and cell-fate specification in development. *Curr. Biol.* 27, R1024–R1035. doi: 10.1016/j.cub.2017.07.010

Cheng, Y., Muroski, M. E., Petit, D. C. M. C., Mansell, R., Vemulkar, T., Morshed, R. A., et al. (2016). Rotating magnetic field induced oscillation of magnetic particles for in vivo mechanical destruction of malignant glioma. *J. Control. Release* 223, 75–84. doi: 10.1016/j.jconrel.2015.12.028

Chithrani, B. D., and Chan, W. C. W. (2007). Elucidating the mechanism of cellular uptake and removal of protein-coated gold nanoparticles of different sizes and shapes. *Nano Lett.* 7, 1542–1550. doi: 10.1021/nl070363y

Chow, A., Stuckey, D. J., Kidher, E., Rocco, M., Jabbour, R. J., Mansfield, C. A., et al. (2017). Human induced pluripotent stem cell-derived cardiomyocyte encapsulating bioactive hydrogels improve rat heart function post myocardial infarction. *Stem Cell Reports* 9, 1415–1422. doi: 10.1016/j.stemcr.2017.09.003

Clark, C. C., Aleman, J., Mutkus, L., and Skardal, A. (2019). Bioprinting A mechanically robust thixotropic collagen and hyaluronic acid bioink supplemented with gelatin nanoparticles. *Bioprinting* 16:e00058. doi: 10.1016/j.bprint.2019.e00058

Compton, B. G., and Lewis, J. A. (2014). 3D-printing of lightweight cellular composites. *Adv. Mater.* 26, 5930–5935. doi: 10.1002/adma.201401804

Cooper, R. J., Menking-Colby, M. N., Humphrey, K. A., Victory, J. H., Kipps, D. W., and Spitzer, N. (2019). Involvement of β-catenin in cytoskeleton disruption following adult neural stem cell exposure to low-level silver nanoparticles. *Neurotoxicology* 71, 102–112. doi: 10.1016/j.neuro.2018.12.010

Cruz-Acuña, R., Quirós, M., Farkas, A. E., Dedhia, P. H., Huang, S., Siuda, D., et al. (2017). Synthetic hydrogels for human intestinal organoid generation and colonic wound repair. *Nat. Cell Biol.* 19, 1326–1335. doi: 10.1038/ncb3632

Davidson, L. A. (2017). Mechanical design in embryos: mechanical signalling, robustness and developmental defects. *Philos. Trans. R. Soc. B Biol. Sci.* 372:20150516. doi: 10.1098/rstb.2015.0516

Davis, G. S., Phillips, H. M., and Steinberg, M. S. (1997). Germ-layer surface tensions and 'tissue affinities' in Rana pipiens gastrulae: quantitative measurements. *Dev. Biol.* 192, 630–644. doi: 10.1006/dbio.1997.8741

Davoudi, Z., Peroutka-Bigus, N., Bellaire, B., Wannemuehler, M., Barrett, T. A., Narasimhan, B., et al. (2018). Intestinal organoids containing poly(lactic-co-glycolic acid) nanoparticles for the treatment of inflammatory bowel diseases. *J. Biomed. Mater. Res. Part A* 106, 876–886. doi: 10.1002/jbm.a.36305

Du, V., Luciani, N., Richard, S., Mary, G., Gay, C., Mazuel, F., et al. (2017). A 3D magnetic tissue stretcher for remote mechanical control of embryonic stem cell differentiation. *Nat. Commun.* 8:400. doi: 10.1038/s41467-017-00543-2

Dupont, S., Morsut, L., Aragona, M., Enzo, E., Giulitti, S., Cordenonsi, M., et al. (2011). Role of YAP/TAZ in mechanotransduction. *Nature* 474, 179–184. doi: 10.1038/nature10137

Engler, A. J., Sen, S., Sweeney, H. L., and Discher, D. E. (2006). Matrix elasticity directs stem cell lineage specification. *Cell* 126, 677–689. doi: 10.1016/j.cell.2006.06.044

Falleroni, F., Torre, V., and Cojoc, D. (2018). Cell mechanotransduction with piconewton forces applied by optical tweezers. *Front. Cell. Neurosci.* 12:130. doi: 10.3389/fncel.2018.00130

Feng, Q., Liu, Y., Huang, J., Chen, K., Huang, J., and Xiao, K. (2018). Uptake, distribution, clearance, and toxicity of iron oxide nanoparticles with different sizes and coatings. *Sci. Rep.* 8:2082. doi: 10.1038/s41598-018-19628-z

Ferreira, J. N., Hasan, R., Urkasemsin, G., Ng, K. K., Adine, C., Muthumariappan, S., et al. (2019). A magnetic three-dimensional levitated primary cell culture system for the development of secretory salivary gland-like organoids. *J. Tissue Eng. Regen. Med.* 13, 495–508. doi: 10.1002/term.2809

Filippi, M., Dasen, B., Guerrero, J., Garello, F., Isu, G., Born, G., et al. (2019). Biomaterials Magnetic nanocomposite hydrogels and static magnetic fi eld stimulate the osteoblastic and vasculogenic pro fi le of adipose-derived cells. *Biomaterials* 223:119468. doi: 10.1016/j.biomaterials.2019.119468

Foroozandeh, P., and Aziz, A. A. (2018). Insight into cellular uptake and intracellular trafficking of nanoparticles. *Nanoscale Res. Lett.* 13:339. doi: 10.1186/s11671-018-2728-6

Frede, A., Neuhaus, B., Klopfleisch, R., Walker, C., Buer, J., Müller, W., et al. (2016). Colonic gene silencing using siRNA-loaded calcium phosphate/PLGA nanoparticles ameliorates intestinal inflammation in vivo. *J. Control. Release* 222, 86–96. doi: 10.1016/j.jconrel.2015.12.021

Gao, D., Ding, W., Nieto-Vesperinas, M., Ding, X., Rahman, M., Zhang, T., et al. (2017). Optical manipulation from the microscale to the nanoscale: fundamentals, advances and prospects. *Light Sci. Appl.* 6:e17039. doi: 10.1038/lsa.2017.39

Gjorevski, N., and Lutolf, M. P. (2017). Synthesis and characterization of well-defined hydrogel matrices and their application to intestinal stem cell and organoid culture. *Nat. Protoc.* 12, 2263–2274. doi: 10.1038/nprot.2017.095

Gjorevski, N., Sachs, N., Manfrin, A., Giger, S., Bragina, M. E., Ordóñez-Morán, P., et al. (2016). Designer matrices for intestinal stem cell and organoid culture. *Nature* 539, 560–564. doi: 10.1038/nature20168

Gonçalves, A. I., Rotherham, M., Markides, H., Rodrigues, M. T., Reis, R. L., Gomes, M. E., et al. (2018). Triggering the activation of Activin A type II receptor in human adipose stem cells towards tenogenic commitment using mechanomagnetic stimulation. *Nanomed Nanotechnol. Biol. Med.* 14, 1149–1159. doi: 10.1016/j.nano.2018.02.008

Grashoff, C., Hoffman, B. D., Brenner, M. D., Zhou, R., Parsons, M., Yang, M. T., et al. (2010). Measuring mechanical tension across vinculin reveals regulation of focal adhesion dynamics. *Nature* 466, 263–266. doi: 10.1038/nature09198

Hennes, A., Held, K., Boretto, M., De Clercq, K., Van den Eynde, C., Vanhie, A., et al. (2019). Functional expression of the mechanosensitive PIEZO1 channel in primary endometrial epithelial cells and endometrial organoids. *Sci. Rep.* 9, 1–14. doi: 10.1038/s41598-018-38376-8

Henstock, J. R., Henstock, M., Rashidi, H., Shakesheff, K. M., and Haj, A. J. (2014). Remotely activated mechanotransduction via magnetic nanoparticles promotes mineralization synergistically with bone morphogenetic protein 2: applications for injectable cell therapy. *Stem Cell Transl. Med.* 3, 1363–1374. doi: 10.5966/sctm.2014-0017

Hoffman, L. M., Jensen, C. C., Chaturvedi, A., Yoshigi, M., and Beckerle, M. C. (2012). Stretch-induced actin remodeling requires targeting of zyxin to stress fibers and recruitment of actin regulators. *Mol. Biol. Cell* 23, 1846–1859. doi: 10.1091/mbc.E11-12-1057

Hoskins, C., Cuschieri, A., and Wang, L. (2012). The cytotoxicity of polycationic iron oxide nanoparticles: common endpoint assays and alternative approaches for improved understanding of cellular response mechanism. *J. Nanobiotechnology* 10:15. doi: 10.1186/1477-3155-10-15

Hsiao, I. L., Fritsch-Decker, S., Leidner, A., Al-Rawi, M., Hug, V., Diabaté, S., et al. (2019). Biocompatibility of amine-functionalized silica nanoparticles: the role of surface coverage. *Small* 15, 1–11. doi: 10.1002/smll.201805400

Hughes, S., Mcbain, S., Dobson, J., and Haj, A. J. (2007). Selective activation of mechanosensitive ion channels using magnetic particles. *J. R. Soc. Interf.* 5, 855–863. doi: 10.1098/rsif.2007.1274

Ito, A., Ino, K., Hayashida, M., Kobayashi, T., Matsunuma, H., Kagami, H., et al. (2005). Novel methodology for fabrication of tissue-engineered tubular constructs using magnetite nanoparticles and magnetic force. *Tissue Eng.* 11, 1553–1561. doi: 10.1089/ten.2005.11.1553

Jestin, J., Cousin, F., Dubais, I., Ménager, C., Schweins, R., Oberdisse, J., et al. (2008). Anisotropic reinforcement of nanocomposites tuned by magnetic orientation of the filler network. *Adv. Mater.* 20, 2533–2540. doi: 10.1002/adma.200702758

Ji, M., Ma, N., and Tian, Y. (2019). 3D Lattice Engineering of Nanoparticles by DNA Shells. *Small* 15, 1–12. doi: 10.1002/smll.201805401

Jorge-Peñas, A., Bové, H., Sanen, K., Vaeyens, M. M., Steuwe, C., Roeffaers, M., et al. (2017). 3D full-field quantification of cell-induced large deformations in fibrillar biomaterials by combining non-rigid image registration with label-free second harmonic generation. *Biomaterials* 136, 86–97. doi: 10.1016/j.biomaterials.2017.05.015

Kim, H., Che, L., Ha, Y., and Ryu, W. (2014). Mechanically-reinforced electrospun composite silk fibroin nanofibers containing hydroxyapatite nanoparticles. *Mater. Sci. Eng. C* 40, 324–335. doi: 10.1016/j.msec.2014.04.012

Kloxin, A. M., Kasko, A. M., Salinas, C. N., and Anseth, K. S. (2009). Photodegradable hydrogels for dynamic tuning of physical and chemical properties. *Science* 324, 59–63. doi: 10.1126/science.1169494

Kokkinis, D., Schaffner, M., and Studart, A. R. (2015). Multimaterial magnetically assisted 3D printing of composite materials. *Nat. Commun.* 6:8643. doi: 10.1038/ncomms9643

Lancaster, M. A., and Huch, M. (2019). Disease modelling in human organoids. *Dis. Model. Mech.* 12:dmm039347. doi: 10.1242/dmm.039347

Lee, W., Kalashnikov, N., Mok, S., Halaoui, R., Kuzmin, E., Putnam, A. J., et al. (2019). Dispersible hydrogel force sensors reveal patterns of solid mechanical stress in multicellular spheroid cultures. *Nat. Commun.* 10, 1–14. doi: 10.1038/s41467-018-07967-4

Leite, P. E. C., Pereira, M. R., Harris, G., Pamies, D., Dos Santos, L. M. G., Granjeiro, J. M., et al. (2019). Suitability of 3D human brain spheroid models to distinguish toxic effects of gold and poly-lactic acid nanoparticles to assess biocompatibility for brain drug delivery. *Part. Fibre Toxicol.* 16, 1–20. doi: 10.1186/s12989-019-0307-3

Li, N., Fan, X., Tang, K., Zheng, X., Liu, J., and Wang, B. (2016). Nanocomposite scaffold with enhanced stability by hydrogen bonds between collagen, polyvinyl pyrrolidone and titanium dioxide. *Coll. Surf. B Biointerf.* 140, 287–296. doi: 10.1016/j.colsurfb.2015.12.005

Li, Q., Lin, H., Wang, O., Qiu, X., Kidambi, S., Deleyrolle, L. P., et al. (2016). Scalable production of glioblastoma tumor-initiating cells in 3 dimension thermoreversible hydrogels. *Sci. Rep.* 6, 1–10. doi: 10.1038/srep31915

Li, Y., Chung, E., Rodrigues, R., Firpo, M., and Healy, K. (2006). Hydrogels as artificial matrices for human embryonic stem cell self-renewal. *J. Biomed. Mater. Res. A* 79, 1–5. doi: 10.1002/jbm.a

Li, Z., Fan, Z., Xu, Y., Lo, W., Wang, X., Niu, H., et al. (2016). PH-sensitive and thermosensitive hydrogels as stem-cell carriers for cardiac therapy. *ACS Appl. Mater. Interf.* 8, 10752–10760. doi: 10.1021/acsami.6b01374

Lian, I., Kim, J., Okazawa, H., Zhao, J., Zhao, B., Yu, J., et al. (2010). The role of YAP transcription coactivator in regulating stem cell self-renewal and differentiation. *Genes Dev.* 24, 1106–1118. doi: 10.1101/gad.1903310

Lin, Y. C., Guo, Y. R., Miyagi, A., Levring, J., MacKinnon, R., and Scheuring, S. (2019). Force-induced conformational changes in PIEZO1. *Nature* 573, 230–234. doi: 10.1038/s41586-019-1499-2

Liu, Z., Liu, Y., Chang, Y., Seyf, H. R., Henry, A., Mattheyses, A. L., et al. (2016). Nanoscale optomechanical actuators for controlling mechanotransduction in living cells. *Nat. Method* 13, 143–146. doi: 10.1038/nmeth.3689

Markides, H., Mclaren, J. S., Telling, N. D., Alom, N., Al-mutheffer, E. A., Oreffo, R. O. C., et al. (2018). Translation of remote control regenerative technologies for bone repair. *NPJ Regen. Med.* 3:9. doi: 10.1038/s41536-018-0048-1

Mcbeath, R., Pirone, D. M., Nelson, C. M., Bhadriraju, K., and Chen, C. S. (2004). Cell shape, cytoskeletal tension, and rhoa regulate stem cell lineage commitment several studies have noted that changes in cell shape themselves can alter the differentiation of precommitted mesenchymal lineages. Spiegelman and Ginty (1983). *Dev. Cell* 6, 483–495. doi: 10.1016/s1534-5807(04)00075-9

Michalet, X., Pinaud, F. F., and Bentolila, L. (2005). Quantum_dots_for_live_cells__i.PDF. *Science* 307, 538–544. doi: 10.1126/science.1104274

Morgan, E., Wupperfeld, D., Morales, D., and Reich, N. (2019). Shape matters: gold nanoparticle shape impacts the biological activity of siRNA delivery. *Bioconjug. Chem.* 30, 853–860. doi: 10.1021/acs.bioconjchem.9b00004

Müller, P., Langenbach, A., Kaminski, A., and Rychly, J. (2013). Modulating the actin cytoskeleton affects mechanically induced signal transduction and differentiation in mesenchymal stem cells. *PLoS One* 8:e0071283. doi: 10.1371/journal.pone.0071283

Nerurkar, N. L., Mahadevan, L., and Tabin, C. J. (2017). BMP signaling controls buckling forces to modulate looping morphogenesis of the gut. *Proc. Natl. Acad. Sci. U.S.A.* 114, 2277–2282. doi: 10.1073/pnas.1700307114

Panariti, A., Miserocchi, G., and Rivolta, I. (2012). The effect of nanoparticle uptake on cellular behavior: disrupting or enabling functions? *Nanotechnol. Sci. Appl.* 5, 87–100. doi: 10.2147/NSA.S25515

Pankhurst, Q. A., Connolly, J., Jones, S. K., and Dobson, J. (2003). Applications of magnetic nanoparticles in biomedicine. *J. Phys. D. Appl. Phys.* 36:R167.

Pathak, M. M., Nourse, J. L., Tran, T., Hwe, J., Arulmoli, J., Le, D. T. T., et al. (2014). Stretch-activated ion channel Piezo1 directs lineage choice in human neural stem cells. *Proc. Natl. Acad. Sci. U.S.A.* 111, 16148–16153. doi: 10.1073/pnas.1409802111

Ranga, A., Girgin, M., Eberle, D., Caiazzo, M., Tanaka, E. M., Ranga, A., et al. (2017). Correction for Ranga et al., Neural tube morphogenesis in synthetic 3D microenvironments. *Proc. Natl. Acad. Sci. U.S.A.* 114, E3163–E3163.

Ranga, A., Gobaa, S., Okawa, Y., Mosiewicz, K., Negro, A., and Lutolf, M. (2014). 3D niche microarrays for systems-level analyses of cell fate. *Nat. Commun.* 5, 1–10. doi: 10.1038/ncomms5324

Rotherham, M., Henstock, J. R., Qutachi, O., and Haj, A. J. (2018). Remote regulation of magnetic particle targeted Wnt signaling for bone tissue engineering. *Nanomed. Nanotechnol. Biol. Med.* 14, 173–184. doi: 10.1016/j.nano.2017.09.008

Saliev, T., Baiskhanova, D. M., Akhmetova, A., Begimbetova, D. A., Akishev, M., Kulsharova, G., et al. (2019). Impact of electromagnetic fields on in vitro toxicity of silver and graphene nanoparticles. *Electromagn. Biol. Med.* 38, 21–31. doi: 10.1080/15368378.2018.1534740

Sanhaji, M., Göring, J., Couleaud, P., Aires, A., Cortajarena, A. L., Courty, J., et al. (2019). The phenotype of target pancreatic cancer cells influences cell death by magnetic hyperthermia with nanoparticles carrying gemicitabine and the pseudo-peptide NucAnt. *Nanomed. Nanotechnol. Biol. Med.* 20:101983. doi: 10.1016/j.nano.2018.12.019

Sapir-lekhovitser, Y., Rotenberg, M. Y., Jopp, J., and Friedman, G. (2016). Magnetically actuated tissue engineered scaffold: insights into mechanism of physical stimulation. *Nanoscal* 8, 3386–3399. doi: 10.1039/c5nr05500h

Schweiger, C., Hartmann, R., Zhang, F., Parak, W. J., Kissel, T. H., and Rivera-Gil, P. (2012). Quantification of the internalization patterns of superparamagnetic iron oxide nanoparticles with opposite charge. *J. Nanobiotechnol.* 10, 1–11. doi: 10.1186/1477-3155-10-28

Scialabba, C., Sciortino, A., Messina, F., Buscarino, G., Cannas, M., Roscigno, G., et al. (2019). Highly homogeneous biotinylated carbon nanodots: red-emitting nanoheaters as theranostic agents toward precision cancer medicine. *ACS Appl. Mater. Interf.* 11, 19854–19866. doi: 10.1021/acsami.9b04925

Shen, Y., Wu, C., Uyeda, T. Q. P., Plaza, G. R., Liu, B., Han, Y., et al. (2017). Elongated nanoparticle aggregates in cancer cells for mechanical destruction with low frequency rotating magnetic field. *Theranostics* 7, 1735–1748. doi: 10.7150/thno.18352

Sokolova, V., Rojas-Sánchez, L., Białas, N., Schulze, N., and Epple, M. (2019). Calcium phosphate nanoparticle-mediated transfection in 2D and 3D mono- and co-culture cell models. *Acta Biomater.* 84, 391–401. doi: 10.1016/j.actbio.2018.11.051

Son, B., Kim, H. D., Kim, M., Kim, J. A., Lee, J., Shin, H., et al. (2015). Physical Stimuli-induced chondrogenic differentiation of mesenchymal stem cells using magnetic nanoparticles. *Adv. Healthc. Mater.* 4, 1339–1347. doi: 10.1002/adhm.201400835

Souza, G. R., Molina, J. R., Raphael, R. M., Ozawa, M. G., Stark, D. J., Levin, C. S., et al. (2010). Three-dimensional tissue culture based on magnetic cell levitation. *Nat. Nanotechnol.* 5, 291–296. doi: 10.1038/nnano.2010.23

Steinberg, M. S. (1963). Reconstruction of tissues by dissociated cells. Some morphogenetic tissue movements and the sorting out of embryonic cells may have a common explanation. *Science* 141, 401–408. doi: 10.1126/science.141.3579.401

Stewart, R. M., Zubek, A. E., Rosowski, K. A., Schreiner, S. M., Horsley, V., and King, M. C. (2015). Nuclear-cytoskeletal linkages facilitate cross talk between the nucleus and intercellular adhesions. *J. Cell Biol.* 209, 403–418. doi: 10.1083/jcb.201502024

Tseng, P., Judy, J. W., and Di Carlo, D. (2012). Magnetic nanoparticle-mediated massively parallel mechanical modulation of single-cell behavior. *Nat. Methods* 9, 1113–1119. doi: 10.1038/nmeth.2210

Veldhuis, J. H., Ehsandar, A., Maître, J. L., Hiiragi, T., Cox, S., and Brodland, G. W. (2017). Inferring cellular forces from image stacks. *Philos. Trans. R. Soc. B Biol. Sci.* 372:20160261. doi: 10.1098/rstb.2016.0261

Wong, E. W., Sheehan, P. E., and Lieber, C. M. (1997). Nanobeam mechanics: elasticity, strength, and toughness of nanorods and nanotubes. *Science* 277, 1971–1975. doi: 10.1126/science.277.5334.1971

Xu, W., Baribault, H., and Adamson, E. D. (1998). Vinculin knockout results in heart and brain defects during embryonic development. *Development* 125, 327–337.

Xue, X., Sun, Y., Resto-Irizarry, A. M., Yuan, Y., Aw Yong, K. M., Zheng, Y., et al. (2018). Mechanics-guided embryonic patterning of neuroectoderm tissue from human pluripotent stem cells. *Nat. Mater.* 17, 633–641. doi: 10.1038/s41563-018-0082-9

Yamamoto, Y., Ito, A., Kato, M., Kawabe, Y., Shimizu, K., Fujita, H., et al. (2009). Preparation of artificial skeletal muscle tissues by a magnetic force-based tissue engineering technique. *J. Biosci. Bioeng.* 108, 538–543. doi: 10.1016/j.jbiosc.2009.05.019

Yang, C., Tibbitt, M. W., Basta, L., and Anseth, K. S. (2014). Mechanical memory and dosing influence stem cell fate. *Nat. Mater.* 13, 645–652. doi: 10.1038/nmat3889

Yue, Z. G., Wei, W., Lv, P. P., Yue, H., Wang, L. Y., Su, Z. G., et al. (2011). Surface charge affects cellular uptake and intracellular trafficking of chitosan-based nanoparticles. *Biomacromolecules* 12, 2440–2446. doi: 10.1021/bm101482r

Zhu, W., Liu, X., Tan, L., Cui, Z., Yang, X., Liang, Y., et al. (2019). AgBr nanoparticles in situ growth on 2D MoS2 nanosheets for rapid bacteria-killing and photodisinfection. *ACS Appl. Mater. Interf.* 11, 34364–34375. doi: 10.1021/acsami.9b12629

Conflict of Interest: The authors declare that the research was conducted in the absence of any commercial or financial relationships that could be construed as a potential conflict of interest.

frontiers in Bioengineering and Biotechnology

ORIGINAL RESEARCH
published: 30 April 2020
doi: 10.3389/fbioe.2020.00315

Development of Multifunctional Biopolymeric Auto-Fluorescent Micro- and Nanogels as a Platform for Biomedical Applications

*Arti Vashist[1], Venkata Atluri[1], Andrea Raymond[1], Ajeet Kaushik[1,2], Tiyash Parira[1], Zaohua Huang[1,3], Andriy Durygin[4], Asahi Tomitaka[1], Roozbeh Nikkhah-Moshaie[1], Atul Vashist[5], Marisela Agudelo[1], Hitendra S. Chand[1], Ilyas Saytashev[6,7], Jessica C. Ramella-Roman[6,7] and Madhavan Nair[1]**

[1] Department of Immunology and Nanomedicine, Center for Personalized Nanomedicine, Herbert Wertheim College of Medicine, Institute of NeuroImmune Pharmacology, Florida International University, Miami, FL, United States, [2] Division of Sciences, Art, and Sciences, Department of Natural Sciences, Florida Polytechnic University, Lakeland, FL, United States, [3] Department of Otolaryngology, University of Miami School of Medicine, Miami, FL, United States, [4] CeSMEC, Florida International University, Miami, FL, United States, [5] Department of Biotechnology, All India Institute of Medical Science, New Delhi, India, [6] Department of Biomedical Engineering, Florida International University, Miami, FL, United States, [7] Department of Cellular Biology, Pharmacology and Ophthalmology, Herbert Wertheim College of Medicine, Miami, FL, United States

OPEN ACCESS

Edited by:
Filippo Rossi,
Politecnico of Milan, Italy

Reviewed by:
Sujit Narayanan Kootala,
Uppsala University, Sweden
Amit Jaiswal,
Indian Institute of Technology Mandi, India

***Correspondence:**
Madhavan Nair
nairm@fiu.edu

Specialty section:
This article was submitted to Nanobiotechnology, a section of the journal Frontiers in Bioengineering and Biotechnology

Received: *23 November 2019*
Accepted: *23 March 2020*
Published: *30 April 2020*

Citation:
Vashist A, Atluri V, Raymond A, Kaushik A, Parira T, Huang Z, Durygin A, Tomitaka A, Nikkhah-Moshaie R, Vashist A, Agudelo M, Chand HS, Saytashev I, Ramella-Roman JC and Nair M (2020) Development of Multifunctional Biopolymeric Auto-Fluorescent Micro- and Nanogels as a Platform for Biomedical Applications. Front. Bioeng. Biotechnol. 8:315. doi: 10.3389/fbioe.2020.00315

The emerging field of theranostics for advanced healthcare has raised the demand for effective and safe delivery systems consisting of therapeutics and diagnostics agents in a single monarchy. This requires the development of multi-functional bio-polymeric systems for efficient image-guided therapeutics. This study reports the development of size-controlled (micro-to-nano) auto-fluorescent biopolymeric hydrogel particles of chitosan and hydroxyethyl cellulose (HEC) synthesized using water-in-oil emulsion polymerization technique. Sustainable resource linseed oil-based polyol is introduced as an element of hydrophobicity with an aim to facilitate their ability to traverse the blood-brain barrier (BBB). These nanogels are demonstrated to have salient features such as biocompatibility, stability, high cellular uptake by a variety of host cells, and ability to transmigrate across an *in vitro* BBB model. Interestingly, these unique nanogel particles exhibited auto-fluorescence at a wide range of wavelengths 450–780 nm on excitation at 405 nm whereas excitation at 710 nm gives emission at 810 nm. In conclusion, this study proposes the developed bio-polymeric fluorescent micro- and nano- gels as a potential theranostic tool for central nervous system (CNS) drug delivery and image-guided therapy.

Keywords: nanogels, microgels, theranostics, nanomedicine, biopolymers

INTRODUCTION

Numerous systems have been developed as theranostics agents, which included multi-functional inorganic nanoparticles (Degli Esposti et al., 2018), quantum dots (Ho and Leong, 2010), and many radiolabeled biomarkers (Kang et al., 2018), however, the clinical applications of these agents have provoked practical challenges. Recently, theranostics have been tuned as a personalized

health-care due to advancements in drug delivery systems (DDS) for enhanced efficacy and least side-effects. The current strategy of developing bio-polymeric theranostic agents has pronounced conviction of incorporating inherent features of no toxicity, biodegradability, biocompatibility and high sensitivity.

In this regard, fluorescent hydrogels have attracted great attention of us and others due to their smart biomaterials like features and have been intensively explored as most convenient tracers and therapeutics for decades. Many studies showed the development of fluorescence-based hydrogels for sensing and tracking the bio-actives and therapeutics *in vitro and in vivo* (Pires et al., 2018). However for these diverse applications, hydrogels need to be developed by tagging the fluorophores by chemical or physical immobilization inside the hydrogel matrix. The entrapment of fluorophores in the hydrogel matrix is tedious and limiting process as the tagging or entrapping fluorescent dyes or compounds and their photobleaching may affect their characteristic features like biocompatibility and biodegradability (Zhang and Yang, 2013). Such DDS has exhibited performance in a personalized manner due to tunable salient features including size, morphology, targeted delivery, and release profile (Allen and Cullis, 2004).

Efforts have been made to develop macro to micro- and nano-size hydrogel particles, exhibiting lower toxicity. Literature reveals both micro and nano range is preferred for various cancer therapies and other biomedical applications (Sahiner et al., 2006; Zhang et al., 2015; Vashist et al., 2018a). Thus, in the present study, the focus was more on the development of bio-polymeric hydrogel particles in both microscale and nanoscale, which have the following features: (i) easy synthesis with high yield; (ii) highly biocompatible to the intracellular environment; (iii) the by-products of the hydrogels are biodegradable and non-toxic to the cellular environment; (iv) have functionality which makes them capable of binding with various bio-actives including drugs, DNA, RNA, proteins, etc.; (v) the biomaterials can be detected *in vitro and in vivo*; and (vi) the cellular uptake and the monitoring or tracking of the carrier for release and degradability should be feasible (Shi et al., 2014). The combination of the above features makes nanogels an excellent drug carrier with extraordinary performance in drug delivery and diagnostics (Hamidi et al., 2008; Jiang et al., 2014; Vashist et al., 2017).

Efforts have been made to develop nanogel based systems as carriers for those drugs that cannot pass through the BBB. Therefore, efficient nanogel carriers have been developed to deliver hydrophobic drugs, oligonucleotides, and other bio-actives across the BBB (Vinogradov et al., 2004; Roney et al., 2005; Juillerat-Jeanneret, 2008). Various cells like pericytes, astrocytes, and endothelial cells constitute BBB. The structure and the functionality of the BBB are related to the tightly-packed endothelial cells. Existing therapies for CNS are defeated by the challenges imposed by the BBB that hinders the entry of several drugs and bioactive across it. Strategies to develop nanoparticles with the potential to traverse the BBB by changing their surface functionality or by the widespread mechanism "Trojan horse," which relates to the engulfment of nanoparticles by the endogenous transport systems (Wohlfart et al., 2012; Wong et al., 2012). The systems which involve inorganic particles and synthetic polymers, are associated with certain drawbacks such as biodegradability, toxicity and other side effects (Hamid Akash et al., 2015). Thus, there is an immense need to develop biodegradable and biocompatible cost-effective DDS. The goal of the present study was to achieve a very simple and stable bio-polymeric hydrogel system, which can be sorted to various sizes for diverse biomedical applications. The developed natural polymer based hydrogel particles are expected to hold potential to deliver various bioactives such as drugs and proteins across the BBB.

It was anticipated that the developed particles when hydrophobically modified using linseed oil-based polyol will develop a surface functionality, which will facilitate them to cross BBB and their entry to the brain through the tight junctions. The synthesis was inspired by the fact that the synergism achieved by the combination of the two biopolymers chitosan and HEC with polyol will result in excellent drug delivery platform whose characteristics can be modulated by imbibing various bioactive or drugs for targeted and sustained delivery. We were able to develop a multi-functional material exhibiting an excellent wide excitation/emission spectrum. For the first time, we demonstrate the development of bio-polymeric auto-fluorescent hydrogels in both micro and nanoscale using natural polymers chitosan, HEC and sustainable linseed oil-based polyol exhibiting complete biocompatibility (in the concentration range 10–100 μg/ml) tested over a wide range of host cells like Astrocytes, PBMCs, and Microglia. Moreover, a dynamic wide range of emission wavelength (450–750 nm), and (710–810 nm) adds to their utility for *in vivo* imaging. The high stability in aqueous solution and physiological pH (water, pH 7.4) contributed to a good shelf-life in solution and dry form at room temperature for 12 months while retaining their auto-fluorescence property. Wide range of size from microscale to nanoscale resulted in cellular uptake and co-localization during *ex vivo* studies with PBMC, Microglia, and Astrocytes. Remarkably, the developed hydrogel particles showed the capability to transmigrate BBB, which highlights their huge potential to be used for the drug delivery to the CNS. These micro- and nanogels have unique and superior properties as compared to the existing theranostic systems (Kunjachan et al., 2012) and thus hold potential for multiple applications including drug delivery, diagnostics, and *in vivo* imaging.

EXPERIMENTAL SECTION

Materials

Chitosan (448877-50G, Sigma-Aldrich), Hydroxyethyl cellulose (22–300 mPa.s, 2% in water at 20°C, TCI, 9004-62-0), Heavy liquid paraffin oil: Density: 0.8660–0.890 Kg/m^3, Tween 80, Ethanol) n-Hexane (Sigma-Aldrich), Glycine (Mwt. 75.0 7g/mol: Density 1.607 g/cm^3, linseed oil, glacial acetic acids, hydrogen peroxide, diethyl ether, acetic anhydride (Sigma-Aldrich) were used as received. Linseed oil polyol was prepared using standard protocols (Sharmin et al., 2007). Cellulase, Trichoderma viride, Millipore Sigma Deionized water from Millipore mille U10 water

purification system was used in the preparation of hydrogels and other *in vitro* experiments.

Methods

Synthesis of Micro/Nano Hydrophobically Modified Chitosan-Hydroxyethyl Cellulose

The micro/nano hydrogel particles of chitosan and hydroxyethyl cellulose (HEC) were prepared by water in oil emulsion polymerization method (Kajjari et al., 2011). Linseed oil-based polyol was used as a hydrophobic modifier (Vashist et al., 2012, 2013). Forty milliliter of 2% (w/v) polymer solution was prepared by using a known amount of chitosan and HEC in 1% (v/v) acetic acid. The different formulation was prepared using medium molecular weight and low molecular weight chitosan. A separate beaker was used to make a mixture of liquid paraffin oil and 1% (w/w) Tween 80. The polymer solution was added dropwise to the mixture of oil and surfactant with a stirring rate of 1400 rpm on a magnetic stirrer. The mixing of the solution was continued for a further 20 min and followed by the addition of glutaraldehyde (5 ml) for another 10 min. The linseed oil polyol was added to the reaction mixture and stirring was continued at 1400 rpm for 6 h. The synthesized hydrogel particles were washed with n-hexane to remove the excess of oil. The excess amount of GA was deactivated by 0.1 M glycine solution (Kajjari et al., 2011). The hydrogel particles were dried for 24 h at room temperature. The throughly washed particles were kept for drying at room temperature, stored in a vaccum dessicator and used for further characterizations.

Characterization of Micro/Nanogels Using FT-IR, Raman, DLS, Zeta Potential, and TEM Analysis

The hydrogel samples were dried under vacuum for overnight till attained the constant weights. The dried samples were then analyzed using model 1750 FT-IR spectrophotometer (PerkinElmer Cetus Instruments, Norwalk, CT, United States). TEM analysis was performed using a Phillips CM-200 200 kV transmission electron microscope with an operating voltage of 80 kV. Particle size distribution of microgels and nanogels particles in PBS was measured by dynamic light scattering (DLS) method using a zetrasizer nano ZS (Malvern Instruments, United Kingdom) The surface charge of the particles was also determined using Zetasizer nanoZS. The hydrogel particle suspension diluted with PBS (0.1 mg/ml) was further used for both particle size and zeta potential measurements.

Cellular Uptake of Nanogels by Human Peripheral Blood Mononuclear Cells (PBMC), Microglial Cell Lines (CHME5), Primary Human Astrocytes, and Primary Human Microglia

PBMCs.

PBMCs were purified from human leukopacks (buffy coat), which were obtained commercially from the community blood bank (One Blood, Miami, FL, United States). PBMCs were isolated as previously described by us (Atluri et al., 2016). The first step involved the dilution of the buffy coat with phosphate buffer saline (PBS) (Invitrogen, Gaithersburg, MD, United States) at room temperature. The diluted buffy coat was overlaid on the top of the Ficoll-Histopaque such as two separate layers of the liquid is formed. These samples were centrifuged at 1,200 g for about 20 min with acceleration = 1, deceleration = 0 at room temperature. A further collection of the PBMC layer formed at the interface was done and the cells were washed with PBS. The pellet was re-suspended in Ammonium-Chloride-Potassium (ACK) lysing buffer to achieve complete lysis of the red blood cells in the samples and kept in ice for 15 min. The washing of the cells with PBS was again done and the total cell number and cell viability were evaluated by trypan blue exclusion (Sigma-Aldrich, St. Louis, MO, United States) in a hemocytometer counting chamber. Finally, the cells were re-suspended in complete culture medium containing Roswell Park Memorial Institute (RPMI) 1640 (Life Technologies, Gaithersburg, MD, United States), 25 mM 4-(2-hydroxyethyl)-1-piperazineethanesulfonic acid (HEPES) (Sigma-Aldrich, St. Louis, MO, United States), 2 mM glutamine (Sigma-Aldrich, St. Louis, MO, United States), 100 μg streptomycin (Sigma-Aldrich, St. Louis, MO, United States), 100 U penicillin (Sigma-Aldrich, St. Louis, MO, United States), and 10% fetal bovine serum (Life Technologies, Gaithersburg, MD, United States) (Figueroa et al., 2016).

CHME5.

For the biocompatibility and uptake study, the microglial cells (CHME-5) were cultured using Dulbecco's Modified Eagle Medium (DMEM) supplemented by a fetal bovine serum (FBS) and antibiotic/antimycotic solution to a final concentration of 500 ml of DMEM + 50 ml of 10% FBS + 5.5 ml of 10X antibiotic/antimycotic solution (Sigma-Aldrich, St. Louis, MO, United States) (Samikkannu et al., 2016).

Primary human astrocytes.

Primary human astrocytes were purchased from ScienCell Research Laboratories (Carlsbad, CA; Cat. # 1800-5). These cells were grown on the astrocyte medium purchased from ScienCell laboratories (Cat. # 1801) containing 2% of fetal bovine serum (ScienCell Cat. # 0010), astrocyte growth supplement (ScienCell Cat. # 1852) and penicillin/streptomycin (ScienCell Cat. # 0503), antibiotic /antimycotic solution (Sigma-Aldrich, St. Louis, MO, United States) (Atluri et al., 2013).

Biocompatibility Analysis Using Primary Human Astrocytes, Microglia (CHME5), and PBMCs

Biocompatibility was assessed using XTT cell viability assay, using sodium 3,3′-(-[(phenylamino)carbonyl]-3,4-tetrazolium)-bis(4-methoxyl-6-nitro)benzene sulfonic acid hydrate) assay. Primary human astrocytes (1×10^4 cells per well) were seeded in a 24-well plate and after 24 h of incubation at 37°C, the medium was replaced with 1 ml of fresh medium containing nanogel 5–100 μg/ml. Cells were treated with various concentrations and incubated for different time points (1, 2, 4, and/or 7 days). XTT 1 mg/ml and 2.5 μl of phenazine methosulfate (PMS) solution was freshly prepared and added (25 μl) to each well. The XTT containing wells were incubated for 4 h at 37°C. A multi-mode microplate reader (Synergy HT), was used to measure absorbance at 450 nm wavelength. All experiments were performed in triplicates ($N = 3$). Results are graphed as

mean ± standard deviation. The statistical analysis was done using Two-way analysis of variance (ANOVA) and also by Tukey's multiple comparison test. Differences were considered significant if $p \leq 0.05$. For experiments with CHME5 and PBMCs, 2×10^5 cells were seeded per well (2×10^5 per well) in 24-well plates. Further, the same protocol described above was followed for each cell type. To maintain the PBMCs for 7 days, fresh media containing IL-2 was added at required intervals.

Determination of Lactate Dehydrogenase (LDH) Cytotoxicity of Nanogel in Microglia (CHME5) and PBMCs

CHME5 cells and PBMCs (10,000 cells per well) were plated in a 96-well plate and incubated at 37°C, 5% CO_2. Various concentrations (10–100 μg/ml) of nanogel formulations were added to the culture media and incubated for 24 h. The Thermo Scientific Pierce LDH cytotoxicity assay kit was used to quantitatively measure lactate dehydrogenase (LDH) released into the media from damaged cells, which act as a biomarker for the cellular cytotoxicity and cytolysis (Decker and Lohmann-Matthes, 1988; Minaeva et al., 2017; Kumar et al., 2018). LDH background activity was determined by including, complete medium control. Additional cells were plated in triplicate for spontaneous LDH activity controls (negative control with water) and maximum LDH activity controls (positive control with 10X lysis buffer). Plates were incubated overnight in a CO2 at 37°C. The cells were treated for 24 h with (10–100 μg/ml) nanogel formulations. Further the Lysis Buffer (10 μl, 10X) was added to the wells serving as maximum LDH activity controls and mixed gently by tapping. Further, the plate was incubated in an incubator at 37°C, 5% CO_2 for 45 min. Fifty microliter of medium from each sample medium (e.g., complete medium, serum-free medium, spontaneous LDH activity controls, compound-treated, and maximum LDH activity controls) was transferred to a 96-well flat-bottom plate in triplicate wells using a multichannel pipette. Further 50 μl of reaction mixture was added to each well and mixed using multichannel pipette. The plate was incubated at room temperature for 30 min in dark. After 30 min of incubation, stop solution (50 μl) was added to each sample well and mixed gently by tapping. Absorbance was measured at 490 and 680 nm. Determination of LDH activity was done by subtracting the 680 nm absorbance value of (background) from the 490 nm absorbance before calculating the percentage of cytotoxicity (Brown et al., 2015) with the following formula:

$$\% \text{ Cytotoxicity} = \frac{\text{Compound treated LDH activity} - \text{Spontaneous LDH activity}}{\text{Maximum LDH activity} - \text{Spontaneous LDH activity}} \times 100$$

Cellular Uptake of Nanogels by Imaging Flow Cytometry

Prior to analyzing cellular uptake, we analyzed the fluorescent properties of nanogels without cells to determine the optimum concentration and maximum fluorescent intensity. Since these nanogels have multi-fluorescent properties and in this FlowSight instrument they are detected through multiple channels, a screening of different concentrations of particles (1–100 μg/ml) was done prior to selecting the optimum concentration and channel use for further analysis. 50 μg/ml of nanogels had the maximum fluorescent intensity detected through channel 8 (ex/em: 405 nm/505–560 nm). Therefore, channel 8 was selected for subsequent analysis.

To determine time-dependent uptake of nanogels, PBMCs and CHME5 (1×10^6) were incubated for up to 24 h with different concentrations (1–100 μg/ml) of nanogels. Cells were harvested at different time points (2, 6, and 24 h) and washed prior to acquisition. Fluorescence intensity and percentage of cells expressing nanogels were analyzed using imaging flow cytometry with Amnis FlowSight instrument (Luminex Corporation). A total of 10,000 events were collected for all individual samples. Analysis was done using Ideas Software.

For all experiments, cells were analyzed and selected based on higher gradient RMS values or cells with better focus and single cells. Gating of focus cells is depicted in histogram (**Supplementary Figure S5**). After focus cells were selected, a scatter plot of brightfield area versus aspect ratio for the focus population was further analyzed to select single cells (**Supplementary Figure S5**), which are characterized by an intermediate area value and a high aspect ratio. The subpopulation of single cells was used to gate based on fluorescent intensity. Region on histogram was drawn based on comparisons between cells without nanogels (control sample) and cells with different concentrations of nanogels. Time-dependent cellular uptake of nanogels for 2 and 6 h is demonstrated in bar graphs included in **Supplementary Figure S5**. Representative histograms showing subpopulation of cells with high fluorecent intensity (MFI) and expressing nanogels (% gated) are depicted in **Supplementary Figure S5**.

Two-Photon Imaging

1×10^6 cells were plated on a 2-chamber slide until cells reached about 80% confluency. The cells were treated with 50 μg/ml of nanogel concentration and incubated for different time points 6 and 24 h at 37°C, 5% CO_2. The control and nanogel treated cells were washed thoroughly using PBS (pH 7.4) and further fixed using 4% paraformaldehyde solution for 20 min. Further the cells were washed 3 times with 1X buffer with gentle agitation for 5 min and stored at −80°C prior to imaging. Two-photon excitation fluorescence imaging with linear confocal channel was used to visualize the uptake of nanogels by primary microglial cells. The laser scanning imaging system was custom built on Thorlabs Cerna microscope chassis (Thorlabs Inc., Newton, NJ, United States) with broadband femtosecond Ti:Sapphire laser (800 nm central wavelength, 85 MHz repetition rate, Element 600, Femtolasers, Vienna, Austria) as an excitation/illumination source. Confocal linear reflectance and TPEF images were acquired reconstructed using data acquisition board (NI PCIe-6351, Austin, TX, United States) from photomultiplier tube detectors (PMT, Hamamatsu, Japan) signals with suitable optical bandpass filters (775–785 nm for confocal; 465–495 nm and 550–633 nm for TPEF, Semrock, Rochester, NY, United States)

at 1.33 frames per second by averaging 120 frames. PMT control voltages for the respective acquisition channels were kept constant between imaging sessions of control and treated samples, while the average laser power was adjusted in the range from 5 to 20 mW. All the acquired data in confocal and TPEF channels were normalized to a maximum value between nanogels treated and control (untreated) samples, final images depict square root of the intensity for visualization purposes. The concentration of nanogel (50 μg/ml) was selected based on the other experiments (flow cytometry) as the optimum concentration to see the time based uptake by the primary microglial cells.

Biodegradation Studies

The hydrolytic and enzymatic degradation of the hydrogel particles was studied using SEM analysis. Nanogel of known concentration 1 mg/ml was suspended in water for 7 days at 37°C. Cellulase, Trichoderma viride, was used for enzymatic degradation. Nanogels (1 mg/ml) were incubated for 7 days containing 10 units/g in 1 ml of water (pH 5.0) and then incubated particles from both the solution water and enzyme were dried on a glass slide and further coated with gold particles followed by SEM analysis to assess the morphology of the degraded particles.

Nanogel Transmigration Across the *in vitro* Blood Brain Barrier (BBB)

The *in vitro* BBB system used in the present study was adapted from previous studies published by Persidsky et al. (1997). Briefly, using a 24-well transwell (3.0 μM pore; Corning Life sciences) plate primary human brain microvascular endothelial cells (HBMEC; Sciencell) (2 × 105 per/well) were cultured in the inner chamber (on the upper membrane face) while primary human astrocytes (HA) and pericytes (at 1:1 ratio) were seeded (2 × 105 per well) on the lower membrane. These cells all together form the *in vitro* BBB transwell system which was co-cultured to confluency (∼7 days) prior to the treatment with different concentrations of nanogels.

Transendothelial electrical resistance (TEER) measurements. The confirmation of BBB integrity was done by the measurement of transendothelial electrical resistance (TEER). The various nanogel concentrations were incubated for 24 h and the electrical resistance across the *in vitro* BBB was measured using an automatic ohmmeter (AutoRems, WPI). Briefly, BBB transwell system was placed on the AutoRem device, and the probes were placed in the inner and outer chamber. The TEER reading was measured at 15 s intervals. Results were normalized to the control/untreated wells.

Dextran-FITC transport assay for permeability assessment. The permeability of the BBB was assessed using a Dextran-FITC transport assay. Briefly, Dextran-FITC solution (50 μl, 2 mg/ml) was added to the inner chamber of BBB transwell and the plate was incubated at 37°C for 3 h. Fluorescence (485/520 nm) in outer wells after 3 h was measured using microplate reader (Synergy HT, multi-mode microplate reader, Biotek). The percentage transport of FITC- dextran transport across the BBB model was compared with the FITC-dextran transported across the inserts without cells (Jayant et al., 2015). Results were normalized to the cell control/untreated post-incubation.

Nanoformulation transmigration efficiency measurement. Transmigration study was carried out by using the auto-fluorescence feature exhibited by the nanogel particles. The nanogel in various concentrations was added to the upper chamber and incubated for 24 h. After the incubation of the media containing the nanogels was collected from the upper as well as the lower chamber. The fluorescence intensity was observed on a plate reader (Synergy HT, multimode microplate reader, BioTek) by adjusting the excitation and emission wavelength to excitation 590/20, emission 645/40.

Transmigration efficiency is measured as:

$$\%\ \text{transmigration efficiency} = \frac{\text{Fluorescence in lower chamber}}{\text{Fluorescence in upper chamber} + \text{Fluorescence in lower chamber}} \times 100$$

The effect of the nanogel exposure on the integrity and permeability of the *in vitro* BBB was determined by measuring the TEER and the FITC dextran transmigration, respectively, using the Millicell ERS microelectrodes (Millipore). Briefly, FITC-dextran was added to the upper chamber and incubated for 4 h. Fluorescence was measured at ex/em 485/520 nm using a microplate reader (Synergy HT, multi-mode microplate reader, BioTek). The percentage of FITC- dextran transported across the BBB was compared with the FITC-dextran transported across the inserts without cells.

Statistical Analysis

Data were represented as mean ± SD of three independent experiments or otherwise indicated. *T*-test was used for statistical comparisons among two groups. For statistical comparisons of more than two groups, one-way ANOVA was used to analyze the significant differences and wherever appropriate *p*-values of less than 0.03 were considered statistically significant. All the experiments were conducted in triplicates and results were expressed as mean ± standard deviation. Other statistical analysis are mentioned with individual figure captions.

RESULTS

Design and Synthesis of Micro- and Nanogels Based Carriers

Efforts have been made to design various hydrogel-based carriers using biopolymers owing to their superior characteristics with no toxicity and complete biodegradability. In the present study, biopolymers chitosan having medium molecular weights (190–310 kDa) and HEC have been used for the development of hydrogel particles. The water-in-oil emulsion polymerization reaction was deployed for the development of hydrogel particles. These hydrogel particles were hydrophobically modified using

sustainable resource "Linseed oil" based polyol (Vashist et al., 2013). It was hypothesized that the hydrophobic modification will restrict the swelling capacity of the polymeric hydrogel particles, which thereby will enhance their hydrophobicity and thus help them traverse through the BBB. The hydrogel particles can be designed in various size ranging from micro to nano (300 μm to 100 nm). Linseed oil-based polyol was synthesized as per protocol reported earlier with some modification (Sharmin et al., 2007). The modulation in the stirring rate 1200–1400 rpm resulted in the development of finer and homogeneous hydrogel particles coded as T-4 in all figures. The reaction time played a crucial role in achieving the high yield of the hydrogel particles. Most importantly, it is worth to mention that there was no crosslinked particle formation when only HEC and polyol was used for the synthesis of nanogel by emulsion polymerization technique. Thus it is very important to highlight that chitosan played a significant role in the formation of crosslinked hydrogel particles. Previously, we reported the formation of inter-penetrating network with the addition of linseed oil derived polyol (Vashist et al., 2012). The concentration of the linseed oil-based polyol was found to modulate the size of the hydrogel particle and a decrease in particle size was observed with the increasing content of polyol in the synthesized hydrogels. Size sorting strategy was opted to obtain different size particles. Briefly, different size mesh filters were used for collecting the desired size particles. Emphasis was given on obtaining both micro and nanoparticles with unique characteristic properties, which can be diversely used as a carrier for therapeutics in cancer, HIV, other neurological disorders and diagnostics. Finally, the particles filtered through 25 μm membrane were used for all downstream experiments. **Figure 1** showed the crosslinking reaction of the matrix materials (chitosan and HEC with glutaraldehyde and the surface modification by hydrophobic polyol was further confirmed by FT-IR analysis (**Figure 2**).

The core-shell structure was obtained by the transmission electron microscopy (TEM) (**Figures 3A,B**) for the designed hydrogel particles. TEM analysis confirmed the spherical shape with core-shell morphology and the nano-size (60–70 nm) of the particles. **Supplementary Figure S1** shows the TEM image of single nanogel particles. The average hydrodynamic size was obtained using zeta sizer for the sorted particles (0.2 and 25 μm membranes) (**Supplementary Figure S2**) which showed that the sorting technique may be used to achieve the desirable hydrodynamic size of the developed micro/nanogel particles. The Zeta Potential measurements demonstrated the surface charge of −1.98 mV in water and −6.56 mV in PBS. It is expected that this near neutral surface charge will help in increased circulation time and also inhibition to plasma protein absorption to the surface of the nanogel particles.

Fluorescence Characteristics of Micro- and Nanogel Particles

Apparently, the two individual biopolymers chitosan and HEC used in the present study for the design of hydrogel particles, show weak intrinsic fluorescence. Chitosan in aqueous solution, owing to its weak intrinsic fluorescence does not serve as a fluorescent probe to detect targets. Therefore, many strategies have been employed to conjugate fluorescent moieties to chitosan (Benediktsdóttir et al., 2012; Bor et al., 2017) and expand the horizon of its applications (Zaitsev et al., 2015; Bor et al., 2017). Chitosan-based polymers are usually tagged with fluorescent dyes/compounds for *in vitro* or *in vivo* biological imaging. Further, present synthesis involves hydrophobic modification using linseed oil-based polyol that was pre-stored for 190 days. Linseed oil shows fluorescence in the range of 600 nm when excited at 337 nm (Miyoshi, 1985; Alam et al., 2014). The confirmation of the auto-fluorescence was done using photoluminescence (PL) measurements, which was conducted using Ocean Optics USB 2000 fiber optic spectrometer and 5 mW, 405 nm diode laser as the excitation source (**Figure 3C**). Interestingly the Raman spectral analysis, which revealed the presence of the strong autofluorescence in the micro- and nanoparticles (**Figure 3D**). Strong fluorescence is known to muddle the weak spontaneous Raman signals which add to challenges in chemical characterization of single particles (Kaiser et al., 1996; Gong et al., 2017). Therefore, the absence of Raman peaks in the Raman spectra was intriguing and pointed toward the presence of high fluorescence exhibited by the particles (**Figure 3D**). To further validate the efficacy of the developed hydrogel particles for *ex vivo* or *in vivo* imaging, the particles were imaged at higher wavelengths using optical filters (emission wavelength/band-width) for red (605/70 nm), far-red (700/75 nm) and near infra-red (810/90 nm) regions. The particles showed a bright emission at all the wavelengths including 810 nm (**Figure 3E**).

Additionally, images were acquired using imaging flow cytometer. Different concentrations (1–100 μg/ml) of nanogel particles without cells were prepared in PBS buffer pH 7.4 to get an emission spectrum of the particles at an excitation of 405 nm and confirmed the presence of fluorescence. Post-acquisition of nanogel particles, analysis was done based on the area and aspect ratio of images, single-particle population and clumps were gated. A concentration-dependent reduction in the fluorescence of diluted samples was observed, which may be attributed to the less availability of single particles on dilutions.

Figure 4A represents the mean fluorescent intensity values of the single-particle population for each channel. The nanogel particles were detected with 405 nm excitation laser and analyzed based on emission in channel 8 (505–560 nm), which exerted the maximum intensity for each concentration. 50 μg/ml nanogel concentration gave the maximum fluorescent intensity (**Figure 4B**). Our results clearly indicate that the polymeric network particles formed by the reaction of chitosan, glutaraldehyde, HEC, and linseed polyol showed wide emission range (460–770 nm) when excited at 405 nm. The crosslinking reaction between chitosan and glutaraldehyde possibly led to the formation of Schiff's bases by condensation reaction between the amino and carbonyl groups of chitosan and glutaraldehyde, respectively. HEC and linseed polyol are stable in the polymeric network due to the formation of hydrogen bonds. Overall, in the polymeric network, as shown in the reaction scheme in **Figure 1**, we have different types of functional groups that may have enhanced the fluorescing ability of the hydrogel network.

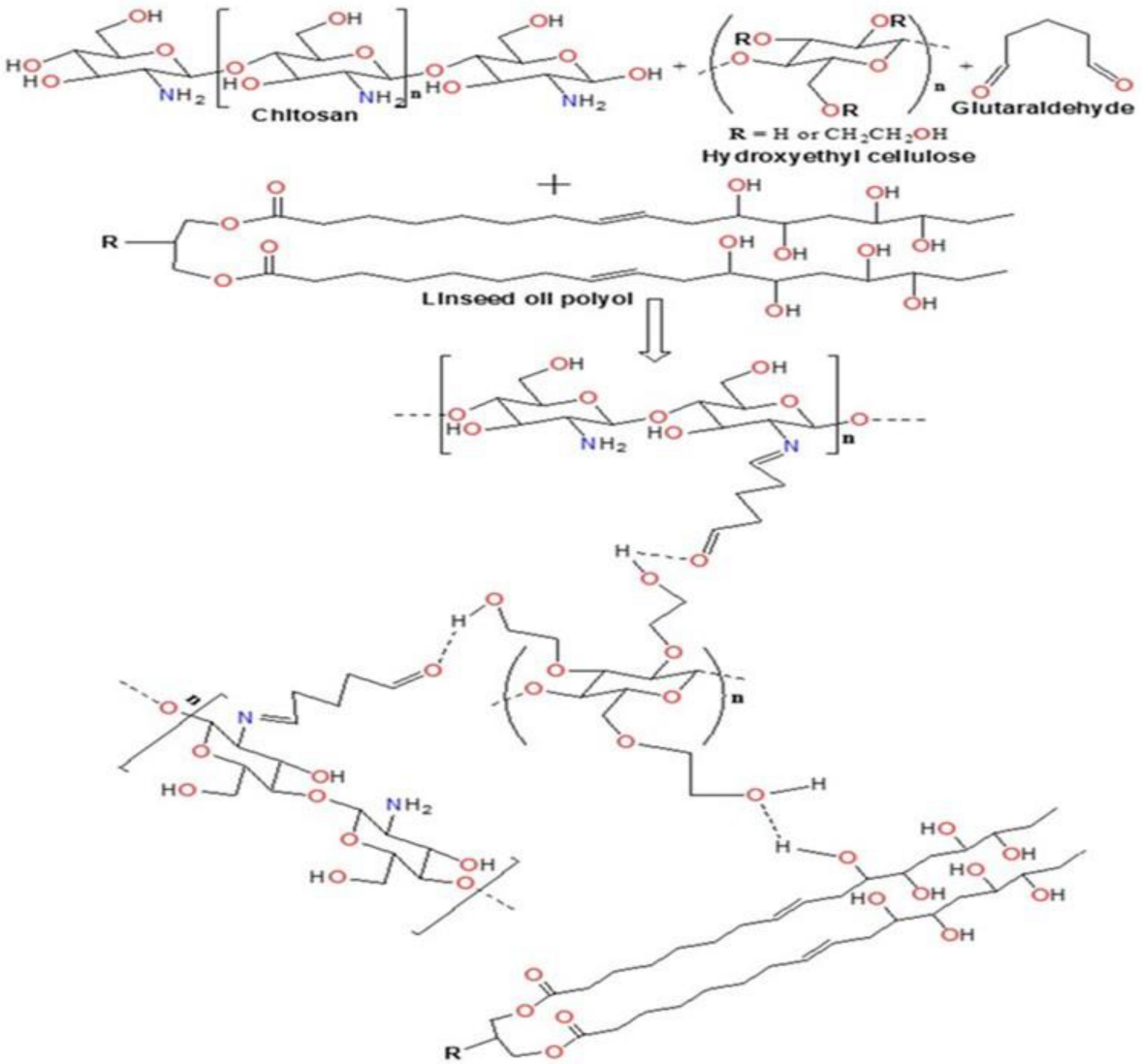

FIGURE 1 | Reaction scheme for the development of micro-and nanogels.

As discussed in the earlier section it is important to highlight that chitosan was the most important constituent in combination with HEC and polyol, which played a crucial role for the presence of high fluorescence in the developed particles. The additive effect of the –OH groups (due to the incorporation of polyol) and the formation of the > C = N- linkages (due to condensation reaction between chitosan and glutaraldehyde) may have enhanced the fluorescing ability of the polymeric network in the wavelength range of 430–630 nm. Overall, the attachment of the linseed polyol containing multiple –OH groups may have contributed largely to the fluorescing capacity of the hydrogel network (460–770 nm). The electronic transitions of particular interest for fluorescence in the reported polymeric network are the low energy $\pi-\pi^*$ and $n-\pi^*$ transitions of > C = N, and high energy $n-\sigma^*$ transitions of –OH groups. The broadening of the peak, when excited at 405 nm, which is centered at 570 nm, may be attributed to the coalescing of the fluorescence bands of the peaks due to –OH groups with slightly different energies.

Biocompatibility Evaluation of Nanogels *in vitro*

To evaluate the biocompatibility of the synthesized nanogels, LDH assay (was performed on neuronal cells Microglia and PBMCs (**Supplementary Figure S3**). Results demonstrated that the nanogels were non-cytotoxic and the viability was similar to the control and thus are safe to the cells. Cytotoxicity of nanogels against the peripheral cells (PBMCs), astrocytes and microglial cells (CHME5) was assessed by XTT assay performed over a concentration range of 10–100 μg/ml. The nanogels were found to be non-toxic in the tested concentrations up to 2 days

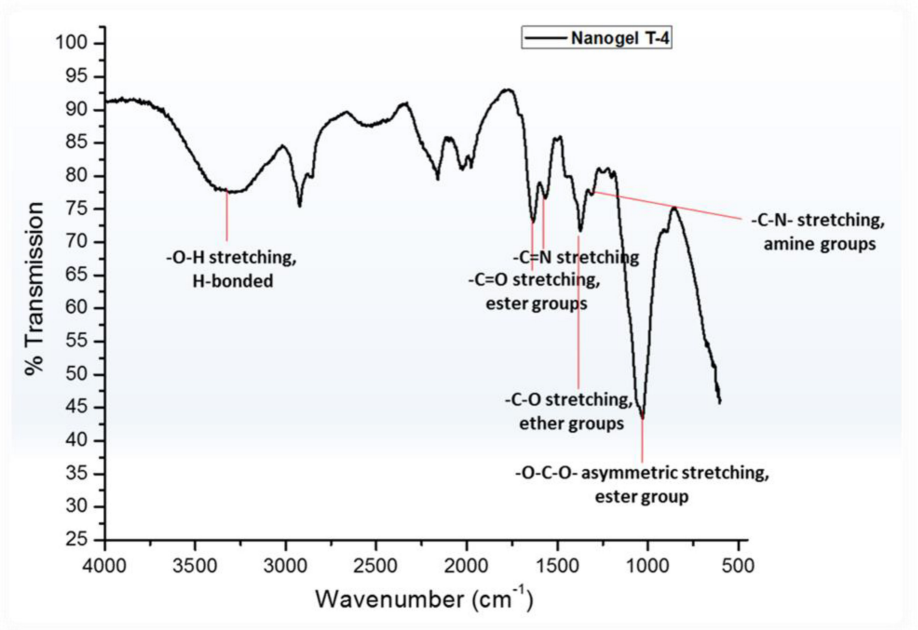

FIGURE 2 | FT-IR analysis of nanogel.

for CHME5. The high cell viability (∼80% and above up to 7 days) and intact morphology confirmed that the developed nanogels are biocompatible with respect to all the cell types tested (**Figure 5**). This may be attributed to the biocompatible biopolymers used for the development of the hydrogel particles and their unique chemical structure resulted after crosslinking, exhibiting biomimetic soft tissue like hydrogel structures. Also, we hypothesize that the enhanced element of hydrophobicity and formation of interpenetrating networks (IPNs) introduced by incorporation of linseed oil-based polyol may result in a stable nanogel system which sustained in the cellular environment.

Toxicity Analysis of Nanogels in Human Astrocytes

Human astrocyte cell line (U87 cells) were cultured for 24 h and were incubated with nanogel particles suspended in PBS at a final concentration of 100 μg/ml. Images were acquired at day 6 (**Supplementary Figure S4**) and day 7 using various optical filters for analyzing fluorescence in the green, red and blue visible region (**Figures 6A,B**) in OLYMPUS IX51 microscopy system. There were no discernible morphological changes in the astrocytes incubated with nanogels compared to untreated cells; therefore, nanogels were deemed as non-toxic for this CNS cells. The longer treatment of astrocytes with nanogels demonstrated cellular uptake of nanogels suggesting longer retention (up to 7 days) of these particles within astrocytes; therefore, confirming the potential use of these nanogels for CNS-targeted theranostics.

Cellular co-localization of particles within astrocytes was demonstrated by imaging the cells that were incubated with the 10 μg/ml of nanogels for 72 h in the Labtech chambered slides at different emission wavelengths (CWL)/Bandwidth (FWHM): 605/70, 700/75, and 810/90 (**Figure 6C**). A differential interference contrast (DIC) image showed the cell morphology, and the merged image analysis with fluorescent images showed the co-localization of the particles within the cells and particles were imaged using the higher wavelength filters. These studies further confirmed the potential for *in vitro* and *in vivo* imaging utility of these novel nanogel particles as they can be imaged in the far-red and near-infrared regions for better imaging penetrance.

Cell Uptake and Toxicity Profiles

In addition to the biocompatibility testing, the nanogels were qualitatively and quantitatively screened for the cellular uptake using single-cell imaging flow cytometry. For this study, CHME5 cell lines and PBMCs were selected. As discussed in the earlier section, different concentrations of nanogels were incubated with cells for up to 24 h. After incubation, cells were harvested, washed with PBS, acquired, and analyzed to quantify the location and distribution of fluorescence. In this process of analysis, we further confirmed the existence of wide emission wavelength and multichannel fluorescence properties of nanogels. The cells treated with nanogel particles were detected with 405 nm excitation laser and analyzed based on emission in channel 8 (505–560 nm), which exerted the maximum intensity for each concentration.

Time and concentration dependent uptake of nanogels by PBMCs and CHME5 (1×10^6) was confirmed using imaging flow cytometry. PBMCs cultured with nanogels at a concentration of 100 μg/ml showed significant uptake of nanogel particles. Similarly, CHME5 cells, showed significant uptake at 50 μg/ml concentration. Images acquired for CHME5

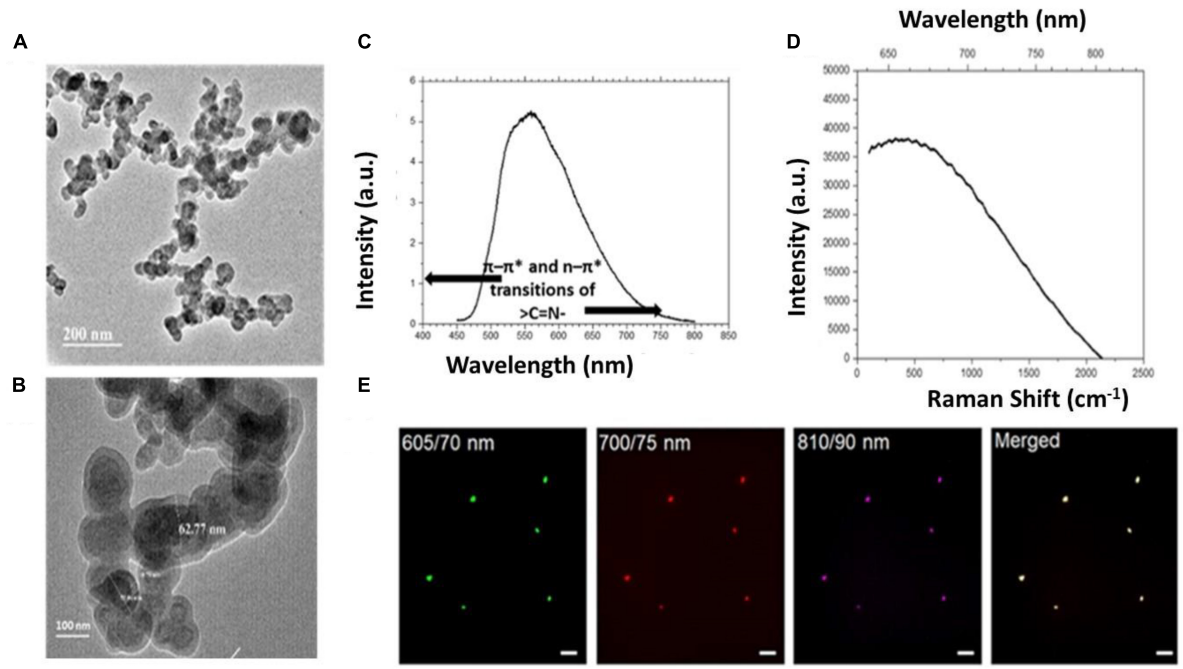

FIGURE 3 | (A,B) TEM analysis for nanogel particles. **(C)** Photoluminescence (PL) measurements 405 nm diode laser as excitation source in Ocean Optics USB 2000 fiber optic spectrometer. **(D)** Raman spectra analysis of the nanogels. **(E)** Representative images showing the autofluorescence exhibited by the nanogels acquired at the wavelength regions (emission wavelength/band-width) for red (605/70 nm), far-red (700/75 nm) and near infra-red (810/90 nm) regions; an overlay of merged image is also shown, scale – 20 μm.

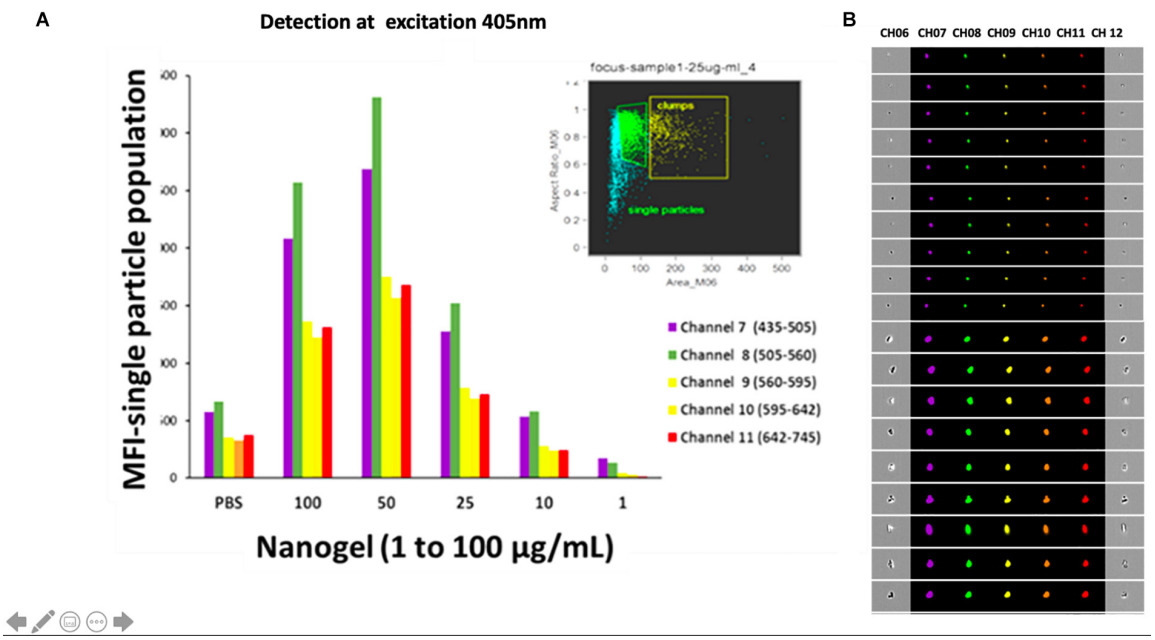

FIGURE 4 | (A) The mean intensity values of the single-particle population for each channel at an excitation wavelength of 405 nm. **(B)** Images acquired for the presence of fluorescence for and aggregated and single particle in each channel at an excitation wavelength of 405 nm.

expressing fluorescence due to nanogel uptake and the mean fluorescent intensity values of the positive cell population are shown in **Figures 7A,B**. Similarly, **Figures 7C,D** demonstrate the percentage of PBMCs expressing fluorescence due to nanogel uptake and the mean fluorescent intensity values of the positive cell population. A time-dependent increased in fluorecence of

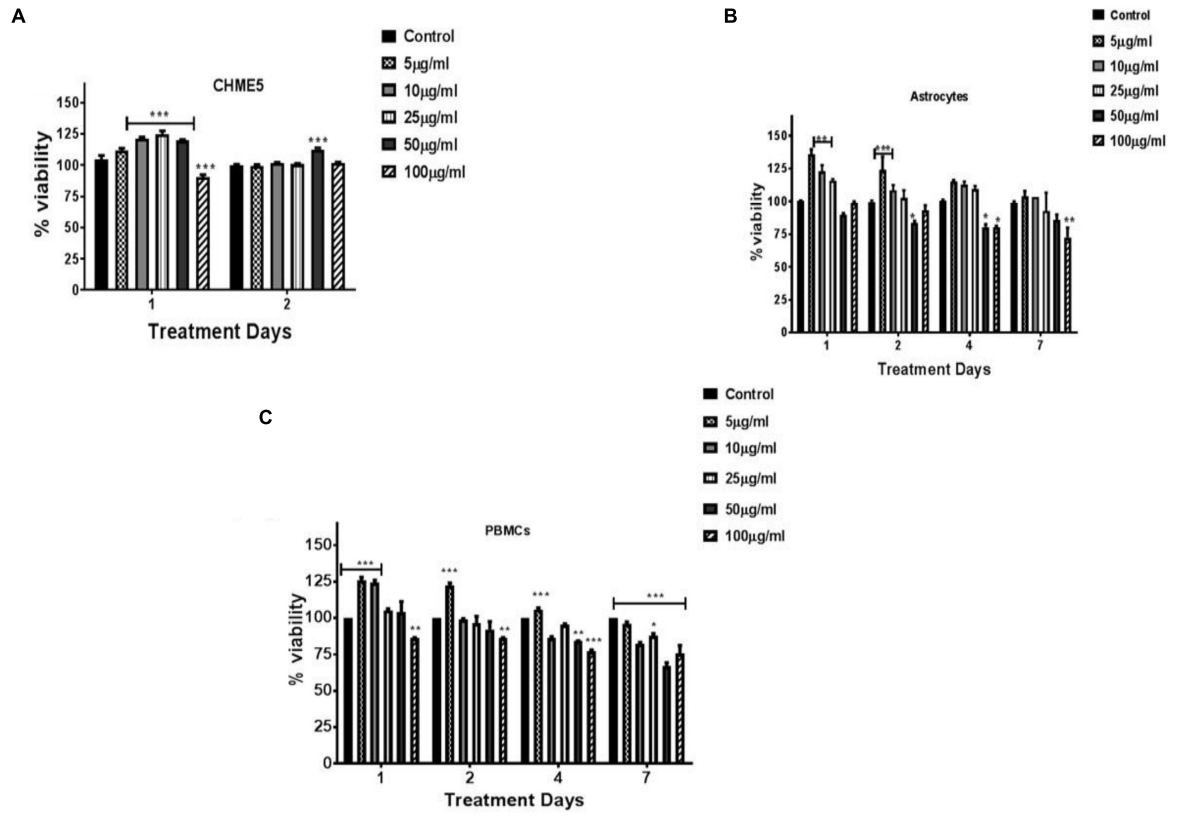

FIGURE 5 | Cytocompatibility testing of nanogels at various concentrations (5–100 μg/ml) as a function of time. **(A)** CHME-5; **(B)** astrocytes; **(C)** PBMCs. Cells were treated with various concentration of nanogel for 1, 2, 4, and/or 7 days. XTT assay performed on cells post nanogel exposure. Statistical significance determined by Two-way ANOVA and *post hoc* (Bonferroni post-tests) analysis, $^{*}p < 0.05$, $^{**}p < 0.01$, and $^{***}p < 0.001$.

cells cultured with nanogels for 2 and 6 h is demonstrated in bar graphs included in **Supplementary Figure S5**. The further increased in fluorecence after culturing cells with nanogels for up to 24 h (**Supplementary Figure S5**) confirmed a time-dependent increase in cellular internalization of nanogels.

Two-Photon Imaging

The two-photon fluorescence imaging also confirmed the cellular uptake of nanogels for up to 24 h. **Figure 8** showed the 6 and 24 h time based uptake of nanogel by primary microglial cells. Control (untreated) and nanogel treated cells were imaged and are depicted in **Figure 8**. The time based uptake showed that there was increased uptake of nanogels in 24 h. Please note that the untreated cells have background endogenous fluorescence (**Figure 8**), which is due to the presence of NADH/FAD fluorescent co-factors in the cytoplasm and cell body. The imaging technique showed the presence of fluorescent nanogel particle in primary microglial cells in 465–495 nm and 550–633 nm channels.

Hydrolytic Degradation and Enzymatic Degradation Study

The nanogel were found to change little in morphology after 7 days of hydrolytic (water) and enzymatic degradation (Cellulase) study as indicated by the SEM analysis (**Supplementary Figure S6**). The hydrolysis and complete degradation of nanogels in 7 days was limited due to the stability achieved by the crosslinking and the hydrophobicity induced by the addition of linseed polyol. Though, it is expected that longer incubation time of the nanogel will induce complete biodegradation of these nanogels due to the biodegradable characteristic of chitosan (Wang et al., 2019) and HEC which is used as the matrix material in the development of hydrogels.

Blood-Brain Barrier (BBB) Transmigration

The BBB poses a great challenge for efficient delivery of various therapeutics owing to its lipid-rich composition (Hawkins et al., 2006). This necessitates the requirement of formulations which provides a hydrophobic environment for ease of transmigration through BBB. Therefore the transmigration of nanogels through the BBB was evaluated using the *in vitro* human BBB model. The intactness of the developed BBB was determined by measurement of TEER values. As the integrity of the BBB was confirmed the nanogels in different concentration (10–100 μg/ml) were added to the different upper wells of BBB. **Figure 9A** shows the TEER values of the control and the treated wells of various concentration of nanogels. There was no significant change in the

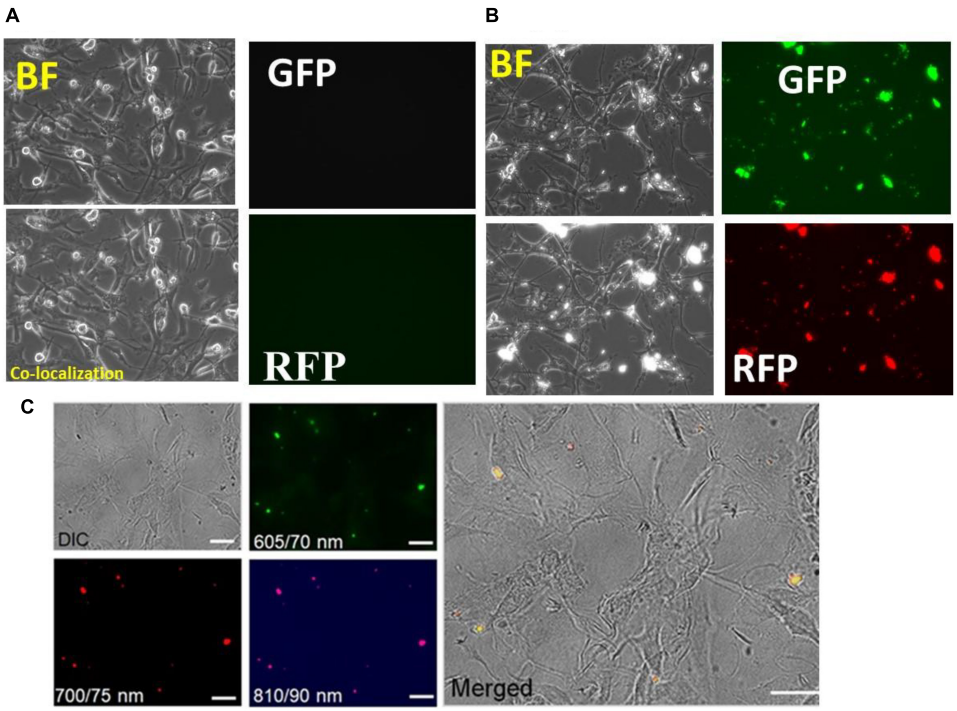

FIGURE 6 | Toxicity profiles and co-localization of nanogels with astrocytes after 7 day treatment of nanogels. **(A)** Control; **(B)** 100 *upmug*/ml. **(C)** Cellular uptake analysis of the nanogels as assessed by the differential interference contrast (DIC) imaging and by the fluorescent imaging at the wavelength/bandwidth range of 605/70, 700/75, and 810/90 nm, scale – 20 μm. The merged image on the right panel shows the overlay of all the images.

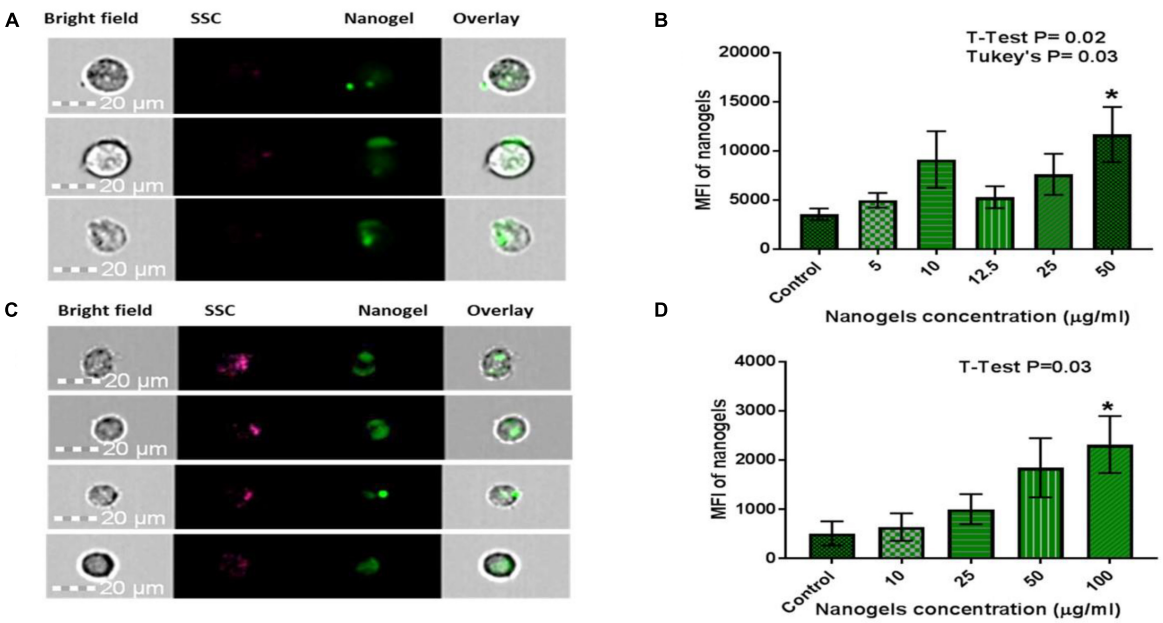

FIGURE 7 | Qualitative and quantitative assessment of cellular uptake of nanogels using Flow Cytometry for **(A,B)** CHME-5: Statistical analysis: Data is represented as Mean ± SEM. Significance was tested by Student's *T*-test which showed T4 50 μg/ml was significantly higher than Control ($P = 0.02$). Significance was also tested by one-way ANOVA which showed significance between columns (treatments), $F(5, 28) = 2.786$, $P = 0.0365$. *Post hoc* analysis with Tukey's multiple comparisons tests showed T4 50 μg/ml was significantly higher than control ($P = 0.03$). **(C,D)** PBMCs: Statistical analysis: Data is represented as Mean ± SEM. Significance was tested by Student's *T*-test which showed T4 100 μg/ml was significantly higher than Control ($P = 0.03$). Significance was also tested by one-way ANOVA which showed significance between columns (treatments), $F(4, 23) = 2.995$, $P = 0.03$. *Post hoc* analysis with Tukey's multiple comparisons tests did not show any further significance. * means it is significant compared to control.

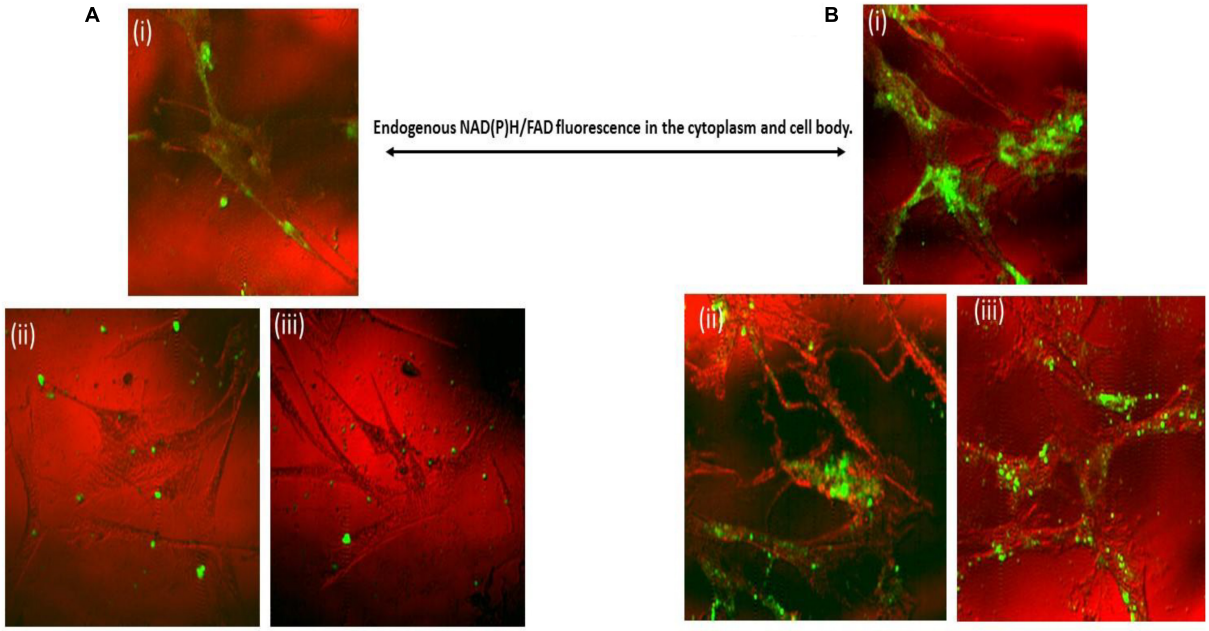

FIGURE 8 | Combined reflectance confocal and two-photon imaging of nanogel uptake by Primary microglial cells at **(A)**: (i) Control; (ii,iii) 6 h treatment; **(B)**: (i) Control; (ii, iii) 24 h treatment of nanogels. Pseudocoloring: Red – confocal (or nearly confocal) reflectance at 780 nm; Green – Two-photon excitation fluorescence (400–633 nm range all together). Average laser power ranging from 5 to 20 mW.

values of TEER as compared to the control, which confirms that the nanogels does not affect the overall integrity of the BBB. The permeability of the BBB was also measured using the paracellular transport of the FI-TC across the BBB as described previously (Jayant et al., 2015). The FI-TC is used as a detection bioactive molecule for the membrane intactness. **Figure 9B** shows that the permeability was not altered with the treatment of nanogels as compared to untreated. The permeability is normalized to the positive control.

The transmigration of the nanogels was measured as the function of fluorescence. The fluorescence intensity recorded in upper and lower chambers using plate reader showed that approximately 10% of nanogels were capable of transmigrating through the tough BBB tight junctions (**Figure 9C**). The hydrogel particles used in this study were polydispersity with PDI of 0.6. Hydrophobically modified nanogels using linseed oil (triglyceride) based polyol which is non-polar in nature have been designed in such a manner which increases their hydrophobicity for enhancing their transmigration across the tight junctions. The crosslinking reaction occurred during the synthesis of nanogels between the biopolymers viz., chitosan, HEC and glutaraldehyde leading to the formation of Schiff base using the condensation reaction and the surface functionalization by the linseed polyol may have facilitated hydrophobic interactions. The transport data revealed that unlike at higher concentration (100 μg/ml), gel particles exhibited better transmigration in BBB model when used at lower concentration of 10 μg/ml. This may be possibly due to the less aggregation and less crowding of the nanogel particles in the upper chamber which may have allowed better diffusion across the tight junctions. The main cause of the lower transmigration of nanogels across the BBB may be due to the polydispersity of the particles and it is anticipated that there may be an increase in the % transport once the polydispersity is lowered down and a monodisperse particle with PDI of >0.4 is used. We hypothesize that slight variation in the content of the polyol, increasing the monodispersity, and the biopolymers may increase the passage of the nanogel through the tight junctions. Thus, these novel auto fluorescent nanogels owe great potential as a DDS for CNS therapy.

DISCUSSION

In recent years, several nano- and micron range drug delivery vehicles have evolved for theranostic applications remarkably due to rise in the demand for multi-functional systems capable of imaging and delivering the drugs or genes to the target site (Shi et al., 2014; Chan and Almutairi, 2016). For example, various nanoparticles based systems have been developed by conjugating with lanthanides, peptides, gold nanoparticles, and quantum dots which contributes to the fluorescence and can also act as a drug delivery vehicle (Lin et al., 2017; Cardoso Dos Santos et al., 2018; Yuan et al., 2018). However, these materials have faced a lot of safety concerns owing to toxicity due to their inorganic nature. Efforts are being made to develop safe autofluorescent biomaterials such as polymers (Yang J. et al., 2009), polymeric nanoparticles (Yang Z. et al., 2009), dendrimers (Wang and Imae, 2004), and nanogels (Gyawali et al., 2018) with significant easy route and high biocompatibility and less toxicity which can be deployed for bio-imaging and

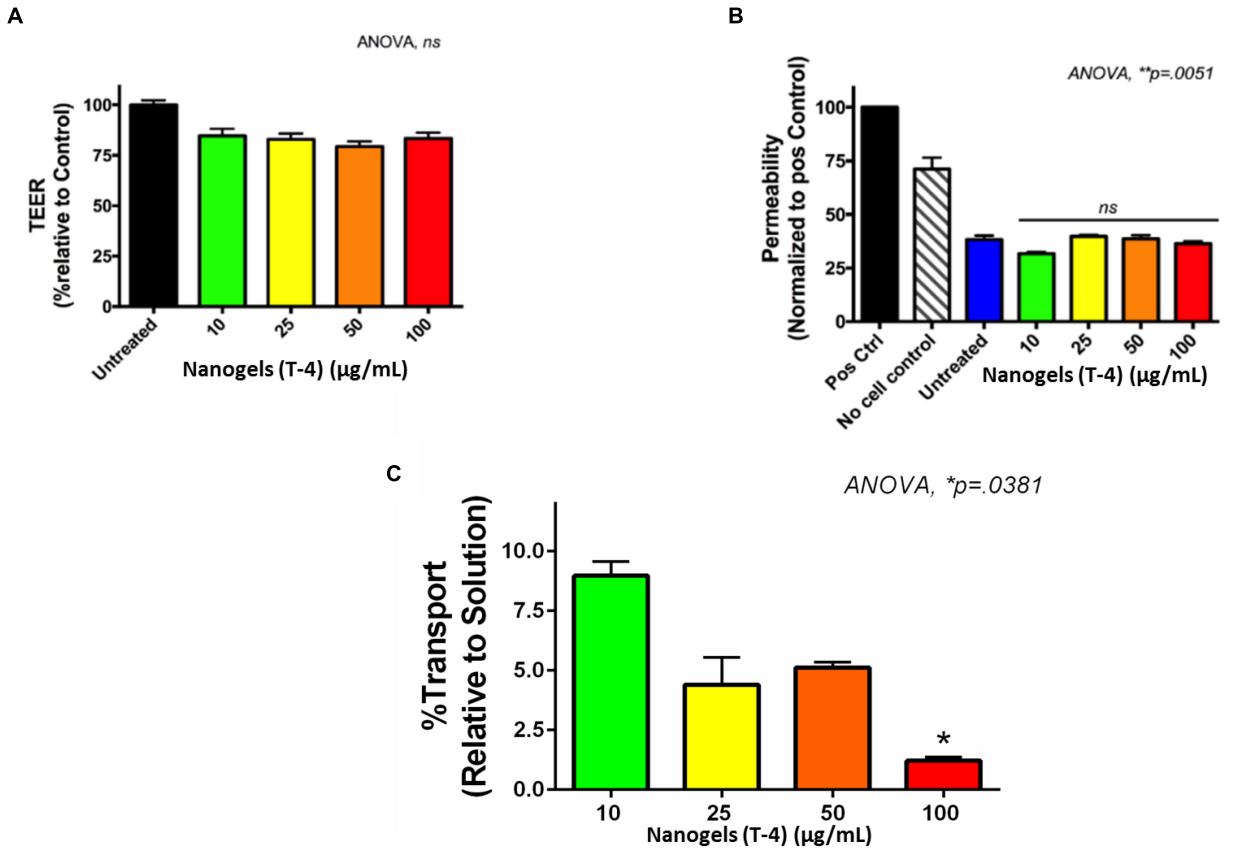

FIGURE 9 | *In vitro*- BBB model. **(A)** The TEER values of the *in vitro* BBB model after exposure of nanogels. **(B)** Permeability of the *in vitro* BBB model after nanogel treatment for 24 h. **(C)** % transport of nanogels across the *in vitro* BBB model.

drug delivery (Vashist et al., 2018b). Our approach utilizes the natural biodegradable and biocompatible polymers and uses a simple method of synthesis developing both micro-and nano range particles exhibiting autofluorescence which could be a promising theranostic system that will mimic a perfect imaging agent and delivery vehicle for CNS drug delivery. The ability of the developed hydrogel particles to fluoresce in wide emission spectrum range and cellular compatibility could potentially translate the present imaging modalities and develop soft nanogel systems for CNS and periphery therapies.

In the present study, we have put forward the advanced and novel bio-polymeric hydrogel system in micro- and nanoscale exhibiting unique autofluorescent feature. This hydrogel system has wide-emission spectrum in the range of 450–780 nm, on excitation at 405 nm as well as excitation at 710 nm gives emission at 810 nm showing its capacity to be used for *in vivo* imaging. Recent trends in theranostics suggest that this wide emission phenomenon from a bio-polymeric biocompatible system offer excellent potential for bright fluorescence probes used for *in vitro* optical imaging used for cellular imaging as well as *in vivo* imaging (Anilkumar et al., 2013).

We showed that the developed nanogel show safe uptake by the microglia and PBMCs. These gel particles owing to their biodegradable and biocompatible constituents showed low cytotoxicity and high biocompatibility with all the cell types viz., PBMCs, CHME5, and astrocytes. The % viability of ∼80% using nanoformulations is considered to be non-toxic in both peripheral and CNS cells (Thorat et al., 2014). The toxicity investigation of the nanogels using the astrocytes long co-culture experiments revealed that the developed nanogel particles were biocompatible with the astrocytes for 7 days and there was co-localization of the nanogel particles with the astrocytes. The revelations of the autofluorescence by the Raman and photoluminescence study was further confirmed by the images acquired by the flow cytometry. This mechanistic study used for imaging nanogel provided proof of the concept to identify the cellular internalization and presence of fluorescence. This study further confirmed the potential application of the developed hydrogel particles in bio-therapeutic delivery by cellular co-localization or internalization (Li et al., 2017).

The developed micro- and nanogel system put forward their advantages as a multi-functional carrier escaping all the limitation offered by the conventional nanocarriers such as tagging with inorganic fluorescent probes, non-toxicity and another adverse side-effects. The exquisiteness of the present system lies in the wide-detection range of the nanogels as multi-channel fluorescence offer the benefit of the detection of the nanogels in various instruments by adjusting the excitation and

emission wavelengths. We could observe the fluorescence on a plate reader (Synergy HT, multimode microplate reader, BioTek) by adjusting the excitation and emission wavelength to excitation 590/20, emission 645/40. This makes the "micro- and nanogel" a unique imaging agent with wide-detection limit and makes it accessible for various instruments. Moreover, the micro- and nanogels do not contain any drug and inorganic nanoparticles imply the presence of autofluorescence and biocompatibility, thus they have the potential to be used as an imaging agent for other bioactive molecules when binding with the developed nanogels.

Radically improved features of the present hydrogel system have advantages over the so far published fluorescent hydrogel systems in the literature (Chang et al., 2009; Ji et al., 2019; Wu et al., 2019). The BBB model explicitly showed the experimental proof for the hypothesized concept of the hydrophobically modified nanogels using linseed oil-based polyol transmigrating across the tight junctions of BBB. The data on the intactness of BBB and permeability after the exposure of the nanogels intriguingly suggest that the designed nanogel system owe great potential of CNS drug delivery. However, the exact mechanism of the transport of these nanogels crossing the BBB has to be explored in depth.

This study provides a room to develop a receptor or ligand-free delivery of nanocarrier for CNS drug delivery. Notably, present multi-functional, size-controlled nanogel showed high fluorescence and biocompatibility and exploits all size range from micro-and nanogels. The future direction of the present study directs for the improvement in the% transport of nanogels across BBB. The intonation in the concentrations of the biopolymers used in the present synthesis, the change in the concentration of hydrophobic polyol including variation in the reaction conditions such as stirring rate and temperature may be utilized to fabricate a new class of nanogels with improved features, i.e., enhanced transmigration through BBB. Thus, we propose these multi-functional nanogel particles as an innovative and effective tool for the CNS targeting and innocuous therapies and owe huge potential to act as an excellent theranostic agent.

CONCLUSION

In summary, we here developed a novel bio-polymeric size-controlled approach for synthesizing micro- and nanogel particles exhibiting unique autofluorescent characteristic, which obviates the requirement of additional tag for their detection inside the intracellular microenvironment and exhibit potential for *in vivo* imaging. These hydrogel particles possess excellent biocompatibility, cell uptake, and surface functionality, which make them superior therapeutic carrier which can be explored for their capability to encapsulate various bioactives inside them. It is anticipated that both the hydrophobic modification by using linseed oil-based polyol and soft porous structure has facilitated the transport the hydrogel particles through the strong CNS BBB. This hydrogel systems strongly directs the technology toward the path of advancement in nanoimaging and therapy, which will provide new avenues for enhanced CNS therapy.

DATA AVAILABILITY STATEMENT

All datasets generated for this study are included in the article/**Supplementary Material**.

AUTHOR CONTRIBUTIONS

ArV planned and coordinated research and was actively involved in all experiments. AtV, AK, and AT helped in data analysis and manuscript writing. TP, MA, and AD helped in the detection of fluorescence by laser and cell uptake studies using flow cytometry measurements. HC contributed the microscopic imaging. VA and ZH performed cytotoxicity studies. RN-M was involved in TEM analysis. AR was involved in the design of BBB *in vitro* model and transport study. IS and JR-R helped us in two-photon imaging of the nanogels. MN was involved in the experimental research plan and continuous supervision.

FUNDING

This work was partially financially supported by FIU Foundation grant AW000000011094 and from the National Institute of Health (NIH) Grants 1R01DA037838-01, 1R01DA040537-01, and R01DA034547. JR-R and IS gratefully acknowledge funding from the Herbert and Nicole Wertheim Professorship Endowment as well as the STROBE: A National Science Foundation Science & Technology Center under Grant No. DMR 1548924.

ACKNOWLEDGMENTS

We acknowledge the Advanced Materials Engineering Research Institute (AMERI) at FIU for SEM and TEM.

SUPPLEMENTARY MATERIAL

The Supplementary Material for this article can be found online at: https://www.frontiersin.org/articles/10.3389/fbioe.2020.00315/full#supplementary-material

REFERENCES

Alam, M., Akram, D., Sharmin, E., Zafar, F., and Ahmad, S. (2014). Vegetable oil based eco-friendly coating materials: a review article. *Arab. J. Chem.* 7, 469–479. doi: 10.1016/j.arabjc.2013.12.023

Allen, T. M., and Cullis, P. R. (2004). Drug delivery systems: entering the mainstream. *Science* 303, 1818–1822. doi: 10.1126/science.1095833

Anilkumar, P., Cao, L., Yu, J.-J., Tackett, K. N., Wang, P., Meziani, M. J., et al. (2013). Crosslinked carbon dots as ultra-bright fluorescence probes. *Small* 9, 545–551. doi: 10.1002/smll.201202000

Atluri, V. S. R., Kanthikeel, S. P., Reddy, P. V., Yndart, A., and Nair, M. P. (2013). Human synaptic plasticity gene expression profile and dendritic spine density changes in HIV-infected human CNS cells: role in HIV-associated neurocognitive disorders (HAND). *PLoS One* 8:e61399. doi: 10.1371/journal.pone.0061399

Atluri, V. S. R., Pilakka-Kanthikeel, S., Garcia, G., Jayant, R. D., Sagar, V., Samikkannu, T., et al. (2016). Effect of cocaine on HIV infection and inflammasome gene expression profile in HIV infected macrophages. *Sci. Rep.* 6:27864. doi: 10.1038/srep27864

Benediktsdóttir, B. E., Sørensen, K. K., Thygesen, M. B., Jensen, K. J., Gudjónsson, T., Baldursson, Ó, et al. (2012). Regioselective fluorescent labeling of N, N, N-trimethyl chitosan via oxime formation. *Carbohydr. Polym.* 90, 1273–1280. doi: 10.1016/j.carbpol.2012.06.070

Bor, G., Üçüncü, M., Emrullahoğlu, M., Tomak, A., and Şanlı-Mohamed, G. (2017). BODIPY-conjugated chitosan nanoparticles as a fluorescent probe. *Drug Chem. Toxicol.* 40, 375–382. doi: 10.1080/01480545.2016.1238481

Brown, C. L., Smith, K., Wall, D. M., and Walker, D. (2015). Activity of species-specific antibiotics against Crohn's disease–associated adherent-invasive *Escherichia coli*. *Inflamm. Bowel Dis.* 21, 2372–2382. doi: 10.1097/mib.0000000000000488

Cardoso Dos Santos, M., Goetz, J., Bartenlian, H., Wong, K.-L., CharbonnieÌre, L., and Hildebrandt, N. (2018). Autofluorescence-free live-cell imaging using terbium nanoparticles. *Bioconjugate Chem.* 29, 1327–1334. doi: 10.1021/acs.bioconjchem.8b00069

Chan, M., and Almutairi, A. (2016). Nanogels as imaging agents for modalities spanning the electromagnetic spectrum. *Mater. Horizons* 3, 21–40. doi: 10.1039/c5mh00161g

Chang, C., Peng, J., Zhang, L., and Pang, D.-W. (2009). Strongly fluorescent hydrogels with quantum dots embedded in cellulose matrices. *J. Mater. Chem.* 19, 7771–7776.

Decker, T., and Lohmann-Matthes, M.-L. (1988). A quick and simple method for the quantitation of lactate dehydrogenase release in measurements of cellular cytotoxicity and tumor necrosis factor (TNF) activity. *J. Immunol. Methods* 115, 61–69. doi: 10.1016/0022-1759(88)90310-9

Degli Esposti, L., Carella, F., and Iafisco, M. (2018). "17 - Inorganic nanoparticles for theranostic use," in *Electrofluidodynamic Technologies (EFDTs) for Biomaterials and Medical Devices*, eds V. Guarino and L. Ambrosio (Sawston: Woodhead Publishing), 351–376. doi: 10.1016/b978-0-08-101745-6.00017-7

Figueroa, G., Parira, T., Laverde, A., Casteleiro, G., El-Mabhouh, A., Nair, M., et al. (2016). Characterization of human Monocyte-derived Dendritic cells by imaging flow Cytometry: a comparison between two Monocyte isolation protocols. *J. Vis. Exp.* 116:e54296. doi: 10.3791/54296

Gong, Z., Pan, Y.-L., Videen, G., and Wang, C. (2017). The temporal evolution process from fluorescence bleaching to clean Raman spectra of single solid particles optically trapped in air. *Chem. Phys. Lett.* 689, 100–104. doi: 10.1016/j.cplett.2017.09.064

Gyawali, D., Kim, J. P., and Yang, J. (2018). Highly photostable nanogels for fluorescence-based theranostics. *Bioact. Mater.* 3, 39–47. doi: 10.1016/j.bioactmat.2017.03.001

Hamid Akash, M. S., Rehman, K., and Chen, S. (2015). Natural and synthetic polymers as drug carriers for delivery of therapeutic proteins. *Polym. Rev.*55, 371–406. doi: 10.1080/15583724.2014.995806

Hamidi, M., Azadi, A., and Rafiei, P. (2008). Hydrogel nanoparticles in drug delivery. *Adv. Drug Deliv. Rev.* 60, 1638–1649. doi: 10.1016/j.addr.2008.08.002

Hawkins, R. A., O'kane, R. L., Simpson, I. A., and Vina, J. R. (2006). Structure of the blood–brain barrier and its role in the transport of amino acids. *J. Nutr.* 136, 218S–226S. doi: 10.1093/jn/136.1.218S

Ho, Y. P., and Leong, K. W. (2010). Quantum dot-based theranostics. *Nanoscale* 2, 60–68. doi: 10.1039/b9nr00178f

Jayant, R. D., Atluri, V. S., Agudelo, M., Sagar, V., Kaushik, A., and Nair, M. (2015). Sustained-release nanoART formulation for the treatment of neuroAIDS. *Int. J. Nanomed.* 10:1077. doi: 10.2147/IJN.S76517

Ji, X., Wang, J., Niu, S., and Ding, C. (2019). Size-controlled DNA-cross-linked hydrogel coated silica nanoparticles served as a ratiometric fluorescent probe for the detection of adenosine triphosphate in living cells. *Chem. Commun.* 55, 5243–5246. doi: 10.1039/c9cc01832h

Jiang, Y., Chen, J., Deng, C., Suuronen, E. J., and Zhong, Z. (2014). Click hydrogels, microgels and nanogels: emerging platforms for drug delivery and tissue engineering. *Biomaterials* 35, 4969–4985. doi: 10.1016/j.biomaterials.2014.03.001

Juillerat-Jeanneret, L. (2008). The targeted delivery of cancer drugs across the blood–brain barrier: chemical modifications of drugs or drug-nanoparticles? *Drug Discov. Today* 13, 1099–1106. doi: 10.1016/j.drudis.2008.09.005

Kaiser, T., Esen, C., Moritz, H., Borchers, M., and Schweiger, G. (1996). Observation of fluorescence background suppression in Raman scattering on single microparticles. *Berichte der Bunsengesellschaft für physikalische Chemie* 100, 119–122. doi: 10.1002/bbpc.19961000206

Kajjari, P. B., Manjeshwar, L. S., and Aminabhavi, T. M. (2011). Novel interpenetrating polymer network hydrogel microspheres of chitosan and Poly(acrylamide)-grafted-Guar gum for controlled release of ciprofloxacin. *Indus. Eng. Chem. Res.* 50, 13280–13287. doi: 10.1021/ie2012856

Kang, L., Jiang, D., Ehlerding, E., Ferreira, C., Yu, B., Barnhart, T., et al. (2018). Theranostics of lymphoma with 89Zr-and 177Lu-labeled daratumumab. *J. Nucl. Med.* 59(Suppl. 1), 74–74.

Kumar, P., Nagarajan, A., and Uchil, P. D. (2018). Analysis of cell viability by the lactate dehydrogenase assay. *Cold Spring Harb. Protoc.* 2018:pdb-prot095497. doi: 10.1101/pdb.prot095497

Kunjachan, S., Jayapaul, J., Mertens, E. M., Storm, G., Kiessling, F., and Lammers, T. (2012). Theranostic systems and strategies for monitoring nanomedicine-mediated drug targeting. *Curr. Pharm. Biotechnol.* 13, 609–622. doi: 10.2174/138920112799436302

Li, D., van Nostrum, C. F., Mastrobattista, E., Vermonden, T., and Hennink, W. E. (2017). Nanogels for intracellular delivery of biotherapeutics. *J. Control. Release* 259, 16–28. doi: 10.1016/j.jconrel.2016.12.020

Lin, W., Zhang, X., Qian, L., Yao, N., Pan, Y., and Zhang, L. (2017). Doxorubicin-loaded unimolecular micelle-stabilized gold nanoparticles as a theranostic nanoplatform for tumor-targeted chemotherapy and computed tomography imaging. *Biomacromolecules* 18, 3869–3880. doi: 10.1021/acs.biomac.7b00810

Minaeva, O. V., Brodovskaya, E. P., Pyataev, M. A., Gerasimov, M. V., Zharkov, M. N., Yurlov, I. A., et al. (2017). Comparative study of cytotoxicity of ferromagnetic nanoparticles and magnetitecontaining polyelectrolyte microcapsules. *J. Phys. Conf. Ser.* 784:012038. doi: 10.1088/1742-6596/784/1/012038

Miyoshi, T. (1985). Fluorescence from oil colours, linseed oil and poppy oil under N2 laser excitation. *Jpn. J. Appl. Phys.* 24, 371–372. doi: 10.1143/jjap.24.371

Persidsky, Y., Stins, M., Way, D., Witte, M. H., Weinand, M., Kim, K. S., et al. (1997). A model for monocyte migration through the blood-brain barrier during HIV-1 encephalitis. *J. Immunol.* 158, 3499–3510.

Pires, R. A., Abul-Haija, Y. M., Reis, R. L., Ulijn, R. V., and Pashkuleva, I. (2018). Hydrogel nanomaterials for cancer diagnosis and therapy. *Hydrogels* 170, 170–183. doi: 10.1016/j.ejpb.2015.03.032

Roney, C., Kulkarni, P., Arora, V., Antich, P., Bonte, F., Wu, A., et al. (2005). Targeted nanoparticles for drug delivery through the blood–brain barrier for Alzheimer's disease. *J. Control. Release* 108, 193–214.

Sahiner, N., Godbey, W., McPherson, G. L., and John, V. T. (2006). Microgel, nanogel and hydrogel–hydrogel semi-IPN composites for biomedical applications: synthesis and characterization. *Colloid Polym. Sci.* 284, 1121–1129. doi: 10.1007/s00396-006-1489-4

Samikkannu, T., Atluri, V. S., and Nair, M. P. (2016). HIV and cocaine impact glial metabolism: energy sensor AMP-activated protein kinase role in mitochondrial biogenesis and epigenetic remodeling. *Sci. Rep.* 6:31784. doi: 10.1038/srep31784

Sharmin, E., Ashraf, S., and Ahmad, S. (2007). Synthesis, characterization, antibacterial and corrosion protective properties of epoxies, epoxy-polyols and epoxy-polyurethane coatings from linseed and(i(Pongamia glabra(/i(seed oils. *Int. J. Biol. Macromol.* 40, 407–422. doi: 10.1016/j.ijbiomac.2006.10.002

Shi, B., Zhang, H., Qiao, S. Z., Bi, J., and Dai, S. (2014). Intracellular microenvironment-responsive label-free autofluorescent nanogels for traceable gene delivery. *Adv. Healthc. Mater.* 3, 1839–1848. doi: 10.1002/adhm.201400187

Thorat, N., Otari, S., Patil, R., Bohara, R., Yadav, H., Koli, V., et al. (2014). Synthesis, characterization and biocompatibility of chitosan functionalized superparamagnetic nanoparticles for heat activated curing of cancer cells. *Dalton Trans.* 43, 17343–17351. doi: 10.1039/c4dt02293a

Vashist, A., Gupta, Y. K., and Ahmad, S. (2012). Interpenetrating biopolymer network based hydrogels for an effective drug delivery system. *Carbohydr. Polym.* 87, 1433–1439. doi: 10.1016/j.carbpol.2011.09.030

Vashist, A., Kaushik, A., Ghosal, A., Nikkhah-Moshaie, R., Vashist, A., Dev Jayant, R., et al. (2018a). "Chapter 1 journey of hydrogels to nanogels: a decade after," in *Nanogels for Biomedical Applications*, eds A. Vashist, A. K. Kaushik, S. Ahmad, and M. Nair (United Kingdom: The Royal Society of Chemistry), 1–8. doi: 10.1039/9781788010481-00001

Vashist, A., Kaushik, A., Vashist, A., Bala, J., Nikkhah-Moshaie, R., Sagar, V., et al. (2018b). Nanogels as potential drug nanocarriers for CNS drug delivery. *Drug Discov. Today* 23, 1436–1443. doi: 10.1016/j.drudis.2018.05.018

Vashist, A., Kaushik, A. K., Ahmad, S., and Nair, M. (2017). *Nanogels for Biomedical Applications*. United Kingdom: Royal Society of Chemistry.

Vashist, A., Shahabuddin, S., Gupta, Y. K., and Ahmad, S. (2013). Polyol induced interpenetrating networks: chitosan-methylmethacrylate based biocompatible and pH responsive hydrogels for drug delivery system. *J. Mater.Chem. B* 1, 168–178. doi: 10.1039/c2tb00021k

Vinogradov, S. V., Batrakova, E. V., and Kabanov, A. V. (2004). Nanogels for oligonucleotide delivery to the brain. *Bioconjug. Chem.* 15, 50–60. doi: 10.1021/bc034164r

Wang, D., and Imae, T. (2004). Fluorescence emission from dendrimers and its pH dependence. *J. Am. Chem. Soc.* 126, 13204–13205. doi: 10.1021/ja0454992

Wang, Z., Yang, L., and Fang, W. (2019). "Chitosan-based hydrogels," in *Chitin and Chitosan: Properties and Applications* eds Lambertus A. M. van den B. and Carmen G. B. (Hoboken, NJ: John Wiley & Sons), 97–144.

Wohlfart, S., Gelperina, S., and Kreuter, J. (2012). Transport of drugs across the blood–brain barrier by nanoparticles. *J. Control. Release* 161, 264–273. doi: 10.1016/j.jconrel.2011.08.017

Wong, H. L., Wu, X. Y., and Bendayan, R. (2012). Nanotechnological advances for the delivery of CNS therapeutics. *Adv. Drug Deliv. Rev.* 64, 686–700. doi: 10.1016/j.addr.2011.10.007

Wu, B. Y., Le, X. X., Jian, Y. K., Lu, W., Yang, Z. Y., Zheng, Z. K., et al. (2019). pH and thermo dual-responsive fluorescent hydrogel actuator. *Macromol. Rapid Commun.* 40:1800648. doi: 10.1002/marc.201800648

Yang, J., Zhang, Y., Gautam, S., Liu, L., Dey, J., Chen, W., et al. (2009). Development of aliphatic biodegradable photoluminescent polymers. *Proc. Natl. Acad. Sci. U.S.A.* 106, 10086–10091. doi: 10.1073/pnas.0900004106

Yang, Z., Leon, J., Martin, M., Harder, J. W., Zhang, R., Liang, D., et al. (2009). Pharmacokinetics and biodistribution of near-infrared fluorescence polymeric nanoparticles. *Nanotechnology* 20:165101. doi: 10.1088/0957-4484/20/16/165101

Yuan, F., Li, Y., Li, X., Zhu, J., Fan, L., Zhou, S., et al. (2018). Nitrogen-Rich D-π-A structural carbon quantum dots with a bright two-photon fluorescence for deep-tissue imaging. *ACS Appl. Bio Mater.* 1, 853–858. doi: 10.1021/acsabm.8b00276

Zaitsev, S. Y., Shaposhnikov, M. N., Solovyeva, D. O., Zaitsev, I. S., and Möbius, D. (2015). Cell staining by photo-activated dye and its conjugate with chitosan. *Cell Biochem. Biophys.* 71, 1475–1481. doi: 10.1007/s12013-014-0370-1

Zhang, X., Malhotra, S., Molina, M., and Haag, R. (2015). Micro-and nanogels with labile crosslinks–from synthesis to biomedical applications. *Chem. Soc. Rev.* 44, 1948–1973. doi: 10.1039/c4cs00341a

Zhang, Y., and Yang, J. (2013). Design strategies for fluorescent biodegradable polymeric biomaterials. *J. Mater. Chem. B* 1, 132–148. doi: 10.1039/c2tb00071g

Conflict of Interest: ArV, MN, and AK have the following competing interest: Florida International University has a US Non-Provisional patent application entitled "Micro/Nano Magnetic Hydrogels with Autofluorescence for Therapeutic and Diagnostic Applications. This work has been granted the U.S. Patent on Micro/Nano Magnetic Hydrogels with Autofluorescence for Therapeutic and Diagnostic Applications US Patent App. 15/907, 703, 2019 with ArV, MN, and AK; as inventors.

The remaining authors declare that the research was conducted in the absence of any commercial or financial relationships that could be construed as a potential conflict of interest.

Advantages of publishing in Frontiers

OPEN ACCESS
Articles are free to read for greatest visibility and readership

FAST PUBLICATION
Around 90 days from submission to decision

HIGH QUALITY PEER-REVIEW
Rigorous, collaborative, and constructive peer-review

TRANSPARENT PEER-REVIEW
Editors and reviewers acknowledged by name on published articles

Frontiers
Avenue du Tribunal-Fédéral 34
1005 Lausanne | Switzerland

Visit us: www.frontiersin.org
Contact us: info@frontiersin.org | +41 21 510 17 00

REPRODUCIBILITY OF RESEARCH
Support open data and methods to enhance research reproducibility

DIGITAL PUBLISHING
Articles designed for optimal readership across devices

FOLLOW US
@frontiersin

IMPACT METRICS
Advanced article metrics track visibility across digital media

EXTENSIVE PROMOTION
Marketing and promotion of impactful research

LOOP RESEARCH NETWORK
Our network increases your article's readership